TRANSPORTATION RESEARCH RECORD 665

Bridge Engineering
Volume 2

Proceedings of a conference conducted by the Transportation Research Board, September 25-27, 1978

TRANSPORTATION RESEARCH BOARD

COMMISSION ON SOCIOTECHNICAL SYSTEMS
NATIONAL RESEARCH COUNCIL

NATIONAL ACADEMY OF SCIENCES
WASHINGTON, D.C. 1978

Transportation Research Record 665
Price $13.40

subject areas
03 rail transport
23 highway drainage
27 bridge design
33 construction
34 general materials
40 general maintenance
62 foundations
63 mechanics

Transportation Research Board publications are available by ordering directly from the board. They may also be obtained on a regular basis through organizational or individual supporting membership in the board; members or library subscribers are eligible for substantial discounts. For further information, write to the Transportation Research Board, National Academy of Sciences, 2101 Constitution Avenue, N.W., Washington, D.C. 20418.

ISBN 0-309-02697-0
Library of Congress Catalog Card No. 78-71939

Sponsorship of the Papers in This Transportation Research Record

GROUP 2—DESIGN AND CONSTRUCTION OF TRANSPORTATION FACILITIES
Eldon J. Yoder, Purdue University, chairman

Conference Steering Committee
Ivan M. Viest, Bethlehem Steel Corporation, chairman
Dan S. Bechly, Roland H. Berger, W. E. Brakensiek, W. Dale Carney, Henry W. Derthick, John W. Fisher, Karl H. Frank, Charles F. Galambos, John M. Hanson, Conrad P. Heins, Wayne Henneberger, Lester A. Herr, Marvin H. Hilton, Robert N. Kamp, Heinz P. Koretzky, John M. Kruegler, Clyde N. Laughter

Lawrence F. Spaine, Adrian G. Clary, Wm. G. Gunderman, and John W. Guinnee, Transportation Research Board staff

Contents

Preface

During the past several decades, an impressive amount of research has been conducted in the development of new materials and technology to design, construct, and maintain vehicular bridges. Much has been learned about these complex problems and should be conveyed to a user community that represents such varied interests as state, federal, and local governments; private transportation agencies; consulting engineering firms; industry; planners; scientists; and engineers. Much remains to be learned, and this user community should be involved in guiding future research programs.

A continuing trend toward heavier loads and increasing traffic volumes, combined with adverse environmental conditions, has resulted in a reduction in the life expectancy of bridges and more rapid deterioration of existing bridges. A comprehensive review of the national bridge inventory by the U.S. Department of Transportation concluded that approximately 40 000 bridges on the Interstate highway system alone are structurally deficient and functionally obsolete. Similar bridge problems are faced by railroad and transit agencies.

The problem is widely recognized; both federal and state appropriations and operating agency appropriations are continually increasing for bridge construction and maintenance. An even larger effort must be made if the nation's surface transportation system is to function efficiently. Because funds are limited for bridge construction and for the repair, rehabilitation, and strengthening of existing bridges, a careful evaluation should be made of all available technology and needed research to ensure the optimum use of resources.

The Bridge Engineering Conference was organized to facilitate an interchange of information on all aspects of design, construction, rehabilitation, and maintenance of vehicular bridges and to have specific emphasis on problems and solutions of interest to highway, railroad, and transit bridge engineers, administrators, and managers. The papers in Transportation Research Records 664 and 665 constitute the proceedings of the conference held September 25-27, 1978, at the Chase-Park Plaza Hotel, St. Louis, Missouri. These two records contain all of the papers prepared in advance of the conference as well as several that were not included in the program due to limitations of time and space.

Organization and direction of the conference were the responsibilities of the Conference Steering Committee, whose members are listed on the reverse side of the title page of this Record.

The Bridge Engineering Conference was partially funded by the Federal Highway Administration and Federal Railroad Administration. The following organizations cooperated to make the conference possible:

COSPONSORS
Federal Highway Administration
Federal Railroad Administration
PARTICIPATING AGENCIES
American Association of State Highway and Transportation Officials
American Railway Engineering Association
American Road and Transportation Builders Association
American Society of Civil Engineers
International Association for Bridge and Structural Engineering
Missouri Pacific Railroad Company
Missouri State Highway Commission
National Association of County Engineers

The Eads Bridge, St. Louis, Missouri, 1874. Designer and builder, Capt. James Buchanan Eads. Designated National Civil Engineering Landmark.

THE DEVELOPMENT OF THE ONTARIO HIGHWAY BRIDGE DESIGN CODE

P.F. Csagoly and R.A. Dorton, Ontario Ministry of Transportation and Communications

At the end of 1975, the Ontario Ministry of Transportation and Communications decided to develop a Code for designing Ontario's highway bridges. Structural research in the Ministry, which began in 1969, has been successful in clarifying several aspects of structural behavior and load-carrying capacity. The activities concentrated on proof-testing existing bridges of questionable strength, inspecting and recording a large number of structures for various common faults; many the result of inadequate design practices. The resulting Ontario Highway Bridge Design Code is based on the existing AASHTO Specifications, but with most provisions for working stress design eliminated. For both serviceability and ultimate limit states, an upper-bound representation of all commercial vehicles observed in Ontario through various load surveys is employed. The use of deflection and stiffness criteria has been re-evaluated for each structural material. Impact and dynamic response is treated as a function of resonance frequencies. While introducing provisions for 0.3% deck reinforcement, crack control is made mandatory. The Code will discourage the use of single load path structures. New provisions on hydrology, drainage and various dimensional requirements are intended to achieve low maintenance structures. New sections are devoted to non-traditional analysis, soil-steel structures and the evaluation of existing bridges.

The objective of this paper is to highlight the new provisions of the Code and to provide information on the background research and study which led to their inclusion.

Background Research and Testing

In 1966 the Ontario Trucking Association made several presentations with the aim to increase the permissible weight of commercial vehicles. Although the legal Ontario weights were nearly twice as large as those recommended by AASHTO (1), the Ontario highway bridges had shown no distress due to overloading. This created skepticism of the validity of the AASHTO Code. The Ministry responded to this skepticism and originated a bridge testing program in 1969, in order to identify the magnitude of extra load-carrying capacity hidden due to the suspected conservatism of the Specifications and the unrefined nature of "traditional" methods of structural analysis.

The testing program, which at the time of writing this paper included over 125 bridges, revealed three significant facts:

1. The actual load-carrying capacity of highway bridges can exceed by a substantial margin the value established by "traditional" methods of analysis.
2. The load-carrying capacity can be predicted with certainty by refined methods of analysis, verified in turn by prototype bridge testing.
3. The margin of unaccounted-for extra capacity was observed to vary between 10% on steel trusses to 3,000% on concrete rigid frames.

Rationale for a New Code

It was considered important to have available a metric design code in 1978, as this is the target date for metric conversion for the construction industry in Canada. The most important factor in the Ministry's final decision to write a new Code was the availability of several significant research and development findings from Ministry work carried out by universities and the Ministry's Research and Development Division. Documentation more substantial than internal research reports was required as bridge designers need the backing of an accepted specification for their regular design activities, and it was thus essential to codify the research findings. The time necessary to incorporate these into either the CSA (2) or AASHTO (1) codes was considered prohibitive. In addition, the uncertainty in these specifications over the use of load factor or limit states design did not coincide with the Ministry's objectives to have a rational limit states format in operation as soon as possible to the exclusion of all other methods.

Preparation of the Code

The task force comprising 95 engineers is governed by an 11 member Code Control Committee,

which is responsible for the general concepts and broad philosophy of the Code as well as the review and acceptance of the technical sections written by sub-committees. The Code Control Committee is represented by MTC, the federal government of Canada, universities, and consulting engineers.

A sub-committee was formed for each of the 17 anticipated Code Sections, with chairmen appointed from MTC or the universities. The average committee size is five, and the sub-committee membership is from governments, universities, consulting engineers and industry of Canada and the United States.

Writing of the Code was begun immediately following a seminar in May 1976, attended by all members. Following reviews of content and outline, the first drafts were submitted in March 1977. These were subjected to detailed review by the Code Control Committee and revised drafts were submitted for editing. These edited drafts were issued for public comment in February 1978 with the final content of the Code scheduled to be completed late in 1978.

Each Section of the Code will consist of four possible subdivisions:

1. The Code proper which will be prescriptive and binding.
2. Charts or diagrams giving detailed data in an Appendix which will be binding.
3. A commentary giving justification or background information on each Code clause.
4. A supplement of background data or research information considered essential for a full understanding of the Code.

General Concepts

The first proposal for a new design load based on survey data on actual truck loadings in Ontario was given in 1973 (3). In addition to the live loading model it defined a load factor approach and a new proposal for dynamics of bridges.

The most important concept established for the Code was that it should be presented in the Limit States format. This was to apply to all Sections and all materials, and meant that the Working Stress method of the present CSA-S6 and the optional Working Stress or Load Factor approach of AASHTO would not be permitted. The Limit States approach requires that load factor and performance factor values be given in the Code, based on statistical data on load and strength variations, and calibrated to a pre-selected value for the Safety Index β.

A major objective of the Code was to transfer the growing knowledge of the actual behavior of existing bridges from the full-scale load test program (4, 5, 6) into definable clauses for the evaluation of the load-carrying capacity of existing bridges. In addition to evaluation methods based on testing experience, the Code defines rating and posting loads that are directly related to the design loads for new bridges and hence the existing trucks on the highway. The increased concern for minimizing maintenance is expressed through new clauses covering bridge hydraulics, deck drainage and durability.

The importance of advanced techniques is evidenced by the addition of a Section on "Methods of Analysis" which gives guidance on analytical methods that are accepted or recommended. The Code is a design code, and hence construction items have only been included if they were considered essential to the designer.

Limit States Design

Background

Limit States Design was developed and adopted for structural design during the 1950s, and has since been widely accepted by many European countries. General use of the method in North America has been somewhat slower, although the basis was established as early as 1963 in the ACI Building Code (7), but under different terminology.

The advantages of the Limit States Design approach towards achieving more uniform structural safety and economy are well documented (9, 10, 11). Safety and Limit States Design are comprehensively defined by MacGregor (9) and were used extensively in the development of the Code. He states: "When a structure or structural element becomes unfit for its intended use it is said to have reached a limit state.

Limit States Design is a design process that involves:

1. Identification of all potential modes of failure, i.e. limit states.
2. Determination of acceptable levels of safety against occurrence of each limit state.
3. Consideration by the designer of the significant Limit States."

The Code defines the Limit States in two groups, Ultimate Limit States and Serviceability Limit States (8).

Ultimate Limit States

The ultimate limit states correspond to the maximum load-carrying capacity of the bridge or a component, and are associated with the extreme loading cases. These states may result from loss of equilibrium, fracture of a section, formation of a mechanism due to plastic hinge development, and buckling.

Elastic methods of analysis are to be used in determining the response of the structure at the ultimate limit states, which is consistent with current North American codes such as AASHTO (1), NBC (7), and ACI (12), and most European codes. While it is true that the structure is unlikely to behave elastically throughout the load range, and that plastic redistribution will occur normally before an ultimate limit state is reached, it is recognized that methods of analysis involving inelastic behavior are not generally available to the designer at present.

The ultimate strength calculation of sections is based on the present well-established North American procedures. For reinforced concrete in flexure the calculation is based upon strain compatibility and an equivalent rectangular concrete stress distribution at the 0.85 f'_c level. For steel sections in flexure, the plastic moment is assumed to be attained for braced compact sections, but the yield moment is used for non-compact and unbraced sections.

For the ultimate limit state design calculations, load factors are applied to all load and force effects, and performance factors to the resistance or strength.

Serviceability Limit States

The serviceability limit states concern the disruption of the functional use of the structure

and are associated with the loadings for normal use. A bridge may be considered to have reached the serviceability limit state because of local damage such as cracking and spalling of concrete, vibration, excessive deflection, and fatigue. Elastic methods of analysis should be used to determine the response, as the structure is expected to behave elastically at the stress level or deflection value specified for these states.

There are two live load levels to be considered for the serviceability limit states. For fatigue, where the accumulation of many repeated events is the criterion, the live load corresponds to one heavy truck train. This service load is also applied to vibration calculations for human response. A multiple truck loading must be considered for states such as local damage and permanent deformation below the ultimate level.

Some serviceability limit states were covered implicitly in the Working Stress Methods of previous codes. They are now more clearly defined, the loadings and checks are more explicit, and many are new to bridge codes.

Human response to vibration, for bridges designed for varying pedestrian use, is covered by a frequency dependent limit on dynamic deflection. For substructure design, settlement is the most important serviceability condition, as any differential settlement causes superstructure and roadway deformations.

The cracking level of deck slabs is a critical criterion for deck durability. Cracking in all reinforced concrete is controlled by a service level limit on tensile reinforcement stresses, with the value dependent upon exposure conditions.

For steel the live load deflection limitations of previous codes have been removed, to be replaced by new dynamic and vibration controls. Inelastic deformation must not take place at the serviceability limit state to prevent permanent set. For high strength friction bolts in shear, the slip of the connected parts is controlled. Fatigue limits are set as a service condition for main members, connections and secondary members in steel.

For bearings and expansion joints, performance under the movements due to temperature, shrinkage, creep, and live load is a service level condition.

The serviceability limit state conditions are many and varied, and each designer will have to ensure that all the states appropriate to the particular structure being designed are properly investigated.

Design Equation

For the ultimate limit state the required design relationship is that the factored resistance must exceed the sum of the factored load effects. Thus:

$$\phi R \geq \Sigma KL \qquad (1)$$

where:

ϕ = Performance Factor
R = Resistance
K = Load Factor
L = Load Effect

The performance factor ϕ is applied to the resistance to account for the variabilities in material properties, dimensions and workmanship, the uncertainties in methods of computing resistance, and the type of failure being avoided. The load factors K are applied to the loads to account for uncertainties in the analytical methods, the unpredictable behavior of the structural system and to account for the variability of the loads themselves.

As the variability in loads would be expected to be non-uniform among dead load, live load and earth pressure, for instance, different values of K could be expected. Similarly the variability in dimensional tolerances between steel beams, cast-in-place concrete and asphalt, for instance, would indicate the same. For simplicity, AASHTO has used a value of K = 1.3 for all loads, and varied the live load magnitude for different load combinations.

In the Ontario Code greater precision has been sought by selecting the best value for the load factor for live load and each of four different dead load effects. The extra work involved in using a number of load factors is justified by the improved accuracy. This is particularly true as spans increase and the variable dead load factors produce a significant improvement in accuracy, and hence in more uniform safety and economy.

The separation of ϕ and K factors has been maintained throughout the Code. This should be borne in mind if a comparison is made with AASHTO, where separation has been maintained for reinforced concrete, but only load factors are given for steel, without performance factors. In actual fact, the load factor given for steel is a combination of both factors, or K/ϕ, but quoted as a load factor (13).

The values of K and ϕ used in the Code were derived as part of the Code calibration process described later.

Design Live Load

That the bridge design live load vehicle should be directly related to the legal highway vehicle appears self-evident. The fact that this relationship is very difficult to discern in many jurisdictions is, however, true. This is probably due to the fact that authors of bridge codes are not usually in a position to set or administer legal truck weights.

The maximum legal weights in 1944 were similar to the 320 kN (72 kip) AASHTO Standard HS 20 truck which was first specified for bridge design in that year. This loading is still commonly accepted in North America, except for those who specify an HS 25 truck. Since 1944 the legal weights have increased substantially reaching a peak value of 623 kN (140 kips) in Ontario.

Maximum Truck Weights

Ontario's present maximum legal weights for trucks were established in 1971 following extensive study of the effects of the proposed increases upon bridge response (14). The formula which determines the allowable gross weight, axle weights, or combinations of axles is known as the Ontario Bridge Formula (OBF). It relates the allowable weight W in kips to the equivalent base length B_M in feet, in the following manner.

$$W = 20 + 2.07B_M - 0.0071B_M^2 \qquad (2)$$

The equivalent base length is defined as the length over which the total weight on a group of axles should be uniformly distributed in order to produce substantially the same response on a bridge as the group of axles itself. B_M is calculated by an equation whose inputs are individual axle weights and interaxle spacings. With this

transformation any vehicle or group of axles can be quickly evaluated for acceptability. The formula has been plotted as the lower curve in Figure 1. The two limits are W = 89 kN (20 kips) when B_M = 0, which is the single axle case, and W = 623 kN (140 kips) when B_M = 24.4 m (80 ft.), which is the maximum B_M value that can be generated with a legal vehicle length limit of 19.8 m (65 ft.). The various axle groups for the HS 20 truck have been plotted on this diagram, and it can be seen that this live load model represents only the lower part of the legal weight curve (OBF).

The legal weight curve can only act as the basis for a design live load if actual weights never exceed the legal weights, which implies perfect enforcement with no tolerance. To ascertain actual truck weights, major surveys have been carried out at truck inspection stations in Ontario. A survey of 7,292 vehicles was taken in 1971 and results were plotted to compare with the legal weight curve. The first effort to establish a bridge design load based on this survey data was made in 1973 (3), using an upper-bound weight curve known as the Maximum Observed Load (MOL) curve. This upper bound was best represented by a curve with a constant band width of 100 kN (22.5 kips) above the legal weight curve (OBF), as shown in Figure 1.

To verify the actual weights surveyed in 1971, another survey of 9,864 vehicles, preselected to be representative of the heavy trucks, was carried out in 1975. It was found that the MOL was still a satisfactory upper-bound curve, but the percentage of trucks falling between the OBF and MOL curves had increased since 1971. In 1978, improved weight enforcement procedures were introduced. The new regulations are based on a modified Bridge Formula in SI units shown in Figure 2. The corresponding modified MOL level was adopted as the basis for a design live load model.

Figure 1. Ontario Bridge Formula (OBF) curve.

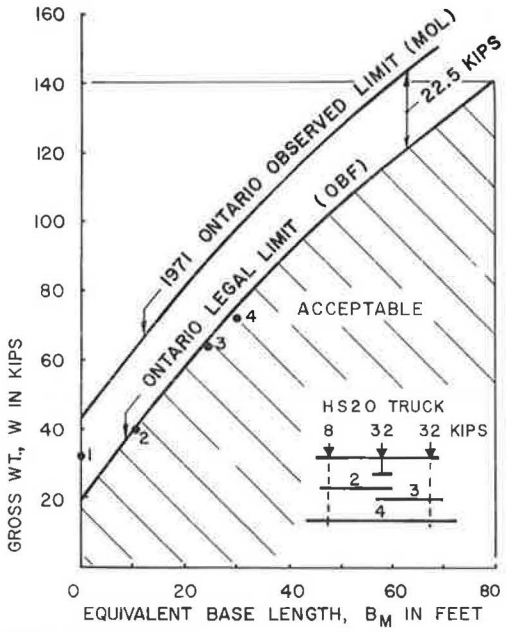

Note: 1 kN = 0.225 kip
1 m = 3.28 ft.

Figure 2. Maximum Observed Load (MOL) curve.

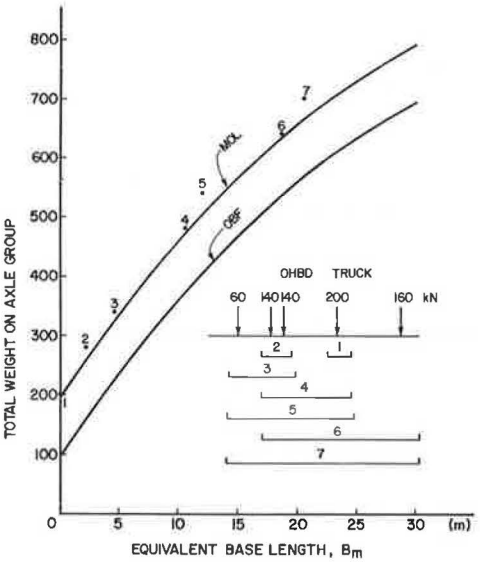

Note: 1 kN = 0.225 kip
1 m = 3.28 ft.

Live Load Design Models

A live load design system must model the following two aspects:

1. One heavy vehicle. This should incorporate the effect of axle loadings for the design of the floor system and short span members. The single vehicle itself will also govern the design of short to intermediate span bridges.
2. The presence of several vehicles. There are two components of multiple presence. First, the presence of more than one vehicle in a lane, and second, the presence of vehicles in more than one lane. The first component applies to bridges above the short span range, and most continuous structures. The second affects all multi-lane structures.

The single heavy vehicle model should be an upper-bound representation of all vehicle weights, as it will be applied to a design for the ultimate limit state. The MOL curve was used as the basis for developing the truck model which has to produce the maximum response for both moment and shear using either the whole truck or individual axles or axle combinations. No single actual truck from the surveys could produce this required response, and hence an idealized 5-axle vehicle was developed (Figure 3) which is referred to as the OHBD truck and rese bles a real truck configuration. The plot of this OHBD truck and four other axle groupings thereof, using the B_M transformation compared to the MOL curve (Figure 2), shows its suitability for capturing maximum responses.

Figure 3. Diagram of Ontario Code design truck.

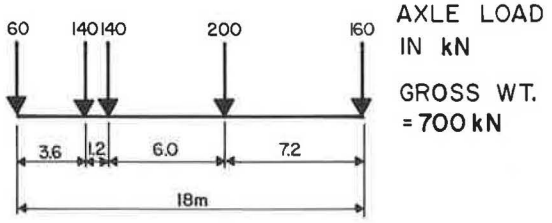

OHBD TRUCK

Note: 1 kN = 0.225 kip
1 m = 3.28 ft.

Determining the suitability of this OHBD truck for the wide variety of continuous structures in use, and developing the multiple presence aspects of a live load system required a large statistical study (15). A statistical description of Ontario truck traffic was developed which included the following:

1. 6,825 trucks taken from the 1975 survey.
2. A probability distribution of gross weight ratio, which is the ratio of gross truck weight to the legal weight limit, based on the 1975 survey.
3. A probability distribution for headway distance between trucks.

The Code's sub-committee responsible for the live load system selected the 700 kN (157.5 kip) OHBD truck as the idealization of one heavy vehicle. This decision was based on the truck's ability to best capture various responses based on the MOL study and the University of Western Ontario report (15), and the fact that it was the simplest and most practical model.

The live load system selected to model the presence of several vehicles uses one 490 kN (110.2 kip) truck in each lane, which is 70% of the OHBD truck, and is combined with a uniformly distributed load (UDL) (Figure 4). Lane reduction factors are applied according to the number of lanes loaded, and the intensity of the UDL varies with the highway classification.

For the serviceability limit states the effect of the mean of the loaded frequently occurring vehicles was required. The service load has been selected as 80% of the OHBD truck, thus having a gross weight of 560 kN (126 kips).

The loading to be used for the evaluation of existing bridges and for posting purposes is the OHBD truck and two subconfigurations of this truck (16). Thus the one basic truck configuration can be used for ultimate and serviceability limit states, for evaluation and posting, with obvious analytical and computer programming advantages.

Dynamic Load and Vibrations

The impact factor in North American bridge codes has remained unchanged for 50 years. It is a very simple formula which attempts to describe a very complex dynamic interaction between the vehicle and bridge structure. Objectionable structural vibration has been addressed by means of a live load deflection limit, or by specifying span to depth ratio limits, neither of which achieve the desired objective with modern highway structures. The new Code makes substantial changes in the area of impact and dynamic response based primarily on the results of full-scale bridge testing. The new Code values may change in the future as further data are gathered, but this is a first step in relating the dynamic design process to a more significant parameter, the first flexural frequency.

Existing Specifications

The present AASHTO Specifications give impact values as a function of span length in percentage of the live load to be applied, i.e. dynamic response is treated as a quasi-static load.

The AASHTO impact formula was first used in 1927, and it appears to have served reasonably well for simple spans and short spans of that period, having been based on impact tests of highway bridges carried out in the early 1920s. It does not, however, contain important parameters found to affect the dynamic behavior of continuous bridges more recently built.

The current slenderness limit of span/depth <25 for beams has had its evolution traced back to the AREA railway specification of 1905. The limitation on deflection was first introduced in railway bridge specifications in 1871, and was very similar to the current AASHTO value of 1/800 of the span for deflection due to live load and impact. These limitations have only been applied to steel bridges and the sole reason for their retention appears to have been expectation that user discomfort from vibrations would be controlled thereby. There is no justification for keeping these controls on deflection today as they are inadequate for their intended use, and criteria relating to user response to vibrations can now be specified.

With the present concern about bridge deck deterioration there has been some reluctance to abandon the deflection limits for fear that increased flexibility would hasten deck deterioration. There appears to be no correlation between flexibility and deck deterioration from investigations reported (17), and the usual deflection controls for steel and concrete bridges have been deleted from the new Code.

Recent Research and Testing

MTC has been investigating bridge dynamics for more than 20 years. The initial work was done at Queen's University, and dealt with human sensitivity to vibration (18) and bridge vibrations measured in the field (19,20). The measurements were carried out on 52 bridges known to vibrate, and recorded mid-span deflections with a simple deflectograph. The frequency of vibration of the loaded structures was generally the first flexural frequency, or a forced frequency usually in the 2 to 7 Hz range, corresponding to the typical truck bounce frequencies.

A plot of the Queen's University 1956-57 results of dynamic deflection ratio against observed bridge frequency (Figure 5) shows a considerable number of bridges with impact over the maximum AASHTO value of 0.3. The dynamic deflection ratio, or impact, is the ratio of live load dynamic deflection to static deflection at mid-span.

Between 1969 and 1971 MTC carried out dynamic response studies on a number of continuous structures, including the voided post-tensioned concrete deck type. MTC's own load test vehicle was used for these tests, being a 5-axle tractor semi-trailer unit with load varied by concrete blocks. The results of 11 tests have been reported (21) and Figure 6 shows the plot of impact against observed bridge frequency. Only one bridge, with a flexural frequency of 5.8 Hz, gave an impact value below the AASHTO figure, and the values ranged up to a maximum of 87% for a 5-span, post-tensioned concrete deck structure. The report suggested that bridges with natural frequencies in the 2 to 5 Hz range should be avoided if possible, due to the high dynamic response observed when bridge and vehicle frequencies match.

The findings of this dynamic testing were incorporated in the impact proposals put forward in 1973 (3) and were used for the design of the Conestogo River Bridge (4,5). For this 3-span continuous plate girder bridge it was economically impossible to avoid the 2 to 5 Hz band for all of the first three flexural frequencies. It was decided to abandon the AASHTO deflection and depth limitations and design a very flexible structure

Figure 4. Truck + UDL, lane load design system.

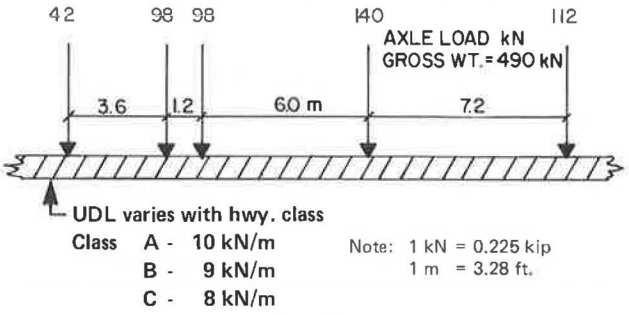

Figure 5. Plot of dynamic deflection ratio against frequency, simple spans 1956.

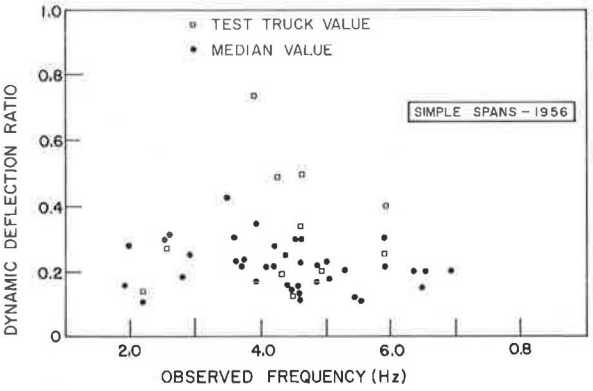

Figure 6. Plot of impact against frequency, continuous spans 1972.

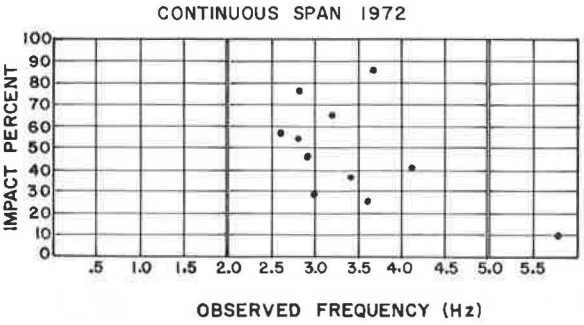

Figure 7. Code diagram of dynamic load allowance.

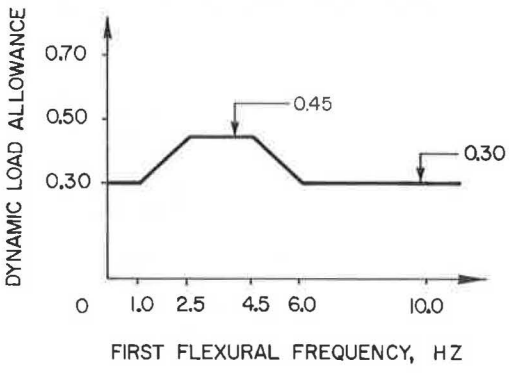

with a first frequency of 1.6 Hz. As the second and third mode frequencies were within the band, an impact value of 0.45 was used.

New Code Provisions - Dynamic Allowance

Although the dynamic and static responses of a bridge structure to load are not identical, codes in the past have assumed that the response is identical as a design convenience. This practice is continued in the new Code by providing for an equivalent static allowance for impact, called the dynamic load allowance. A general clause does allow the use of advanced theoretical or experimental dynamic analysis of the vehicle-bridge system to establish the values of the dynamic load allowance. Such an analysis would require the knowledge of representative vehicle loadings and vehicle suspension systems, a representative bridge structure including damping characteristics, and the variations in axle loads caused by irregularities in the riding surface. Because such an analytical method is not generally available or practical to use on a particular structure, a quasi-static representation is proposed for design purposes.

The dynamic load allowances are given in terms of one OHBD Truck or part thereof, or the lane load for the ultimate limit state, and the service loading or part thereof for the serviceability limit states. As two or more trucks on a bridge are unlikely to be dynamically identical and in-phase, it is expected that the maximum dynamic effects due to one truck are greater than the maximum effect per truck when more than one truck is present. For this reason modification factors (Table 1) are applied to loading cases of more than one truck.

Table 1. Modification factors for dynamic load allowance.

Loading Case	Modification Factor
More than one OHBD Truck	0.7
More than two OHBD Trucks	0.6
Four or more OHBD Trucks	0.5

The specified dynamic load allowance values apply to all construction materials except wood. The typical damping values for wooden structures are about three times the values observed for steel or concrete structures of similar frequency, and for this reason the dynamic load allowance for wood has been reduced to 0.7 of the specified values and is only applied to certain structural types.

A dynamic load allowance of not less than 0.4 is specified for deck slabs and deck systems, the designs of which are controlled by wheel loads. This value covers the impactive action of wheel loads where the approach riding surface has been paved to normal standards, and assumes that the dynamic response effects are insignificant. For floor beams and stringers spanning less than 12 m (39 ft.), the specified value is $\geqslant 0.35$.

For main members the dynamic load allowance is specified as a function of the first flexural frequency of the members as shown in Figure 7. To avoid undue refinement in the calculations, a variation of ±10% in the calculated frequency must be allowed in selecting the dynamic load allowance, reflecting a degree of uncertainty in the frequency calculation.

For flexible, long-span structures with a frequency of less than 1 Hz, and short-span structures with a frequency greater than 6 Hz, the maximum AASHTO impact value of 0.3 is retained for the dynamic load allowance. For structures where a resonance condition is possible, values are reaching a maximum value of 0.45 in the band of 2.5 Hz to 4.5 Hz. The pitch and bounce frequencies of most heavy commercial vehicles in Ontario fall within this band.

New Code Provisions - Vibration Control

A serviceability limit state has been specified to control objectionable vibrations for pedestrian users of various types of bridges. To achieve this control, a restriction has been placed on deflection in relation to the first flexural frequency of the bridge.

Structures have been placed in four classes, each class having its own deflection-frequency limit curve. These curves have been based on a number of studies of human response to vertical vibration (18,22), with the acceleration parameter changed to the equivalent deflection parameter for ease of calculation.

Methods of Analysis

The present AASHTO Specifications give little guidance on methods of static analysis for bridge superstructures, except for the clauses on distribution of loads. In the new Ontario Code, the section on methods of analysis replaces the load distribution clauses and expands the coverage to indicate approved methods of design analysis.

Background

It has long been recognized that the distribution factors given in AASHTO are lower-bound values to cover a wide variety of cases, and thus lead to overdesign for some structures. There has always been a general clause which allows a rational analysis to replace an empirical formula, but there has been little active encouragement to use advanced methods of analysis.

The removal of the deflection limitation for steel beams could lead to more flexible structures, for which the load distribution is better than for present structures. As an example, the Conestogo River Bridge (4) had an equivalent distribution factor of S/7.5 based on a grid analysis, compared to the AASHTO empirical value of S/5.5. While the simple distribution factor approach has served well in the past, and was necessary when more complex analysis was very time-consuming, the availability of computer programs for advanced methods of analysis means the empirical approach is not appropriate for all structures today.

For these reasons the distribution factor approach has been reconsidered, and where still found acceptable, has been given in a more accurate format, but much of the simplicity of the old method has been retained. For the areas considered unacceptable, preferred methods of refined analysis are given for different categories of structures. In addition, guidance is given on conditions affecting the selection of the method of analysis and on the idealization of structures for analysis.

Simplified Methods

Two simplified methods of analysis are allowed, subject to prescribed conditions being fulfilled. One is a distribution coefficient method and the other is the beam analogy method.

The distribution coefficient method is comparable to the AASHTO distribution factor method, the application being similar by the use of a load fraction S/D applied to the wheel loads. D is given a value in AASHTO according to bridge type, but is selected from charts for each bridge by the Ontario Code in accordance with the number of lanes and the stiffness properties of the particular structure, thus providing improved accuracy. The method is approved for use in calculating longitudinal moments and shears in bridges with shallow superstructures, subject to restrictions on continuity, skew, curvature, beam spacing, and variations in section. The shallow superstructures to which the method applies include solid slabs, shallow voided slabs, slabs on girders, grillages and shear connected beams.

The procedure for longitudinal moments is to calculate the torsional parameter α, which is a function of the longitudinal and transverse bending stiffnesses and torsional stiffnesses, and the flexural parameter Θ, which is a function of the bending stiffnesses in the two directions, the bridge width and span length. With these values of α and Θ, a chart is selected based on span and number of lanes which gives D as a function of α and Θ. A typical chart for a 2-lane bridge is shown in Figure 8. Separate charts are provided for moment and shear. The Code gives methods and charts for calculating the various stiffness parameters and hence α and Θ for all the shallow superstructure types listed. The charts were derived by the use of a computer program based on orthotropic plate theory (23).

The beam analogy method, whereby the whole or part of a bridge superstructure is analyzed assuming it to be a one-dimensional beam, is limited to the evaluation of longitudinal moments and shears due to dead loads. In addition, the cross section of the bridge must be substantially uniform, the skew smaller than a specified value depending upon the bridge properties, and the supports either line supports or uniformly spaced discrete supports.

Figure 8. Chart of distribution coefficient D values.

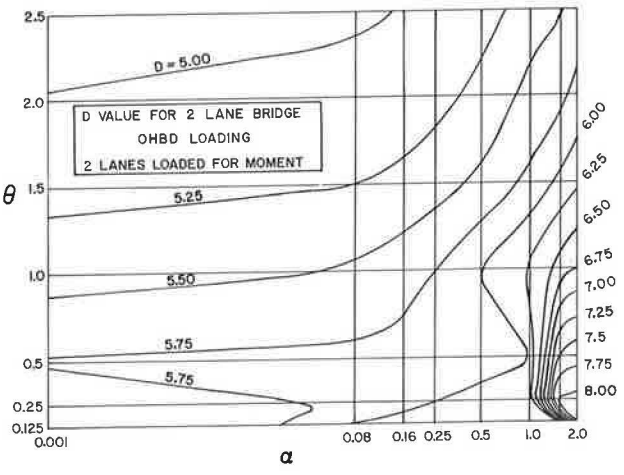

Refined Methods

The following methods are approved for general use for the analyses of the appropriate bridge types:

1. Grillage analogy methods.
2. Orthotropic plate theory methods.
3. Finite element methods.
4. Finite strip methods.
5. Folded plate methods.

These refined methods are well reported in the technical literature and the Code gives reference to representative papers without further detailing of the methods. The Code does, however, give detailed guidance on the idealization of shallow structures for analysis by both 2-dimensional and 3-dimensional analytical methods.

Selection of Methods of Analysis

A number of approved methods of analysis have been identified, and the structural responses to be considered for each type of structure are shown in Table 2, and factors affecting structural response in Table 3. The Code gives tables for each bridge type A to L in Table 2, relating the responses and factors affecting responses to the approved methods of analysis. These tables show the analytical methods which can satisfactorily model each response and response factor. Approval is required for the use of any method of analysis which does not comply with the requirements of the appropriate table for the bridge type under consideration.

Table 2. Types of bridges and structural responses.

Bridge Types	Structural Responses										
	Longitudinal Moment	Transverse Moment	Longitudinal Torsion	Longitudinal Shear	Transverse Shear	In-Plane Forces	Deformation	Torsional Warping	Distortional Warping	Axial Forces for Line Members	Moments & Shears for Line Members
A. Slabs	X	X		X		X					
B. Slabs on Girders	X	X		X		X					
C. Shallow Voided Slabs	X	X		X		X					
D. Grillages	X	X		X	X						
E. Shear Connected Beams	X	X		X	X	X					
F. Single Cell Box Girders	X	X	X	X	X	X		X	X		
G. Multi-Cell Box Girders	X	X	X	X	X	X		X	X		
H. Multi-Spine Box Girders	X	X	X	X	X	X		X	X		
I. Rigid Frames	X	X		X	X	X					
J. Trusses										X	
K. Arches										X	X
L. Wood Beams, Decks	X	X		X	X		X				

Table 3. Factors affecting structural responses.

A.	Continuity of spans
B.	Plan geometry
C.	Edge stiffening
D.	Variation of transverse cross section
E.	Variation of longitudinal cross section
F.	Diaphragms and Cross Frames
G.	Wind bracing
H.	Yielding supports and supports for skew spans
I.	Temperature effects
J.	Creep and Shrinkage
K.	Floor system interaction

This specific guidance on the selection of methods of analysis is new to North American bridge codes and has been provided to ensure the use of the most suitable methods for each bridge design, and encourage the use of refined methods rather than simplified or empirical methods whenever appropriate.

It is expected that the new provisions for refined methods of analysis will require more design time than before. It has been shown (24) that, on the average, the cost of the computational part of design does not exceed one percent of the total cost of a bridge. Considering that a refined method of analysis may lead to reduction of structural component sizes, elimination of certain secondary members, simplification and uniformity in detailing, even a one hundred percent increase in actual design time would appear justified.

Miscellaneous Provisions

General Features of Design

Hydraulic aspects are a major cause of bridge and culvert problems. A recent international survey of major bridge failures (25) showed that 66 of the 143 failures were due to scour. To emphasize the requirements for proper hydraulic design, it was decided to expand the coverage considerably and include it in the Code.

The hydraulic design aspects are largely based on the procedures established by the MTC Hydrology Section, and include requirements for all sizes of bridges and culverts and their appurtenant works, including design flood criteria, scour calculations and protection, and backwater design.

In general, the Code is aiming at self-protecting bridge superstructures. Other than spalling of the deck surface, most deterioration problems were found to be related to inadequate drainage facilities. Provisions will require:

1. Improved design for drain-pipes;
2. Improved location of drain-pipes such that brine is not spilled on other structural components;
3. Continuous drip around the perimeter of the superstructure;
4. Minimum slopes of all previously horizontal surfaces to eliminate ponding;
5. Minimum 8 in. gap between the end of the superstructure and the abutment to permit inspection and to ensure proper ventilation.
6. Minimum number of deck joints.

Miscellaneous Loads and Movements

Equivalent static wind loads for bridges are based on the geographically dependent reference wind pressure for a 50-year return period, modified by given factors for exposure and gust effect, and by a horizontal force coefficient which varies with the superstructure type.

Thermal gradient effects have received little consideration in the past, but recent realization of the magnitude of the possible stresses induced has caused concern. Values for the temperature differentials through the depth of different types of structure are given, and the magnitude of the resulting induced moments can be determined from the nondimensional curvature-depth relationships given.

Substructure and Retaining Walls

The limit states format produced the major change in this section. The limit states calculations cover both the substructure and piles acting as structural members and the geotechnical capacity of the supporting soil. Because the Code is the first one in North America to use the limit states format for substructures and soil capacity, much original work was required in selecting the soil performance factors, and establishing the ultimate and serviceability limit states.

Concrete Deck Slabs

For the design of concrete deck slabs supported by beams or girders, the current AASHTO Specifications assume that wheel loads are distributed over a given length of slab, and the transverse spanning slab strips are then designed as reinforced concrete beams by the usual flexural theory. Such slabs usually develop compressive membrane, or arching forces, which allow a substantial reduction in reinforcing steel (26,27).

Provided the deck system supplies sufficient horizontal rigidity for the development of arching forces, the specified empirical design method may be used. The required reinforcing steel ratio of 0.3%, for each direction top and bottom, is little more than the minimum normally supplied for shrinkage and temperature effects, and the method thus becomes a prescription for the amount of steel, provided the appropriate boundary conditions are satisfied. These boundary conditions are met by most existing composite slabs, and include the following:

1. A solid slab of constant thickness with a minimum value of 200 mm (8 in.) with edge stiffening.
2. Span of the slab perpendicular to the direction of traffic no greater than 3.66 m (12 ft.).
3. Span/Thickness ratio of the slab not over 15.

The prescribed reinforcing is adequate to carry all local wheel loads on slabs spanning between girders, and is normally adequate to cover the transverse bending effects due to load distribution between girders. However, torsionally stiff box girder systems should be analyzed for transverse moments and shears in the slab due to differential deflection of the girders. Details of the background research and testing for the empirical method are given in other conference papers (28,29).

Reinforced Concrete

Apart from the limit states format, the major changes in the Code concern shear and torsion.

The shear provisions given for beams and compression members are based mainly on the shear provisions of the ACI Building Code 318-71 (30) and the recent report of ACI-ASCE Committee 426 (31). The shear stress carried by the concrete is a function of the concrete strength and longitudinal steel ratio, and is constant for a particular beam whether or not the beam has stirrups (31,32). It is assumed that axial compression will increase the shear resistance of members and that axial tension will reduce the shear resistance. Shear friction is included and conditions when the concept may be applied are given.

For members loaded in torsion, the clauses are based primarily on the provisions of CSA Standard A23.3 (33). The basic equations for determining the amount of torsional steel required to provide a certain torsional strength are based on the 45^{o} space truss analogy (34).

Prestressed Concrete

Among several changes to the prestressed concrete provisions are the following:

1. The maximum permissible compressive stress in members produced in certified plants has been increased since the final concrete strength is controlled by that required at transfer, and the 28-day strength is generally higher than the specified strength.
2. A limit has been imposed on the maximum effective prestress in voided slabs to prevent longitudinal cracking due to stress concentrations over the voids (35).
3. To fully utilize the economic advantages of low relaxation steels, the stress limit at transfer and the stress limit at jacking have been increased. The latter increase is limited to post-tensioned construction.
4. The method of calculating prestress losses differs from other codes, and the losses at transfer and the losses after transfer are computed separately.
5. The effect on shear capacity of the presence of post-tensioned ducts in thin webs is covered by an expression for equivalent web width (36).
6. New expressions for the development length of prestressing strands are specified to provide bond integrity for the load capacity of the member.

Structural Steel

Among the numerous changes in the structural steel section are the following:

1. Unlike the AASHTO Specifications, the Code specifies a separate performance factor ϕ value for structural steel.
2. Steels specified for primary tension elements are required to meet minimum specified CVN values for notch toughness (37).
3. The AASHTO formula for the strength of compression members was found to give inconsistent safety levels for different slenderness ratios and has been replaced by the CSA Standards S16.1 formulae (38,39).
4. The requirements for bottom lateral bracing for beam and girder bridges have been made less restrictive and such bracing is now required only for spans of 45 m (150 ft.) or greater.

Structural Fatigue

The Code requires that members, subject to cyclic tensile stress during passage of the live load, be proportioned on the basis of an allowable stress range, F_{SR}, corresponding to a specified number of stress cycles, N.

The stress range concept means that only live load and dynamic load allowance stresses need be considered when designing a particular detail for fatigue.

The number of cycles of maximum stress range for the Code was determined from available studies of Ontario's truck traffic. The load spectrum from the 1975 survey was evaluated against the response of a single OHBD Truck for several simple spans between 6.1 m (20 ft.) and 61 m (200 ft.) for shear and moment.

The number of constant stress range cycles to be

considered for the design of bridges on the three Ontario road classifications are given in Table 4.

Table 4. Stress range cycles, N.

Type of Road	Average Daily Truck Traffic (ADTT)	Single Service Loads
Class A	1000 or more	over 2,000,000
Class B	250 - 1000	2,000,000
Class C-1	50 - 250	500,000
Class C-2	0 - 50	100,000

The stress range is calculated using a single service load crossing the bridge, the service load being 80% of a single OHBD Truck amplified by the corresponding dynamic load allowance. To discourage the design of single load path structures, the Code requires that allowable stress range be reduced by 25% for this type of structure. The Code emphasizes that a minimum number of secondary members be used and their components be appropriately designed for both ultimate and service limit states (40).

Soil-Steel Structures

The Code provides tables for the design thicknesses of corrugated conduit walls for spans up to 7.9 m (26 ft.). These tables are the same as presently provided by the corrugated metal pipe industry. However, by the application of the limit states design method given in the Code, conduit wall thicknesses smaller than those given in the tables may be possible. The prescribed limit states method must be used for spans over 7.9 m (26 ft.), unless a finite element method or other approved refined method is employed. Special patented techniques, such as longitudinal beams, relieving slabs, steel ribs and squeeze blocks, may be used provided all the Code requirements are met. The buckling computation is a refinement of the conventional ring compression method. The calculation of loads differs from AASHTO by allowing for active earth pressure on the top of the conduit combined with passive pressure below.

The deformations of the conduit walls during the backfilling operation have to be controlled so that the conduit wall stresses do not exceed 90% of the yield stress of the steel. A simple formula is given for the maximum crown deflection at which this stress is reached.

Wood Structures

The change from working stress design to limit states design has been more difficult for wood than for steel and concrete. There is no North American wood specification in the limit states format, and little of the test data needed for the transformation was immediately available. A large program of in-grade testing is currently under way at the University of British Columbia, and the availability of the test results from this and other projects will determine many of the values and provisions appearing in the Code.

The most common form of wooden bridge in Ontario is the longitudinally laminated deck type. The Code covers load sharing between laminations for asphalt covered decks and composite wood-concrete deck superstructures.

Rating of Existing Bridges

There is today a growing concern about bridge maintenance, and an increased emphasis on preserving and strengthening existing bridges when possible, rather than replacing them. Maintenance and bridge rating have traditionally not had the same attention as new construction methods, design and analysis, and in comparison many of the existing techniques appear outdated. The full-scale bridge testing program started in 1969 in Ontario was aimed at a better understanding of the actual behavior of bridges so that any built-in conservatism could be identified and accounted for in evaluating load-carrying capacity (6). The results of this test program have had a large influence on a number of the Code sections for new bridges as well as contributing to the provisions of this section.

The aim of the new Code is to apply the refined methods of analysis to bridge evaluation as well as new designs, particularly when a posting limit or possible replacement is being considered. The limit states approach is the only method accepted in keeping with the rest of the Code, and the rating and posting loads are directly related to the design live loads established through the latest truck surveys (16).

The given performance factors ϕ, and load factors K, have been derived for new bridge designs. They may be subject to change for bridge evaluation where the future life expectancy or possible use of the bridge differs from new construction.

Bearings and Deck Joints

The design or selection of bearings and deck joints, the calculation of structure movements, and provisions for structure articulation are all covered in a systematic and comprehensive manner in one section of the Code. The ultimate and serviceability limit states to be considered are defined and performance requirements are given.

The performance requirements have been set to minimize maintenance and improve the durability of structures. Inadequate anchorage of deck joints has caused many maintenance problems in the past, and minimum anchorage requirements are now specified.

Accessories

The accessories section applies to the structural design of supports for highway signs, luminaires and traffic signals, and of bridge railings. The design of supports has been covered by AASHTO in a separate specification (41), but the required provisions are incorporated into the bridge specification for the Ontario Code.

Construction and Temporary Works

This section covers loading of the structure during construction by specifying loads and factors different from those prescribed for the completed structure.

Temporary works include the design for those structural works necessary for the building of a bridge, but not forming part of the finished bridge. The design methods are covered by other sections of the Code, and the temporary works section primarily specifies the loads and forces to be used.

Code Calibration

The calibration process is the selection of the values of the following design equation parameters to achieve the objectives of the selected code format:

Performance factors, ϕ
Load factors, K

The principal objective in using the limit states format was to achieve more uniform structural safety than provided by the previously used working stress format. The calibration was carried out in two phases. The first phase was the initial selection of values for the parameters based on available statistical data using second moment reliability theory and a target safety index β. The second phase consisted of a comparison of a number of bridge designs carried out to the working stress methods of the AASHTO Specification with designs to the new Code using the initial values of the design parameters. The parameters were then adjusted in light of this comparison and the final safety levels assessed.

Background

When ultimate strength design methods were first introduced in North America with the 1956 ACI Building Code, the values for load factors were selected based largely on engineering judgement (9). As probabilistic theories developed and some statistical data on strength and load variation became available, the safety provisions and design parameters were revised accordingly. Another method used to effect a change from one format to another is to calibrate the new format parameters so that the resulting structures have much the same strength as structures designed to the old format. This method was used when load factor design in steel was first introduced into the AASHTO Specifications (13), and the single calibration point was for a simple span of 12.2 m (40 ft.). For other span lengths, the strengths or safety levels would be different by the two formats.

The method used for the AASHTO Specification was not considered satisfactory for calibration of the Ontario Code, as it presupposes a satisfactory safety level for a particular span length using old designs and does not take advantage of the statistical data which are increasingly available. When full data are available on all materials, all loads and load combinations for a full sample of bridge types, then the application of probability theory based on an acceptable risk of failure will be possible. This situation still appears to be some years away, and the application of a lower level of calibration is the only practical option today, taking advantage of what statistical data are available from various sources.

The safety index β is the basic measurement of structural safety in current probability methods, and was used in both phases of the calibration of the Ontario Code.

First Phase Calibration

A second moment reliability method (42) was used for the first calculation of load factor and performance factor values.

A starting value of $\beta = 3.5$ was selected, based on current typical values considered acceptable for building design. The committees for each material then calculated starting ϕ values based on available statistical data. Data was often lacking or inadequate for bridges, and typical values had to be selected from general construction experience.

These initial values of design parameters were used in the second phase for comparative designs using the first draft of the new Code.

Second Phase Calibration

The second phase calibration method (43) required data on a number of structures designed to the current standards. MTC provided information on bridges designed to the AASHTO loading by working stress methods, from which 11 were selected (Table 5) as being representative of the most common types presently used in Ontario. The selected bridges covered the usual span ranges in each group, and the typical span for each group was identified for use in the weighting process. For uniform comparison of live load effects all the selected bridges have two traffic lanes, and are located on Class A highways.

Table 5. Comparison of safety indices β by new Code and by AASHTO.

Category	Limit State	Span Length m	Safety Indices β	
			AASHTO	New Code
Steel I-Girders	Moment	18.3	5.19	4.00
	Moment	27.5	2.14	4.20
	Moment	37.8	2.59	3.80
	Shear	18.3	6.51	5.00
	Shear	27.5	4.27	4.80
	Shear	37.8	4.82	4.15
Steel Box Girders	Moment	42.7	2.69	3.85
	Shear	42.7	6.05	3.95
Pretensioned Concrete AASHTO Beams	Moment	18.3	4.72	3.50
	Moment	27.5	4.05	3.70
	Moment	29.9	3.60	3.55
	Moment	33.5	3.66	3.40
	Shear	18.3	2.88	4.00
	Shear	27.5	3.97	3.80
	Shear	29.9	2.91	3.75
	Shear	33.5	3.58	3.65
Post-Tensioned Concrete Decks	Moment	32.0	4.93	3.90
	Moment	38.1	4.45	4.10
	Moment	40.3	3.77	3.85
	Shear	32.0	3.73	3.35
	Shear	38.1	3.29	3.45
1 m = 3.28 ft.	Shear	40.3	3.07	3.40

These bridges were analyzed to obtain values of structural safety in terms of the safety index β (44):

$$\beta = \frac{\ln (\bar{R}/\bar{S})}{\sqrt{V_R^2 + V_S^2}} \qquad (3)$$

where:

$\bar{R}$ and V_R = mean and coefficient of variation of resistance,

$\bar{S}$ and V_S = mean and coefficient of variation of load.

The load and resistance data were used in equation 3 to calculate the safety index β for moment and shear for each bridge.

The β values in Table 5 for current AASHTO bridges vary from a low of 2.14 to a high of 6.51. This range of β values justified the selected starting value of $\beta = 3.5$, and it was confirmed as the target β value for the next phase of calibration.

The selected structures were then redesigned to the new Code, using the starting performance factor ϕ

values given by the sub-committees, and the starting load factor K values from the first phase calibration.

The objective of the subsequent calibration process (43) was to reduce the scatter of β values by adjustment of the starting values of the design equation parameters. With the calibrated values of these parameters, the β values were recalculated to check the variation from the target value of 3.5. The results are shown in Table 5, and the β value scatter has been reduced to between 3.35 and 4.2 (45), except for steel girders in shear.

These calibrated values of the design parameters were used in the draft of the Code distributed for public comment, and are shown in Tables 6 and 7. The values may be changed as further calibration work is performed, before the Code is published.

Table 6. Calibrated values of load factors K.

Load Factor Description	Load Factor Values
Live Load K_L.	1.35
Dynamic Load Allowance K_I.	1.35
Dead Load K_{D_1} for factory produced structural components.	1.15
Dead Load K_{D_2} for cast-in-field structural components and all non-structural components.	1.25
Dead Load K_{D_3} for asphalt wearing surface.	1.7

Table 7. Calibrated values of performance factors ϕ.

Category	Limit State	ϕ Value
Steel Girders	Moment	0.90
	Shear	0.90
Pretensioned Concrete Beams	Moment	0.85
	Shear	0.65
Post-Tensioned Concrete Decks	Moment	0.85
	Shear	0.65

Closing Remarks

The Ontario Highway Bridge Design Code will be published in late 1978, and work will then begin on a revised edition to be issued one year later.

The primary objective of the change to Limit States Format - the provision of more uniform safety levels - appears to have been achieved. Whether improved economy has also been attained can only be assessed when an adequate sample of bridges has been designed to the new Code. However, it is expected that the increased design live load can be accommodated and still produce a 10% saving in structural materials.

References

1. Standard Specifications for Highway Bridges. AASHTO 1977.
2. CSA Standard S6-1974. Design of Highway Bridges.
3. P.F. Csagoly and R.A. Dorton. Proposed Ontario Bridge Design Load. MTC, RR186, 1973.
4. R.A. Dorton, M. Holowka and J.P.C. King. The Conestogo River Bridge – Design and Testing. CJCE, Vol. 4, No. 1, March 1977.
5. J.P.C. King, M. Holowka, R.A. Dorton and A.C. Agarwal. Test Results from the Conestogo River Bridge. Bridge Engineering Conf., TRB, 1978.
6. B. Bakht and P.F. Csagoly. Testing of Perley Bridge. Research and Development Division, MTC, 1977, RR207.
7. ACI Comm. 318. Building Code Requirements for Reinforced Concrete. ACI-318-63, 1963.
8. National Building Code. NRC, 1975.
9. J.G. MacGregor. Safety and Limit States Design for Reinforced Concrete. CJCE, Vol. 3, No. 4, 1976.
10. D.J.L. Kennedy. Limit States Design – An Innovation in Design Standards for Steel Structures. CJCE, Vol. 1, No. 1, 1974.
11. D.E. Allen. Limit States Design – A Probabilistic Study. CJCE, Vol. 2, No. 1, 1975.
12. ACI Comm. 443. Analysis and Design of Reinforced Concrete Bridge Structures. 1977.
13. G.S. Vincent. Tentative Criteria for Load Factor Design of Steel Highway Bridges. American Iron and Steel Inst. N.Y., February 1968.
14. F.W. Jung and A.A. Witecki. Determining the Maximum Permissible Weights of Vehicles on Bridges. MTC, RR175, 1971.
15. D. Harman and A.G. Davenport. The Formulation of Vehicular Loading for the Design of Highway Bridges in Ontario. U. of Western Ontario, December, 1976.
16. A.C. Agarwal and P.F. Csagoly. Evaluation and Posting of Bridges in Ontario. Bridge Engineering Conf. TRB, 1978.
17. R.N. Wright and W.H. Walker. Vibration and Deflection of Steel Bridges. AISC Engineering Journal. January 1972.
18. D.T. Wright and R. Green. Human Sensitivity to Vibration. Ontario Joint Highway Research Program Report. February 1958.
19. D.T. Wright and R. Green. Highway Bridge Vibrations. Ontario Joint Highway Research Program Report. May 1964.
20. R. Green. The Motion of Highway Bridges under Moving Loads. MSc Thesis, Queen's University, 1958.
21. P.F. Csagoly, T.I. Campbell and A.C. Agarwal. Bridge Vibration Study. MTC, RR 181, 1972.
22. H. Reigher and F.J. Meister. The Effect of Vibration and People. Hq. Air Material Command, Wright Field, Ohio, 1946, F-TS-616-RE.
23. B. Bakht and R.C. Bullen. Analysis of Orthotropic Right Bridge Decks. Dept. of the Environment, London, Eng., 1974. HECB/B/15 (ORTHOP).
24. B. Bakht, P.F. Csagoly and L.G. Jaeger. Effect of Computers on Economy of Bridge Design. Proc. of the CSCE Specialty Conf. on Computers in Structural Engineering Practice. Montreal, October 1977.
25. D.W. Smith. Bridge Failures. Proc. of the Institution of Civil Engineers. U.K., August 1976.
26. J.F. Brotchie and M.H. Holley. Membrane Action in Slabs. ACI, Detroit. SP-30, 1971.
27. P.Y. Tong and B. deV. Batchelor. Compressive Membrane Enhancement in Two-Way Bridge Slabs. ACI, Detroit. SP-30, 1971.
28. B. deV. Batchelor, B.E. Hewitt, P.F. Csagoly and M. Holowka. An Investigation of the Ultimate Strength of Deck Slabs of Composite Steel/Concrete Bridges. Bridge Engineering Conf. TRB, 1978.
29. P.F. Csagoly, M. Holowka and R.A. Dorton. The True Behavior of Thin Concrete Bridge Decks. Bridge Engineering Conf. TRB, 1978.
30. ACI Comm. 318. Building Code Requirements for Reinforced Concrete. ACI-318-71, 1971.
31. ACI-ASCE Comm. 426. Suggested Revisions to Shear Provisions of Building Codes. ACI Journal, Vol. 74, No. 9. September 1977.
32. ACI-ASCE Comm. 426. The Shear Strength of Reinforced Concrete Members. Journal of the Structural Div., ASCE. Vol. 99, No. ST 6, June 1973.
33. Code for the Design of Concrete Structures for Buildings. CSA Standard A23.3-1973. CSA, Ontario, 1973.
34. P. Lampert and M.P. Collins. Torsion, Bending and Confusion – An Attempt to Establish the Facts. ACI Journal, Vol. 69, No. 8. Aug. 1972.
35. P.F. Csagoly and M. Holowka. Cracking of Voided Post-Tensioned Concrete Decks. MTC, RR 193, 1974.
36. L. Chitnuyanondh. Shear Failure of Concrete I-Beams with Prestressing Ducts in the Web. PhD Thesis, Queen's University, 1976.
37. S.T. Rolfe. Fracture Mechanics and the AASHTO Material Toughness Requirements for Bridge Steels. Proc. CSE Conf. 1976. Canadian Steel Industries Construction Council, Toronto.
38. Steel Structures for Buildings, Limit States Design. CSA Standard S16.1-1974. CSA, Ontario, 1974.
39. Limit States Design Steel Manual, Canadian Institute for Steel Construction, Toronto, 1977.
40. J.W. Fisher, A.W. Pense and R. Roberts. Evaluation of Fracture of Lafayette Street Bridge. Journal of the Structural Div., ASCE, Vol. 103, No. ST 7, July 1977.
41. Standard Specifications for Structural Supports for Highway Signs, Luminaires and Traffic Signals. AASHTO, 1975.
42. M.K. Ravindra, N.C. Lind and W.C. Siu. Illustrations of Reliability Based Design. Journal of the Structural Div. ASCE, Vol. 100, No. ST 9, September 1974.
43. W.C. Siu, S.R. Parimi and N.C. Lind. Practical Approach to Code Calibration. Journal of the Structural Div., ASCE, Vol. 101, No. ST 7, July 1975.
44. E. Rosenblueth and L. Esteva. Reliability Basis for Some Mexican Codes. ACI, Detroit. Publication SP-31, 1972.
45. A.S. Nowak and N.C. Lind. Calibration of the OHB Design Code. Ontario Highway Bridge Design Code Report. University of Waterloo. 1977.

FATIGUE TESTS OF PRESTRESSED GIRDERS WITH BLANKETED AND DRAPED STRANDS

B. G. Rabbat, P. H. Kaar, H. G. Russell, Portland Cement Association
R. N. Bruce, Jr., Tulane University

In pretensioned girders, draping of strands can be avoided by using straight tendons having unbonded "blanketed" lengths at the ends of girders. An experimental investigation was carried out to determine the effect of repetitive loading on the behavior and strength of girders with draped and blanketed strands. Six full-size Type II AASHTO-PCI girders were tested. Two girders contained draped strands. The other girders had straight strands with four tendons blanketed at each end. The effects of load level, development length, and confining ties were investigated. The test program called for 5-million cycles of loading followed by a static test to destruction. The paper presents results of the investigation and shows that blanketed strands can be used successfully if adequate strand development length is provided. Fatigue fracture of strands was observed in pre-cracked beams where load level produced tensile stress in the precompressed concrete.

Highlights

Use of draped strands in pretensioned girders presents problems for designers, fabricators and inspectors. The tensioning procedure is time consuming, costly, and may leave doubt as to the actual prestress level obtained throughout the length of the strand. Draping of strands can be avoided by using straight tendons having unbonded "blanketed" lengths at the ends of girders.

Test Program

An experimental investigation was carried out at the Portland Cement Association Laboratories to determine the effect of repetitive loading on the behavior and strength of girders with blanketed strands.

Six full-size Type II AASHTO-PCI girders, each 15.24-m (50-ft) long, were tested. Two girders contained draped strands. The other four had straight strands with four tendons blanketed at each end.

Controlled variables in the test program were load level, development length, and use of ties to confine the concrete in the stress transfer region of the blanketed strands. All specimens were cracked prior to fatigue loading.

The test program called for 5-million cycles of loading between dead load and dead load plus live load. Static tests to full dead load plus live load were performed before cyclic loading and after 1, 2-1/2 and 5-million cycles. At the completion of 5-million cycles, the girders were tested to destruction under static load.

This paper summarizes the experimental investigation (1) and presents the results of the tests.

Conclusions

The results of the fatigue tests of this investigation indicate the following:

1. In prestressed bridge girders, concrete stresses may be controlled by either draping strands or, alternatively, using straight strands having unbonded "blanketed" lengths at the ends of girders.
2. For similar loading conditions, the behavior and strength were the same for girders having either blanketed or draped strands.
3. The fatigue life of specimens designed for a tensile stress of $0.5\sqrt{f'_c}$ MPa ($6\sqrt{f'_c}$ psi) under full service load was significantly less than that of specimens designed for zero tension.
4. In specimens designed for zero tension in the concrete under service load condition, and having blanketed strands designed for one development length, ℓ_d, as defined in ACI 318-71, Clause 12.11.1, the behavior and strength of the specimens with blanketed strands were similar to those of conventional girders with draped strands.
5. In the specimen designed for a tensile stress of $0.5\sqrt{f'_c}$ MPa ($6\sqrt{f'_c}$ psi) in the uncracked concrete under full service load and having blanketed strands designed for twice the development length, $2\ \ell_d$, only small slip of the strands occurred. This indicated adequate bond of the blanketed strands for about 3-million cycles of repetitive loading.
6. In the specimen designed for a tensile stress of $0.5\sqrt{f'_c}$ MPa ($6\sqrt{f'_c}$ psi) in the uncracked

concrete under full service load and having blanketed strands designed for one development length, ℓ_d, the blanketed strands slipped indicating bond fatigue.

7. In the three specimens where cyclic loading produced a tension of $0.5\sqrt{f'_c}$ MPa ($6\sqrt{f'_c}$ psi) in the concrete, fatigue fracture of the strands occurred at about 3-million cycles of repetitive loading. These specimens included a control girder with draped strands. The calculated minimum and maximum stresses in the strands were between 980 and 1040 MPa (142 and 151 ksi), respectively.

8. Use of ties to confine the concrete in the stress transfer region of blanketed strands in one specimen did not cause any substantial improvement in the behavior of that specimen.

Recommendations

Based on the test results and the conclusions outlined above, it is recommended that:

1. In bridge girders, blanketed strands may be used as an alternative for draped strands.
2. In bridge girders designed for no allowable tension in the concrete under service load conditions, the blanketed length of strands should be calculated allowing for at least one development length, ℓ_d, as defined by ACI 318-71, Clause 12.11.1. In most girders, the development length can be greater than ℓ_d without exceeding the allowable concrete stress at the end of the girders. A length greater than ℓ_d will result in less strand lengths to be blanketed and, therefore, would be more economical to manufacture.
3. In bridge girders designed for an allowable tensile stress of $0.5\sqrt{f'_c}$ MPa ($6\sqrt{f'_c}$ psi) in the uncracked concrete under service load condition, the blanketed length of strands should be calculated allowing for at least two development lengths, $2\,\ell_d$. In most girders, the development length can be greater than $2\,\ell_d$ without exceeding the allowable concrete stress at the end of the girders. A length greater than $2\,\ell_d$ will result in less strand lengths to be blanketed and, therefore, would be more economical to manufacture.
4. Use of ties to confine the concrete in the stress transfer region of blanketed strands is not necessary.
5. When tension is allowed in the concrete under service load conditions, design of the girders to prevent strand fatigue should be a consideration.
6. Further research is needed to determine the fatigue properties of prestressing strands. The results can then be incorporated into specifications and codes. Currently the designer is not provided with any guidance regarding design of strands for fatigue.
7. Research is needed to determine the level of tension in the concrete at which pretensioned girders would be able to withstand traffic loading without strand fatigue during their design service life.
8. Research is needed to determine how far strands should be extended beyond the point where they are not needed. In reinforced concrete members, the cut-off point of a reinforcing bar is governed by either a development length measured from the critical section, or a minimum distance (e.g., 15 bar diameters) (2) measured from the theoretical point where the bars are not needed. Presently, specifications do not provide the designer with a minimum distance criterion for prestressing steel.

Introduction

Strands are draped at the ends of prestressed girders to control concrete stresses. Draping of strands can be avoided by using straight tendons as long as the concrete stresses at the ends of the beams remain within the allowable limits. This can be achieved by using the "blanketing" concept. The effect of prestressing is eliminated in a given strand by preventing bond with the concrete. This can be achieved by greasing the strand, coating it with retarder, or covering it with plastic tubing. Greasing or using a retarder is risky because of the possibility of affecting other than the specified strands. Plastic tubing is preferred because it also provides an easy means of inspection.

The blanketing technique has been tested previously (3,4). However, further tests were needed since recent Codes (5) and Specifications (2) permit tension in the precompressed fibers under service loads.

Therefore, the aims of this investigation were to:

1. Determine whether tension in the concrete under service load condition affects the development length.
2. Determine whether one or two development lengths, ℓ_d, (as defined by ACI 318-71, Clause 12.11.1) are required.
3. Determine whether ties to confine the concrete in the stress transfer region of blanketed strands are beneficial.

Design of Specimens

Six full-size Type II AASHTO-PCI specimens were tested in this investigation. Table 1 summarizes the test variables. Cross sections, reinforcing details and the loading pattern are shown in Fig. 1.

Test specimens were designed according to the 1973 AASHO Specifications (2) and the 1974 and 1975 AASHTO Interim Specifications (6,7).

Concrete strength at transfer of prestress, was assumed to be at least 27.6 MPa (4,000 psi). The concrete design strength at 28 days was taken as 34.5 MPa (5,000 psi).

The strands used were 11.1-mm (7/16-in.) diameter with a nominal strength of 1724 MPa (250 ksi). Prestress losses at service condition were assumed to be 20%.

A minimum number of strands were blanketed to ensure that the top and bottom concrete stresses of the end regions remained within the allowable values. At each end, four strands were blanketed in all girders having straight tendons only.

The blanketing location was determined from the concept of development length. The procedure is similar to that for stopping rebars in reinforced concrete members.

One development length was calculated (2) to be 1.68-m (5 ft - 6 in.). Location of blanketing tubing relative to the position of the applied loads is shown in Fig. 2. Strands were blanketed in pairs to maintain symmetry. Only strands in the bottom layer were blanketed.

Development length was measured from the locations where the strands were required to exhibit their full strength. To force the cracks to occur at these critical locations, crack forming devices were placed in the test girders at the locations shown in Fig. 2. The crack formers consisted of 55x454-mm (2-3/16x17-7/8-in.) pieces of 1.6-mm (1/16-in.) thick sheet metal.

Ties to confine the concrete in the end transfer region of all girders conformed with the Louisiana "typical details for prestressed concrete girder construction". The same confining tie details were used at the stress transfer regions of the blanketed strands of Specimen G14.

The choice of the range of loads for the fatigue testing of Specimens G11, G13 and G10 was governed by the following criteria:

1. Under full service load, tensile stress in the precompressed concrete fiber was $0.5\sqrt{f'_c}$ MPa ($6\sqrt{f'_c}$ psi). Therefore, the dead load moment, M_D, plus the live load moment, M_L, caused a tensile stress of $0.5\sqrt{f'_c}$ MPa ($6\sqrt{f'_c}$ psi) in the bottom concrete fibers at midspan.
2. Calculated flexural capacity, M_u, of the girder at midspan was:

$$M_U = 1.3\ M_D + 2.167\ M_L$$

These two conditions yielded the fatigue loads P_{min} and P_{max} for Specimens G11, G13 and G10. Load P_{min} corresponds to dead load moment in addition to the selfweight moment. Load P_{max} corresponds to total dead load plus live load moments.

For Specimens G14, G12 and G10-A, the maximum service load, P_{max}, was chosen to correspond to a midspan bottom concrete fiber stress of zero tension. The minimum load, P_{min}, was chosen to be a nominal 2.7 kN (600 lbs.) required to keep the rams in contact with the top of the girders. Table 2 summarizes calculated values for range of fatigue loads, the corresponding midspan moments, stresses in the bottom layer of strands and stress range in these strands. Note that the loads P_{min} and P_{max} are the inner point loads of Fig. 2. The outer point loads are 2.5 times the magnitude of the listed loads.

Present Codes (5) and Specifications (2) do not provide the designer with any guidance concerning allowable stress range to prevent fatigue failure in prestressing strands. The calculated stress levels listed in Table 2 are much smaller than the allowable stresses recommended by ACI Committees 215 (8) and 443 (9).

Test Program

Two loading systems were used to test each specimen. The first was basically for dynamic loading, and the second for static tests to destruction. The second system is shown in Fig. 3.

Dynamic loading was applied through four rams. Each ram was secured to a concrete frame prestressed to the laboratory floor. In Fig. 3, the stems of two rams are in the retracted position.

To accommodate the large deflections required to test the specimens to destruction, the test setup was modified. The second loading system consisted of cross heads and tie rods. Loads were applied by hydraulic rams reacting against the underside of the test floor (10).

Instrumentation was first installed during manufacture of the girders in the plant. Quantities measured included prestressing force, strand strains, confining tie strains, and camber.

In the laboratory, measurements of applied loads, deflections, strand strains, confining tie strains and strand slip were recorded during the static tests.

During the dynamic tests, measurements recorded were strand slip and number of cycles of repetitive loading.

Ends of the specimens were supported on a 127-mm (5-in.) diameter roller located between two steel plates. A jig was erected at each support to prevent the girder from rolling longitudinally during the dynamic testing.

Testing started with 3 cycles of static loading between P_{min} and P_{max}. These predetermined loads are listed in Table 2. To ensure that Specimens G14, G12 and G10-A would crack, they were loaded up to P_{max} = 65 kN (14.6 kips) during the static tests only.

Repetitive loading was applied at the testing machine rate of 265 cycles/min. The large mass of the girder necessitated a dynamic correction. This correction was accounted for by controlling the loads such that the deflections produced due to cyclic loading corresponded with the measured minimum and maximum static deflections.

To determine the effect of the cyclic loading on the girder's response, dynamic loading was interrupted at 1-million and 2.5-million cycles and a static test was conducted between P_{min} and P_{max}. After 5-million cycles, the repetitive loading was stopped. The loading system was then modified and the specimen loaded statically in increments to destruction.

The concrete compressive strength was determined from 152x305-mm (6x12-in.) concrete cylinders. At test time, the concrete strength of the girders ranged between 40.7 and 52.4 MPa (5900 and 7600 psi). Strength of the deck concrete was between 34.5 and 41.4 MPa (5000 and 6000 psi).

All strands were stress-relieved. They were manufactured in Japan. Coupons from the same strands used in the girders were tested in the laboratory. These coupons were instrumented with strain gages similar to those used in instrumenting strands in the girders. The modulus of elasticity was found to be 230,600 MPa (33,440 ksi). It was used to convert the measured strand strains into strand stresses. The measured modulus was high because the strain gages were placed along a wire, i.e., along a spiral.

When unrolled from their coils, the strand had a shiny surface. For about ten days the strands were exposed to high humidity due to rain and curing steam from adjacent prestressing beds. This resulted in brown surface rusting of the strands.

Behavior of Specimens

The following is a description of the behavior of each specimen. Specimens are discussed in the sequence of testing.

Specimen G11

For Specimen G11, increasing slip of the blanketed strands was measured as the dynamic test progressed. After 3.78-million cycles, fatigue loading was stopped because of the formation of a large crack at the outer east crack former. The stiffness of specimen had decreased considerably. The specimen was then unloaded and the loading system modified in preparation for the final static test to destruction.

During the test to destruction, sudden fracture of the specimen occurred at a load very close to the specified service load level. All distress occurred at the section where the large crack had formed. No other cracks appeared. Only two of the

22 strands did not fracture. These were blanketed over a longer length and slipped inside the end portion of the girder. A plot of the applied load versus midspan deflection is shown in Fig. 4.

Specimen G13

After 3.2-million cycles of repetitive loading, a large crack had extended high into the web at the inner east crack former of Specimen G13. Slip of the blanketed strands was negligible. The stiffness of the girder had decreased.

Specimen G13 was cut open at the critical section to inspect the strands. Six strands were found to be fully fractured in fatigue. Six strands had one to five of the seven wires fractured in fatigue. Only 10 of the 22 strands had no visible evidence of fatigue.

While removing the concrete cover at the critical section, the position of the crack former with respect to the bottom layer of strands was carefully observed. The outside strands of the bottom layer were bearing against the crack former while the intermediate strands were clear. Of the two strands, one was intact, and the other had fatigue fracture about 38-mm (1.5-in.) away from the crack former.

To determine whether the fatigue had affected the properties of the intact strands that crossed the critical section, coupons were extracted from the girder. These were tested statically in tension. The breaking strength of these strands corresponded to the manufacturers strand strength.

To obtain further information from Specimen G13, the strands at the inner west crack former were exposed. A crack of limited height had formed at this section. There were no external visible signs of damage. After exposing the tendons, it was found that one strand of the second layer and one wire from a bottom layer strand were fractured in fatigue.

Specimen G10

Behavior of Specimen G10 was very similar to that of the two previous specimens. After 3.63-million cycles, the dynamic loading was intentionally stopped after observing the formation of a large crack at the inner west crack former. This was the location of a hold-down device.

Specimen G10 was then loaded statically to destruction. It fractured prematurely and suddenly as illustrated by the applied load versus midspan deflection curve of Fig. 4. The failure was concentrated at the critical section. No new cracks appeared along the beam.

After separating the two segments of the girder, the fractured surface of all strands was inspected. It was possible to identify the strands that failed due to fatigue and the ones that failed due to tension. The two modes of fracture are very distinct as illustrated by Fig. 5. Six strands were found to be fully fractured in fatigue. Eight strands had one to four of the seven wires fractured in fatigue.

As observed earlier in Specimen G13, it was noticed that the two outer strands of the bottom layer were touching the crack former while all the intermediate ones were clear. The outer strands had fractured in tension. It is interesting to note that the hold-down device did not seem to be the cause of fatigue of strands. The distribution of fatigued wires and strands was random.

Specimen G14

Specimen G14 survived 5-million cycles. Only small cracks had formed at the four crack formers. Strand strains and confining tie strains remained stable during the test. Slip of the blanketed strands did not exceed 0.11-mm (0.0045-in.).

Specimen G14 was then loaded statically to destruction. Figure 4 illustrates the applied load versus midspan deflection curve. The specimen exhibited ductile behavior. Uniformly spaced cracks formed over the center 8.5-m (28-ft) of the specimen. After reaching a midspan deflection of 0.7-m (28-in.), the specimen fractured. The measured strength exceeded that calculated by 4%.

During the initial and intermediate static tests, the gages attached to the confining ties did not record any significant strains. It was only during the final static test, after closely spaced cracks were opening that some gages recorded strains.

Specimen G12

Specimen G12 was similar to Specimen G14 in every respect except that it did not contain confining ties in the stress transfer regions of the blanketed strands. Specimen G12 was tested in a similar manner and the response was similar. The measured strand slips were a little larger.

During the static test to destruction, Specimen G12 exhibited very ductile behavior as illustrated by the applied load versus midspan deflection curve of Fig. 4. The test was stopped after a midspan deflection of 0.8-m (31-in.) was reached. Measured strength exceeded that calculated by about 2%.

Specimen G10-A

Specimen G10-A had draped strands and was similar to Specimen G10. The only difference was the stress level during cyclic loading. Under cyclic loading, no tension was allowed in the bottom fibers at midspan.

Applied load versus midspan deflection curve during the final static test is shown in Fig. 4. The strength of Specimen G10-A exceeded that calculated by about 4%.

Analysis of Test Results

Based on the data collected from each test, comparisons of performance of the specimens is given in this section. Significant test observations are also discussed.

Level of Fatigue Loading

In Specimens G11, G13 and G10, the higher limit of repetitive loading corresponded to a tensile stress of $0.5\sqrt{f'_c}$ MPa ($6\sqrt{f'_c}$ psi) in the bottom concrete fibers at midspan. The specimens were cracked prior to fatigue loading. In these three specimens, strands fractured due to fatigue after 3.2 to 3.7-million cycles.

In Specimens G14, G12 and G10-A, the repetitive loading did not cause tension in the concrete. All three specimens survived 5-million-cycles of repetitive loading. In subsequent static tests to destruction, all three specimens exhibited ductile behavior as illustrated by Fig. 4. Strength of

Specimens G14, G12 and G10-A exceeded that calculated by 2% to 4%.

Strand Stress Range

Stress range is defined as the difference between maximum and minimum strand stresses corresponding to the respective maximum and minimum loads. Stress range was calculated through strain compatibility, equilibrium of internal forces and a knowledge of the actual material properties. The stress range was also measured by means of strain gages applied to the strands. To eliminate the time-dependent effects of creep and shrinkage, and any possible temperature effects, the stress range of each static test is used for comparison purposes.

Table 3 lists the highest measured range of strand strain corresponding to maximum and minimum inner loads of 65 kN (14.6 kips) and 18.2 kN (4.1 kips), respectively. Measured strand strains were converted to stresses using the experimentally determined modulus of elasticity. Specimen G10-A was not instrumented for strand strains.

Calculations for internal stresses indicate that stress range is a function of the effective prestress. For example at a 21% loss of prestress, the calculated stress range corresponding to maximum and minimum inner loads of 65 kN (14.6 kips) and 18.2 kN (4.1 kips) is 58 MPa (8.4 ksi). At 27% loss, the calculated stress range corresponding to the same loads is 82.7 MPa (12 ksi). The stress range as affected by prestress is shown in Fig. 6.

For all specimens, the measured stress range increased with increase of the cycles of repetitive loading as shown in Table 3. However, in Specimens G11, G13 and G10, the rate of increase in stress range was much higher. These three specimens were subjected to higher load levels. Strands of the above three specimens fractured due to fatigue between 3.2 and 3.7-million cycles of repetitive loading.

Figure 7 is a plot of the calculated stress range in the strands at 20% loss of prestress versus the fatigue life of Specimens G11, G13, and G10. The S-N curve was adapted from Fig. 12 of a report prepared by ACI Committee 215, Fatigue of Concrete (8). Their curve was obtained through a regression analysis of fatigue test results (11). It can be seen that the fatigue strength of Specimens G11, G13, and G10 was lower than previous fatigue test results.

Slip of Blanketed Strand

Strand slip measured with a dial gage provided a good indication of the effectiveness of the development length. Figure 8 illustrates the load versus slip recorded during the static tests. For each girder, the blanketed strand that had the largest slip is plotted. As shown in Fig. 8a for Specimen G11, slip increased with repeated load. This denoted bond fatigue (12,13). When Specimen G11 was loaded to destruction, two strands slipped inside the end portion of the girder.

Figure 8b is for Specimen G13. Slip stabilized after the initial elastic slip. Even after 3.2-million cycles, the increase in slip was negligible denoting good anchorage of the blanketed strands. Specimen G13 had double the development length specified in ACI 318-71, Clause 12.11.1.

Figures 8c and 8d are for Specimens G14 and G12, respectively. Slip of Specimen G14 was smaller than strand slip of Specimen G12. This suggests some beneficial effect of the extra confining ties. However the effect was not significant enough to justify the use of the ties. Slip in Specimen G14 also remained smaller during the static test to destruction as shown in Fig. 9. The maximum strand movements of Specimens G14 and G12 were small up to 5-million cycles. The small slip did not affect the strength and behavior of the two beams.

The effect of the number of cycles of repetitive loading on strand slip is illustrated in Fig. 10. For each specimen, the strand with the largest slip is plotted. This plot denotes rapid bond deterioration of Specimen G11.

It can be seen that for Specimens G12 and G14, magnitudes of slip plotted in Fig. 8 are different from those of Fig. 10. During the repetitive loading of Specimens G14 and G12, the maximum applied inner load, P_{max}, was 48.5 kN (10.9 kips). During the static tests, the maximum applied inner load was 65 kN (14.6 kips). Thus the slip measured during the static tests was larger.

Development Length

Specimen G13 was designed for two development lengths, 2 ℓ_d. Specimen G11 was designed for one development length. Both specimens were cycled at the higher load level corresponding to a tensile stress of $0.5\sqrt{f'_c}$ MPa ($6\sqrt{f'_c}$ psi) in the concrete. Both specimens had fatigue fracture of the strands. The main difference in behavior was that, in Specimen G11, slip of the strands kept increasing with cyclic loading as shown in Fig. 10.

A bond fatigue failure of the blanketed strands of Specimen G11 was observed. On the other hand, in Specimen G13, slip of strands remained virtually unchanged after the initial elastic slip up to 3.2-million cycles of repetitive loading as shown in Fig. 8b. Therefore, twice the development length, 2 ℓ_d, used in Specimen G13 provided good anchorage of the blanketed strands.

Specimens G14 and G12 were designed for one development length. They were tested at a load level corresponding to zero tension in the concrete. Both specimens survived 5-million cycles of repetitive loading. In the subsequent static test to destruction, both specimens reached their calculated strength. No bond fatigue of the strands was observed. Therefore, when the cyclic load corresponded to zero tension in the concrete, one development length was adequate.

Surface Condition of Strands

In the present investigation, strands used in the test specimens had brown surface rust. It is well known that the surface condition affects the required development length. However, the surface condition of the strands was not one of the control variables of this investigation. It is possible that the surface condition of the strands may have affected both development length and fatigue properties.

Confining Ties

Strains measured on the confining ties at service load levels were negligible. Significant strains were measured only at very high loads following the formation of large cracks, during the static test to destruction.

Smaller slip of the blanketed strands was measured in Specimen G14, with confining ties than in

Specimen G12. However, the behavior and strength of Specimen G14 do not indicate any significant beneficial effect of the confining ties.

Concluding Remarks

The tests of this investigation have confirmed that blanketing of strands is a feasible technique that could lead to safer and more economic manufacturing of pretensioned bridge girders.

The tests have also indicated that fatigue of strands may be an important consideration in prestressed girders designed according to recent Codes where a concrete tensile stress of $0.5\sqrt{f'_c}$ MPa ($6\sqrt{f'_c}$ psi) is permitted under service loads. Present Codes do not provide the designer with guidance regarding fatigue of strands.

Conclusions and Recommendations based on this investigation are listed in the section entitled HIGHLIGHTS at the beginning of the paper.

Acknowledgments

This investigation was sponsored by the Louisiana Department of Transportation and Development, represented by Messrs. J. W. Lyon, Research and Development Engineer, J. E. Ross, Concrete Research Engineer, and J. W. Porter, Assistant Bridge Design Engineer.

The girders tested in this investigation were manufactured at the Prestressed Concrete Products Company, Inc., in Mandeville, Louisiana. Special thanks to Mr. C. L. Sloan, Chief Engineer for allowing instrumentation and preliminary tests in the plant.

The experimental work was carried out in the Structural Development Section under Dr. W. G. Corley, Director, Engineering Development Department. Particular credit is due to N. W. Hanson for advice on instrumentation, to J. N. Chhauda for assistance on the project, and to B. W. Fullhart, W. H. Graves, W. Hummerich Jr., B. J. Doepp, J. P. McCarthy and D. R. Thompson for their assistance in the manufacture, instrumentation and testing of the specimens.

Disclaimer

References

1. Rabbat, B.G., Kaar, P.H., Russell, H.G., and Bruce, R.N., Jr., "Fatigue Tests of Full-Size Prestressed Girders", Research Report No. 113 prepared by the Portland Cement Association for the Louisiana Department of Transportation and Development, June 1978, 140 pp.
2. "Standard Specifications for Highway Bridges", American Association of State Highway Officials, Eleventh Edition, Washington, D.C., 1973, 469 pp.
3. Kaar, P.H. and Magura, D.D., "Effect of Strand Blanketing on Performance of Pretensioned Girders", Journal of the Prestressed Concrete Institute, Vol. 10, No. 6, pp. 20-34, December 1965.
4. Dane, J., III and Bruce, R.N., Jr., "Elimination of Draped Strands in Prestressed Concrete Girders", Civil Engineering Department, Tulane University, New Orleans, Submitted to the Louisiana Department of Highways, State Project No. 736-01-65, Technical Report No. 107, pp. 147, 1975.
5. "Building Code Requirements for Reinforced Concrete", ACI 318-71, American Concrete Institute, Detroit, November 1970, 78 pp.
6. Subcommittee on Bridges and Structures, "Interim Specifications, Bridges", American Association of State Highway and Transportation Officials, Washington, D.C., 1974, 133 pp.
7. Subcommitte on Bridges and Structures, "Interim Specifications, Bridges", American Association of State Highway and Transportation Officials, Washington, D.C., 1975, 100 pp.
8. ACI Committee 215, "Considerations for Design of Concrete Structures Subjected to Fatigue Loading", Journal of the American Concrete Institute, March 1974, pp. 97-121.
9. ACI Committee 443 Report, "Analysis and Design of Reinforced Concrete Bridge Structures", American Concrete Institute, Detroit, Michigan, 1977, 116 pp.
10. Hognestad, E., Hanson, N.W., Kriz, L.B., and Kurvits, O.A., "Facilities and Test Methods of PCA Structural Laboratory", Journal of the PCA Research and Development Laboratories, Vol. 1, No. 1, pp. 12-20 and pp. 40-45, January 1959; Vol. 1, No. 2, pp. 30-37, May 1959; Vol. 1, No. 3, pp. 35-41, September 1959. Reprinted as Development Department Bulletin D33, Portland Cement Association, Skokie, Illinois.
11. Warner, R.F, and Hulsbos, C.L., "Probable Fatigue Life of Prestressed Concrete Beams", Journal of the Prestressed Concrete Institute, Vol. 11, No. 2, April 1966, pp. 16-39.
12. Kaar, P.H., Hanson, N.W., Corley, W.G., and Hognestad, E., "Bond Fatigue Tests of Pretensioned Concrete Crossties", Presented at FIP/PCI VII Congress, New York, 1974.
13. Kaar, P.H. and Hanson, N.W., "Bond Fatigue Tests of Beams Simulating Pretensioned Concrete Crossties", Journal of the Prestressed Concrete Institute, Vol. 20, No. 5, pp. 65-80, September 1975. Also PCA Research and Development Bulletin RD042.01R.

Table 1. Test specimens.

Specimen	Stress Level	Development Length	Confinement Reinforcement
G11	Tension in	d	No
G13	Bottom Fiber	2 d	No
G10	$0.5\sqrt{f'_c}$ MPa	Draped	No
G14	No Tension	d	Yes
G12	under Service	d	No
G10-A	Load	Draped	No

$0.5\sqrt{f'_c}$ MPa = $6\sqrt{f'_c}$ psi

Table 2. Fatigue loads and stress levels.

Remarks	Specimen No.	
	G11,G13,G10	G14,G12,G10A
Applied Load, kN, P_{min}	18.2	2.7
P_{max}	65.0	48.5
Moment (Constant Moment Zone), kN.m, Min.	549	303
Max.	1275	1024
Strand Stress (Bottom Layer), MPa, Min.	983	968
Max.	1041	1010
Strand Stress Range, MPa	58	42
Midspan Bottom Fiber Concrete Stress at P_{max}	$0.5\sqrt{f'_c}$ MPa	0

Note: Strand Stresses are calculated assuming 20% loss of prestress

1 kN = 0.225 kip 1 kN.m = 0.738 ft kip 1 MPa = 0.145 ksi

Table 3. Measured strains and corresponding stress ranges.

P_{min} = 18.2 kN P_{max} = 65.0 kN

Number of Cycles	Strain, millionths				
	G11	G13	G10	G14	G12
1	318	369	255	352	379
2	314	380	223	-	-
3	320	383	237	-	-
1.0×10^6	424	412	583	386	426
2.5×10^6	544	602	569	382	462
5.0×10^6	-	-	-	400	464

Corresponding stress range based on E = 230,603 MPa

Number of Cycles	Stress, MPa				
	G11	G13	G10	G14	G12
1	73	85	59	81	87
2	72	88	51	-	-
3	74	88	55	-	-
1.0×10^6	98	95	134	89	98
2.5×10^6	125	139	131	88	107
5.0×10^6	-	-	-	92	107

1 kN = 0.225 kip
1 MPa = 0.145 ksi

Figure 1. Cross section and reinforcing details of test specimens.

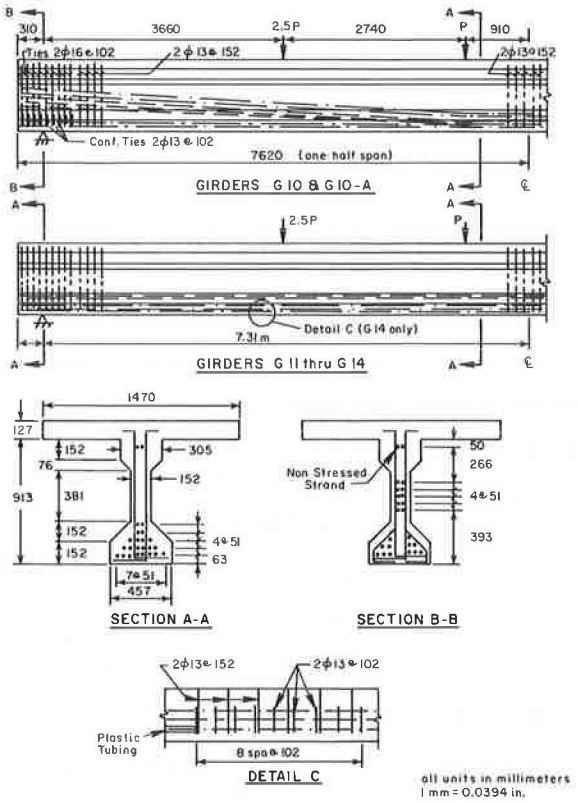

Figure 2. Location of blanketing tubing and crack formers relative to position of loading points.

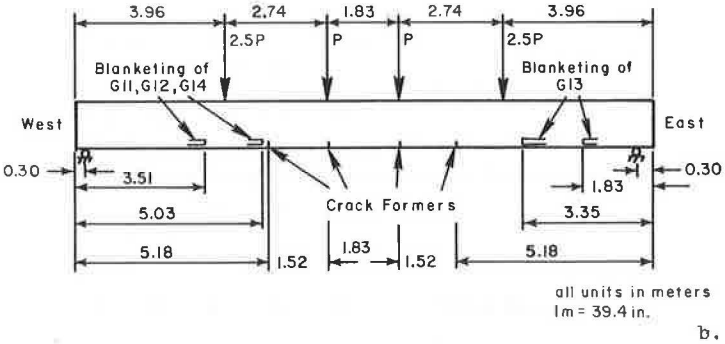

Figure 3. Test setup.

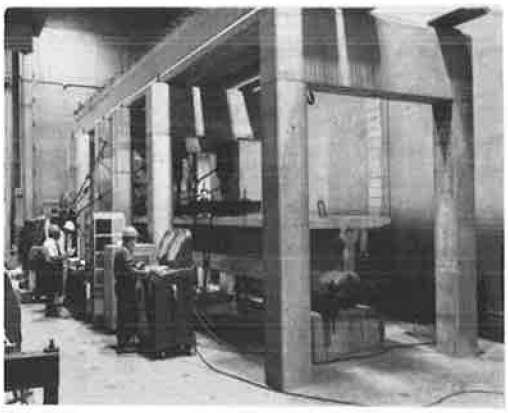

Figure 4. Load versus midspan deflection envelopes for static tests to destruction.

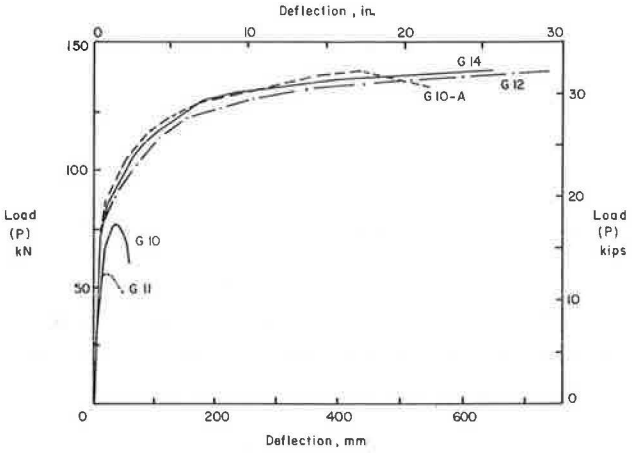

Figure 5. Fatigue and tension fracture surfaces of strands.

a. Fatigue fracture.

b. Combined fatigue and tension fracture.

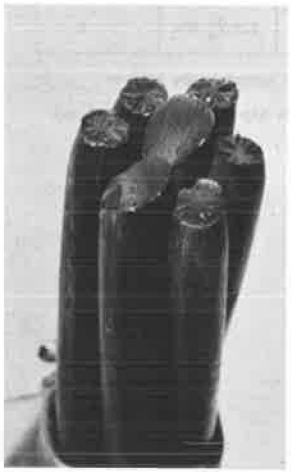

c. Cup and cone tension fracture.

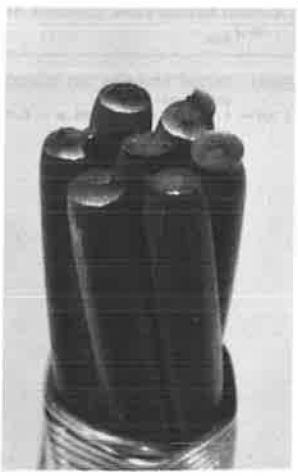

Figure 6. Calculated stress range versus percentage loss of prestress.

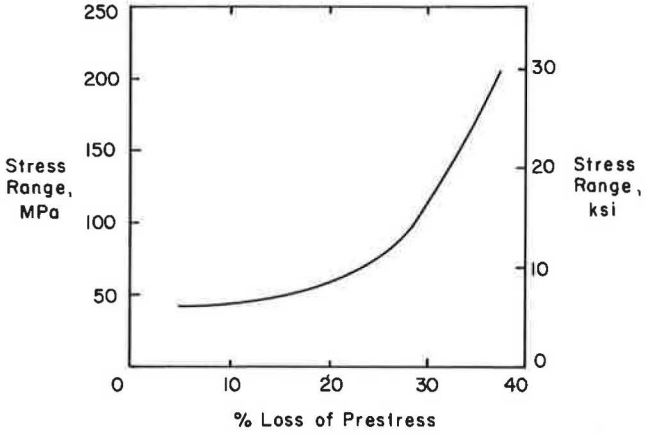

Figure 7. S-N curve for 7/16 in. diameter strands.

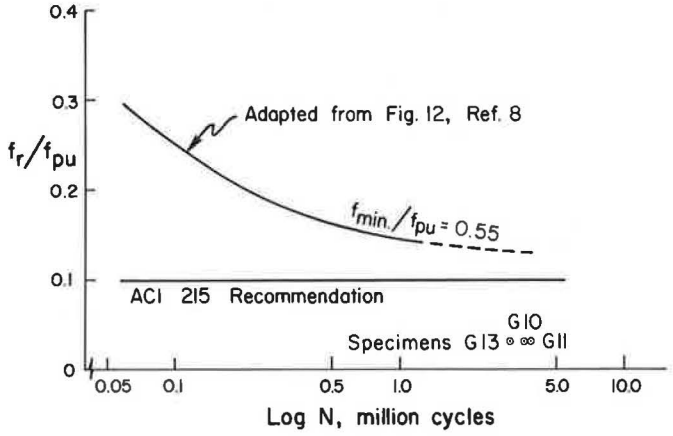

Figure 8. Measured load versus slip at different cycles.

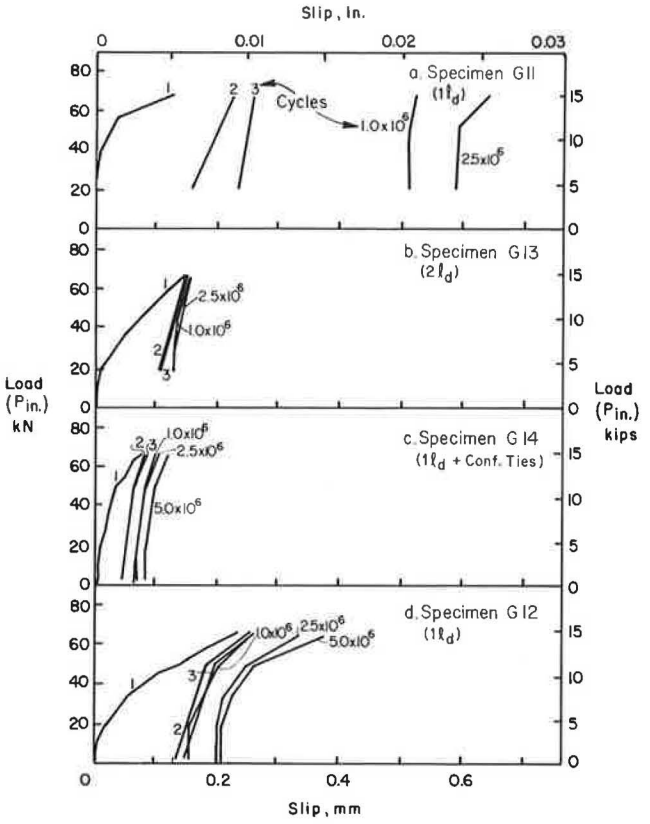

Figure 9. Load versus slip during static test to destruction.

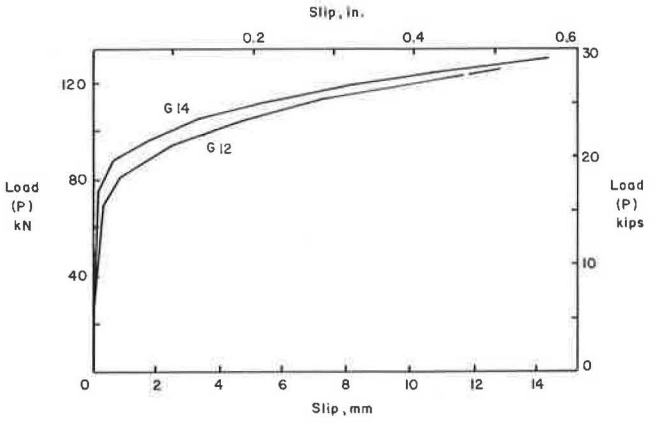

Figure 10. Variation of slip with applied cycles of repetitive loading.

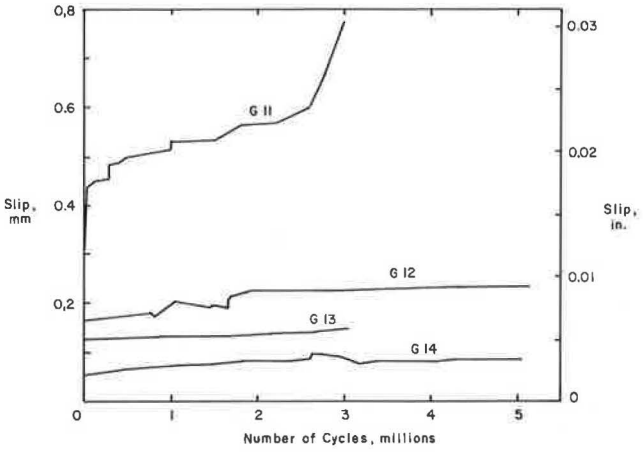

PRACTICAL BRIDGE RETROFIT CONCEPTS TO REDUCE DAMAGE PRODUCED BY SEISMIC MOTIONS

A. Longinow and R. R. Robinson, IIT Research Institute, Chicago, Illinois
W. Podolny, Federal Highway Administration, Washington, D.C.
K. H. Chu, Illinois Institute of Technology, Chicago, Illinois
D. S. Albert, Hazalet & Erdal, Consulting Engineers, Chicago, Illinois

This paper presents design criteria and design details on eight bridge retrofit concepts which were developed for implementation on existing highway bridges so as to minimize damage and hazard to life in the event of an earthquake. Retrofit categories were selected on the basis of observed damage experienced by highway bridges in previous earthquakes. The eight retrofit concepts are:

1. Concrete box girder hinge longitudinal restrainer.
2. Girder longitudinal displacement stopper at abutment.
3. Steel girder vertical displacement restrainer.
4. Steel girder hinge expansion joint longitudinal restrainer.
5. Pier footing strengthening.
6. Reinforced concrete bent column strengthening.
7. Girder bearing area widening.
8. Steel girder pin bearing vertical and lateral displacement restrainer.

This narrative describes the bridge retrofit process and illustrates the individual concepts in terms of intended function and structural details. The design method employed is illustrated by including the step by step design of one of the eight retrofit concepts.

The work described herein is at least in part motivated by the damage that was sustained by highway bridges during the February 9, 1971 San Fernando earthquake. This earthquake clearly pointed out a number of deficiencies in bridge design specifications. It also focused on the fact that numerous existing bridges may be expected to fail in some major way during their remaining life if subjected to strong motion seismic loads. Bridge failures are clearly undesirable since a bridge may be a vital link in a road network. When a portion of the road network has been disrupted by the collapse of a bridge, vital services to the surrounding communities are disrupted for the time required to find an alternate route or for the bridge to be repaired or replaced. Depending on the extent of other physical damage and casualties produced by the earthquake, the loss of vital bridges, i.e., those that provide access to hospitals for example, can magnify the effects of the disaster.

Following the February 9, 1971 San Fernando earthquake, Federal Highway Administration (FHWA) launched a study (1) whose objective was to identify and define practical techniques and criteria for retrofitting existing highway bridges so as to increase their resistance to seismic forces. This was followed by another effort which produced a design reference manual (2). The objective was to illustrate retrofit concepts that can be applied to existing bridges, which will enhance the probability of survival of the structure when it is subjected to postulated seismic motions. This narrative is based on the results of this effort.

Bridge Retrofit Decision Process

In determining whether a given bridge warrants retrofitting these three steps (as a minimum) should be considered:

1. Will the bridge suffer a critical failure (i.e., so extensive that the bridge could not remain in even emergency use) if subjected to the probable earthquake ground motions for the bridge site? If the structural analysis produces a negative answer to this question one need go no further. If the answer is affirmative the second step is:

2. Determine the level of importance of the bridge to the given locality by considering the type of highway, traffic volume, accessibility of other crossings, etc. A recommended procedure for deciding on the importance of the bridge is given in (3). If it is determined that the bridge is unimportant to the locality, it may be decided that retrofitting is not feasible even though the answer to step 1 was affirmative. If however, it is decided that the bridge is important to the area, the third step is:

3. Determine the type or types of retrofit measure(s) to employ. This decision is based on the following considerations: (a) probable mode of failure; (b) how will the chosen retrofit measure(s) influence the performance of other parts of the bridge under seismic as well as normal service loading;

(c) a comparison of expected interference with traffic flow on and under the bridge for different retrofit measures; (d) a comparison of expected costs of fabrication and installation of different retrofit measures. This comparison is based on, but not necessarily limited to: accessibility of the area to be retrofitted (e.g., it would be more costly to enlarge a footing if the existing footing were under water as opposed to normal backfill on dry land); the type and quantity of construction materials (e.g., type of steel, concrete); type and quantity needed for installation; length of time needed for installation; the number and qualifications of men needed to do the work; number of bridges; if a large number of bridges in a given area are identified for retrofitting, there are practical considerations in contracting and inspection. A greater degree of efficiency is achieved if a number of bridges in one area can be included under a single contract. It is more efficient to prepare plans and let contracts for several large jobs than a large number of single bridge contracts. A large contract can also be inspected more efficiently by a single inspector. Bridges in a single contract should be reasonably close together (4).

Two of the key items in the bridge retrofit decision process that need emphasizing are (a) the determination of probable ground motions and (b) selection of appropriate structural analysis method and a sufficiently accurate structural model of the bridge.

The probable "earthquake" at a given bridge site can be determined on a statistical basis by the use of historic earthquake data previously compiled for the given geographic area. The earthquake at the site can be expressed in terms of maximum ground acceleration, an "effective" acceleration, a response spectrum or a motion history. A number of sources for such information are currently available and several levels of "accuracy" are possible (5,6). An approximate procedure for selecting a probable ground acceleration at a bridge site is included in (7).

The unique aspect of earthquakes is the fact that motions generally persist for a "long time" relative to the natural periods of bridge components. A component can therefore experience many load cycles of varying magnitude during the passage of the principal portion of an earthquake. Many cycles of "low" magnitude can be more effective in producing damage than a single cycle of "high" magnitude and short duration. Analysis methods capable of considering such random motions and predicting the corresponding behavior of a structure in whatever phase (elastic, nonelastic) it chooses to respond, are still very much in the research phase. Presently the problem is in part hampered by lack of reliable data on the cyclic behavior of reinforced concrete past the linear range. However, the major problem is still the quantity of computer time required to solve a reasonably sized model of the structure. To overcome some of these difficulties, a simplified analysis method was developed and verified as part of the effort (7) described. The method is a practical engineering approach which considers only the dominant modes of response. It is an iterative procedure in the sense that several models of varying complexity may be required to zero-in on the answer. This method has the advantage of providing reliable answers in a relatively short period of time without reliance on any specific computer program. However, it places a great deal of reliance on the basic engineering intuition and practical experience of the user.

Bridge Retrofit Measures

Bridge retrofit measures considered were selected on the basis of the type of failure modes and damage experienced by highway bridges in previous earthquakes. Observed failure modes can be grouped into two categories, i.e., substructure (pier or abutment) failures and hence loss of superstructure capacity, and superstructure collapse due to excessive relative motion of the support bearings. Both of these types of failure occurred during the San Fernando earthquake (8).

Structural failures and damage to bridges are also caused by inadequate foundation strength or load-bearing degradation during the course of seismic loading. Soil liquefaction is an example of this failure mode.

Severe motion of the soil supporting the foundation can cause large horizontal and vertical deformations of the support point. These transient motions create relative movement between the support points which can lead to the failures described.

Based on highway bridge damage observed in previous earthquakes, eight retrofit measures were identified:

1. Concrete box girder hinge longitudinal restrainer.
2. Girder longitudinal displacement stopper at abutment.
3. Steel girder vertical displacement restrainer.
4. Steel girder hinge expansion joint longitudinal restrainer.
5. Pier footing strengthening.
6. Reinforced concrete bent column strengthening.
7. Girder bearing area widening.
8. Steel girder pin bearing vertical and lateral displacement restrainer.

Each of these retrofits is addressed to increasing either the rigid body stability of the superstructure or the strength of the substructure. Thus the retrofit measures, if appropriately designed, will enhance bridge resistance to the dominant failure modes that have been observed from severe seismic loading.

Since the emphasis of the study described (2) was on retrofit concepts rather than on bridge analysis, seismic forces that the various retrofit measures were designed to resist were not determined by analyzing each given bridge when subjected to a probable earthquake. Rather, these forces were determined as follows.

Horizontal motion restrainers were designed for a force of 0.25 times the contributing dead load. For a simply supported span fixed at one end and free to translate at the other, the contributing dead load is the total superstructure weight at the fixed end for longitudinal seismic loading and one-half of the superstructure weight at each end for transverse loading. Other examples of contributing dead load are given in (9).

Vertical motion restrainers connected between the superstructure and the substructure across the bearings were designed to withstand a separation force equal to 0.10 times the bearing dead load reaction (10).

In actual bridge retrofit efforts such forces would be determined from the bridge response analysis if a detailed analysis method is used, or from criteria given in (7) if the IITRI simplified analysis method is used.

To keep the illustrations simple, only one component of earthquake motion was considered with each retrofit concept. Obviously in the actual case of bridge retrofit analysis, all three components (lateral, longitudinal and vertical) would need to be

considered.

In general, the retrofit design concepts are based on earthquake loading considerations consistent with AASHTO Load Factor Design - Group VII loading (11). Therefore the earthquake load is multiplied by 1.3 and yield stresses are generally permitted for the materials. If a working stress design is used for a particular retrofit, the basic unit allowable stress can be increased by 33 percent as indicated in the 1975 Interim (11).

The new materials that are employed in the retrofit measures are listed in Table 1. It is noted that conventional materials and moderately high strength concrete have been employed for the retrofit measures.

It is not considered practical to design bridges that will economically serve normal transportation needs and also will not be damaged to some extent when subjected to severe seismic motions. Thus the basis of retrofitting a given bridge should not be intended to allow no damage whatsoever, but should be such as to limit the damage to the extent that the bridge does not collapse and that traffic may be maintained at least in the immediate period after an earthquake, with minimum emergency repairs to the bridge.

Seven of the eight retrofit measures are described in general term in the following paragraphs. Retrofit 8, Steel Girder Pin Bearing Vertical and Lateral Displacement Restrainer is described in the last section along with its step by step design.

Concrete Box Girder Hinge Longitudinal Restrainer

A four-span grade separation bridge (Figure 1) of multiple concrete box girder construction is cited to illustrate this retrofit concept. The original design employs a single transverse expansion joint hinge such that no longitudinal force can be transmitted across the joint.

The purpose of the hinge longitudinal restrainer is to restrict relative longitudinal motion across the hinge during an earthquake. The device consists of 12 restrainer rods (Figures 1 and 2) used to tie the bridge together. Excess openings (see Figure 2) are provided in the lower part of the box girder for implementing the device. With this device, the portion of the superstructure supported at the hinge will not fall off the hinge seat due to excessive relative motion. In the design, a certain amount of free thermal expansion travel is permitted to take place before the motion restrainers exert resistance.

Girder Longitudinal Displacement Stopper at Abutment

The objective of the longitudinal girder stopper is to restrict the relative longitudinal motion between the superstructure and the abutment at the expansion bearings during an earthquake. Using this retrofit measure will limit the bearing motion and eliminate bearing instability from toppling or falling off the abutment due to excessive motion. A certain amount of free travel from thermal expansion effects and allowable earthquake motion is permitted to take place before the stopper exerts resistance to the motion. To illustrate the stopper retrofit concept, a 27.43 m (90 ft) simple span I-beam bridge, adapted from (1) was chosen with the stopper applied at the expansion bearing (Figure 3). Stopper details which resulted from the design effort are shown in Figure 4.

Steel Girder Vertical Displacement Restrainer

The objective of the vertical displacement restrainer is to restrict the relative vertical motion between the superstructure and the pier or abutment seat during an earthquake with a strong vertical component. The use of this retrofit will limit the vertical separation that can occur at the support bearings and eliminate bearing instability and hence loss of superstructure support.

To illustrate the design of this concept, a bridge was considered with longitudinal girders supported by bearings which do not provide a positive

Table 1. New Materials for retrofit design.

Material	AASHTO (ASTM) Spc.	F_y ksi	F_u ksi	Comments
1. Structural steel	M183 (A36)	36	58-80	
2. Low-carbon steel	(A307)		60-100	Machine bolts, grade B
3. High strength bolts	M164 (A325)	92	120	1/2 inch to 1 inch diameter
		81	105	1-1/8 inch to 1-1/2 inch diameter
4. Reinforcing steel	M31 (A615*)	60	90	Billet steel, grade 60
5. Sponge rubber	M153 (D1752)			Type I density $\geq$ 30 pcf
6. Fabric pads	AASHTO 1973 Std. Specification, Art. 2.10.3 (L)			
7. Carbon steel bars	M227 (A306)	30	60-72	Anchor bars, grade 60
8. Concrete	AASHTO 1973 Std. Specification, Art. 2.4, f'_c = 5 ksi			
9. Grout	PCI 1971, Part B, Guide Specifications for Posttensioning Materials, Art. 4.3 (page B-27), f'_c = 6 ksi			

Note: 1 in. = 2.54 cm. 1 ksi = 6.89 MPa. 1 pcf = 16.02 Kg/m^3.

restraint to uplift forces. The piers are reinforced concrete frames with sufficient open space under the cap beam to accommodate the restrainer details. Figure 5 illustrates the resulting concept.

Figure 1. Box girder hinge longitudinal restrainer retrofit concept.

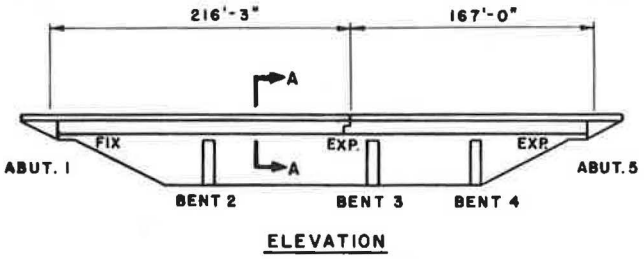

Note: 1 ft = 0.305 m. 1 in. = 2.54 cm.

Figure 2. Restrainer detail.

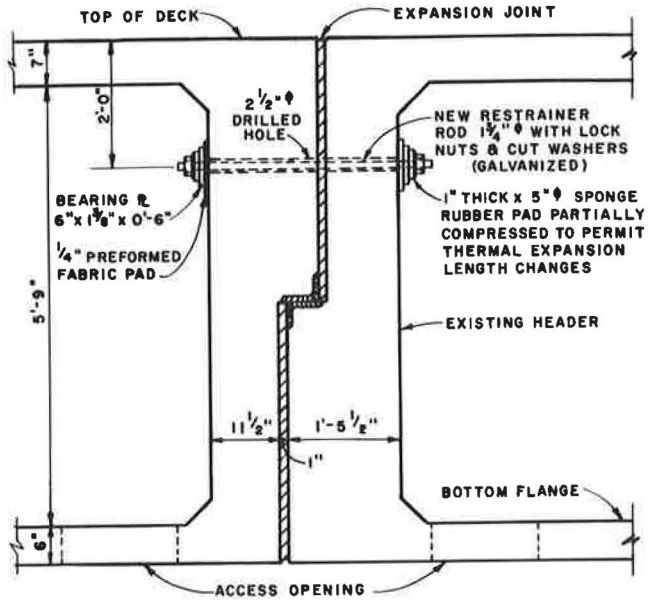

Note: 1 ft = 0.305 m. 1 in. = 2.54 cm.

Figure 3. Girder longitudinal displacement stopper at abutment retrofit concept.

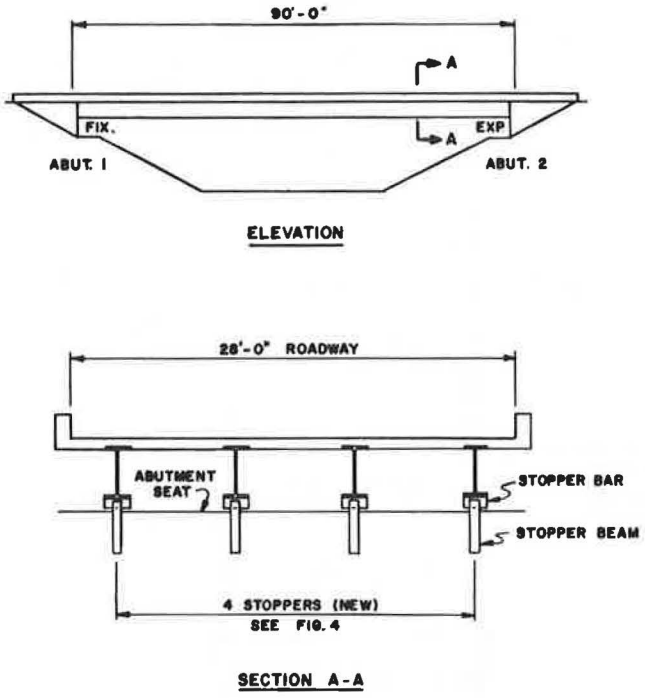

Note: 1 ft = 0.305 m. 1 in. = 2.54 cm.

Figure 4. Stopper detail.

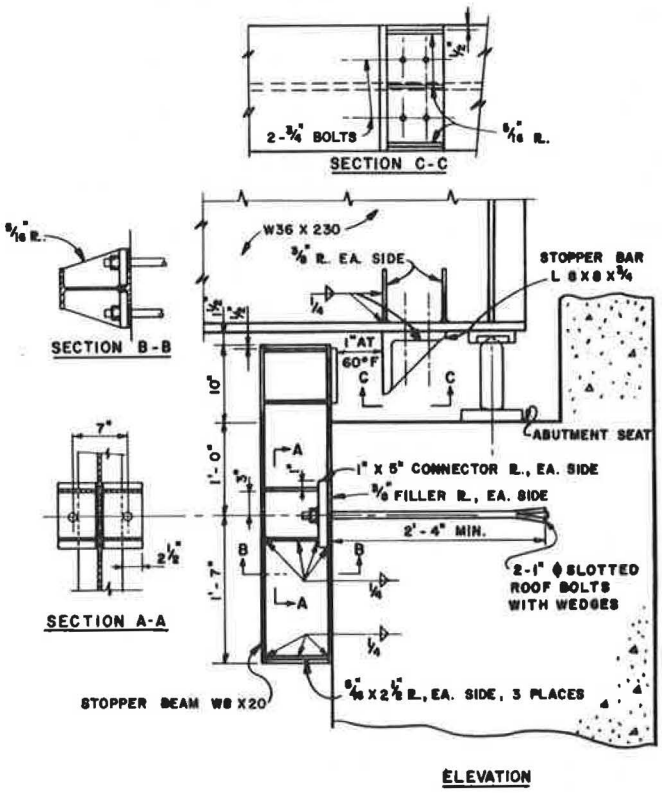

Note: 1 ft = 0.305 m. 1 in. = 2.54 cm.

Figure 5. Steel girder vertical restrainer retrofit concept.

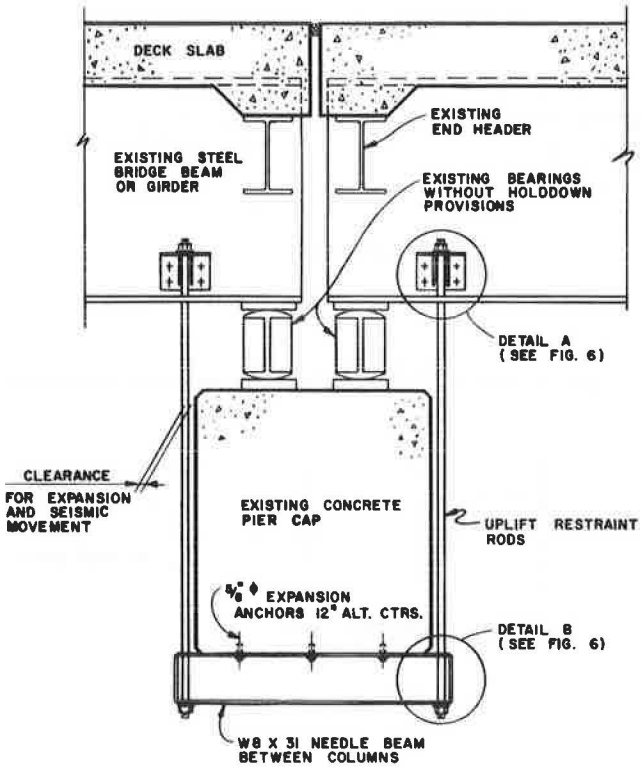

Note: 1 ft = 0.305 m. 1 in. = 2.54 cm.

Steel Girder Hinge Expansion Joint Longitudinal Restrainer

As with the box girder discussed previously, the purpose of the expansion joint longitudinal restrainer is to restrict the relative longitudinal motion across the expansion joint during an earthquake. Using this retrofit concept, excessive separation displacements across the hinge are reduced and hinge failures created by this effect are thus eliminated. A certain amount of free thermal expansion is permitted at the hinge before resistance is encountered.

A typical four-span grade separation of cantilever and suspended span construction illustrates the use of this retrofit concept. The original design of the expansion joint is such that no longitudinal force can be transmitted across the joint.

The retrofit concept makes use of existing headers (see Figure 6) located at either side of the expansion joints. Restrainer rods located close to the bridge girders are used to tie the bridge together. Since in this particular case the headers are not by themselves sufficiently strong, steel channels (see Figure 7) provide a diagonal brace to transfer the design load from the restrainer rods to the girder web.

Pier Footing Strengthening

The objective of this retrofit is to increase the longitudinal load resistance of a pier footing so that substructure failure will not occur during a high intensity seismic disturbance. The technique employed involves the addition of new piles around the perimeter of the footing and widening and deepening the footing so as to tie-in the new piles.

Figure 6. Steel girder hinge expansion joint longitudinal restrainer retrofit concept.

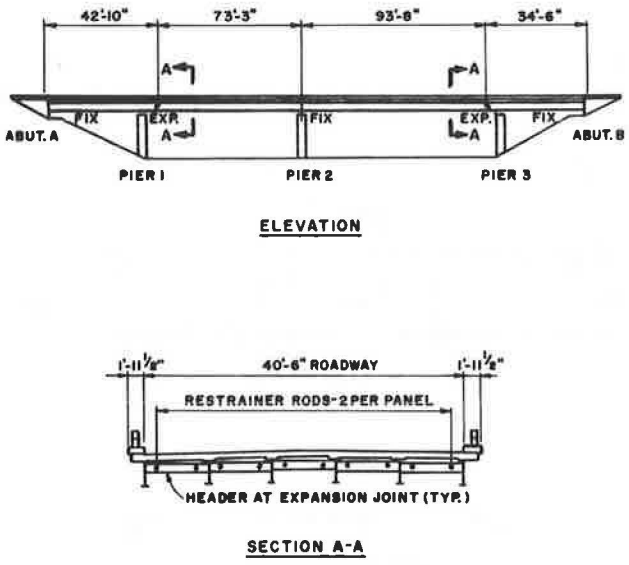

Note: 1 ft = 0.305 m. 1 in. = 2.54 cm.

Figure 7. Hinge expansion joint longitudinal restrainer details.

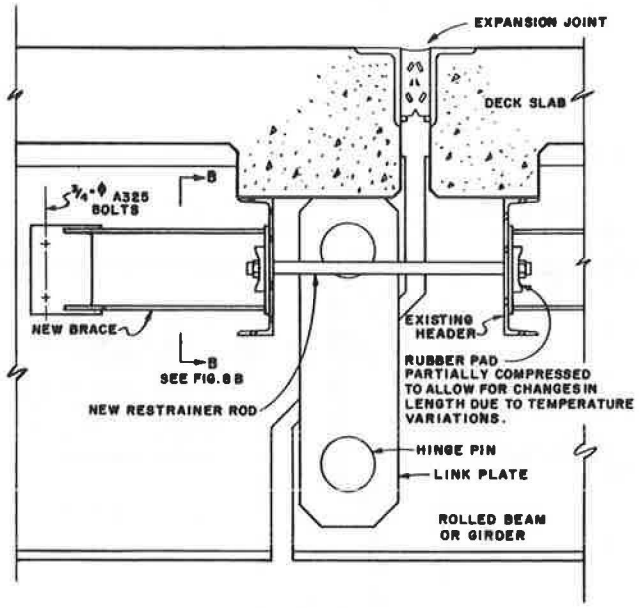

Note: 1 ft = 0.305 m. 1 in. = 2.54 cm.

The added strength is such that the footing will be capable of resisting the bending moment and shear forces induced by the earthquake loading.

To illustrate the retrofit concept, a 3.66 m x 4.57 m x 0.91 m (12 ft x 15 ft x 3 ft) footing with 20 reinforced concrete piles is modified to withstand the longitudinal seismic shear and moment forces that significantly exceed the existing pile capacity. The footing supports a single 1.83 m (6-ft) diam reinforced concrete column. Modifications determined as the result of the analysis performed are shown in Figures 8 and 9.

Figure 8. Pier footing strengthening retrofit - elevation.

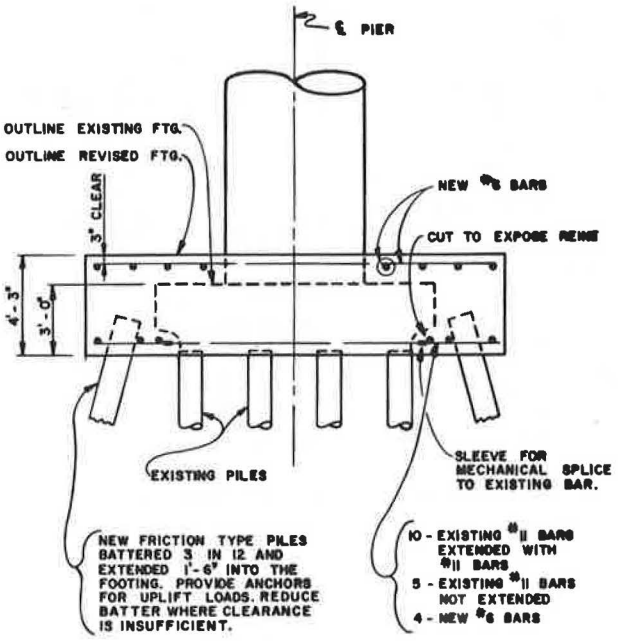

Note: 1 ft = 0.305 m. 1 in. = 2.54 cm.

Reinforced Concrete Bent Column Strengthening

The objective of this retrofit is to increase the flexural capacity of a bent column so that bent failure will not occur during a strong motion earthquake. The method used provided additional longitudinal reinforcement to the exterior of the column which is connected to the bent cap and footing by grouting the new bars in drilled holes. Lateral dowels are also introduced to enhance the monolithic behavior of the new addition to the parent column.

A representative two-span reinforced concrete box girder bridge is used to demonstrate the retrofit measure. The original design employed a single column pier with the cap monolithic with the superstructure and a pile spread footing. The structural characteristics of the retrofit are shown in Figure 10.

Girder Bearing Area Widening

The purpose of widening a bearing area is to provide additional width at the girder support points in the event that strong motion seismic loading pulls the superstructure off the bearings. Using this retrofit the displaced girders are expected to impact on the widened bearing area thus averting

Figure 9. Pier footing strengthening retrofit - pile and bottom reinforcement details.

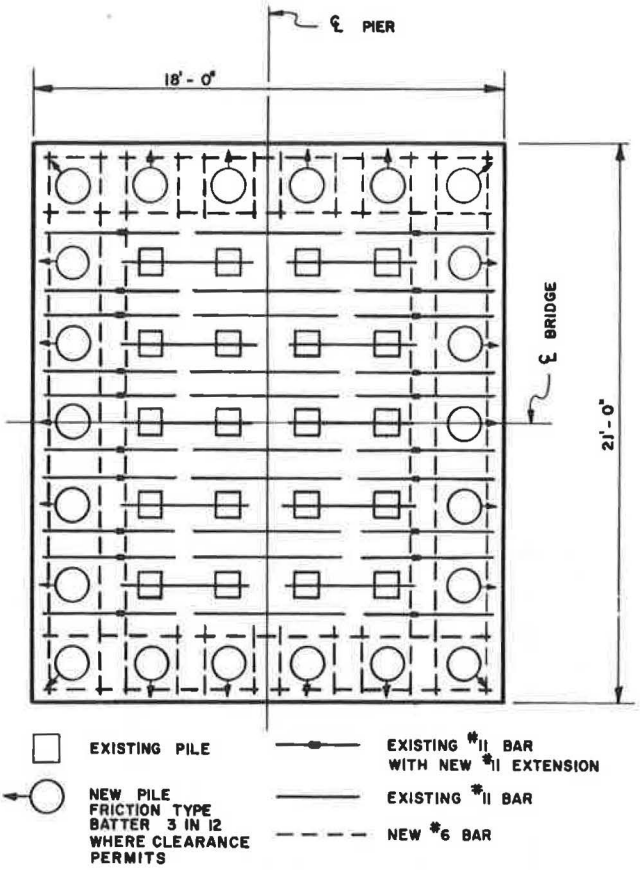

Note: 1 ft = 0.305 m. 1 in. = 2.54 cm.

Figure 10. Reinforced concrete bent column strengthening retrofit concept.

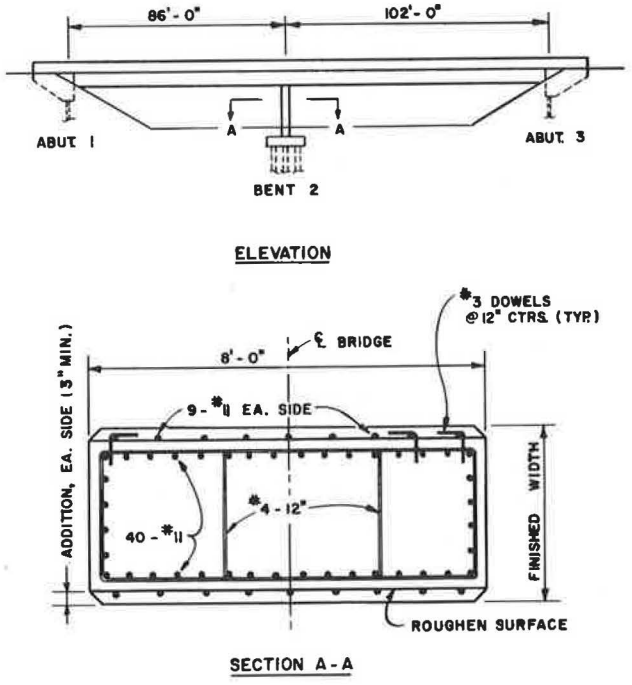

Note: 1 ft = 0.305 m. 1 in. = 2.54 cm.

collapse of the superstructure.

To illustrate this retrofit a 0.99 m (3 ft-3 inch) wide reinforced concrete pier cap is postulated and a 0.30 m (12 inch) width addition, on one side of the cap, is designed to withstand the loading associated with the impact of the girders on the widened area (Figure 11). The superstructure girders are spaced at 1.83 m (6 ft) centers and the load on the widened area is assumed to be centered at 0.15 m (6 inches) from the existing pier cap face. The addition to the pier cap is designed using the shear friction design method (12).

Figure 11. Girder bearing area widening retrofit details.

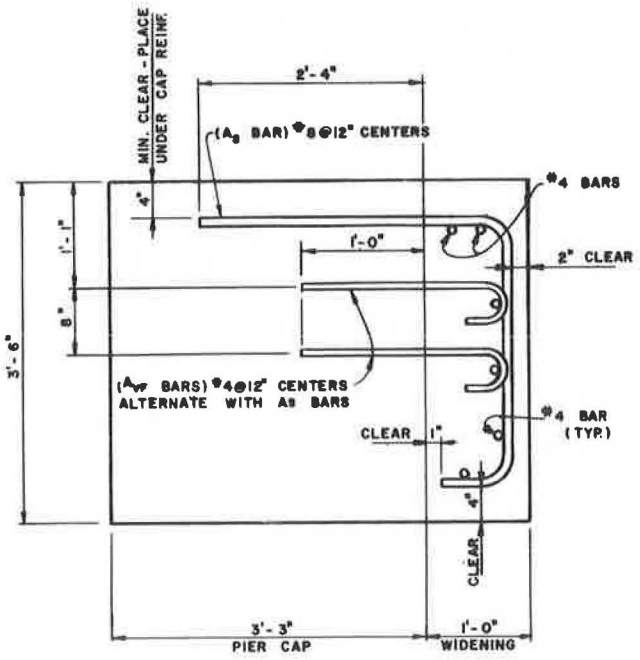

Note: 1 ft = 0.305 m. 1 in. = 2.54 cm.

Design of Bridge Retrofit Concepts

This section contains the step-by-step design of the Steel Girder Pin Bearing Vertical and Lateral Displacement Restrainer bridge retrofit concept. The purpose is to demonstrate the procedure employed in design.

Steel Girder Pin Bearing Vertical and Lateral Displacement Restrainer

The objective of the pin bearing displacement restrainer is to inhibit essentially all of the relative vertical and lateral motion across the bearing that could take place during an earthquake. With this retrofit, potential vertical and lateral motions during an earthquake are arrested by the addition of a bracket and stopper bar arrangement welded to the webs of the girders. The joint is also effectively restrained against relative longitudinal motion during an earthquake by the new vertical restraint which prevents the suspended span from rolling over the pin.

The retrofit method is applicable to any bridge with longitudinal girders supported by hinged bearings which do not provide positive restraint against uplift or lateral motion. A 200 kip (889.64 kN) dead load vertical reaction at the pin bearing was assumed to illustrate the concept. The brackets are fabricated from stiffened W6 x 25 beams that are positioned horizontally across the bearing joint opening with one of the bracket flanges welded to the suspended girder web only. A 2 inch (50.8 mm) square, 0.5 inch (12.7 mm) thick stop bar is welded to the girder web on the other side of the bearing joint above the bracket (Figures 12 and 13).

Figure 12. Steel girder pin-type bearing vertical and lateral displacement restrainer.

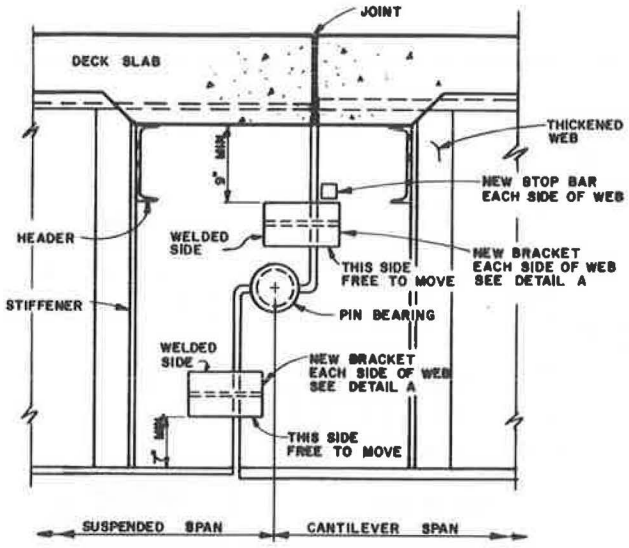

Note: 1 ft - 0.305 m. 1 in. = 2.54 cm.

Figure 13. Steel girder restrainer details.

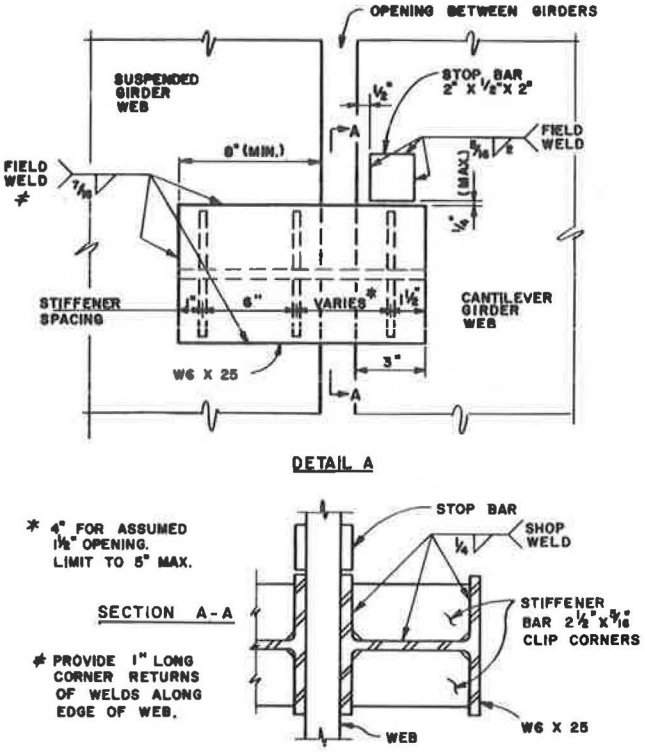

Note: 1 ft = 0.305 m. 1 in. = 2.54 cm.

Earthquake Loading. Suspended span girder reaction = 200 kips/girder (889.64 kN/girder)

Lateral earthquake load

EQ = 0.25 x contributing dead load = 50 kips (222.41 kN)

Vertical earthquake load

0.1 x 200 = 20 kips (88.96 kN)

AASHTO 1975
Art. 1.2.20(D)

Lateral Restrainer Design

Pin bearings may have a rim projection which provides resistance to lateral loads; however, no lateral force will be assumed as transferred through the bearing. Cantilever brackets (W6 x 25) welded to each side of the suspended span web plate above and below the bearing pin will provide adequate lateral load transfer. Each pair of brackets will be assumed to transfer one-half of the vertical load. The top pair of brackets will also function as a vertical uplift restrainer.

Use load factor design

Design load per unit = 1.3 x 50/2 = 32.5 kips (144.57 kN)

AASHTO 1975
Art. 1.2.22

This lateral force must be resisted in either direction.

Size of Cantilever Brackets. Opening between girders assumed to be 1.5 in. (38.10 mm).

Cantiler arm = 3.0 + $\overline{X}$ = 7.67 in. (194.82 mm), where $\overline{X}$ = 4.67 in. (118.62 mm)
(see bracket connection calculation)

Moment = 32.5 x 7.67 = 249.3 inch-kips (28.2 kN·m)

Use W6 x 25 brackets

S_{xx} = 16.7 inches^3 (273664.6 mm^3)

f = 249.3/16.7 = 14.9 ksi <36 ksi (102.7 MPa < 248.2 MPa) o.k.

Attachment of Lateral Restrainers to Girders. Field weld cantilever brackets to suspended span web with 7/16 inch (11.11 mm) fillet weld. Provide proper corner returns (1 inch, 25.4 mm) so that welds are capable of withstanding loads normal to the web.

Properties of Bracket Weld

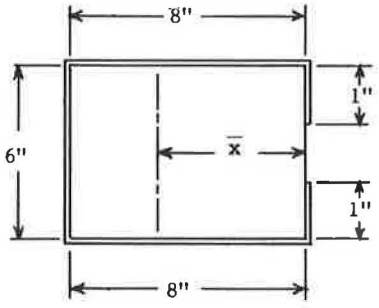

	A	x	Ax	I_{oo}	Ax^2
8 x 2	16	4	64	85.3	256
6 x 1	6	8	48	-	384
1 x 2	2	0	0	-	0
	24		112	85.3	640.0
					85.3

$\overline{x}$ = 112/24 = 4.67 in. (118.62 mm) $-A\overline{x}^2$ = -522.7

S = $I/\overline{x}$ = 43.4(in.)^3 (711200.1 mm^3) I = 202.6(in.)^4 (84328400.6 mm^4)

AASHTO 1973
Art. 1.7.28(B)

Allowable Weld Stress

0.45 x 58 = 26.1 ksi (178. MPa)

7/16 in. weld strength = 26.1 (7/16) 0.707
= 8.1 kips/inch (1418.5 kN/m)

AASHTO 1973
Art. 1.7.135(A)

Bracket Weld Stress from Lateral Load

$\frac{32.5}{24} \pm \frac{249.3}{43.4}$ = 1.35 ± 5.74 = 7.1 kips/in.<8.1 kips/in. (1243.4 kN/m) < 1418.5 kN/m) o.k.

Girder Web Stiffness. The webs are assumed to be at least 2 inches (50.8 mm) thick and this thickness is adequate to withstand the lateral loads from the brackets without additional stiffeners.

Vertical Restrainer Design

Use a pair of restrainer units at each girder. Each unit to consist of two stop bars and cantilever brackets field welded to the girder webs.

Use load factor design

Design load per unit = 20 x 1.3/2 = 13 kips (57.83 kN)

AASHTO 1975
Art. 1.2.22

Size of Stop Bars

A = 13/36 = 0.36 sq in. (232.26 mm^2)
Use 2 x 1/2 bar (A = 1 sq in., 645.16 mm^2)

Size of Cantilever Brackets

Cantilever arm = 7.67 in. (194.82 mm)
M = 13 x 7.67 = 99.7 inch-kips (11.26 kN·m)

Use the pair of upper W6 x 25 brackets that were provided for the lateral restrainer. These cantilever brackets will be employed to resist both the vertical and lateral restraint loads. Assume vertical load is resisted only by the connected flange.

S = 0.456 $(6)^2/6$ = 2.74 inches^3 (44900.65 mm^3)

f_b = 99.7/2.74 = 36.4 ksi (250.97 MPa) (allow. 36 ksi, 248.21 MPa o.k.)

Connection of Uplift Restrainer to Girder

Stop Bar. Field weld to cantilever span web with 5/16 inch (7.94 mm) fillet weld.

Allowable weld stress = 0.45 x 58 = 26.1 ksi (179.95 MPa)

5/16 inch weld strength = 26.1 (5/16) 0.707
= 5.77 kips/inch
(1010.48 kN/m)
AASHTO 1973
Art. 1.7.135(A)

Required length = 26.1/5.77 = 4.5 inches (114.3 mm)

Weld around three sides = 6 inches (152.4 mm)

No weld along bottom to permit full bearing of bracket flange.

Cantilever bracket. Check 7/16 inch (11.11 mm) weld stress (see lateral restrainer calculations for weld properties) 7/16"

Weld strength = 8.1 kips/inch (1418.54 kN/m)

Loads P = 13 kips (57.83 kN); M = 99.7 inch-kips (11.26 kN·m);

Min. Sec. Modulus = 43.4 $inch^3$ (711200.1 mm^3)

Bracket weld stress from vertical load

$\frac{13}{24} \pm \frac{99.7}{43.4} = 0.54 \pm 2.30 = 2.8$ kips/inch (490.36 kN/m) <8.1 kips/inch (1418.54 kN/m) o.k.

Conclusion

Bridges that are located on high risk seismic zones that were designed for earthquake loading according to the pre-1975 AASHTO Design Criteria may suffer substantial structural damage, and in some cases, collapse can be anticipated. This conclusion is based on analyses performed for several bridges and reported in (1). Each bridge was subjected to a postulated seismic load of the highest severity that will occur during the life of the structure at the bridge site.

This set of bridge retrofit concepts and the simplified analysis method given in (7) are intended to provide the practicing bridge engineer with basic guidelines, information and examples that may be used in planning and executing a bridge retrofit program.

It is believed that most bridges can be modified, if required, to dramatically increase their seismic strength. A number of the retrofit concepts can be relatively economically implemented especially when compared with the cost of structural failure.

The philosophy to be employed for determining the type and need for a retrofit measure is one of a balanced risk concept. Retrofitting should not be based on a need for eliminating all damage, but to limit the damage such that collapse does not occur and traffic can be maintained or restored after minimal repairs. A good deal of yielding and damage can be absorbed by the piers and other ductile components before collapse of the structure.

Acknowledgements

This work was supported by the Federal Highway Administration under Contract DOT-FH-11-8847. The period of performance was June 30, 1975 to May 31, 1977.

References

1. Robinson, R. R., et al, "Structural Analysis and Retrofitting of Existing Highway Bridges Subjected to Strong Motion Seismic Loading", Report FHWA-RD-75-94, Federal Highway Administration, Office of Research and Development, Washington, D.C. 20590, May 1975
2. Robinson, R. R., Longinow, A., and Albert, D. S. "Seismic Retrofit Measures for Highway Bridges - Design Reference Manual for Retrofitting Bridges to Withstand Earthquakes", for Federal Highway Administration Contract DOT-FH-11-8847, Final Report - Volume 2, June 1977 (in draft form)
3. Longinow, A., Bergman, E. and Cooper, J. D., "Bridge Retrofitting - Selection of Critical Bridges in a Road Network", Proceedings Technical Council on Lifeline Earthquake Engineering, Specialty Conference, University of California, Los Angeles, California, August 30-31, 1977
4. Degenkolb, O. H., "Retrofitting Highway Structures to Increase Seismic Resistance", Proceedings Technical Council on Lifeline Earthquake Engineering, Specialty Conference, University of California, Los Angeles, California, August 30-31, 1977
5. Newmark, N. M., Blume, J. A., and Kapur, K. K., "Seismic Design Spectra for Nuclear Power Division, American Society of Civil Engineers, November 1973
6. Algermissen, S. T. and Perkins, D. M., "A Probabilistic Estimate of Maximum Acceleration in Rock in the Contiguous United States", U.S. Geological Survey, Open File Report 76-416, 1976
7. Longinow, A., Robinson, R. R. and Chu, K. H., "Seismic Retrofit Measures for Highway Bridges-Training Course Material", for Federal Highway Administration Contract DOT-FH-11-8847, Final Report, Volume 1, June 1977 (in draft form)
8. "San Fernando, California, Earthquake of February 9, 1971", Volume II, Utilities, Transportation, and Sociological Aspects, U.S. Department of Commerce, 1973
9. 1975 Interim Specifications, Interim 2, Section 2 - Loads (Earthquake Stresses), Standard Specifications for Highway Bridges, AASHTO
10. Japan Road Association, "Specifications for Earthquake Resistance Design of Highway Bridges" quoted in, Iwasaki, T., Penzien, J., Clough, R., "An Investigation of the Effectiveness of Existing Bridge Design Methodology in Providing Adequate Structures Resistance to Seismic Disturbance. Phase 1: Literature Survey", FHWA-RD-73-13, November 1973
11. 1975 Interim Specifications, Interim 3, Loading Combinations, Standard Specifications for Highway Bridges, AASHTO.
12. 1974 Interim Revision, Section 5 - Reinforced Concrete Design, Standard Specifications for Highway Bridges, AASHTO

INCREASING THE SEISMIC RESISTANCE OF EXISTING HIGHWAY BRIDGES

Oris H. Degenkolb, California Department of Transportation
Presented by: Guy D. Mancarti, California Department of Transportation.

Prior to the 1971 San Fernando Earthquake, bridges in California experienced only minor seismic related damage. The San Fernando event demonstrated that structures designed by AASHTO Specifications in use at that time are vulnerable to seismic shaking. Failure of these bridges during an earthquake could be hazardous to highway users and block vital transportation lifelines. The State of California initiated a bridge retrofitting program in 1971 in order to increase the seismic resistance of bridges built before that time. The most prevalent deficiency of pre-1971 bridges is a lack of longitudinal restraint of girders at hinges and end supports. California has developed devices which will have been used to retrofit more than 649 bridges at a cost of $22 million by 1980. An evaluation of all state owned bridges is currently being made in order to complete the program. Many of the bridge columns which were designed according to specifications prior to 1971 were proven to be seismically deficient because they had too few ties to adequately confine the concrete. This paper and presentation will cover a brief background, philosophy, magnitude of the problem, design criteria, details and costs.

Introduction

Prior to 1971, very little earthquake damage was experienced by bridges in the mainland 48 states. The little damage that did occur was generally limited to minor cracking and spalling of concrete, damaged bearings and grout pads, and slight displacements of spans. The bridges involved were generally quite low with rather short spans.

The 1971 San Fernando earthquake provided a test of modern bridges which had spans as long as 191 feet and heights of 150 feet. Much of the damage to these bridges was caused by vibration induced by ground motion.

The San Fernando earthquake occurred at 6:00 a.m., before peak morning traffic, and before the completion of two major highway interchanges which were under construction in the area. As a consequence, there was relatively little inconvenience to the travelling public and only two fatal injuries. If the same quake had occurred a few months later and a few hours later in the day, the inconvenience to the public and number of fatalities could have been dramatically different.

Deficiencies In Existing Bridges

The 1971 earthquake pointed out a number of deficiencies in bridge design specifications and detailing practices. Although the level of seismic design forces and methods of applying those forces proved to be inadequate, the most serious deficiencies were attributed to details. Segments of superstructures were not properly tied together. Some concrete columns were seismically inadequate because they had an insufficient amount of spiral and tie reinforcement, the ties and spirals were inadequately detailed, and main column reinforcement frequently had insufficient splice length and end anchorage. The column deficiencies are especially critical in bridges with single column bents.

Retrofitting Philosophy

It is not practical or economical to design new bridges or retrofit existing bridges that will serve normal transportation needs but not be damaged to some extent if subjected to severe seismic shaking. The aim is to make structures seismically resistant to the extent that they may sustain damage but not collapse completely. It is also desirable that they be capable of carrying at least a limited amount of emergency traffic even though they may be damaged. Although retrofitting existing structures will increase their seismic resistance considerably, a designer is limited by the capabilities and features of the existing facilities and economics. Portions of some existing structures have to be strengthened to accommodate the anchorage forces which restrainers require. In some cases restrainers which would develop the forces required to hold the segments of a bridge together would pull the ends out of the spans or pull over the columns. When hinges are not restrained, segments of a bridge can act independently and forces in the columns can be significantly greater than if hinge movements are

limited. Thus, retrofitting hinges with restrainers can significantly reduce the probability of column failures.

Prioritizing Retrofitting Work

It was realized immediately after the 1971 earthquake that existing bridges should be retrofitted in order to increase their seismic resistance. A prioritizing system was devised which assigned weighted values to:

1. Type of bearings
2. Width of hinge or bearing seat
3. Restraint of supports
4. Height of structure
5. Type of supports
6. Flexibility of supports
7. Curvature in alignment
8. Probable earthquake intensity
9. Hazard to public on and under structure
10. Disruption to traffic and utilities
11. Danger to buildings or facilities under the structure.

This system worked well for identifying candidate structures for immediate retrofitting. However, the prioritizing numbers obtained did not always reflect the true relative importance of some structures. The input is largely a matter of judgment, but under certain circumstances a single factor might be important enough to justify a high priority regardless of all other factors. A less important structure could rate lower in a number of less important categories but get a higher overall rating. The results from any prioritizing system should be subject to adjustment by good judgment.

There are also practical considerations which can, to some extent, override the strict adherence to a prioritizing system. If a large number of bridges spread over a very large area are identified for retrofitting, there are considerations in contracting and inspection which should not be overlooked. Although there are not any definitive rules which can be followed, there are general guidelines which should be considered. A greater degree of efficiency can be achieved if a number of bridges in one area can be included in a single contract. It is more efficient to prepare plans and let contracts for a few large jobs than a great number of single bridge contracts. A contractor's mobilization costs can be spread out and personnel can be trained and used more efficiently on a contract with a number of bridges. A large contract can be inspected efficiently, but a single inspector on too small a job will have time to waste unless he can be given other work to do. For efficiency, it is obvious that bridges in a contract should be located reasonably close together. It is generally true that groups of bridges in different contracts should not ordinarily overlap. If individual structures are prioritized by an inflexible system, it is highly unlikely that structures with nearly equal priorities will be geographically located to form logical contracts.

Hinge And Bearing Restrainers

Restrainers should be capable of developing a minimum force equal to 25% of the weight of the lighter segment of superstructure connected, based on working strength design. This rule of thumb is satisfactory for relatively short structures where the influence of the abutment backfill on the superstructure is uncertain. However, dynamic analysis should be made for larger and more complex structures and provisions made for larger forces, if required. All of California's seismic dynamic analyses are based on load factor methods and a ductility factor of one is used for restrainers.

California has used 3/4-inch pre-formed 6x19 galvanized cables (ASTM Designation A-603) with a minimum breaking strength of 23 tons (205 kN) as the basic unit for its restraining devices. Swaged end fittings are used which are required to develop the minimum breaking strength of the cable. This type of cable and end anchorages have been used in highway barrier systems for many years. They are being tested on a regular basis and have an excellent performance record. 1¼-inch diameter galvanized ASTM A-722 (with supplementary requirements) steel bars which have a specified minimum elongation of 7% measured in 10-bar diameters are also being used.

The ideal restrainer should absorb and dissipate energy. Although a number of such devices have been considered, they have not been regarded as being economically practical for routine retrofitting work. The steel cables and rods can store energy, but transfer it back into the structure as they pull the segments of superstructure back together. Much of the energy is probably dissipated by the pounding of the superstructure elements when they come together. The damage caused by this action is repairable and should not cause the bridge to collapse.

When the hinge and bearing retrofitting program was started, most of the designs were done by working strength methods. A working load of 50% of the ultimate strength for galvanized cables plus an overstress of 33% permitted for seismic conditions gives a total allowable load of 30.6 kips (136 kN) per cable. For load factor design methods, a yield strength of 85% of ultimate load, or 39.1 kips (174 kN) per 3/4-inch cable is assumed. The design yield stress for 1¼-inch high strength bars is 120 k.s.i. (827 k Pa) or 150 kips (667 kN) per bar. These bars are particularly useful in cases where it is impractical or undesirable to use the number of 3/4-inch cables required to obtain the necessary resisting force. Many older bridges which are being retrofitted have shear keys which are inadequate for keeping the two sides of the hinge aligned longitudinally if the structure is subjected to seismic shaking. Since a transverse shearing action at the hinge could cause the rods to fail and become ineffective in tension, supplemental solid mild steel rods are installed through the

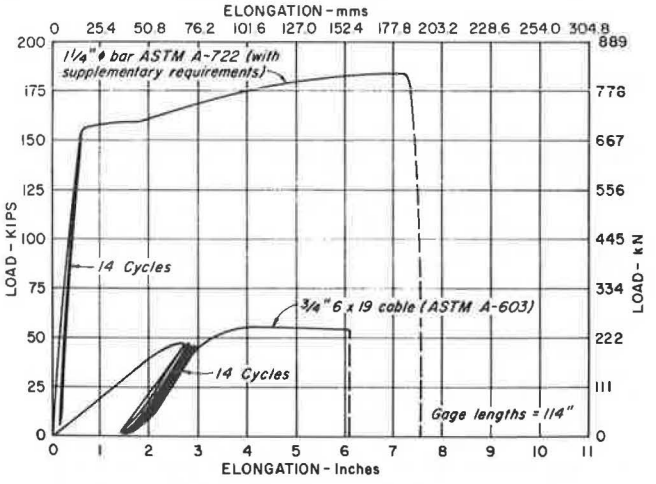

Figure 1

hinges in order to provide additional shear resistance.

California has conducted a number of tests of 3/4" cables and 1¼" ϕ bars to compare their qualities as restrainers. Figure 1 shows the stress-strain relationship of specimens tensioned from near zero stress to specified minimum yield stress (assumed to be 0.85 Fy for cables) for 14 cycles and then to failure.

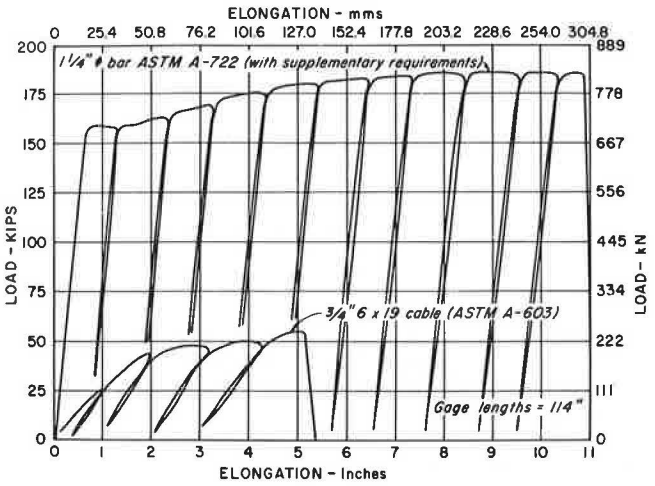

Figure 2

Figure 2 shows stress-strain relationships for cables and bars tensioned to failure but releasing the load to nearly zero at approximately one inch increments of stretching.

Cycling 3/4" cables within the elastic range required more than twice the amount of energy than cycling an equivalent number of 1¼ ϕ bars of the same length for the same number of cycles. This is due to the fact that bars have a greater modulus of elasticity and the elongation within the elastic limit is less than for cables. Within this range the cables and bars store energy but do not dissipate any significant amount.

The bars stretched and cycled beyond the elastic limit dissipated approximately 3 times as much energy as the equivalent number of the same length cables.

If restrainers are permitted to yield, greater joint openings and column deflections will be realized. Once either type of restrainer is stretched beyond its elastic limit it obviously will not assist in closing the joint to its normal position. Although bars will dissipate more energy than cables when failure occurs, the elongation will also be much greater. This could be an extra factor of safety in some structures but could be disastrous in structures with relatively short, stiff columns. When a restrainer is stretched to its ultimate limit, the structure is vulnerable to any additional shocks.

Considering the impreciseness of predicting a bridge's response to a possible future earthquake, it is generally not prudent to depend on restrainers acting beyond their elastic limit.

Restrainer Details

Figure 3 shows the most commonly used detail for retrofitting hinges of existing concrete box girder bridges. The concrete bolsters are generally required to spread out the concentrated forces of the restrainers so that they don't destroy the hinge

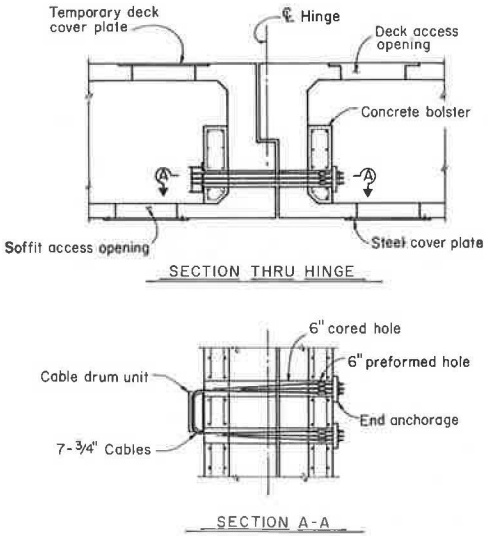

Figure 3

diaphragms. A minimum of one 7-cable (428 kip, 1,900 kN) unit placed in each exterior cell at each hinge is generally considered to be a minimum requirement in order to provide maximum resistance to transverse bending of the entire superstructure. Access to the cells is made through the soffit whenever possible in order to avoid interfering with traffic on the bridge. If access through the soffit is not possible or desirable due to conflicts with traffic under the structure, or other reasons, work is done through deck openings. In this case, traffic handling may become critical and work limited to off-peak hours. Steel plates set flush with the roadway surface are used to carry traffic across the access holes between working periods. Deck access holes must be permanently closed when work is completed. Holes in the soffit are covered with galvanized steel plates which can be readily removed for future inspections.

Figure 4 is a modification of the concept shown in Figure 3. It is generally restricted to hinges and end supports of shorter span T-beam bridges where the restraining force requirements are considerably lower.

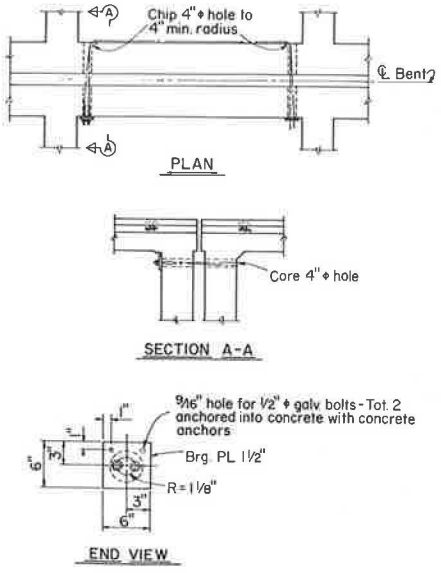

Figure 4

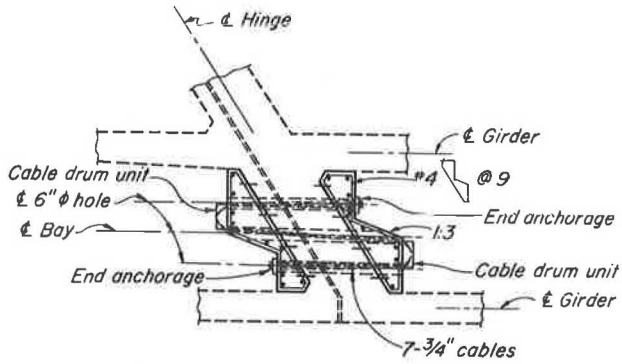

Figure 5

Figure 5 is another modification of Figure 3 and has been used in a few situations where the existing diaphragms are capable of resisting the greater force provided by the seven cables which pass through the joint three times.

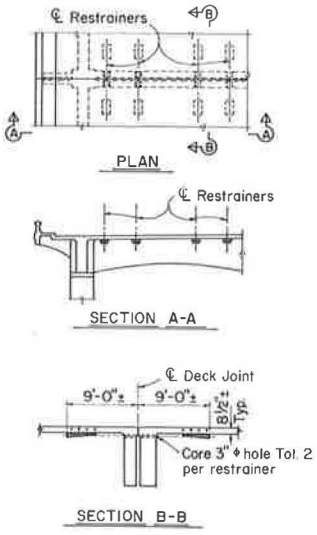

Figure 6

The detail shown in Figure 6 has been used on a limited basis where the diaphragms are not capable of being adequately strengthened and it would have been less desirable to attach restrainers directly to the girder stems. In this particular case it was necessary to place the cable anchorages far enough from the ends of the deck slab so that they would not pull the ends out of the spans.

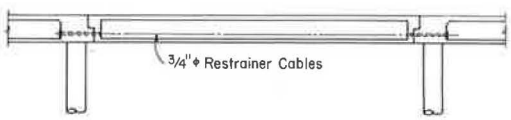

Figure 7

Variations of Figure 7 have been used in a number of instances where drop-in spans could be expected to fall if the structure were shaken in an earthquake. If the hinge seats are very narrow and the cables very long, additional cables might be required in order to limit the amount of stretching under seismic loading. This method is uneconomical in very long span.

An installation using high strength rods is illustrated in Figure 8. Cables could also be used in this scheme.

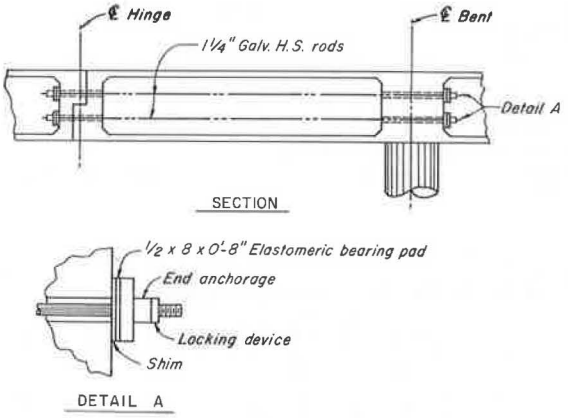

HIGH STRENGTH ROD RESTRAINER

Figure 8

Figure 9 shows a commonly used detail for restraining steel girders which are in line with each other. When girders in adjacent spans are offset, transverse beams are attached to the bottom girder flanges which are used for anchoring the restrainer cables, as shown in Figure 10.

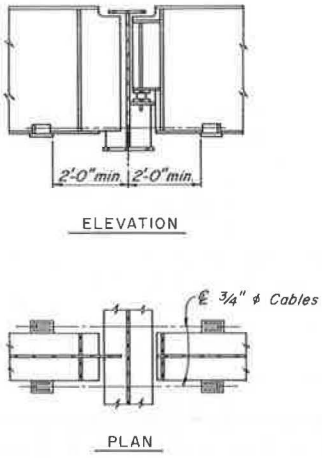

Figure 9

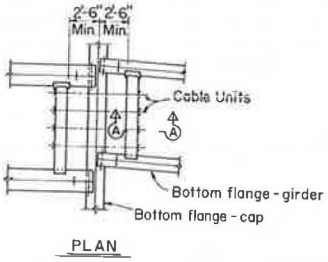

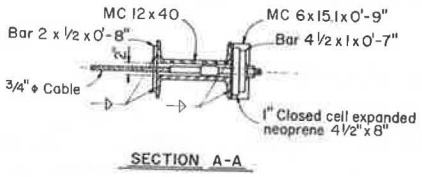

Figure 10

Figure 11 illustrates a method of attaching the ends of steel girders directly to the supporting concrete bents.

The restrainers illustrated above are only a few of the many types we have used to date. Each bridge has its own peculiarities and requires special attention and details.

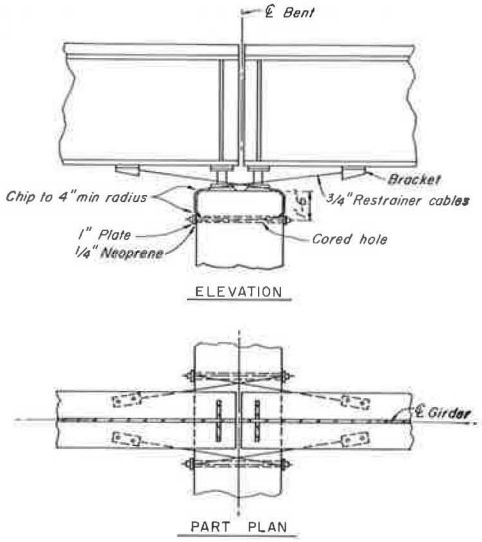

Figure 11

Costs

The following contract unit prices are taken from a large number of recent contracts which were bid competitively:

	Low	Avg.	High	
Deck access openings	$200.	$230.	$300.	/each
Soffit " "	200.	228.	300.	/each
Miscellaneous metal (cables, fittings, brackets, etc.)	1.50	1.75	5.00	/pound
Core 6" holes	38.	42.	62.	/lin.ft.
Core 4" holes	26.	33.	55.	/lin.ft.
Core 2" holes	18.	23.	30.	/lin.ft.
Diaphragm bolsters	200.	253.	300.	/each
Close deck access openings.	200.	251.	350.	/each

Installation of Restrainers

One of the main problems in connection with retrofitting existing bridges is minimizing interference with existing traffic. It is frequently necessary to limit work to off-peak hours. When retrofitting box girder bridges, the designer is given the option of specifying access to the girders through either the deck or soffit. Deck and soffit openings are generally made quite close to the hinges where tensile stresses in the girder reinforcement and compressive stresses in the concrete are relatively low, but far enough away so that the openings are not an inconvenience to the workmen.

Steel cover plates are generally required over the deck openings to provide for traffic during non-working hours. The 5/8-inch thick cover plates were placed on top of the deck in earlier contracts but were found to be hazardous to certain vehicles. Plates are now required to be recessed into the deck so they provide a flush riding surface. After work inside the girder cells is completed, extensions are welded to the ends of the cut reinforcing steel in the deck, to provide lap splices, and the opening is filled with concrete.

It is not considered necessary to replace reinforcement and concrete in soffit openings. Exposed ends of the reinforcing steel are painted with zinc-rich paint and a galvanized steel plate bolted over the opening.

Some contractors have expressed a preference for doing all of their work through the soffits whenever possible, in order to avoid conflicts with traffic on the bridge deck. Present equipment allows them to work as much as 100 feet from ground underneath a structure. A preference has also been expressed for gaining access to a temporary platform suspended underneath narrower structures from the bridge deck.

Retrofitting Columns

The second greatest weakness of Pre-1971 structures pointed out by the San Fernando earthquake was that the reinforcing steel ties in columns did not provide adequate confinement of the concrete. Bridges with single column bents are particularly vulnerable. Since the restraining of the superstructure at hinges and bearings was judged to be a more serious problem, and providing that restraint alleviated the seriousness of the column deficiency, more can be obtained for the money by retrofitting the hinges and bearings first. Methods of retrofitting columns to make them more earthquake resistant are being investigated and a developmental contract will be let in the near future for trying out some of the schemes.

All bridges which might require column retrofitting are currently being identified. When the developmental contract is completed a program to retrofit the columns of some of the state's more critical structures will be considered.

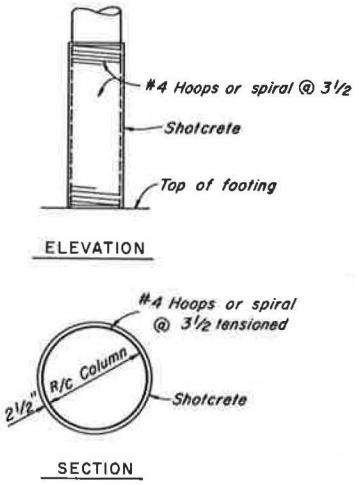

COLUMN RETROFITTING

Figure 12

FOX INDUSTRIES

Figure 13

Figure 12 illustrates reinforcing steel hoops that are prestressed on the outer face of the column which is then covered with shotcrete. The device shown in Figure 13 was especially designed for this purpose. It is basically a turnbuckle which develops the strength of the reinforcing steel and places an initial pre-stress in the hoop.

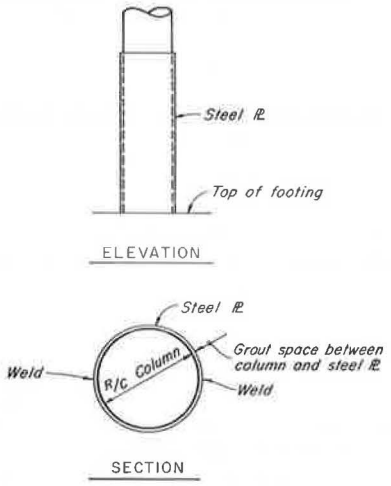

COLUMN RETROFITTING

Figure 14

The column retrofitting method shown in Figure 14 consists of wrapping a column with tensioned prestressing wire and applying a protective coat of shotcrete.

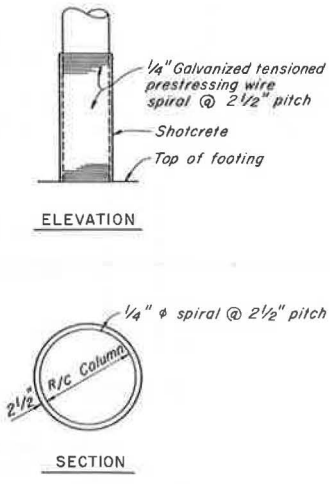

COLUMN RETROFITTING

Figure 15

Figure 15 illustrates a method which consists of welding a steel shell around an existing column and filling the space between the shell and column with grout. "Weathered" steel can be used for achieving an architectural effect, if desired, or ordinary steel can be used and painted.

Conclusions

Many bridges which were designed by pre-1971 specifications and standards have serious seismic deficiencies. California has a program for retrofitting many of those bridges to make them more seismically resistant.

During an earthquake, each bridge abutment and pier can rotate in any direction independently, in phase or out of phase with any other pier or abutment. Ground between piers can distort elastically and in some cases may rupture or liquify. The seismic analysis of bridges and criteria for retrofitting bridges to increase their seismic resistance is, at the present time, a developing state-of-the-art process. Engineering judgment is an important factor in retrofitting bridges to make them more seismically resistant.

DEVELOPMENT OF A SIMPLIFIED METHOD OF LATERAL LOAD DISTRIBUTION FOR BRIDGE SUPERSTRUCTURES

Tarek S. Aziz, Acres Consulting Services Limited
M.S. Cheung, Public Works Canada
Baidar Bakht, Ontario Ministry of Transportation and Communications

A new simplified method for establishing the live load design moments in most common types of bridges is presented. The proposed method was developed by using orthotropic plate theory and was checked by the grillage analogy method. The basis of the method together with the details of development methodology are discussed. Different variables which may affect load distribution in bridges were examined, and the main variables governing the distribution factors were selected for the present study. The study deals mainly with single span right bridges which can be analysed using the orthotropic plate theory or grillage analogy. However the limits of applicability of the distribution factors to continuous and skew bridges and bridges with diaphragms and edge beams are also discussed.

Vehicle loading on a highway bridge is distributed transversely to the main longitudinal girders by the floor system, which consists of deck slab and supporting members. The interaction between the different components of a highway bridge is difficult to determine, thus the complete structural analysis of a bridge is a complex undertaking. For the purpose of designing new bridges or evaluating existing ones, most codes (including American (1) and Canadian (2) bridge codes) provide empirical rules for transverse load distribution. Currently, both AASHTO and CSA-S6 permit each longitudinal girder in the bridge to be designed for some portion of the wheel loads of the standard truck. In 1973, the AASHTO code introduced more realistic empirical rules for load distribution in box girder bridges. The formulae were based on work carried out by Motarjemi and Van Horn (3). Further research on three categories of bridges, mainly beam and slab bridges, box girder bridges and multibeam bridges, was carried out by Sanders and Elleby (4). Based on the results of this research, distribution formulae for multibeam bridges have been incorporated in AASHTO Interim Bridge Specifications 1974 (5).

A new simplified method for establishing the live load design moments in most types of single and multi-span bridges (see Figure 1) is proposed in this paper.

The method is intended to be used in the design of new bridges as well as the evaluation of load-carrying capacity of existing ones. The method allows a bridge engineer to determine the maximum bending moment in any girder due to the worst loading condition without having to carry out a computer analysis (grids, orthotropic plate or finite element analysis). Because the load distribution phenomenon is treated more realistically in this method, some of the unnecessary built-in conservatism of the old standards can be eliminated. At the same time, the simplicity of the current AASHTO approach is maintained in the format of presentation.

The method may be used to derive load distribution factors for any other type of truck configurations. Recently, similar distribution factors have been developed by the authors for the Ontario loading and are now incorporated in a new bridge code for Ontario (6).

At present, distribution factors are used in four sections of the AASHTO code. The number of variables considered in each section is different, and, in each case, distribution factors are based on studies done on a particular type of bridge. It is appropriate at this stage to make several comments on the current AASHTO specifications.

1. In the current AASHTO Code, bridge type and girder spacing are considered to be the two most important parameters affecting the distribution of lateral loads. However, for some bridge types (box girders, composite box girders, and multibeam) distribution formulae also include other parameters.

2. Apart from the Interim Specifications (5) for multibeam bridges, AASHTO formulae do not account for variation of the member stiffness and its effect on structural behaviour. The formulae, in general, appear to consider only the geometrical variables of the bridge.

3. Reduction factors for multi-lane bridges are either included implicitly in the distribution formulae or neglected intentionally. Thus the stochastic nature of the live loading phenomenon may not be accounted for properly.

Variables that Govern Lateral Load Distribution

In general, the following variables may affect load distribution in bridges. Each of them have been studied and their effects on lateral load distribution are accounted for in the development of the simplified load distribution charts proposed in this paper.

The Stiffness Characteristics of the Bridge

These variables affect the behaviour in many ways. For example, if an equivalent orthotropic plate is used to model the bridge, its stiffness parameters (7) D_x, D_y, D_{xy}, D_{yx}, D_1, D_2 appear directly in the governing equation of the orthotropic plate, and their effect is self-evident.

Through a mapping process (7) the above stiffness variables can be reduced into two characteristic nondimensional variables α and Θ where:

$$\alpha = \frac{D_{xy} + D_{yx} + D_1 + D_2}{2\,(D_x D_y)^{0.5}} \qquad (1)$$

and

$$\Theta = \frac{W}{2L}\left(\frac{D_x}{D_y}\right)^{0.25} \qquad (2)$$

In which D_x, D_y, D_{xy}, D_{yx}, D_1 and D_2 are stiffness parameters, W is the width of the bridge and L is the length of the bridge.

Figure (1) shows the variation of α and Θ for different types of bridges. The practical range of α is between 0 and 2 while the practical range of Θ is between 0.125 and 2.50. The values of α and Θ for some 80 existing bridges are plotted on the α-Θ space. It can be seen from the figure that different types of bridges fall into different locations of the α-Θ space (for example, floor systems incorporating timber beams have an α between 0.0001 and 0.01 with a great variation of Θ, while concrete slab bridges have a constant α of 1.0).

The Width of the Bridge (W)

This variable affects the behaviour of the bridge by determining its maximum number of lanes (design lanes) and also by defining the aspect ratio, W/L. The larger the aspect ratio, the higher the flexural parameter, Θ of the bridge. Bridges with small aspect ratios usually tend to have better load distribution characteristics.

The Number of Lanes (N_L)

In general, as the number of loaded lanes on a given bridge is increased, the girders tend to share the load more equally and thus the moment distribution in the transverse direction becomes more uniform.

The Number of Girders (N_G)

The load per girder decreases as the number of girders increases. In addition, the number of girders affects the values of both α and Θ.

Truck Locations on the Deck

The transverse location of the truck may affect the load distribution factors significantly. The edge distance, defined as the distance between the edge of the bridge and the outer most line of wheel loads, and the distance between trucks could result in very different load distribution factors. Various combinations of truck locations and edge distances have been studied. Critical positions are used to determine the load distribution factors.

Axle Width of the Truck

Axle width of the truck affects the load distribution factors significantly. Different axle widths may result in entirely different load distribution factors, even if all the other variables are kept the same. Therefore, strictly speaking, the load distribution factors are applicable only to the type of trucks that have the same axle width as those used in the development of the distribution factors. Fortunately, for the majority of trucks, the axle width is a standard 1.83 m (6 feet). Thus this variable has been eliminated from the study.

Longitudinal Axle Spacing

Longitudinal axle spacing has very little effect on the transverse load distributions. Load distribution factors developed for a particular axle spacing may be used for any other types of truck configuration without sacrificing accuracy within practical limits, provided the axle width is standard (1.83 m).

Size of Patch Loads

For the types of bridges considered in this study, this variable is known to have little effect on the lateral load distribution. The sizes of the equivalent patch load for different wheel loads shown in Figure 2 have been used in this study.

Methods of Analysis

Two well-established methods of analysis were used in the current investigation; the orthotropic plate analysis and the grillage analogy.

In the orthotropic plate analysis, the structure is idealized as a plate of constant thickness having different flexural and torsional properties in two mutually perpendicular directions. The series solution presented by Cusens and Pama (7) was used. It covers the torsionally stiff and torsionally soft decks, as well as the isotropic decks. This solution was applied through a well-established computer program, ORTHOP (8). The area of loading for the different wheels is taken into account (Figure 2) and edge beams, if present, are accounted for.

In the grillage analogy method, a structure

is idealized as an assembly of beams. This method was applied through a well-established computer program, GRIDS (9). The grillage analogy method was used to provide independent checks on the ORTHOP results as well as to study the effect of diaphragms reported elsewhere (10).

Development of Distribution Schemes

Development of distribution schemes for a code is a complicated task made difficult by the number of variables involved and the need to account for all of them while maintaining simplicity. In this study the task was accomplished in two phases.

1. Preliminary and pilot studies of the different variables and their effect on the load distribution were made in an attempt to determine the importance of each variable and the minimum number of variables to be maintained.
2. Analyses were made for different groups of bridges that cover the practical ranges of variables defined in the first phase. A total of 1,344 hypothetical cases of bridges were analyzed in this phase and the results formed the data base for the suggested schemes.

Figure 3 shows a flow chart of the general methodology used for the development of the distribution schemes.

Observations from the Pilot Studies

To determine effects of different variables on the governing values of moments, pilot studies were conducted on a series of bridges. For each analysis conducted the following three items were extracted:

1. The maximum moments,
2. Intensity factors (defined as the ratio of maximum moment to the average moment in the bridge), and
3. The theoretical equivalent width D (as used in AASHTO to obtain the distribution factor S/D).

Some observations made on the effects of the variables involved in the pilot studies appear below.

Bridge Width

The width of the bridge has an effect on the governing values of the moments in addition to its contribution to the values of θ. Figure 4 shows a typical behavior for the effect of width on the D values for two-lane bridges.

Girder Spacing

The theoretical D values are dependent on the girder spacings. However, it was found that for girder spacing of more than 1.52 m (5 feet), the change in the theoretical D value with girder spacing is small (less than five percent) for all the practical ranges of α and θ.

Bridge Span

A series of analyses for two families of bridges was conducted. The first family had a constant span of 18.29 m (60 feet) while the other family had a constant span of 36.58 m (120 feet). All the possible variations of the properties were considered (for example, α was varied from 0.0 to 2.0 while θ was varied from 0.125 to 2.50). Figure 5 shows a typical member of each family. It was observed that bridges which had the same α and θ resulted in the same theoretical D value independent of the absolute value of the span. Thus, while the critical D value is dependent on α and θ; it is independent of the absolute value of the span. (Note that θ itself is dependent on the span). This approach was repeated for different bridge widths and different numbers of lanes. The conclusion was that two bridges of different lengths but identical α and θ have the same distribution coefficients or D values. As part of these analyses the theoretical D values were calculated for different places within the span. The results showed conclusively that the theoretical D values are constant for most of the span.

Number of Loaded Lanes

The number of loaded lanes affect the values of D substantially, in particular for bridges with low values of θ. Figure 6 shows a typical behavior for a two lane bridge. The behaviour shown in this figure suggests that the governing loading case in a design may not necessarily be the fully loaded case since reduction factors for multi-lane bridges have to be introduced first to arrive at the governing design moments.

Edge Distance

Edge distance, defined as the distance between the edge of the bridge and the outermost line of wheel loads, has a major effect on the governing values of the moments, especially when the governing moments are in the vicinity of the free edge. For example, Figure 7 shows a typical behavior of the effect of the edge distance on the theoretically derived D values for a two-lane, 8.84 m (29 feet) bridge with α equal to 0.16.

Other Effects on the Load Distribution

Additional factors that affect the load distribution have been studied and the results have been reported recently by Aziz and Alizadeh (10). Some of the observations that have a bearing on this study are summarized below.

Continuity

While continuity of the bridge may affect the absolute values of the moments, it does not change the moment distribution pattern of the bridge. The zones of negative moments in a continuous bridge behave in a similar manner as the zones of positive moments. The proposed method, although developed from analyses for single span bridges, was found applicable with good accuracy to both positive and negative moments. The only adjustment required for continuous bridges is to utilize the effective span (the distance between contraflexure points) in calculating θ.

Skew

Skew bridges with skew angle less than 15 degrees can be analysed by the proposed method treating them as right bridges. From actual analyses, it was confirmed the error arising from this simplification was small and can be neglected.

Diaphragms

Although the proposed method was developed for bridges without diaphragms, studies on the effects of diaphragms on the transverse distribution of live loads using grillage analogy methods (10,11) concluded that the method is also adequate for bridges with diaphragms. In this case, the proposed method would generally result in a slightly conservative estimate of the distribution factors.

Distribution Charts for AASHTO Loading

Following the pilot studies, a total of 1,344 hypothetical cases of bridges were analyzed by ORTHOP to develop the distribution charts given in Figures 8, 9, 10 and 11 for the AASHTO HS truck. All bridges were assumed to have a minimum curb width of 45.72 cm (1 foot 6 inches) on each side. Thus, the edge distance in these analyses was maintained at a practical limit of 1.07 m (3 feet 6 inches). The values of Θ and α were varied in the range of 0.125 to 2.50 and 0.0 to 2.00 respectively. This should be sufficient to cover all practical bridges.

All the possible loading combinations were considered, from the worst concentric case of loading to the worst eccentric case of loading. In accordance with the AASHTO specifications, when there were three or four lanes loaded, reduction factors of 0.9 or 0.75 respectively were used. All the partial loading possibilities were considered as well. The bridges were loaded to produce the maximum bending moment. The governing theoretical D values were calculated from the moments integrated over a 1.52 m (5 feet) width. The differences observed between an outside girder and an inside girder were not significant enough to justify a special treatment or presentation for each. Finally, contours were drawn to represent the D values for each category of bridge (two lane, three lane and four lane). Because the width of a bridge has an effect on the load distribution in addition to its contribution in Θ, a correction factor chart was devised to deal with bridges having lane widths larger or smaller than 3.35 m (11 feet) (for which the basic contours were drawn). While this correction, C_f, was found to be less than 15 per cent in most cases, it was decided that by developing such a chart the proposed method would be made even more accurate. Finally, a total of 100 bridges were analyzed by the developed charts as well as by ORTHOP and GRIDS. The maximum error observed was very small.

Steps in Applying the Method

After discussing the foregoing distribution charts and the derivation procedures, it is appropriate to summarize here the steps to apply the proposed method, in a format similar to that used in the AASHTO code.

For shallow superstructures (shown in Figure 1) having either right spans or skew angles smaller than 15 degrees, the longitudinal moment due to HS loading is computed as follows.

1. The values of α, Θ and μ are calculated from:

$$\alpha = \frac{D_{xy} + D_{yx} + D_1 + D_2}{2\sqrt{D_x D_y}} \qquad (1)$$

$$\Theta = \frac{W}{2L}\left(\frac{D_x}{D_y}\right)^{0.25} \qquad (2)$$

$$\mu = \frac{\text{Lane width} - 3.35\ \text{m}}{0.61} \quad \text{(for SI units)}$$

$$\text{(Maximum of 1.0)} \qquad (3)$$

$$\mu = \frac{\text{Lane width} - 11\ \text{feet}}{2} \quad \text{(for Imperial units)}$$

where:

W = Width of the bridge.
L = Span of the bridge or equivalent simple span for a continuous bridge (span between contraflexure points for positive or negative moment regions).

2. Corresponding to the values of α and Θ determined previously, D_{design} is found by reading a D value from the applicable chart (Figures 8, 9, and 10), and a correction factor "C_f" from a variation chart (Figure 11), and substituting in the following expression.

$$D_{design} = D\left[1 + \frac{\mu C_f}{100}\right] \qquad (4)$$

3. The governing design bending moment is the fraction S/D_{design} of the moment resulting from one line of wheel loads, applied to a girder, or a web of a voided slab, or a unit width of a solid slab,

where:

S = the actual spacing of longitudinal girders; or,
S = spacing of webs, in the case of voided slabs; or,
S = a unit width, in the case of solid slabs or laminated timber bridges.

Examples of the use of these analysis charts appears below.

Examples

1. The proposed method is applied to a three-lane beam and slab bridge with a span of 18.29 m (60 feet) and a width of 13.72 m (45 feet). The cross section of the bridge is shown in Figure 12. The steps in arriving at D_{design}, are:

D_x = EI/ (beam spacing)

= E (5629033.8 cm^4)/236.22 cm

= 23829.62 E

D_y = E (slab thickness)^3 /12

= E (19.05 cm)^3 /12

= 576.11 E

neglecting the contribution of the steel I beam to the torsional inertia; since the torsional inertia of an I beam is very small.

$D_{xy} = D_{yx}$ = G(slab thickness)^3 /6

$$= \frac{E}{2\,(1 + 0.15)} \quad \frac{(19.05\ cm)^3}{6}$$

= 500.96 E

$D_1 = D_2 = \nu$ (lesser of D_x and D_y)

= 0.15 x 576.11 E

= 86.42 E

α = 0.5 (500.96 + 500.96 + 86.42 + 86.42) / (23829.62 x 576.11)$^{0.5}$

= 0.16

Θ = 0.5 x 1371.53 (23829.62/576.11)$^{0.25}$ / (1828.71)

= 0.95

The lane width is 4.27 m (14 feet), therefore

$\mu = 0.5 \quad \frac{(4.27-3.35)}{0.61}$

= 1.5 > 1.0

Use μ = 1.0

from Figure 9, the value of D for α = 0.16 and Θ = 0.95 is 1.74 m (5.70 feet) and from Figure 11 the value of C_f is 5.8. Therefore,

D_{design} = 1.70 m (1 + 1.0 x 5.8/100)

= 1.84 m (6.10 ft).

(The corresponding value of D_{design} according to the current AASHTO method is 1.67 m (5.5 feet.))

2. In this example, the proposed method is used to calculate the load distribution factors for the Conestogo River Bridge, a 2 lane, 3 span continuous plate girder bridge (Figure 13) with a central span of 44.20 m (145 feet) and side spans of 34.75 m (114 feet). The distribution factor for the central span of the bridge was calculated and the results are compared with AASHTO load distribution factors and field test values in Table 1.

While the above examples indicate that use of the AASHTO load distribution formulae generally result in over conservative load distributions, it has also been found (13) that for certain cases, these AASHTO load distribution factors can be unconservative. On the other hand, consistently safe but economical load distribution factors were obtained from the proposed load distribution charts for all cases.

Table 1. Comparison of distribution factors obtained by AASHTO, proposed method and reference 12

Methods	Distribution Factors (Wheel Load)	D_{design} Meters	D_{design} Feet
AASHTO Code	1.58	1.67	5.5
Proposed Method	1.44	1.83	6.0[a]
	1.31	2.01	6.6[b]
Testing (12)	1.04	2.43	8.0

[a] If μ is limited to Maximum Value of 1.0
[b] If actual μ is used (μ = 3.0)

Conclusions

A simplified lateral load distribution procedure has been presented. The method is believed to provide a more accurate load distribution than the AASHTO and CSA-S6 codes while maintaining the simplicity of an AASHTO-type approach. Analysis charts have been developed and presented for AASHTO HS vehicles. It was confirmed that the longitudinal axle spacing of the truck has little effect on the lateral load distribution factors. Therefore, the analysis charts developed for AASHTO loading may be used with reasonable accuracy for other truck configurations, provided that the reduction factors for multi-lane loading are the same as those in the AASHTO specifications. This has in fact been done for the Ontario Highway Bridge Design Load proposed for the new Ontario Bridge Code (10, 13).

The methodology for developing a simplified method as presented, can be utilized for developing distribution factors for other types of trucks and reduction factors.

Acknowledgements

The original concept and objective to develop a rational and simplified method of analysis for lateral load distribution for highway bridge decks was initiated by the Transportation group, Public Works Canada. The project was sponsored and funded by Public Works Canada and the Department of Supply and Services.

References

1. American Association of State Highway and Transportation Officials. Standard Specifications for Highway Bridges. Eleventh Edition, Washington, D.C., 1973
2. Canadian Standards Association, S6-1974. Design of Highway Bridges. Ontario, 1974.
3. D. Motarjemi and D.A. Van Horn. Theoretical Analysis of Load Distribution in Prestressed Concrete Box-Beam Bridges. Lehigh University, Fritz Engineering Laboratory Report 315.9, October 1969, Bethlehem, Pennsylvania.
4. W.W. Sanders Jr. and H.A. Elleby. Distribution of Wheel Loads on Highway Bridges. National Cooperative Highway Research Program Report 83, 1970.
5. American Association of State Highway and Transportation Officials. Interim Specifications, Bridges. Washington, D.C., 1974.
6. R.A. Dorton and P.F. Csagoly. The Development of the Ontario Bridge Code. Paper prepared for the 1977 National Lecture Tour of the Canadian Society for Civil Engineering,

Structural Division.
7. A.R. Cusens and R.P. Pama. Bridge Deck Analysis. John Wiley and Sons Ltd., London, 1975.
8. B. Bakht and R.C. Bullen. Analysis of Orthotropic Right Bridge Decks. Highway Engineering Computer Branch/B/15 (ORTHOP), Department of Environment. U.K.
9. R. Sen. Pogram for the Grillage Analysis of Slab or Pseudo-Slab Bridge Decks. Highway Engineering Computer Branch/B/9 - GRIDS, Department of Environment U.K.
10. T.S. Aziz and A. Alizadeh. Transverse Distribution of Vehicle Loads on Highway Bridges. Report for the Technological Research and Development Branch, Public Works Canada, 1978.
11. G.A. Culham and A. Ghali. Distribution of Wheel Loads on Bridge Girders. Canadian Journal of Civil Engineering, Vol. 4, Number 1, 1977.
12. R.A. Dorton, M. Holowka and J.P. King. The Conestogo River Bridge - Design and Testing. Canadian Journal of Civil Engineering, Volume 4, Number 1, 1977.
13. B. Bakht, M.S. Cheung and T.S. Aziz. Application of A Simplified Method of Calculating Longitudinal Moments to the Proposed Ontario Highway Bridge Code. To be published in Canadian Journal of Civil Engineering.

Notation

C_f = A correction factor for width effects.
D = Load distribution factor.
D_{design} = Load distribution factor, used in design.
D_x = Longitudinal flexural rigidity per unit width.
D_{xy} = Longitudinal torsional rigidity per unit width.
D_y = Transverse torsional rigidity per unit span.
D_1 = Coupling rigidity per unit width.
D_2 = Coupling rigidity per unit span.
E = Young's Modulus.
G = Shear Modulus.
I = Moment of Inertia.
L = Span of bridge.
N_L = Number of lanes
N_G = Number of girders.
S = Girder spacing
W = Width of bridge.
α = Torsional parameter

$$\frac{D_{xy} + D_{yx} + D_1 + D_2}{2(D_x D_y)^{0.5}}$$

θ = Flexural paramater

$$\frac{W}{2L}\left(\frac{D_x}{D_y}\right)^{0.25}$$

ν = Poisson's ratio.

Figure 1. Bridges of common use for which the proposed method applies.

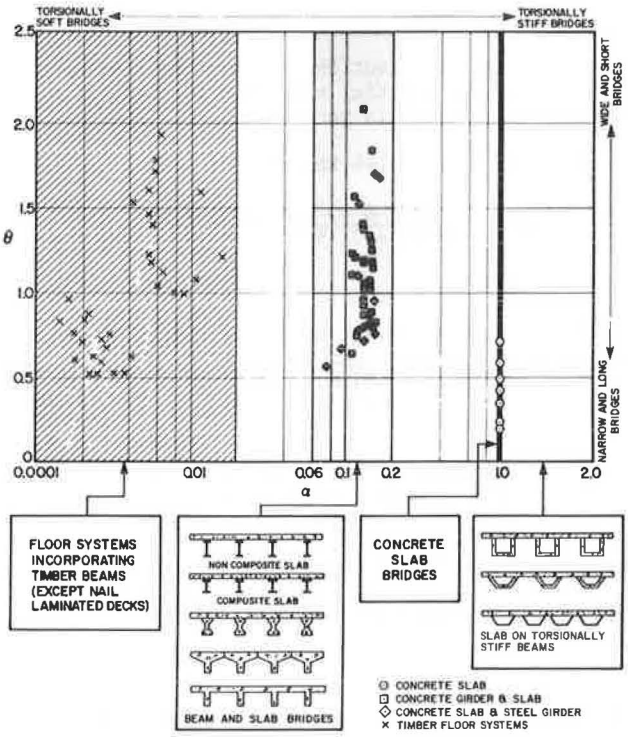

Figure 2. Wheel bearing area at the surface, and load area at the center of the deck.

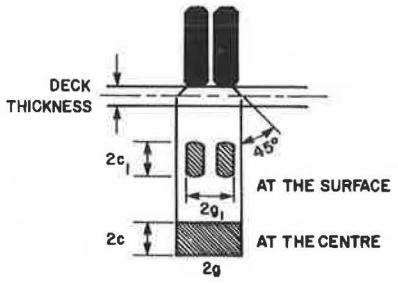

NOMINAL WHEEL LOAD		DIMENSIONS OF THE LOAD AREA AT THE CENTRE OF THE DECK			
		2g		2c	
kN	Tons	cm	in.	cm	in.
35.59	4	71.12	28	45.72	18
35.38	6	71.12	28	45.72	18
71.17	8	81.28	32	45.72	18

Figure 3. Analysis flow chart.

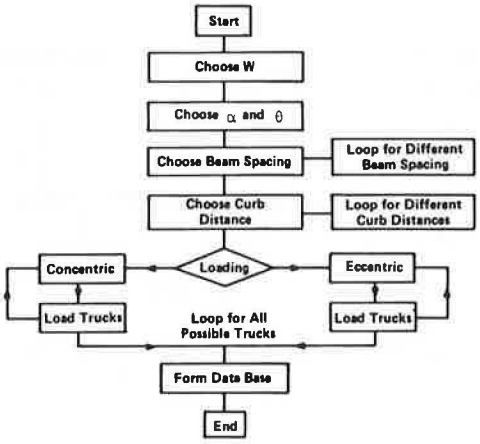

Figure 4. Effect of width on D values for beam and slab bridges.

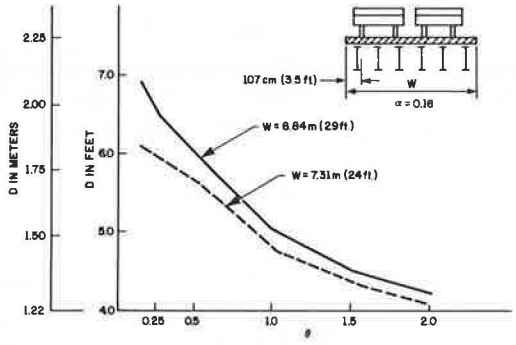

Figure 5. Critical positions for moment.

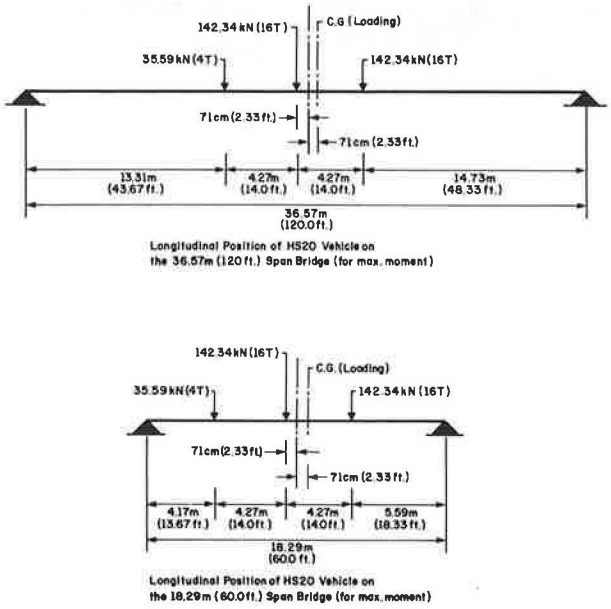

Figure 6. Effect of number of loaded lanes on D values for beam and slab bridges.

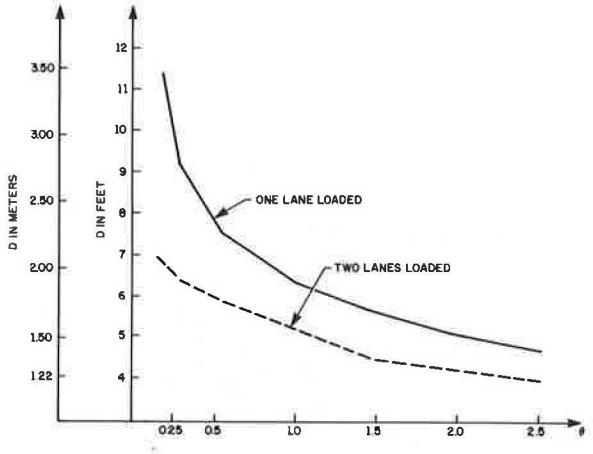

Figure 7. Effect of edge distance on D values for beam and slab bridges.

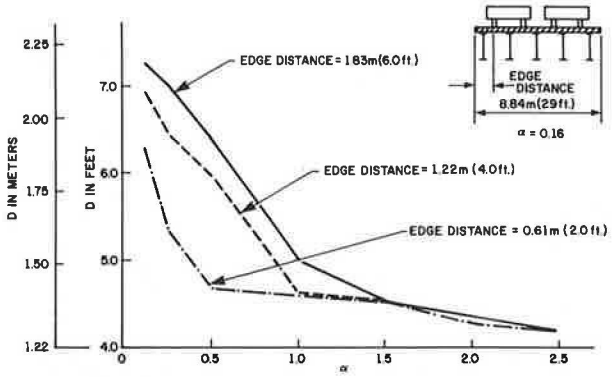

Figure 8. D values for 2 lane bridges - AASHTO loading.

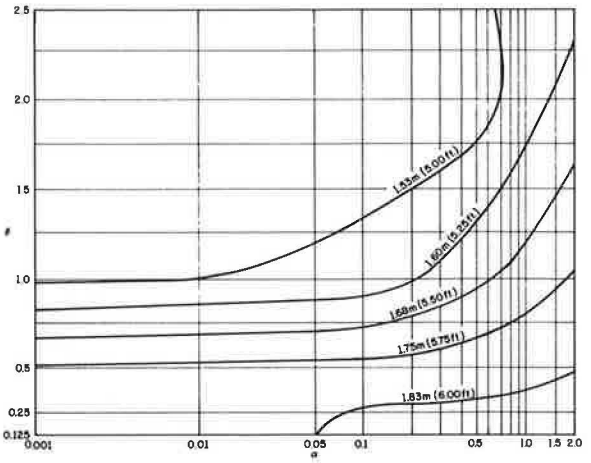

Figure 9. D values for 3 lane bridges - AASHTO loading.

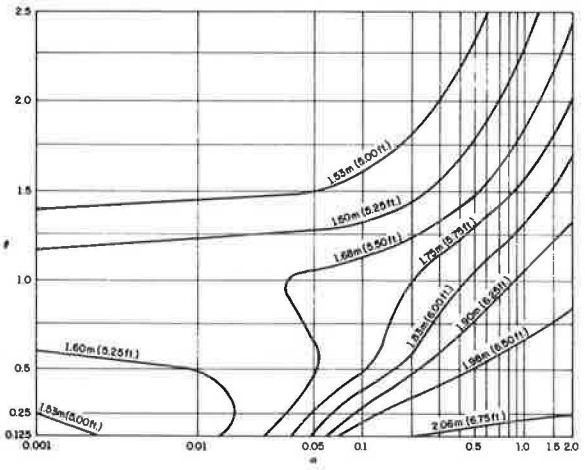

Figure 10. D values for 4 lane bridges - AASHTO loading.

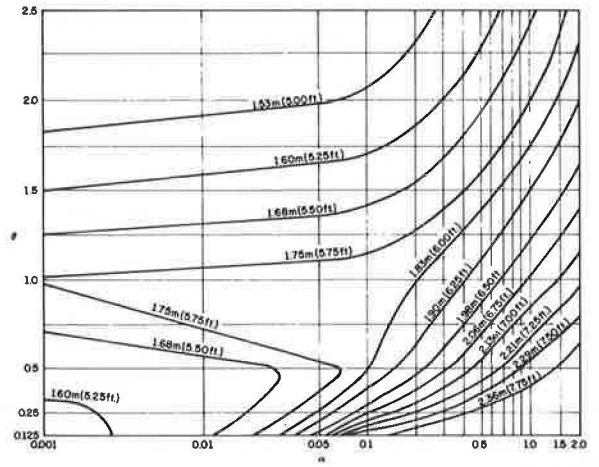

Figure 11. Variations of correction factors for AASHTO loading - 2, 3 and 4 lanes (percent).

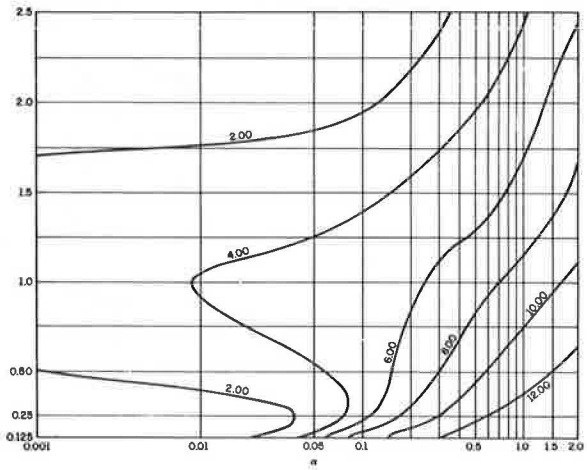

Figure 12. Example bridge number 1.

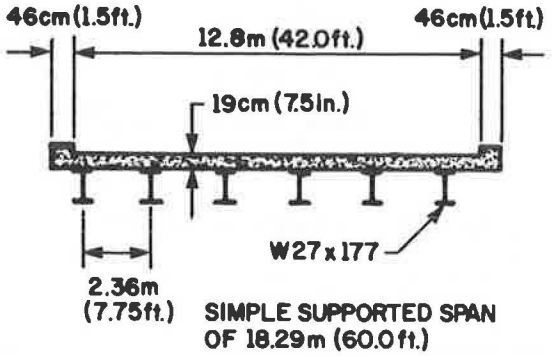

Figure 13. Example bridge number 2 (Conestogo River Bridge).

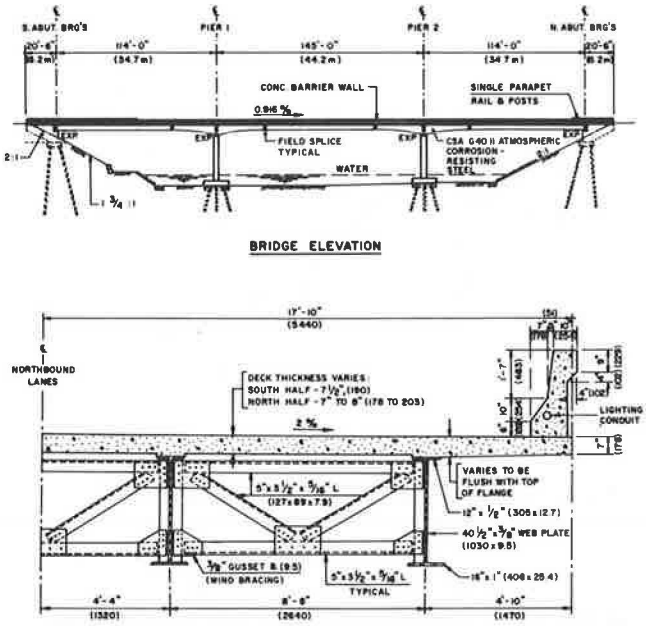

WEB STRESSES IN PRESTRESSED CONCRETE BRIDGE BEAMS HAVING DISCONTINUOUS TENDONS

James R. Libby, President, James R. Libby & Associates, San Diego, California
G. Krishnamoorthy, Professor of Civil Engineering, San Diego State University, San Diego, California
John Revels, Construction Inspector, City of San Diego, San Diego, California

Prestressed concrete bridge girders are sometimes designed with prestressing tendons that terminate within the span rather than at the ends of the girders or at their supports. Tendons of this type are normally significantly inclined at their anchorages due to the clearances required for construction because of the inclination of the tendons at their anchorages. Significant vertical components of prestressing are imposed on the girder. The AASHTO Specifications for Highway Bridges and the Building Code Requirements for Reinforced Concrete (ACI 318-71) do not specify specific methods of analysis for this condition. A finite element analysis of an actual bridge girder was made to determine the conditions of stress in the vicinity of intermediate anchorages. The results of this analysis were compared to those obtained with a principal tensile stress analysis using methods normally employed by bridge designers. It was found both methods of analysis predicted principal tensile stresses of similar magnitude and orientation. The predicted locations of the greatest principal tensile stresses were different for the two methods of analysis. The fact that the greatest principal tensile stresses occur on planes approximately parallel to the paths of some of the post-tensioning ducts is demonstrated.

Description of the Problem

For reasons of economy of prestressing steel, and in some instances in order to confine flexural stresses to acceptable levels, post-tensioning tendons are sometimes terminated within a span rather than at the ends of a girder or at the supports. Bridges containing overhanging girders and a suspended span, as shown in Figure 1, are structures where details of this type of arrangement of tendons are frequently found. The post-tensioning tendons in the overhanging girders may be a combination of tendons that extend from one end of the girder to the other together with tendons that do not. This condition is illustrated in Figure 2, where three groups of tendons are shown. In this case, tendon Groups 1 and 2 can be stressed before the suspended girders are in place but the stressing of tendon Group 3 must be deferred until the suspended girders are in place. This sequence must be followed in order to avoid flexural overstressing of the concrete in the vicinity of the pier. The area of the girder under consideration in this paper is shown in Figure 2 and in detail in Figure 3, showing the individual tendons of tendon Groups 1, 2, and 3 respectively.

A characteristic of the overhanging girders used in bridges of this type is that the conditions of moment in the girders vary as the construction progresses. At the time tendon Groups 1 and 2 are stressed, the suspended span is not in place. Therefore the maximum positive dead load moment between the supports is larger than it is after the suspended span is in place. In the completed structure, the moments of various sections along the span are very similar to those found in a continuous bridge. In the portion of the girders shown in Figure 3, the moments are relatively low in the completed structure while the prestressing is relatively high.

Tendons which terminate within a span normally have to be inclined rather steeply in order to provide the clearances required to stress the tendon. These tendons may be inclined as much as 30 degrees or more as shown in Figure 3. The relatively great inclinations of the tendons result in vertical components of the prestressing force that are quite significant. The various combinations of the effects of prestressing, dead load and live load that occur during the life of a girder of this type result in interesting and variable conditions of stress states in the vicinity of the intermediate anchorages. The analysis of these stresses is normally referred to as shear design.

The prestressed concrete design provisions of the AASHTO Standard Specifications for Highway Bridges (Reference 1) are based upon the assumption that concrete can withstand a shear force causing a unit stress of 1.242 MPa (180 psi) for concrete strengths of 20.7 MPa (3000 psi) or more without web reinforcement. If the shear force is greater than that which the concrete can carry by itself, web reinforcement must be provided to carry the excess force. These provisions originally appeared in "Tentative Recommendations for Prestressed Concrete" of the ACI-ASCE Joint Committee 323 in 1958

Figure 1. Elevation of girders.

Figure 2. Girder and center line of cables-profile.

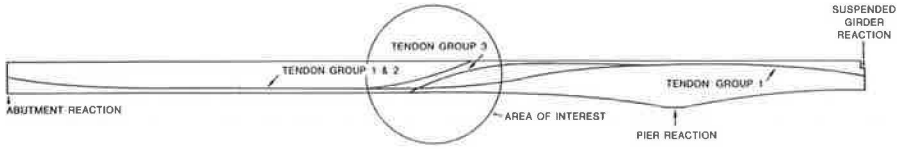

Figure 3. Non-composite cross section.

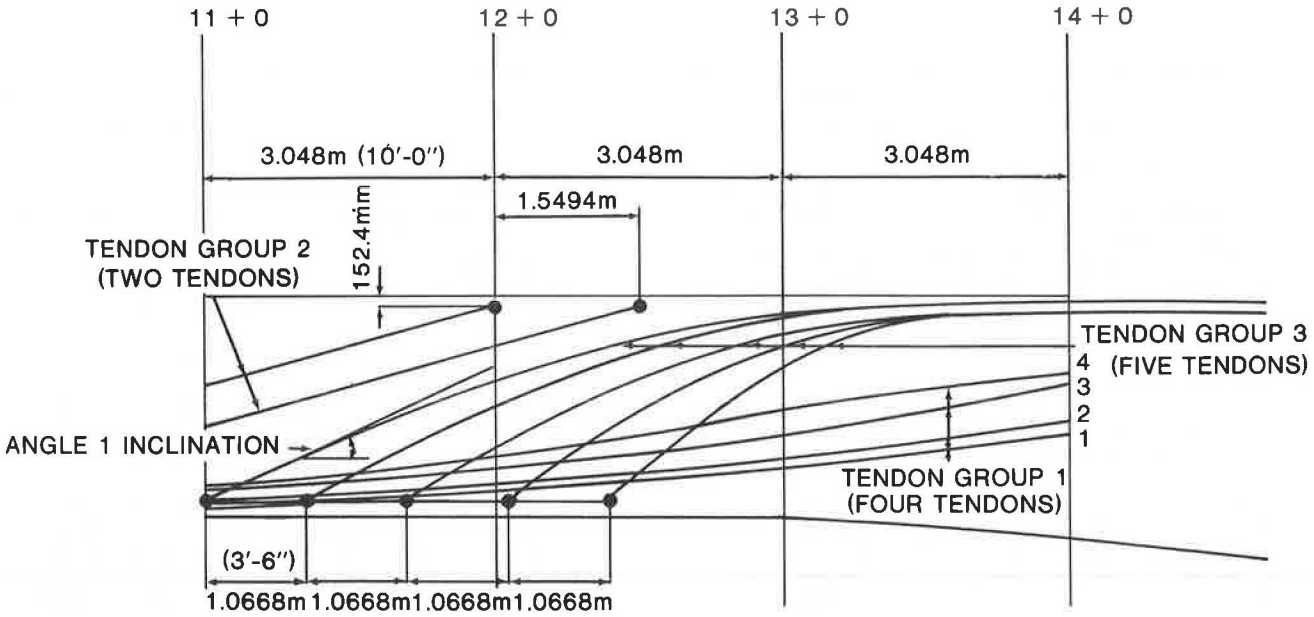

(Reference 2) which were based upon a limited number of tests on beams conducted at the University of Illinois. These requirements were intended to be conservative as the test data available at that time were limited.

Subsequently additional tests were performed at the University of Illinois on beams with moving loads to simulate bridge beams. The results of the later test result in the shear provisions which appeared in the 1963 edition of the Building Code Requirements for Reinforced Concrete (ACI 318-63) (Reference 3). They are also included in ACI 318-77 (Reference 4) in a slightly simplified version. Comparison of the results obtained with the current ACI & AASHTO relationships will reveal the AASHTO Specifications are conservative in areas where flexural cracking is precluded and unconservative in areas where flexural cracking can occur.

Two type of shear-related cracking are now recognized. The first of these is termed flexural-shear cracking and the second is referred to as web cracking. The analysis of the former involves an investigation of the flexural cracking that can occur under the design loads. Web cracking is predicted by the determination of the conditions of loading that result in a principal tensile stress equal to the tensile strength of the concrete.

In the area of the beam under consideration, the conditions of prestressing and moments due to the dead and live loads preclude flexural cracking and hence, the analysis of the safety of the member can be made by determining the principal tensile stresses that exist in the member under various conditions of loading and comparing these to the tensile strength of the concrete. The tensile strength of the concrete is normally taken as $0.33\sqrt{f'_c}$ MPA ($4\sqrt{f'_c}$ psi).

Stress analysis in the vicinity of curved tendons, which terminate at various locations such as shown in Figure 3, is very complex due to the effects of the anchorage zone stresses, the vertical component of the prestressing resulting from the curvature of the tendon and the reduced width of the web resulting from the presence of the post-tensioning duct. These factors have to be taken into account

for a realistic analysis.

Principal Tensile Stress Analysis

For beams prestressed longitudinally, not provided with prestressed stirrups and subject to transverse loads, stress analysis is generally confined to the investigation of the principal tensile stresses at the centroidal axis of the member. Vertical prestressing of the web resulting from the vertical curvature of the tendons is normally neglected because it cannot be easily evaluated, and the effect of neglecting this is generally small. This is a conservative procedure. Because the moment due to transverse loads do not cause flexural stresses at the centroidal axis, the principal tensile stresses are computed from the shear stresses resulting from the transverse loads and the axial stresses due to prestressing. It should be recognized the stress at the centroidal axis due to the longitudinal component of the prestressing is the quotient of this force and the area of the beam cross-section. The shear stress can be computed using the classical flexural-shear stress relationship:

$$v = \frac{VQ}{Ib} \qquad (1)$$

in which:

b = horizontal width of the beam at the centroidal axis.

I = moment of inertia of the beam cross section with respect to the horizontal plane passing through the centroidal axis.

Q = the first moment of the beam area lying above or below the horizontal plane passing through the centroidal axis, with respect to the plane.

V = the shear force at the section under consideration

v = unit shear stress

Figure 4. Non-composite cross section.

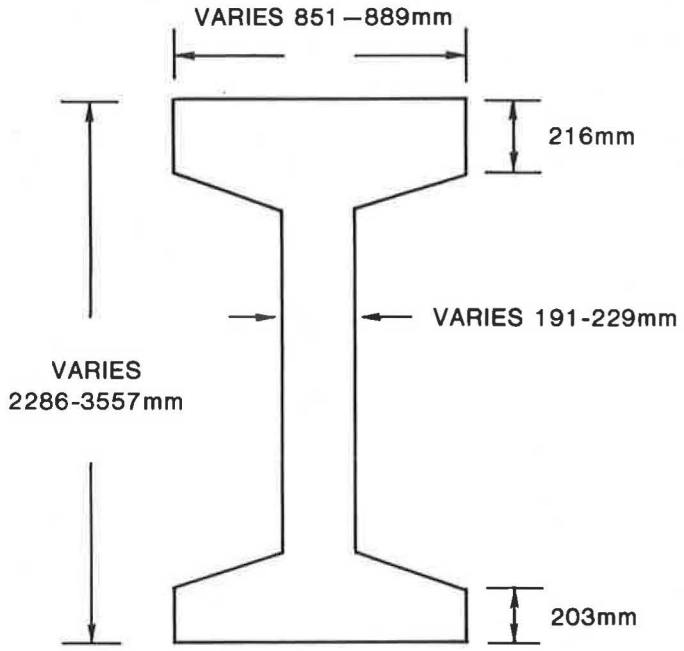

Table 1. Principal tensile stresses at centroidal axis-gross web thickness MPa (psi).

Station	All of tendon group 1 plus tendons 1-4 of group 3 Without shear stress from 5 of group 3	All of tendon group 1 plus tendons 1-4 of group 3 Including shear stress from tendon 5 of group 3	All of tendon groups 1-3 Including shear stress from tendon 5 of group 3
12 + 4	1.566 (227)		
12 + 5	7.015 (292)		
12 + 6	0.794 (115)	1.69 (245)	1.532 (222)
12 + 7		1.518 (220)	1.373 (199)
12 + 8		1.359 (197)	1.228 (178)

Table 2. Principal tensile stresses at centroidal axis--net net thickness MPa (psi).

Station	All of tendon group 1 plus tendons 1-4 of group 3 Without shear stress from 5 of group 3	All of tendon group 1 plus tendons 1-4 of group 3 Including shear stress from tendon 5 of group 3	All of tendon groups 1-3 Including shear stress from tendon 5 of group 3
12 + 4	2,167 (314)		
12 + 5	2,015 (292)		
12 + 6	1,097 (159)	2,339 (339)	2,125 (308)
12 + 7		2,104 (305)	1,904 (276)
12 + 8		1,884 (273)	1,697 (246)

The cross sectional dimensions of the beam studied in this paper vary as shown in Figure 4. Principal tensile stresses, computed by usual methods, for several stations along the beam shown in Tables 1 and 2. The stresses listed in Table 1 are based upon the gross web thickness of 228.6 mm (9 in.) while those in Table 2 are based upon the net web thickness of 165.1 mm (6.5 in.). Based upon this analysis, which ignores the effect of vertical prestressing resulting from the curvature of the group 3 tendons, the greatest principal tensile stress occurs at (station 12 + 6). This is the case if the shear stress resulting from the vertical component of group 3 tendon 5 is or is not considered to be effective at this station.

Finite Element Analysis

The structural model consisted of a simply supported span of 9.15 m (30 feet) with cantilevers of 3.05 m (10 feet) on each end as shown in Figure 5. This configuration was selected as a means of simulating the moments and shears acting upon the beam between stations 11 + 0 and 14 + 0 where the principal tensile stresses were under study. This model permitted moments to be applied through forces of variable intensity at the ends of the cantilevers while the shears were applied through the reactions at stations 11 + 0 and 14 + 0. The effects of prestressing were modeled with forces as illustrated in Figure 6. The post-tensioning ducts were not included in the finite element model used in this study.

The analysis of the structure was conducted by using SAP IV computer program (Structural Analysis Program for Static and Dynamic Response of Linear Systems) developed at University of California Berkeley, (Reference 5). The beam was modeled using three dimensional finite elements with three translational degrees of freedom. In the flanges, three dimensional variable node isoparametric elements (i.e., more than eight nodes) were used. In the web, eight node "brick" elements which employ incompatible modes were used. Isotropic properties were assumed. The elastic modulus and Poissons ratio employed were 27,600 MPa (4000 ksi) and 0.20, respectively. Additional dead and live loads within the span were simulated by surface pressure loads. The two typical cross sections assumed for the analyses are shown in Figures 4 and 7.

The structure was modeled with 1498 nodes and 639 three dimensional finite elements for the non-composite case. Additional 368 nodes and 275 elements were added for analyzing the composite case.

In the first set of analysis, the finite element model was restrained along the lateral direction of the girder. In order to ascertain the effect of Poisson's ratio, the model with all the degrees of freedom was also analyzed. It was found that for planar loadings of the type considered here, the effect of Poisson's ratio was not significant.

The analysis resulted in six global stresses at the centroid of each finite element. From these stresses, the magnitude and direction of principal tensile stresses at various locations of the girder were computed and plotted.

The following load conditions were analyzed and the maximum principal tensile stresses were plotted in order to obtain the critical load case.

1. Dead Load + Diaphragm and drop in girder + Slab + 90% initial load due to tendon group 1 and tendon group 2 + 100% initial load due to tendon group 3.
2. Dead Load* + 80% initial load due to tendon groups 1, 2, and 3 + Maximum moment (Mmax) + shear (V).
3. Dead load + 80% initial load due to tendon groups 1, 2, and 3, + Mmin and V concomitant.
4. Dead load + 80% initial load due to tendon groups 1, 2, and 3 + Vmin and M concomitant.
5. Dead load + 80% initial load due to tendon groups 1, 2, and 3, + Vmax and M concomitant.

*Girder + Diaphragm + Drop in Girder + Slab + Curb + Railing + Future D.L.

Condition 1 was analyzed with the non-composite section; the remaining with the composite section. The principal tensile stresses for the above beam sections and loading conditions are plotted in Figures 8 - 12.

Figure 5. Structural model.

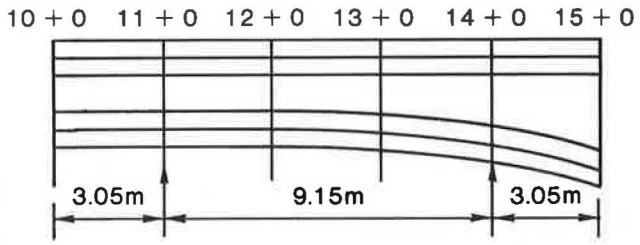

Figure 6. Forces in prestressed cables.

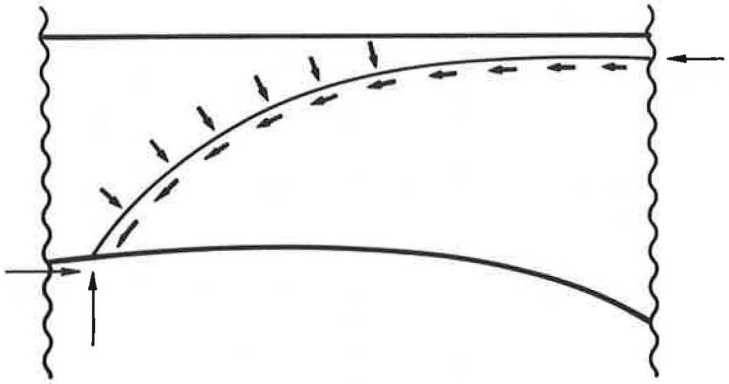

Figure 7. Composite cross section (see Figure 4. for dimensions not shown).

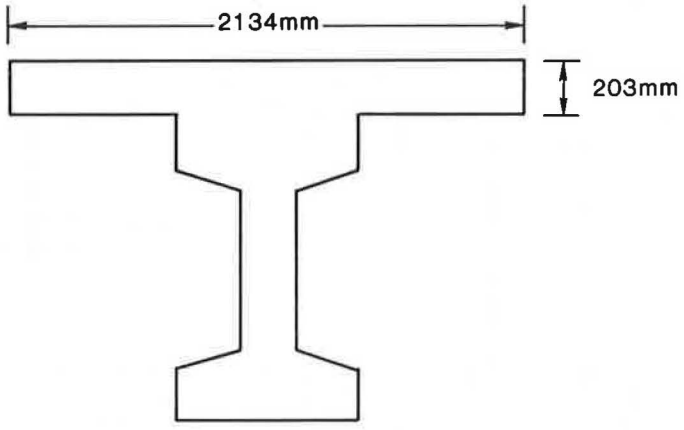

Conclusions

Comparing the principal stresses obtained by conventional methods of computation, as shown in Table 1, to those obtained by the use of the finite element method, as illustrated in Figures 8 - 12, leads one to conclude the former method is conservative for the conditions studied. The former method predicts maximum values of maximum principal tensile stress at locations different from those predicted by a finite element analysis. The difference in magnitude and location of principal tensile stresses predicted by the two methods is at least partially explained by the effects of vertical prestressing of the web being neglected in the conventional computations but not in the more sophisticated method.

The orientation of the principal tensile stresses as shown in Figure 9 shows the direction of these stresses approximately follow the paths of the group 3 tendons. Comparison of the values of the principal tensile stresses shown in Table 1 and 2 clearly illustrates the importance of basing principal tensile stress computations on net rather than gross web thicknesses in conditions such as these.

Conventional methods of computing principal tensile stresses are adequate for usual cases encountered in bridge design. The cost of three dimensional finite element analysis can only be justified under unusual circumstances.

Figure 8. Principal tensile stress plot MPa (psi) for load condition 1.

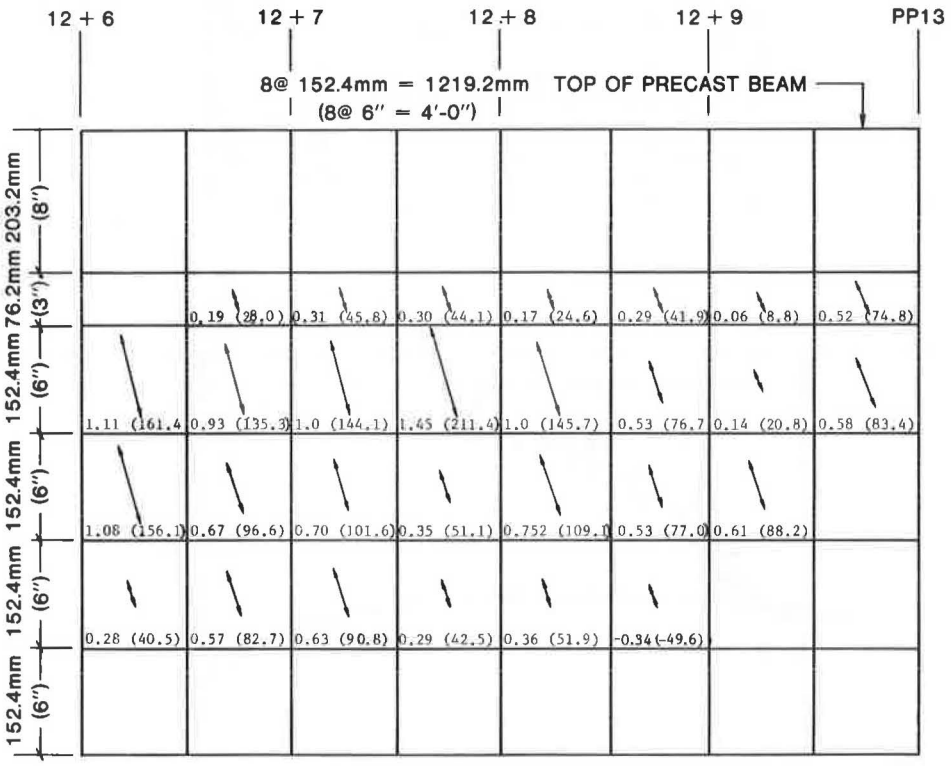

Figure 9. Principal tensile stress plot MPa (psi) for load condition 2.

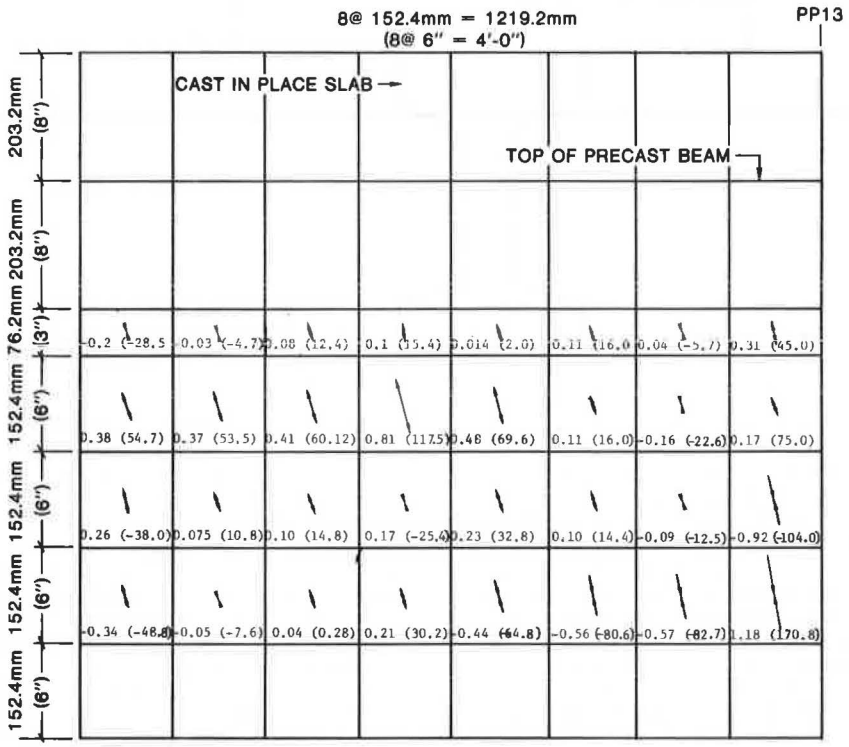

Figure 10. Principal tensile stress plot MPa (psi) for load condition 3.

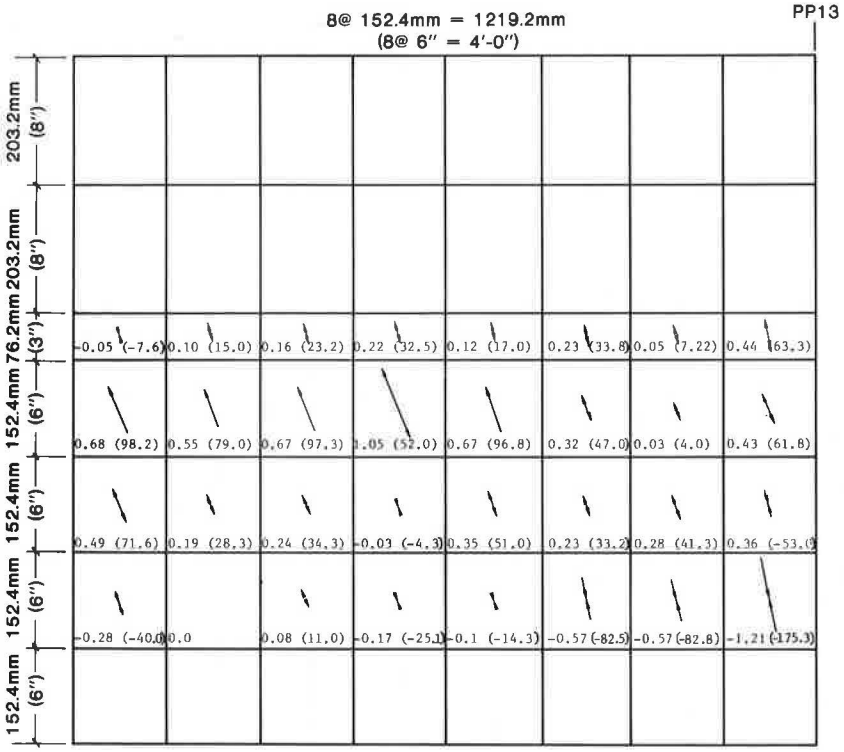

Figure 11. Principal tensile stress plot MPa (psi) for load condition 4.

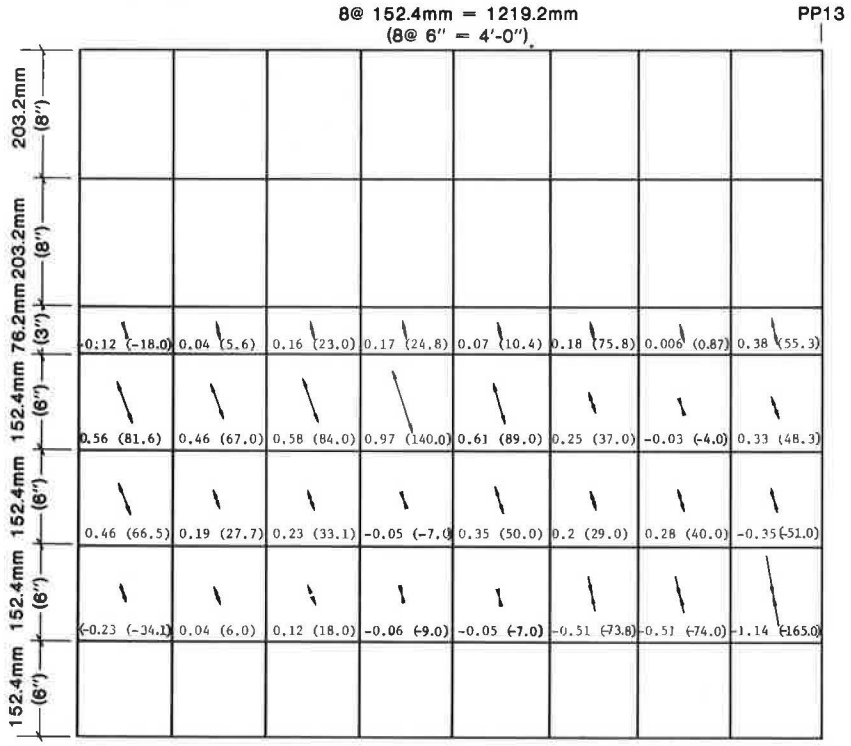

Figure 12. Principal tensile stress plot MPa (psi) for load condition 5.

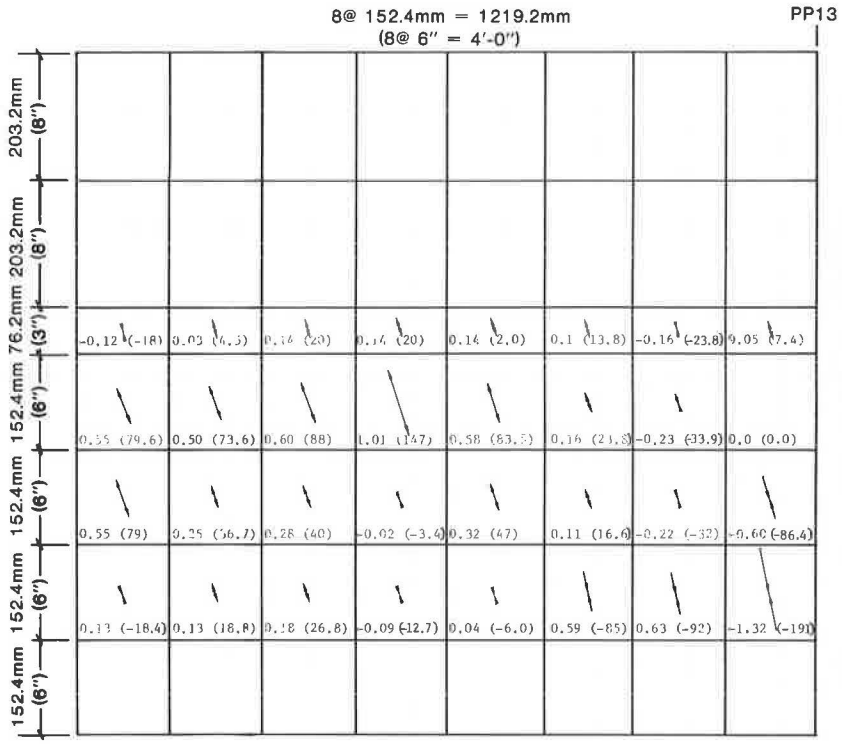

References

1. American Association of State Highway and Transportation Officials. Standard Specifications for Highway Bridges. 11th ed., Washington D.C., 1973.
2. ACI-ASCE Joint Committee 323. Tentative Recommendations for Prestressed Concrete. Journal of the American Concrete Institute. 29, No. 7, pp. 545-578 (January 1958).
3. ACI Committee 318. Building Code Requirements of Reinforced Concrete. American Concrete Institute. Detroit, 1963.
4. ACI Committee 318. Building Code Requirements of Reinforced Concrete. American Concrete Institute. Detroit, 1971.
5. K. Bathe, E. Wilson, and F. Peterson. SAP IV, A Structural Analysis Program for Static and Dynamic Response of Linear Systems. Report No. EERC 73-11, June 1973, College of Engineering, University of California, Berkeley, California.

MODEL STUDIES OF DOUBLE-CELL BOX GIRDER BRIDGE WITH INTERMEDIATE DIAPHRAGMS

Ricardo P. Pama and Pichai Nimityongskul, Asian Institute of Technology, Bangkok, Thailand
Daniel Z. Pribadi, Petra Christian University, Surabaya, Indonesia
Seng-Lip Lee, University of Singapore, Singapore

An experimental study on the influence of intermediate cross-bracing diaphragms on the behavior of a simply supported double-cell box girder bridge has been carried out. A perspex model was tested under various loading conditions and the test results, namely the displacements, cross-sectional distortion, longitudinal and transverse normal forces were compared with theoretical values suggested by Nimityongskul, Pama and Lee [1]. In this analysis, the elements in the box section are treated as rectangular plates subjected to lateral and in-plane boundary forces. The end diaphragms are assumed to be infinitely rigid in and flexible normal to their planes. The intermediate diaphragm is assumed to act in such a way that it exerts only concentrated vertical and horizontal reactions on the joints of the box section without introducing resisting moments against joint rotations. Test results indicated that the distortion of the cross-section of a box girder without intermediate diaphragm is more prominent when loaded along the side-joints. With one intermediate diaphragm the distortion at the loaded section remains practically the same when the diaphragm is sufficiently away from the applied loads, but is considerably reduced when the diaphragm is near the load. The use of intermediate diaphragm decreases effectively the cross-sectional distortion, increases the overall stiffness of the bridge and redistributes the longitudinal normal forces. In general, the experimental values confirm the theoretical predictions on the influence of intermediate diaphragms on the load distribution in a double-cell box girder bridge. Careful considerations must be taken in designing these intermediate cross-bracing diaphragms to satisfy the assumptions made in the theory.

Introduction

Box girders which may be either straight or curved in plan are currently used for highway bridges. The cross-section may be single-cell or multi-cell depending on the width of the bridge. A lot of analytical and experimental studies have been reported lately as evidence of the increasing use of box girder bridges in the last few years. Quite a few dealt with the influence of transverse stiffeners or diaphragms which are used to prevent cross-sectional distortion of the box elements. The experimental work reported so far has been limited to single-cell box girders with solid diaphragms.

An extensive review of the methods for analysing box girder can be found in the progress report of the Subcommittee on Box Girders of the ASCE-AASHO Task Committee on Flexural Members [1]. ARENDTS and SANDERS [2] used the concept of replacing the actual cellular structure of a concrete box girder highway bridge with a uniform plate whose structural properties are equivalent to those of the actual bridge. An analysis of box girders of deformable cross-section based on an analogy of beams on elastic foundation was separately studied by WRIGHT, ABDEL-SAMAD and ROBINSON [3] and CAMPBELL-ALLEN and WEDGWOOD [4]. The effects of rigid or deformable interior diaphragms are also treated by determining the stiffness for the beam on elastic foundation. SAWKO and COPE [5] used modified finite element technique for the analysis of multi-cell bridges without transverse diaphragm. ABDUL-SAMAD, WRIGHT and ROBINSON [6] applied thin-walled beam theory to box girders of deformable cross-section. Thin-walled beam theory is extended to cover stiffened plate elements and the effects of deformable interior diaphragms. A further simplified formulation was studied by DALTON and RICHMOND [7] to obtain the solution for girders of trapezoidal cross-section by assuming that only the diaphragms or cross-frames resist the cross-sectional distortion. SCORDELIS [8] applied folded plate theory to obtain the solution for a simply supported box girder bridge. The analysis is limited to straight prismatic box girder composed of isotropic plate elements without intermediate diaphragms. An analysis of box girder by finite strip method was presented by CHEUNG [9], in which harmonic functions which fitted the boundary conditions in the longitudinal directions are used in conjunction with single polynomials as displacement function in the transverse direction.

Recently NIMITYONGSKUL, PAMA and LEE [10] presented an accurate and efficient method of analysis for box girder bridges and takes into account the influence of intermediate diaphragms. The elements in the box section are treated as rectangular plates subjected to lateral and in-plane boundary forces. The solutions due to unit vertical and horizontal loads applied at the joints for the case without intermediate diaphragm are obtained and used as influence coefficinets to derive the solutions for any combination of concentrated live loads applied at the joints as well as the effect of intermediate diaphragms.

MYERS and COOPER [11] experimentally studied the effects of interior diaphragms in a simply supported single-cell box girder bridge and compared the results with those obtained based on the beam on elastic foundation analogy. HEINS, BONAKDARPOUR and BELL [12] presented the results of an experimental study on the behavior of a plexiglass three-cell curved beam model subjected to static loads and compared the deflections and strains with those predicted by the slope deflection theory. GODDEN and ASLAM [13] presented the results of an experimental study on the static response of skew box girder bridges and theoretical result based on a finite element analysis was used for comparison. An experimental investigation to study the behavior of composite simply supported box girder bridge with end diaphragms was carried out by MATTOCK and JOHNSTON [14] and the result agreed well with those obtained by the folded plate theory. ANEJA and ROLL [15] carried out an experimental investigation on a horizontally curved box beam highway bridge model subjected to various loading conditions. A model analysis of a curved prestressed concrete cellular bridge was presented by CHUNG and GARDNER [16]. A 1/24 scale perspex model was used to predict the elastic properties and a 1/6 scale prestressed concrete model to determine the load factor. DAVIS, SHEFFEY, CASTLETON and EVANS [17] presented a model and prototype studies of box girder bridge and correlated the results with the prototype behavior and that predicted by the folded plate analysis.

This paper describes an experimental investigation which was conducted to determine the influence of intermediate diaphragms on the behavior of a simply supported straight double-cell box girder bridge. The intermediate diaphragms are in the form of rigid cross-bracing as shown in Fig. 1. The experimental results are compared with theoretical values suggested by NIMITYONGSKUL, PAMA and LEE [10].

General Theoretical Consideration

A double-cell straight box girder bridge with or without intermediate diaphragms, simply supported at the ends by means of supporting diaphragms, and subjected to a concentrated load acting at a joint is shown in Fig. 1. A vertical concentrated load acting on a joint of the top deck can be resolved into symmetrical and antisymmetrical components as shown in Fig. 2. The solution for the antisymmetrical component is treated in detail by NIMITYONGSKUL, PAMA and LEE [10]. The effect of symmetrical component is localized and can be obtained by suitable approximation for design purposes. The elements in the box section are treated as rectangular plates subjected to lateral and in-plane boundary forces. It is assumed that the influence of in-plane forces on the bending of the plate may be disregarded. This leads to two fourth order partial differential equations, which govern the bending of the plate under the action of the normal load components and the membrane action of the plate under in-plane load components (Fig. 3).

Treatment of Intermediate Diaphragm

The end diaphragms are assumed to be infinitely rigid in and flexible normal to their planes. The intermediate diaphragm is assumed to act in such a way that it exerts concentrated vertical and horizontal reactions only at the joints of the box section without introducing resisting moments against joint rotations. It is assumed to be infinitely rigid in its own plane and, under general loading, it undergoes rigid body displacement, i.e., vertical and horizontal deflections as well as rotation about the axis of the bridge. The values of the reactive forces are determined from the conditions that the rigid body displacements of the intermediate diaphragm are compatible with the joint displacements, under the simultaneous effect of the applied loads and the reactive forces, and that reactive forces on the diaphragm are in self equilibrium. Numerical results for a simply supported double-cell box girder bridge subjected to unit loads applied separately at the middle and side joints are initially obtained for the case without intermediate diaphragms. These results are then used as influence coefficients in developing the solutions for cases with one intermediate diaphragm at midspan and three intermediate diaphragms at quarter points.

Experimental Program

Model Design and Fabrication

Tests were conducted on a model of a double-cell straight box girder bridge. The simply supported span of the model is 1520 mm and the cross-section is shown in Fig. 1. All components of the box girder were made of perspex. The parameters suggested by NIMITYONGSKUL, PAMA and LEE [10] were used except that the thickness of the top and bottom decks and the webs were made the same because of the unavailability of perspex plates of different thicknesses. The model was designed such that there is substantial deformation of the cross-section under load. In constructing the model, the side and middle webs were glued into positions on the bottom deck and then all the necessary electrical strain gages were attached to their proper locations as shown in Fig. 4. The intermediate diaphragms were positioned properly at midspan and quarter-span of the bridge girder. Finally, the top deck was glued to the webs and interior diaphragms. Detachable end diaphragms were fixed to the box element by using screws. Circular holes were drilled on the end diaphragms to allow the wires of the electrical strain gages inside the girder to pass through.

Instrumentation

Electrical resistance rectangular strain rosettes were attached to the model as shown in Fig. 4. At quarter-span and midspan, six rectangular strain rosettes were fixed at each section. At three-eighth-span section, twenty-four rectangular strain rosettes were provided. Mechanical dial gages were used for measuring deflections. Temperature effect on strain gages attached to the model which has poor heat diffusion properties was compensated by using dummy gages.

Determination of Material Properties

Prior to testing the model, the mechanical properties of the model materials were determined. Representative samples of each of the box girder components were subjected to axial tension test. Longitudinal and transverse strains were measured by means of electrical strain gages attached to one side of the specimens. The test results gave an average value for the modulus of elasticity E of 2.90×10^6 KN/m^2 and Poissons ratio ν of 0.365. Tensile creep test was conducted on the control specimens and it was observed that the rate of creep diminished appreciably after approximately three minutes of loading.

Test Set-Up and Measurements

The box girder was supported on steel bearing plates (50 mm x 350 mm) with a 15 mm diameter steel rollers. Ball bearings were also provided to prevent the uplift due to eccentric loading but this proved unnecessary during the test. Static point loads were applied monotonically in increments to the box girder by means of a hydraulic jack as shown in Fig. 5. Since it was established that the effect of creep became negligible three minutes after initial loading, strain measurements were only taken after this time interval has elapsed. The strains were automatically recorded by a data logger.

Test Programs

The test program was divided into three major parts corresponding to the number of intermediate diaphragms present. Each test series consists of six minor test programs depending on the variation of the point of application of the load spanwise and transversewise on the top deck. Incremental point loads of 220 N, starting from 880 N to 1540 N were applied at quarter-span, three-eighth-span and midspan on the top left edge and on the middle joint of the cross-section. The application of an initial load was necessary to remove the slack in the loading system. The test series started with three intermediate diaphragms present. After this test the two diaphragms at quarter-span were sawed off by a jacksaw and a similar set of tests repeated. Finally the diaphragm at midspan was removed and another set of tests was conducted on the model. The test results are compared with theoretical values obtained by the use of a digital computer.

Test Results and Discussions

Deflections

Deflections were recorded at mid-joint and side-joints of the cross-section at quarter-span, three-eighth-span, midspan, and three-quarter-span. Figures 6 to 8 show the average experimental deflections and the corresponding theoretical values of the simply-supported box girder for the case without diaphragm, with one diaphragm, and with three diaphragms due to unit loads acting at quarter-span, midspan, and three-eighth-span respectively. The horizontal displacements observed from the experiment were small and were not included. The experimental values are generally in good agreement with the corresponding theoretical values. It is observed that for the case with one diaphragm (Figs. 6b, 7a and 8c) the deflected shape of the model at the diaphragm section especially for the case of unit loads acting at the left edge is slightly different from that obtained theoretically. This difference is due to the fact that the box section did not distort as a rigid body as predicted in the theory. In other words, there was still a certain degree of local distortion even at the intermediate diaphragm section. It is to be noted that the intermediate diaphragm is assumed in the analysis to be infinitely rigid in its own plane and, under general loading undergoes rigid body displacement only. The type of intermediate diaphragms used in this test is in the form of cross-bracings and therefore they are not as rigid as those assumed theoretically. This effect is less evident for the case with three diaphragms. On the whole, the correlation between the experimental and theoretical deflections is good.

Cross-Sectional Distortion

The influence of intermediate diaphragms can be observed clearly for loads acting at quarter-span. The distortion of the cross-section remains practically unchanged (Fig. 6) when an intermediate diaphragm is introduced at midspan, whereas, this distortion vanished when three intermediate diaphragms were provided. For loads acting at midspan and three-eighth-span respectively as shown in Figs. 7 and 8, the distortion is considerably reduced by adding one diaphragm only at midspan. The cross-sectional distortion was further reduced when three intermediate diaphragms were present. As expected, the twisting of the box section for cases with one and three intermediate diaphragms is less than for the case without diaphragm when the loads act at the side-joint.

Longitudinal Normal Forces

Figures 9 to 11 show the experimental and theoretical results for the longitudinal normal forces N_y at various locations indicated in Fig. 4. In general the strain readings varied linearly with the applied load. The experimental values are generally in good agreement with the theoretical values. The influence of intermediate diaphragm can be seen clearly for points at the loaded section in which values of longitudinal normal forces for loads at mid-joints and side-joints are getting closer to each other or almost the same for the case with one and with three intermediate diaphragms. Without intermediate diaphragm, the values of N_y are significantly higher at the locations near the loaded joint. For loads applied at the side-joints, the values of N_y at the point near the loaded joint are slightly decreased by the addition of a diaphragm at the loaded section and the transverse distribution of load is evident from the distribution of N_y to the other point of the loaded section. For sections sufficiently away from the diaphragm, the values of N_y are hardly influenced by the presence of intermediate diaphragm as can be seen in Fig. 12.

Transverse Normal Forces

The experimental and theoretical results for transverse normal forces N_y are summarized in Tables 1, 2 and 3. The agreement between the experimental and theoretical values are in general not very good. The experimental results give smaller values but it can be clearly seen that the transverse normal force is insignificant for the model without intermediate diaphragm except in the vicinity of the loaded joint. With intermediate diaphragms, the concentrated dia-

phragm reactions introduce significant values of N_x locally in the neighborhood of the joints. For values at three-eighth-span, the influence of the intermediate diaphragms on N_x are hardly evident. The difference between experimental and theoretical values may be due to the convergence of the series solution in the theory. Also, at the loaded section, the theory does not take into account the effect of symmetrical loading on the transverse normal force in the web. Moreover, the cross-bracing diaphragm attached to the plate element may be giving additional transverse stiffness to the plate element which may also contribute to this discrepancy between the theoretical and experimental results for N_x.

Conclusions and Practical Applications

1. The distortion of the cross-section of a box girder without intermediate diaphragm is more prominent when loaded along the side-joints. With one intermediate diaphragm the distortion at the loaded section remains practically the same when the diaphragm is sufficiently away from the applied loads, but is considerably reduced when the diaphragm is near the load.

2. The use of intermediate diaphragm decreases effectively the cross-sectional distortion, increases the overall stiffness of the bridge and redistributes the longitudinal normal forces.

3. For side-joint loading, the deflection along the left profile passing through the loaded joints for the case without intermediate diaphragm is larger than that for the case with intermediate diaphragms while the situation is reversed at the other side-joint.

4. In general, the experimental values confirm the theoretical predictions on the influence of intermediate diaphragms on the load distribution in a double-cell box girder bridge. Careful consideration must be taken in designing these intermediate cross-bracing diaphragms to satisfy the assumptions made in the theory. For model studies, it is recommended to use a different material for the intermediate diaphragms especially one which is considerably stiffer compared with the other components of the model and to make it slender enough to eliminate the occurrence of resisting moments at the joint as much as possible.

5. Since transverse stresses are relatively small, transverse stiffness is therefore more significant than transverse strength in the design of intermediate diaphragms.

The reversible nature of the transverse normal stresses necessitates that restrictions should be imposed in the design such that low strength limits are prescribed in order to avoid fatique failures.

List of Symbols

b	=	span length of the bridge
D	=	flexural rigidities of decks and webs
E	=	modulus of elasticity
M_x, M_y	=	transverse and longitudinal bending moment per unit length respectively
M_{xy}, M_{yx}	=	torsional moment per unit length
N_x, N_y	=	transverse and longitudinal normal forces
P	=	vertical concentrated load
t	=	thickness of decks and webs
w	=	vertical displacement
y	=	longitudinal position of cross-section
ν	=	Poisson's ratio

References

1. The Subcommittee on Box Girders of the ASCE-AASHO Task Committee on Flexural Members. Progress Report on Steel Box Girder Bridges. J. Struc. Div., ASCE, Vol. 97, No. ST4, Proc. Paper 8068, April 1971, pp. 1175-1185.
2. Arendts, J.G. and Sanders, W.W. Concrete Box Girder Bridges as Sandwich Plates. J. Struc. Div., ASCE, Vol. 96, No. ST11, Proc. Paper 7695, November 1970, pp. 2353-2371.
3. Wright, R.N., Abdel-Samad, S.R. and Robinson, A.R. BEF Analogy for Analysis of Box Girders. J. Struc. Div., ASCE, Vol. 97, No. ST7, July 1968, pp. 1719-1743.
4. Campbell-Allen, D. and Wedgwood, R.J.L. Need for Diaphragms in Concrete Box Girder. J. Struc. Div., ASCE, Vol. 97, No. ST3, March 1971, pp. 825-842.
5. Sawko, F. and Cope, R.J. Analysis of Multi-Cell Bridges without Transverse Diaphragm - a Finite Element Approach. The Struc. Eng., Vol. 47, No. 11, November 1969, pp. 455-461.
6. Abdel-Samad, S.R., Wright, R.N. and Robinson, A.R. Analysis of Box Girders with Diaphragms. J. Struc. Div., ASCE, Vol. 94, No. ST10, October 1968, pp. 2231-2370.
7. Dalton, D.C. and Richmond, B. Twisting of Thin-Walled Box Girders of Trapezoidal Cross-Section. Proc. ICE, Vol. 39, January 1968, pp. 61-73.
8. Scordelis, A.G. Analysis of Simply Supported Box Girder Bridges. Report No. SESM 66-77, Dept. of Civil Engineering, U. of Calif., Berkeley, 1966.
9. Cheung, Y.K. Analysis of Box Girder Bridges by the Finite Strip Method. ACI, Second International Symposium of Concrete Bridge Design, Chicago, Paper Sp. 26-15, April 1969.
10. Nimityongskul, P., Pama, R.P. and Lee, S.L. Influence of Intermediate Diaphragms on Load Distribution in Box Girder Bridges. Fourth Australasian Conference on Mechanics of Structures and Materials, Brisbane, Australia, August 1973.
11. Myers, D.E. and Cooper, P.B. Box Girder Model Studies. J. Struc. Div., ASCE, Vol. 95, No. ST12, December 1969, pp. 2845-2861.
12. Heins, C.P., Bonakdarpour, B. and Bell, L.C. Multicell Curved Girder Model Studies. J. Struc. Div., ASCE, Vol. 98, No. ST4, April 1972, pp. 831-843.
13. Godden, W.G. and Aslam, M. Model Studies of Skew Multi-Cell Girder Bridges. J. Eng. Mech. Div., ASCE, Vol. 99, No. EM1, February 1973, pp. 201-223.
14. Mattock, A.H. and Johnston, S.B. Behavior under Load of Composite Box Girder Bridges. J. Struc. Div., ASCE, Vol. 94, No. ST10, October 1968, pp. 2351-2370.
15. Aneja, I. and Roll, F. Experimental and Analytical Investigation of a Horizontally Curved Box-Beam Highway Bridge Model. ACI, Second International Symposium on Concrete Bridge Design, Chicago, Paper Sp. 26-16, April 1969.
16. Chung, H.W. and Gardner, N.J. Model Analysis of a Curved Prestressed Concrete Cellular Bridge. ACI, Second International Symposium on Concrete Bridge Design, Chicago, Paper Sp. 26-14, April 1969.
17. Davis, R.E., Sheffey, C.E., Castleton, G.A. and Evans, E.E. Model and Prototype Studies of Box Girder Bridge. J. Struc. Div., ASCE, Vol. 98, No. ST1, January 1972, pp. 165-183.

Summary

An experimental study on the influence of intermediate cross-bracing diaphragms on the behavior of a simply supported double-cell box girder bridge has been carried out. A model made of perspex was tested under various loading conditions and the test results are compared with theoretical values suggested by NIMITYONGSKUL, PAMA and LEE [10]. The experimental results for deflection and longitudinal normal forces are shown to be in good agreement with the theoretical results. This study showed that the use of intermediate diaphragm decreases effectively the cross-sectional distortion throughout the span, increases the overall stiffness of the bridge and redistributes the longitudinal normal forces.

Table 1. Transverse normal forces $N_x b$ due to unit load at quarter-span.

(a) Unit load at left edge

Point	Theoretical Results			Experimental Results		
	Without Diaphragm	One Diaphragm	Three Diaphragms	Without Diaphragm	One Diaphragm	Three Diaphragms
M_1	-0.560	1.470	2.475	0.400	1.000	1.400
M_2	0.150	1.170	0.235	0.100	1.250	0.100
M_3	0.300	17.370	11.800	0.600	3.200	3.100
Q_1	4.310	3.940	3.990	4.230	4.100	-8.850
Q_2	24.840	24.670	20.600	-10.800	-13.400	-16.550
Q_3	4.435	4.045	16.910	4.350	5.700	10.800

(b) Unit load at center

Point	Theoretical Results			Experimental Results		
	Without Diaphragm	One Diaphragm	Three Diaphragms	Without Diaphragm	One Diaphragm	Three Diaphgrams
M_1	0.100	3.370	3.335	0.215	1.720	1.700
M_2	0.350	2.000	0.180	0.650	1.400	0.430
M_3	0.150	10.350	10.420	0.220	0.800	0.820
Q_1	0.100	0.150	12.135	0.170	0.450	14.650
Q_2	6.020	8.035	9.360	5.000	2.900	8.630
Q_3	-12.040	-12.150	6.260	19.500	-3.350	2.820

Table 2. Transverse normal forces $N_x b$ due to unit load at three-eighth-span.

(a) Unit load at left edge

Point	Theoretical Results			Experimental Results		
	Without Diaphragm	One Diaphragm	Three Diaphragms	Without Diaphragm	One Diaphragm	Three Diaphragms
M_1	-0.210	0.570	-4.030	0.105	0.300	-3.100
M_2	0.225	-1.795	-1.250	0.150	-1.500	-1.000
M_3	0.510	19.615	24.300	0.200	1.750	4.250
TE_1	2.830	2.340	3.740	2.400	2.250	3.050
TE_4	46.170	46.150	46.680	26.200	24.500	23.000
TE_5	4.065	4.640	3.815	3.950	4.600	4.000
Q_1	-0.640	-0.120	5.140	-0.420	3.750	-7.500
Q_2	-0.330	-0.980	-1.880	-0.050	-1.700	-2.000
Q_3	0.435	0.320	10.800	-0.050	-7.050	2.000

(b) Unit load at center

Point	Theoretical Results			Experimental Results		
	Without Diaphragm	One Diaphragm	Three Diaphragms	Without Diaphragm	One Diaphragm	Three Diaphragms
M_1	0.185	4.535	6.055	0.395	5.050	7.400
M_2	0.205	10.465	3.875	0.550	6.200	3.700
M_3	0.365	13.665	14.000	0.160	5.250	5.500
TE_1	0.570	0.570	0.270	0.850	0.900	0.700
TE_4	3.470	9.650	6.460	3.000	8.300	5.500
TE_5	-1.960	-1.290	-1.460	-1.400	-1.000	-1.100
Q_1	0.285	0.375	10.420	0.120	0.700	9.000
Q_2	0.140	0.470	4.290	0.050	0.200	3.100
Q_3	-0.010	0.105	4.970	-0.100	0.060	6.500

Table 3. Transverse normal forces $N_x b$ due to unit load at mid-span.

(a) Unit load at left edge

Point	Theoretical Results			Experimental Results		
	Without Diaphragm	One Diaphragm	Three Diaphragms	Without Diaphragm	One Diaphragm	Three Diaphragms
M_1	2.310	-6.020	-7.310	3.100	-3.200	-3.100
M_2	0.220	3.500	-2.920	-0.250	3.300	0.250
M_3	0.710	28.040	30.670	1.050	5.050	6.055
Q_1	-0.590	-0.090	8.125	-0.205	-0.200	5.850
Q_2	-0.190	-0.035	0.690	0.150	-0.600	0.950
Q_3	-0.255	-0.015	4.765	0.550	-0.550	4.640

(b) Unit load at center

Point	Theoretical Results			Experimental Results		
	Without Diaphragm	One Diaphragm	Three Diaphragms	Without Diaphragm	One Diaphragm	Three Diaphragms
M_1	-1.880	6.075	6.815	-1.650	4.850	4.650
M_2	4.040	6.550	7.420	3.300	6.055	6.920
M_3	0.575	16.780	17.800	0.650	6.400	7.040
Q_1	0.315	-0.025	8.995	0.300	-0.240	7.250
Q_2	0.070	-0.005	0.795	-0.150	0.550	1.625
Q_3	0.500	-0.080	3.800	-0.640	-1.050	3.700

Figure 1. Simply supported double-cell box girder bridge.

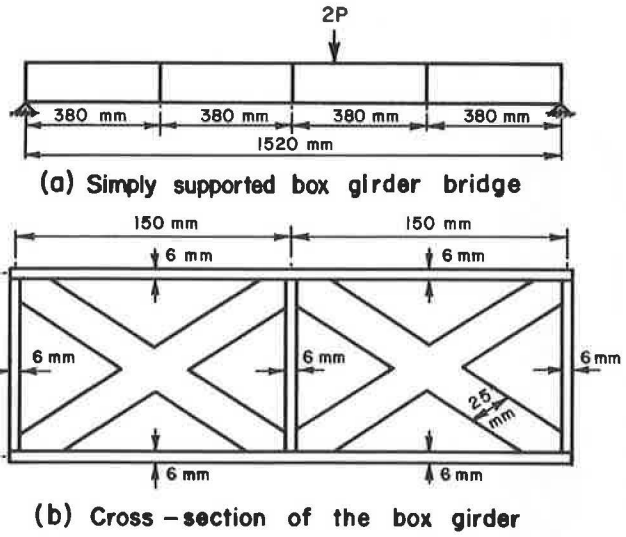

Figure 2. Components of loading.

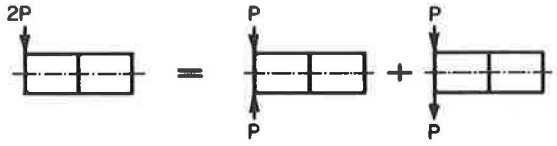

Figure 3. Positive directions of bending and membrane stress resultant.

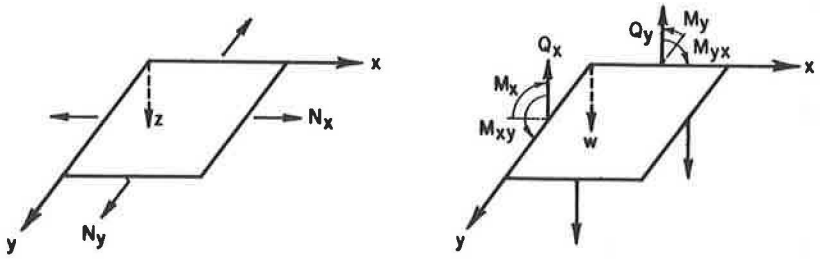

Figure 4. Location of strain gages.

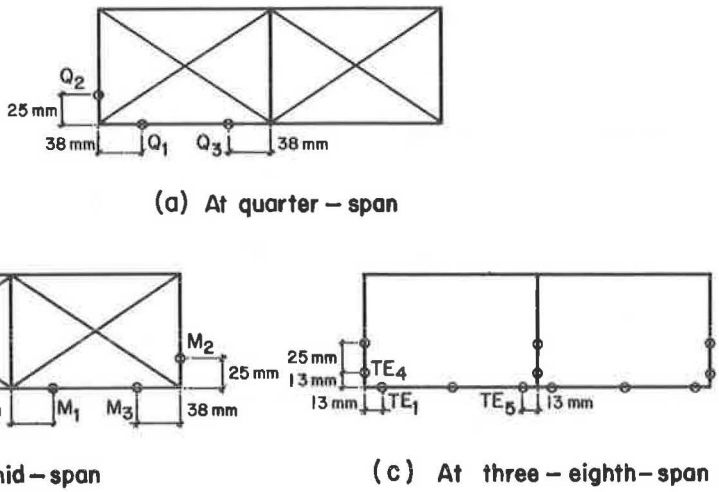

Figure 5. Test set-up.

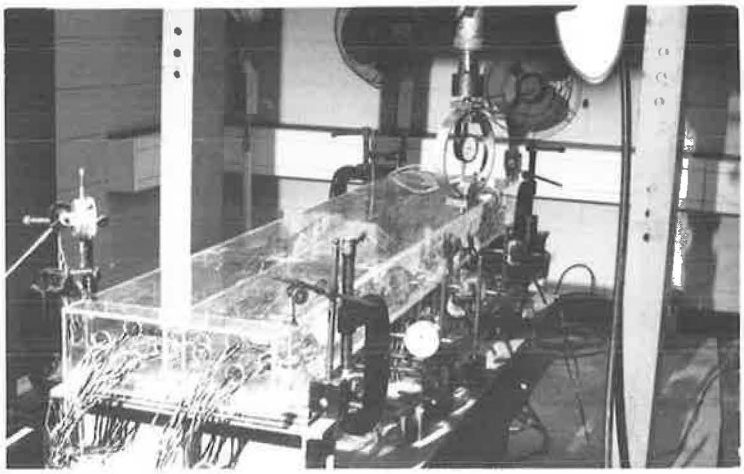

Figure 6. Deflections $(w)(D/b^2) \times 10^4$ due to unit load at quarter-span.

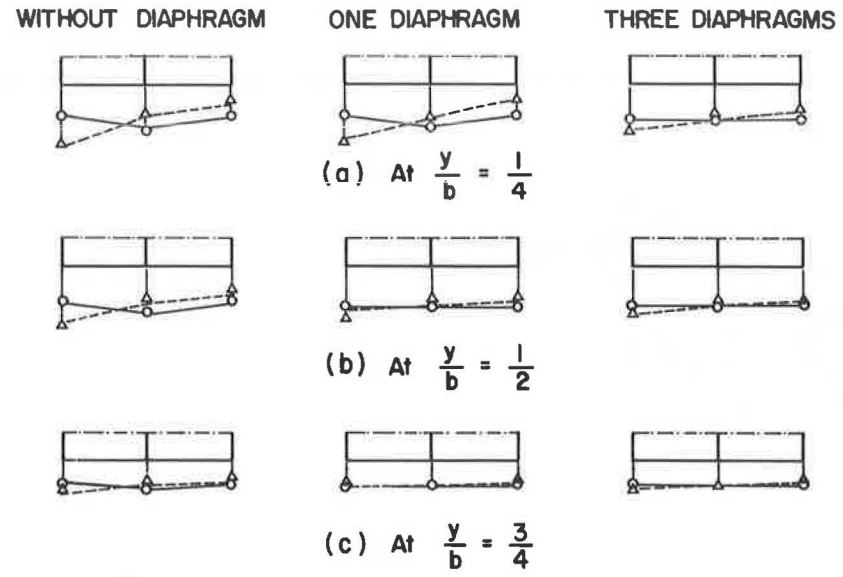

Figure 7. Deflections $(w)(D/b^2) \times 10^4$ due to unit load at midspan.

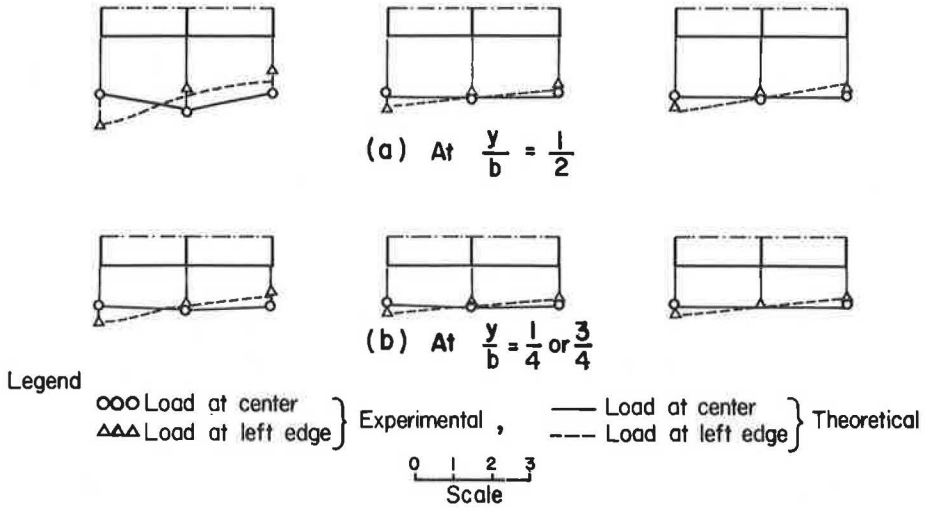

Figure 8. Deflections $(w)(D/b^2) \times 10^4$ due to load at three-eighth-span.

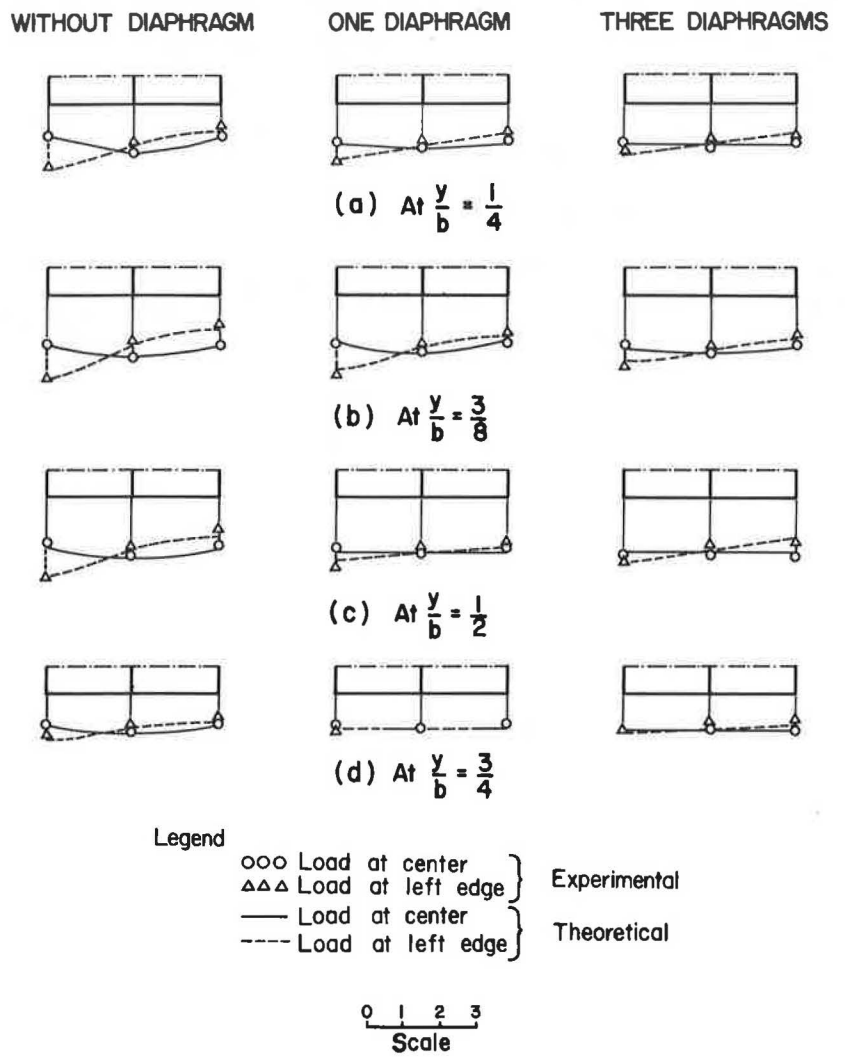

Figure 9. Longitudinal normal forces $(N_y/t) \times 10^{-2}$ at M_1 and M_3.

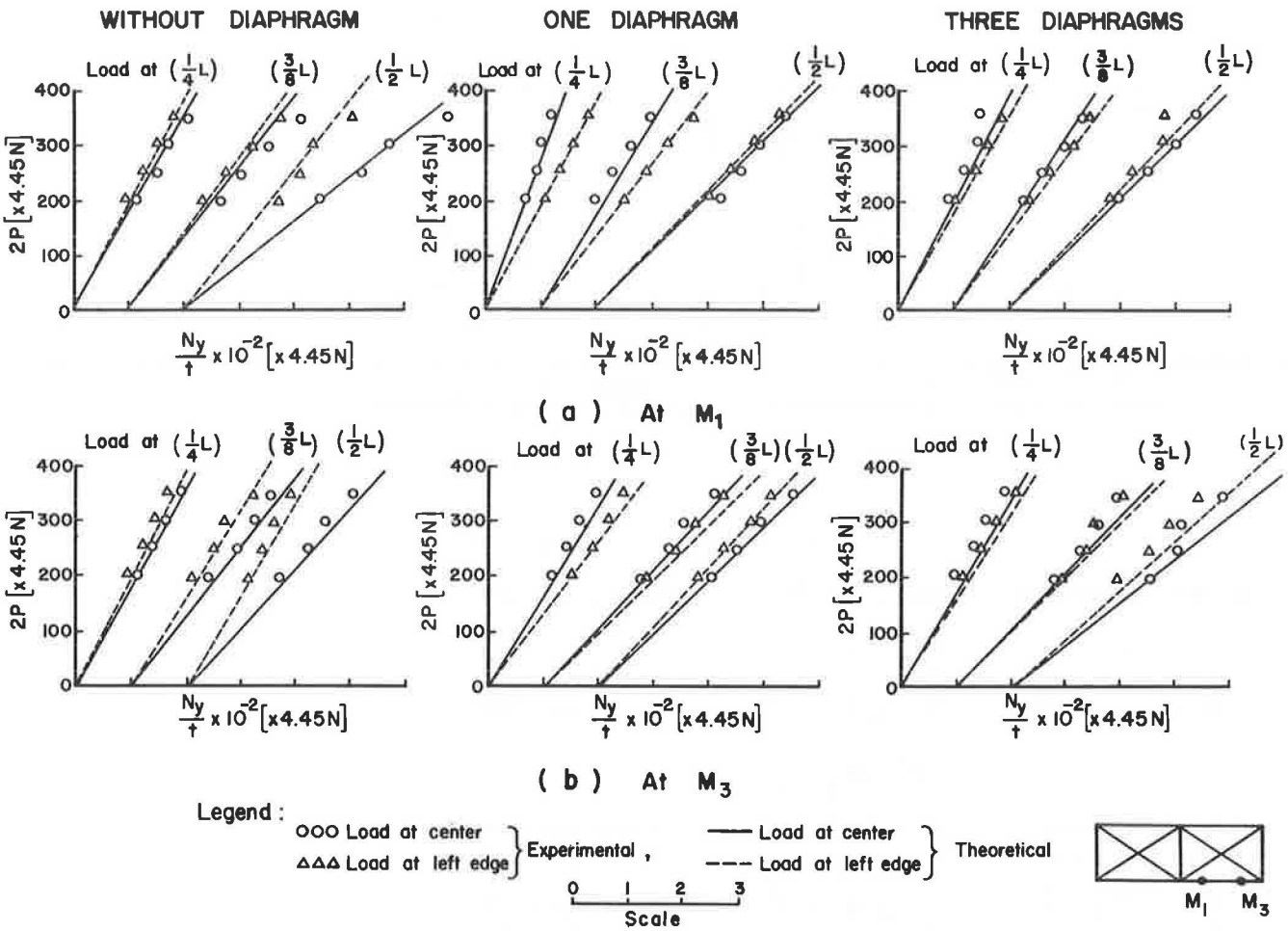

Figure 10. Longitudinal normal forces $(N_y/t) \times 10^{-2}$ at M_2 and Q_2.

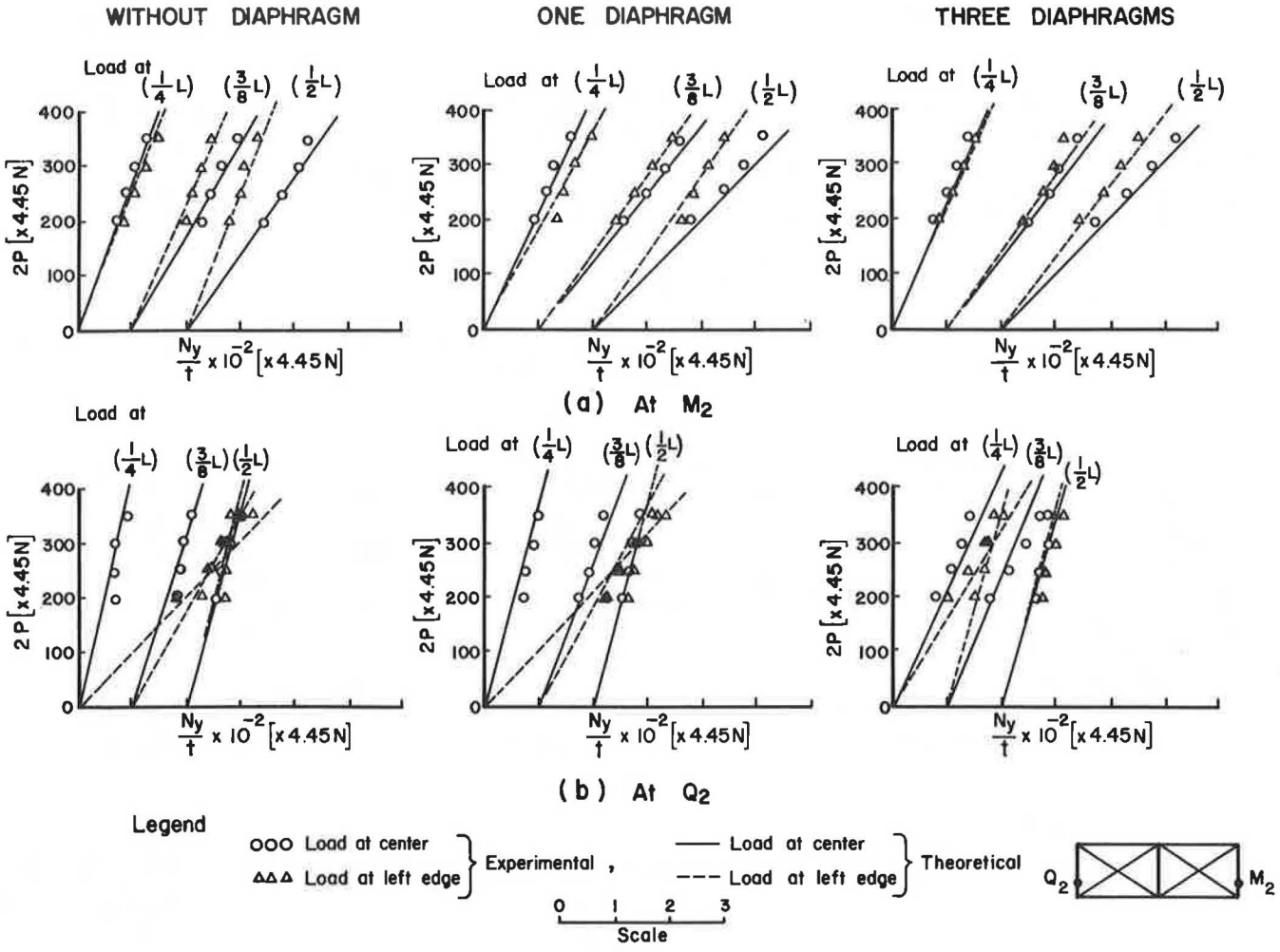

Figure 11. Longitudinal normal forces $(N_y/t) \times 10^{-2}$ at Q_1 and Q_3.

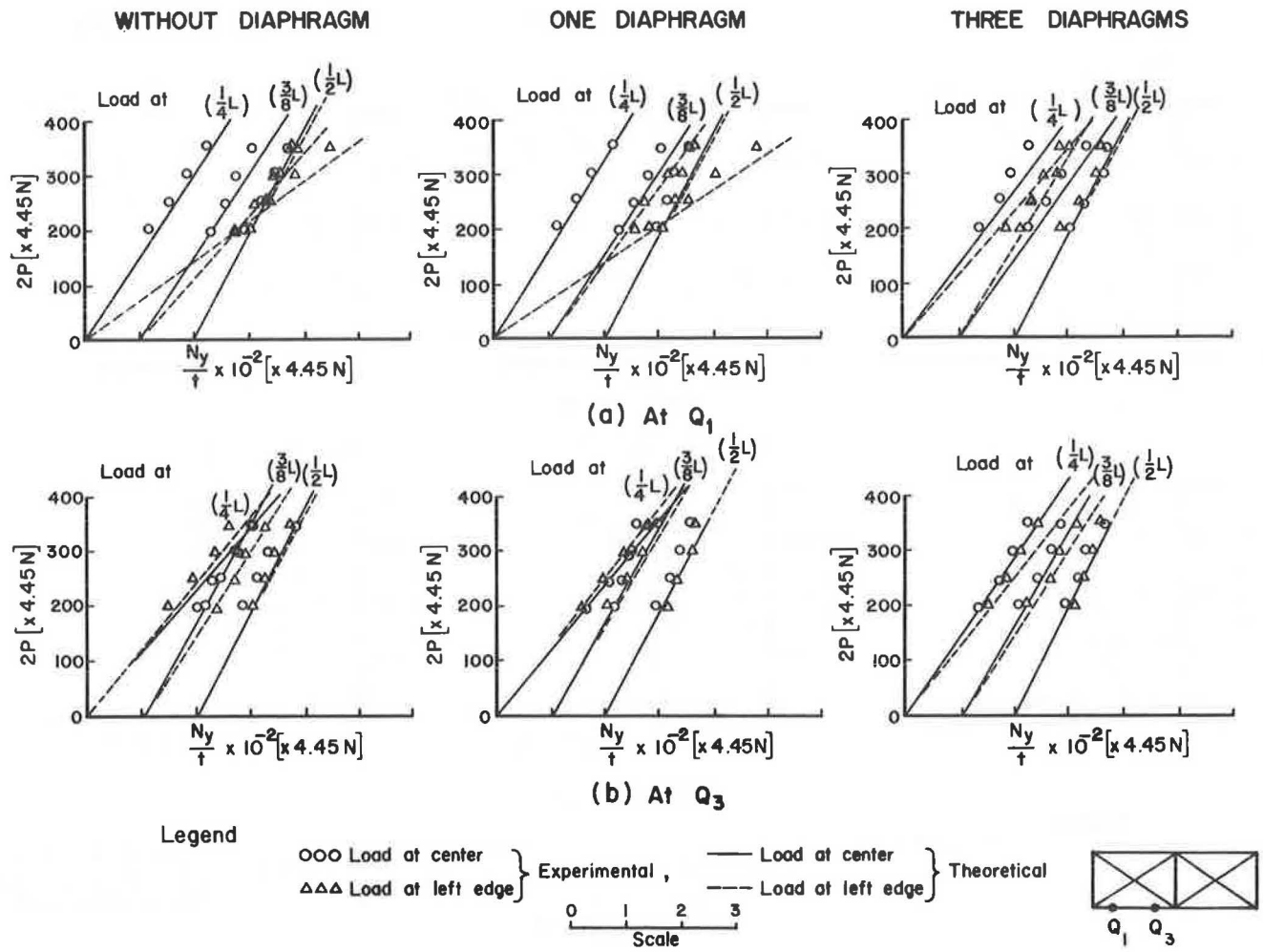

Figure 12. Longitudinal normal forces $N_y b$ at y/b = 3/8 due to unit load at three-eighth-span.

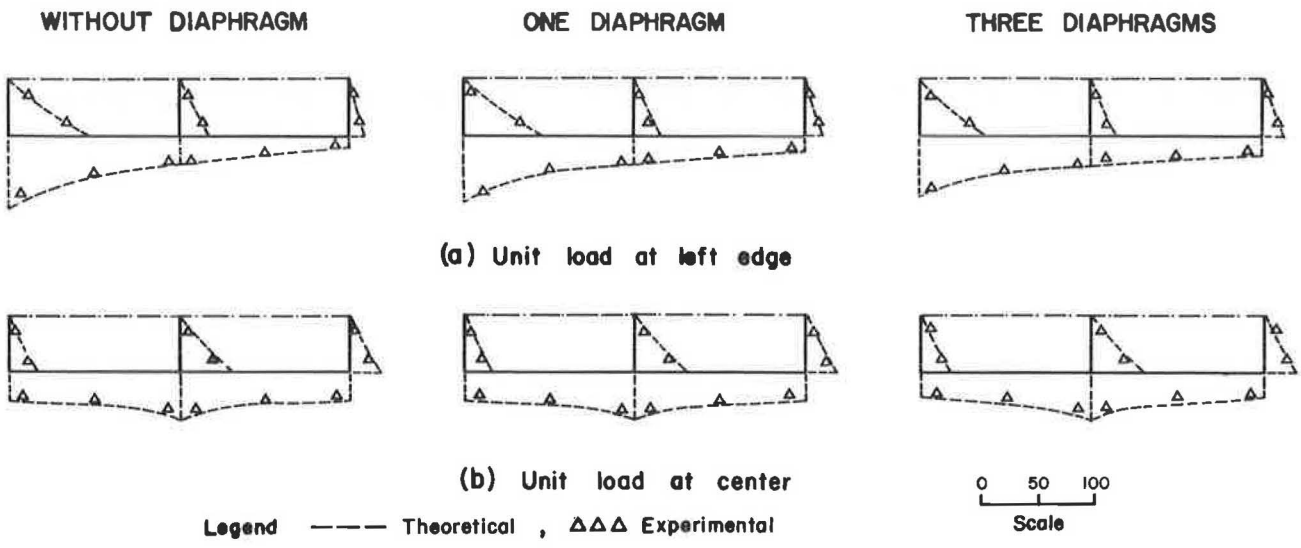

DYNAMIC RESPONSE OF BRIDGES

G P Tilly, Transport and Road Research Laboratory

Bridges can be excited by the action of wind, vehicles, or pedestrians. Whereas there are well developed methods to calculate dynamic behaviour, there have been comparatively few correlations with full scale measurements. The Transport and Road Research Laboratory has therefore undertaken a programme of research to measure the response of selected bridges to such loading. The work has also included tests in which the bridges were excited by an energy input device and damping values were measured from free decays.

Response to wind has been measured for two steel box girder bridges having orthotropic decks. Automatic self-switching equipment was used to record bridge acceleration, wind speed and direction, when wind speeds exceed a threshold level. Response to traffic has been measured for a multi-span steel box girder viaduct having a concrete deck. Response to pedestrians has been measured for a variety of types of footbridge.

Measured values of bridge response are compared with calculated values using procedures recommended in the new British Design Standard.

The dynamic response of bridges is an important aspect of design which has attracted a very considerable volume of research. Most examples of vibration leading to collapse have been due to excitation by wind, for example the Brighton Chain Pier in 1833 and other cases up to the more recent and well publicised Tacoma Narrows Bridge. There have also been cases of serious damage due to pedestrian induced vibration dating as far back as the Broughton case iron chain bridge which collapsed in 1831 and several footbridges have been 'bounced' off their bearings in recent years. There are no known cases of damage to main components due to traffic induced vibrations but there have been examples of fatigue failure of components, such as cross-bracing, that can resonate.

Despite the depth of the literature on dynamic behaviour, it has been found that there are inadequate data in several important areas. For example there have been surprisingly few well documented studies of the damping behaviour of modern steel structures and prior to the work described in this paper no damping data were available for welded steel box girder bridges. Similarly, there have been few comprehensive measurements of response to wind and it has not been possible to check the accuracy of design analyses beyond confirming that behaviour is stable. The situation with regard to traffic induced vibration is more satisfactory and there have been a number of measurements of movements and stresses. Nevertheless, these have been mostly concerned with relatively short span bridges and less attention has been given to the longer spans which are often very lively. Vibration of footbridges is not generally considered to be a major problem because unduly lively behaviour can usually be rectified relatively cheaply. There is however the question of human tolerance. Although active people can tolerate high levels of vibration, elderly and infirm people have a much lower tolerance. In addition it is unwise to build bridges that can deliberately be excited to high amplitudes of vibrations by vandals. Recent work by TRRL on footbridges has been to determine what constitutes lively behaviour and to compare measured response with calculations using formulae given in the new British Standard.

1. Damping

Damping is the term used to describe the dissipation of energy in a vibrating structure. There are a variety of mathematical expressions used to represent damping, the most common ones being logarithmic decrement and fraction of critical. Logarithmic decrement, δ, is most conveniently measured from a free decay and is given by

$$\delta = \frac{1}{n} \text{Log}_e \frac{a_m}{a_{m+n}}$$

where a is amplitude of vibration, m is the number of cycles along the decay at which measurement is started, and n is the number over which the measurement is made. Fraction of critical damping, ζ, often expressed as a percentage, is given by $\frac{C}{C_c}$ where C is damping and C_c is critical damping. The relationship between ζ and δ is $\zeta = \frac{\delta}{2\pi}$ for low values of damping typical of those in the range of superstructure

behaviour. In this paper logarithmic decrement is used exclusively.

Values of damping are required for calculation of structural response to transient or cyclic forces. In a recent review of the literature (1) attention was drawn to the distinction between different types of damping. Material damping is related to the steel or concrete and is a function of the energy dissipation by internal mechanisms. Numerous tests have been conducted on a laboratory scale and relatively wide ranges of values have been reported. After elimination of some extreme values and one or two questionable results, consensus ranges of damping are as given in Table 1. (Component damping refers to individual beams).

Table 1. Typical values of damping

Material	Component	Bridge
Steel		
0.002 to 0.008	0.004 to 0.03	0.02 to 0.06
Concrete		
0.01 to 0.06	0.02 to 0.06	0.02 to 0.1

Values of component damping are higher than for the constituent materials because there are additional losses of energy associated with the fabricated product. This is less apparent for concrete whose main mechanism of damping is associated with relative movements at cracks and internal flaws which are present in both the basic material and in cast beams. The belief that prestressed concrete exhibits lower damping than reinforced concrete is not supported by such data as are available; laboratory tests on beams with and without prestress have not shown any significant differences in damping (2) (3). Steel has damping values which are approximately one tenth of those for concrete. Damping is influenced by the type of steel but values are unlikely to differ significantly for different constructional steels. Steel beams have differing damping according to the method of fabrication, see Table 2. (derived from references 4 - 8)

In making comparisons between the different forms of fabrication it should be noted that values are influenced not only by testing techniques but are also dependent on amplitude of vibration. Hence comparisons may not be like with like because some investigations involve lower amplitudes than others. Nevertheless the general trends given in Tables 1 and 2 are intuitively correct and are confirmed where different investigations have overlapped. The dependence of damping on amplitude of vibration occurs for both concrete and steel. In all cases the trend is for logarithmic damping to increase with amplitude by up to 500 per cent.

Damping values of bridges are higher than for either the constituent materials or the components, as shown in Table 1. The increases are due to extra forms of energy dissipation such as relative movement at joints and interaction with substructure. Although concrete bridges tend to have slightly higher values of damping than steel bridges, structural form is the dominant feature in determining performance. Few comparisons can be made between steel and concrete because design philosphies differ and it is difficult to find comparable bridges having main features that are similar.

Testing steel bridges presents problems because the most important structures have long spans which require special techniques. Furthermore long-span bridges are usually situated on major roads which cannot be closed to traffic even for brief times during off-peak periods. A variety of methods of excitation have been adopted by different investigators such as the use of a test vehicle driven across a plank, sudden release of deflection, single-pulse loading (rockets) and resonant loading. The latter method has been used almost exclusively in the TRRL work. The excitation equipment, called an energy input device, has a set of weights which are reciprocated in a vertical plane by hydraulic actuators (10), Figure 1. In one exceptional case the

Figure 1. Energy input device and towing vehicle

Table 2. Damping values for different types of steel beam

Rolled I-Beams	Bolted	Riveted	Welded	Attached to Concrete Slab
	Loose			
0.003 to 0.007	0.01 to 0.07	0.006 to 0.02	0.004 to 0.008	0.04 to 0.11
	Tight			
	0.005 to 0.03			

main 213m span of the Cleddau Bridge at Milford Haven was excited by the sudden release of deflection produced by suspending a 32.7Mg weight (11), Figure 2. Because of the difficulties in testing

Figure 2. Excitation of the Cleddau Bridge

Figure 3. Influence of amplitude on damping

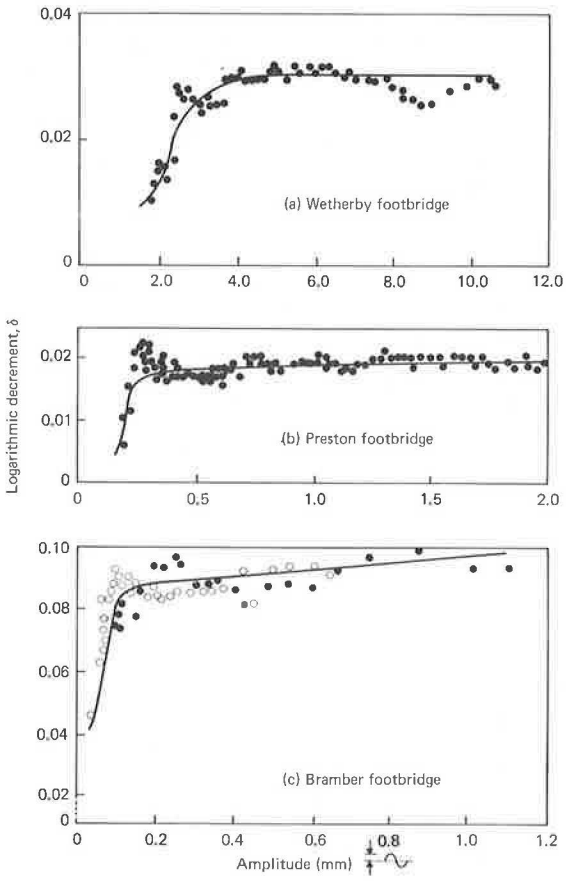

long-span bridges a programme of tests was conducted on steel footbridges having relevant configurations. The resulting values of damping for six footbridges, had extremes of 0.015 to 0.10 and typical values of 0.02 to 0.06. The measurements of the long-span Cleddau bridge gave damping of 0.043 to 0.059 which is within this range and gives some support to the belief that behaviour of footbridges is relevant to the general study. Typical curves of damping against amplitude of vibration are given in Figure 3. The relationship, shown schematically in Figure 4, involves values of damping which increase from a low value close to the constituent material damping to an upper-level at higher amplitudes. The former

Figure 4. Schematic representation of damping behaviour.

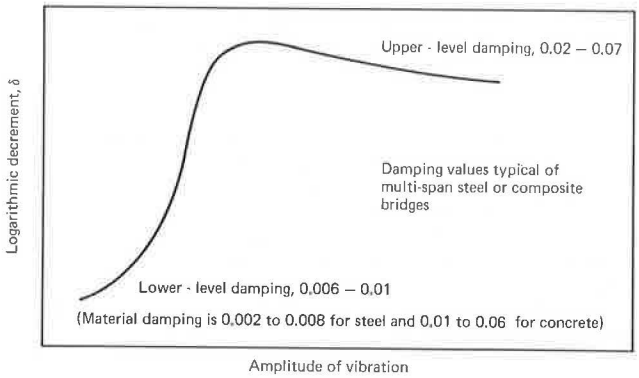

occurs at amplitudes which are too low to have structural significance and it is the upper-level damping that is usually relevant to calculation of bridge response. Values quoted in this paper as being typical are representative of upper-level damping.

When composite bridges were introduced, having concrete decks structurally attached to steel beams, there was concern that the response to traffic induced vibration could be livelier than for earlier types of bridges. As a result several research projects were set up and measurements were made of dynamic characteristics of different types of composite bridge. The damping values from these investigations are in the range 0.05 to 0.10 which is higher than values for wholly steel bridges but similar to slender concrete bridges (1). In the programme of tests by TRRL on sixteen composite bridges (9), damping ranged between extremes of 0.02 to 0.13 but typical values were between 0.05 and 0.07. One of the main points to emerge from the tests on steel and composite bridges was that single-span structures exhibit higher damping values, 0.05 to 0.13, than multi-spans which have values of 0.01 to 0.08, Figure 5. In cases where measurements were made on different parts of the substructure, it was found that significant vibrations occurred so that a substantial contribution to damping may be made at interfaces such as between the ground and an abutment. The higher damping exhibited by single-span steel bridges is a general trend that emerged from the testing of typical examples of modern bridges but it does not follow that single-span bridges need necessarily have high damping. Clearly it is possible to have weak links to the superstructure so that significant movements are not transmitted to the substructure. In cases where damping is associated with the superstructure alone the situation is akin to vibration of a beam and damping values

Figure 5. Damping values for single and multi-span bridges

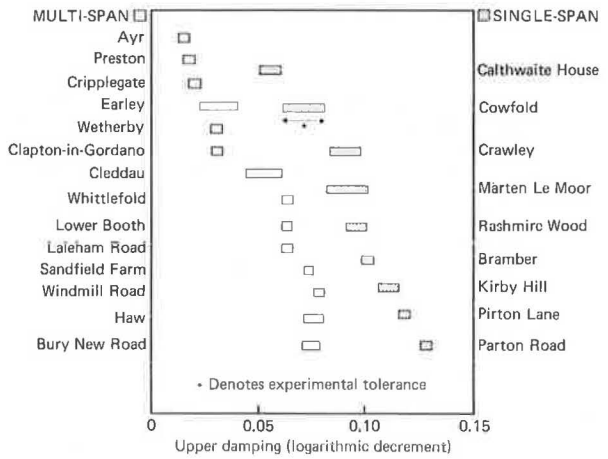

can be very low. Welded box girders, whether having steel or concrete decks, can have very low damping. Of eighteen steel box girder bridges tested, four had upper-level damping values of less than 0.03. These low values are partly due to the low damping of welded plates as distinct from older types of construction such as trusses and partly due to simple supports which permit little interaction with the superstructure.

In order to be able to study damping of steel box girders under more closely controlled conditions, a 30m rectangular steel beam has been erected at TRRL. The beam is 2.44m wide and 0.92m deep, and is supported on concrete piers, Figure 6. The

Figure 6. 30m experimental steel box girder

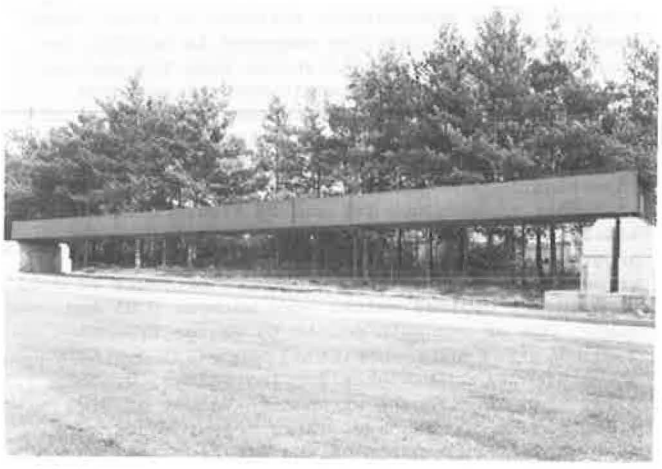

testing programme involves measurements of damping for several types of bearing and with the addition of different types of surfacing, eg concrete or mastic asphalt. It is intended to assess the contributions to overall damping of these different features, using full scale components in a manner not previously possible. In the work to date, it has been found that with the beam supported on simple rubber pads at each end, the damping is 0,008. This is in the range for intrinsic material damping of steel and it is clear that there is little if any contribution from other mechanisms. With a system composed of rocker bearings at one end and sliding bearings at the other, considerable movement was transmitted to the piers and the damping was 0.012. The extra component was due to dissipation of energy at the sliding bearings and between the piers and the ground.

Most reported work on concrete bridges has been on relatively short spans and there have been very few tests on modern longer span concrete structures. Measured values of damping, excluding some extreme values, are in the range 0.02 to 0.10. There is no clear evidence to support the generally held view that damping of prestressed bridges is any lower than that of reinforced bridges. Two similar concrete footbridges were tested by TRRL, one reinforced the other post-tensioned. The respective span lengths were 10.7m - 36.8m - 10.7m and 15.3m - 33.6m - 15.2m, both had suspended centre spans. The reinforced footbridge had a damping value of 0.044 whereas the post-tensioned footbridge had a value of 0.065. There are several reported cases of prestressed structures having very low damping but this may be due to slim superstructures which can vibrate without interaction with abutments or piers, rather than the fact that the concrete is prestressed.

2. Measured Bridge Response

2.1 Wind Induced Vibration

Measurements of wind induced vibrations by TRRL have been made on two long-span steel box girder bridges (12). The first was the Cleddau Bridge at Milford Haven mentioned in Section 2. Earlier wind tunnel tests had predicted that large wind induced vibrations could develop and consequently a damping device was fitted inside the box (13). Measurements were made of wind induced vibrations during a 5½ month period to check behaviour with the damper inoperative. Accelerometers were positioned at the centre of the span and at quarter points. Wind speed and direction were measured using an anemometer and wind vane at the top of a 6m high mast positioned at the leading edge of the structure for winds blowing onshore. The indicated wind speed was corrected to free stream wind speed using a factor of 20 per cent which was obtained from wind tunnel tests. During the time the measurements were taken, the predicted critical wind speeds of 21 and 23m/s were experienced on several occasions. The maximum amplitude of movement never exceeded ±28mm in any of the occurrences and was substantially lower than predicted by the wind tunnel tests for either laminar or turbulent flow, Figure 7. However the response could be under-estimated from these measurements because there are insufficient data for the higher wind speeds and it is possible that the maximum respones could develop at speeds above the predicted values. Furthermore, the wind speeds may not have been sustained for long enough to cause the bridge to develop maximum response.

The second bridge whose wind response has been monitored is the Wye Bridge which has a 235m cable-stayed main span. During the first two years in service, between 1966 and 1968, there were several reported instances of relatively severe vibration but since that time the response has apparently been considerably less. Wind tunnel tests have predicted that a response of ±64mm can develop for damping of 0.03 and a wind blowing at 7.8 to 9.2m/s normal to the superstructure. The measurements on Wye Bridge were after the work on Cleddau Bridge and used

Figure 7. Comparison of measured and predicted deflection for Cleddau Bridge

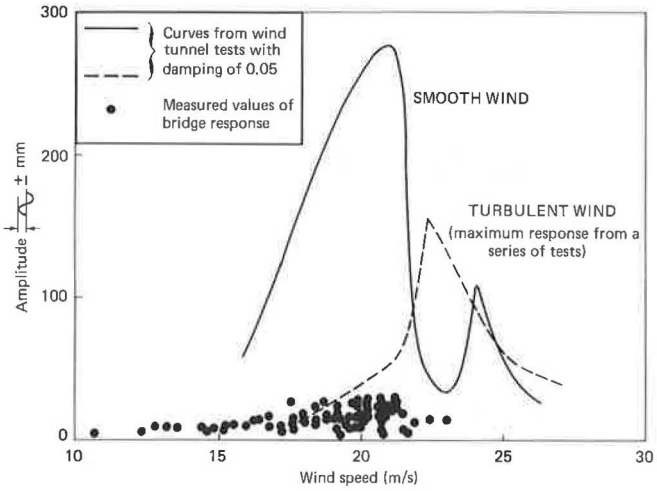

specially constructed equipment for automatic data acquisition, ADA, not previously available (12). This equipment constantly monitors three anemometers and an accelerometer. The anemometers are mounted orthogonally at the end of a 7m long horizontal boom positioned outwards from the leading edge at the centre of the span. The accelerometer is fixed inside the box also at the centre of the span. By suitable combinations of the signals from the anemometers the ADA is constantly informed of the direction and magnitude of the wind vector. When it is in the horizontal plane, within $\pm 40^{o}$ of the normal to the bridge, and its magnitude exceeds a predetermined level, outputs of the four sensors are recorded on analogue tape for a period of 8 minutes. The equipment was first installed on the bridge in March 1976 and will remain in use for several years. It has not been continually operational because it was necessary to move it when maintenance operations were carried out on the box. Up to 1978 there have been a number of occasions when sustained oscillations developed in the structure. The maximum measured response is ±18mm at 0.46Hz.

2.2 Traffic Induced Vibration

Measurements of traffic induced vibrations have been made on the Tinsley Viaduct. This structure had been found to require extra strengthening when reassessed using updated design criteria. It was decided to measure traffic induced vibrations before the strengthening in order to assess the dynamic performance. The bridge is two-level with twenty spans and a total length of 1032m. The superstructure is composed of steel box girders with concrete decks (12). Measurements were made of the deflections of the upper motorway level of the eighteenth span under normal traffic, using a cantilever deflection gauge. The data were recorded on analogue tape during four one-hour periods. The superstructure deflected as a continuous beam so that uplift as well as downward deflections were recorded. Vehicles were assessed by observation and those which appeared to be less than 15kN were excluded. During the four hours recording there were 914 north-bound vehicles and 744 south-bound vehicles exceeding 15kN. It was found that the maximum uplift was 5mm and the maximum downward deflection was 14.4mm. Most occurrences were in the range ±2mm, see histograms in Figure 8. These move-

Figure 8. Histograms of traffic induced deflections measured on Tinsley Viaduct

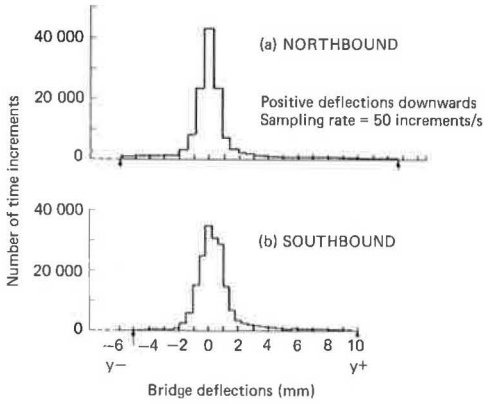

ments are very small in relation to the size of the structure; the maximum vibration component of ±2.6mm is less than half the recommended tolerance limit to pedestrian comfort.

Measurements of traffic induced vibrations on other bridges have given similar data.

2.3 Response to Pedestrians

Modern long-span bridges, although designed to be stable under the action of wind, tend to be lively under traffic. The vibration is often very noticeable to pedestrians and may be uncomfortable to motorists in stationary vehicles because movements can be amplified by the suspension system. This is not usually considered to be a serious problem because the vibrations generate negligible stresses in the superstructure. The consideration of human tolerance in such cases has not been a serious issue either. This is partly because the vibrations are not high enough to cause serious concern and partly because pedestrians who walk along heavily trafficked long-span bridges tend to have a higher tolerance. Footbridges excited by the pedestrians themselves present a different situation because they serve a large proportion of elderly and infirm people. In several cases it has been neccesary to amend designs at a late state in construction or after completion. The question of pedestrian tolerances is very subjective and limits are dependent on features such as frequency and amplitude of vibration, duration of exposure, whether walking or standing, and the psychological attitude of the pedestrian. After consideration of earlier work, the tolerance limit proposed for the British Standard is an acceleration of $\pm \frac{1}{2}\sqrt{f_o}$ where f_o is the fundamental natural bending frequency in Hz. Frequencies above 5Hz are not considered to present any problem. The background to the recommendations is given in

Reference 14. Simplified and generalised formulae are given for calculation of bridge response. For bridges of up to three spans the simplified method gives acceleration by the expression

$$4\pi^2 f_o^2 Y_s K\psi \quad m/s^2$$

where y_s is static deflection due to a vertical load of 700 Newtons at mid point of the longest span.

K is a configuration factor

ψ is a dynamic response factor depending on damping. Values recommended for damping are 0.03 for steel, 0.04 for composite (steel beams with concrete deck) and 0.05 for concrete bridges.

For frequencies greater than 4Hz the calculated acceleration may be reduced by an amount varying linearly from zero reduction at 4Hz to 70 per cent reduction at 5Hz. Alternatively response can be calculated by a general method where the load applied by a pedestrian is given by 180 Sin $2\pi f_o$ t Newtons, moving at a speed of 0.9 f_o m/s, t being time in seconds.

In the tests on footbridges by TRRL characteristics that are measured include static stiffness under concentrated loading, bending frequencies, mode shapes, damping, and response to pedestrians. Measured data of this type can be used to check the accuracy of calculated frequencies and response. Although considerable attention has been given to the development of accurate methods to calculate dynamic behaviour, few comparisons have been made with field measurements. In practice, the accuracy of calculations is influenced by features such as the support conditions which are difficult to express numerically. The methods and assumptions used to calculate dynamic behaviour of superstructures in the TRRL work have been described by Wills (15). Briefly, the calculations of frequency were made for free undamped vibration. Effects of rotary inertia and shear deformation are neglected. Bridge superstructures of variable depths have been considered. In calculating flexural rigidities, the whole cross-section including parapet upstands for continuous superstructures, is assumed to contribute fully to stiffness without reduction for shear lag. Hand rails and surfacings are ignored. Reinforcement is neglected and the dynamic modulus of concrete is used. This varies with concrete strength but gives a modular ratio of 5 to 6. Using these assumptions, the fundamental frequency can usually be calculated to within ±10 per cent of the measured value. Four of the lively footbridges, two steel and two concrete, are examined in relation to calculated response to pedestrians, Table 3. The resulting figures confirm that the two formulae give similar results. Furthermore the calculated accelerations correlate reasonably well with the measured ranges which are themselves very dependent on the pedestrians in question. The calculated response for the Wetherby footbridge exceeds the tolerance limit but measured responses for a single pedestrian on all the bridges were below the tolerance limit. Where responses were measured for two pedestrians walking in step, the values were approximately twice as high as for single pedestrians. Responses for walking and running across the two concrete footbridges are shown in Figure 9.

Figure 9. Responses of concrete footbridges to one person walking and running, measured at mid-span

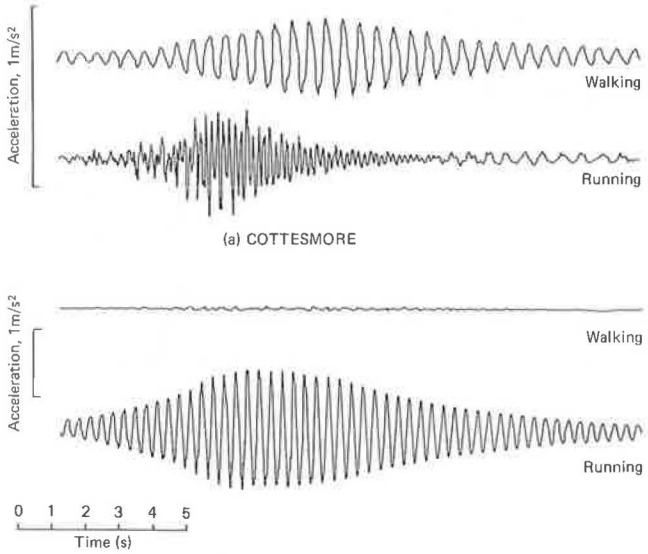

In cases where bridges are found to be unduly lively remedial action can usually be taken relatively easily. This is illustrated by a slender steel box girder footbridge at Clapton-in-Gordano which could not be adequately assessed before construction due to doubts about what damping value should be assumed. When built, the bridge was found to have damping of 0.005 for amplitudes of vibration of up to ±6mm. This damping is unusually low and permitted unacceptably lively behaviour because the tolerance limit converted into deflection, is ±6mm, which could easily be exceeded by a pedestrian. The lively behaviour was cured by fitting friction dampers against the abutment at the free end of the bridge and in the sleeve joints between the hand rails. The addition of the handrail damper increased the overall damping to 0.012 at ±4mm rising to 0.035 at ±24mm. The damper at the bearing raised the values to 0.055 at ±3mm, Figure 10. The small reduction in damping at higher amplitudes is typical of friction damping. In cases of continuous multi-span bridges it may not be convenient to add friction devices and use of tuned dynamic absorbers is a more attractive solution. Vibration absorbers have been used successfully for bridges found to be susceptible to wind induced vibration (13) (16). Their performance has been demonstrated recently on the 30m steel box girder at TRRL. The dynamic characteristics were investigated by exciting the beam using a small version of the energy input device ie a vibrating mass reciprocated in a vertical plane by a hydraulic actuator. The excitation was carried out at different frequencies so that response/time curves could be plotted for the beam with and without addition of the dynamic absorber, Figure 11. The reduction in response can be seen to be very significant.

Table 3. Calculated and measured values of dynamic response of footbridges

Bridge	Frequency, f_o, Hz		Calculated response m/s^2		Measured response m/s^2	Tolerance limit $\pm\frac{1}{2}\sqrt{f_o}$
	Calculated	Measured	Simplified method	General method		
Steel						
Craigie Park, Ayr	3.30	3.11	0.58	0.57	0.09-0.54	0.91
River Wharfe, Wetherby	2.62	2.62	0.97	0.88	0.06-0.49	0.81
Concrete						
Brackendale Road, Camberley	3.04	2.82				0.87
1 pedestrian			0.24	0.20	0.16-0.63	
2 pedestrian			0.48	0.40	0.58-1.03	
Cottesmore, Oxford	1.69	1.89				0.65
1 pedestrian			0.28	0.22	0.37-0.55*	
2 pedestrian			0.56	0.44	0.83-1.03*	

*Pedestrians walking in step with a metronome

Figure 10. Influence of extra dampers on first mode behaviour of Clapton-in-Gordano footbridge

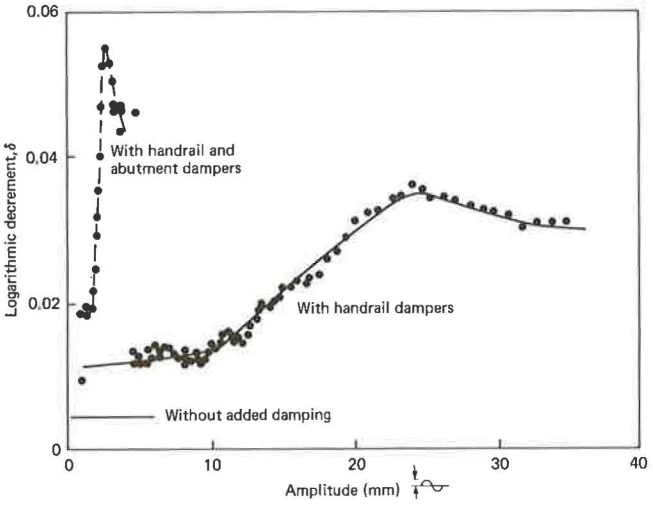

Figure 11. Effect of tuned absorber on vibration of 30m steel box girder

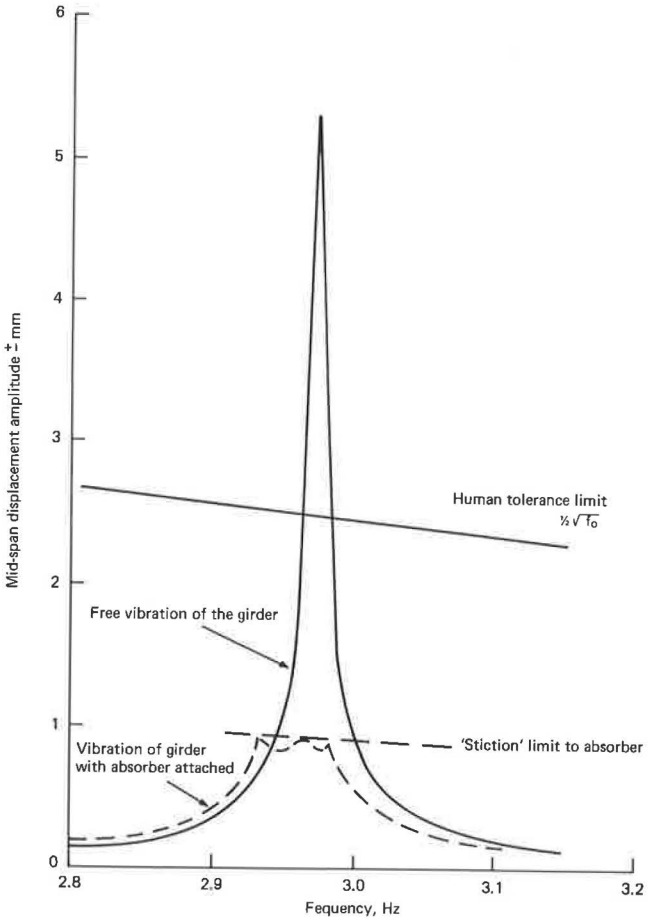

3. Conclusions

1. Damping values of bridges and their component materials increase with amplitude of vibration. Typical upper-level values are 0.02 to 0.06 for steel, 0.05 to 0.10 for composite (steel beams with concrete decks) and 0.02 to 0.10 for concrete bridges.

2. Measurements made to date, of the response of two long span steel bridges to wind, indicate that amplitudes of vibrations are less than values predicted from wind tunnel tests.

3. Traffic induced vibrations are not a serious problem for modern bridges. Amplitudes of movement are relatively low and involve low stresses and accelerations below the levels for human tolerance.

4. Pedestrian induced vibration of footbridges can sometimes present problems. However calculated responses correlate with measured behaviour and show that proposed design procedures give adequate guidance.

5. Lively bridges can be deadened by the addition of extra damping or vibration absorbers. Such methods are considered preferable to structural modifications such as stiffening the superstructure or reducing span lengths.

Acknowledgements

The work described in this Paper forms part of the programme of the Transport and Road Research Laboratory and is published by permission of the Director. The testing programme was carried out by R Eyre. The tuned absorber was designed and tested by R Jones, University of Reading.

References

1. G.P. Tilly. Damping of Highway Bridges: A Review, Paper 1, pp. 1-9. Symposium on Dynamic Behaviour of Bridges, TRRL Report SR 275 UC, Crowthorne 1977.
2. J. Penzien. Damping of characteristics of pre-stressed concrete. Journal of ACI, Proc V61, No 9, Sept 1964, pp 1125-1148.
3. M.L. James, L.D. Lutes and G.M. Smith. Dynamic properties of reinforced and prestressed concrete structural components. J of ACI Proc V61 No 11, Nov 1964 pp. 1359-1382.
4. R. Eyre. Unpublished work at Transport and Road Research Laboratory, 1977.
5. Y. Yamada. Studies on vibration damping of steel structure. IABSE Symposium, Lisbon, 1973, pp. 101-106.
6. R.C. Duffield, H.J. Salane, A.R. Olsen and R.R. Wells. Damping characteristics of composite beams, Proc ASCE, J of Struc. Div. Vol 103 No ST1 Jan 1977 pp. 105-118.
7. L.W. Teller and G.W. Wiles. Tests on structural damping. Public Roads, Vol 27, No 10, Oct 1973, pp. 203-233.
8. I. Holland. Damping of vibrations in simply supported prestressed beams. Inst. Struc. Mechs., Tech Univ of Norway - Trondheim April 1962.
9. R. Eyre and G.P. Tilly. Damping Measurements on Steel and Composite Bridges, Paper 3, pp. 22-39 Symposium on Dynamic Behaviour of Bridges, TRRL Report SR 275 UC Crowthorne 1977.
10. D.R. Leonard. Dynamic tests on highway bridges - test procedures and equipment, TRRL Report LR 654 Crowthorne 1974.
11. R. Eyre. Dynamic tests on the Cleddau Bridge at Milford Haven. TRRL Report SR 200 UC. Crowthorne 1976.
12. R. Eyre and I.J. Smith. Dynamic response to Traffic and Wind. Paper 5, pp. 56-69, Symposium on Dynamic Behaviour of Bridges, TRRL Report SR 275 UC, Crowthorne 1977.
13. C.W. Brown. An engineer's approach to dynamic aspects of bridge design. Paper 8. pp. 107-111 Symposium on Dynamic Behaviour of Bridges, TRRL Report SR 275 UC, Crowthorne 1977.
14. J. Blanchard, B.L. Davies and J.W. Smith. Design criteria and analysis for dynamic loading of footbridges. Paper 7 pp. 90-106 Symposium on Dynamic Behaviour of Bridges, TRRL Report SR 275 UC, Crowthorne 1977.
15. J. Wills. Correlation of calculated and measured dynamic behaviour of bridges Paper 6 pp. 70-89
Bridges, TRRL Report SR 275 UC Crowthorne, 1977.
16. V.A.L. Chasteu. The use of tuned vibration absorbers to reduce wind excited oscillations of a steel footbridge. The Civil Engineer in South Africa, Vol 15 No 6 pp. 147-154 June 1973.

DYNAMIC RESPONSE OF A SINGLE TRACK RAILWAY TRUSS BRIDGE

C. L. Dhar and K. H. Chu, Illinois Institute of Technology.
V. K. Garg, Association of American Railroads

A lumped mass model of a railway truss bridge is developed. The model considers only the vertical degree of freedom of each truss joint. The vehicle system is idealized as a three degree of freedom model consisting of the carbody and wheel-axle sets. Dynamic interaction equations for the bridge-vehicle system are derived and solved using the numerical integration method. Impact factors for member forces and nodal deflections are generated under the action of a single or a series of three moving vehicles. Finally, a limited parametric study is performed to determine the influence of vehicle speed, vehicle suspension characteristics and sprung mass on impact factors.

The subject of bridge impact* has been of great interest to many investigators and researchers since the middle of nineteenth century. A detailed review on this subject has been given in [1]. During the past two decades, a considerable amount of analytical and experimental research work has been conducted for highway bridges. A general scheme for analysing the vibration problem of highway bridges due to moving vehicles has been given in [2]. This method includes a realistic model of the vehicle to study the interaction between the bridge and the vehicle. To date, only a very limited amount of theoretical work has been done to study such interaction for railway bridges.

The first analytical approach to the railway bridge vibration problem was suggested by Willis [3] in 1849. Subsequently, Robinson [4] in 1884 conducted bridge impact tests and compared them to a simplified analysis. In the early 20th century, significant contributions to the development of a general theory of bridge vibration were made by Timoshenko [5] and Inglis [6]. Schallenkamp [7] in 1937, presented a rigorous closed form solution for the case of a smoothly rolling load in which he included both the mass of the load and the mass of the bridge. Looney [8] in 1944, using a numerical procedure, obtained solutions of the problem with multiple masses.

In the U.S.A.the most complete series of tests on railroad bridges were conducted by the sub-committee of American Railway Engineering Association (AREA) under the direction of Turneaure [9] in 1911. The results of these tests were impact formula that were used in the design of railroad bridges until 1935.

In 1935, Hunley [10] collected data for static and dynamic deflection of 39 different railroad bridges under approximately 300 different locomotives. He also secured additional data on damping coefficients for bridges. The AREA (American Railway Engineering Association) design specifications for railroad bridges were revised in accordance with Hunley's recommendation for impact effects and were used until 1948. Subsequently, extensive field and laboratory tests were conducted by the Association of American Railroads for steel, concrete and timber railroad bridges. These tests are described by Ruble [11]. More recent tests are published in AREA proceedings. Based on these tests the present AREA design specifications for impact on railroad bridges were developed.

The objective of this study is to examine the vertical dynamic response of a truss railway bridge to the passage of one or a series of railway vehicles. Only vehicle in its normal operating condition has been considered. The effects of vehicle hunting or vehicle breaking resulting in lateral or longitudinal motion of the bridge are neglected. The bridge is analyzed as a multi-degree of freedom system; and the vehicle is represented realistically as a four-axle sprung load unit with three degrees of freedom. In the analysis, input due to track irregularities is neglected and only the elastic interaction between the bridge and vehicle is considered. The equations of motion for the vehicle-bridge system, including the vehicle-bridge interaction, are developed and solved to generate dynamic impact factors for member forces and nodal deflections. A limited parametric study has been performed to determine the influence of vehicle speed, vehicle suspension characteristics and sprung mass on impact factors.

Vehicle-Bridge System Model

A lumped mass model of the truss bridge in which the masses are assumed to be concentrated at each truss joint, is considered. The truss joints are assumed to be pin-connected. Half of the mass of each member is contributed to the joints it connects. The floor system of floor-beams, stringers and the track system is lumped to the bottom chord joints. The cross-beams are assumed to be pin-connected to the truss joints and secondary effects are neglected. The wheels of the vehicle are assumed to remain in contact with the track at all times. All displacements are assumed to be small. Only the vertical degree of freedom is assigned to each truss joint. The truss flexibility coefficients are obtained by the deflections caused by a unit load applied at each joint one at a time. The effect of rotary inertia and non-linearity of material or deformation are neglected in the analysis.

The vehicle system is idealized as a three degree of freedom model of a railway vehicle consisting of a rigid car body and four axle sets, Fig.1. The two, 2-axle trucks are assumed to form a part of the car body as in the actual vehicle. The three degrees of freedom assigned to the vehicle correspond to bounce, pitch and roll motion. In the model, the primary and secondary suspension system are considered as linear springs in series and replaced by an equivalent spring. Damping in the suspension systems is small and consequently neglected. This simplified model has been chosen, after it was found that its bounce, pitch and roll frequencies are quite close to the test values and to a more complex ten degree of freedom model of the vehicle.

Equations of Motion

D'Alembert's principle of dynamic equilibrium is used to write the equations of motion. By equating the external and internal forces we get:

$$[M]\ddot{[D]} + [C]\dot{[D]} + [K][D] = [F(x,t)] \tag{1}$$

where

$[M]$ = Mass matrix of the truss

$[K]$ = Stiffness matrix of the truss

$[C]$ = Damping matrix of the truss

or $[C] = a\omega_1[M]+b[K]$, where a and b are scalar constant and ω_1 is the fundamental circular frequency. In the analysis

$$[C] = a\omega_1[M] \tag{2}$$

is used.

$[F(x,t)]$ = vector of applied nodal loads, due to interaction between the moving vehicle and the bridge.

$[D] = [v_1, v_2, \text{----}v_n]^T$ = joint displacement vector.

Here v is the vertical displacement and subscript denotes the joint number.

$\dot{[D]}$, $\ddot{[D]}$ = joint velocities and accelerations. Equations of motion for vehicle: v_b^i is the vertical displacement of the bridge associated with the ith wheel of the vehicle at any time t, Fig.2b. The equation of motion of vehicle are expressed as:

$$M^b\ddot{y}^b + \sum_{i=1}^{8} k_y(y^b \pm l_i\phi^b \pm b\theta^b - v_b^i) = 0 \tag{3}$$

$$I^b\ddot{\phi}^b + \sum_{i=1}^{8} k_y(y^b \pm l_i\phi^b \pm b\theta^b - v_b^i)(\pm l_i) = 0 \tag{4}$$

$$J^b\ddot{\theta}^b + \sum_{i=1}^{8} k_y(y^b \pm l_i\phi^b \pm b\theta^b - v_b^i)(\pm b) = 0 \tag{5}$$

Where M^b, I^b and J^b are the mass, pitch moment of inertia and roll moment of inertia of the vehicle; y^b, ϕ^b, and θ^b refer to vertical, pitch and roll displacement of the vehicle; k_y is the equivalent spring stiffness of each vertical suspension element; l_i is the distance of the centroid of the vehicle to the ith wheel, and b is the half distance of wheel contact points. A dot superscript denotes differentiation with respect to time.

The interacting force p^i between the rail and the ith wheel of the vehicle is expressed as

$$p^i = M_u(g-\ddot{v}_b^i) + k_y(y^b \pm l_i\phi^b \pm b\theta^b - v_b^i) + M_s g \tag{6}$$

where

M_u = Unsprung mass

$M_s = \frac{M^b}{8}$ = sprung mass

If the ith wheel is on track segment lving between kth and (k+1) joint, Fig.2a, then v_b^i is expressed in terms of v_k^i and v_{k+1}^i by linear interpolation

$$v_b^i = \frac{x^i}{l_p} v_{k+1}^i + (1-\frac{x^i}{l_p})v_k^i = \alpha^i v_{k+1}^i + \beta^i v_k^i \tag{7}$$

where

x^i = distance of ith wheel from joint k

l_p = panel length of truss

$\alpha^i = x^i/l_p$

$\beta^i = (1-\alpha^i)$

Similarly,

$$\ddot{v}_b^i = \alpha^i\ddot{v}_{k+1}^i + \beta^i\ddot{v}_k^i \tag{8}$$

The load transmitted from the ith wheel to the kth and (k+1)th joints are

$$p_k^i = \beta^i(\frac{c-d}{c})\ p^i$$

$$p_{k+1}^i = \alpha^i(\frac{c-d}{c})\ p^i \tag{9}$$

where

c = center to center distance of trusses

d = distance between truss and rail

Substituting v_b^i, $\ddot{v}_b^i$ and p^i from equations (6), (7) and (8) into equation (9) gives

$$p^i = \beta^i(\frac{c-d}{c})\ [(M_s+M_u)g + k_y(y^b \pm l_i\phi^b \pm b\theta^b - \alpha^i v_{k+1}^i - \beta^i v_k^i) - M_u(\alpha^i\ddot{v}_{k+1}^i + \beta^i\ddot{v}_k^i)] \tag{10a}$$

$$p_{k+1}^i = \alpha^i(\frac{c-d}{c})\ [(M_s+M_u)g + k_y(y^b \pm l_i\phi^b \pm b\theta^b - \alpha^i v_{k+1}^i - \beta^i v_k^i) - M_u(\alpha^i\ddot{v}_{k+1}^i + \beta^i\ddot{v}_k^i)] \tag{10b}$$

Substituting equations (3), (4), (5) and (10) into equation (1) the following dynamic equation is obtained.

$$[M]_R\begin{bmatrix}\ddot{D} \\ \hline [\ddot{y}^b, \ddot{\phi}^b, \ddot{\theta}^b]^T\end{bmatrix} + [C]_R\begin{bmatrix}\dot{D} \\ \hline [\dot{y}^b, \dot{\phi}^b, \dot{\theta}^b]^T\end{bmatrix} + [K]_R\begin{bmatrix}D \\ \hline [y^b, \phi^b, \theta^b]^T\end{bmatrix} = [F]_R \tag{11}$$

where

$[D]$ = the vector consisting of vertical displacements of truss joints

$[M]_R$ = Mass matrix of bridge-vehicle system including interaction effect

$[C]_R$ = Damping matrix of bridge system

$[K]_R$ = Stiffness matrix of bridge-vehicle system including interaction effect. The stiffness matrix of the bridge is obtained by inverting the flexibility matrix.

$[F]_R$ = Time dependent force vector resulting from bridge-vehicle interaction.

The resulting equations of motion for the bridge vehicle system, (11), are solved using the following step-by-step procedure:

1) Establish a distance vector based on the configuration of axles and the distance between the vehicles. This vector stores the distances between wheel loads.
2) Calculate the position of the wheels and determine the wheel loads on the span.
3) For every load on the span determine its position with regard to the truss panel it occupies.
4) Compute α^i and β^i
5) Form $[M]_R$, $[K]_R$ and $[F]_R$
6) Compute static displacements at truss joints and stresses in truss members.
7) Calculate dynamic deflections using step-by-step numerical integration technique.
8) Compute dynamic load vector by [K] [D] where [K] is the stiffness matrix of the bridge.

Dynamic Response of a Single Track Truss Bridge

Using the formulation discussed previously, a computer program was developed to determine the dynamic response of a single track truss bridge subjected to a single or three moving vehicles system. The bridge analyzed is taken from reference [12] and the main geometry of the bridge is shown in Fig.3. Other relevant data, such as member properties of the bridge etc., and vehicle data is given in Appendix A.

The dynamic response for the single moving vehicle at 60 mph is obtained for two conditions, undamped and damped, using two percent structural damping. The dynamic response for the three moving vehicle system corresponds to the undamped condition at 60 mph. The vehicles are assumed to have no initial vertical motion at the time of entry into the bridge.

Time histories of the static and dynamic amplification factors for mid-span deflection and "worst case" member stresses are shown in Figs.4 through 8. The amplification factor Λ_d and Λ_s for dynamic (Γ_d) and static (Γ_s) response are defined as

$$\Lambda_d = \frac{\Gamma_d}{\Gamma_{sm}} \quad ; \quad \Lambda_s = \frac{\Gamma_s}{\Gamma_{sm}}$$

where Γ_{sm} is the maximum static response. The impact factor I is defined as $I=\max|\Lambda_d|-1$. Table 1 lists the impact factors for the bridge under damped and undamped condition for both single and three vehicle loading. It may be seen that the maximum impact factor for mid-span displacement is about 5% for a single vehicle without damping and 4% with damping. For the three vehicle system the impact factor is about 23%. This indicates that impact under multiple vehicle loading is significantly larger than the sum of the impact factors resulted from the individual vehicles. Similar observation can be made for member force impact factor, where a single vehicle under undamped condition generates a maximum impact factor of about 6.3% whereas the three vehicles case yields a maximum impact factor of about 26%. It should be noted that the member force impact factors are reduced by including structural damping into the system.

A limited parametric study has been performed for the dynamic response of the bridge under a single moving vehicle without structural damping. The study has been performed to establish the influence of vehicle suspension parameters, vehicle speed and sprung mass on impact factors. Fig.9, 10 and 11 show the results of this study. The impact factor for mid-span deflection is increased from about 3.5% to about 8% when the vehicle speed is increased from 40 mph to 80 mph. It may be noted from Fig.9 that as speed is increased from 60 to 80 mph the member force impact factor shows an increase of about 3%.

Fig.10 shows that a stiffer suspension system will result in larger impact factors as expected. Fig.11 indicates that impact factors are somewhat linearly proportional to the sprung mass of the vehicle.

Conclusions

Equations of motion for the bridge-vehicle system have been developed to analyse dynamic response of a single-lane truss bridge under a single vehicle or a three moving vehicle system. It has been found that the impact factors under the multiple vehicles are significantly larger than the sum of the impact factors due to individual vehicles. Incorporation of structural damping into the bridge system resulted in a reduction of the deflection and force impact factors. A limited parametric study shows that largest impact factors result at high speed with a stiff suspension system. Impact factor appears to increase linearly with respect to sprung mass of the vehicle.

References

1. T. Haung. Vibration of Bridges, Shock & Vibration Digest, Vol.8, No.3, March 1976 p.61-76.
2. A.S. Veletsos and T. Haung. Analysis of Dynamic Response of Highway Bridges, ASCE, J. Engr.Mech.Division, Vol.96, EM5, October,1970.
3. R. Willis. Appendix Report of the Commissioners Appointed to Inquire into the Application of Iron to Railway structures. Stationery Office, London, 1849.
4. S.W. Robinson. Special Report to the Commissioners of Railroads and Telegraphs of Ohio, for the year 1884-85.
5. S. Timoshenko. Vibration of Bridges. Trans. ASME. Vol.53, 1928.
6. C.E. Inglis. Mathematical Treatise on Vibrations of Railway Bridges. Cambridge University, Press.London 1934.
7. A. Schallenkamp. Schwingungen Von Tragen Bei Bewwgten Lasten. Vol.8, No.3, 1937. pp.187.
8. C.T. Looney. Impact on Railway Bridges. University of Illinois, Bulletin Series No.352 1944.
9. F.E. Turneaure, et al. Report of Committee on Impact. Proceedings, AREA Vol.12, Part II-1911.
10. J.B. Hunley. Impact in Steel Railway Bridges of Simple Span, as derived from tests made on the Cleveland, Cincinnati, Chicago & St.Louis Railway, 1931-34. Bulletin AREA, Vol.37, No.380. October 1935.
11. E.J. Ruble. Impact in Railroad Bridges. ASCE Proceedings, Separate No.736, July 1955.
12. L.C. Urquhart and C.E. O'Rourke. Design of Steel Structures. McGraw-Hill Book Company, Inc.New York, 1930.

APPENDIX A

Member Properties and Pertinent Data
For Single-Track Truss Bridge

Member	Section	Area (Gross)
Top Chord	cov.24" x 9/16"	
U_0U_1, U_1U_2	2-L3½" x 3½" x 5/8"	
	2-L3½" x 3½" x 5/8"	58.5 in^2
U_2U_3, U_3U_4	2-web 20" x 11/16"	
	Double Lat.2½" x ½"	
Bottom Chord		
L_0L_1, L_1L_2	4-L3½" x 3½" x ½"	36.63 in^2
L_4L_5, L_5L_6	2-web 21" x 9/16"	
L_2L_3, L_3L_4	4-L3½" x 3½" x 5/8"	63.51 in^2
	4-web 21" x 9/16"	
Intermediate Posts		
L_1U_0, L_2U_1	4-L6" x 4" x 3/8"	19.34 in^2
L_3U_2, L_4U_3	Web 13" x 3/8"	
L_5U_4		
Diagonals		
U_0L_2, L_4U_4	4-L6" x 4" x 11/16"	
	Web 13" x 5/8"	34.25 in^2
L_2U_2, U_2L_4	2[15x50	
	Double Lat.2½" x ½"	30.53 in^2
End Posts		
L_0U_0, U_4L_6	cov.24" x 5/8"	
	2-L2½" x 3½" x 5/8"	62.5 in^2
	2-L3½" x 3½" x 5/8"	
	2-Web 20" x 3/4"	
	Double Lat.2½" x ½"	

Wt. of each stringer = 6611 lbs.
Wt. of each cross beam = 4160 lbs.
Wt.of track system coming at each bottom chord joints - 65000 lbs.

Basic Data For a 4-Axle Railway Vehicle

Dimensional Data:

$\bar{b}$ -	Half length of wheel base	= 54 in (137 cms)
b -	Half distance between wheel contact points	= 29.5 in (75 cms)
L -	Half distance between truck centers	= 204 in (518 cms)

Mass & Inertia Data:

M^b	Carbody Mass	= 546 lbs-sec^2/in (247 kg)
	Truck frame mass	= 19.4 lbs-sec^2/in (8.7 kg)
M^u -	Wheel set mass	= 22.1 lbs-sec^2/in (10 kg)
I^b -	Carbody roll moment of inertia	= 1.2×10^6 lbs-in-sec^2 (1.36×10^{10} kg-cm^2)
J^b -	Carbody pitch moment of inertia	= 1.8×10^7 lbs-in-sec^2 (2.04×10^{11} kg-cm^2)

Spring Rates Data:

k_y - Vertical spring stiffness/wheel (Includes Primary & Secondary stiffness)	= 7,000 lbs/in (12,250 N/cm)
Distance from last wheel of front vehicle to the first wheel of rear vehicle	= 81.5 in (217 cm)

Table 1 - Maximum Axial Forces in Members of a Truss Bridge and Impact Factor in Percentages

Note: All Forces are in KIPS

Member Number	Member Forces Under dead load	SINGLE VEHICLE CASE			3 VEHICLE CASE				
		Max.Live Load Static Force	Undamped Bridge		2% Bridge Damping			Undamped Bridge	
			Max.L.L. Dynamic Force	Impact Factor	Max.L.L. Dynamic Force	Impact Factor	Max.L.L. Static Force	Max.L.L. Dynamic Force	Impact Factor
2 or 3	76.35	82.06	84.38	2.83	83.19	1.4	158.2	186.7	18.02
4 or 5	139.6	139.6	145.9	4.51	141.3	1.22	274.5	342.3	24.7
6 or 7	76.35	81.62	86.37	5.82	84.63	3.69	159.1	190.1	19.48
8	19.79	54.3	54.88	1.07	54.82	0.96	90.46	108.0	19.39
9	69.66	92.42	94.44	2.19	94.36	2.1	154.5 -11.95	181.4 -16.4	17.41 -
11	-23.74	34.15 -63.62	35.65 -66.18	4.39 4.02	35.04 -66.03	2.6 3.8	34.98 -77.86	35.82 -87.48	2.0 12.36
12	22.68	54.99	58.48	6.3	56.61	2.95	90.46	102.0	12.76
13	-23.74	34.7 -65.96	29.79 -69.24	4.9	32.87 -67.79	2.77	34.93 -79.01	36.77 -85.7	5.0 8.48
15	69.66	91.77 -11.73	94.94 -7.814	3.45	95.2	3.73	154.4 -8.99	188.5 -16.4	22.09 -
16	19.79	55.26	56.77	2.73	55.89	1.14	90.46	114.0	26.0
18 or 19	-123.5	-128.9	-131.9	2.33	-130.1	0.93	-252.0	-308.9	22.58
20 or 21	-123.5	-128.7	-130.4	1.32	-129.8	0.77	-252.0	-312.8	24.13

Figure 1. Idealized vehicle model.

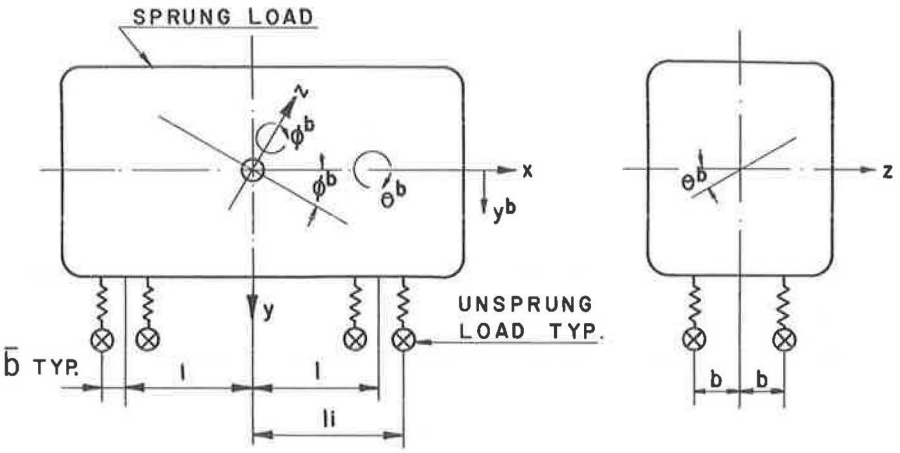

Figure 2a. Plan view of configuration of wheel load in a panel of bridge span.

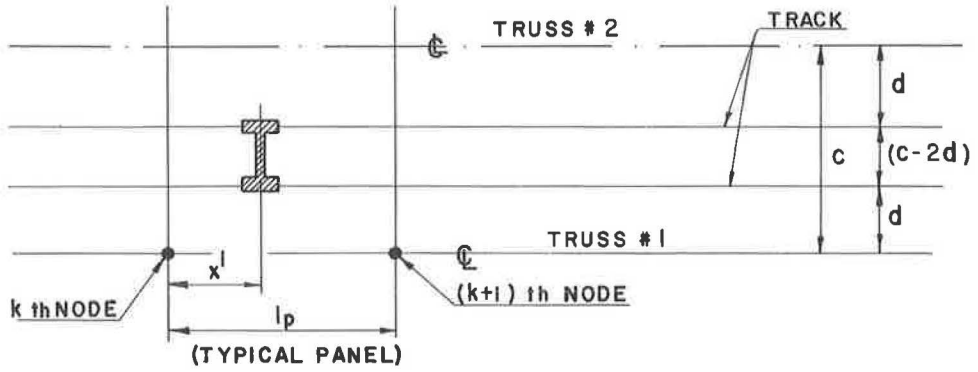

Figure 2b. Conversion of wheel loads into joint loads.

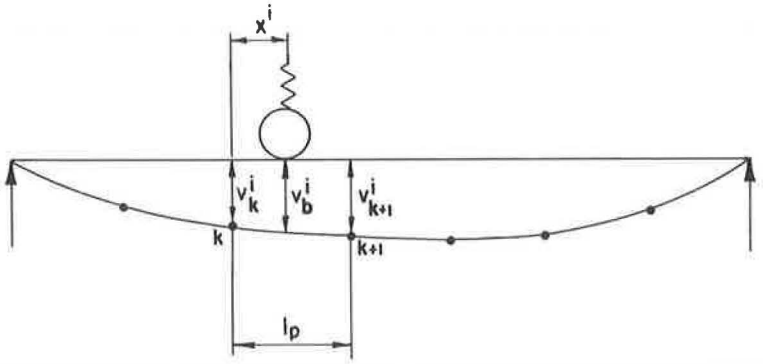

Figure 3. Geometry of the bridge and masses concentrated at each joint.

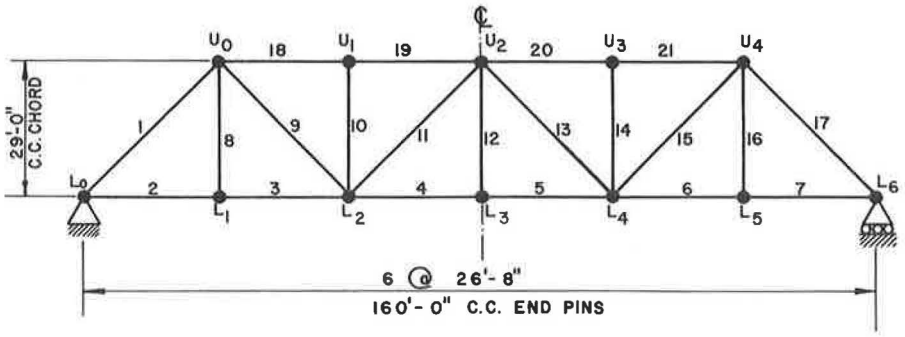

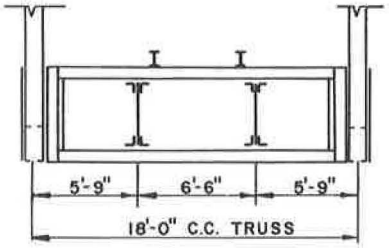

Figure 4. History curves of mid span deflection of truss bridge w/o damp.

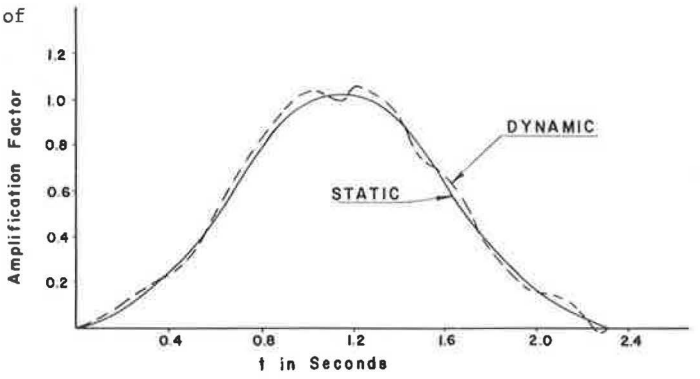

Figure 5. History curves of mid span deflection of truss bridge w/2% damping.

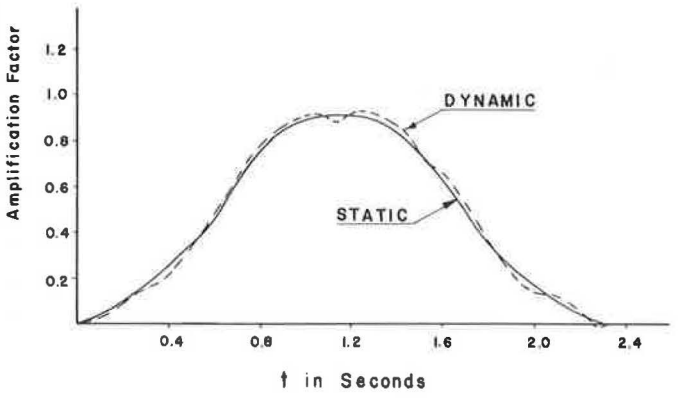

Figure 6. History curves of stress in member U_2L_3 w/one vehicle.

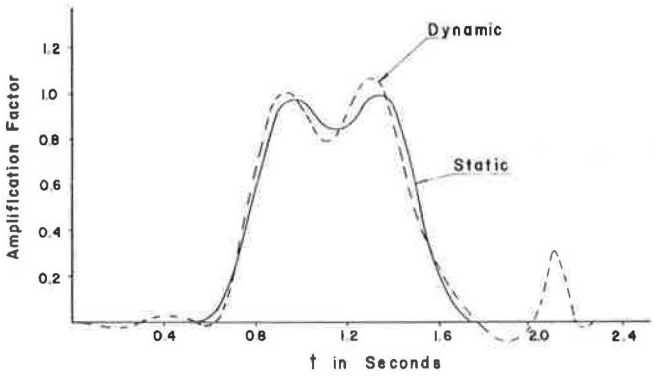

Figure 7. History curves for mid span deflection for single track truss bridge w/3 vehicles w/o damping.

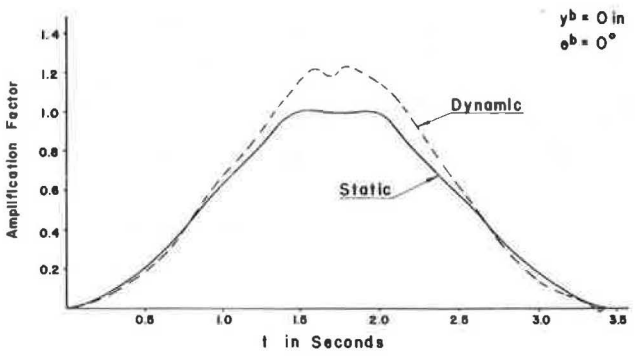

Figure 8. History curves for forces in member L_5U_4 w/3 vehicles w/o damping.

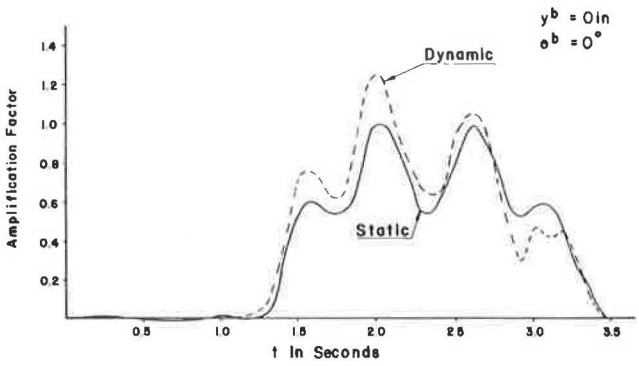

Figure 9. Impact percentage versus speed of vehicle (single vehicle on bridge).

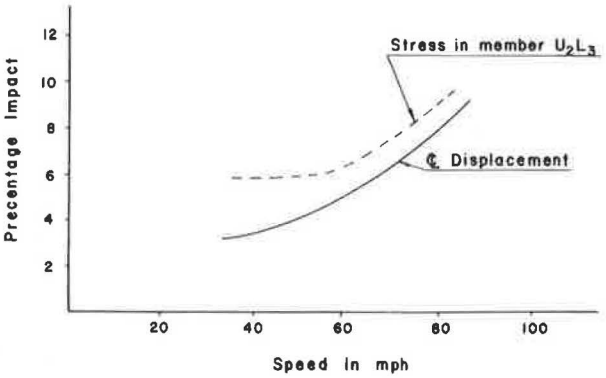

Figure 10. Impact percentage versus spring stiffness (single vehicle on bridge).

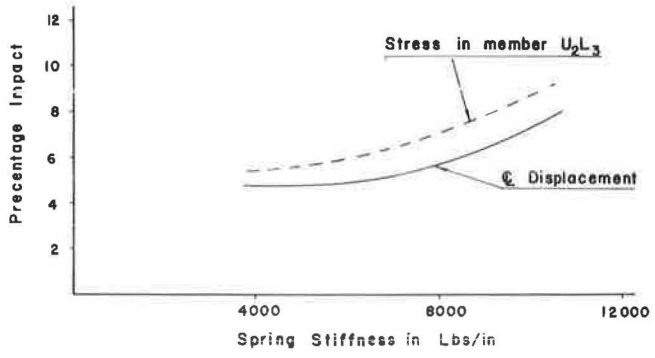

Figure 11. Impact percentage versus sprung load (single vehicle on bridge).

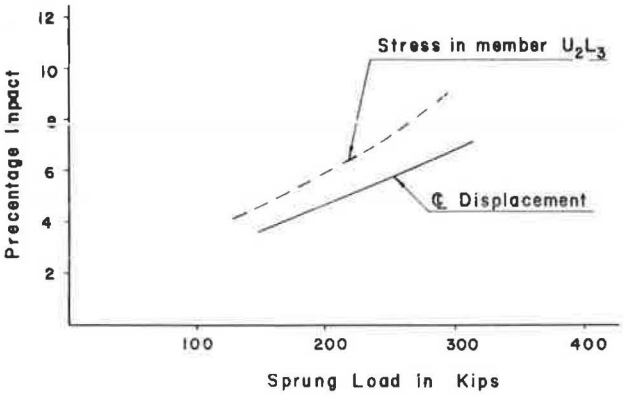

ANALYSIS AND TESTING OF A TRAPEZOIDAL BOX GIRDER BRIDGE

Michael Holowka, Ontario Ministry of Transportation and Communications

Bridge construction using open steel box girders and a concrete deck slab acting composite is aesthetically pleasing and ideally suited for grade separations and river crossings for spans varying between 21 m and 110 m (70 ft. and 360 ft.). Current design specifications for this construction, however, are considered to be incomplete and do not provide sufficient guidance during construction. In a number of cases, due to lack of bracings and/or diaphragms, excessive displacements have occurred during construction. To clarify this problem, a typical, single span, 2-lane bridge was extensively instrumented and tested. The purpose of the testing program was to investigate the behaviour of a torsionally stiff bridge during and after construction and to compare the experimental data with analytical results. The concrete deck, which was constructed with 0.3% isotropic reinforcement rather than 1.0% orthotropic reinforcement to comply with the AASHTO Specifications, was also monitored. Test data consisted of structural and reinforcing steel strains, deflections, reactions for construction, and live load and temperature effects. The experimental deck was constructed in two stages. A preliminary review of the data indicated that, for this bridge geometry, construction effects were within the predicted values as no excessive deflections or strains were observed. The concrete deck with the dramatically reduced reinforcement was adequate for modern highway traffic provided sufficient diaphragms were present. The overall structural behaviour can be accurately predicted by analysis and, with diaphragms present, can be analyzed by beam theory and proper load distribution factors.

Ontario's recent use of steel box girders with a concrete deck acting composite has produced several unique problems during and after bridge construction. It was decided that monitoring the structural response of a typical, 2-lane bridge would allow the engineer an opportunity to compare the actual bridge behaviour with the design specifications. The bridge chosen for study was the first deck having 0.3% isotropic reinforcing steel in both directions for the entire bridge length. The deck was constructed in two lifts; the second being a concrete overlay.

The testing of the bridge was multi-fold and included the following:

1. Measurement of reaction forces and structural steel strains due to dead load, temperature and live load.
2. Measurement of reinforcing steel strains due to live load.
3. Measurement of strains in the cross-bracing and intermediate diaphragms due to live load and temperature.
4. Determination of the existence of bond between the two concrete lifts.
5. Measurement of concrete deck displacements due to concentrated wheel loads.
6. Comparison of test data with analytic results whenever feasible.

Temperature and construction cross-bracing effects on overall slab behaviour are not discussed in this report.

Description of Bridge

The West Arm Lake Nipissing (North Branch) Bridge is located in Ontario approximately 50 km (30 mi.) southwest of Sturgeon Falls on Highway 64. The 2-lane bridge, spanning a navigable waterway, is a simply supported structure 42.7 m (140 ft.) long and 10.4 m (34 ft.) wide. The roadway width is 8.5 m (28 ft.) and the two curbs and barrier walls are 0.9 m (3 ft.) wide. The bridge has zero skew and no superelevation except for a 2% standard crossfall. (Refer to Figure1.)

The bridge superstructure consists of two trapezoidal steel box girders composite with the concrete deck. The steel girders consist of atmospheric corrosion resistant structural steel with a specified yield point of 345 MPa (50 ksi). The top flanges of the girders are at 2.54 m (8 ft. 4 in.) centers with a bottom flange width of 1.83 m (1 ft. 0 in.). The webs are inclined at a 12^{o} angle and have a vertical depth of 1.63 m (5 ft. 4 in.). Plate diaphragms at each abutment and five intermediate cross-bracings at 7.1 m (23 ft.) centers are also present.

The overall thickness of the deck is 200 mm (8 in.) and consists of a 150 mm (6 in.) first lift and a 50 mm (2 in.) concrete overlay. The two layers were bonded together with a cement/sand slurry. All reinforcing steel is contained in the first layer. The second layer, consisting of a high quality

concrete, is expected to provide protection for the reinforcing steel against corrosion. This deck is part of the Ministry's experimental project on developing self-protecting, durable bridge decks. Corrugated stay-in-place formwork was used inside the steel boxes except for a 6.1 m (20 ft.) section at mid-span of the east box girder. At this section between the two boxes and for the cantilever, normal plywood forms were used. AASHTO (1) and CSA (2) design specifications were used for the entire bridge design except for the concrete deck. (Refer to Figure 2.)

The reinforcing steel requirements for the deck were based on the proposed specification of the Ontario Highway Bridge Design Code. The reinforcing consists of 15 mm (#4) bars at 254 mm (10 in.) centers in both longitudinal and transverse directions. This is equivalent to four layers of 0.3% isotropic steel. This percentage is based on an effective depth of 165 mm (6.5 in.). The reinforcing steel requirement for the 1.37 m (4 ft. 6 in.) cantilever part of the deck follows the current AASHTO Specifications.

Instrumentation

The bridge was thoroughly instrumented to monitor reactions, strains, deflections and temperatures during various stages of the testing program. Deflection meters, optical levelling equipment, electrical and mechanic strain gauges, load cells and thermocouples were employed.

Load Cells

Load cells were used to temporarily replace the normal bearings for the duration of the test program. These load cells in the form of a barbell were available prior to the start of the project. Appropriate fixing hardware was fabricated to permit their proper installation. The load cells, as shown in Figure 3, provided a positive connection between the superstructure and the bearing plates. Consequently, the uplift forces as well as the normal reaction forces could be monitored. The individual cells had a vertical load capacity of 1780 kN (400 kips) in compression and 1110 kN (250 kips) in tension. The load cells could record both vertical and horizontal forces; however, only vertical forces were measured. The south bearings were fixed while the north bearings were free to move in the longitudinal direction to accommodate ambient temperature changes.

Reinforcing Steel Strain Gauges

The reinforcing steel strains were monitored by two 90^{o} T-rosettes mounted on a ground section of the rebar and wired to form a 4-arm wheatstone bridge. The gauge centerlines were located around the circumference of the bar 180^{o} apart. By this arrangement, only axial forces in the bars were measured.

Grinding to prepare the bars for strain gauging application resulted in a non-uniform reduced cross section. Consequently, each bar had to be individually calibrated. A plot of load versus strain output was obtained for each bar from which a strain reduction factor was determined to account for the variability of the cross section. This calibration assumed the normal initial sectional area as specified for that particular bar size. The reinforcing steel was strain gauged in the Ministry's laboratory and then properly positioned in the deck. A total of 14 locations were monitored. Four traverse bars, two top bars and two bottom bars were monitored at four locations. The two longitudinal locations were at the centerline of the span and 3.8 m (12 ft. 6 in.) south of the centerline of the bridge, respectively. The transverse positions were at the longitudinal centerline of the bridge over both top flanges of the east girder and at the center of the east girder. Four longitudinal bars, two top bars and two bottom bars were also monitored at the mid-span and 3.8 m (12 ft. 6 in.) south of the centerline. The bars were located at the longitudinal centerline of the deck and at the centerline of the east girder. Four cantilever bars were also monitored.

Bond Indicators

With the two-stage construction technique, there was a need to determine if the bond between the two lifts of concrete was stable when subjected to a heavy concentrated wheel load. Precast concrete cylinders 50 mm (2 in.) in diameter were strain gauged and the gauged section was subsequently located at the interface between the base course and the overlay. The 50 mm strain gauge was oriented along the vertical axis of the core.

After construction of the deck, 50 mm (2 in.) diameter holes were drilled at predetermined locations in the deck. The bond indicator was inserted and then bonded with epoxy to the existing concrete. This indicator shows only if a bond is present or absent between the two concrete layers. Provided the strain gauge is working, the bond exists. If the two layers separate, the cylinder breaks and the strain gauge stops functioning.

The 10 bond indicators placed in the concrete deck were located 4.57 m (15 ft.) to 21.34 m (70 ft.) from the south abutment and in both the positive and negative transverse moment zones.

Deflections

An Ni-1 Carl Zeiss level was employed to monitor deflections. Special level rods were suspended from the underside of the bridge at the quarter span, three-eighths span and mid-span. The rods were located across the width of the bridge to provide a transverse deflection profile at these locations.

Structural Steel Strain Gauges

A total of 68 uniaxial strain gauges were installed to monitor strains in the structural steel. The gauge configuration was chosen so that only strains in selected directions were measured. A single active arm of an SR4 gauge, type FAE-50-1256 (G.F. = 2.06 ± 1%, 120.0 ± 0.2 ohm), was used with a 3-arm bridge completion tab. All gauges were applied at the structural steel fabricators shop prior to erection. Figure 4 shows the location of the gauges.

The trapezoidal box girders were instrumented at mid-span only. The east girder (site 1E) was heavily gauged at 12 locations with 34 strain gauges. The inside and outside of each girder were instrumented so that bending and axial forces could be monitored. Longitudinal strains were monitored with 18 gauges, transverse strains with 16 gauges. The west girder site 1W was instrumented with 10 gauges on the inside of the girder to check the symmetrical behaviour of the girders.

Cross-bracing strains were monitored at seven locations with 24 strain gauges. Cross-bracings were instrumented inside the girders and between each girder at mid-span and at 7.11 m (23 ft. 4 in.) from the south bearing, as shown in Figure 4. The

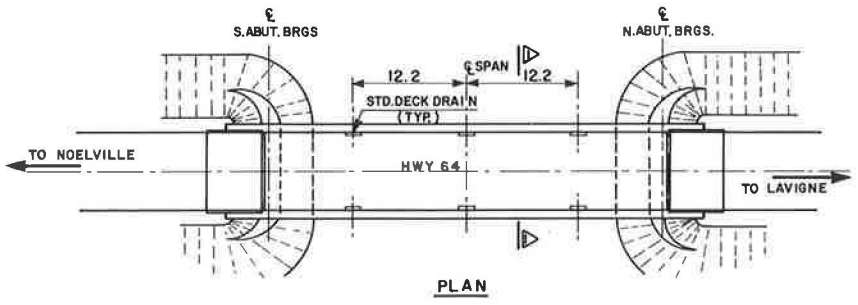

Figure 1. General layout of the West Arm Lake Nipissing Bridge.

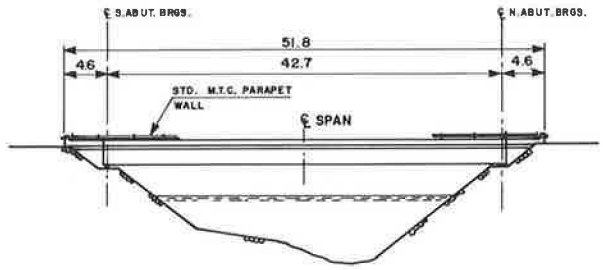

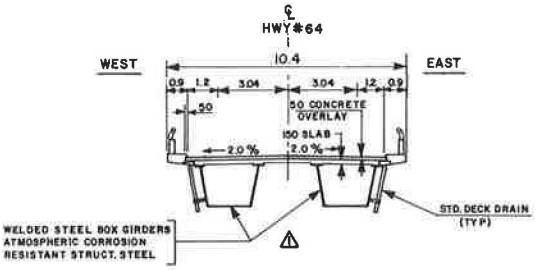

Figure 2. Cross section of bridge.

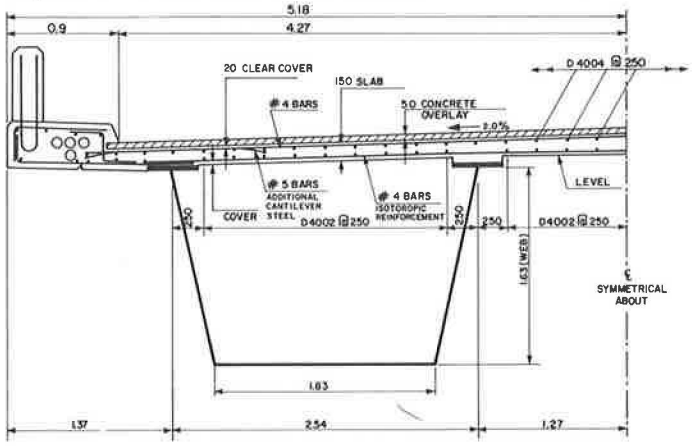

Figure 3. View of installed load cells.

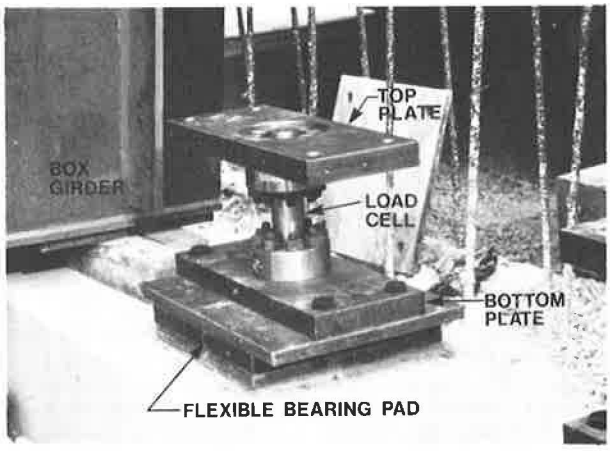

Figure 4. Plan view of location of strain gauges on structural steel.

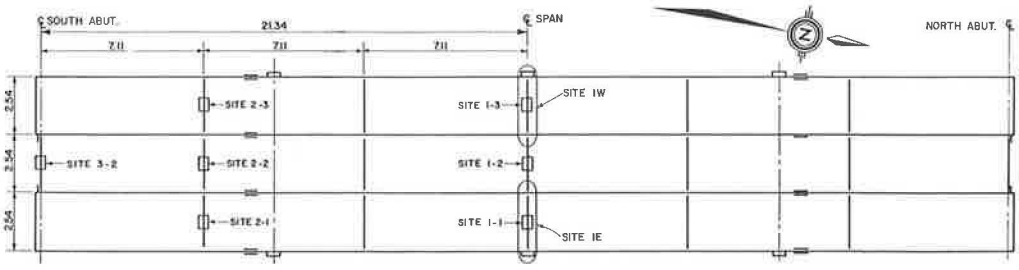

Figure 5. Overall view of test vehicles.

diaphragm at the south abutment between the two girders was also monitored with 6 strain gauges. This diaphragm consisted of a wide flange steel beam plus 3 steel angles. Each angle, both flanges and the web of the beam were instrumented.

Thermocouples

Twenty-three thermocouples were installed to monitor the temperature gradient through the whole cross section of the bridge at the mid-span. Additional thermocouples were employed to measure the ambient air temperature. The thermocouples were located inside the steel box girder and on both the top and bottom faces of the concrete deck.

Data Acquisition System

The data acquisition equipment used to monitor strain gauges and load cells was a 100-channel system which sequentially scans, measures and stores data in a memory buffer. The system was specially designed for the Ministry by Vidar Autodata Inc. and is Type Autodata 5600. The system is permanently housed in a mobile testing van.

During the testing, the information stored in the memory buffer was processed. A hard copy of the data was available for data analysis and reference during testing. Simultaneously, a punched paper tape with the data in binary format was produced which could subsequently be used for computerized data reduction. The PDP-8 mini computer of the system converted all strain data to engineering units of stress, load etc., via separate calibration factors for each input channel.

Test Loading

The two test vehicles used were 5-axle tractor semi-trailer combinations (Figure 5). The magnitude of the axle loads could be varied by placing on the trailer concrete ballast blocks each weighing 9.5 kN (2.125 kips). The number and position of blocks controlled the axle weights with a maximum gross vehicle weight of approximately 890 kN (200 kips).

Four load levels ranging in gross test vehicle weight from 490 kN (110 kips) to 890 kN (200 kips) were used to monitor the linearity of structural responses to incremental loading. With this setup, test data could be immediately examined at the lower loads to determine if any overloading would occur and to provide a warning signal against unexpected failures. Axle weights are given in Table 1.

Numerous static load tests were carried out with the test vehicle in different longitudinal and transverse positions to cover significant and governing design cases. Figure 6 shows the eight longitudinal line configurations and Figure 7 the six load locations along the length of the bridge. These were designed to provide concentric and eccentric loads and checks on symmetry by employing one and/or two trucks per lane. Generally, load location 4 gave the maximum overall flexural effect. Deflections, strains and reactions were monitored for 48 load positions for each load level.

The concrete deck was tested to measure the response of the concrete slab to a concentrated point load. A concentrated point load of 445 kN (100 kips) was applied to the deck at 14 different locations. The point load was applied by an hydraulic ram through two neoprene pads 250 mm by 250 mm (10 in. by 10 in.) in size, which model the effective footprint of a dual tire wheel. The load was positioned along a top flange, the centerline of the bridge and the centerline of the east girder. The reinforcing steel strains, the localized concrete deck deflections and the applied load were simultaneously monitored.

Test Results and Comparison

Static Load and Reactions

The individual reactions at both north and south abutments were monitored for all load locations and load levels. Table 2 gives the total reaction for both the south and north ends for load level 3. This value is the algebraic sum of the four load cells at each end. Table 2 also shows the total reaction at each support by assuming the bridge to be a simply-supported beam. The maximum deviation between theoretical and experimental values was 53.4 kN (12 kips) except for line 5, load location 4. In most cases, the experimental values were less than the theoretical results. On the average, test data were approximately 5% lower than expected. There are a number of possible sources of error to explain this variation such as calibration error, vehicle weight and location error, lead wire attenuation error and the transfer of load to abutment through barrier wall, guardrail or deck expansion joint.

The maximum observed reaction at load level 3 due to one vehicle loading or one vehicle per lane loading was 445 kN (100 kips), and was caused by one lane loaded with the vehicle adjacent to the east curb. This represents 73% of the total end reactions produced by the loading. The current design practice in Ontario is to distribute the load in equal proportions to each bearing; in this case 50%. This practice may seriously underestimate the actual reactions by approximately 50% and consequently cause overloading in the bearing. By using 75%, the revised design dead load plus the live load of 868 kN (195 kips) would just overload the bearings originally proposed which had a capacity of 846 kN (190 kips). The Quest program (3) adequately predicts within 10% the maximum reaction for a bearing.

Figure 8 illustrates the distribution of reactions at a girder end for the eccentric load case of line 2 and the concentric load case of line 5 for load level 4. It can be seen that reactions are not uniformly distributed and in fact are governed by one vehicle positioned adjacent to the curb. This maximum reaction is approximately 20% greater than that due to a uniform distribution of reactions caused by a single vehicle per lane loading. Figure 8 also shows the analytical reactions from the Quest program (3) for load location 4.

Deflections

Typical deflection data at the centerline of the span are shown in Figure 9. Due to time and weather limitations, only load levels 1, 2 and 3 at various selected locations were monitored for deflection. A total of 11 readings at each test section were taken. For symmetric loading the deflection was constant across the section; an example is test 3-4-4. For eccentric loading, the deflections were linear; an example is test 1-6-4. This linearity of deflection is believed to be the consequence of the high torsional rigidity of the closed sections.

The comparison between experimental and theoretical results indicate a good correlation. In all cases, the analytical deflections were numerically greater than the experimental ones; however, the pattern of deflections was identical. This discrep-

Figure 6. Longitudinal line locations.

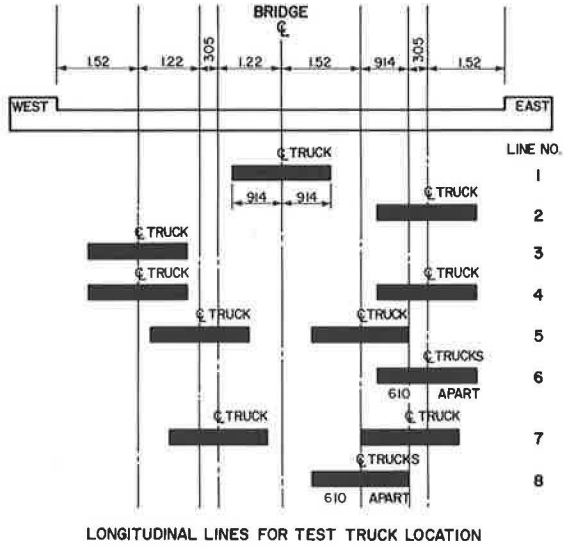

Figure 7. Load location along the length of the bridge.

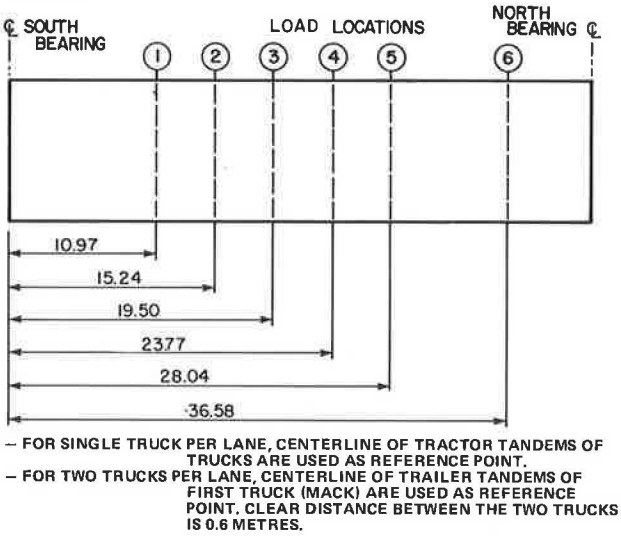

Figure 8. Plot of individual reactions for various loadings.

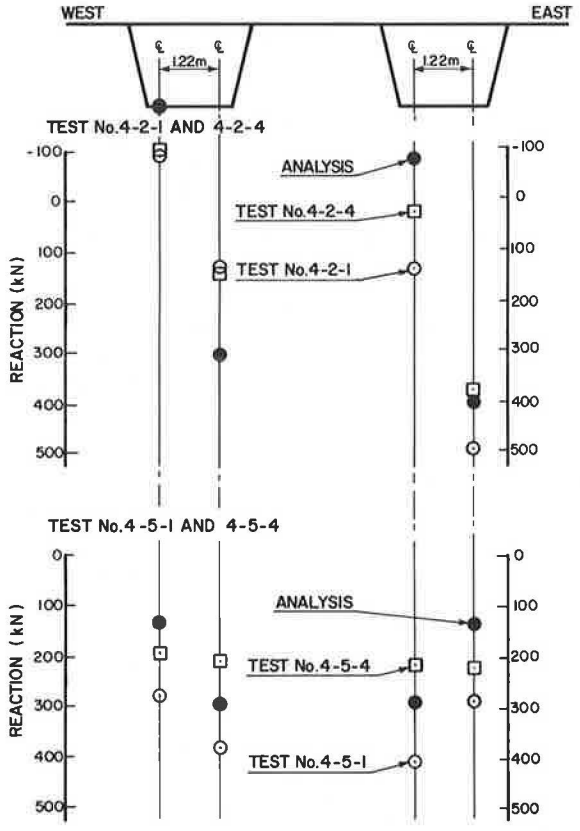

Figure 9. Transverse deflections at centerline of span.

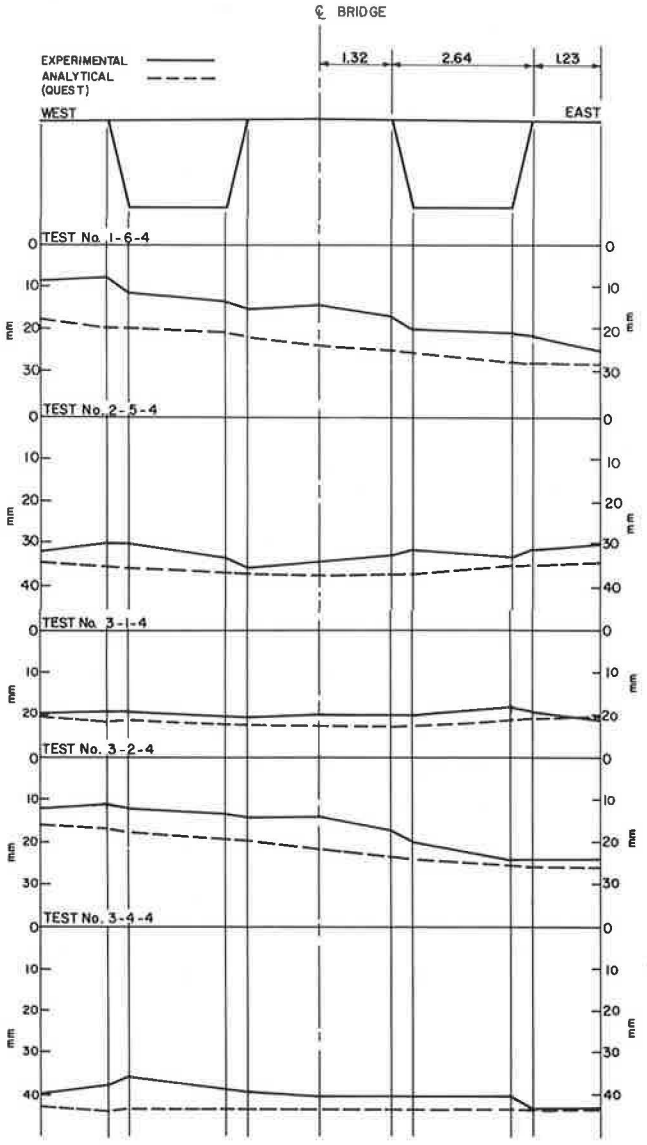

Table 1. Axle weights of testing trucks.

Load Level	Load Values (Kenworth) kN				Load Values (Mack) kN			
	Total	Front Axle	Tractor Tandem	Trailer Tandem	Total	Front Axle	Tractor Tandem	Trailer Tandem
1	500.2	53.4	223.8	222.9	504.6	64.1	218.9	221.2
2	629.2	51.6	282.1	294.1	655.5	67.6	291.9	295.9
3	769.4	54.7	358.2	356.4	778.8	70.3	353.3	355.1
4	892.7	57.9	417.4	417.4	911.8	73.0	420.1	418.7

ancy could be eliminated by assuming a modulus of elasticity for the concrete greater than that based on 27 600 kPa (4000 psi) compressive strength or by normalizing the deflections.

Twenty-eight day cylinder results indicated an average compressive strength of approximately 34 450 kPa (5000 psi), thereby confirming the above assumption.

Cross-Bracing Strains

The instrumented cross-bracings were monitored during construction and load testing. The maximum strain observed during construction of the 6-inch base course of the deck was 150 microstrain. This represents a maximum stress of 29 000 kPa (4350 psi). Only the horizontal members showed any strains; strains for the diagonal members were essentially zero. Immediately after placing the concrete, the strains varied between 35 and 150 microstrain. At the end of the monitoring period, 24 h after the finish of the pour, the strains ranged between 0 and 60 microstrain. The bracing at the south abutment showed the largest variation in strain (+150 to -100 microstrain). It can be concluded that only minimal bracing is required for this typical 2-lane bridge.

During the live load testing and with the construction bracing in place, the maximum observed strain was 218 microstrain or a stress of 43 600 kPa (6300 psi) in tension. Maximum compressive stress was 39 600 kPa (5700 psi). With the construction bracing removed, the maximum observed cross-bracing stresses showed no significant change from the observations with the construction bracing in place. This was expected since the construction bracing was required only during the deck placing to compensate for possible eccentric construction loading since the individual boxes would be torsionally weak at this stage.

Structural Steel Strains

The trapezoidal box girders were monitored at mid-span for steel strains in both the longitudinal and transverse directions for all the load positions outlined in Figures 6 and 7. The observed strains were then compared with theoretical results obtained from the Quest program (3). In all cases the correlation between the experimental and theoretical longitudinal strains was very good. For brevity, only a limited number of results and comparisons are presented in this paper.

The Quest program was developed in England by the Ministry of Environment for the linear elastic analysis of box girder bridges using the finite element method. The box girder bridge was modelled by quadrilateral thin shell finite elements which are capable of simulating membrane and flexural behaviour. The program considers six degrees of freedom at each node of the element mesh. The input consists of the overall geometry of the bridge, the material properties, and the loading and boundary conditions. The output includes nodal displacements, boundary reactions, and element nodal stress resultants and extreme fibre stresses.

A total of 263 nodes and 293 elements were used to model the bridge. The effect of the barrier wall and curbs was also included by approximation of the cross section. The analysis was performed for girders with and without constructing bracing and indicated that there was no significant difference in the strain levels of the trapezoidal girders under live load.

Figure 10 shows typical longitudinal strain results for various load positions. A comparison of results at the centerline of the span with the test vehicles at load location number 4 is available. Only the final load level number 4 results, corresponding to total truck loads of approximately 900 kN (202.5 kips), are shown. Results from load levels 1 to 3 were used to indicate linearity with load. Linearity was excellent and consequently the lower level loading showed the same distribution and comparison of strain except for smaller magnitudes. Strain data is shown in: 10a for one truck concentric; 10b for one truck eccentric; 10c and d for two trucks side by side with one truck per lane; and 10e for two trucks per lane eccentric. In Figures b, c, and e, the truck is adjacent to the curb.

The strain data for both exterior and interior surfaces of the steel box is given. The analytical results are indicated by a solid line. The maximum observed strain due to live load was 385 microstrain or 76.9 MPa (11,200 psi) and occurred when both lanes were loaded with one truck each. This represents a symmetric loading and consequently the load is uniformly distributed across the width of the bridge. With only one truck on the bridge, the maximum observed strain was 237 microstrain or 47.4 MPa (6,900 psi) and corresponded to 62% of the maximum observed strain caused by two trucks.

In most cases the longitudinal strains measured in the web showed good agreement with theoretical predictions. The largest strain discrepancies occurred at the top flange. This was perhaps due to the fact that the corresponding nodal point was at mid-depth of the concrete deck in the idealization procedure. This change in location for theoretical and experimental points probably caused the strain differences.

Based on the experimental strains, the load distribution factor for this bridge may be considered to be one lane per girder. The corresponding AASHTO distribution factor for the bridge is specified as 2.225 times a wheel load. This is equivalent to 1.113 times a truck or lane loading and consequently overestimates the actual distribution by about 11%.

Further investigation was made to determine the effect of the barrier wall on the longitudinal steel strains. Figure 11 shows the effect of the barrier wall for two load cases. Figure 11a shows the barrier wall effect when the bridge is loaded by the critical governing load case, while Figure 11b shows the barrier wall effect when the bridge is subjected to an eccentric load. For the critical load cases and with no barrier wall, the strains increased by an average of 11.75% for both box girders. For the eccentric load, the strains increased by 10% for the west girder and by 16% for the east girder. It should be noted that the barrier walls had no significant effect on the pattern of load distribution for the governing load location.

Using the standard Ministry design program and design approach, the maximum stress due to one test vehicle per lane was 95.4 MPa (13.85 ksi). The maximum observed strain and hence stress was 76.9 MPa (11.2 ksi). If the observed values are increased by 10% to account for the barrier wall effect, the maximum observed stress is 11% lower than the stress based on design assumptions. This is acceptable and indicates that simple beam theory, with the correct section idealization plus the correct distribution factor, can be used to accurately design this type of bridge.

Figure 10. Structural steel box girder longitudinal strains.

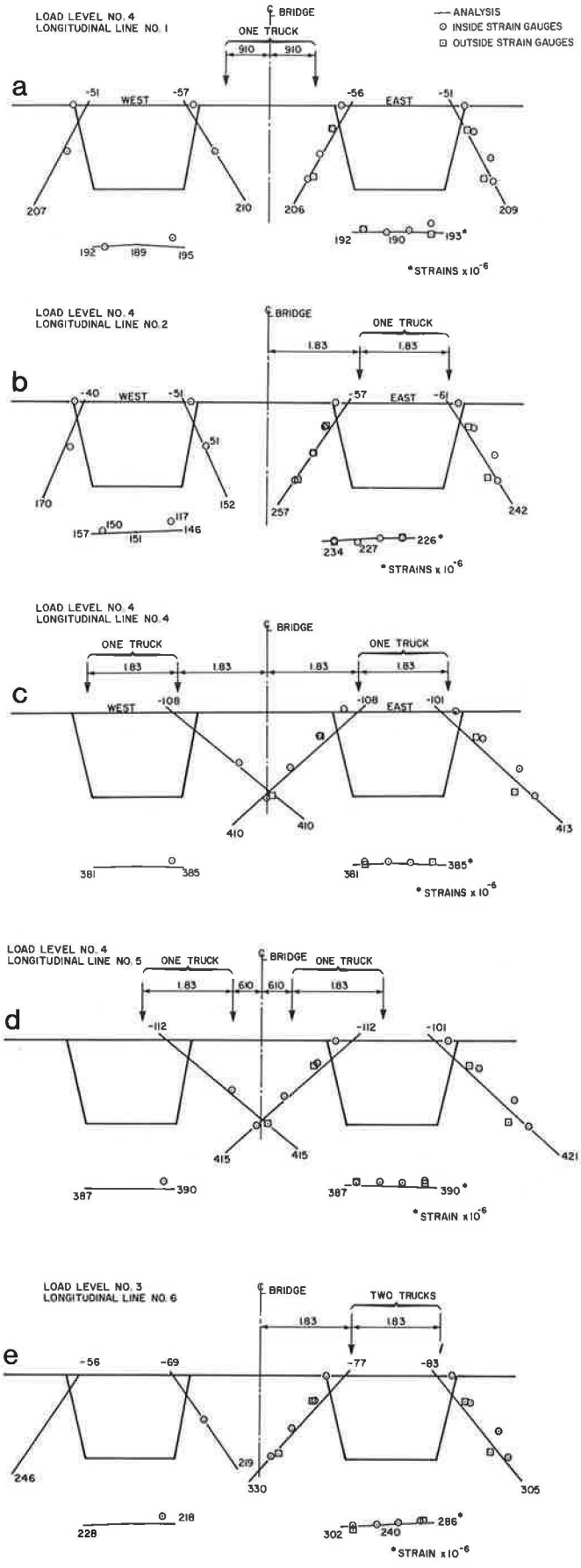

Figure 11. Effect of barrier walls on longitudinal strains.

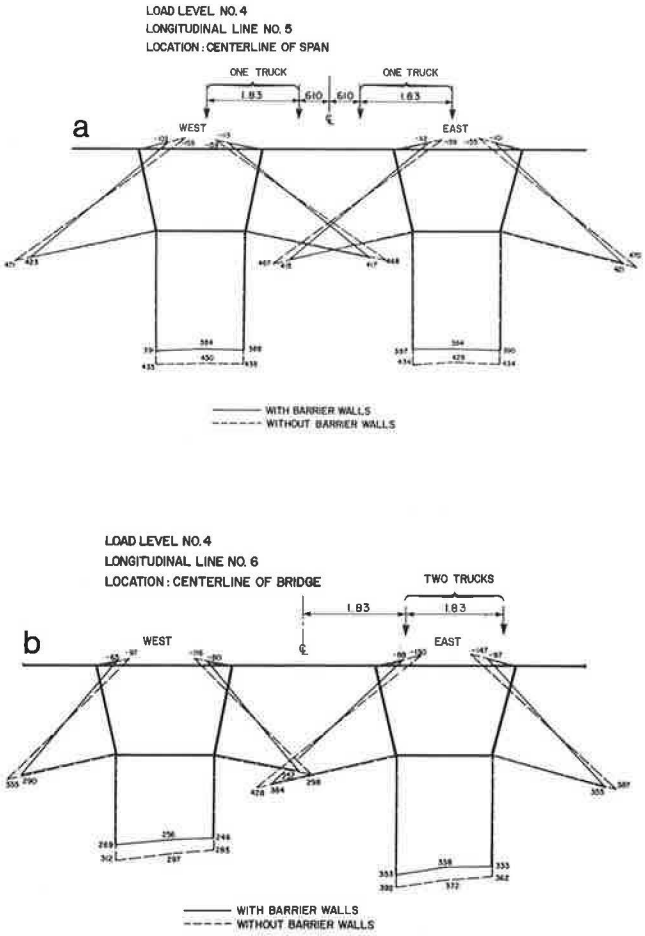

Concrete Deck

The deck was tested to evaluate the bond between the two concrete lifts and to monitor the behaviour under a concentrated load.

Ten locations were tested with the 445 kN (100 kips) concentrated load. The load was applied adjacent to the bond indicator gauges which were continuously monitored during testing. No failure of any gauge occurred thereby indicating the absence of any bond failure. After the completion of the overall load tests, these gauges were again checked and found functioning; thereby, indicating no loss of bond between the two concrete lifts.

Typical load versus deflection plots are given in Figure 12. The load is plotted on the vertical axis with the vertical displacement on the horizontal axis. The vertical displacement at the centerline of the two pads was continuously measured as the load was applied. This vertical displacement was measured with respect to the displacement rig supports which were remote from the concentrated load and generally located directly over the top flanges of the box girders. The load was cycled between 0 and 445 kN (100 kips) until the load deflection curve was repeatable. As Figure 12 shows, the number of load cycles required was 3 to 4. The initial loading cycle was offset minimally due to initial microcracking of the concrete deck so that internal arching action could be developed.

The load/deflection plot of Panel 1-3 was typical of the concrete deck, with stay-in-place formwork between the top flanges of a box. Panel 1-4 was typical of the concrete deck, without stay-in-place formwork, between the top flanges of a box. The load/deflection curve of the concrete deck between the two boxes was between the two plots given in Figure 12. Table 3 lists the vertical deflection under the concentrated load for six positions along the span for the concrete deck spanning between the boxes and spanning from top flange to top flange of the east box. The deflections ranged from 0.737 mm to 1.88 mm (0.029 in. to 0.074 in.). This corresponds to a span/deflection ratio of 1350 to 3450. The two panels corresponding to the design assumptions indicated restraint factors, based on deflections, of between 0.75 and 1.0. The design process assumes a minimum restraint factor of 0.50.

The only difference in the bridge between the November 1976 and May 1977 tests was the removal of the construction cross-bracing between the two box girders. The average difference in the vertical deflection under the concentrated load between the two series of tests was 1.6% (Table 3). Therefore, no significant difference existed between the two tests. Consequently, the construction cross-bracing did not affect the behaviour of the slab with respect to isolated wheel loads.

Approximately 3 months after the load testing of May 1977, a hairline crack appeared in the concrete overlay adjacent to the interior top flange of the west girder. The crack extended 20 m (65 ft.) and from approximately quarter span to quarter span. This crack had not been visible at the time of load testing.

Subsequent analysis of the bridge, with and without the construction cross-bracing, indicated that maximum concrete stresses in the order of 3240 kPa (325 psi) could be developed at the above location once the cross-bracing had been removed (Figure 13). These stresses were caused by a test vehicle at load level 4 adjacent to the east curb and barrier wall. For the same load but with the construction cross-bracing in place, maximum concrete strains of only 1100 kPa (160 psi) could be expected above the interior top flange of the west girder. Stresses at the crack location increased by approximately 100% when the construction cross-bracing was removed.

Consequently, the cross-bracing between twin box girders should have been left in place to achieve a crack free concrete deck.

Reinforcing Steel Stresses

Reinforcing steel stresses in both the longitudinal and transverse direction were monitored at 17.56 m (56.5 ft.) and 21.34 m (70 ft.) from the centerline of the south bearings. For the concentrated wheel load testing, significant reinforcing steel stresses occurred only when the load was at the same location as the gauges. Maximum observed transverse reinforcing steel stresses were 128 MPa (18.64 ksi) and longitudinal stresses were 100 MPa (14.5 ksi). Maximum reinforcing steel stress in the top steel over the top flanges was found to be negligible. The above stresses were caused by a 445 kN (100 kips) simulated wheel load. These reinforcing steel stress levels were less than that permitted by the AASHTO Specifications for working stress design even though the load was 4.8 times greater and the reinforcing steel quantity approximately 3 times less. This is another indication that deck slabs do not behave as assumed in design but rather by internal arching action (4).

The deck exhibited similar responses to a concentrated wheel load similar to the test panels of the Conestogo River Bridge (5).

Reinforcing steel stresses were also monitored during the load testing portion of the overall program. With the bridge loaded with two 890 kN (200 kips) trucks, the maximum reinforcing steel stresses observed were 68.9 MPa (10 ksi) in tension and 20.7 MPa (3 ksi) in compression. For this bridge, the testing of the slab with the concentrated wheel load was a more severe case than with the overall heavy truck loads.

Conclusions

1. For this type of cross section, no eccentric construction loading was present and consequently no substantial construction cross-bracing strains were observed, indicating that only minimal construction bracing is required.
2. With the two-stage concrete deck construction technique, only a good natural bond between the two layers is required to prevent slip at their interface.
3. The concrete deck with 0.3% isotropic reinforcement is adequate for modern highway loading. However, to prevent longitudinal deck cracking over the top flange, the construction bracing of the type used for this bridge should be left in place.
4. Deflections, reactions and stresses can be adequately predicted by proper analysis (3). It appears that beam theory and correct distribution factors are adequate for the design of bridges similar to the bridge geometry tested.

References

1. AASHTO. Standard Specifications for Highway Bridges. American Association of State Highway and Transportation Officials, eleventh edition, 1973.
2. CSA. Design of Highway Bridges. CSA Standard S6 - 1974, Canadian Standards Association.
3. HECB/B/14 (Quest). Highway Engineering Computer Branch, Department of the Environment, London, England.
4. B.E. Hewitt and B. deV Batchelor. Punching Shear Strength of Restraint Slabs. Journal of the Structural Division ASCE, No. ST9, September, 1975.
5. R.A. Dorton, M. Holowka and J.P.C. King. The Conestogo River Bridge - Design and Testing. Canadian Journal of Civil Engineering, V4, No. 1, pp. 18-39, 1977.

Figure 12. Typical load-deflection plots of concrete deck.

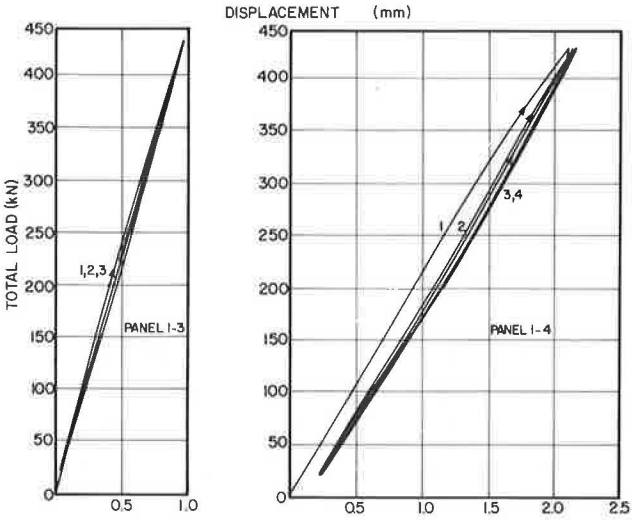

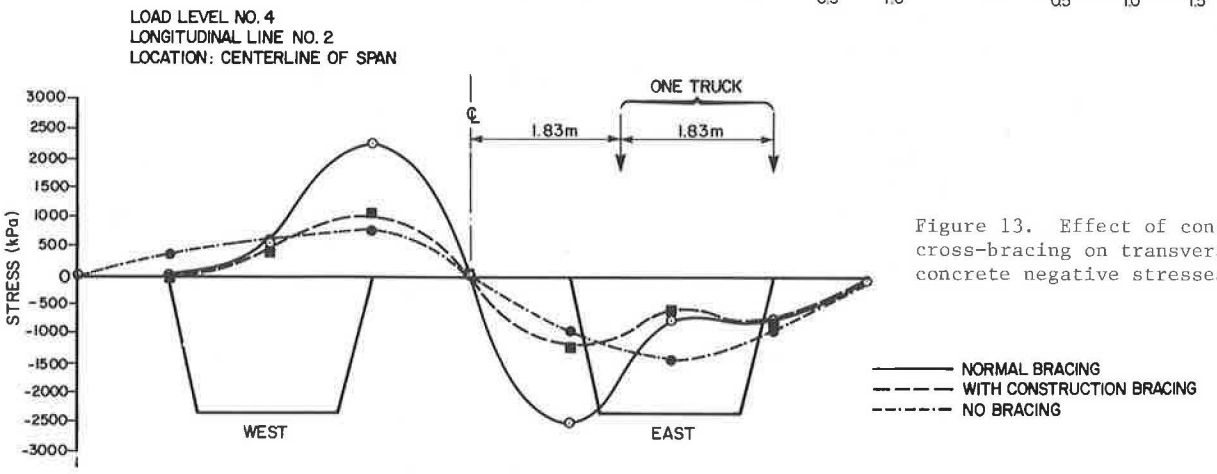

Figure 13. Effect of construction cross-bracing on transverse concrete negative stresses.

Table 2. Reaction data - test and analysis

Load Location	Beam Analysis R_{South}	Beam Analysis R_{North}	Experimental Results Line 1 R_{South}	Line 1 R_{North}	Line 2 R_{South}	Line 2 R_{North}	Line 3 R_{South}	Line 3 R_{North}
1	623.5*	145.9	596.3	125.5	609.5	131.4	598.0	130.9
2	546.5	222.9	520.4	197.1	546.5	205.9	524.5	199.5
3	469.6	299.8	445.8	271.4	475.7	279.8	447.5	284.0
4	390.3	379.1	372.2	345.1	402.0	351.5	376.5	346.0
5	315.7	453.7	303.8	397.1	321.5	435.8	295.2	418.9
6	161.8	607.6	154.8	578.5	156.5	589.1	150.3	575.0

Load Location	Beam Analysis R_{South}	Beam Analysis R_{North}	Line 4 R_{South}	Line 4 R_{North}	Line 5 R_{South}	Line 5 R_{North}	Line 6 R_{South}	Line 6 R_{North}
1	1249.1	299.0	1193.1	269.3	1193.5	271.0	1193.2	275.3
2	1094.3	453.9	1042.0	415.8	1044.7	429.5	1042.5	429.3
3	939.8	608.3	891.4	566.4	897.8	574.9	897.2	570.3
4	786.3	761.8	749.4	717.7	896.5	653.6	805.4	725.2
5	631.0	917.1	598.2	875.5	603.3	876.2	619.0	869.8
6	320.4	1227.8	301.8	1182.9	303.8	1182.6	301.4	1184.1

Load Location	Beam Analysis R_{South}	Beam Analysis R_{North}	Line 7 R_{South}	Line 7 R_{North}	Line 8 R_{South}	Line 8 R_{North}
1	879.8	311.9	844.2	288.0	840.7	281.1
2	934.5	435.7	937.6	401.5	893.8	406.5
3	957.6	590.5	977.4	553.0	924.8	554.4
4	833.9	745.4	833.4	715.4	782.6	699.5
5	648.4	899.8	689.8	863.9	635.6	853.0
6	425.4	946.1	419.4	904.9	339.9	878.3

*All values in kN.

Table 3. Slab deflections due to concentrated wheel load.

Panel Location	Maximum Slab Deflection (mm) November 1976	Maximum Slab Deflection (mm) May 1977
Centerline of east box girder – 4.57 m from centerline of south bearings – stay-in-place forms present.	0.838	0.838
Centerline of east box girder – 9.14 m from centerline of south bearings – stay-in-place forms present.	0.838	0.838
Centerline of east box girder – 13.72 m from centerline of south bearings – stay-in-place forms present.	0.737	0.787
Centerline of east box girder – 17.56 m from centerline of south bearings.	1.854	1.880
Centerline of east box girder – 21.34 m from centerline of south bearings.	1.422	1.676
Centerline of east box girder – 25.91 m from centerline of south bearings – stay-in-place forms present.	0.864	0.914
Centerline of bridge – 4.57 m from centerline of south bearings.	–	0.991
Centerline of bridge – 9.14 m from centerline of south bearings.	1.067	1.041
Centerline of bridge – 13.72 m from centerline of south bearings.	1.143	1.270
Centerline of bridge – 17.56 m from centerline of south bearings.	1.219	1.041
Centerline of bridge – 21.34 m from centerline of south bearings.	1.041	1.143
Centerline of bridge – 25.91 m from centerline of south bearings.	0.914	0.940

TEST RESULTS FROM THE CONESTOGO RIVER BRIDGE

J. P. C. King, The University of Western Ontario
M. Holowka, R. A. Dorton, A. C. Agarwal, Ontario Ministry of Transportation and Communications

The Conestogo River Bridge is a three span continuous steel plate girder structure with a concrete deck longitudinally prestressed for full composite action. The design live loading was an upper-bound representation of all observed truck loadings in Ontario, and a grid analysis was used instead of the usual live load distribution factors. A new load factor method was employed, and deflection and impact values provided by the AASHTO Specifications were abandoned in favour of a dynamic analysis, resulting in a very flexible structure with low natural frequencies. Other features include the use of high strength bolts as shear connectors, and slab test panels designed for membrane action with greatly reduced reinforcing steel percentages. On the basis of full scale load tests, the advisability of the regular use of these features on future bridges is determined. The testing program was conducted using two test vehicles, each of which could be loaded to 890 kN (200 kips). Static tests indicate good correlation between analytical and experimental strains, with load distribution significantly better than predicted by AASHTO Specifications. Dynamic tests indicate that this very flexible bridge, with a first mode frequency below the usual range of commercial vehicle frequencies, behaves as anticipated. The valuable information obtained from this project is incorporated in the new Ontario Highway Bridge Design Code.

The Ontario Ministry of Transportation and Communications has a research program comprised of in-house research and that performed by associated university and consulting engineering groups. The findings of these various research projects have culminated in the design and subsequent testing of a prototype bridge, under actual highway and environmental conditions. Proposals on such items as live loading, bridge dynamics, distribution factors, load factor design, shear connectors and slab membrane action could be assessed prior to the possible inclusion in the new Ontario Highway Bridge Design Code.

The crossing of the Conestogo River near Waterloo Ontario on Highway 85 was selected as the location of the prototype bridge. The structure was designed by the Structural Group of the Research and Development Division of the Ministry in 1973 with construction completed in the summer of 1975. Testing of the bridge began during construction, with much of the initial load testing conducted in 1975. Further static and dynamic tests have taken place since this first series and future tests are anticipated with the structure in use.

The resulting bridge is a three-span continuous,steel plate girder structure with an overall length of 113.7 m (373 ft) and a central span of 44.2 m (145 ft) as shown in Figures 1 and 2. The welded girders are haunched to a depth of 2.13 m (7 ft) over the piers, and 1.07 m (3 ft 6 in) at midspan. The deck between barrier walls is 10.36 m (34 ft) with two 3.66 m (12 ft) travelled lanes and two 1.52 m (5 ft) shoulders. Four girders are spaced at 2.64 m (8 ft 8 in) with cross frames at a maximum of 7.47 m (24 ft 6 in) centres, and bottom laterals connecting the outer pairs of girders (Figures 3 and 4). Composite action in the negative moment region is achieved by the longitudinal prestressing of the nominal 190 mm (7½ in) thick slab. The structure thus acts in a fully composite manner for the full length of the bridge under both superimposed dead load (consisting of sidewalk, curb and future waterproofing) and live load.

Design and Construction

The recommendations as outlined in the Proposed Ontario Bridge Design Load (POBDL) report (1) were used for most of the Conestogo River Bridge design. Items not covered in this report (web stiffening, fatigue, flange buckling, splices and connections) were designed using the applicable sections of the 1973 AASHTO Specifications (2) for Load Factor Design.

The POBDL live load – Case 3 (Figure 5) representing a design vehicle of 722.8 kN (162.5 kips), generally governed for the moment design. A maximum number of four vehicles (two per lane) was used since the structure is on a expressway class highway. Where critical moments arose by the loading of a shorter length influence line, a reduced UDL was used as in POBDL Case 2.

AASHTO specifies a distribution factor of S/1.68 (where S is the girder spacing in metres) for two or more traffic lanes on a concrete slab on steel girder type of bridge. It is generally accepted that this value tends to be overly conservative for certain types of bridges. A grid analysis program was used with the POBDL load to obtain the appropriate distribution factors for flexural effects at 0.4 end span, pier and 0.5 centre span. The computed distribution factors were found to vary with vehicle location. A value of S/2.29 was selected for use in the flexural design. Although somewhat unconservative for the exterior girder at the piers, it was felt that since the maximum negative moment did not occur with the vehicles directly over

Figure 1. The Conestogo River Bridge Under Static Test

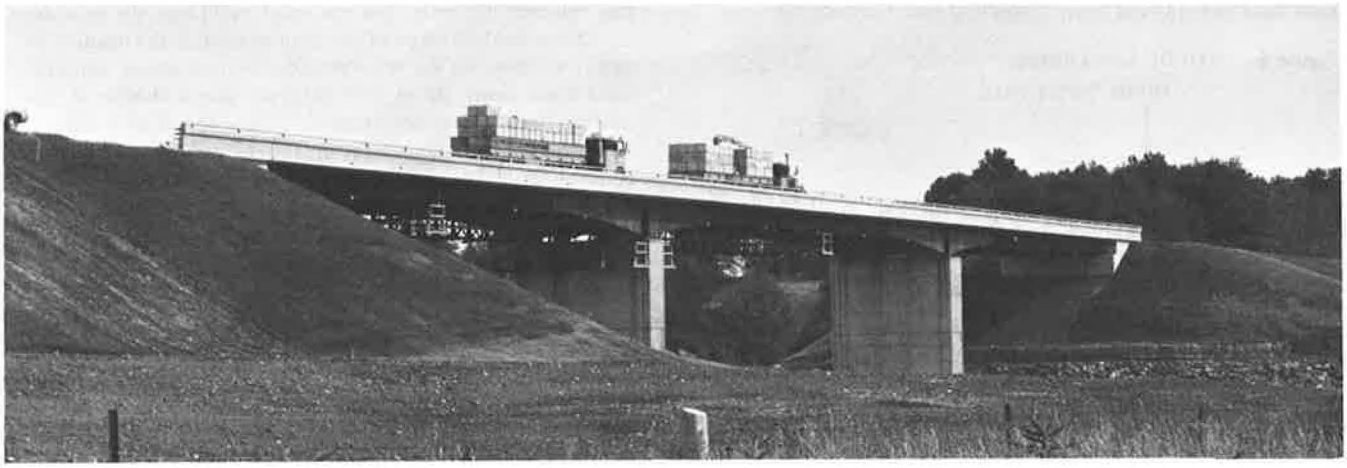

Figure 2. Bridge Elevation

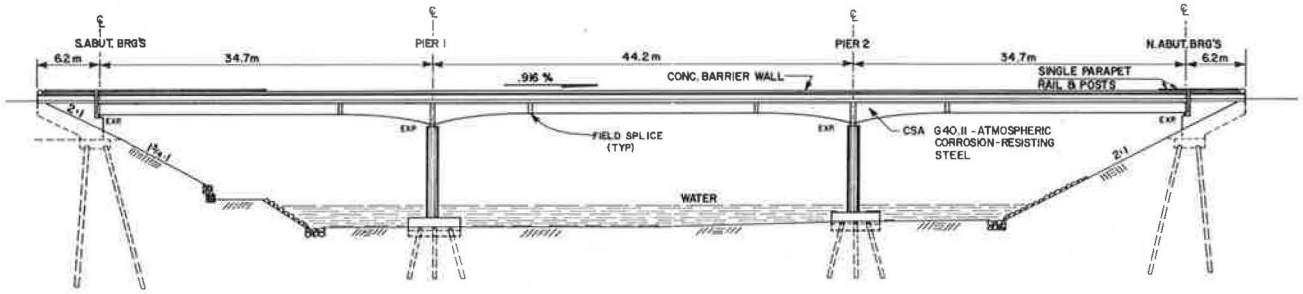

Figure 3. Half Bottom Chord Plan

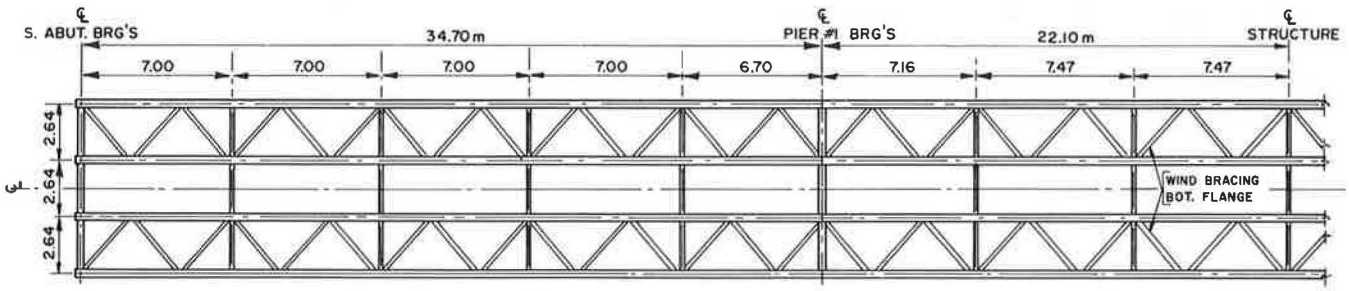

Figure 4. Half Cross Section

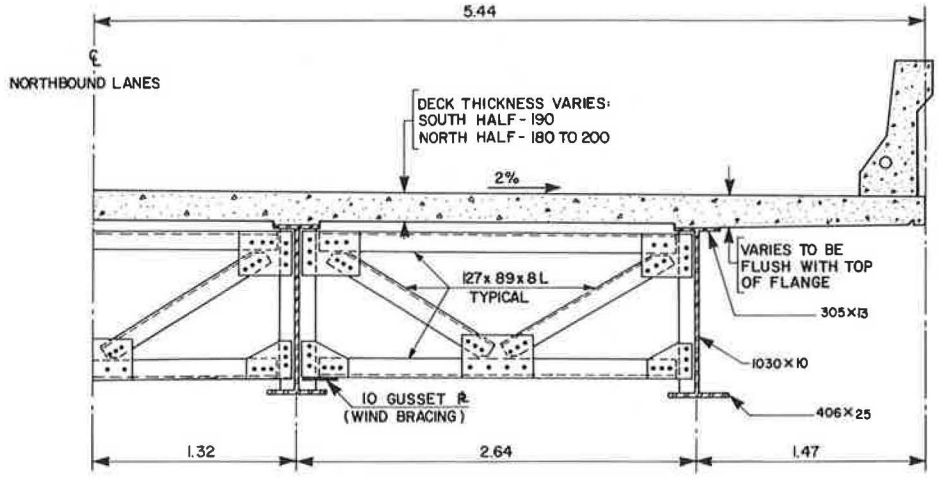

the pier, the values selected would be adequate for design purposes. This compares quite favourably with that observed in both field tests (3) and other theoretical investigations (4).

Figure 5. POBDL Live Loading

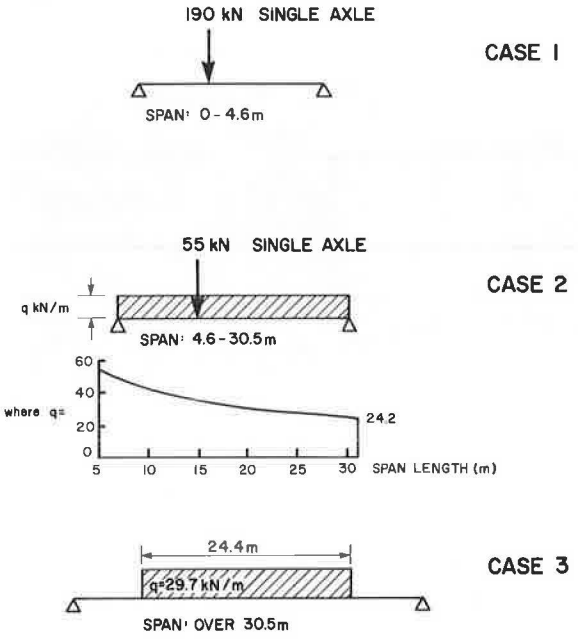

A live load variability factor of 1.10 (to account for the possibility of an illegal overload) was used in addition to the live load factor inherent in the 722.8 kN (162.5 kip) POBDL vehicle. This results in an overall live load factor of 1.276 on the maximum legally permitted load of 622.7 kN (140 kips). Dead load factors reflecting the variability of in-situ material weight vary with construction and fabrication methods (1.10 for structural steel and concrete deck slabs, 1.15 for concrete barrier wall, 1.33 for asphalt). In addition to these load factors, a capacity reduction factor of 0.85 was applied to the yield stress limit state for steel.

The impact factor is of the same configuration as the standard AASHTO provision, however its magnitude was chosen after a careful appraisal of the expected bridge-vehicle interaction. It was felt that if the first mode frequency could be sufficiently removed from the 2 to 5 Hz band of vehicle frequencies, the dynamic effects would be significantly lower than the almost 90 percent impact value measured in several field tests where such a frequency match was evident (5). A one-dimensional lumped mass analytical model was used to predict the natural frequencies. The resulting first mode frequency was 1.53 Hz with the second and third modes falling in the 2 to 5 Hz band. To control the likelihood of resonance and obtain a reliable design impact factor, a model of the bridge was constructed and tested with a vehicle of variable natural frequency and mass. The tests confirmed that resonance was unlikely in all but the second and third modes, and then only when the vehicle had been pre-excited by a bump prior to entry on to the bridge. A constant impact value of 45 percent of the maximum mid-span moment was used for design.

Girder bending stiffness was lowered considerably in order to remove the first mode frequency from the 2 to 5 Hz band. This increased deflections so that the live load deflection at mid-span was 100 mm (3.9 in) or 1/450 of the central span length. The current specification of 1/800 of the span length is based upon the theory that by limiting deflection, the causes of "objectionable" vibrations as perceived by pedestrians, would be alleviated. Since the Conestogo structure is on a limited access highway, pedestrians would not normally be on the structure and thus this deflection constraint could logically be waived.

Since the UDL type of live load as used in the bending design is not as severe for shear considerations as several concentrated loads, design shears were obtained using a number of axle configurations and vehicle weights. A load factor of 1.276 was used with a distribution factor of S/2.16 for computation of girder shear, while a simple span type of distribution was used for girder reactions at abutment and pier.

In order to prevent the concrete deck from cracking in the negative moment region and thus losing the fully composite action, it became necessary to longitudinally prestress the deck. The bolt configuration (Figure 6) consisting of a 22.2 mm (7/8 in) A325 Type 3 bolt with extra threaded length and two nuts in bearing on the top flange. A two nut system was required to pre-set the location of the bolt in the hole. The bolts were to be placed to one end of oversized holes in the top flange to allow shrinkage and elastic shortening from the slab stressing to take place freely without stressing the steelwork. These high strength bolt shear connectors were designed initially in accordance with the AASHTO Specifications for welded stud connectors and load factor design, using POBDL loading and substituting bolts for studs. They were thus designed for ultimate strength, then checked for fatigue.

Figure 6. Shear Connector Details

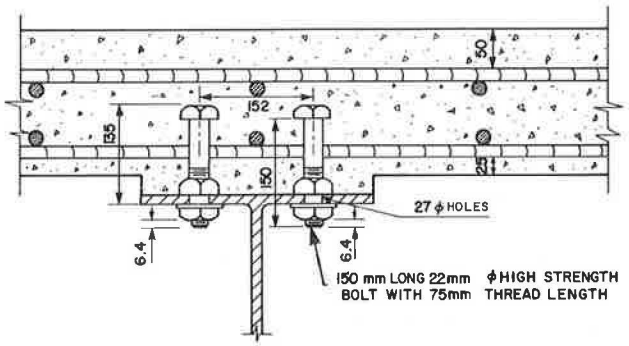

Although the use of high strength bolts as shear connectors has been studied (6), this particular assembly has not been tested before. Consequently a testing program was established to check if such a bolt would form as a shear connector at least as well as an equivalent diameter standard welded stud connector, if the load-slip relationship would be affected by the 4.8 mm (3/16 in) oversize hole and if the presence of threads in the shear plane would affect the fatigue life of the connector.

The results of the static slip tests are shown in Figure 7. Rapid slip takes place at 78 kN (17.5 kips) to 89 kN (20 kips) until the bolts come into bearing. This slip load is in excellent agreement with the proposed Ontario Highway Bridge Design Code value for slip resistance at the serviceability limit state for grit blasted studs of 79 kN (17.8 kips).

One specimen was taken to ultimate load, when the bolts sheared at an average load of 206 kN (46.2 kips) each. With the concrete strength of the slabs at 29.6 MPa (4300 psi), the calculated ultimate strength of an equivalent diameter stud shear connector is 167 kN (37.6 kips). Excluding the performance factor for the bolt of 0.67, the shear resistance of the bolt, according to the Ontario Highway Bridge Design Code is 185 kN (41.5 kips).

A second specimen was fatigue tested at a load range of

44.5 kN (10 kips) per bolt for 500,000 cycles with no slip. The load was incrementally increased, reaching 111 kN (25 kips) at 1,000,000 cycles with no slip. The test was terminated at 1,835,000 cycles because of fatigue failure of the steel testing beam. As also observed in Reference (7), fatigue is not a design factor for high strength bolt shear connectors.

Figure 7. High Strength Bolt Static Slip Test

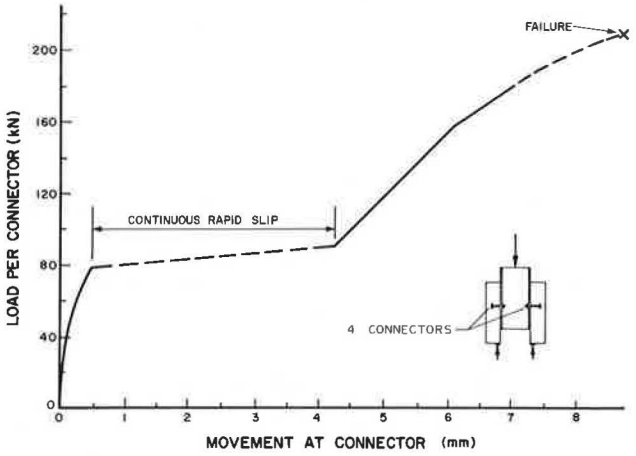

From this testing, it is confirmed that an A325 bolt, torqued to the specified tension, can be used as a shear connector. It can be designed as a bolt in shear, since its ultimate strength is not defined by the crushing of the concrete around the base of the shear connector as is the case of welded studs.

A portion of the deck was divided into test panels with varying slab thickness, transverse steel percentage and concrete cover. The slab design was based upon extensive theoretical and modelling research (8). This research indicated that deck slabs fail in punching shear, not in the assumed flexural mode, and have exhibited a very large factor of safety when compared with the AASHTO Specifications. The design and testing of these deck panels (in which the minimum transverse steel percentage is 0.2 percent) are covered in detail in reference (8). Except for these test panels, the deck slab was designed for transverse bending by the AASHTO working stress method and the distribution of wheel loads was in accordance with Article 1.3.2 (2). Consequently 19 mm (3/4 in) reinforcing bars were used at 190 mm (7½ in) centers (almost 1.0 percent), top and bottom with extra top steel for the cantilever slab portion. Due to longitudinal prestressing, the distribution steel was reduced to 13 mm (½ in) bars at 305 mm (12 in) centers top and bottom throughout.

A check on the capacity of the bridge was carried out using both the AASHTO working stress and load factor methods. Compariative results are plotted in Figure 8. AASHTO working stress shows an overstress condition of a maximum of 12 percent at the piers with the load factor method showing a similar capacity to the POBDL method. Since the differences between the capacities predicted by the three methods were sufficiently small, there was no concern over the adequacy of the Conestogo Bridge as designed with the new POBDL criteria.

Fabrication and erection of the structural steel followed conventional methods, with special emphasis placed on camber control. A vertical tolerance of ± 3.2 mm (± 1/8 in) was placed upon the setting of the formwork, reinforcing steel and prestressing ducts. This was necessary to allow a direct comparison between the slab design and the punching shear test results.

Figure 8. Design Moment Capacity Comparisons

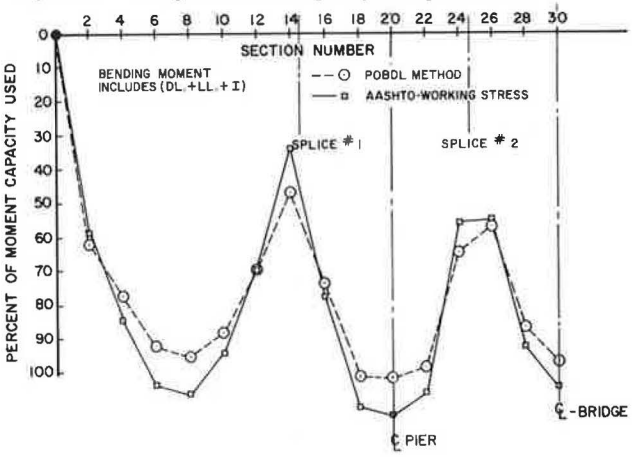

A) AASHTO WORKING STRESS VS. POBDL

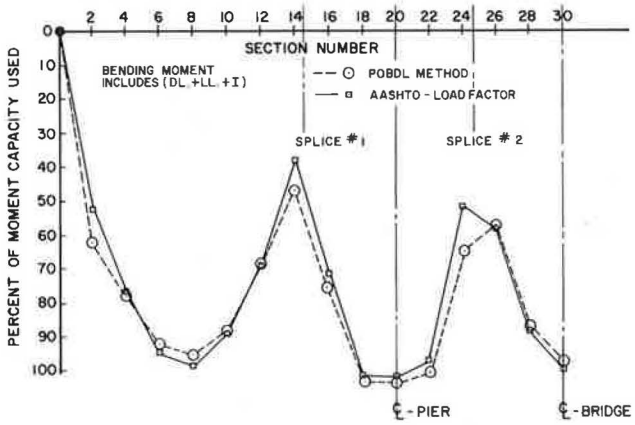

B) AASHTO LOAD FACTOR VS. POBDL

The original construction method called for the high strength bolt shear connectors to be offset in oversize flange holes and remain in position during the placing of the deck slab. It was thought that a low torque could initially be placed on the bolts and consequently no movement would take place throughout the deck forming, re-bar placing and deck pour operations, yet allow relatively free movement of the slab during the post-tensioning procedure. However, a number of shear connectors were found to be out of place when a spot check was made after the deck was poured. More than 10 percent of the bolts would be incapable of the required movement, thus it was decided to abandon the concept of free slab movement and to fully torque the shear connectors prior to the stressing operation. From a design point of view, the additional prestress transfer load could be taken by the shear connectors without fear of slippage, and the compressive prestress in the steel girders would not be severe. It was felt that the some 15 percent loss of prestress at the pier would be offset in part by the increase in concrete strength that is normally found in the field, over that specified. The presence of the prestressing force is not considered to effect the ultimate load carrying capacity of the bridge.

Instrumentation and Testing

The test program and corresponding instrumentation were designed to answer the questions that arose with the formulation of the design and construction methods. It was hoped that information relative to the following subjects could be

obtained from the prototype tests.

1. Girder erection stresses and deflected shape.
2. Nature and degree of prestress.
3. Theory of slab membrane action.
4. Effect of the barrier wall, sway frames and slab on distribution of load between girders.
5. Dynamic performance.

Reference (9) contains complete information concerning the variety of instrumentation used to monitor load, strain and deflection for the static and dynamic testing of the structure.

Prior to the construction of the barrier walls, a dynamic pull-down test was carried out. Top and bottom flange strains were recorded while jacking against a bulldozer on the shallow river bed at midspan. The results were compared to a similar test after the construction of the barrier walls.

Twelve static load locations were selected to produce maximum effects in the positive and negative moment regions. An incremental loading procedure was followed, using six load lifts with a maximum load of two 890 kN (200 kip) test vehicles. To explore the effect of the sway frames on the distribution of load to the girders, a set of static tests was repeated with a single test vehicle in a critical location for positive moments in the north end span. Strains were recorded with three instrumented sway frames in various combinations of unbolted and fully bolted conditions. In order to produce influence surfaces for bending moment, a single vehicle was successively positioned along the structure in 3.0 m (10.0 ft) increments in each of five test lanes. Top and bottom flange strains in the centrespan, pier and endspan were recorded.

The test vehicle, loaded to a weight of 368 kN (82.7 kips) made runs at 48, 64 and 80 km/h (30, 40 and 50 mph) in both directions in three lanes. The strain gauge output was recorded while the vehicle was on the bridge, and for 30 – 60 seconds of free vibration after the vehicle had left the bridge.

Analysis and Test Results

Construction and Dead Load

Good agreement was obtained between a continuous beam model and the measured cross sectional average values of bending moment and deflection. However, there was up to a 22% variation between girders in the mid-span deflections. This variation is due to slight differences in camber and a rotation of the pier sections allowed by the nominal clearance in the bolted girder splices. Significant erection stresses (172.3 MPa or 25 ksi) were observed in the bracing members since the sway frames were used to realign the girders. Apparent axial forces are present, even prior to stressing of the deck, and can be considered using the top and bottom flange strains as outlined in Reference (9). Average axial compressive strains of 110 micro-strain in the centre span were computed from the recorded top and bottom flange strains, which is of the correct order of magnitude for typical shrinkage strains. Very small axial strains were computed at the pier section.

Since the stressing of the deck was applied to the composite section and not the slab done as originally hoped, recording the resulting strains in the girders enabled slab prestress to be determined. Based upon top and bottom flange strains, the computed average sectional slab prestress compares very favourably with the design prestress, and in all cases is greater than the required service level prestress (Figure 9). The maximum steel prestress at the pier was of the order of 24.1 MPa (3.5 ksi) compression in the top flange (which is opposed by tensile live load stresses), with negligible stress in the bottom flange. Maximum top and bottom flange stresses were about 29.0 and 18.6 MPa (4.2 and 2.7 ksi) respectively in the centre span. It is felt that these stresses will pose no problems as in all cases where high compressive stress exists, the live load stress is either very small or tensile in nature. The axial forces are fairly uniform between girders indicating the prestressing effects were evenly distributed and there was an even shear transfer between the slab and girder.

Thermally induced stresses, were generally rather small over the period of observation. The largest stresses were found in the bottom chord member of the central sway frame (27.6 MPa or 4 ksi) for a cyclic ambient temperature variation of 9.4 C^{O} (17 F^{O}), which corresponds very closely to the stress one would expect if the member were fully restrained. Top chord and diagonal member stresses were very small as were the stresses in the bottom laterals. Since the stresses in the bottom chords of the exterior sway frames were also quite small, temperature stresses appear to be most significant in the interior panels where the largest degree of restraint against free movement is provided by girders.

Static Tests

Grid analysis techniques have been used by several researchers (9) to model beam and slab bridges. Good results can be obtained with a careful choice of grid configuration and stiffness parameters. The choice of these parameters becomes more difficult with increasing girder depth and idealizations of the three-dimensional structure must be made.

A gridwork of elements was used conforming as closely as possible to the configuration of the structural steel. Longitudinal members were located at each main girder, with transverse members at each diaphragm or sway frame position. Bending and torsional moments of inertia, cross sectional area, bending and shear moduli of elasticity were required for each member. Since the varying haunch thicknesses at any given section resulted in less than a two percent difference in section properties, girder inertias were assumed to vary in the longitudinal direction only.

The barrier wall, cast in 6.1 m (20 ft) lengths with 3 expansion joints, could increase the stiffness of the exterior element

Figure 9. Longitudinal Deck Prestress

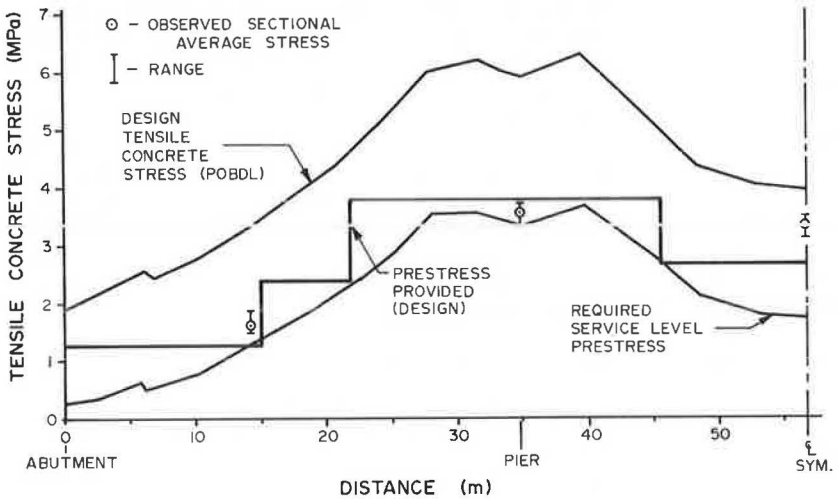

by almost 70 percent if fully active. However, the static pull down tests performed at the centerline of the bridge showed that there was no appreciable difference in either the mid-span deflection or girder stress for this symmetric loading. Good agreement was obtained between the test results assuming no contribution from the barrier wall to the section properties of the exterior element.

Several models of longitudinal element torsional stiffness were examined before suitable transverse stiffness was evident. It was found that by simply taking the torsional stiffness of the slab element by itself, the deflections and moments under non symmetric loading were overestimated by as much as 30 percent. The best model found assumed that the bottom lateral and sway frame systems provided lateral support to the exterior and interior girders. This in effect is similar to a closed section with the lateral system representing the bottom flange of the torsionally stiff box section. Each approach considered was examined statistically, comparing experimental and predicted response, with the above representation providing the necessary torsional stiffness to model the response satisfactorily.

Figure 10 shows two of the static test comparisons for the final load lift of 890 kN (200 kip) test vehicles. Linear behaviour was observed in all respects for the preceding load lifts.

A distribution factor was calculated at each of the three critical sections for every vehicle position in the static tests. A separate factor was obtained for interior and exterior girders shown in Figure 11 for positive and negative moment. In most cases the distribution factor computed from test data was considerably lower than that used for design purposes. The factors that exceeded the design value were accompanied by low sectional moments and were not critical. The only case that might be considered to be significant is when two vehicles are outside the design traffic lane, almost directly over the exterior girder, resulting in a large negative bending moment at the pier in the exterior girder. However, as in all of the tests with a truck on the shoulder, this respresents a more severe situation than normally contemplated in design. Similar trends in the variation of the distribution factor with load position were seen in the single vehicle crawl runs.

Axial forces in the instrumented sway frames were obtained for all static tests from the strain gauge data. In general, the largest forces were found in the bottom chord member of the sway frame closest to the loaded area. Maximum live load stresses were 86.6 MPa tensile (12. 4 ksi) and 61.5 MPa compressive (8.8 ksi). These stresses by themselves are not severe, however when coupled with observed erection stresses of up to 209.5 MPa (30 ksi), a severe stress condition could result in the connections. These observed live load stresses in the sway frame members agree quite favourably with those computed from

Figure 10. Static Bending Moments And Deflections

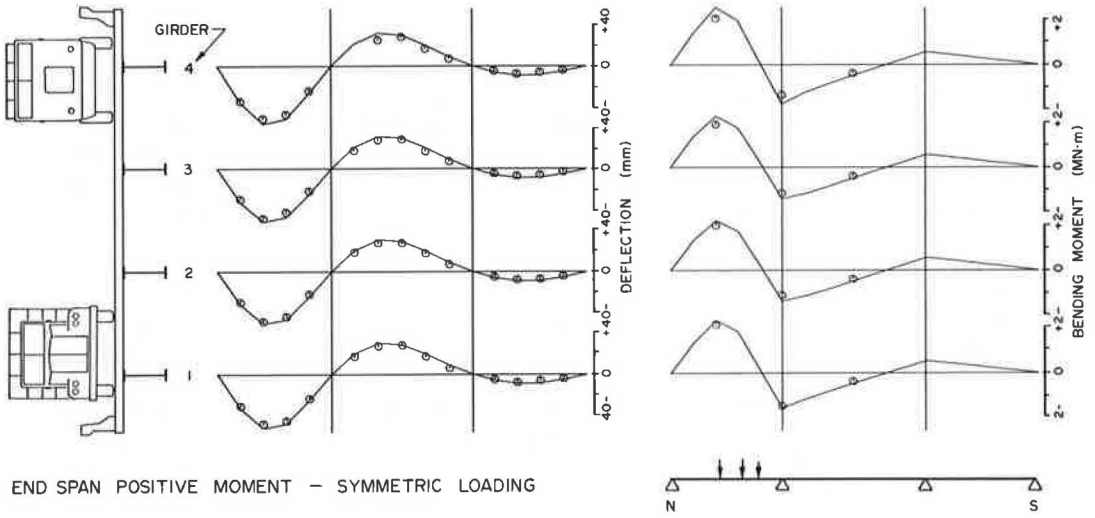

END SPAN POSITIVE MOMENT – SYMMETRIC LOADING

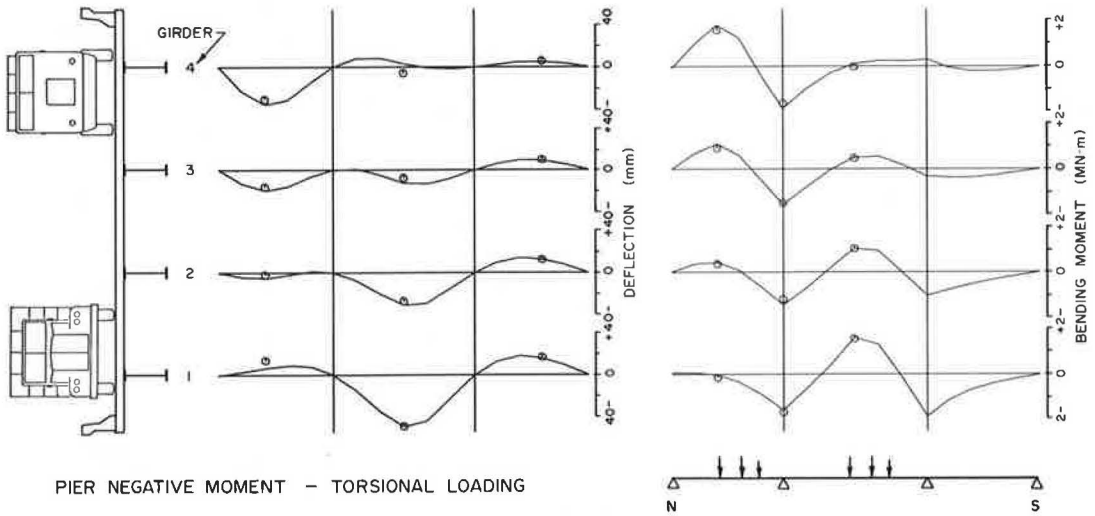

PIER NEGATIVE MOMENT – TORSIONAL LOADING

Figure 11. Distribution Factors From Static Tests

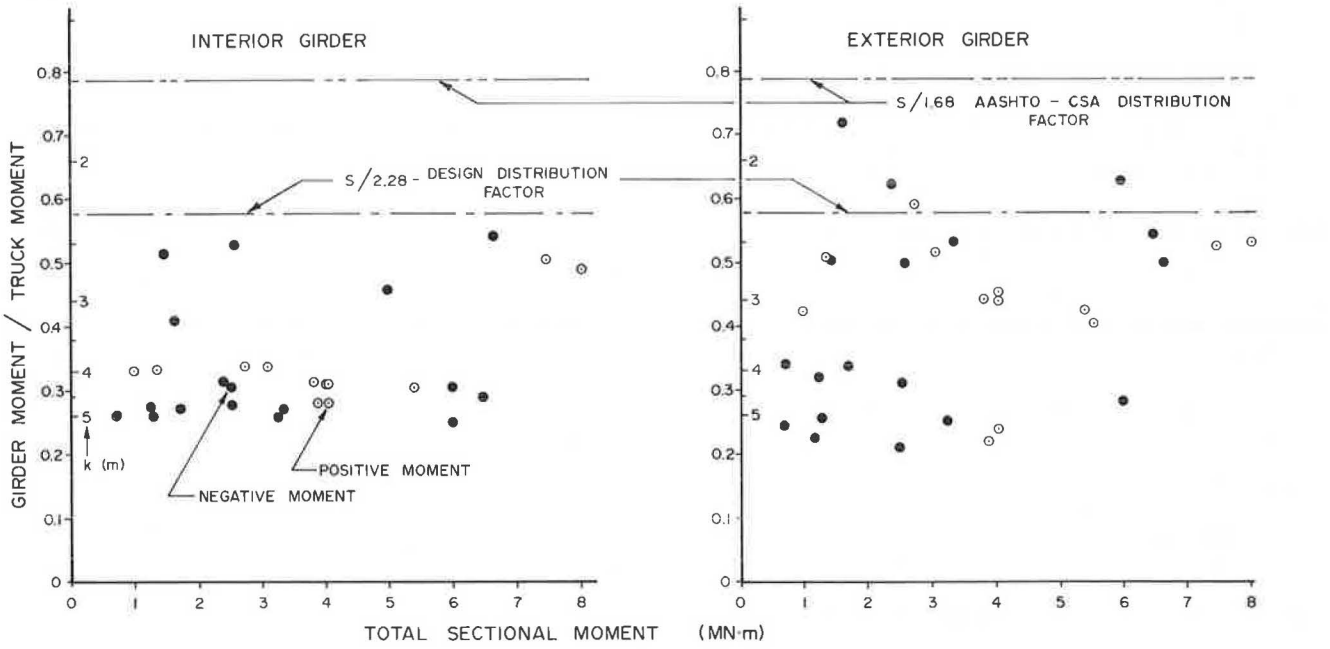

transverse moments and shears as determined from the grid analysis.

Similarly, forces were obtained for the instrumented bottom lateral members. In symmetrically loaded spans the stresses were tensile in the order of 14.0 MPa (2 ksi). Eccentric loading, producing longitudinal shear between an exterior pair of girders, engages the bottom laterals in a truss-like action. Alternate tensile and compressive forces were seen in adjacent members with a maximum observed stress of 64.3 MPa tension (9.2 ksi) and 55.9 MPa compression (8.0 ksi).

Transverse reinforcing bar stresses were obtained near the position of maximum positive longitudinal bending moment in the endspan. The maximum tensile stress found was 82.4 MPa (11.8 ksi) in the positive moment reinforcement of the central panel.

Stresses in the longitudinal reinforcing bars over the pier substantiated the design claim of full composite action throughout the length of the bridge superstructure. Applicable stresses are shown in Figure 12 showing definite composite action over the pier for several loading conditions. Maximum recorded live load tensile stresses in the longitudinal reinforcement at the pier was 10.5 MPa (1.5 ksi) corresponding to a concrete stress of 1.75 MPa (250 psi) which is well below the design tensile stress of 2.65 MPa (380 psi) shown in Figure 9.

Due to the high degree of preload in the sway frame members, they were not able to be completely removed as originally planned in the distribution tests. However, even in a semi-connected state there was enough restraint provided to the bottom flange of the girders to prevent a significant change in load distribution. The resulting changes in sway frame stresses were as much as $\pm$ 50% of their fixed state stresses. It is hoped that future tests may clarify the role that the bracing members play in the distribution of load.

From these results it is evident that the standard AASHTO distribution factor is extremely conservative while the figure of S/2.29 used in the design and substantiated by field tests is closer to reality. Researchers have recognized this problem and several methods have been proposed to account for the added lateral stiffness present in modern composite structures. Figure 13 shows the results of one such method (11) that involves the determination of actual stiffness parameters before a distribution factor can be obtained. The resulting distribution factors using the stiffness parameters from the Conestogo structure are not greatly different from that observed during the prototype tests or that used in the design.

Dynamic Tests

A natural frequency of 1.61 Hz was observed during the pull down tests with no discernable difference in frequency between the tests conducted before and after the barrier wall was constructed. The power spectrum shown in Figure 14 clearly identifies vibration modes at 1.68, 2.32, 2.66, 3.12, 3.44, 3.62, 6.08, 6.42 Hz. If the natural frequencies reported in Reference (10) for the bending modes are increased by a factor which gives a first mode frequency of 1.68 Hz, then frequencies of 1.68, 2.71, 3.63, 6.42 Hz are obtained which are in very close agreement with certain of the values from the field tests. The character of the damping is a mixture of Coulomb and viscous, with the Coulomb component dominant. The damping is between 0.3 and 0.5 percent of critical for both the second and third bending modes, if a viscous model is assumed and the values obtained using their logarithmic decrement. This value of damping is quite low when compared with that of non prestressed structures.

The dynamic amplification of bridge motion due to a vehicle passage was obtained by examination of the time histories of bridge response in the period while the vehicle was on the bridge and is considered to be representative of the impact factor used for bridge design. The distribution of dynamic amplification, although quite scattered, gave a mean dynamic amplification of 0.2 with a standard deviation of 0.09, giving a coefficient of variation of 0.45. If a normal distribution is assumed, these statistics give a probability of exceedance of the design impact factor of 0.45 of 2.75×10^{-3}.

Additional dynamic testing including the simultaneous presence of vehicles need still to be analysed to provide a complete view of the dynamic response of the bridge.

Figure 12. Stress Distributions At North Pier

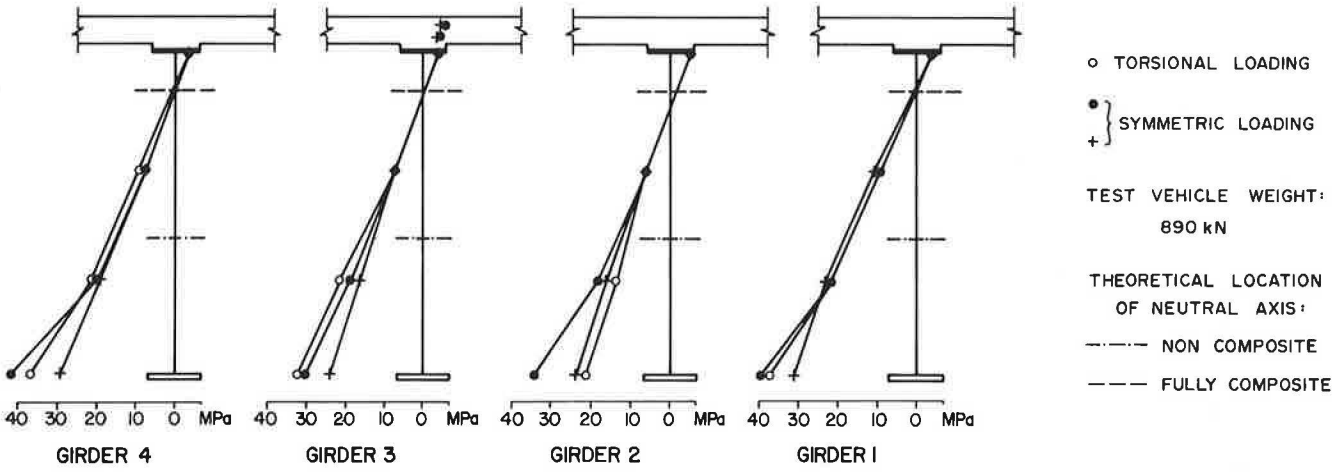

Figure 13. Variable Distribution Factor (After Sanders)

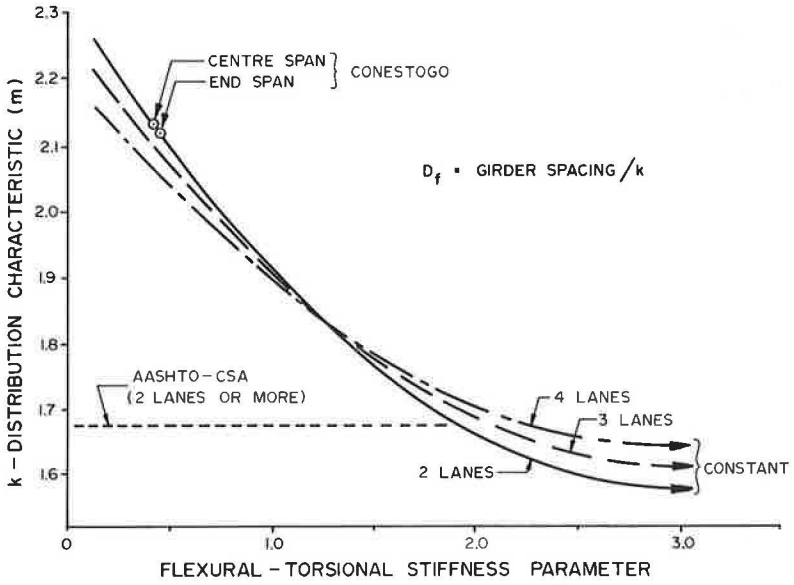

Figure 14. Typical Frequency Analysis Of Bridge Vibrations

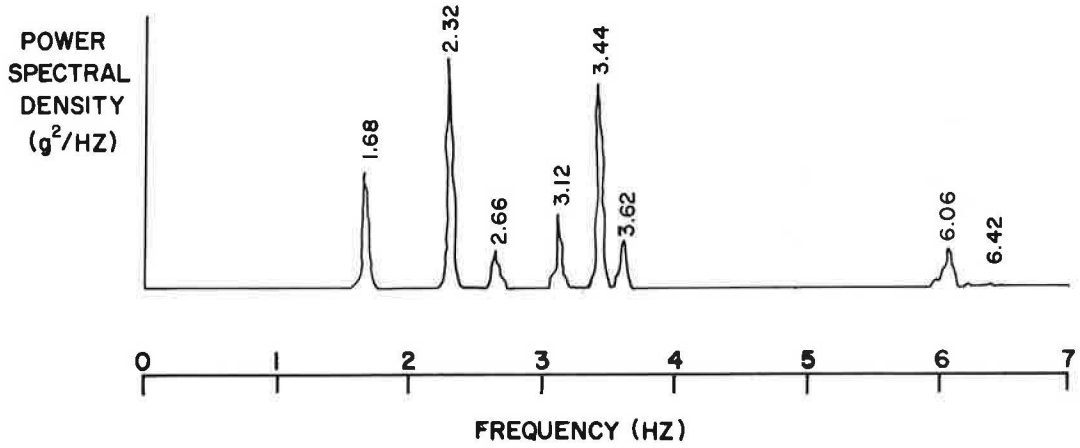

Conclusions

1. Full composite action has been achieved for the entire length of the bridge using the method of longitudinal prestressing.

2. For this structure, the design criteria and methods used enable increased vehicle weights to be safely accommodated at no increase in materal compared to designs by AASHTO.

3. High strength bolts provide a satisfactory shear connection between the girder and slab.

4. The observed load distribution was significantly better than that suggested in present AASHTO specifications. The distribution factor used in the design is substantiated by the test results and current research.

5. The bracing system provides lateral restraint to the girder bottom flanges, increasing the torsional stiffness of the structure and considerably improving the distribution of load.

6. This very flexible structure with a first natural frequency below the usual range of vehicle frequencies appears to have satisfactory dynamic properties.

7. The Conestogo River Bridge responds in a manner which is consistent with the design assumptions.

References

1. Csagoly, P. F. and Dorton, R. A., "Proposed Ontario Bridge Design Load", RR 186, Ministry of Transportation and Communications, Ontario, 1973, 32 pp.
2. "Standard Specifications for Highway Bridges", American Association of State Highway and Transportation Officials, 1973.
3. King, J. P. C., Csagoly, P. F., and Fisher, J. W., "Field Testing of the Aguasabon River Bridge, Ontario", TRR 576, Transportation Research Board, Washington, D.C. 1975, pp. 48-60.
4. Wright, R. N., and Walker, W. H., "Criteria for the Deflection of Steel Bridges", Bulletin No. 19, American Iron and Steel Institute, November 1971, 75 pp.
5. Csagoly, P. F., Campbell, T. I., and Agarwal, A. C., "Bridge Vibration Study", RR. 181, Ministry of Transportation and Communications, Ontario, 1972, 30 pp.
6. Rankine, C. R. S., "High Strength Bolts as Shear Connectors", MTC Project Q45, MSc. thesis, Queens University, Kingston, Ontario, 1971.
7. Dallam, L. N., "Static and Fatigue Properties of High Strength Bolt Shear Connectors", Report 70-2, Missouri Cooperative Highway Research Program, 1970.
8. Hewitt, B. E., and Batchelor, B. de V., "Punching Shear Strength of Restrained Slabs", Journal of the Structural Division ASCE, No. ST9, September 1975, pp. 1837 – 1853.
9. King, J. P. C., "Structural Behaviour of the Conestogo River Bridge", MTC Project L5, MESc. thesis, University of Western Ontario, London, Ontario, 1978, 120 pp.
10. Dorton, R. A., Holowka, M., and King, J. P. C., "The Conestogo River Bridge – Design and Testing", Canadian Journal of Civil Engineering, V4, No. 1, 1977, pp. 18-39.
11. Sanders, W. W., "Wheel Load Distribution in Highway and Railway Bridges – Developments in Bridge Design and Construction", Rockey, Bannister and Evans Ed., Crosby, Lockwood and Sons Ltd., London, 1971, pp. 540-556.

LABORATORY AND FIELD STUDIES OF A PEDESTRIAN BRIDGE COMPOSED OF GLASS REINFORCED PLASTIC

Fred C. McCormick, Consultant, Virginia Highway and Transportation Research Council

The design, fabrication, and load-testing procedures are described for girders composed entirely of glass-reinforced polyester (GRP) resin. The girders are 4.9 m (16 ft.) long and have geometric features which include trussed webs, a solid flange plate, and a triangular-shaped cross section. Three of the girders were attached laterally by a GRP cover plate in the laboratory to provide a complete superstructure for a pedestrian bridge 4.9 x 2.1 m (16 x 7 ft.). The lightweight, high strength, and formability of the GRP materials permitted fabrication and handling of both the components and the completely assembled structure without the use of heavy equipment. The weight of the GRP superstructure was approximately 360 kg (800 lb.). Laboratory tests were conducted to ascertain the load transfer characteristics at the GRP plate and concrete deck interface. Live load tests were performed to measure strains, deflections, and the creep behavior of a full-scale girder exposed to prevailing climactic conditions. Comparisons of theoretical and experimental results ranged from nearly zero up to 20% in which the experimental results were usually lower than the predicted values for deflections and strains. The bridge is scheduled for field erection in 1978 and observations will be made for five years to monitor its structural behavior, the effects of weathering, and user abuse.

The structural use of glass fiber-reinforced plastics (GRP) has been evident in the automotive, aircraft, and boat industries for a number of years. Civil engineers in general, and bridge engineers in particular, have been slow in exploring the application of structural plastics. Three principal factors which discouraged a consideration and earlier use of synthetic composite materials were (1) a deficiency of basic data on the properties of the materials and field experience necessary for design, (2) a ready source of available materials in familiar geometric configurations, and (3) a continuing source of the relatively cheaper conventional construction materials. In recent years, these factors have changed to the extent that a consideration of synthetic composites as an alternate construction material has become feasible. This is not to say that all former inhibitions and obstacles to the selection of a composite material for a given structure or bridge have been eliminated. There is still a great deal to learn about both the short- and long-term properties of these materials, but each passing year catalogues additional valuable data gained from in-service structures upon which confidence and design procedures can be established. A number of professional groups from the camps of both the producers and users have issued guidelines and specifications which are useful to designers. Chief among these efforts is the forthcoming ASCE Manual for the Design of Structural Plastics prepared under the direction of the Structural Plastics Council of the American Society of Civil Engineers.

The introduction over a decade ago of GRP shapes similar in geometry to structural steel shapes provided some motivation for designers to consider synthetic composites for structural applications where appropriate. However, the low elastic modulus (approximately 10% that of steel) and flamability characteristics of these products have limited structural applications to services demanding high corrosion resistance and electrical insulation.

Cost considerations for GRP materials were improving rapidly until 1974, when the price of petrochemical products increased drastically. Currently, the rates of rise in costs are approximately equal for both synthetic resins and the conventional materials of construction. The raw material components in popular GRP systems now cost approximately $1.32 per kg ($0.60 per pound) and fabricated structural shapes in the range of $3.30 per kg ($1.50 per pound). Even though these unit costs are higher than those for steel and concrete materials, strength-to-weight ratios, fabrication procedures, lifetime maintenance costs, and other considerations provide a cost-benefit advantage for GRP composites in a growing number of structural applications.

An experimental study of a GRP light-duty bridge is described in this paper. A reduction in cost from that incurred in the use of conventional materials and construction procedures was anticipated from (1) the use of industrialized fabrication techniques, (2) a short erection time, (3) reduced dead weights, and (4) a maintenance-free life of many years. The development of a trussed girder as the principal structural member of the bridge evolved over the period from September 1971 to June 1976 and is described in several publications.(1,2,3,4) Recommendations have been made to pursue a study of a

full-scale, in-service bridge in order to investigate variables of force, temperature, moisture, sunlight, and abuser use.(2) Approval for the project has been obtained under the classification of an "Experimental Feature" in the construction of a recreational rest area located along Interstate 66 approximately 5 km (3 miles) northwest of Front Royal, Virginia.

Functional and esthetic considerations of the site dictate a pedestrian bridge 4.9 m long by 2.1 m wide (16 feet x 7 feet), which will span a small creek and blend with the natural appearance of a wooded area. The esthetic requirements are to be satisfied by using exposed aggregate concrete as the bridge deck to match adjacent gravel paths, timber handrails, and green glass-reinforced plastic (GRP) plates over the trusses to blend with the trees and summer flora.

The research project was planned to be carried out in two phases. Phase I, which has been completed, was devoted to the fabrication and load testing of a single, full-scaled girder. Phase II deals with the fabrication, erection, load testing, and related matters of the prototype bridge structure. The entire bridge has been fabricated and completely assembled in the Composite Materials Laboratory at the University of Virginia. Precast concrete seats for the bridge have been cast to ensure an accurate fit and to minimize the time needed to erect the superstructure at the site.

Objectives

Specific objectives of Phase I were:

1. To perfect design and fabrication procedures for a girder dimensionally scaled up from previous specimens.
2. To compare analytically predicted deflections with deflections which occurred when the concrete slab was cast on the top plate of the girder.
3. To observe the behavior of the composite girder during a live load test of 4,060 Pa (85 psf).
4. To observe the behavior of the composite girder under static load for an extended period of time.

Specific objectives of Phase II are:

1. To design, fabricate, assemble, and instrument the complete bridge structure.
2. To establish procedures for expeditious field erection of the superstructure, placement of concrete deck, and installation of handrails.
3. To observe the behavior of the bridge under a live load test equivalent to the design load of 4,060 Pa (85 psf).
4. To monitor the bridge for a period of five years to determine the effects of materials creep, weathering, and user abuse.

Phase I — Preliminary Test Girder

Design

The preliminary test girder was designated TTG-13 (triangular-trussed girder specimen number 13) and was basically a scaled-up version of TTG-12, which is described in reference 1. Figure 1 is a view of TTG-12 with the principal features of the girder identified. The overall length of TTG-13 was 4.9 m (16 ft.), the width of the top cover plate was 71 cm (28 in.), and the depth from the top plate to the lower chord was 40 cm (16 in.). The depth was considered to be relatively shallow compared to the width, but was adopted to satisfy anticipated site conditions.

A criterion of 13-mm (0.5-in.) deflection at midspan under a uniformly distributed live load of 4,060 Pa (85 psf) was used for designing the fiberglass elements. The concrete deck slab was assumed to act as a portion of the top flange of the girder in meeting the criterion for live load. Because of the shallow depth of the girder and the deflection limitation, the predicted design stresses in the tension elements were low relative to a potential working stress of 172 M Pa (25,000 psi). The maximum computed stress was 36 M Pa (5,300 psi) and occurred in a lower chord element. The final sizes of the bottom chord and web diagonals were determined by means of a computer program based on the finite element analysis described in reference 2. The total numbers of strands of glass roving used in the elements are shown in Figure 2.

Figure 1. Typical test specimen of a triangular trussed girder showing the principal features.

Fabrication

Specimen TTG-13 was fabricated in essentially the same way as previous girders had been fabricated; namely, by cutting and fitting the pultruded rods, tubes, and lower chord connectors; bonding the top plate and stiffeners; mounting the top plate on a mandrel and attaching vertical stiffeners and lower chord connectors; and winding and curing the tension elements. (The pultruding process is used to form structural shapes by simultaneously pulling a number of continuous strands of resin-impregnated glass roving through a heated die which cures the resin within several minutes.) Figure 3 shows the specimen mounted on the mandrel just prior to winding and Figure 4 shows the completed girder in the curing oven. Both views show the girder in an inverted position. A description of the glass, resin, and other materials used is given at the end of the paper.

No metallic fasteners were used in any of the connections. Resin-impregnated wooden bolts were used along with an epoxy adhesive to attach the top plate to the transverse stiffeners. Pultruded fiberglass rods 0.9 mm (3/8 in.) in diameter were used to fasten the ends of the vertical stiffeners to the transverse stiffeners, and 0.6 mm (1/4 in.)

Figure 2. Comparison of winding paths and number of strands for TTG-13 and TTG-WC.

Total tension strands and winding pattern for TTG-13. Dashed lines are stiffeners and plate.)

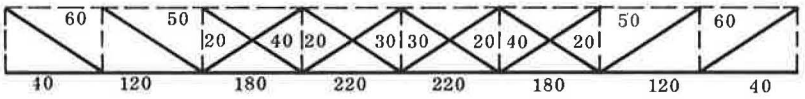

Winding paths and total tension strands for TTG-WC. (Dashed lines are stiffeners and plate.)

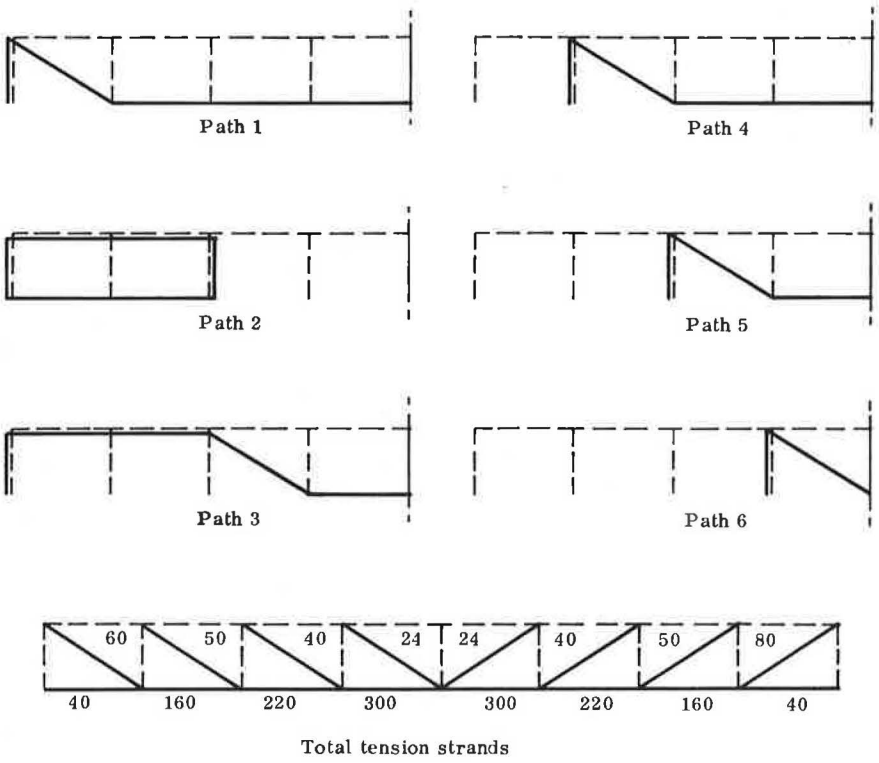

Figure 3. Stiffener and flange plate mounted on mandrel prior to winding the tension elements.

Figure 4. A completed girder in an oven for post-curing resin at 54.4°C (130°F).

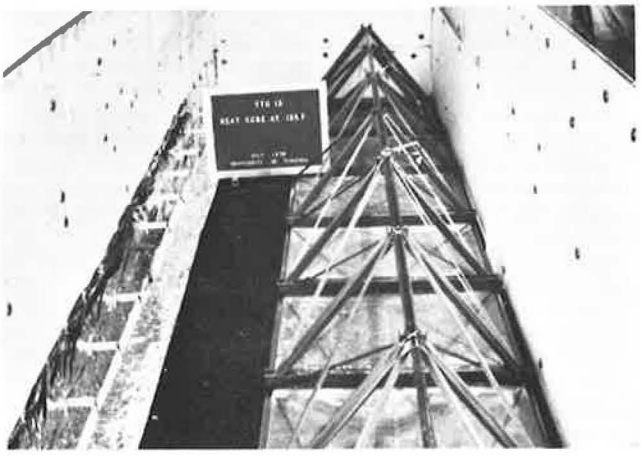

diameter rods were used to fasten the stiffeners and lower chord connectors.

Two strands (3,120 fibers per strand) of glass roving were simultaneously impregnated with resin and used to build up the tension elements by continuously winding the strands manually around anchor points formed by the transverse stiffeners and the lower chord connectors. The winding paths and the number of strands used in the development of the tension elements are included in Figure 2. Cross diagonals were included in all of the panels in TTG-13 to satisfy anticipated shear force requirements generated by partial live loading on the top plate. However, with the subsequent application of the concrete deck, it was determined that the design live load did not impose a tensile stress upon the cross diagonals, so they were not included in the prototype structure. A cover plate 0.6 mm (1/4 in.) thick was bonded to the top plate of the girder prior to placing the concrete deck.

The manpower requirement for the fabrication of the 4.9 m (16 ft.) long specimens was limited to one person for all cutting and assembly operations, except on occasion when the cumbersome mandrel or top plate had to be moved. Winding the tension elements was more efficiently accomplished by the use of three persons, one of whom rotated the mandrel and kept count of the number of strands as they were placed. Approximately six man-hours were required to wind TTG-13.

Instrumentation

Six electrical resistance strain gages were bonded with an adhesive to selected elements in the specimen. The gages were Type EA-06-250-BF-350, supplied by the Micro-Measurements Company, and were bonded with M-bond 200 (Methyl-2-cyanocrylate adhesive). Deflections at several panel points during load tests were measured by mechanical dial indicators with least readings of 0.025 mm (0.001 in.). Data from these instruments will be presented and discussed later.

Concrete Deck Placement

The test specimen was supported at both ends by wooden frames built to fit the V shape formed by the inclined stiffeners. No support was applied directly to the lower chord stiffener connector. A wooden side form for the 76 mm (3 in.) thick concrete slab was placed adjacent to the outside edges of the top plate and supported along its length so that the member could deflect independently from the form as the concrete was applied to the girder. Consequently, the finished depth of the concrete varied from 98 mm (3-7/8 in.) at the center of the girder to 83 mm (3-1/4 in.) at the ends. Just prior to placing the concrete, the fiberglass plate was sanded, cleaned with an acetate solvent, and coated with an epoxy adhesive especially formulated to bond fresh concrete to solid materials. With a unit weight of 2,224 Kg/m^3 (139 pcf), the concrete slab weighed approximately 680 kg (1,500 lb.). Cylinder tests of the concrete indicated a compressive strength of 36 M Pa (5,300 psi) and a compressive modulus of elasticity of approximately 24,800 M Pa (3,600,000 psi) after moist curing for 32 days. Using the rule of mixtures for the concrete and plate, an equivalent modulus for the top flange of the girder was computed as 23,400 M Pa (3,400,000 psi). This value was used in the analytical determination of live load deflections and stresses.

Live Load Tests

A uniformly distributed live load of 3,680 Pa (77 psf) was applied to the girder by placing steel barrels on the concrete slab and filling them with water. Figure 5 shows this test in progress. The load was removed from the girder as soon as strain and deflection measurements were recorded. No signs of distress in the girder were noted during or after the test. Figure 6 shows a comparison of the measured and computed deflections at various locations on the girder. The experimental data indicate nearly linear relationships between the load and deflection. These curves also indicate that the deflections were approximately 70% of the computed values.

Subsequently, the barrels were filled with sand to apply an equivalent uniform live load of 4,300 Pa (90 psf) to the slab. The barrels were filled progressively from one end of the girder to observe the behavior of the cross diagonals throughout the member. Computations had predicted that the cross diagonals would go into tension under a live load of 4,060 Pa (85 psf) applied to one-half of the girder length. However, the partial load caused no shear reversal in the unloaded panels so that the cross diagonals remained in compression during the test. It was planned to leave this load on the girder for an indefinite period of time to observe possible creep deflections and weathering effects. Four days after loading, the joint at the lower chord connectors and the stiffeners at both ends of the member failed due to the lateral force exerted on the stiffeners by the V supports. Figure 7 shows the displacement of the stiffener and distortion of the joint after failure occurred. While this was considered to be a serious failure of the girder, the member apparently lost no strength nor stability. Therefore, the load was not removed. Periodic creep deflection measurements and inspections for weathering were continued for several months. Figure 8 shows the net deflection of the top surface of the girder at midspan and at the supports over a period of time. These data were obtained with a surveyor's level and rod. The settlement at the supports was due to deformation of an asphalt pavement beneath the supports. The fluctuations observed at the centerline of the girder were attributed to thermal effects or measurement errors.

Figure 5. Live load test of TTG-13 with water-filled barrels for a distributed load of 3,680 Pa (77 psf).

Figure 6. Comparison of theoretical and experimental deflections for live load test of TTG-13. 25.4 mm = 1 in.; 47.8 N/m^2 = 1 psf.

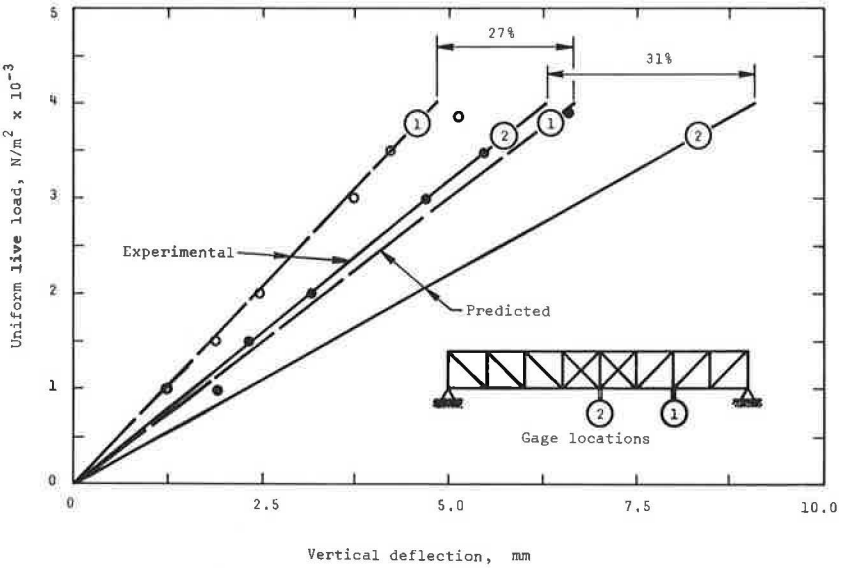

Figure 7. End view of girder TTG-13 showing the failure of a joint at a lower chord connector due to the seat bearing load.

Figure 8. Creep of TTG-13 at center span and settlement of the supports with a constant live load of 4,300 N/m^2 (90 psf).

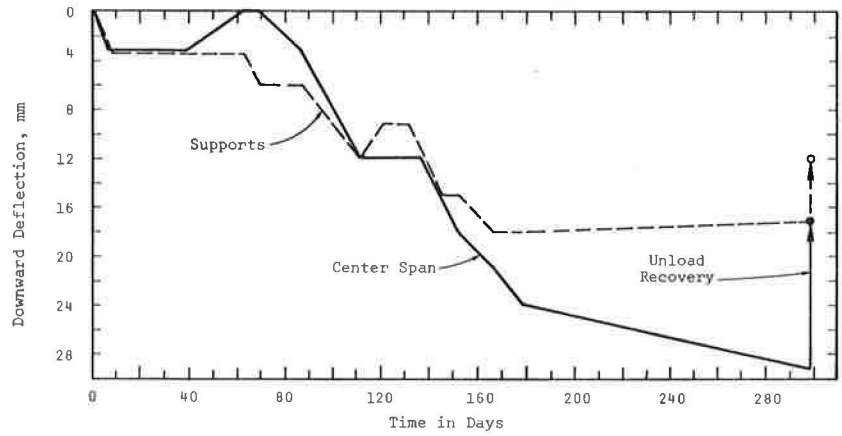

There appeared to be little, if any, creep deflection at the center of the girder for the first three months of the test. Over the next three months, however, a fairly constant rate of approximately 0.23 mm (0.009 in.) per day was observed. Subsequently, the rate decreased to approximately 0.04 mm (0.002 in.) per day. During this time it was noticed that the wooden supports were deforming at the joints and altering the bearing conditions of the girder appreciably. Therefore, it is not known whether the observed flexural creep of the girder was due to (uncompensated) movement of the supports or the yielding of the GRP materials within the girder. Figure 9 shows the terminal deflection of 76 mm (3 in.) of the center of the girder just prior to removal of the live load.

Quantitative weathering measurements (such as weight loss of coupons) were not made. However, it was noted that bleaching of the original greenish tint of the resin occurred gradually with time. Some "blooming" of the fibers (exposure of glass fibers due to erosion of the resin from the surface) was also noted after about six months on exposed surfaces of the pultruded shapes. Fiber blooming increased progressively over the test period but did not appear to influence the serviceability nor the performance of the girder in any way.

Figure 9. Deflection of TTG-13 at midspan relative to the ends of the girder just prior to removing the live load.

Creep Test of TTG-12

Experience with the fabrication and testing of TTG-13 indicated the need to study further the consequences of casting the concrete deck slab on a girder with temporary intermediate supports. Therefore, an experiment was conducted with specimen TTG-12 to investigate stress transfer from the fiberglass girder to a concrete slab cast on the top plate. An effort was made also to evaluate the integrity of the epoxy joint between the girder plate and the concrete slab as a load was applied to the composite girder. It was recognized that the deflection of the girder would be excessive under the weight of the fresh concrete because composite action of the fiberglass girder and the bonded concrete slab would not become effective until after the concrete developed compressive strength. It was reasoned that the deflection of the girder should be reduced by supporting it with falsework along its length until the concrete hardened, but it was not known how the top plate of the girder and the concrete slab would interact when the falsework shoring was removed. The experiment with TTG-12 was therefore planned to observe the behavior of the girder (a) as the concrete slab was cast, (b) when the interior supports were removed, and (c) following the load transfer to the slab.

Procedure. The test specimen was instrumented with electrical resistance strain gages and dial indicators and was supported temporarily at the two panel points adjacent to the center stiffeners. Placement of a concrete slab 76 mm (3 in.) thick followed the application of a coating of epoxy adhesive to the top plate of the girder. The slab was moist cured for 8 days during which time the compressive strength reached 21 MPa (3,000 psi). At that time, the interior supports were removed and strain and deflection measurements were initiated. Deflections were measured for 145 days and strain measurements were made for 16 days.

Experimental Results. As was expected, placement of the concrete slab caused downward deflections of the top plate of the girder between supports. The deflections increased equally 0.3 mm (0.012 in.) at each dial indicator during the first 48 hours after placement. Additional deflections of approximately 0.25 mm (0.010 in.) were measured at each gage over the next 6 days. Removal of the interior supports caused a fairly uniform downward displacement of the girder of approximately 1.5 mm (0.060 in.). Displacements occurring after the interior supports were removed are shown in Figure 10.

Discussion of Results. Overall, the test data indicated that considerable time was required for the test specimen to be transformed from a three-span continuous member with an inactive (concrete slab) compression flange to a single-span member with the concrete slab acting as the compression flange. The strain data from the top plate clearly showed that the neutral surface of the girder immediately moved into the concrete slab when the interior supports were removed. These data also indicated that the adhesive bond between the concrete and the girder plate initially was adequate to transfer whatever shear stresses developed at the interface. However, the long-term deflection data shown in Figure 10 are subject to speculative interpretation. One interpretation would suggest that the concrete slab continued to cure and shrink, with consequent increased deflection of the girder. It might also be argued that the concrete deformed due to compressive stresses and that the reinforced plastic tension elements also underwent creep deformation, but the relatively low stress levels involved do not support this contention. Relaxation or progressive failure of the adhesive at the concrete-GRP plate interface also could have caused the deflections observed.

The data of Figure 10 are believed to be reasonably accurate but they do present several disparities. First, it would be expected that the midspan deflection would be greater than that at the points closer to the end supports. The data indicate that all three points deflected approximately equally for the first month of observation. Secondly, there appears to be a significant change in the rate of the deflection at two of the gages approximately 30 days from the time the interior supports were removed. This behavior could occur if the adhesive bond at the concrete slab-plate interface failed suddenly, but if the bond did fail, it seems unlikely that only two of the gages would have been affected.

In summary, the data from this experiment did not clearly identify principal mechanisms controlling the behavior of the girder, but the test procedure and results did provide insight for the anticipated behavior and construction procedures for the prototype structure. Modifications in the design and erection procedures for the prototype resulting from these observations will be described later.

Phase II – Prototype Bridge

The prototype bridge (TTG-WC) was 4.9 m (16 ft.) long and 2.1 m (7 ft.) wide. It consisted of three identical girders, similar to TTG-13, connected by bonding a cover plate to each of the top flange plates and by tieing the lower chords together with strands of resin-impregnated glass roving. Each girder was 71 cm (28 in.) wide and 46 cm (18 in.) deep. Elimination of the cross diagonal elements included in TTG-13 required some changes in the lay-up pattern of the roving in the chord and diagonal elements. The final configuration used is shown in Figure 2 in comparison with that used for TTG-13. Approximately the same amounts of glass were used in the elements for both patterns. An increase in depth to 46 cm (18 in.) from the 40 cm (16 in.) used for TTG-13 reduced the predicted deflections and stresses from those determined for TTG-13. The design dead load was 2,250 Pa (47 psf) and the design live load was 4,062 Pa (85 psf).

Several modifications in the design were made to TTG-WC as a result of the tests conducted with TTG-12 and TTG-13.

1. The cross diagonal elements were omitted in all of the panels. These were considered unnecessary for the stability of the member.
2. End plates of 12 mm (1/2 in.) thick material salvaged from scraps of the top flange plate were fitted and bonded in the triangular space between the stiffeners at the ends of the girders to preclude the type of failure experienced with TTG-13.
3. Narrow strips of 12 mm (1/2 in.) thick plate were bonded to the top of the cover plate in a direction perpendicular to the length of the bridge. These strips served as mechanical shear connectors between the cover plate and the concrete slab. They also were used as clamps during the bonding of the

Figure 10. Deflections observed in TTG-12 during stress transfer from flange plates to the concrete slab.

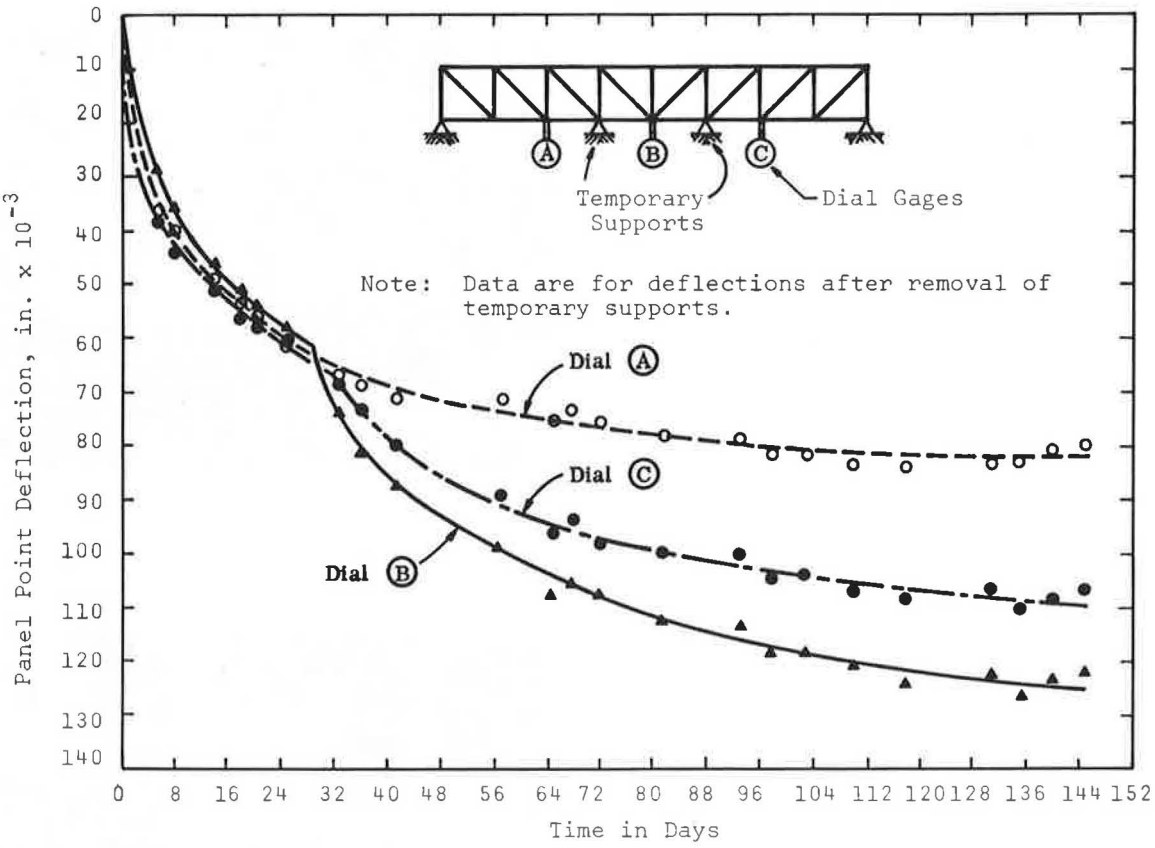

cover plate by bolting them securely to the flange plate of each girder.

4. The dimensions of the lower chord connector were altered slightly to provide better end bearing support for the mating stiffeners.

Fabrication of Girders

The fabrication of TTG-WC closely paralleled that of TTG-13 with some modifications. These modifications included the replacement of wooden bolts with brass bolts in the flange-to-stiffener connection, the elimination of positioning pins in the joint between the stiffeners and the lower chord connectors, and sandblasting of all bonded surfaces. A corrosion resistant metallic bolt was used to provide more strength than that available from the wooden bolts. The 6 mm (1/4 in.) diameter pins were omitted from the lower chord connector because they were determined to be structurally ineffective and were not required for the assembly procedure. All mating surfaces which were to be bonded with an epoxy adhesive were sandblasted to assure removal of the release agent used in the manufacture of the pultruded products. A No. 1 silica sand was used in a sandblaster at an air pressure of 275 Pa (40 psi) to clean the surfaces of plates and stiffeners. This operation was time-consuming but provided a better bond surface than previously obtained by belt sanding. The manpower requirement for the winding operation of each of the three girders was approximately the same (six man-hours) as that for TTG-13.

Assembly of Bridge

The three identical girders were assembled to form the prototype structure by bonding a common cover plate (6 mm [1/4 in.] thick) to the top flange plate and by connecting the lower chords with strands of glass-impregnated roving. It was essential that the adhesive joint between the girder flange and cover plate should be as free from voids as possible to develop the shear strength required for the integrity of the compression element for the bridge. Experience in bonding large surface areas during the assembly of TTG-8 (see reference 2) had provided an indication of the difficulty in achieving a void-free joint. The two primary contributing factors in the assembly problem was the inherent warpage of the pultruded plates and the bending, or distortion, of the top plate resulting from the attachment of stiffeners and tension strands during the fabrication of the girder. While both of these factors were individually small, there was some concern that the distortion could be eliminated in order to provide contact over most of the plate area within the 0.075 mm (0.003 in.) thickness required by the glue line. It was obvious that a normal clamping force would be required to hold the surfaces together while the adhesive cured. Because of the large areas involved and the time required to complete the joint, an epoxy that cured at room temperature was selected as the adhesive.

In view of the above considerations, steel beams were placed transversely beneath all three girders and supported at the ends so that the top plate of each girder rested directly upon the steel beam. Careful leveling of the beams and alignment of the

girders longitudinally achieved a reasonably rectangular and planar configuration for the overall surface for the bridge. The cover plates, 1.2 m (4 ft.) wide, were cut to lengths of 2.1 m (7 ft.) to eliminate all longitudinal joints and to simplify the bonding procedure. Four cover plates were therefore used to cover the entire bridge area. Prior to applying adhesive to both plates, the surfaces were cleaned thoroughly with an acetate solvent. Contact between mating plate surfaces was achieved by applying C-clamps along the edges, bolting three clamping strips per cover plate, and applying pressure through an air bag over the center portion of the plate. Figure 11 shows a typical arrangement for bonding one of the cover plates. The supporting steel beams may be seen in the lower right of the figure. The air bag was in contact over the full width of the bridge along a strip slightly less than 1 m (3 ft.) wide. The adhesive was permitted to cure under pressure for at least 5 days at a room temperature of approximately 23°C (70°F). Inspection of the bonded joint after curing was made by visual observation around the edges of the plates and by scanning portions of the plates with an ultrasonic detector. The visual inspection revealed that most, but not all, of the peripheral joints were free of open cracks.

Several regions which were either considered to be well-bonded or had a likelihood of improper bonds were selected for ultrasonic scanning. The well-bonded regions included the central portions of the contact surfaces over which the air bag had been pressurized. The regions of questionable bonds were along the interior edges of the cover plates, the interior edges of the flange plates, and particularly the "corner" areas formed at the intersections of the joints in the flange and cover plates. As described previously, the inherent curvature in the respective plates and the inability to provide positive clamping along the interior edges of the cover plates during assembly raised some doubts as to the nature of the bonded joint in these areas. The ultrasonic inspection was made with a V-Scope, Model C-4960, manufactured by James Electronics of Chicago, as shown in Figure 12. The V-Scope measured the time required for a high frequency audio wave to pass through the two plates and epoxy joint. Calibration of the instrument with a "good" joint and one with an extensive void established a well-defined measurement of the time delay due to the void. Approximately 50 points along the joined edges of the plates were surveyed. Nearly one-half indicated the presence of voids. However, the voids did not appear to extend beyond 75 mm (3 in.) from the edge of the plate. One point (at one of the corner intersections) strongly indicated a crack or a separation of the plates extending approximately 75 mm (3 in.) from the edge. None of the points checked with the V-Scope in the central regions of the plates (presumably well-bonded areas) showed any indication of voids or cracks. From the visual inspections and ultrasonic surveys of the bonded plates, the plate assembly procedure appeared to be successful even though it was tedious and required intermittent steps.

After the cover plate was bonded to the top plate of the girders, the entire structure was inverted and the lower chord connectors of parallel girders were tied together with strands of roving as described previously. This operation was quite simple and was completed within several hours. Figure 13 shows this operation. However, inverting the structure without exerting undesirable forces or distortion on the plates or chords required special efforts and fixtures. Wooden braces were attached

Figure 11. Bonding of cover plates on TTG-WC with pressure applied by C-clamps and by means of an air bag.

Figure 12. Inspection of bonded plate joints by means of an ultrasonic scanner.

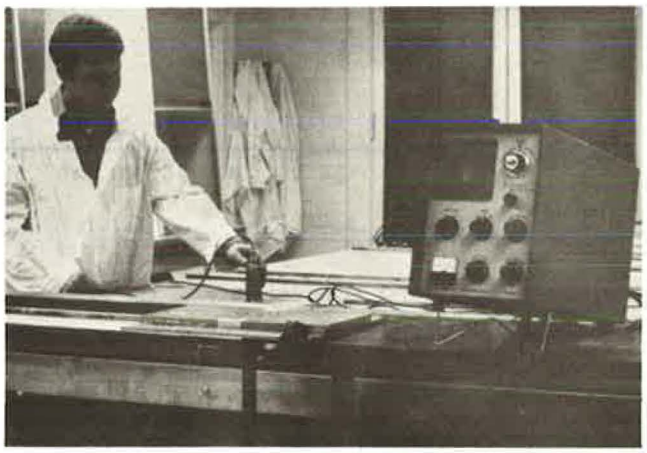

Figure 13. Connecting the lower chords of TTG-WC with continuous strands of resin-impregnated fiberglass.

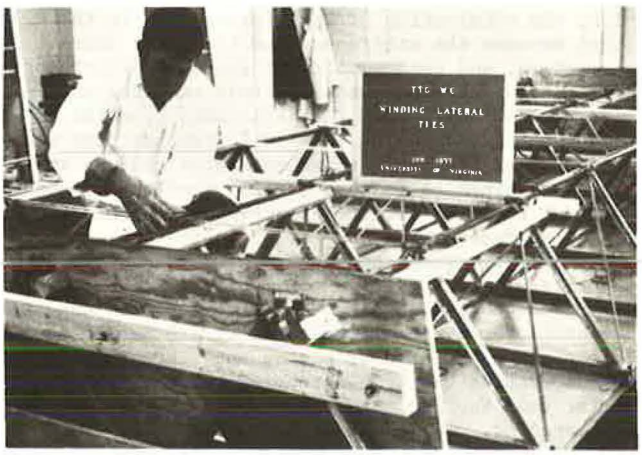

throughout the bridge and movable wooden towers were built to support the structure as it was rotated.

Instrumentation

The bridge was instrumented with electrical resistance strain gages to monitor the deformation of various diagonals, chords, and plates. A total of 20 electrical strain gages (Micro Measurements CEA-06-250-UW-350) were bonded (epoxy, M-Bond AE 15) to the surfaces at selected locations to measure strains in various stranded elements and plates.

Prefabricated Concrete Seats

Concrete seats were designed and prefabricated in the laboratory to match exactly the sawtooth profile of the ends of the assembled bridge. The seats were designed to provide bearing over approximately the middle one-third length of each end stiffener with sufficient clearance around the lower chord connector to preclude any bearing on the stiffener after settlement in the supports. A 6 mm (1/4 in.) thick layer of elastomeric material was cast into the concrete surfaces along the bearing length to assure uniform pressure on the stiffener surfaces. The width of the seat was 10 cm (4 in.) to accommodate the full width of the double stiffener assembly at the ends of the girders. Attachment to an abutment in the field was provided by dowels extended from the back face of the seat which were anchored when the backwall was cast. No anchorage provision was made to hold the bridge in the seat as the dead weight of the completed structure should compensate for any uplift which might be anticipated.

Schedule for Field Studies

Originally, the erection of the pedestrian bridge was scheduled for the spring of 1977. However, certain environmental considerations at the highway rest area postponed the advertisement of bids for construction. At the time of this writing, it is anticipated that the bridge will be erected during the summer of 1978. Therefore, data from load tests and evaluations of erection procedures of the prototype structure will appear in the final report of the project to be issued upon completion of all proposed work.

Materials Used in Fabrication

The following materials were used for the fabrication of the girders.

1. Pultruded square tubes and plates were obtained from Morrison Molded Fiberglass Company, Bristol, Virginia. All materials were grade Extren 500.
2. Fiberglass reinforcement was obtained from Owens Corning Fiberglass Company, Toledo, Ohio. Type 30, E glass roving was used for winding all tensile elements.
3. Polyester resin, Type E 447, used to impregnate the glass roving, was also obtained from Owens Corning Fiberglass Company. Small quantities of MEKP were used as the catalyst to provide a gel time of approximately 50 minutes.
4. Joints between pultruded sections and plates were bonded with epoxy adhesives furnished by Morrison Molded Fiberglass Company (Kit 502) and H. B. Fuller Company, St. Paul, Minnesota, (Resiweld FE7004).
5. The bonded joint between the cover plates and the concrete slab was made with an epoxy, Sikadur Hi-Mod, obtained from Sika Chemical Corporation, Lyndhurst, New Jersey. This epoxy was a two-component material consisting of 1-1/2 parts epichlorohydrin bisphenol A to 1 part of the reaction product of an aliphatic polyamine and monofunctional epoxide modified with 2.46 tri (dimethylaminomethyl) phenol. The initial viscosity for the blended adhesive was specified as 2,000 cps and a tensile strength of 24.1 MPa (3,500 psi) was to be developed after curing for 14 days.

Acknowledgements

The reported research is being sponsored jointly by the Virginia Department of Highways and Transportation and the Federal Highway Administration. Administrative oversight is being provided by the Virginia Highway and Transportation Research Council. Special recognition for assistance is given to Husamettin Alper and Wayne Burton, graduate research assistants, and to John Stulting, James Mills, and Clyde Giannini, members of the technical staff of the Virginia Highway and Transportation Research Council.

The opinions, findings and conclusions expressed in this report are those of the author and not necessarily those of the sponsoring agencies.

References

1. McCormick, F. C., "Modification Studies for a Bridge Girder of Reinforced Plastics," Virginia Highway & Transportation Research Council, Report No. VHTRC 77-R5, July 1976, 29 pp.
2. McCormick, F. C., and H. Alper, "Further Studies of a Trussed-Web Girder Composed of Reinforced Plastics," Virginia Highway & Transportation Research Council, Report No. VHTRC 76-R16, November 1975, 78 pp.
3. McCormick, F. C., "Study of a Trussed Girder Composed of a Reinforced Plastic," Virginia Highway & Transportation Research Council, Report No. VHTRC 75-R6, August 1974, 40 pp.
4. _____, "Initial Studies of a Flexural Member Composed of Glass-Fiber Reinforced Polyester Resin," Virginia Highway & Transportation Research Council, July 1973, 28 pp.

Selected Bibliography

1. Baer, Eric, Editor, Engineering Design for Plastics, Reinhold Publishing Corp., New York, 1964.
2. Benjamin, B. S., Structural Design with Plastics, Van Nostrand Reinhold Co., New York, 1969.
3. "Composite Materials: Testing and Design", American Society for Testing and Materials, Philadelphia, STP 546, 1973.
4. "Composite Reliability", American Society for Testing and Materials, Philadelphia, STP 580, 1975.
5. Structural Plastics: Properties and Possibilities, American Society of Civil Engineers, New York, 1969.

METHODS OF CALCULATION OF THE WIND-INDUCED RESPONSES OF SUSPENDED-SPAN BRIDGES

Robert H. Scanlan
Department of Civil Engineering
Princeton University
Princeton, New Jersey

Abstract

An outline is given of the manner in which expressions for the buffeting forces of the wind, together with those for the self-excited aerodynamic forces due to resulting bridge motion, may be used to predict the random response of a long-span bridge to the action of the natural wind. The problem is examined in terms of the individual responses of the several modes of the structure as they are randomly excited, both in space and in time, by wind gusts. The bridge deck modes in question are each considered to have vertical, torsional and lateral sway components. Recent formulations for wind horizontal and vertical gust spectra are employed. More complete literature references are cited for the details of the methodology used.

Introduction

The wind-induced responses of suspended-span bridges include vortex-induced activity, flutter, galloping, and buffeting. Basically, the intrinsic character of each of these phenomena is determined in the first instance by the geometry of the deck cross-section. It has become the practice in the last ten years to abstract the measured unsteady aerodynamics characteristics of the deck— once its geometry is set— from its particular structural characteristics. The two may then be reunited later in whatever way is dictated as appropriate by the structural dynamics of the full bridge.

The aerodynamic forces consist of a) the steady forces, b) the gust, or buffeting forces, and c) the self-excited forces (related to motions of the bridge). Any analysis must provide for all of these.

In modern bridges the vertical, torsional, and sway components of any given natural structural mode must all be considered; modes are not correctly characterized uniquely as being uncoupled in each of these motions. The motion in one component sense will engender structural and aerodynamic forces in one of the others, and these interact. Hence analytic provision must be made for all possible forces as a study progresses.

While section models of bridges remain the investigatory method of choice, they should now be conceived of only as purely geometric sources of aerodynamic data, never as proper analogs of the full prototype. This is true because conditions under which a section model can be conceived of as truly representative of a prototype are indeed very restrictive; the bridge deck must be straight; bending and torsion modes must be strictly uncoupled, and they must possess identical modal form distribution over the entire span. Otherwise, a section model can be a misleading object of study. Further, section models should not be tested exclusively in laminar flow, but the effects of turbulence included (or considered) in order to verify its local effect up deck-section aerodynamic properties.

Structural Modes

It will be assumed here that a single, linear spanwise coordinate x suffices to define any point along the bridge span (even if the latter is curved in plan or elevation). Since the full bridge is three-dimensional, with displacement components h(x), α(x), p(x) in vertical, torsional, and sway directions, respectively, the total deck section displacement may be represented as a superposition of the components in modes i:

$$h(x,t) = \sum_i h_i(x)\ B\ \xi_i(t) \tag{1a}$$

$$\alpha(x,t) = \sum_i \alpha_i(x)\ \xi_i(t) \tag{1b}$$

$$p(x,t) = \sum_i p_i(x)\ B\ \xi_i(t) \tag{1c}$$

where B, the deck width, is a reference length.

Steady Aerodynamic Forces

These are simply given for unit span by

$$\text{Lift:}\quad L_s = \tfrac{1}{2}\rho U^2 (B)\ C_L\ (\alpha) \tag{2a}$$

$$\text{Drag:}\quad D_s = \tfrac{1}{2}\rho U^2\ A\ C_D\ (\alpha) \tag{2b}$$

$$\text{Moment:}\quad M_s = \tfrac{1}{2}\rho U^2\ B^2\ C_M\ (\alpha) \tag{2c}$$

where A is projected area (normal to the horizontal wind) per unit span, ρ is air density, U is mean wind velocity (assumed normal to the span).

Self-Excited Forces

These are given [1] in linearized form (per unit span) by

$$\text{Lift:}\quad L_{s.e.} = \tfrac{1}{2}\rho U^2 (2B)\ [K\ H_1^*\ \frac{\dot{h}}{U} +,$$

$$K\ H_2^*\ \frac{B\dot{\alpha}}{U} + K^2\ H_3^*\ \alpha] \tag{3a}$$

$$\text{Drag:}\quad D_{s.e.} = \tfrac{1}{2}\rho U^2 (2B)\ [K\ P_1^*\ \frac{\dot{p}}{U}] \tag{3b}$$

$$\text{Moment:}\quad M_{s.e.} = \tfrac{1}{2}\rho U^2 (2B^2)[K\ A_1^*\ \frac{\dot{h}}{U} +,$$

$$K\ A_2^*\ \frac{B\dot{\alpha}}{U} + K^2\ A_3^*\ \alpha] \tag{3c}$$

where $K = B\omega/U$ is reduced frequency parameter, and H_i^*, A_i^*, (i = 1,2,3) functions of K, are self-excited aerodynamic coefficients.

In the case of vortex-induced oscillations, particularly, the above model may require upgrading by inclusion of nonlinear terms. Typical third-degree additional terms appropriate to lift and moment are

$$\text{Lift:}\quad (L_{s.e.})_{n.\ell.} = \tfrac{1}{2}\rho U^2 (2B)\ [K\ H_o^* (\frac{h}{U})^3] \tag{4a}$$

$$\text{Moment:}\quad (M_{s.e.})_{n.\ell.} = \tfrac{1}{2}\rho U^2 (2B^2)[K\ A_o^* (\frac{B\dot{\alpha}}{U})^3] \tag{4b}$$

These forces must be determined by recourse to model experiment, as described in Refs. [1], [2].

Buffeting Forces

These are given [3] (per unit span) by the forms

$$\text{Lift:}\quad L_b(x,t) = -\rho U^2 B[C_L(\alpha_o)\frac{u(x,t)}{U} +,$$

$$\tfrac{1}{2}\frac{dC_L}{d\alpha}\Big|_{\alpha=\alpha_o} + \frac{A}{B}\ C_D(\alpha_o)\ \frac{v(x,t)}{U}] \tag{5a}$$

$$\text{Drag:}\quad D_b(x,t) = \rho U^2 B\ [\frac{A}{B}\ C_D\ \frac{u(x,t)}{U}] \tag{5b}$$

$$\text{Moment:}\quad M_b(x,t) = \rho U^2 B^2\ [C_M(\alpha_o)\ \frac{u(x,t)}{U} +,$$

$$\tfrac{1}{2}\frac{dC_M}{d\alpha}\Big|_{\alpha=\alpha_o}\ \frac{v(x,t)}{U}] \tag{5c}$$

where α_o is the steady net twist under the mean wind velocity U; C_L, C_D, C_M (functions of bridge deck angle of attack α) are steady lift-, drag-, and moment-coefficients, respectively, and u(x,t), v(x,t) are respectively the horizontal and vertical gust components of the wind.

Net Equations of Motion

These take the form

$$[(M_V+M_L)\ B^2+I]_i\ [\ddot{\xi}_i+2\zeta_i\ \omega_i\ \dot{\xi}_i+\omega_i^2\xi] =,$$

$$Q_i(t) \tag{6}$$

where M_V, M_L, I are the generalized inertias of mass m(x) and mass moment of inertia $I_{c.g.}(x)$ about the deck c.g. calculated for the modal components h(x), p(x), α(x):

$$(M_V)_i = \int_{\text{span}} m(x)\ h_i^2(x)\ dx \tag{7a}$$

$$(M_L)_i = \int_{\text{span}} m(x)\ p_i^2(x)\ dx \tag{7b}$$

$$(I)_i = \int_{\text{span}} I_{c.g.}(x)\ \alpha_i^2(x)\ dx \tag{7c}$$

and ζ_i is the mechanical (structural) damping in mode i, which has the natural circular frequency ω_i.

The generalized force Q_i is calculated by noting that

$$\delta W = Q_i \, \delta\xi_i = (L_{s.e.}+L_b)\, \delta h + (D_{s.e.}+D_b)\, \delta p + (M_{s.e.}+M_D)\, \delta\alpha \quad (8)$$

where

$$\delta h = hB \, \delta\xi_i \quad (9a)$$

$$\delta p = pB \, \delta\xi_i \quad (9b)$$

$$\delta\alpha = \alpha \delta\xi_i \quad (9c)$$

The details of Q_i involve intermodal coupling which may be ascribable to the aerodynamics. It is not fruitful here to reproduce full details on the form of Q_i when several modes enter the response. Suffice it to give the flavor of Q_i for the case when one mode alone is assumed to respond tentatively assuming negligible aerodynamic influences from other modes:

$$\begin{aligned} Q_i(t) = Q(t) = \rho U^2 B^2 \{ & [K H_1^*(K) G_{hh} + K H_2^*(K) G_{h\alpha} + K A_1^*(K) G_{h\alpha} \\ & + K A_2^*(K) G_{\alpha\alpha} + K P_1^*(K) G_{pp}] \frac{B\dot{\xi}}{U} \\ & + [K^2 H_3^*(K) G_{h\alpha} + K^2 A_3^*(K) G_{\alpha\alpha}] \xi \\ & + \int_{span} \{ [-C_u h(x) + C_{M1} \alpha(x) + C_p p(x)] \frac{u(x,t)}{U} \\ & + [-C_v h(x) + C_{M2} \alpha(x)] \frac{v(x,t)}{U} \} \, dx \end{aligned} \quad (10)$$

with the definitions

$$G_{hh} = \int_{span} h^2(x)\, dx \qquad G_{h\alpha} = \int_{span} \alpha(x)\, h(x)\, dx$$

$$G_{\alpha\alpha} = \int_{span} \alpha^2(x)\, dx \qquad G_{pp} = \int_{span} p^2(x)\, dx$$

$$C_u = C_L(\alpha_o) \qquad C_v = \frac{1}{2}\left(\frac{dC_L}{d\alpha}\bigg|_{\alpha=\alpha_o} + \frac{A}{B} C_D(\alpha_o)\right)$$

$$C_{M1} = C_M(\alpha_o) \qquad C_{M2} = \frac{1}{2} \frac{dC_M}{d\alpha}\bigg|_{\alpha=\alpha_o}$$

$$C_p = \frac{A}{B} C_D$$

Comments on Aerodynamic Response

In principle, with proper section model background experiments, the entire gamut of responses to aerodynamic input can now be calculated, based on the above theory. This is being routinely done on several modern bridges. However, it is often possible, through initial model experiments, to establish bridge deck geometric shapes that are such as to minimize vortex shedding, incipient galloping and flutter [4]. When this type of modern attention to aerodynamic contour treatment is properly paid in the design stage, it typically results in deck sections having $H_1^* < 0$, $A_2^* < 0$, $H_2^* \tilde{=} 0$, $H_3^* \tilde{=} 0$, $A_1^* \tilde{=} 0$, $A_3^* \tilde{=} 0$ for wide ranges of the parameter K. This can considerably simplify the treatment.

For example, the criterion for flutter in the single mode ξ becomes

$$\zeta = \frac{\rho B^4}{2[(M_V+M_L)\, B^2+I]} \{ G_{hh} H_1^* + G_{h\alpha} H_2^* + G_{h\alpha} A_1^* + G_{\alpha\alpha} A_2^* + G_{pp} P_1^* \} \quad (11)$$

when, by varying K, values of H_i^*, A_i^* (i=1,2) and P_1^* are determined such that the above is satisfied, flutter is present; however, note that if the criteria listed above are already achieved, flutter becomes an impossibility since the righthand side of (11) is intrinsically negative.

There remains only the buffeting problem to examine. This problem remains present even for stable geometric configurations. Many modern bridges that are not flutter-prone have nonetheless not been examined analytically for buffeting. Theory given in [2], [3] and the present paper point out how this calculation can be carried out.

Buffeting Responses

Only the basic outline of this calculation will be reproduced here, the details lying beyond the scope of the present paper. We consider here only the case of buffeting wherein intermodal coupling is negligible.

"Overall" damping $\tilde{\zeta}$, including aerodynamic and structural, can be expressed in the form:

$$\tilde{\zeta} = \zeta_i - \frac{\rho B^4}{2[(M_V+M_L)\, B^2+I]_i} \{ G_{hh} H_1^* + G_{h\alpha}(H_2^*+A_1^*) + G_{\alpha\alpha} A_2^* + P_1^* G_{pp} \} \quad (12)$$

and the (slightly) modified natural circular frequency can be given by

$$\tilde{\omega}^2 = \omega^2 \{ 1 - \frac{\rho B^4}{[(M_V+M_L)\, B^2+I]_i} H_3^* G_{h\alpha} + A_3^* G_{\alpha\alpha}] \} \quad (13)$$

Under these conventions, the power spectral density of response ξ_i is given by

$$S_{\xi_i}(\omega) = \frac{1}{(\tilde{\omega}^2-\omega^2)^2 + (2\tilde{\xi}\tilde{\omega}\omega)^2} \left[\frac{\rho U^2 B^2}{[(M_V+M_L)\,B^2+I]_i}\right] S_F(\omega) \qquad (14)$$

where

$$U^2 S_F = \int_{\text{span}}\int_{\text{span}} [D_u(x_1)\, D_u(x_2)\, S_u(x_1,x_2,\omega) + D_v(x_1)\, D_v(x_2)\, S_v(x_1,x_2,\omega)]\, dx_1 dx_2 \qquad (15)$$

In (15) the definitions are used:

$$S_{u,v}(x_1,x_2,\omega) = S_{u,v}(\tilde{\omega})\, e^{-C(x_1-x_2)/L} \qquad (16)$$

$$C = \frac{16\,\tilde{n}\,L}{U} \qquad (17)$$

where L = span, $\tilde{\omega} = 2\pi\,\tilde{n}$, and S_u, S_v define "standard" wind spectra.

From (14) formulas can be derived (as in [3]) which enable the calculation of the variance of the displacement components h, α, or p. As an example the formula for the single-mode variance $\sigma_h^2(x)$ of the vertical displacement of a bridge curved in plan but with negligible sway is given as

$$\sigma_h^2(x) = \frac{\pi h^2(x)}{4(2\pi\tilde{n})^3\tilde{\zeta}} \left[\frac{\rho B^3 L}{M_V B^2 + I}\right]^2 \left[\frac{2(C-1)}{C^2}\right] \times \left[G_{Du}\, S_u(n) + G_{Dv}\, S_v(n)\right] U^2 \qquad (18)$$

where

$$G_{Du} = \frac{1}{L}\left[C_u^2\, G_{hh} - 2\, C_u C_{M1}\, G_{h\alpha} + C_{M1}^2\, G_{\alpha\alpha}\right] \qquad (19a)$$

$$G_{Dv} = \frac{1}{L}\left[C_v^2\, G_{hh} - 2\, C_v C_{M2}\, G_{h\alpha} + C_{M2}^2\, G_{\alpha\alpha}\right] \qquad (19b)$$

Typical results for high excursions $3\sigma_h$ at the center of the hypothetical bridge are listed below for various mean wind velocities at bridge height:

U(mph)	40	50	60	70	80	90	100	110
$3\sigma_h$(ft)	0.43	0.64	0.89	1.27	1.56	1.86	2.26	2.68

Full details on the example bridge being omitted, the above results are merely illustrative as to trends. A very complete expose' of the methods described here, with additional commentary on stability under buffeting, is given in Ref. 5.

Summary

The present paper has sketched, though extremely briefly, the methods and approaches available to the calculation of aerodynamic responses of suspended-span bridges. It has been pointed out how the necessary bases for analytical insights into the problem can be obtained and used. Intrinsic to the method is the postulated use of aerodynamic data developed from bridge deck section models.

The point of the study is that if basic section model data of the proper sort are first made available, extensive prototype response calculations can be made reliably on a theoretical basis.

The methods alluded to briefly herein permit of considerable extensions and generalizations beyond those mentioned. A notable one of these is to demonstrate the fact that flutter of a full bridge under turbulent flow may be delayed to a higher velocity when many modes participate, due to buffeting; and the general buffeting response will exhibit an evergrowing mean square amplitude with increasing mean velocity U.

References

1. Scanlan, R. H. and Tomko, J. J.: "Airfoil and Bridge Deck Flutter Derivatives" Jnl. Eng. Mech. Div. ASCE, Vol. 97, No. EM6, Dec. 1971, pp. 1717-1737.

2. Simiu, E. and Scanlan, R. H.: Wind Effects on Structures New York, John Wiley and Sons. (in press, 1978).

3. Scanlan, R. H. and Gade, R. H.: "Motion of Suspended Bridge Spans Under Gusty Wind" Jnl. Struct. Div. ASCE, No. ST.9. Sept. 1977, pp. 1867-1883.

4. Scanlan, R. H. and Wardlaw, R. L.: "Aerodynamic Stability of Bridge Decks and Structural Members" Proc. Symposium on Cable-Stayed Bridges, Federal Highway Administration Pasco, Wash., Dec. 6-7, 1977.

5. Scanlan, R. H.: "The Action of Flexible Bridges under Wind: I. Flutter Theory; II. Buffeting Theory" Jnl. Sound and Vibration Southampton, U.K. (in press, 1978).

AERODYNAMIC STABILITY OF TWO CABLE-STAYED BRIDGES

Harold R. Bosch and Lloyd R. Cayes, Federal Highway Administration

The trend in long-span bridge development has been toward increased spans and flexibility and decreased dead weight and damping through use of higher strength materials, refinements in design procedures, and modern fabrication techniques. In some cases, this makes the structure, especially cable-stayed and suspension bridges, sensitive to wind-induced oscillations. Three types of vibrations, namely flexural, torsional (or coupling of the two), and flutter, should be investigated in the design. There is presently no purely analytical or theoretical procedure for the investigation of any of these types of oscillations. Aerodynamic stability information must be obtained from field observations or wind tunnel testing of models. Cable-stayed bridge concepts are receiving popularity in this country. Current cable-stayed designs are subject to the same fundamental wind excitation as the classical suspension bridge; however, the inherent increase in stiffness of the cable-stay box-girder does place it in a different realm of response. With this in mind, several wind tunnel aerodynamic studies have been conducted and recently completed. This paper discusses the results of two such studies. Information is presented regarding vortex shedding response amplitude and acceleration, critical flutter velocity, flutter derivatives, and static force coefficients.

This paper describes the procedures and presents the results of wind tunnel aerodynamic investigations of two cable-stayed bridges presently under construction in the United States. The first bridge investigated is a four-lane structure comprised of double trapezoidal steel box girders with an orthotropic deck and will cross the Mississippi River at Luling, Louisiana. The second is a two-lane structure with a single steel box and will cross the Ohio River at Huntington, West Virginia. Elevation and cross-sectional views are presented in Figures 1 and 2. Both studies were conducted in the George S. Vincent Wind Tunnel by the Federal Highway Administration (FHWA) for the Louisiana Department of Transportation and Development and West Virginia Department of Highways, respectively. The objective of each investigation was to determine bridge dynamic deflection and acceleration under vortex shedding excitation and the critical wind velocity for flutter instability.

It has been well known for many years that serious vibration problems can arise with suspended bridge structures as a result of wind action. Perhaps one of the earliest well documented examples is the failure of the Brighton Chain Pier Bridge in England in 1836 which was witnessed and reported on by Lt. Col. William Reid of the British Army. In fact, as noted by Farquharson (1), 10 suspension bridges suffered major damage or total collapse during the period 1818 to 1889. Most of these failures were of bridges of relatively short spans.

The half century following the 1889 failure of the 384.1-m (1,260-ft) span Niagara-Clifton Bridge marked a period of rapid advances in design and construction techniques as well as materials production and led to the appearance of lighter structures with significantly increased span lengths. The original Tacoma Narrows Bridge was the product of such progress, and its dramatic failure in 1940 is, perhaps, the best known example of an aeroelastic bridge deck instability. Investigations into the causes of the Tacoma Narrows disaster were immediately undertaken at the University of Washington (1), where wind tunnel tests on a scale model reproduced quite faithfully the observed behavior of the bridge during its brief life. The stability of the proposed design for the new bridge was then established by wind tunnel testing. Further research revealed that a section model representing a limited length of the bridge and mounted on springs to reproduce to scale the frequency of a significant mode of motion could be used to determine the response of the bridge in a normal wind at various vertical angles of attack.

During the past decade there has been considerable interest in employing wind tunnel techniques for the determination of the aerodynamic stability derivatives of suspended bridge models (2). These derivatives represent purely aerodynamic data, as opposed to overall dynamic response observations, which are the consequence, uniquely, of bridge cross section geometry.

In earlier wind tunnel tests, bridge deck section models were elastically suspended, with properly scaled vertical and torsional natural frequencies, and observed primarily for their

tendencies to flutter at some air speed. The present practice is to extract the purely aerodynamic characteristics of the model first and then employ these in the dynamic response calculations for the full bridge. This practice has the inherent advantage of divorcing test results from all model structural properties, such as inertia, damping, and frequency, except for geometry.

There are two basic types of wind effects on structures, static and dynamic. The static effect is the pressure that the moving air mass exerts against the structure, and it varies in direct proportion to the square of the mean velocity. The dynamic effects are the forces generated by flow separation and turbulence of the moving air as it passes around the structure or by changes in wind speed such as gusting.

In consideration of the static stability of bridge structures under steady wind, the critical wind direction is normally taken to be perpendicular to the longitudinal axis of the bridge. Lift, drag, and moment coefficients are estimated or measured in the wind tunnel for use in calculating the respective uplift, side thrust, or twist forces on the structure. When lift or drag forces become excessive, an unstable bridge may undergo lateral buckling or torsional divergence.

One form of wind-induced vibrations of bridges is that of vortex shedding response. When wind blows across a slender, bluff object, such as a bridge superstructure, the large wake that is formed consists of an array of vortices which are spaced in a characteristic pattern. The vortices form alternately on either side of the body in a periodic fashion, with the shedding frequency proportional to wind speed. The fluctuating nature of the wake causes an oscillatory force on the bridge, and as shedding frequency approaches the natural frequency of the structure, it is possible for vibrations to result. This response occurs over a range of wind velocities in the vicinity of the resonant value, with maximum amplitude obtained when the "lock-in" condition is achieved. Both the velocity range and maximum amplitude are functions of structural damping and degree of streamlining. Since vortex shedding response is amplitude limited, structural problems arising from this mechanism are seldom catastrophic, although local fatigue damage and human discomfort are possible and warrant consideration.

Another form of instability, and perhaps the most important, is commonly referred to as flutter, following terminology developed in early work on aeroelastic instabilities of aircraft. In this case, wind forces interact with bridge deck motions to create a self-excited oscillation of growing amplitude, possibly leading to destruction. Unlike the vortex shedding problem, the flutter phenomenon is not limited to a velocity range beyond which structural stability returns. Increasing velocity beyond the threshold value causes oscillations to buildup more rapidly and leads to more violent action.

Basic Theory and Mathematical Modeling

The susceptibility of the prototype structure to aerodynamic instability is determined by wind tunnel tests. These tests are conducted on a section model of the bridge which is subjected to laminar flow.

To extract detailed aerodynamic derivative data from the wind tunnel section model studies, it is necessary to provide an analytical model of the physical situation. For this purpose, a symmetrical two-degree-of-freedom system is assumed. As discussed by Scanlan (3), the equations of motion for the sectional structure may be written in the form:

$$m\left(\ddot{h} + 2\zeta_h\omega_h\dot{h} + \omega_h^2 h\right) = L \tag{1}$$

$$I\left(\ddot{\alpha} + 2\zeta_\alpha\omega_\alpha\dot{\alpha} + \omega_\alpha^2\alpha\right) = M \tag{2}$$

where I and m are mass moment of inertia and mass per unit span of model; h and α are vertical and torsional deflections of the given deck section (assumed uniform); ζ is the damping ratio-to-critical; ω is the circular frequency; and L and M are the dynamic lift and moment per unit span. For the self-excited flutter problem, L and M are taken as linear functions and may be written in the form:

$$L = m\left(H_1\dot{h} + H_2\dot{\alpha} + H_3\alpha\right) \tag{3}$$

$$M = I\left(A_1\dot{h} + A_2\dot{\alpha} + A_3\alpha\right) \tag{4}$$

where H_i and A_i (i = 1, 2, 3) are dimensional aerodynamic derivatives determined by experiment, with inertial factors introduced for convenience. By noting the fact that L and M are essentially functions of the "reduced frequency" or dimensionless parameter $K = B\omega/U$, nondimensional derivatives or coefficients may be obtained as:

$$L = 1/2\rho U^2(2B)\left(KH_1^*\frac{\dot{h}}{U} + KH_2^*\frac{B\dot{\alpha}}{U} + K^2H_3^*\alpha\right) \tag{5}$$

$$M = 1/2\rho U^2(2B)\left(KA_1^*\frac{\dot{h}}{U} + KA_2^*\frac{B\dot{\alpha}}{U} + K^2A_3^*\alpha\right) \tag{6}$$

where H_i^* and A_i^* (i = 1, 2, 3) are nondimensional aerodynamic coefficients; B is deck width; U is oncoming wind velocity; and ρ is air density. These equations have been reduced to experimental form to enable direct use, and the details of this reduction are included in reference 3. Essentially, test observations produce time histories of h and α; then with all quantities on the left-hand sides of equations 1 and 2 known, the coefficients are matched by system identification techniques to the test observations as functions of K.

The coefficients are important in evaluating the stability characteristics of a section. The A_2^* coefficient measures aerodynamic damping in the torsion mode and thus is an indicator of single-degree flutter in that mode. The A_3^* coefficient is usually small and is sometimes assumed zero in analysis. In general, it is a measure of the aerodynamic stiffening effect upon frequency. The H_1^* coefficient measures the aerodynamic damping in the vertical mode.

When vortex shedding response is exhibited either indirectly in the aerodynamic coefficients or directly in observations of the model test, the aforementioned mathematical model must be augmented to be applicable to the region of response (4). This can be done for the case of purely vertical motion by providing equation 5 with a special forcing function:

$$L(t) = \frac{1}{2}\rho U^2(2B)C_{L_o}\sin\omega_s t. \tag{7}$$

The resulting combined equation takes on the form:

$$m\left(\ddot{h} + 2\zeta_h\omega_h\dot{h} + \omega_h^2 h\right) = \frac{1}{2}\rho U^2(2B)$$

$$x\left(KH_o^*\frac{\dot{h}}{U} + C_{Lo}\sin\omega_s t\right) \qquad (8)$$

where H_o^* is an aerodynamic damping coefficient for decay to a resonant response amplitude; C_{Lo} is an oscillating lift coefficient; and ω_s is the Strouhal circular frequency. It should be noted here that a completely analogous model could be developed for the torsional case. The parameters above are determined experimentally from records of oscillations at the vortex "lock-in" condition and enable the ultimate prediction of prototype response amplitude.

The "strip" equation for the prototype deck section is expressed as:

$$M\left(\ddot{\eta} + 2\gamma_s\omega_s\dot{\eta} + \omega_s^2\eta\right) = P\sin\omega_s t, \qquad (9)$$

and the maximum mid-span amplitude is computed as:

$$\eta_{max} = \frac{P}{2M\omega_s^2\gamma_s} \qquad (10)$$

where $\gamma_s = \zeta - \frac{\rho B^2 H_o^*}{2m}$,

$P = \rho U^2 B C_{Lo}\int_{span}\Psi(x)dx$ = generalized force amplitude,

$M = m\int_{span}\Psi^2(x)dx$ = generalized mass,

$\Psi(x)$ = normalized span deflection.

$\Psi(x)$ is approximated by assuming that the main span deflected shape is represented by a half wave sine curve.

Design and Construction of Models

A section model of a suspended bridge superstructure is a geometrically similar copy of a typical length of the suspended structure only. Any cables or hangers are not modeled because their aerodynamic effects are considered negligible. The section model is rigidly constructed to ensure that all elastic behavior takes place in the springs from which it is suspended. The vertical and rotational movement of the section model supported by its spring suspension simulate the vertical bending and torsional twist of the prototype structure.

Four basic section models with 15 potential configurations were designed and constructed for the Luling test program. All models were designed to a geometric length scale of 1:60 to ensure adequate reproduction of significant structural details. Model length was set at 1.524 m (60 in) inside to inside of end plates, representing a 91.46-m (300-ft) section of prototype span. Model widths vary from .4281 m (16.85 in) to .5070 m (19.95 in), resulting in aspect ratios between 3.56 and 3.00. Details are given in Table 1 and illustrated in Figure 3.

For the Huntington test program, one basic section model with five potential configurations was designed and constructed to a scale of 1:45, with the 1.524-m (60-in) length representing 68.58 m (225 ft) of prototype. The width of the model is .2446 m (9.6 in), resulting in an aspect ratio of 6.25. Details are given in Table 1 and illustrated in Figure 3.

End plates were employed so that two-dimensional flow could be maintained near the model ends. The models were scaled according to Froude number criterion for wind speed and vertical natural frequency. Due to practical limitations of simulating the relatively high prototype torsional characteristics, torsional natural frequency does not, however, achieve Froude scaling.

To maintain proper weight and weight distribution, develop sharp edges, and provide necessary model strength and rigidity, a variety of lightweight materials were incorporated into the model designs. Girder webs, floor beams, and asphalt decks are constructed of aircraft birch plywood. Girder and beam flanges, edge strips, and railing lips are aluminum. Balsa wood was used for diaphrams, ribs, traffic barriers, stiffeners, and concrete decks. The end plates are of "sandwich" construction, with balsa wood between aluminum sheets. Edges were tapered to reduce drag effects, and an elliptical shape was chosen to minimize weight and polar mass moment of inertia. Trusses with tubular aluminum members were extended from the end plates to provide crossbars 2.286 m (90 in) apart for attachment of the supporting springs. Traffic barriers are attached with machine screws to facilitate removal for modification of the cross section. Details of the experimental arrangement can be seen in Figure 4.

Test Procedure and Instrumentation

The tests were conducted in the FHWA open circuit, low velocity wind tunnel which was designed particularly for testing bridge section models. A blower forces air through a diffusing section with a series of stainless steel wire screens into a cylindrical pressure chamber and through the nozzle from which the air is discharged onto the model. The velocity over the cross section of the wind stream is very uniform to a point 1.8 m (6 ft) beyond the end of the nozzle.

A steady wind velocity, with a range of 0 to 9.1 m/sec (0 to 30 ft/sec), is maintained with a micro-control rheostat in the blower circuit. The wind velocity is computed from the dynamic pressure head of the wind stream obtained by direct measurement with a pitot-static tube and an inclined manometer. Corrections are made for changes in air or fluid temperature and barometric pressure.

The nozzle can be rotated about the horizontal axis of the pressure chamber, allowing tests at various wind angles of attack. The angle of attack is the vertical angle between the wind velocity vector and a horizontal plane; a positive angle of attack indicates an upward wind.

The section models were suspended in front of the wind tunnel nozzle by means of four supports with upper and lower coil springs at each support, as illustrated in Figure 4. The vertical length of the springs was adjusted to set the proper vertical frequency of oscillation. The torsional frequency was set by adjusting the spacing between the springs at each end of the model. Although it was not possible to attain the relatively high torsional frequency desired, attempts were made to obtain as high a frequency as possible. The total mass of the section model, end plates, support trusses, end bracket crossbars, and "moving" springs was tuned to the desired scaled quantity by the addition of small weights to the end plates at the model center of gravity.

Horizontal restraining wires were attached to the end bracket crossbars at the center of gravity of the model to prohibit longitudinal or lateral movement during the tests. The restraining wires, which were tensioned with 0.9-kg (2-lb) weights, were of sufficient length that their vertical components would have no significant effect upon the vertical or torsional motion of the model.

Electrical resistance strain gages were attached to beryllium copper flexure plates above the coil springs. The strain gages at one end of the model were wired to indicate the vertical component of oscillation, and those at the other end were wired to indicate the torsional component. Strain gage outputs were amplified and the two components were recorded side-by-side on an oscillograph.

The models were tested only under laminar flow conditions. The tests were conducted at wind angles of attack varying from +6° to -4°. While maintaining a steady wind velocity at each of a series of increasing values, the models were displaced in the respective vertical and torsional degrees-of-freedom, released, and the oscillatory dynamic response recorded. For the vertical mode, the initial displacement was accomplished manually. For torsion, however, it was necessary to "hold" the model at a 4° displacement and release it using solenoids. The velocity and response data were processed on the FHWA computer system to obtain the aerodynamic derivatives and vortex response information discussed earlier.

The damping values of the model setup were determined by displacing and then releasing the model in a no-wind condition and recording the rate of decay. For the Luling study, tests were conducted at the values of model damping exhibited, and results were extrapolated for other values of damping as necessary. In the Huntington tests, however, various amounts of artificial damping were added during testing to yield results for a range of damping values.

Discussion of Results

Test results for each of the seven Luling configurations and the one Huntington configuration (Model 3-2.4-.01) are summarized in Figures 5 through 10.

No vertical flutter (self-excited, divergent, vertical oscillations) was exhibited by any of the model configurations during laboratory testing. This observation is verified by the computer plots of the aerodynamic derivatives. The H_1^* derivative, the function for aerodynamic damping of vertical oscillations, shows positive damping over the full test range. A typical plot of this derivative is presented in Figure 5. Torsional critical flutter velocities at zero damping and 1 percent damping are illustrated for prototype wind speed and wind angle (angle of attack) in Figures 6 and 7. Torsional flutter (self-excited, divergent, torsional oscillations) was exhibited at horizontal wind speeds greater than equivalent prototype design requirements of 240 km/h (150 mph) for Luling and 200 km/h (125 mph) for Huntington. The greatest flutter stability was demonstrated by the most "streamlined" models, C-6-C-A, C-6-C-B, and C-2C-A, with critical velocities in excess of 400 km/h (250 mph). As angle of attack increases in the positive direction, flutter stability generally decreases for the Luling configurations. Flutter stability of the Huntington model, however, is insensitive to angle of attack.

Since high wind velocities at high angles of attack are not considered likely in view of data obtained at the Severn and Newport Bridges (5), critical flutter velocities of less than design wind speed at high angles of attack are not considered a point of concern. Again, these observations are verified by computer plots of the A_2^* derivative, indicative of torsional aerodynamic damping. When A_2^* becomes positive, self-excitation tendencies are restrained only by the structural damping. A typical plot of this derivative is presented in Figure 8.

An excitation of the bridge deck in vertical and torsional modes by the resonant action of the periodic shedding of vortices in the wake of the structure was exhibited by all models. This amplitude-limited oscillation can be an unacceptable characteristic of the design when it occurs at moderate wind speeds, and resulting accelerations could be disturbing to the user. Generally, vertical vortex shedding response was exhibited at various velocities or ranges of velocities between 24 and 48 km/h (15 and 30 mph), while torsional vortex shedding response was exhibited between 96 and 160 km/h (60 and 100 mph). Since torsional response occurs at relatively high velocities, its effect on the user may be disregarded. For the vertical response which occurs at moderate wind speeds, deck accelerations of 2 percent of "G" are considered acceptable. Estimates of prototype accelerations are illustrated in Figure 9 for vertical response in a horizontal wind. Models C-2C-C and C-2C-A demonstrated the least overall vertical response, while the Huntington model, 3-2.4-.01, exhibited the most. These estimates are considered conservative since it is probable the real wind over the bridge span will be gusty enough to cause poor spanwise correlation and decrease the likelihood of "lock-in" to occur.

Drag coefficients were obtained for the preferred Luling cross section, C-2C-A, and its three erection stages as illustrated in Figure 10. For stage A1, the median barrier was removed; A2, median barrier and fairings removed; A3, median barrier, fairings, and railings removed. Horizontal pressures were computed from the coefficients for a moderate wind angle of +2° and were found to be somewhat less than recommended AASHTO values for configuration C-2C-A and about equal to the AASHTO values for stage A2.

Conclusions

This paper summarizes the results of comprehensive wind tunnel studies of two major bridge structures. The two bridges studied are examples of the cable-stayed, box-girder type which, until recently, has not often been constructed in the United States. In general, all the cross sections tested in a horizontal wind have critical velocities for flutter in excess of the appropriate design wind speeds. At other wind inclinations, the critical velocities remain high enough to exceed expected winds. Varying degrees of vertical motion are caused by vortex shedding at speeds between 24 and 48 km/h (15 and 30 mph). For the Luling, Louisiana, Bridge, vertical vortex shedding response amplitudes and accelerations are minimal and considered neither damaging to the structure nor discomforting to the user. In the case of the Huntington, West Virginia, Bridge, vortex-induced oscillations also are not a threat to bridge safety; however, due to the larger accelerations, pedestrians or passengers in stationary vehicles may feel some vertical motion. Drag forces measured in the wind tunnel appear reasonable relative to recommended design values. Further

details regarding this research may be found in the two recent study reports: "Aerodynamic Investigations of the Luling, Louisiana, Cable-Stayed Bridge," FHWA-RD-77-161 and "Aerodynamic Stability of Proposed Ohio River Cable-Stayed Bridge," FHWA-RD-77-157.

Acknowledgments

These projects were carried out at the request of the Louisiana Department of Transportation and Development and West Virginia Department of Highways. The authors gratefully acknowledge the technical support and guidance provided by Mr. Richard H. Gade, Project Manager for FCP Project 5A. Despite Mr. Gade's failing health in recent years, he never ceased to serve as a guiding force on these and other projects in the Wind Engineering field. Regretfully, Mr. Gade died on September 25, 1977, and he will be deeply missed by all those who knew him.

References

1. F. B. Farquharson et al. Aerodynamic Stability of Suspension Bridges with Special Reference to the Tacoma Narrows Bridge. University of Washington Engineering Experiment Station, Bulletin No. 116, Parts I-V, June 1949 to June 1954.
2. R. H. Gade and R. H. Scanlan. Experimental Measurement and Interpretation of Aerodynamic Stability Coefficients for the Decks of Two Cable-Stayed Bridges. Proceedings of ASCE and EMD Symposium on Dynamic Response of Structures, UCLA, March 1976, pp. 478-486.
3. R. H. Scanlan and J. J. Tomko. Airfoil and Bridge Deck Flutter Derivatives. Journal of Engineering Mechanics, Vol. 97, ASCE, December 1971, pp. 1717-1737.
4. R. H. Scanlan. Recent Methods in the Application of Test Results to the Wind Design of Long, Suspended-Span Bridges. Federal Highway Administration, Report No. FHWA-RD-75-115, October 1975.
5. R. H. Gade, H. R. Bosch, and W. Podolny, Jr. Recent Aerodynamic Studies of Long-Span Bridges. Journal of the Structural Division, Vol. 102, ASCE, July 1976, pp. 1299-1315.

Table 1. Cross-sectional data.

Section model designation (1)	Prototype section depth, in feet (2)	Roadway surface (3)	Railing type (4)	Vertical natural frequency, in cycles per second (5)	Torsional natural frequency, in cycles per second (6)
C-2-C-1	14	Concrete	Basic	2.62	5.29
C-2-C-2	14	Concrete	Alternate	2.56	5.20
C-2C-C	14	Concrete	Alternate	2.56	5.35
C-2C-A	14	Asphalt	Alternate	2.80	5.25
C-2A-C-1	12	Concrete	Basic	2.53	5.24
C-6-C-B	14	Concrete	Basic	2.49	5.33
C-6-C-A	14	Concrete	Alternate	2.48	5.24
3-2.4-.01	9.6	Asphalt	Basic	2.51	6.80

1 ft = 0.3048m

Figure 1. Bridge elevation and cross sections - Luling, La. Bridge.

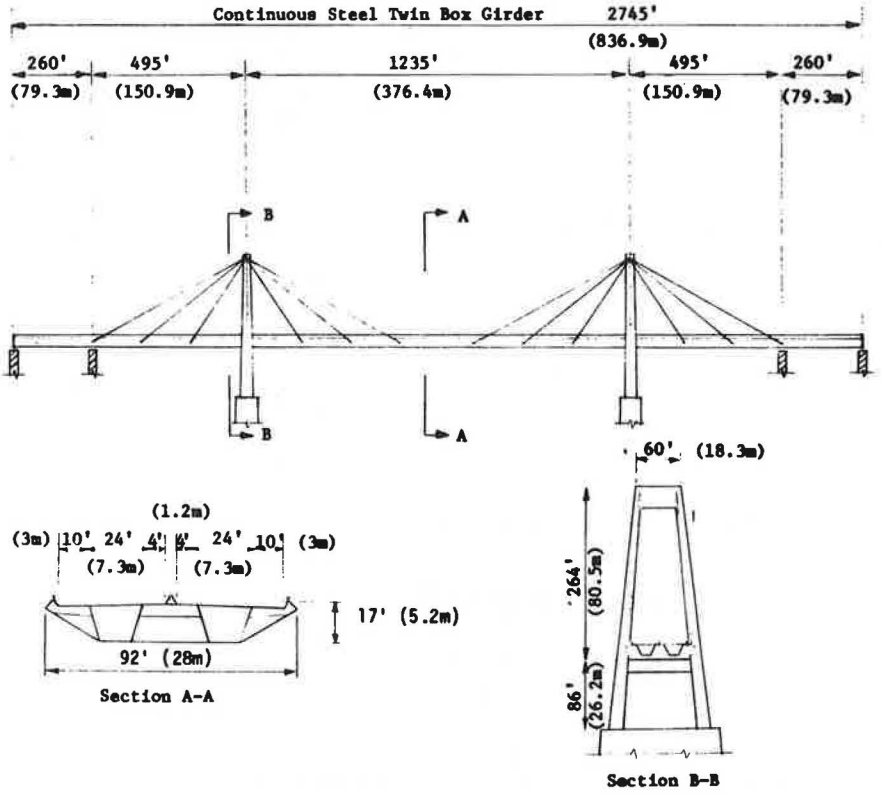

Figure 2. General elevation of prototype - Huntington, W. Va. Bridge.

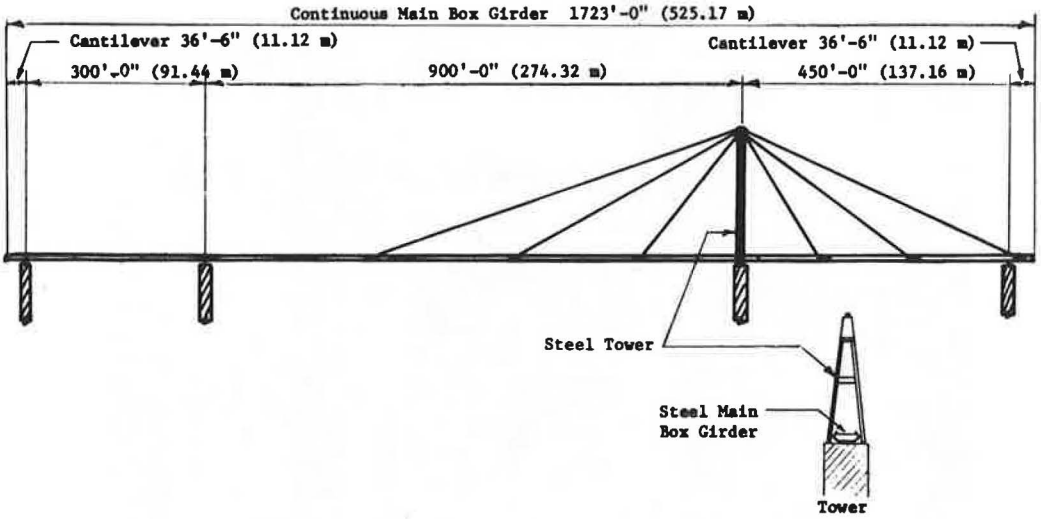

Figure 3. Model configurations and dimensions (1 inch = 25.4 mm).

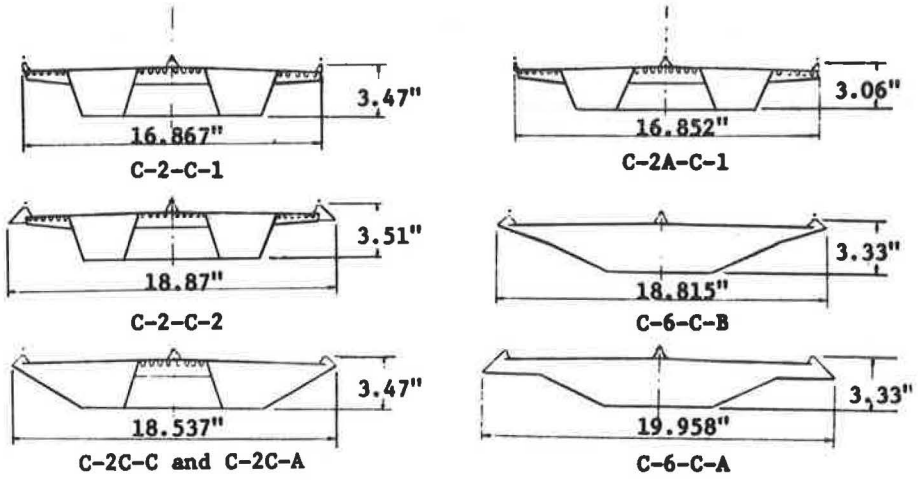

Luling, La. 1:60 Scale Section Models

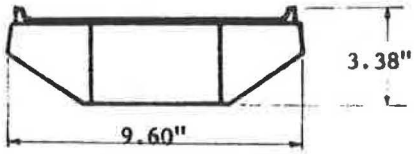

3-2.4-.01

Huntington, W.VA. 1:45 Scale Section Model

Figure 4. Model in wind tunnel.

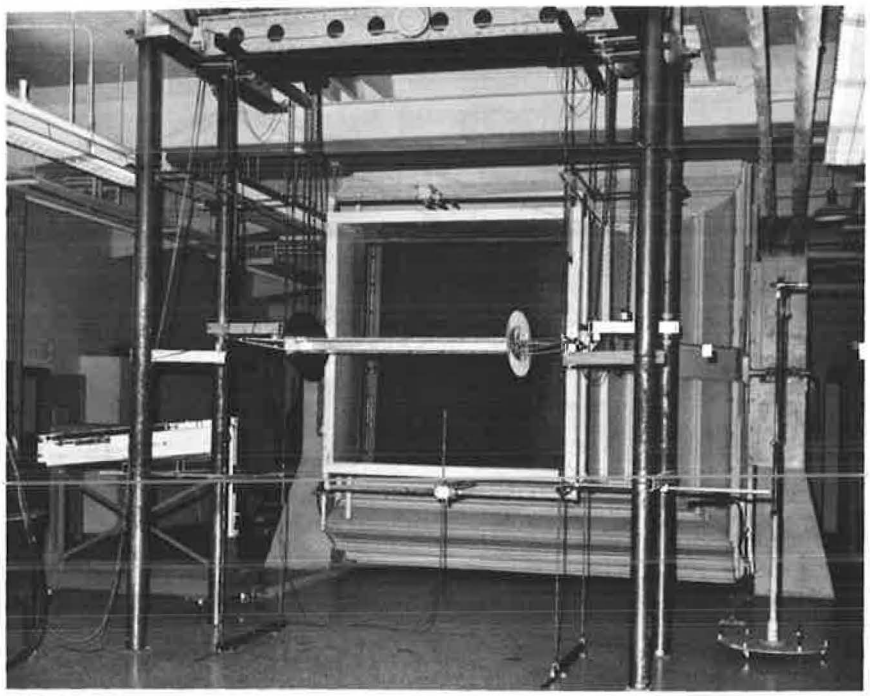

Figure 5. Flutter derivative for vertical - angle of attack = 0°.

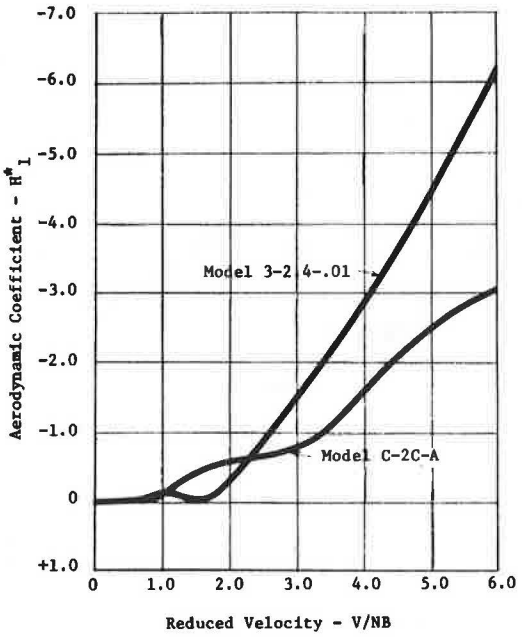

Figure 6. Critical flutter velocity - no damping.

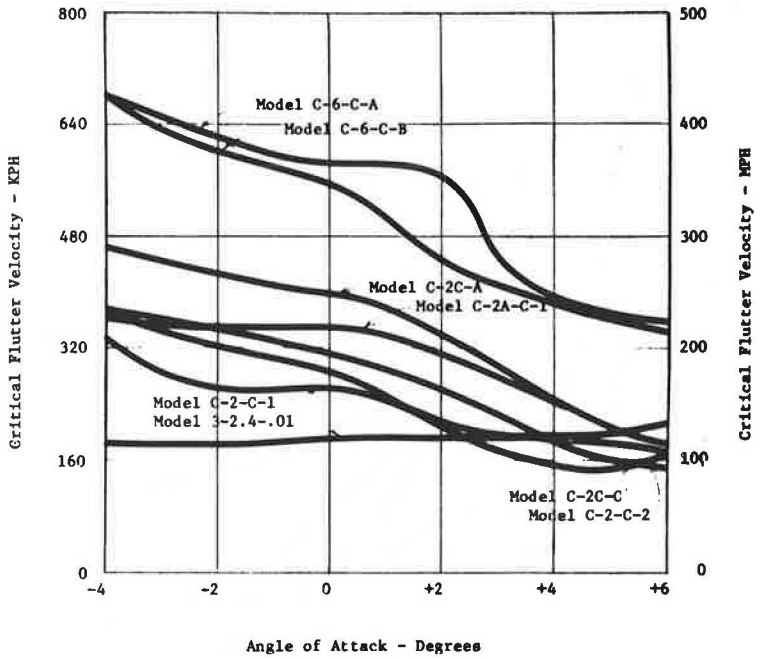

Figure 7. Critical flutter velocity - 1% critical damping.

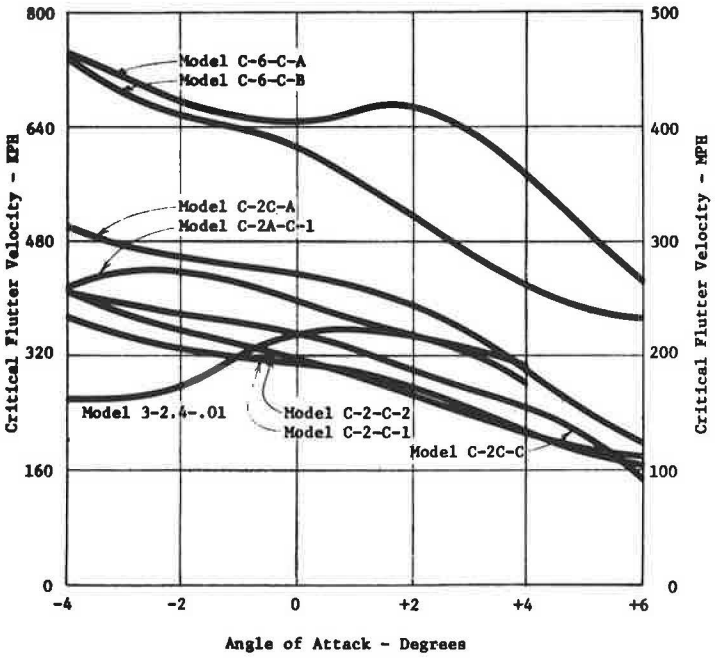

Figure 8. Flutter derivative for torsion - angle of attack = 0°.

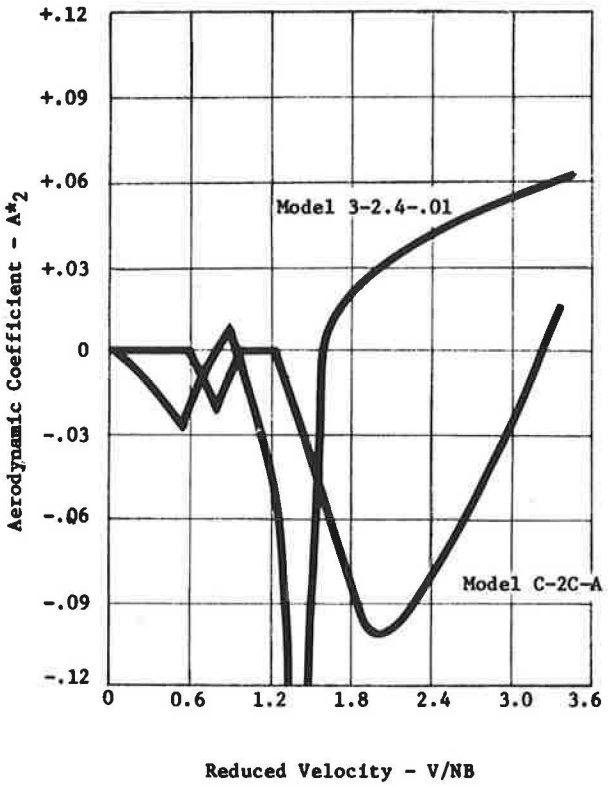

Figure 9. Estimate of prototype accelerations resulting from vertical vortex excitation - angle of attack = 0°.

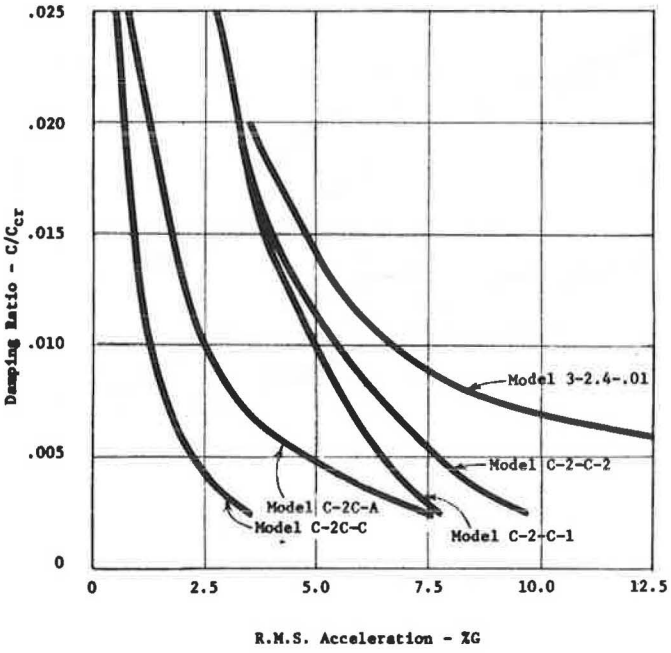

Figure 10. Drag coefficients.

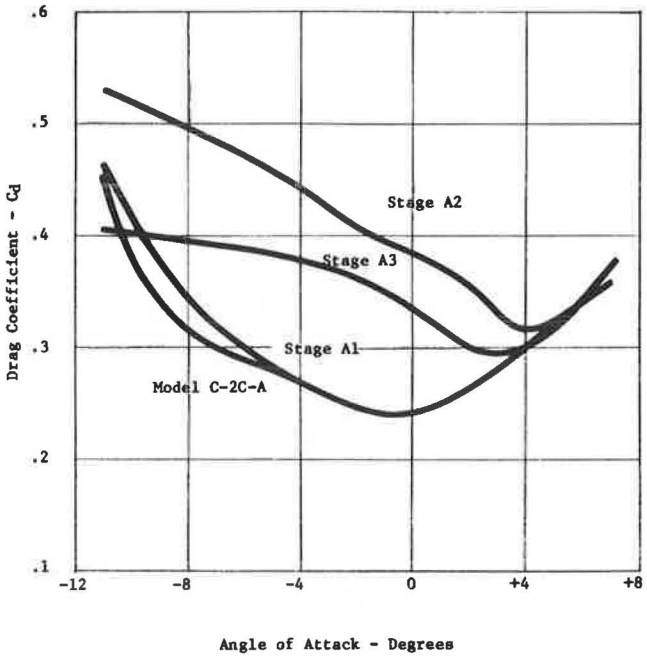

CONCRETE CABLE-STAYED BRIDGES

Walter Podolny, Jr., Federal Highway Administration

This paper presents a comprehensive review on a case-study basis of concrete cable-stay bridges either completed, under construction or in design, with the intent of encouraging designers to consider the feasibility of this type of structure. Evolution of concrete cable-stay bridges is traced from Torroja's Tempul Aqueduct in Spain, completed in 1925, to present day design concepts. Particular attention is given to structure concept, geometric configuration, design considerations, structural details, and method of construction. As late as 1970, the practical span limit of steel cable-stay bridges was considered to be 300 m (1,000 ft). Recently, concrete cable-stayed bridges are considered technically feasible with spans approaching 500 m (1,600 ft). It has been projected that with an aerodynamically shaped composite concrete and steel deck a span of 700 m (2,300 ft) can be achieved. With today's technology of prefabrication, prestressing, and segmental cantilever construction, it is obvious that cable-stay bridges are extending the competitive span range of concrete construction to dimensions that had previously been considered impossible. The technological means exist, they only require implementation.

The concept of supporting a beam or bridge by inclined cable stays is not new and the historical evolution of this type of structure has been discussed in the literature (1-3). The modern renaissance of cable-stay bridges is said to have begun in 1955 with the construction of the Strömsund Bridge in Sweden. This steel structure was built by a German contractor in collaboration with a German engineer, Professor F. Dischinger, who is reported to have rediscovered the stayed bridge in 1938 (4). Since 1955 approximately 80 cable-stay bridges have been built, are under construction, in design, or have been abandonded for one reason or another.

Although most cable-stay structures have been of steel construction a few have been of concrete. It is generally recognized that the first modern concrete cable-stay bridge was Morandi's Lake Maracaibo Bridge constructed in 1962. Since 1962, approximately 15 concrete cable-stayed bridges have been built and others are under construction or in design. Perhaps what is least known is that the first concrete structure to utilize cable stays was the Tempul Aqueduct crossing the Guadalete River in Spain (5). This structure, designed by the Spanish engineer Torroja, was built in 1926 and thus preceeds Dischinger's rediscovery in 1938.

This paper presents a comprehensive review of concrete cable-stay bridges on a case study basis with the intent of encouraging designers to consider the feasibility of this type structure which in some instances might be a more appropriate choice. A tabulation of proportions and ratios of the cable-stay bridges discussed in this paper is given in Table 1 for comparative purposes.

Lake Maracaibo Bridge, Venezuela

The first modern prestressed concrete cable-stay bridge was built over Lake Maracaibo in Venezuela in 1962 and was designed by Professor Riccardo Morandi of Rome University. It ranks as one of the longest cable-stayed bridges in the world, having a superstructure of reinforced and prestressed concrete construction, Figure 1.

Figure 1. Lake Maracaibo Bridge.

This structure has a total length of 8.7 km (5.4 miles). Navigation requirements dicated a horizontal clearance of 200 m (656.2 ft) and a vertical clearance of 45 m (147.6 ft). The five main navigation openings consist of prestressed concrete cantilevered cable-stayed structures with suspended spans hav-

Table 1. Concrete cable-stay bridge proportions and configuration

Bridge	No. of Cable-Stayed Spans	Total Length of Cable-Stayed Spans (m)	Major Span Length (m)	Ratio of Total Length to Major Span	Girder Depth (m)	Span to Girder Depth Ratio	Girder Construction Type[c]
Lake Maracaibo	5	1175	235	5	5	47	CIP with PC drop-in span
Polcevera Viaduct	3	550	210	2.6	4.6	45.7	CIP with PC drop-in span
Wadi Kuf	3	475	280	1.7	4 to 7	70	CIP with PC drop-in span
Magliana Viaduct	2	198.6	145	1.37	-	-	CIP with PC drop-in span
Chaco/Corrientes	3	572.4	245	2.3	3.5	70	PC with CIP drop-in span
Danish Great Belt[a]	-	-	345	-	7.2	48	PC segments
Danish Great Belt[b]	-	-	351	-	0.9	390	CIP segments
Dnieper Harbor	3	276	144	1.9	1.47	98	PC
Tiel	3	457	267	1.7	3.5	76	combination PC and CIP
River Foyle	3	350	210	1.67	3.48	60	PC
Mainbrücke	4	259	148.23	1.75	2.6	57	CIP
Barranquilla	3	279	140	2	3	47	CIP segments
Kwang Fu	4	402	134	3	-	-	PC
Danube Canal	3	230.4	119	1.94	2.8	42.5	combination PC and CIP
Pont de Brotonne	3	607	320	1.9	3.8	84.2	combination PC and CIP
Pasco-Kennewick	3	547	299	1.83	2	150	PC segments
Dame Point	3	792.48	396.24	2	1.85	214	combination PC and CIP

Note: 1 m = 3.28 ft.
[a]Design by White, Young and Partners
[b]Design by Finsterwalder
[c]CIP = cast-in-place, PC = precast

ing a total span of 235 m (771 ft). To preclude any possible damage as a result of unequal foundation settlement or earthquake forces the central spans had to be statically determinate. Thus, a main span is divided into cantilever sections with a simply supported suspended center portion. The suspended spans are composed of four prestressed T-sections.

With a 200 m (656.2 ft) clear span requirement and a 46 m (150.9 ft) suspended span, the cantilever arm extends 77 m (252.6 ft) beyond the pier foundation. To avoid the large depth associated with a cantilever of this dimension cable stays were used as a supporting system from the 92.5 m (303.5 ft) high towers. Any other system of support would have required deeper girders and thus changed the roadway elevation or infringed upon the required navigational clearance.

The cantilever span is supported on X-frames while the cable stays are supported on two A-frames with a portal member at the top. There is no connection anywhere between the X and A-frames, the continuous cantilever girder is a three cell box girder 5 m deep by 14.22 m wide (16.4 ft by 46.7 ft). An axial prestress force is induced into the girder as a result of the horizontal component of cable force, thus, for the most part, only conventional reinforcement is required. Additional prestress tendons were required for negative moment above the X-frame support and transverse cable stay anchorage beams (6).

The pier cap consists of the three cell box girder with the X-frames continued up into the girder to act as transverse diaphragms, Figure 2. After completion of the pier, service girders are raised into position to be used in the construction of the cantilever arm. As a result of the additional moment produced, during this construction stage, by the service girder and weight of the cantilever arm, additional concentric prestress was required in the pier cap. To avoid overstressing of the X-frames during this operation temporary horizontal ties were installed and tensioned.

The anchorages for the cable stays are located in a 22.5 m (73.8 ft) long prestressed inclined transverse girder. The reinforcing cages for these members were fabricated on shore in a position corresponding to the inclination of the cables, and contained seventy prestressing tendons. The cable stays are housed in thick walled steel pipes which were welded to steel plates at their extremity. A special steel spreader beam was used to erect the fabricated cage in its proper orientation.

Figure 2. Pier cap of a main span.

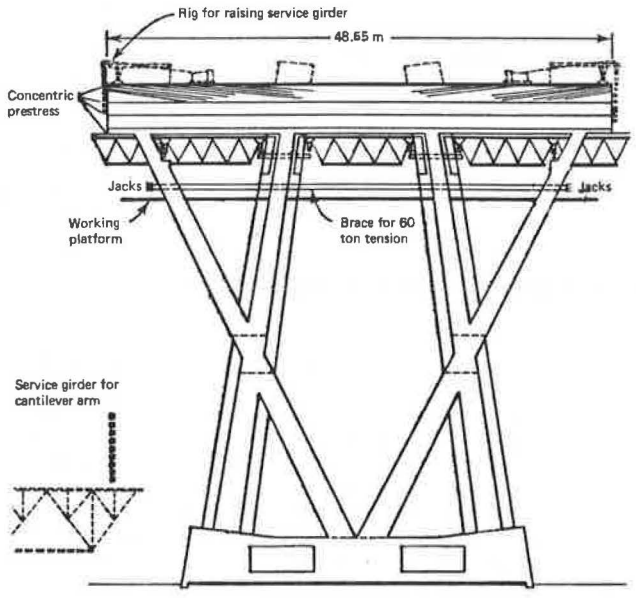

Polcevera Viaduct, Italy

The Polcevera Viaduct in Genoa, Italy was also designed by Professor Morandi and is very similar in design and appearance to the Maracaibo Bridge, Figure 3. It is a high level viaduct 1100 m (3,600 ft) long with the roadway at an elevation of 55 m (181 ft) above the terrain. The three main cable-stayed spans have lengths of 200, 210 and 140 m (664, 689 and 460

Figure 3. Polcevera Viaduct.

ft) (7). It carries the Genoa-Savona Motorway over an area composed of railway yards, roads, industrial plants and the "Polcevera" Creek. The top of the cable-stayed supporting A-frame is 42.5 m (139.5 ft) above the roadway elevation, as in the Maracaibo structure the A-frame has a longitudinal girder at the roadway level and a transverse girder at the top. The deck girder in this structure is a five cell box girder. Center suspended girders have a length of 36 m (118 ft). The transverse cable stay anchorage girders in this structure are box girders requiring that the cable stays divide above the roadway and anchor through the webs of the anchorage girder. The cable stays are composed of pretensioned high tensile steel strands encased in a protective concrete shell (7).

Wadi Kuf Bridge, Libiya

The Wadi Kuf Bridge in Libiya, another Morandi design, is a three span structure with a center span of 280 m (925 ft) and end spans of 98 m (320 ft) with a total length of 475 m (1,565 ft). Figure 4. The familiar A-frame towers are 140 and 122 m (459 and 400 ft) high with the deck clearing the valley at its lowest point by 182 m (597 ft). The superstructure is a single cell box girder of variable depth with cantilever flanges forming a 13 m (42.7 ft) deck (8).

Figure 4. Wadi Kuf Bridge.

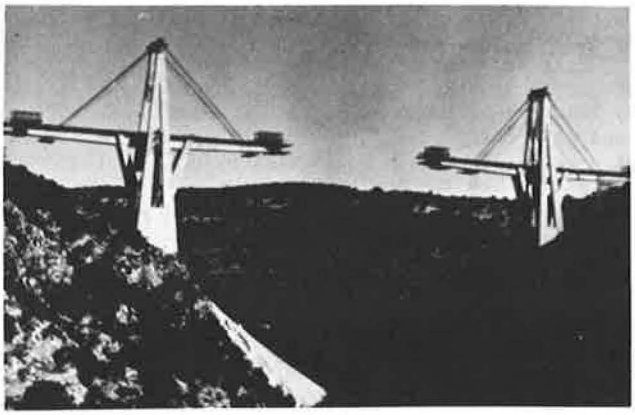

Because of the height and difficult terrain the contractor utilized traveling forms to construct the box girder and deck in a balanced cantilever construction. Temporary cable stays were used to support the cantilever arms during construction as they progressed in both directions from the tower until the permanent stays were installed. The simply supported "drop-in" center portion of the span consisted of three 55 m (180 ft) long double-T beams (7).

Magliana Viaduct, Italy

The Magliana Viaduct in Italy is still another of Morandi's structures. It carries the roadway of the Rome-Fiumicino Airport over a swamp formed by a bend of the Tiber River. This structure as shown in Figure 5 has a single portal type tower and a total length of 198.6 m (652 ft) with spans of 145 and 53, 6 m (476 and 176 ft). The 145 m (476 ft) span is composed of a 63 m (206 ft) suspended span and a 82 m (269 ft) cantilever span which is supported by a forestay at 69 m (226 ft) from the tower. The structure is further complicated in that the roadway has a horizontal curve of 475 m (1,558 ft) radius. The seven cell box girder cantilever deck is 21.5 m (70.5 ft) wide plus the variable overhang on each side to make up a 24.2 m (79 ft) roadway width. The suspended span is composed of eight prestressed T-beams (9).

Figure 5. Magliana Viaduct
(a) plan (b) section (c) elevation

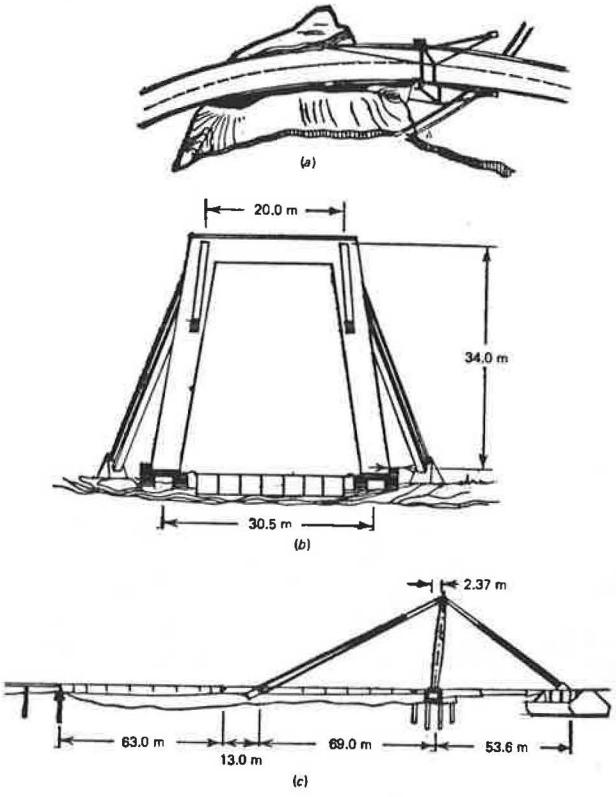

Morandi, in this structure, abandoned the fixity achieved by the X-shaped piers and A-frame towers in his previous structures and resorted to a fully articulated structure. The tower is hinged at its base. Also, the cantilever span contains hinges at the tower and the anchor span. The hinges are large radius steel lined concrete surfaces that extend the full width of the deck. The transverse stay anchorage beam is a box section that is 8 m (26 ft) deep and 2.7 m (8.8 ft) wide and similar to the Polcevera Viaduct, the forestay divides to accommodate anchorage into

each web, Figure 6. Prestressing for the anchorage beam consists of 76 cables of 16 - 5 mm (0.2 in) diameter wires.

Figure 6. Magliana Viaduct.

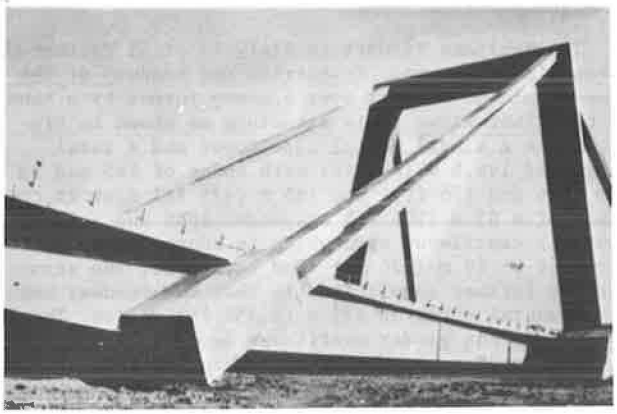

Chaco/Corrientes Bridge, Argentina

This structure, designed by the firm of Amman and Whitney, crosses the Parana River between the provinces of Chaco and Corrientes in the North-East of Argentina and represents an important link in one of the highways between Brazil and Argentina Figure 7. It has a navigation span of 245 m (804 ft), side spans of 163.7 m (537 ft) and a number of 82.6 m (271 ft) approach spans on both sides of the river (10,11).

Figure 7. Chaco/Corrientes Bridge.

In appearance, the structure very much resembles the Lake Maracaibo Bridge. Although the structure has the same dominating portal A-frame pylon it does not have the X-frame supporting the deck structure in the vicinity of the pylon, instead inclined struts are used from the pylon base of the pylon legs to the underside of the deck. Although the pier cap section of the deck, between the inclined struts, is cast-in-place, the cantilever girder is precast segmentally and post-tensioned, in contrast to the Maracaibo Bridge which was cast-in-place. The drop-in spans are cast-in-place as opposed to precast sections in the Maracaibo Bridge. Further, in elevation, this structure has two stays in each plane radiating from each side of the pylon as opposed to one.

Danish Great Belt Bridge Competition

A third prize winner in the 1967 Danish Great Belt Bridge competition was the Morandi style design proposed by the English consulting firm of White, Young and Partners, Figure 8. Design requirements were for three lanes of road traffic in each direction and a single rail traffic in each direction. Rail traffic was based upon speeds of up to 161 km/hr (100 m/hr) (12). Navigation requirements dictated a bridge deck height of 67 m (220 ft) above water level and a clear width of 345 m (1,130 ft).

Figure 8. Danish Great Belt.

This structure is noteable in that the cable-stay configuration in a transverse direction consists of three vertical planes. The deck is envisioned as two parallel single cell box girders, where the rail traffic would be carried inside the box on the bottom flange and the road traffic would be carried on the surface of the top flange. The box girder contemplated a depth of 7.2 m (23.5 ft) and width of 8.45m (27.75 ft) with the top flange cantilevered out 3.7m (12 ft) on each side.

Up to this point all of the concrete cable-stay bridges discussed have been designed by Morandi or have been strongly influenced by his style. They have been typified, for the most part, by the transverse A-frame pylon with auxiliary X-frame support for the girder. However, another entry in the Danish Great Belt competition by Ulrich Finsterwalder of the German firm of Dyckerhoff & Widmann deviated from this style and was awarded a second prize.

Finsterwalder proposed a multiple span, multi-stay system using Dywidag bars for the stays, Figure 9. This proposal contemplated a spacing between pylons of 350 m (1,148 ft) and a spacing of the stays at deck level of 10 m (32.8 ft). Pylon height above water level is 158.5 m (520 ft). In a transverse cross section the deck is 44.5 m (146 ft) wide with

Figure 9. Danish Great Belt.

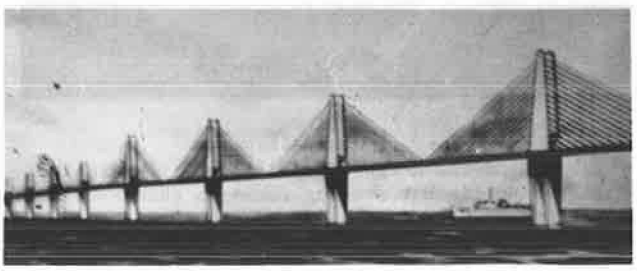

two centrally located vertical stay planes 12 m (39.4 ft) apart to accommodate the two rail traffic lanes and three automobile traffic lanes in each direction outboard of the stay planes, Figure 10. The solid concrete deck has a thickness of 0.9 m (2.95 ft) in the transverse center portion, under the rail traffic, and tapers to 0.4 m (1.3 ft) thickness at the edges. The deck is constructed by the cast-in-place balanced cantilever segmental method with each segment being supported by a set of stays.

Figure 10. Danish Great Belt.

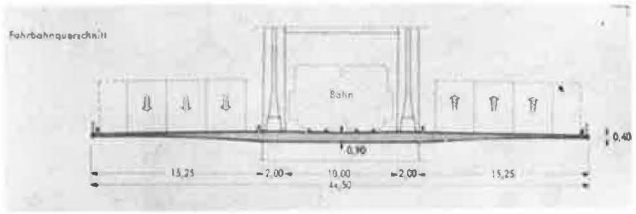

Dnieper Harbor Bridge, U.S.S.R.

The Dnieper Harbor Bridge in Kiev was completed in 1963, Figure 11. The superstructure of this bridge consists of precast reinforced units with a 144 m (472 ft) center span and side spans of 66 m (216.5 ft). Height of the reinforced concrete portal type pylon is 42 m (138 ft). The cable stays are in two vertical planes with three stays emanating from each side of the pylon.

Figure 11. Dnieper Harbor Bridge.

Tiel Bridge, Netherlands

The Tiel Bridge, Figure 12, crosses the Waal River providing a needed traffic link between the town of Tiel and the South of the country and is part of a major North-South route. The required navigation clearance is 260 m (853 ft) in width and 9.1 m (30 ft) in height.

The structure has an overall length of 1,419 m (4,656 ft) and consists of a 807 m (2,648 ft) curved viaduct on a 6,000 m (19,685 ft) radius, which includes 10 continuous 78.5 m (258 ft) long spans and a 612 m (2,008 ft) straight main structure comprising three stayed spans of 95-267-95 m (311.7-876-311.7 ft) and two 77.5 m (254.3 ft) side spans (13). The cross section consists of two precast concrete boxes each supporting two vehicular and one bicycle lane. The total width of the superstructure, which is 27.2 m (89.2 ft) in the access viaduct, is enlarged to 31.5 m (103.3 ft) over the main structure because of the space necessary for the towers supporting the stays.

Figure 12. Tiel Bridge

The main structure is symmetrical about its centerline and consists of an unstayed 77.5 m (254.3 ft) span, a stayed side span of 95 m (311.7 ft) and a center stayed cantilever span of 101 m (331.4 ft) The center gap between the two cantilever ends is connected by a 65 m (213.2 ft) suspended span. The double box superstructure has a constant depth of 3.5 m (11.5 ft). The suspended span consists of four lightweight concrete girders. The portal tower is fixed to the pier and passes freely through the superstructure.

As far as the stays are concerned, two alternates were possible: a multiple stay system supporting the deck almost continuously and a system consisting of a few large stays. As prestressed concrete stays had been selected, the second solution became obvious. Construction of prestressed concrete stays is a costly operation requiring extensive high scaffolding. Thus, it is advantageous to reduce the number of stays. However, there is another school of thought that maintains a multi-stay system is more structurally efficient and economical.

River Foyle Bridge, Ireland

This proposed structure was planned to cross the River Foyle at Madam's Bank near Londonderry, Northern Ireland, Figure 13. It would have consisted of dual three lane roadways with a centrally located walkway. The cable system is a single plane arrangement located along the center-line of the superstructure which uses an inverted Y-pylon and a main central spine deck girder for the cable stay anchorage. The main span has a vertical clearance of 32 m (105 ft) to satisfy navigational requirements. The cable-stay design was not selected for construction because of civil unrest and concern regarding susceptibility to sabotage, a self-anchored suspension bridge was the final choice. However, the cable-stay design does suggest a unique concept for the site.

The approach spans from the west abutment to the tower were to be one at 50 m (164 ft) and two at 70m (229.7 ft). The center span on the east side of the tower is 210 m (689 ft) followed by six approach spans of 70 m (229.7 ft) and one at 50 m (164 ft). The superstructure was designed as a single trapezoidal prestressed box girder with side cantilevers of constant depth and continuous over the total length of the bridge. The box girders were to be precast units, bonded together in place at the tower. The two back stays were to be anchored to the piers, thus increasing the rigidity of the entire bridge structure (14).

Figure 13. River Foyle Bridge

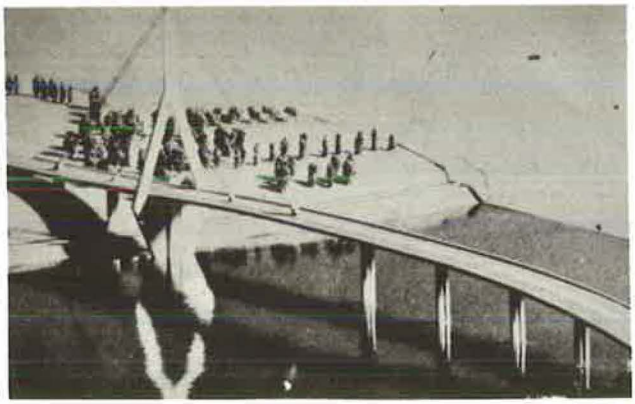

Mainbrücke, Germany

The Mainbrücke Bridge near Hoechst, a suburb of Frankfurt, constructed in 1971 is a prestressed cable-stay structure that connects the Fabwerke Hoechst's chemical industrial complex on both sides of the River Main in West Germany, Figure 14. This structure is a successor of Finsterwald's Danish Great Belt Bridge proposal and represents the first practical application of the Dywidag bar stay.

Figure 14. Mainbrücke.

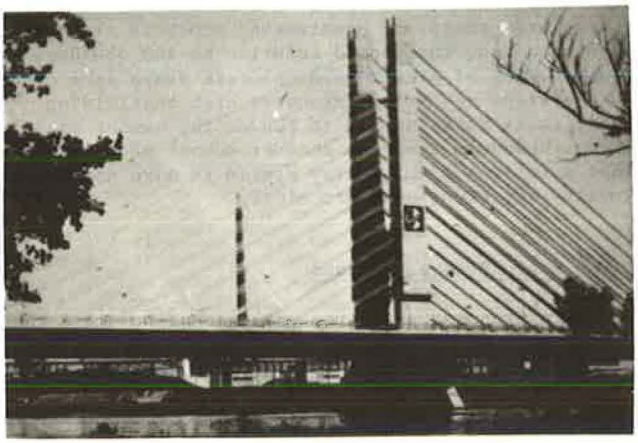

Total length of the structure is 300 m (984.3 ft) with a river span of 148 m (485.6 ft). It carries two three lane roads separated by a railway track and pipelines. The railway and pipelines are in the median between the two vertical planes of stays and cantilever towers and is supported by a 2.6 m (8.5 ft) deep, torsionally stiff box girder. The centerline of the longitudinal webs of the box girder coincide with the centerline of the individual cantilever pylons and are 8 m (26.25 ft) apart. Transverse cross beams at 3 m (9.8 ft) centers form diaphragms for the box and cantilevers, which extend 11.95 m (39 ft) on one side and 11 m (36 ft) on the other side of the central box to support the two roadways. The ends of the transverse cross beams are connected by secondary longitudinal beams, which improve the load distribution of concentrated loads.

Figure 15 shows the partially completed structure and the falsework necessary to install the stays. The costly falsework necessary to install this type of stay is a serious disadvantage to this type of construction. In this structure, each stay is composed of 25 - 16 mm (5/8 in) diameter Dywidag bars encased in a metal sheath, which is grouted for corrosion protection similar to post-tensioned concrete construction.

Figure 15. Mainbrücke.

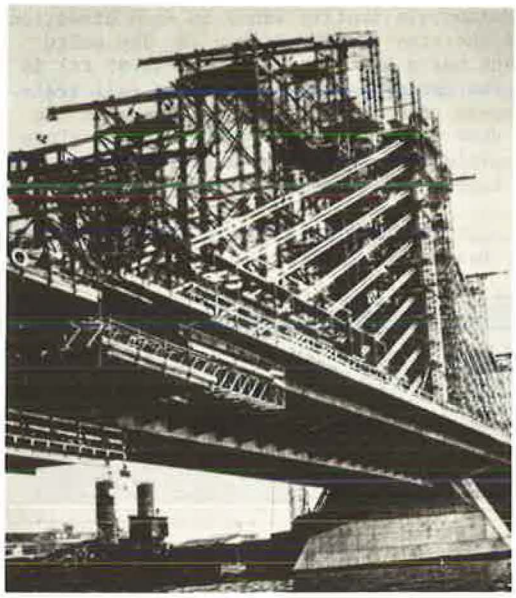

Barranquilla Bridge, Columbia

This bridge, the longest bridge in Columbia, is a 3.86 km (2.4 m) crossing that spans the Magdalena River at Barranquilla on the north coast of Columbia, Figure 16. It includes a three-span stayed concrete box girder main structure and 26 simply supported approach spans with prestressed concrete beams. It is the fourth of the general type designed by Morandi. It has a main span of 140 m (459 ft) flanked by 69.5 M (228 ft) back-spans. Morandi's other stayed concrete structures have drop-in sections in the center of their main spans, while this one is continuously prestressed, making the superstructure and towers more slender.

Travelers cantilevered the box spans simultaneously from both main piers. The box has a constant depth of 3 m (10 ft) and is rectangular with cantilevered sidewalk wings that bring the total deck

Figure 16. Barranquilla Bridge.

width to 11.3 m (37 ft). The stays anchored on the sides of the deck are grouted into post-tensioned concrete casings, so they act compositely, which considerably decreases deflection of the deck under live load. The system is the reverse of that used on the bridge over the Main River in Germany where stressed rods were grouted into steel casings (15).

Kwang Fu Bridge, Taiwan

The Kwang Fu Bridge in Taiwan is shown in Figure 17 under construction in 1976. Each panel of this cable-stayed bridge is made up of several precast linear segments of beams, which are supported on falsework at each panel point. A cross girder is then poured in place across the panel point and the stayed cables are installed and post-tensioned to carry the entire vertical load at that panel. In other words, each set of cables will eventually take the place of the falsework bent, which will then be removed. This bridge has two main spans of 134 m (439.6 ft) and end spans of 67 m (219.8 ft). The contractor elected to place the cables along half steel pipes, which are then covered with the other half and welded together. Inside the pipe, the cables are grouted to offer protection as well as additional stiffening (16).

Figure 17. Kwang Fu Bridge.

Danube Canal Bridge, Austria

This structure is located on the West Motorway (Vienna Airport Motorway) and crosses the Danube Canal at an angle of 45°, it has a 119 m (390 ft) center span with 55.7 m (182.7 ft) side span, Figure 18. The structure is unique because of its construction technique. Because construction was not allowed to interfere with navigation on the canal the structure was built in two 110 m (360.8 ft) halves on each bank and parallel to the canal. Upon completion the two halves were swung into final position and a cast-in-place closure joint was made, Figure 19. In other words, each half was constructed as a one time swing span.

The bridge superstructure is a 15.8 m (51,8 ft) wide trapezoidal three-cell box girder, Figure 20. The central box is cast in 7.6 m (30 ft) long segments on falsework, after the precast inclined webs are placed the top slab is cast. Each half structure has two cantilever towers fixed in a heavily prestressed trapezoidal crosshead protruding under the deck with a two point bearing on the pier, Figure 21. At the deck level the stays attach to steel brackets connected to prestressed cross beams.

Each stay consists of 8 cables, two horizontal by four vertical. At the top of the pylon each cable is seated in a cast iron saddle. The cable saddles are stacked four high and are fixed to each other as well as those in the adjacent plane. The cables are first layed out on the deck, fixed to a saddle, and then lifted by a crane for placement at the top of the pylon. The cables are then pulled at each end by a winch rope to their attachment point at the deck

Figure 18. Danube Canal Bridge - Elevation.

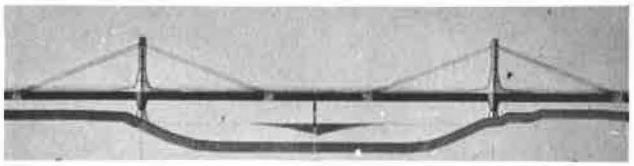

Figure 19. Danube Canal Bridge - Plan.

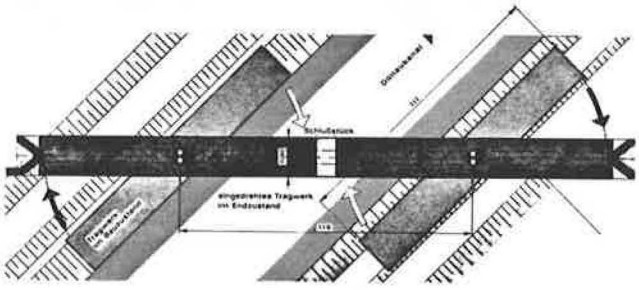

Figure 20. Danube Canal Bridge - Section.

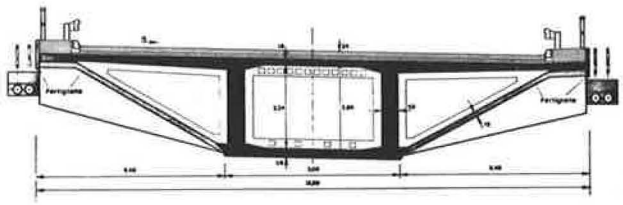

Figure 21. Danube Canal Bridge.

level.

After rotation the superstructure is lowered to permanent bearings. The two halves of the structure are then connected by a cast-in-place closure joint and continuity tendons are placed and stressed (17)

Pont de Brotonne, France

The Pont de Brotonne Bridge, designed and built by Campenon Bernard of Paris, crosses the Seine River downstream from Rouen in France. An artist's rendering, Figure 22, shows the general configuration of the bridge. The box girder will carry four lanes and replace ferry service between two major highways that run north and south of the Seine. Because large ships use this portion of the river to approach the inland

Figure 22. Pont de Brotonne.

port of Rouen 35 km (22 m) to the east, vertical navigation clearance was 50 m (164 ft) above water level, which results in a 6.5% grade for its longer approach (18).

Total length of structure is 1,278.4 m (4,194 ft), divided into three continuous sections: the left bank approach viaduct, the main bridge crossing the Seine, and the right bank approach viaduct. The three sections are separated by expansion joints located at points of contraflexure in the viaduct spans on either side of the cable-stay portion of the structure. The central river crossing includes a 320 m (1,050 ft) center span and 143.5 m (471 ft) side spans. At present, this structure holds the record length for a cable stayed bridge of prestressed concrete.

The deck structure is balanced cantilever out from the pylon pier. Dimensions of the deck segments are, top flange 19.2 m (63 ft) wide, bottom flange 8 m (26 ft) wide, constant depth of 3.8 m (12.5 ft). Web and top flange are 0.2 m (7.8 in) thick, bottom flange is 0.18 m (7 in) thick. Each segment is 3 m (9.8 ft) long, Figure 23. The only part of the trapezoidal box girder that is precast is its sloping webs. The 3 m (9.8 ft) long, 4 m (13 ft) wide precast web elements are precast at the site and are from 0.2 m (7.8 in) to 0.4 m (15.6 in) thick. The balance of the cross section, including top and bottom flanges and its interior stiffening struts and cable-stay anchorages are cast-in-place.

Preceding placement of the precast web units, the bridge's 14 octagonal piers are slipformed, nine on the left bank and three on the right bank. Span length in the approaches are, for the left bank, 38.9 m (127.6 ft) and eight at 58.5 m (192 ft); for the right bank, from the abutment, 39 m (128 ft), 55.5 m (182 ft), and 70 m (230 ft). Approach piers vary in height from 10 to 50 m (33 to 164 ft). The two central pylons rise 120 m (394 ft) above the water level of the Seine. When the slipforming of the piers reached the deck level, the piers were pre-

Figure 23. Pont de Brotonne - Section.

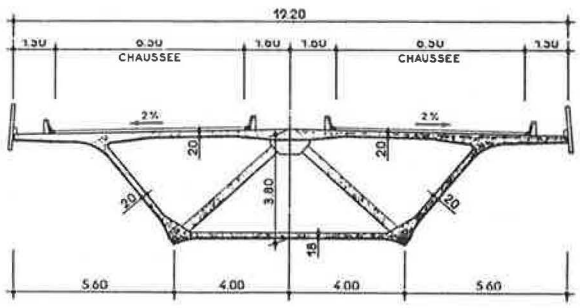

stressed to their foundations so as to stabilize the piers for erection of the deck segments. As the precast deck units were erected, the pylon was constructed using conventional forming methods.

In constructing the girder the first operation was to extend the bottom flange form from a traveling form at the completed segment, place the precast web units which form the basic shape and act as a guide for the remaining traveling form used to cast the upper flange and interior struts. Tower cranes at the pylon placed, as far as they could reach in both directions, the precast webs in a symmetrical manner to balance the loads. Beyond the range of the tower cranes, gantry cranes running on rails on the top flange and extending 3 m (9.8 ft) beyond the end of a completed section were used to place new pieces. After placement of the precast webs the interior steel form is jacked forward to cast the bottom flange, struts, and top flange.

Final support for the deck units is provided by 21 stays continuous through the pylon and varying from 84 to 340 m (275 to 1,115 ft) in length and lie in a vertical plane along the longitudinal axis of the structure. Spacing of the stays at deck level is 6 m (19.6 ft), thus, every other segment has a stay anchor, Figure 24 shows an isometric of a segment and the orientation of prestressing and stay.

Figure 24. Pont de Brotonne - Isometric

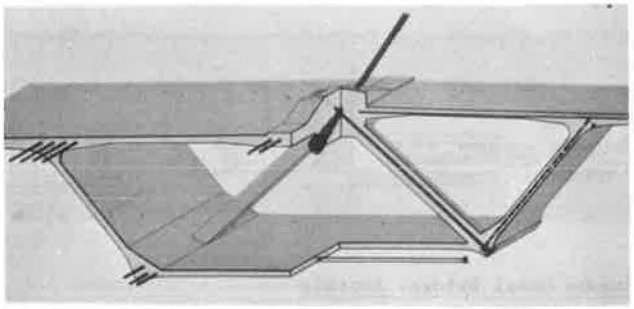

Pasco-Kennewick Bridge, U.S.A.

The first cable-stayed bridge with a concrete superstructure to be built in the United States is the Pasco-Kennewick Intercity Bridge crossing the Columbia River in the State of Washington. The overall length of this structure is 763 m (2,503 ft). The center cable-stay span is 299 m (981 ft) and the stayed flanking spans are 124 m (406.5 ft). The deck is continuous without expansion joints from abutment to abutment, being fixed at the Pasco end and having an expansion joint at the Kennewick abutment. The three main spans are assembled from precast, prestressed concrete segments. Figure 25, while the approach spans are cast-in-place.

The concrete bridge girder is of a uniform cross section, of constant 2 m (7 ft) depth along its entire length and 24.3 m (79 ft 10 in) wide. The shallow girder, and the long main span are necessary to reduce the roadway grades to a minimum, to provide the greatest possible navigation clearances below, and to reduce the number of piers in the 21.3 m (70 ft) deep river.

Segments are precast about 1.6 km (1 m) down stream from the bridge site, each segment weighs about 272 mt (300 t). The sections are barged directly beneath their place in the bridge and hoisted into position. It takes approximately six hours to lift each segment into position, Figure 26. Fifty-eight precast, transversely prestressed concrete bridge

Figure 25. Pasco-Kennewick Bridge.

Figure 26. Pasco-Kennewick Bridge.

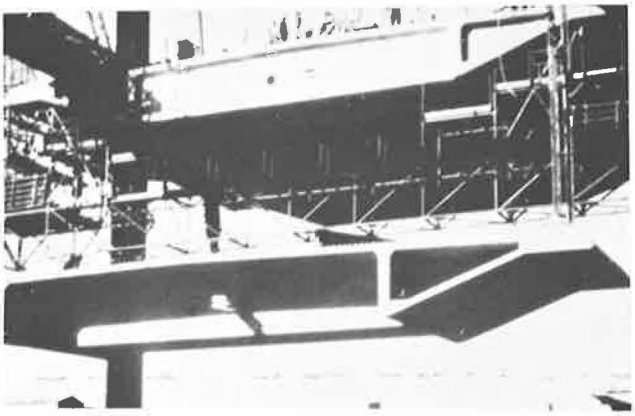

girder segments are required. The segments are match cast, prestressed, cured and then transfered to the bridge, and erected symmetrically about the two main bridge towers, epoxy joined, longitudinally prestressed against the previously erected ones, and suspended from the bridge stays. Each segment is 8.2 m (27 ft) long and consists of three transverse girders and a roadway slab joined along the segment edges with a hollow trangular box, Figure 26. A large part of the longitudinal prestressing force in the bridge girder is provided by the compression resulting from the horizontal component of cable force.

The stays are arranged in two parallel planes with 72 stays in each, that is, 18 stays on each side of each pylon. They are held at each tower top, 54.9 m (180 ft) above the bridge roadway in a steel weldment. The stays are made up of 6.35 mm (0.25 in) diameter parallel high strength steel wires. Stay anchors in the bridge deck are spaced at 8.2 m (27 ft). The prefabricated stays arrive on the job site on reels, and contain from 87 to 283 wires each, are covered with a polyethylene pipe, and after installation and final adjustment are protected against corrosion by pressure injected cement grout. Stay outside diameters range from 0.11 to 0.16 m (4.3 to 6.3 in). Design stress level for the stays is 751.5 MPa (109 ksi). This structure was deisgned by Arvid Grant and Assoc., Inc. in professional collaboration with Leonhardt and Andra of Stuttgart.

Dame Point Bridge, U.S.A.

The proposed Dame Point Bridge over the St. Johns River in Jacksonville, Florida is presently being designed by the firm of Howard Needles Tammen & Bergendoff, Figure 27. Navigation requirements dictate a 381 m (1,250 ft) minimum horizontal opening and a vertical clearance of 46.3 m (152 ft) above mean high water at the centerline of the clear opening. The proposed concrete cable-stay structure will have a 396.24 m (1,300 ft) central span with 198.12 m (650 ft) side spans.

Figure 27. Dame Point Bridge.

The bridge deck, which will carry three lanes of traffic in each direction, will span between longitudinal edge girders on each side. The longitudinal edge girder is in turn supported by a vertical plane of stays arranged in a harp configuration. The concrete deck and edge girders take local and overall bending from dead and live load in addition to the horizontal thrust from the stays (19).

The bridge deck consists of single-T precast floor beams spaning between longitudinal girders and a cast-in-place topping. The precast T's are prestressed for erection loads. After erection the entire deck is post-tensioned to provide positive precompression between edge girders under all conditions of loading. Erection of the deck will be by the balanced cantilever method.

This structure, which extends Finsterwalder's concept in the Danish Great Belt and the Mainbrücke, is still in the design stage and a number of alternates will be available to the contractor at his option. If this structure is consumated in concrete, it will certainly take the record for the longest cable-stay bridge in concrete.

Closing Remarks

As late as 1970, the practical span limit of steel cable-stay bridges was considered to be 305 m (1,000 ft). As seen in the examples of the Danish Great Belt Bridge, the Pont de Brotonne, and the Pasco-Kennewick Bridge, spans of about 305 m (1,000 ft) have been accomplished with concrete cable-stay bridges. The practical span length has been extended to 400 m (1,300 ft) in the Dame Point Bridge, and spans approaching 500 m (1,600 ft) are considered technically feasible. It has been projected that with an aerodynamically shaped composite concrete and steel deck a span of 1,500 m (2,300 ft) can be achieved (20).

In evaluating a concrete cable-stay bridge the designer should be aware of the following advantages: by use of proper aerodynamic streamlining and multi-stays the deck structure can be slim and not portray a massive visual impression, concrete is inherently a material with favorable damping caharacteristics which is important in aerodynamic considerations, the horizontal component of stay force is advanta-

geous in that it produces a prestress force in the concrete and concrete is at its best in compression. With today's technology of prefabrication, prestressing, and segmental cantilever construction, it is obvious that cable-stay bridges are extending the competitive span range of concrete construction to dimensions that had previously been considered impossible. The technological means exist, they only require implementation.

Acknowledgments

The following individuals and firms have been instrumental in obtaining data and illustrations: Julius Berger, Bauboag Aktiengesellschaft, Wiesbaden (Maracaibo). Prof. Morandi (Wadi Kuf). Dr. Gaetano Bologna, l Industria Italiana del Cemento (Magliana Viaduct). Normer Gray (Chaco/Corrientes). White, Young, and Partners (Danish Great Belt). Ulrich Finsterwalder (Danish Great Belt and Mainbrücke). Juhani Virola (Dnieper Harbor). Jean Muller and T. R. Scanlan (Tiel, Danube Canal and Pont de Brotonne). Civil Engineering and Public Works Review, London (River Foyle). Prof. T. Y. Lin (Kwang Fu). L. A. Garrido (Barranquilla). Arvid Grant (Pasco-Kennewick). G. F. Fox and H. J. Graham (Dame Point).

References

1. Feige, A., "The evolution of German Cable-Stayed Bridges - An Overall Survey," Acier-Stahl-Steel (English Version), No. 12, December 1966.
2. Podolny, W., Jr., and Fleming, J. F., "Historical Development of Cable-Stayed Bridges," Journal of the Structural Division, ASCE, Vol. 98, No. ST9, Proc. Paper 9201, September 1972.
3. Podolny, W., Jr., and Scalzi, J. B., "Construction and Design of Cable-Stayed Bridges," John Wiley & Sons, Inc., New York, 1976.
4. Dischinger, F., "Hängebrücken für Schwerste Verkehrslasten," Der Bauingenieur, March 1949.
5. Torroja, E., "Philosophy of Structures," English Version by J. J. Polivka and Milos Polivka, Univ. of California Press, Berkley and Los Angles, 1958
6. "The Bridge Spanning Lake Maracaibo in Venesuela" Wiesbaden, Berlin: Bauverlag GmbH., 1963.
7. Morrandi, R., "Some Types of Tied Bridges in Prestressed Concrete," First International Symposium Concrete Bridge Design, ACI Publication SP-23, Paper SP 23-25, American Concrete Institute, Detroit, 1969.
8. "Longest Concrete Cable-Stayed Span Cantilevered Over Tough Terrain," Engineering News-Record, July 15, 1971.
9. Morandi, R., "Il Viadutto dell Ansa della Magliana per la Autostrada Roma-Aeroporto di Fiumicino," l 'Industria Italiana del Cemento (Rome), Anno XXXVIII, March 1968.
10. Gray, N., "Chaco/Dorrientes Bridge in Argentina," Municipal Engineers Journal, Paper No. 380, Vol. 59, Fourth Quarter, 1973.
11. Rothman, H. B. and Chang, F. K., "Longest Precast Concrete Box Girder Bridge in Western Hemisphere" Civil Engineering, ASCE, March 1974.
12. "Morandi - Style Design Allows Constant Suspended Spans," Consulting Engineer (London), March 1967.
13. "Tiel Bridge," Freyssinet International, STUP Bulletin, March-April 1973.
14. "River Foyle Bridge," Civil Engineering and Public Works Review (London), Vol. 66, No. 780, July 1971.
15. "Rigid stays slim box girder bridge and reduce deflection," Engineering News-Record, June 20, 1974.
16. "Bridging the Gaps," Engineering Bulletin, T. Y. Lin International, Vol. 5, No. 2, October 1967.
17. "The Danube Canal Bridge (Austria)," Freyssinet International, STUP Bulletin, May-June 1975.
18. "Cable-stayed bridge goes to a record with hybrid girder design," Engineering News-Record, October 28, 1976.
19. "Dames Point Bridge," Design Report, Howard Needles Tammen & Bergendoff, November 1976.
20. Leonhardt, F., "Latest Developments of Cable-Stayed Bridges for Long Spans," Saertryk af Bygningsstatiske Meodelelser (Denmark), Vol. 45, No. 4, 1974.

STRUCTURAL PROBLEMS FOR THE MESSINA NARROWS BRIDGE

Leo Finzi, F.A.S.C.E., vCh. I.A.B.S.E., Professor at the Technical University of Milan, Italy

In the past few years a lot of work has been done in Italy on where and how to build the Messina Narrows Bridge. The main problems were the nature and strength of the soil, dangerous currents, winds, faults and relevant earthquakes. At the same time many solutions for a double "one mile" span stayed or suspension bridge and a simple "two mile" span suspension bridge were suggested.
This paper gives a survey of the present state of knowledge with special reference to the technical problems connected with the single span solutions, where aeroelastic stability governs the design of the deck and the cables. On the other hand the 380 m towers are themselves a problem in a heavily seismic area.

1. History.

Italy is a long boot-shaped country. Two miles from the tip of the toe is the island of Sicily (fig. 1).

Two cities face each over the Narrows: Reggio Calabria on the mainland and Messina on the island. A ferry-boat shuttle service has so far been the only transportation service across the Narrows both for trains and cars.

The first idea for a permanent connection across the straits is, as far as we know, in a doctoral thesis of 1870 and at that time the cost of the suggested railway tunnel was estimated as less than 40,000 dollars!

However, systematic studies were starded only after World War I, but the decisive step was the foundation in 1955 of the GPM Gruppo Ponte Messina (Messina Bridge Group). In fact the Gruppo Ponte Messina began to analyze, through the collection of the available data and specific experiments, the situation in the area involved in terms of the sea, the air, the soil and the traffic (1).

In 1969 ANAS, the Italian Highway State Agency, together with the State Railways Administration asked on a worlwide basis for ideas to be submitted on possible solutions for the Messina Narrows crossing, both with a highway and a railway.

Figure 1. The Boot of Italy.

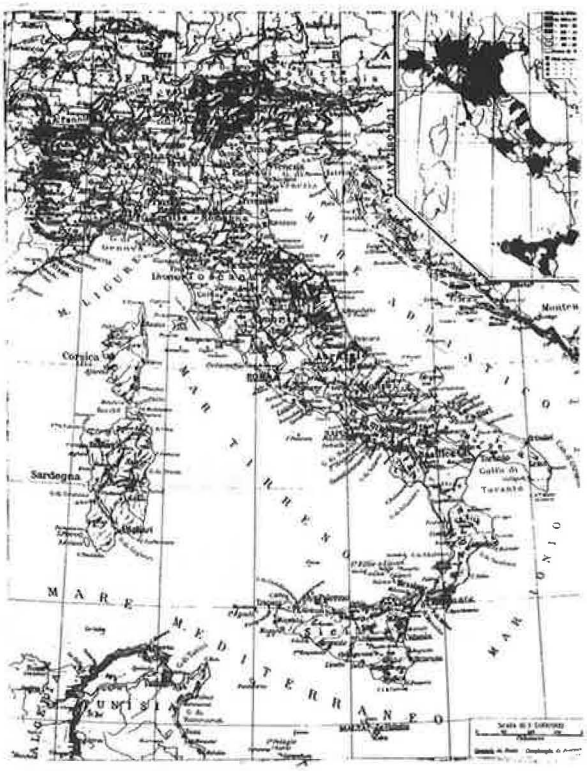

There were 144 participants. Fig. 2 shows the suggestions that were judged the best. Five main possibilities can be distinguished (2) (3).

1. A multispan bridge with intermediate supports;
2. A single 2 mile span bridge;
3. A midwater tunnel;
4. A tunnel buried in the body of a submarine dike;
5. An underground tunnel.

But were all of them really feasbile and, for those that were, which of them were economically competitive?

Figure 2. The 1969 designs.

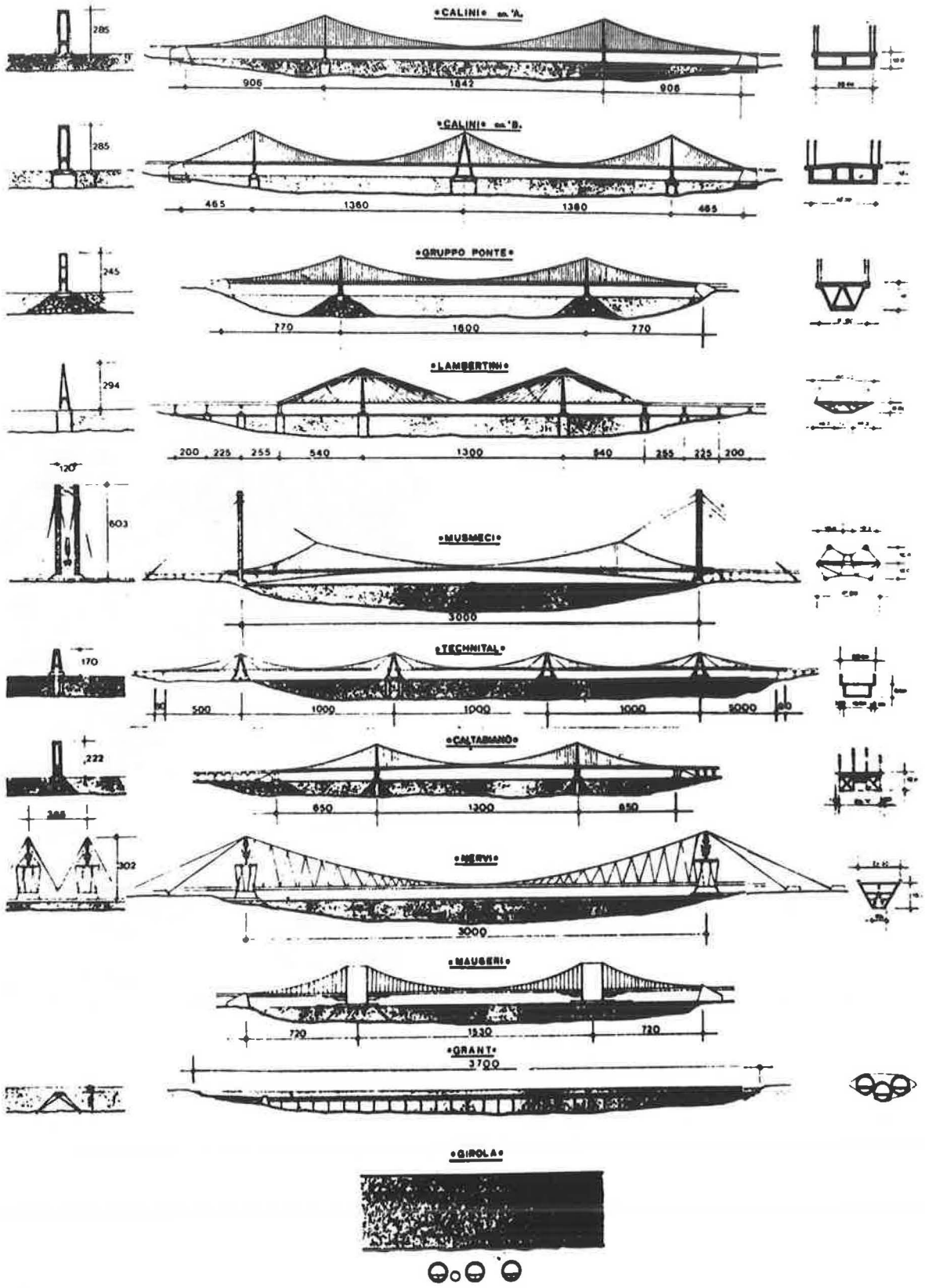

The Gruppo Ponte di Messina has devoted the last eight years to finding a realistic answer to these questions. In doing so better ideas and solutions were discovered in the field of the double and single span bridges.

2. The Environement.

2.1. The Sea.

Most of the problems in the Messina Narrows derive from the fact that here two different seas, the Tirrenian and the Ionic, meet through a submarine saddle (fig. 3) more than 100 m deep.

The difference of tidal regimes (fig. 4), of temperatures, of density and of depth give rise to a turbulent current going North to South and vice versa four times a day with a speed of more than 3 m sec^{-1}.

In winter waves 4 m high must be considered as possible although in summer the situation is much better.

All through the year many ships of up to 500.000 tons pass through the Narrows and numerous collisions occur, as this Scylla and Charibdis effects is notoriously difficult for navigation.

Figure 3. The sea-bed saddle.

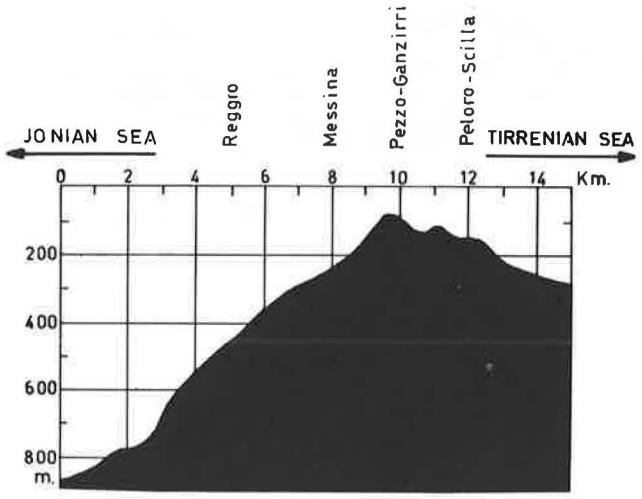

Figure 4. Tidal level in the Narrows.

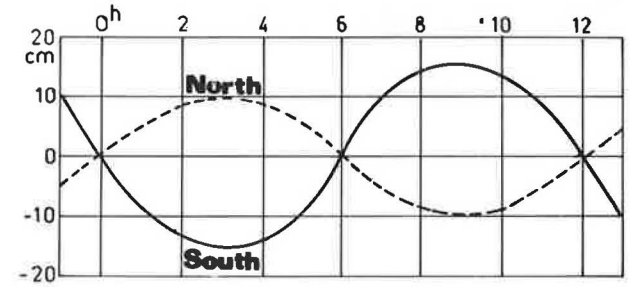

2.2. The Air.

The wind velocity at ground level is well known through the records of the Air Force and Naval stations, but not so at the level of a possible suspension bridge. For this reason since 1977 many anemometers were placed and are at work at different levels (between the sea level and up to 390 m above) on the existing ENEL transmission towers (fig. 5).

For the moment this seems to indicate a design wind speed of 50 m sec^{-1}.

No tornadoes were registered or are expected in the Messina area.

2.3. The Soil.

It was still very difficult for the geologists and soil mechanics people to get a clear idea of the situation in the straits as it varies widely in the different zones.

Nevertheless, looking at the situation of possible foundations near the coasts and in the middle, it appears like this:

1. Coast: sand and sand with gravel not affected by possible liquefaction phenomena; allowable pressure 50 N cm^{-2};
2. Central saddle: almost 60 m of organogenous limestone on the top, then 25 m of sandstone and finally sand and clay.

In general the bedrock is very deep, more than 300 m under the upper layers.

This is in a highly seismic zone and a possible earthquake of Magnitude 7.5 in the vicinity of the crossing has to be allowed for.

This means an horizontal maximum acceleration at bedrock of 0.5 g with a return period of 1.000 years.

At the same time we have faults that are known, and therefore can be avoided, on the coasts, but that could not and probably cannot be discovered in between.

Figure 5. The 223 m high ENEL transmission towers.

Figure 6. The requested traffic lanes and railway tracks.

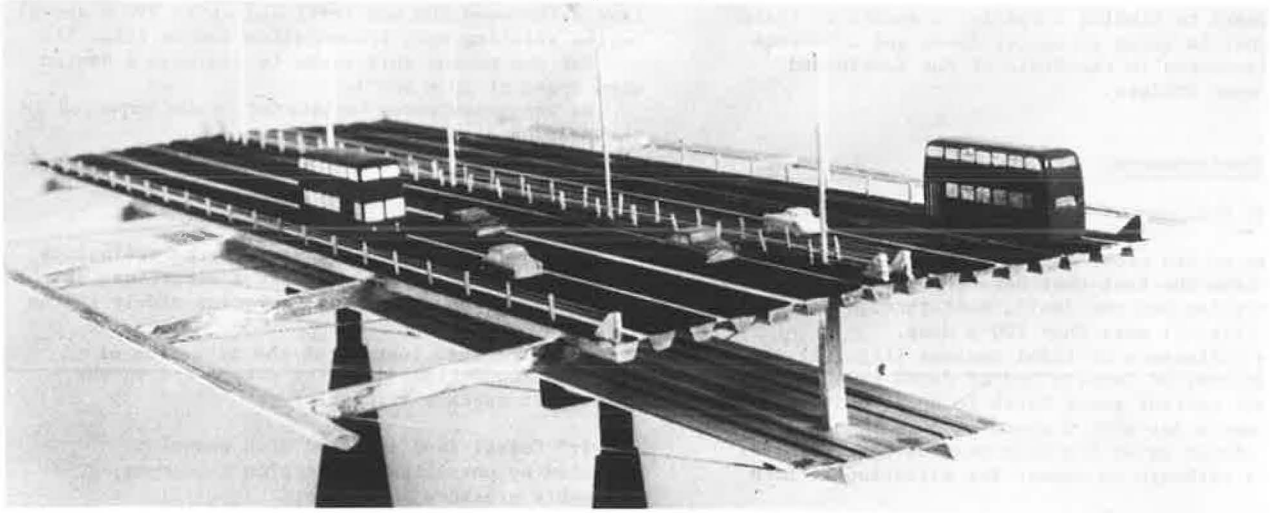

Figure 7. A suggested multispan stayed bridge.

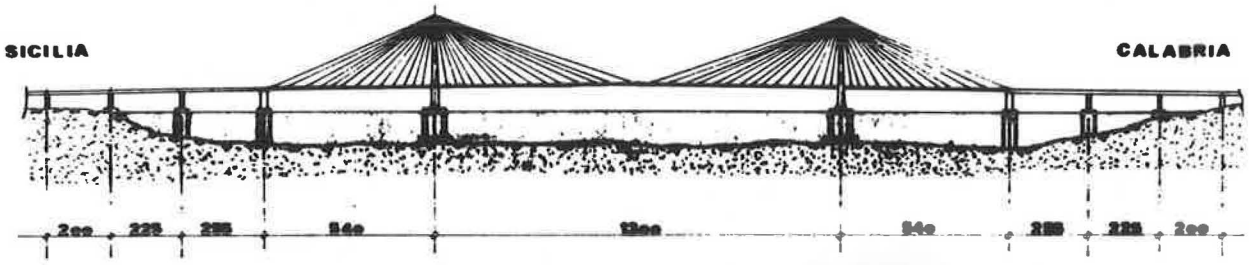

Figure 8. A gradually sinking pier.

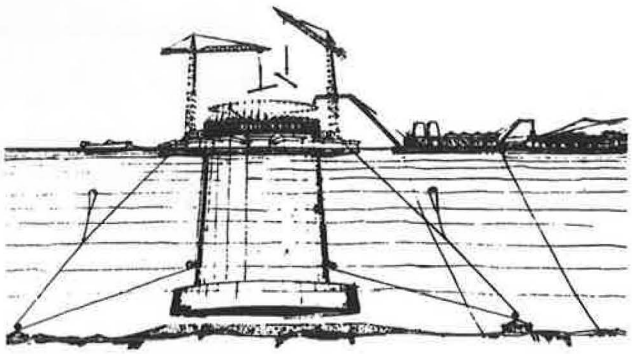

Thus a possible pier, island or dike must risk a fault and a consequent possible dislocation of about 3 m.

As we are between two famous volcanoes, Etna and Stromboli, one might think that the Messina Narrows area would suffer from volcanic activity.

This is not the case, as Etna and Stromboli are of very different natures, and no connection between the two has been shown by the volcanologists.

2.4. The Traffic.

A bridge or tunnel accross the Messina Narrows must allow for the following traffic (fig. 6):

3 + 3 highway lanes
2 railway tracks.

Due to the great length of the crossing a mean value of 80,000 N m^{-1} of total service load should be adequate. 50% of that is due to the railway, which also placed severe limits on the maximum slope. A limit of 1.3 - 1.4% must not be exceeded.

2.5. The Temperature.

The temperature of exposed structures will go below - 10° C and over 70° C.

The sea temperature varies between 13° and 24° C during the year.

3. The Intermediate Supports.

If one discards the ideas of a tunnel under the sea due to the length (more than 35 km) and to the problems connected with three faults (one of them across the Narrows) the main choice is between a multiple span bridge or single span bridge.

A multiple span bridge is possible if one can build one or more intermediate supports in a crowded sea lane with a depth of almost 120 m and with variable currents up to 3 m sec^{-1} and more.

There are mainly two possibilities: piers or artificial islands.

First, let us underline that a solution like that shown in fig. 7 (4) with many intermediate piers is ruled out by navigation needs: in fact two channels almost 1600 m wide are required.

That is, only one intermediate support is allowed, and thus the choice is only between a two span or single span bridge.

Many interesting suggestions were given for a possible pier, such as a gradually sinking one (fig. 8) but, besides the enormous difficulties of building it, such monolithic structures are not able to resist earthquakes due to the inertial effects of the surrounding sea water. But a lattice pier like that suggested by G.P.M. (fig.11) could be earthquake resistant. However, a very sophisticated step by step technique would be needed to erect such a pier in such a sea.

Not such heavy technological problems arise if one thinks of an artificial island in the middle of the crossing (fig.9).

It is clear that in this case one would need an impressive quantity of rock (approximately 20 Mm^3), but this can be easily obtained from the slopes of the nearby volcano Etna.

Lava, in fact, is an excellent material for building and artificial island, and would have the further advantage of not disrupting the wonderful landscape of the zone.

As a conclusion, one can say that only one intermediate support in the Narrows is permissible and that both a lattice pier or an artificial island are possible.

4. The Double-Span Bridge.

If one decides to have a double-span bridge the length of each span would be approximately 1750 m (fig. 12). This is far beyond the largest span built until now (the Humber bridge in Great Britain with a

Figure 9. The G.P.M. artificial island.

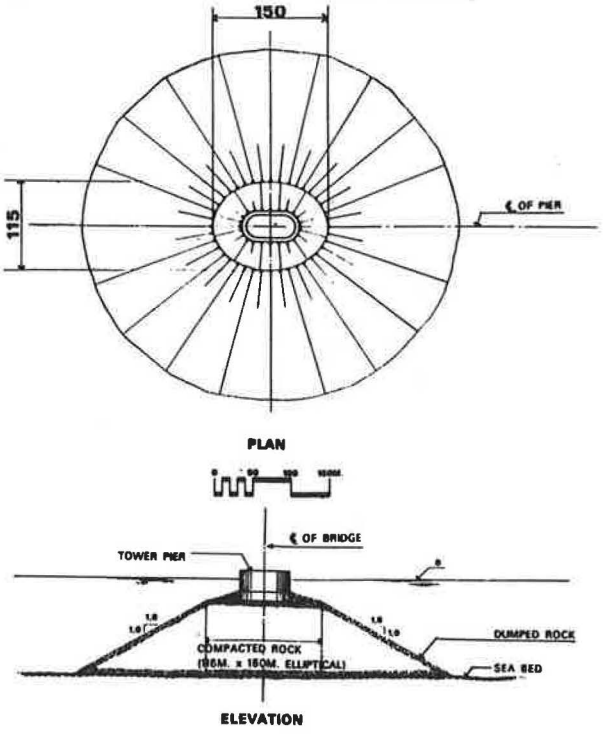

Figure 10. The deck of the double span bridge.

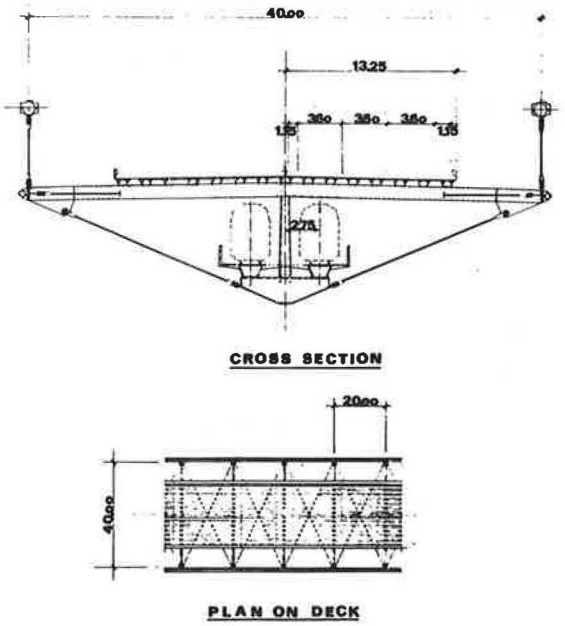

Figure 11. The lattice G.P.M. pier.

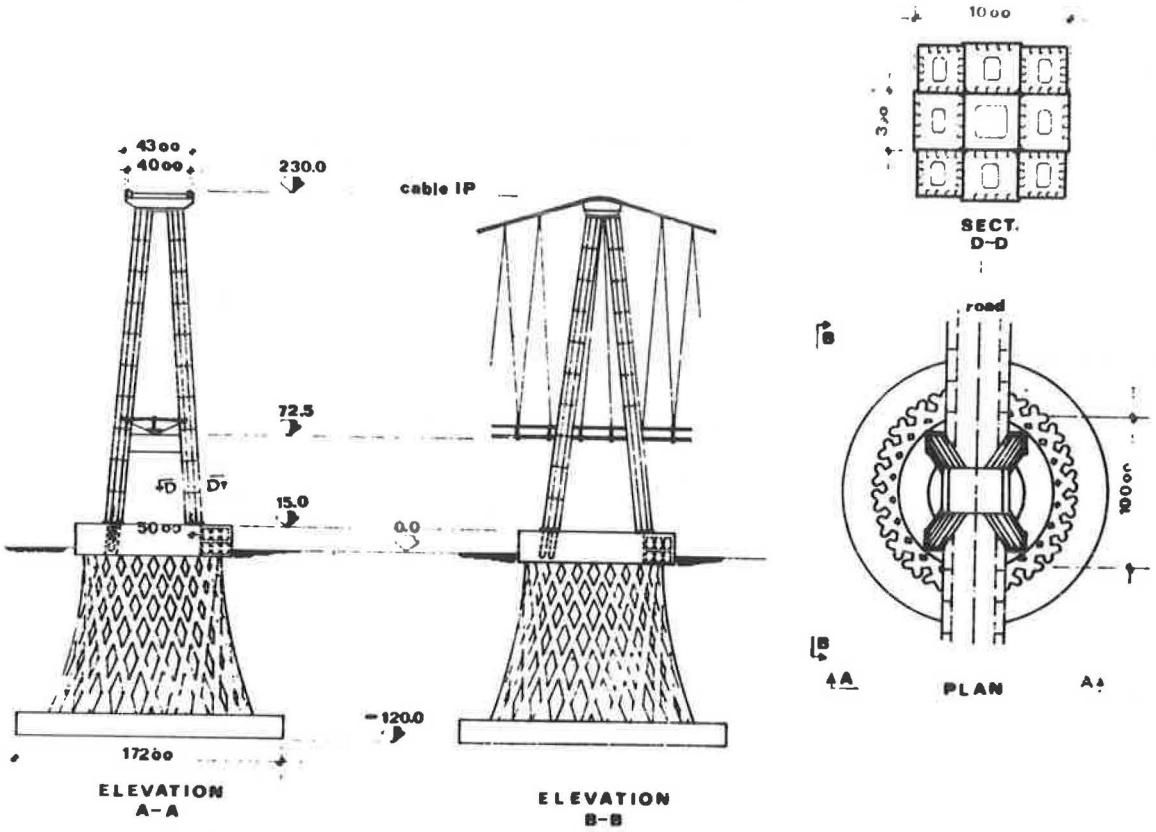

Figure 12. The G.P.M. double span bridge.

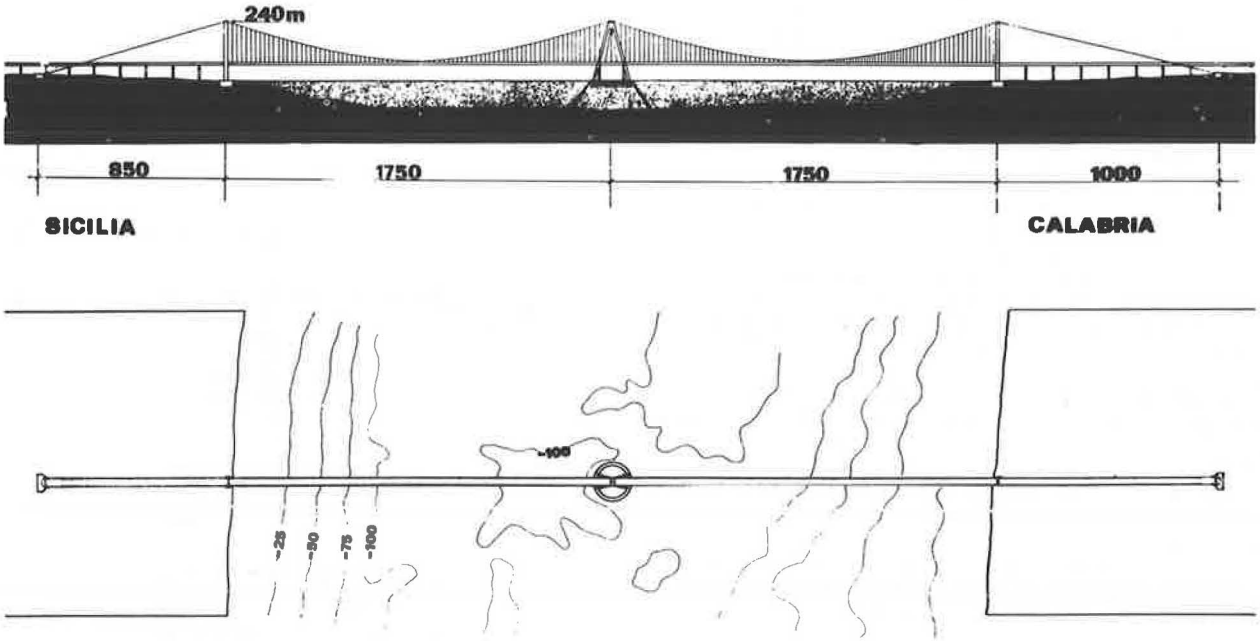

Figure 13. The Musmeci pretensioned hanging bridge.

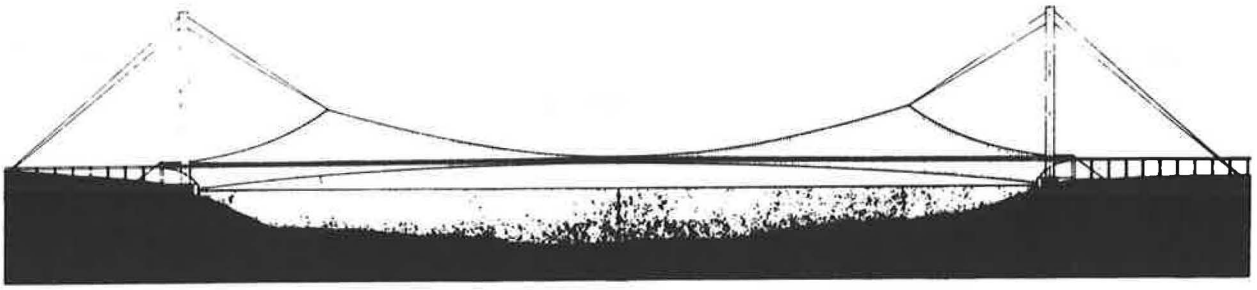

Figure 14. The Musmeci bridge cross-section.

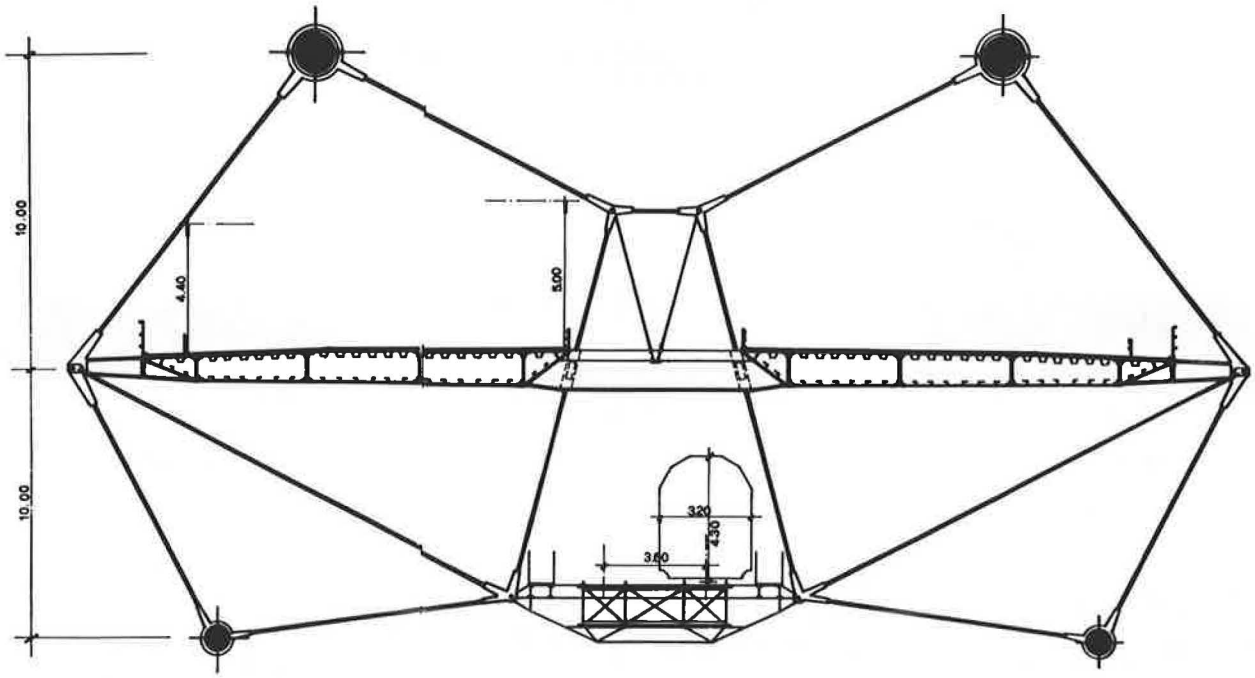

Figure 15. The Danieli hanging structure.

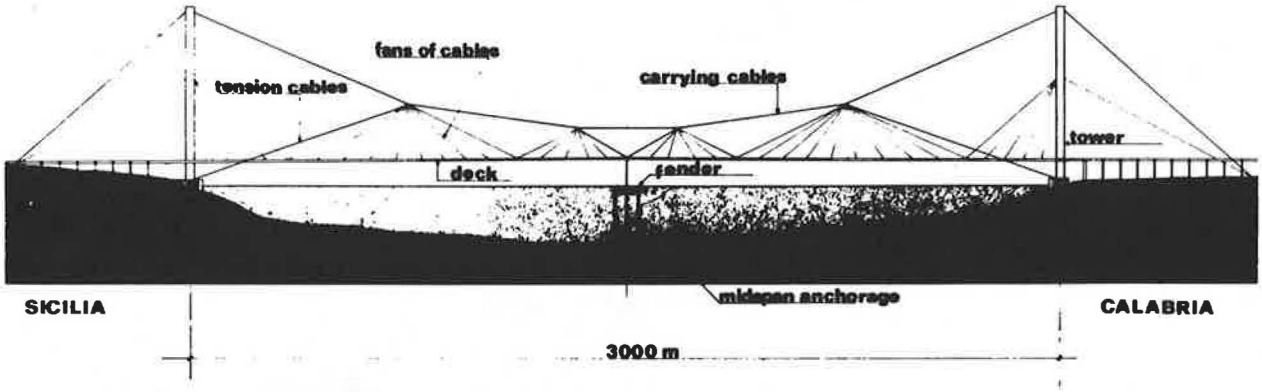

Figure 16. The G.P.M. single span bridge cross-section.

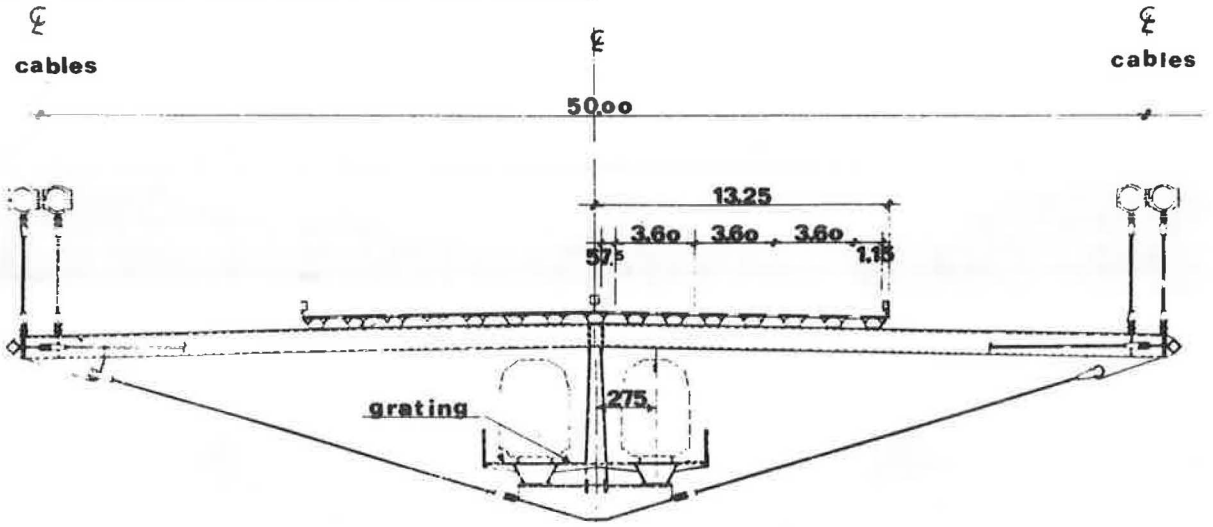

Figure 17. The G.P.M. single span bridge.

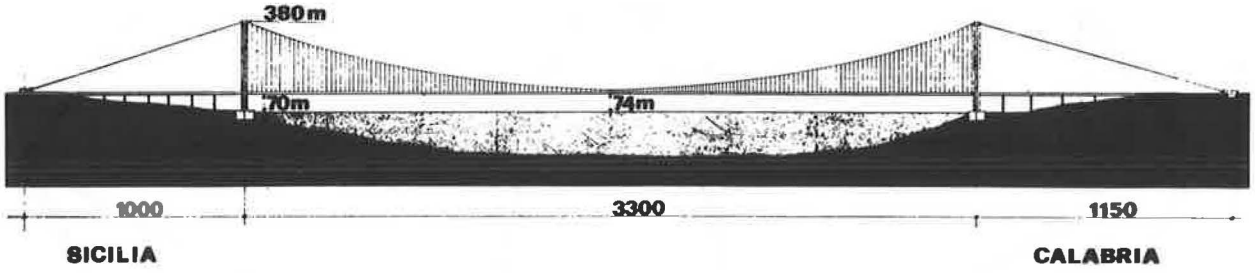

Figure 18. General view of the G.P.M. single span bridge.

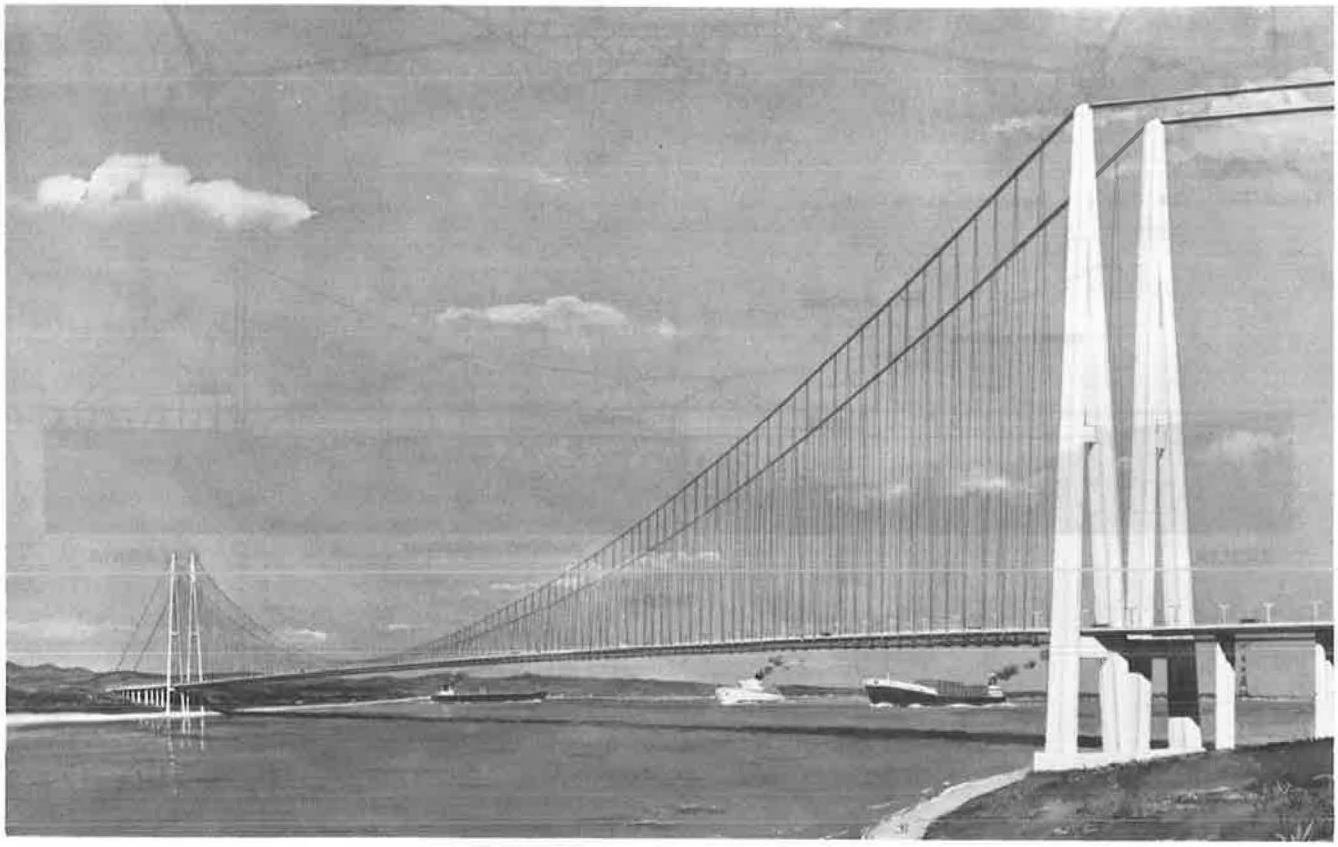

central span of 1410 m). Moreover it may be pointed out that it is unusual, at least in Europe, to see heavy trains passing over suspension bridges.

Nevertheless the studies sponsored by G.P.M. have shown that with a ratio of about 12 between span and sag and a moderately expanded cross section (fig. 10) only two 1 m size cables are sufficient and flutter problems can be properly overcome for a design wind speed of 50 m sec^{-1}.

Towers 230 m are required and the central one must be capital delta shaped.

Great help to G.P.M. came both from British experience in this field and from advanced studies done in Italy both through a numerical simulation and experiments in the FIAT wind tunnel.

5. The Single-Span Bridge.

A single-span bridge offers the enormous advantage of not needing a support in the middle of the Narrows, but on the other hand the required span is 3300 m.

The man in the street might think that going from 1410 m of the Humber bridge to the 1750 m of the double span bridge discussed above asks for a reasonable amount of progress in knowledge and technology, but a 3300 m bridge would be far too long.

In our opinion this is not so, but it would be necessary to change the philosophy of design, rather than simply extrapolate present techniques.

A decisive step in this direction was taken by Musmeci. He thought of the simple span bridge more in terms of a hanging structure than as a traditional suspension bridge (fig. 13). That is, he postulated not only carrying cables but also tension cables. A notable advantage in stiffness and a light super structure were the result (fig. 14).

A similar idea was developed by Danieli (5) but he divided the tension cables into two spans, which therefore demanded midspan anchorage (fig. 15).

The above mentioned two proposals had their Achilles heel however, in the aeroelastic stability and in the horizontal stiffness.

In fact avoiding flutter is the main problem for the simple span bridge.

The G.P.M. people saw this clearly and devoted most of their energy to finding an answer to the aeroelastic problem.

A sophisticated numerical simulation was made first and then a series of 1:10 scale experiments on sections of the bridge were performed in the FIAT wind tunnel.

As varying parameters, the ratio between full and empty surfaces of the deck (fig. 16) and the influence of transversally crossed hangers were considered.

Another main advantage of the G.P.M. design was an exceptionally high span/sag ratio (about 12). Such a choice asks for a large amount of steel in the cables(4 cables Ø 1 m) and the percentage influence of the traffic loads is less than 20%. This allows for slopes much less than the maximum required by the Railway Administration.

The result is a bridge like the one shown in fig. 17 where the cross section is spread through a width of 50 m.

An optimal percentage of empty strips and a well calibrated distribution of parallel and transversally crossed hangers allows for flutter wind speed above the fixed limit of 50 m sec^{-1}.

To prevent excessive horizontal deflection the lateral towers had to be split into two independent ones (fig. 18).

As a final result the estimated cost of the single span bridge is less than for the two span bridge or a possible tunnel. That is, it seems the best solution for the Messina Narrows crossing.

References.

1. Gruppo Ponte Messina s.p.a., Roma. Presentazione del rapporto di fattibilità. GPM 1/299. 1977.
2. L'ingegnere, Roma, n° 11. 1971.
3. Attraversamento dello Stretto di Messina. L'industria delle Costruzioni, Roma, n° 22, 1971.
4. F. De Miranda. Il ponte strallato. Soluzione attuale del problema dei ponti di grande luce. Costruzioni metalliche, Milano, n° 1, 1971.
5. D. Danieli and G. Mazzoli. Una tensostruttura per l'attraversamento dello Stretto di Messina. Giornate della Costruzione in Acciaio. Tema D. Verona, oct. 1977.

THE DESIGN AND CONSTRUCTION OF THE NEW RIVER GORGE BRIDGE

C. V. Knudsen, ASCE-F, Chief Engineer - Structures, Michael Baker, Jr., Inc.
J. F. Cain, Engineer, American Bridge Division, U.S. Steel Corporation

The world's longest steel arch bridge, spanning the New River Gorge in West Virginia, was opened to traffic on October 22, 1977. The overall length of the structure is 923.6 m (3,030 feet), with the main arch spanning a distance of 518.2 m (1,700 feet). During the preliminary design stages, various bridge types were considered. The final decision to build a steel arch was based on a combination of cost and aesthetic considerations. By using a high-strength, corrosion-resistant steel, the weight of the structure was kept to a minimum with the added benefit of maintenance-free steelwork blending with the surrounding rugged terrain. Surface conditions in the coal mining region presented problems during foundation design. Special methods were employed to provide for subsurface stabilization where support bents were located in the proximity of mined-out areas. The computer was a major tool in both the design and erection of the bridge. The computer made it possible to determine the most economical configuration for the main arch, and it was used to study many complicated loading and erecting conditions. Erection of the steelwork presented a tremendous challenge. The height of the structure, 267 m (876 feet) above the river, and the heavy member weights dictated the use of a twin 1,067-m (3,500-foot)-cableway system. Construction of the arch across the gorge proceeded from both sides simultaneously utilizing the unique tieback system to support the cantilevered arch truss halves. The 34-million-dollar structure will be a major link in West Virginia's Appalachian Corridor "L" Expressway System.

The world's longest steel arch bridge spanning the New River Gorge in south central West Virginia was opened to traffic on October 22, 1977. The bridge was designed by Michael Baker, Jr., Inc. for the West Virginia Department of Highways and constructed by the American Bridge Division of United States Steel Corporation. (See Figure 1.)

The total length of the bridge is 923.6 m (3,030 feet). The main 518.2-m (1,700-foot)-arch span is flanked by five 38.6-m (126.5-foot)-continuous deck truss spans on the south and four 43.7-m (143.5-foot)-continuous deck truss spans on the north. Fourteen continuous deck truss spans at 39.5 m (129.75 feet) support the deck over the arch span. The deck of the bridge is 267 m

Figure 1. Elevation View of New River Gorge Bridge.

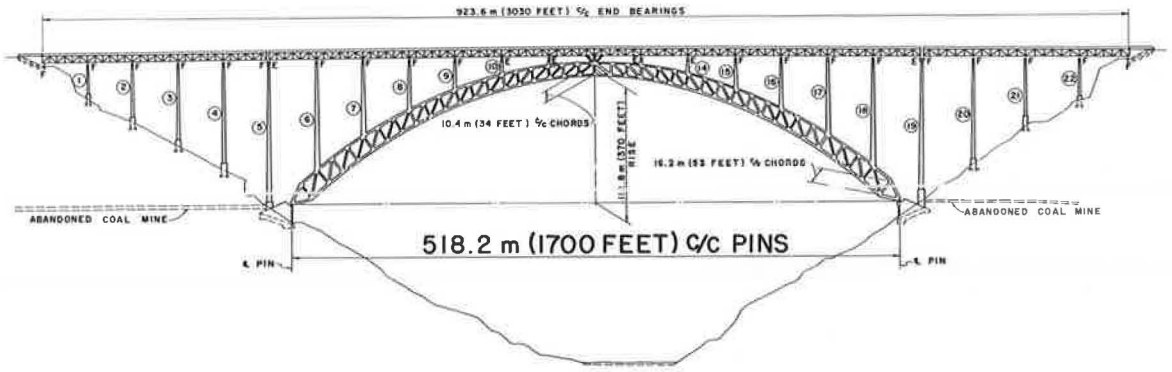

(876 feet) above the waters of the New River, a height exceeded only in the United States by the Royal Gorge Bridge in Colorado. By way of comparison, the Bayonne, New Jersey arch, built in 1932, has a span of 503.5 m (1,652 feet). The Sidney, Australia harbor arch, also built in 1932, has a span of 502.9 m (1,650 feet).

The overall width of the deck is 22.4 m (73.4 feet) providing space for four traffic lanes, adequate shoulders, and a safety type median barrier. The deck is reinforced concrete with a laytex modified mortar overlay.

The bridge is a part of the Appalachian Development Highway System and will open up a long-needed north-south route across the State of West Virginia. Route U.S. 19 will cross the bridge and will be the connecting link between Interstate 79 and Interstate 77, West Virginia Turnpike.

The cost is shared by the West Virginia Department of Highways and the Federal Department of Transportation. The bid for the construction of the bridge was $34,000,000. The lump sum bid for the superstructure was $25,180,000 for 19,410 M tons (21,400 tons) of steel.

Location Studies

In April, 1967, the West Virginia Department of Highways contracted with Michael Baker, Jr., Inc. for professional services to study a section of Corridor "L" from the north end of the existing Oak Hill Expressway to the vicinity of United States Route 60 near Hico, a distance of approximately 18 km (11 miles). The preliminary report indicated a road to be built within a corridor having a width of from 3 to 5 km (2 to 3 miles). After nearly two years of comprehensive alignment and cost studies, the recommended line was accepted by the State and Federal Departments of Transportation.

New River Gorge was the major obstacle between the two terminals. Due to the steep profile, the cost would have been prohibitive to construct a highway at ground level along the sides of the gorge and crossing the river at low elevation. Thus, studies were directed toward the location of the best alignment for the bridge. Aerial and USGS maps were used to locate the shortest span on an alignment that could be projected to tie in with the approach roads.

Foundation Exploration

A limited number of deep-core borings were drilled on the recommended line to determine subsurface conditions. The area in the vicinity of the proposed crossing had been mined. Preliminary core borings verified open mine shafts and remaining coal support columns. The borings confirmed that the proposed alignment was satisfactory as far as subsurface conditions were concerned. After structure type approval, additional core holes were drilled at the exact locations of each of the substructure units.

The overburden above the coal seam is largely sandstone and of good quality. The abutments for the main arch span are founded on rock below the coal bed seam. Except for the first bent adjacent to both ends of the arch, the distance between the coal bed and the bottom of the footings was well over 30 m (100 feet). The overburden of sandstone was considered adequate to support the superimposed loads from the approach spans.

The proposed bottom of footing for the two bents adjacent to the arch was approximately 18 m (60 feet) above the roof of the coal mine shaft. The mined-out areas were located by drilling a number of 150-mm (6-inch)-diameter holes from the bottom of the footings to the cavities. These holes were used to make a photographic survey of the existing subsurface conditions.

The remaining coal columns appeared stable; however, to assure against possible future subsidence, the mined-out areas below the footings of two bents were filled with a sand-gravel grout mixture. The sand-gravel mixture was dropped through the drilled holes to form a cone with a 1.8-m (6-foot)-diameter against the mine roof. The sand-gravel cones were stabilized by injecting cement flyash into the axis of the cone. The condition of the cones were verified by photographs taken with a camera suspended in unfilled holes.

Span Studies

The recommended alignment required a bridge with an overall length of approximately 915 m (3,000 feet). Various lengths of suspension spans were considered. Due to the height of towers above the gorge and/or difficult tower construction on the sides of the gorge, a suspension-type bridge was not favored.

Continuous deck girder and cantilever truss-type spans were also studied. Numerous piers would have been required that would have been costly and difficult to construct.

By a process of elimination of other types, studies were directed toward a steel arch. Due to the heavy thrust and reaction, it was determined that the abutments for the arch should be founded below the level of the existing coal beds. Existing Route 82 crossed the proposed centerline of the bridge at an elevation near the bottom of the coal bed. Both of these features entered into the selection of the positions for the abutments. Natural features controlled the deck elevation and the elevations and locations of the arch abutments. These features also influenced the geometry of the arch.

Design of the Arch

The existing features were instrumental in arriving at a span of 518.2 m (1,700 feet) with a rise of 112.8 m (370 feet) or a span-depth ratio of 4.6. A two-hinged, truss-type arch was selected. The shape of the arch was adjusted to conform to the dead load reaction thrust curve. Live loads and thermal conditions also influence the truss depth and geometrics. Numerous trial runs were made on the computer with variations in shape and depth of truss. The aim was to balance thrusts so that top and bottom chords were practically of equal size, and so that their areas were not significantly affected by secondary stresses due to thermal stresses or wind loads. The depth of the arch truss was varied from 10.3 m (34 feet) at the center span of span to 16.2 m (53 feet) at the first panel from the pin. The top and bottom chords merged to join at the hinge. Geometrically, the arch is a five-centered curve constructed on chords between panel points. At panel points, the ends of the top and bottom chords intersect on

radial lines with vertical truss members being on radial lines. This greatly simplified fabrication details for the truss members, lateral bracing, and vertical bracing as compared to similar details if the vertical members had been made truly vertical.

The arch rests on four cast steel bearing shoes. The normal thrust on the abutment is almost at a 45° angle. The shoes and the embedded grillages were positioned to transmit a maximum thrust of 9,070 M tons (10,000 tons) into the massive abutments. The pins connecting the arch to the shoes are 690 mm (27 inches) in diameter and free to rotate on the bearing shoes. The ends of the bearing pins were fabricated to include a connection for a strut between the pins. The wind bracing from the upper and lower chords was brought down to intersect and be connected to the strut between the pins. This detail turned out to be simple and effective compared to the usual method of either connecting the lateral bracing to the truss or to a shear key in the abutment. A connection of the lateral bracing to the truss was discouraged by the fact that bolts in the area already extended through metal 360 mm (14 inches) thick.

The top and bottom chords are box members. Webs are 1.47 m (58 inches) deep and covers are 1.0 m (39 inches) wide. Members were kept as small as possible, satisfying L/R and thickness of plate requirements. Full depth cross struts were connected to the top and bottom flanges of the chord members but reduced in depth between connections. Thus, wind areas were reduced which in turn reduced lateral bracing requirements. The slenderness of the members actually enhances the beauty of the structure.

The plans and specifications required all truss members to be fabricated to lengths corrected for dead load deformations and to a temperature of 16°C (60°F). Contact surfaces at the ends of the chord members were to be milled and shop assembled for check. At least 75 percent of the contact area was to be in full bearing. For the remainder, a separation not to exceed 0.25 mm (.01 inches) would be permitted. This condition was attained during construction.

The close tolerance may have added to the cost of fabrication; however, the added costs was more than offset by a reduction in size and thickness of gusset plates, splice plates, and number of bolts in the connections. Joints were designed on the basis that 50 percent of the load in the member was carried through by end bearing and the other 50 percent by the bolts. (The 50 percent bolting was adequate for the cantilever during construction.)

Except for minor items, all structural steel in the bridge is ASTM-A588. This is a high-strength, weathering-type steel. High-strength steels are economical for long span bridges. This was especially true for the New River Gorge Bridge. Difficult erection conditions made it imperative that the weight of each individual piece be kept to a minimum. The combined weights of all members, being less by using high-strength steel, tended to further reduce the weights of individual members.

The New River Bridge is in an ideal area for the use of weathering-type steel. The atmosphere is clear of fumes or acids that could contribute to corrosion. Due to the extreme height, the structure would have been costly to paint. The steel has not been painted and has weathered to a dark rustic brown that blends well with the mountainous surroundings. Many dollars were saved during construction and will contribute to additional savings in future maintenance costs.

Approach Spans

The approach spans at both ends of the arch span and the spans over the arch are a series of continuous deck trusses. These spans rest on rectangular box columns. The columns are 1.2 x 1.2 m (4 x 4 feet) at the top, varying to a maximum of 1.2 x 3.5 m (4 x 11.5 feet) at the bottom. All columns in the approach spans were anchored to the concrete foundation by anchor bolts, tensioned to introduce a positive reaction on the base plate. There are thirty-four 83 mm (3-1/4 inch) anchor bolts in the highest column, and each bolt was pretensioned with a force of 103 M tons (235,000 pounds). The tensioning served to anchor the bents prior to erection of the superstructure and to resist lateral wind loads after the bridge was constructed. Due to the terrain, steel bents were more economical to construct than the more conventional concrete piers. The bents and deck trusses are constructed of A588 steel and are not painted.

Fabrication of Steelwork

The deck system was fabricated using numerically-controlled drilling equipment. Because of the recognized accuracy of these mechanisms, the specification's required only 10% of the main truss chord field splices, which were non-bearing, to be shop assembled for fit verification. The field splices for the remainder of the deck system were not assembled until they were finally placed in the field.

Specification's called for progressive assembly of the bent columns in the shop. Segments were completely welded and milled to length. Following this, successive segments were assembled, with the milled ends in bearing, and the field splice holes were drilled using the pre-drilled splice material as a template.

Numerically-controlled drilling equipment was also used to fabricate the arch members. After the box chord members had been welded, drilled and milled to length, the progressive chord method of assembly was followed to verify fit, bearing at the milled joints, and geometry.

All main bridge members were fabricated using shop welded connections. Exposed welds were made using class E80 electrodes to provide a filler metal compatible with the strength and atmospheric corrosion properties of ASTM A588 material. Field connections were bolted using ASTM A325 Type 3 (weathering type) high strength bolts.

Erection Scheme

The rugged, mountainous terrain presented a tremendous challenge in the erection of the arch. In the early planning stages of construction, engineering studies considered many erection schemes. Because of the gorge's great depth, the use of falsework was ruled out. Finally, the decision was made to cantilever the arch trusses out from both sides of the gorge, using a tieback system for temporary support.

An economical method was needed to move the heavy arch truss members into position over the

Figure 2. Cableway and Arch Tieback System.

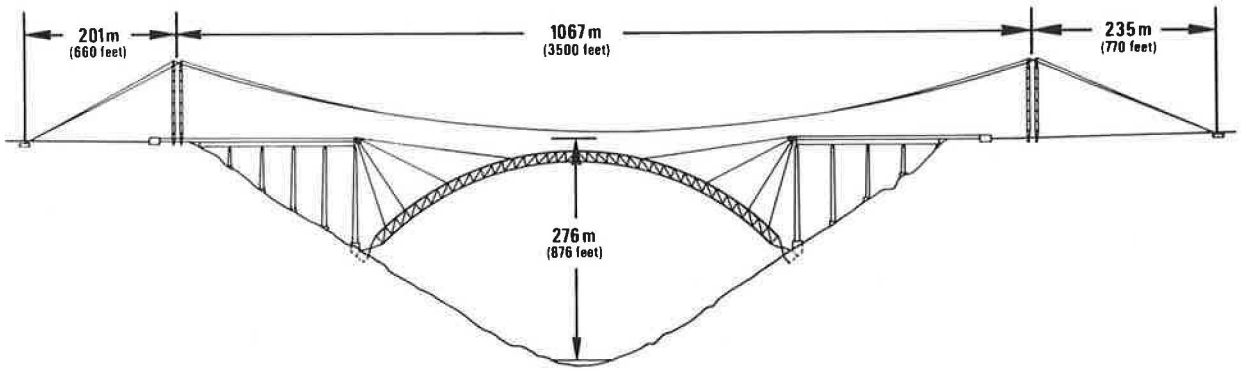

gorge. The use of travelling derricks that would move along the top chord of the arch was considered, but this would have imposed prohibitive loads on the steelwork and the tieback system; also, it presented problems in delivering steel to the derricks. The cableway system finally adopted provided the most economical method for both fabrication and erection, minimizing requirements for reinforcement of the main truss members for erection stresses (See Figure 2).

All structural steel was erected using the cableway system. The land bents and approach deck trusses were completed first. Then, the arch trusses were cantilevered out from both sides of the gorge supported by the temporary tieback system. The arch trusses were joined at mid-span, and the tiebacks were removed. Finally, the arch bents and arch deck trusses were erected, completing the steelwork.

Cableway System

Cableways have been used in the past to erect structures over deep canyons, but the twin system developed for the New River Gorge Bridge is in a class by itself. The 1067 m (3,500 foot) span and 90 M ton (100 ton) lifting capacity made it the largest yet constructed.

Each cableway carried a 45 M ton (50-ton) trolley and hoist on two 76 mm (3 inch) diameter track cables that were supported by a 101 m (330 foot) tower on each side of the gorge. The tower bases were set 2.4 m (8 feet) on either side of the bridge center line, and were pinned to permit lateral tilting, or luffing, of each tower. By luffing the towers, the track cables could be positioned over any portion of the 22 m (72 foot) bridge width (See Figure 3).

Figure 3. Luffing Diagram for Cableway Towers.

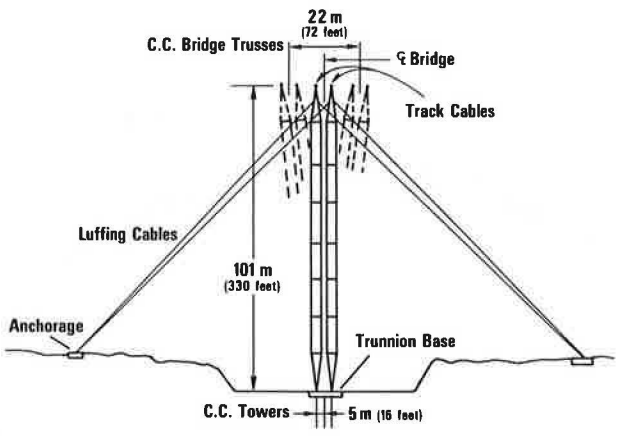

The cableways were operated independently for lifts up to 45 M tons (50 tons); for heavier lifts, the two cableways were operated in unison, providing a lifting capacity of 90 M tons (100 tons).

Arch Tieback System

The tieback system was primarily designed to support the massive arch structure; however, it also included a jacking system that played an important role in the arch closing procedure. Each of the cantilevered arch trusses was independently supported by a concrete anchorage located approximately 70 m (200 feet) behind the abutment at each corner of the bridge (See Figure 4).

Figure 4. Plan of Arch Tieback Anchorage.

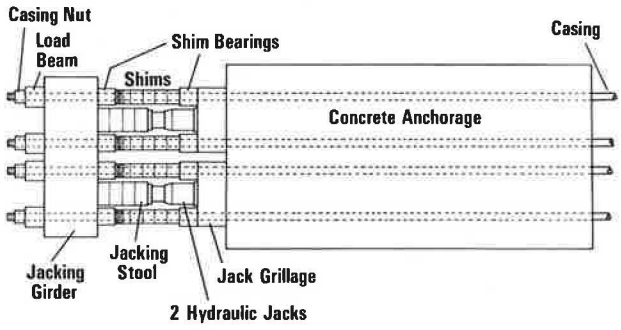

Four strings of pipe casing passed through the anchorage and connected to a moveable steel jacking girder. Behind the anchorage were four 1134 M ton (1250-ton) hydraulic jacks that were used to adjust the position of the moveable jacking girder. Shim blocks placed over the casing between the girder and anchorage transferred the tieback load from the girder to the anchorage.

The four strings of tieback casing extended out on the approach steelwork, where they connected to a rocker and linkage device located at the end approach bent (See Figure 5).

Figure 5. Plan and Elevation of Rocker and Linkage Device.

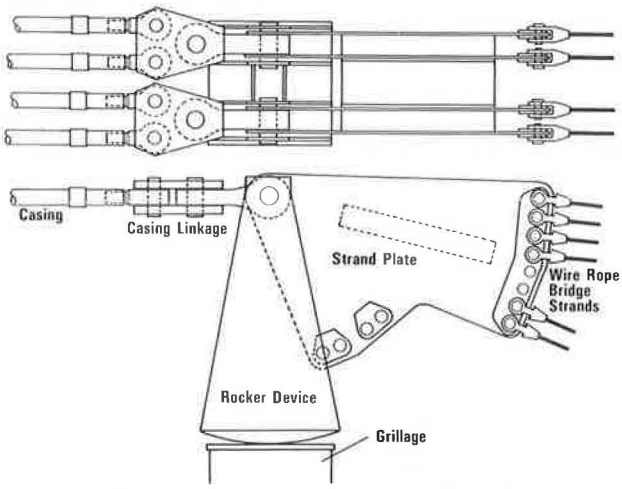

Figure 6. Elevation of Adjusting Device for Arch Tieback Strands.

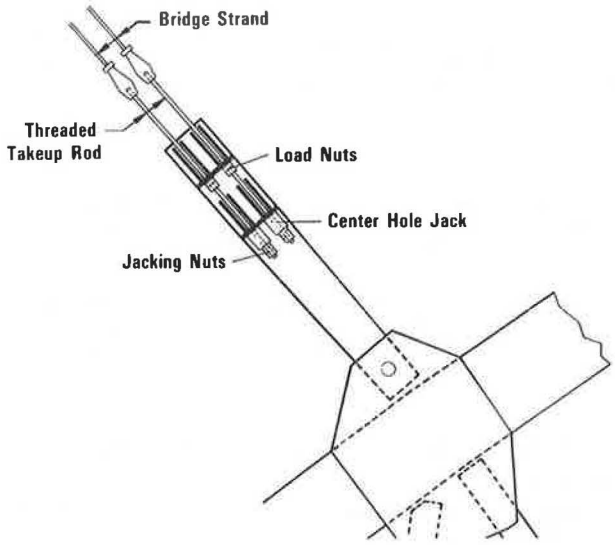

The rocker device had four strand plates with pin holes for connecting wire rope bridge strands that extended down to various support points on the arch truss. The strands were connected to the arch steelwork using a special tieback adjusting device (See Figure 6).

By means of center hole jacks mounted in the device, the strands were adjusted to equal lengths and equal loads. The tieback strands progressively supported the truss at panel points 2, 4 and 8. While supported at panel point 8, the steelwork was cantilevered out to panel point 14, where another set of tieback strands were connected. Because of the weight of the structure at this stage of erection, tiebacks at both panel points 8 and 14 were used to support the steelwork as it was cantilevered out to mid-span at panel point 20 (See Figure 7).

Arch Closing Procedure

Previously, major arch bridges had been closed by inserting jacks in the gap between the two arch halves to attain the design stress, then filling the gap with a custom-made steel insert piece. The New River Gorge Bridge was the first major arch bridge to be closed without an adjustable closing member.

Deflection calculations showed that the top chord splice points would come into contact first during the closing operation. Therefore, during fabrication, the design details for the top chord splice points were modified, adding pins in each web plate to control alignment (See Figure 8).

Figure 8. Top Chord Web Alignment Pin.

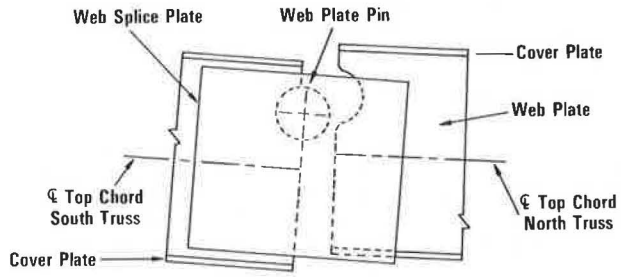

Figure 7. Elevation of Steelwork Cantilevered to Mid-Span While Supported at Panel Points 8 and 14.

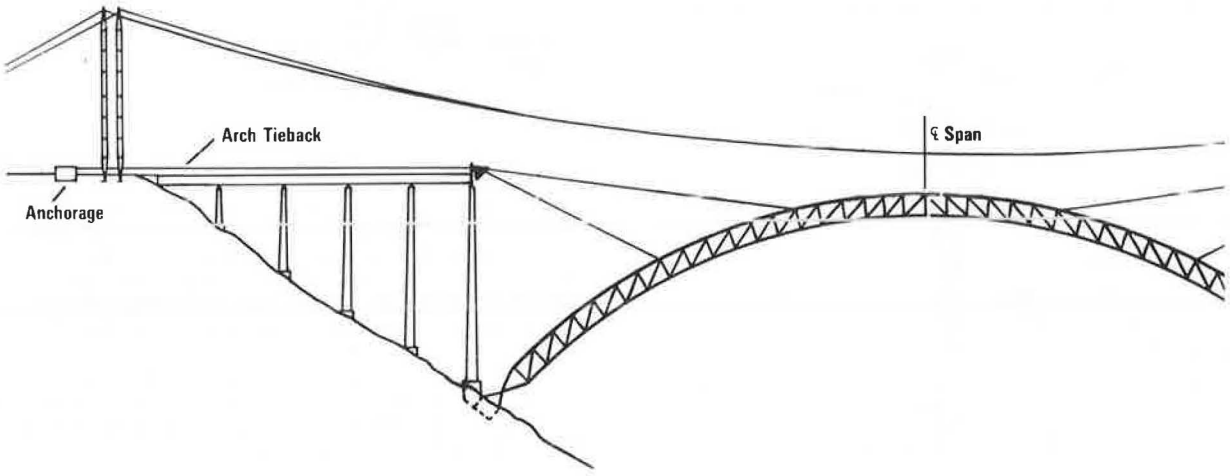

The erection procedure called for the truss halves to be erected high. Then, to close the arch, the tieback system was gradually released using the anchorage jacking system. This caused the truss halves to rotate about their hinges and seated the web pins at the top chord splice points (See Figure 9).

Figure 9. Top Chord Web Alignment Pin in Contact, With Bottom Chord on Alignment Shoe.

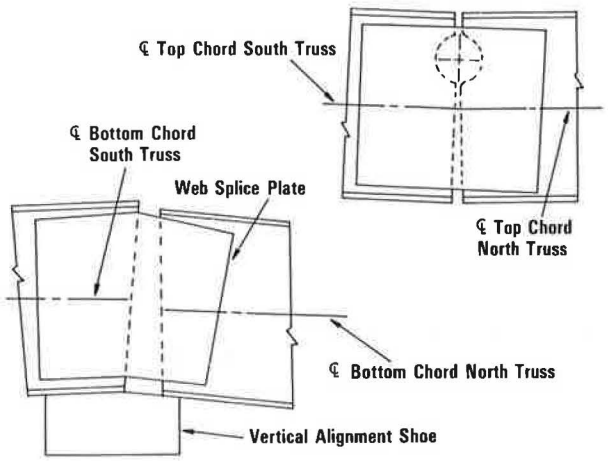

With the web pins in contact, further relaxation of the tie-backs induced compression forces in the top chords, causing the crown of the arch to rise and the top chords to rotate about the web pins, thereby closing the gap at the bottom chord points. When the bottom chords came into bearing, the top and bottom chord splices were pinned and bolted. The tieback system was then released completely, thereby "swinging" the arch span.

Construction Time

Shortly after the contract was awarded in June 1973, construction work began on the bridge abutments and approach bent foundations. Also, foundations were installed for the cableway system; then the cableway was erected and made operational.

Erection of the approach steelwork began in May 1974 and, following the installation of the arch tieback system, the arch erection was started in July 1975. In May 1976 the arch was closed, and the final deck truss steelwork over the arch was placed in November 1976. The deck slab over the arch, along with the parapets and median were poured in the Spring of 1977; in October 1977 the structure was opened to traffic.

TRAFFIC LOADING OF LONG SPAN BRIDGES

Peter G. Buckland and John P. McBryde, Buckland and Taylor Ltd.
Francis P.D. Navin and James V. Zidek, University of British Columbia

To estimate the traffic loading on long span bridges two independent statistical techniques were developed. One was purely analytical, the other used a computer to generate random "traffic" and calculate the maximum load on the bridge. The two methods gave remarkably similar results. Further research produced not only maximum loads, but also maximum moments and shears. From this work the following results emerge:

a) With a knowledge of the average mix of traffic, a design loading can be estimated with a good degree of confidence using the techniques developed.

b) The loading can be accurately represented by a uniform load and a concentrated load in the traditional manner.

c) Unlike the AASHO loading, one set of uniform and concentrated loads can be used to represent both maximum moment and maximum shear.

d) As expected, the uniform load per foot reduces as the loaded length is increased.

e) Unlike AASHO and previous assumptions, it is found that the concentrated load increases as the loaded length increases.

f) When several lanes are loaded simultaneously they do not, as suggested by AASHTO, all carry the same load. A simple distribution formula has been found.

These results have significant implications for the designers of long span bridges; and typical results have been produced for various types of traffic.

It has been recognized by several authorities (e.g. references 2, 4, 6, 7) that the traffic loading per unit length on a bridge diminishes as the loaded length increases. When faced with the need to accurately estimate the load on a bridge (8), however, the authors could find no satisfactory theory available and were obliged to develop their own methods. Having developed the techniques, they have now been applied to the general bridge as reported herein.

Two completely different methods were derived. One was an analytical solution of probability equations and has been described in reference 9. The other uses the random scatter capability of the computer to simulate traffic coming onto the bridge and has been described in reference 5. These two methods served as an excellent check on each other.

From this work, summarized in reference 5, four main conclusions emerged:

1. The maximum loading occurs with traffic stationary. Video-samplings of traffic from the tower of a suspension bridge confirmed this finding by Asplund (2). When traffic starts to move the vehicles separate such that the loading intensity is reduced, even if an allowance is added for impact.(Fig. 0)

Fig. 0. Dense traffic travelling on a long span bridge. Moving traffic clearly spaces out to produce a less severe loading case than that caused by stationary "bumper-to-bumper" vehicles.

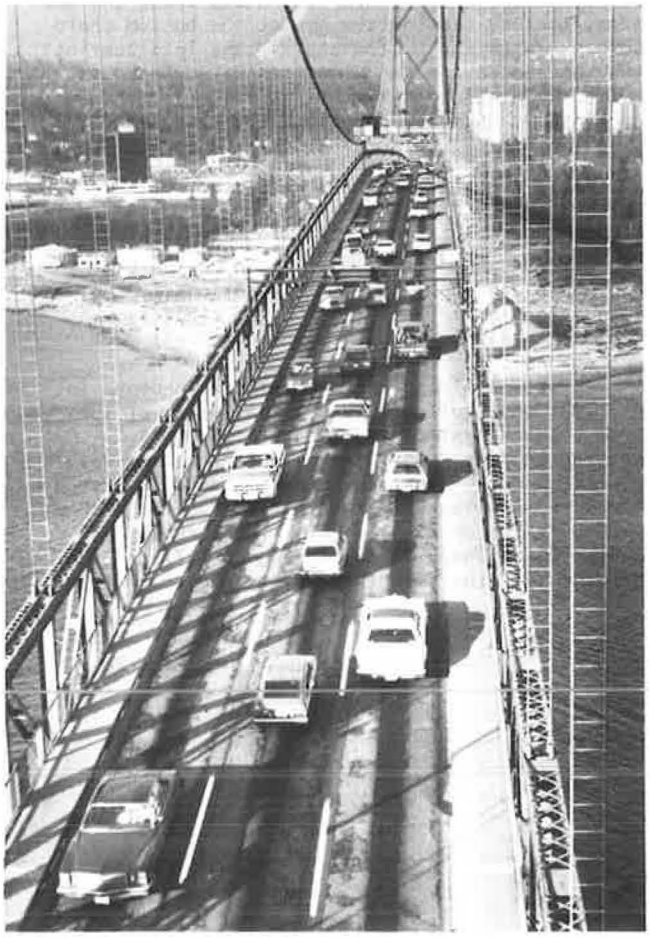

2. The loading can be represented as a uniform load and a concentrated load in the traditional manner, as shown in Fig. 1. This will predict maximum shears and moments on a span with reasonable accuracy, irrespective of the end conditions of the span. Multiple span loadings have not been studied in depth.

3. Unlike AASHTO loading a single pair of loads, the concentrated load, P, and uniform load, U, will produce both maximum shears and maximum moments. Reference to Fig. 1 will show that the maximum moment, M, shear, S, and total weight, W, can be produced by the expressions

$$M = \frac{PL}{4} + \frac{UL^2}{8} \qquad 1$$

$$S = P + \frac{UL}{2} \qquad 2$$

$$W = P + UL \qquad 3$$

Equations 1, 2 cannot be solved simultaneously, but it is found empirically (see ref. 5) that P, U derived from the solution of equations 2, 3 provide good approximations to the solution of equation 1.

4. Unlike traditional loading, the concentrated load (P in figure 1) increases as the loaded length increases. The uniform load decreases as expected.

This paper offers loading for four widely differing types of traffic, comments on their accuracy, compares them with established loading codes and discusses cross-lane distribution.

FIGURE - 1
UNIFORM AND CONCENTRATED LOADS FOR SIMPLE SPANS

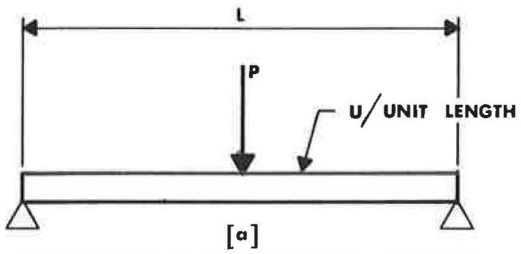

[a]
CONFIGURATION FOR MAXIMUM MOMENT

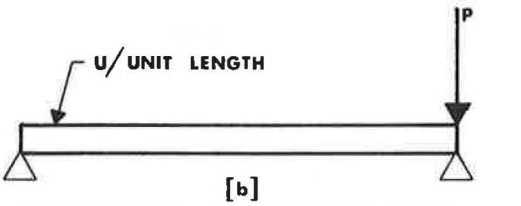

[b]
CONFIGURATION FOR MAXIMUM SHEAR

SIMULATION PROGRAM

The computer program which is used to calculate weights, shears and moments for spans up to about 2000 m (6400 ft.) operates by simulating random traffic crossing over the bridge.

It allows random stoppages of traffic in one or more lanes, on or off the bridge. It then scans the stopped traffic, searching for the maximum load, moment or shear on any length of 15, 30, 61, 122, 244, 488, 975 and 1951 m (50, 100, 200, 400, 800, 1600, 3200 and 6400 ft.). These are referred to as the loaded lengths. The maximum values for each length found during a simulated 3 month period are retained in the memory.

Having found the maxima in one lane, it then searches for the maxima in the other lanes. The traffic in these lanes may be stopped or moving.

The maximum values for each time period of 3 months are printed out, and the mean and standard deviation of these maxima are calculated. A Gumbel extreme value distribution is then used to predict the maximum loading, shear or moment for any required return period, using the formula:

$$Y_R = \bar{Y}_T + K\sigma_T$$

where Y_R is the maximum value expected with a return period R, R is expressed in units of 3 month time periods, $\bar{Y}_T$ is the mean of maximum values observed over T time periods, σ_T is the standard deviation of maximum values in T time periods, and K is a constant depending on R and T.

Although the loading can thus be predicted for any return period, certain rare loading conditions can produce a large standard deviation which will produce unrealistically conservative results if a long return period is used (i.e. K is large). A return period of 5 years has therefore been taken by the authors.

Input to the program falls into four main categories:

Fixed or Arbitrary Data

This includes the length of bridge and approaches on which a stoppage may affect traffic on the bridge, the number of lanes, and the number of 3 month time periods for which the bridge is run.

Bridge Dependent Data

The number and type of stoppages (accidents or breakdowns) and the number of affected lanes for each stoppage can be varied. Stoppages occur randomly in time and position, but a bias can be built in to have more stoppages in some places than others, or at certain times. The length of time to clear a stoppage is random, but the limits are controllable and are different for accidents and breakdowns. The volume of traffic and its average speed are variable by hour of day, as are the number of cars, buses and trucks. The overall percentage of each type of vehicle in each lane is variable.

Driver Dependent Data

For stationary traffic the distance between vehicles is taken as constant, for moving traffic this distance is increased linearly depending on the speed. The speed of "trickle" past an accident is taken as a fraction of the average speed and can be different in each direction.

Vehicle Dependent Data

Cars and buses are each assumed to be of constant length and weight. Trucks are allowed to vary independently in both weight and length. Although the program will handle many mixtures of truck types, insufficient data are available about the traffic, mainly because most authorities study only heavy trucks, not empty or lightly laden ones.

CALCULATED LOADS

Although there is no doubt that more data are needed to ensure accuracy of the results, the authors have nevertheless studied four loading cases which can be considered as a guide.

Case 1 – is based on a two-day observation of traffic on the Second Narrows Bridge in Vancouver, B.C., and is considered fairly typical highway loading. The daily volume on 6 lanes has been taken as 85,900 cars, 351 buses and 6,510 trucks for a total of 92,761 vehicles, of which 7.4% are "heavy vehicles", i.e. buses and trucks over 53 kN (12,000 lb.). The maximum truck weight has been taken as 534 kN (120,000 lb.). The return period is 5 years, with 2000 stoppages per year.

Case 2 – is as for Case 1, but with the proportion of heavy vehicles increased by a factor of four to 29.6%.

Case 3 – again has the same data except that the proportion of heavy vehicles has gone up to 100%. This hypothetical condition represents an "upper limit" of bridge loading for this mix of heavy vehicles.

Case 4 – has very light traffic taken from a seven-day count on Lions' Gate Bridge in Vancouver where a weight restriction is in force. The proportion of heavy vehicles is 2.4% and the heaviest vehicle is 178 kN (40,000 lb.).

PARAMETERS P, U

When the concentrated load, P and the uniform load, U, are calculated for the 4 load cases, the smoothed curves of Figure 2 can be derived. The interesting point, mentioned earlier, is that the concentrated load, P, increases as the loaded length increases. Values of P, U are tabulated in Table 1.

The degree of accuracy obtained by using P, U for simply supported weights, shears and moments for the case with 7.4% heavy vehicles can be seen in Fig. 3, which shows that the average weight is least accurate although, presumably, least important. The shear is within 2% from 61 m (200 ft.) to 975 m (3200 ft.) and the moment is over-estimated by 6% or less, except at 61 m (200 ft.) where the error is safe by 9%.

FIGURE - 2
PARAMETERS P,u FOR DIFFERENT PERCENTAGES OF HEAVY VEHICLES (H.V.)

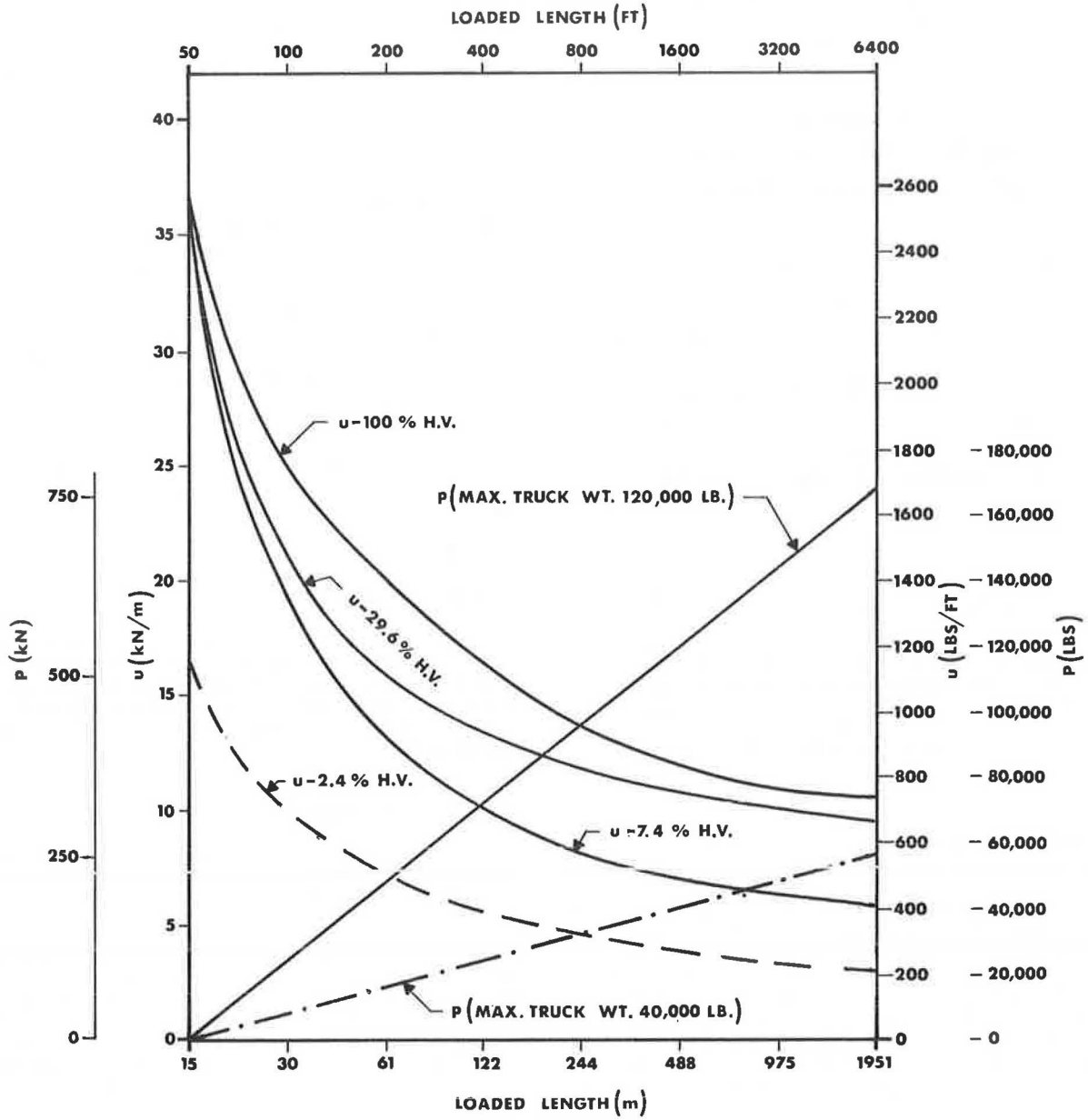

TABLE I. Proposed uniform and concentrated loads for design of long span bridges

Loaded Length		Concentrated Load (P) with 7.4% 29.6% 100% H.V.[a]		Uniform Load (U) kN/m (lbs./ft.) 7.4% H.V.		29.6% H.V.		100% H.V.		Concentrated Load (P) with 2.4% H.V.		Uniform Load (U) 2.4% H.V.	
m.	(ft.)	kN.	(lbs.)							kN	(lbs.)	kN/m	(lbs/ft.)
	(1)		(2)		(3)		(4)		(5)		(6)		(7)
15.25	(50)		0	38	(2600)	38	(2600)	38	(2600)		0	16.8	(1150)
30.5	(100)	107	(24,000)	20.4	(1400)	21.9	(1500)	25.5	(1750)	35.6	(8,000)	10	(690)
61	(200)	214	(48,000)	13.7	(940)	16	(1100)	20.8	(1425)	71.2	(16,000)	7.6	(520)
122	(400)	320	(72,000)	10.4	(710)	13.9	(950)	17.1	(1170)	107	(24,000)	6	(410)
244	(800)	427	(96,000)	8.3	(570)	12.1	(830)	14	(960)	142	(32,000)	4.8	(330)
488	(1600)	534	(120,000)	7.1	(485)	10.8	(740)	12.3	(840)	178	(40,000)	3.9	(270)
975	(3200)	640	(144,000)	6.4	(440)	10.2	(700)	11.2	(770)	213.5	(48,000)	3.4	(235)
1950	(6400)	747	(168,000)	5.8	(400)	9.9	(680)	10.5	(720)	249	(56,000)	3	(210)

Note: [a]% H.V. denotes percentage of heavy vehicles over 53 kN (12,000 lbs.) in the traffic.

FIGURE-3
ACCURACY OF PARAMETERS

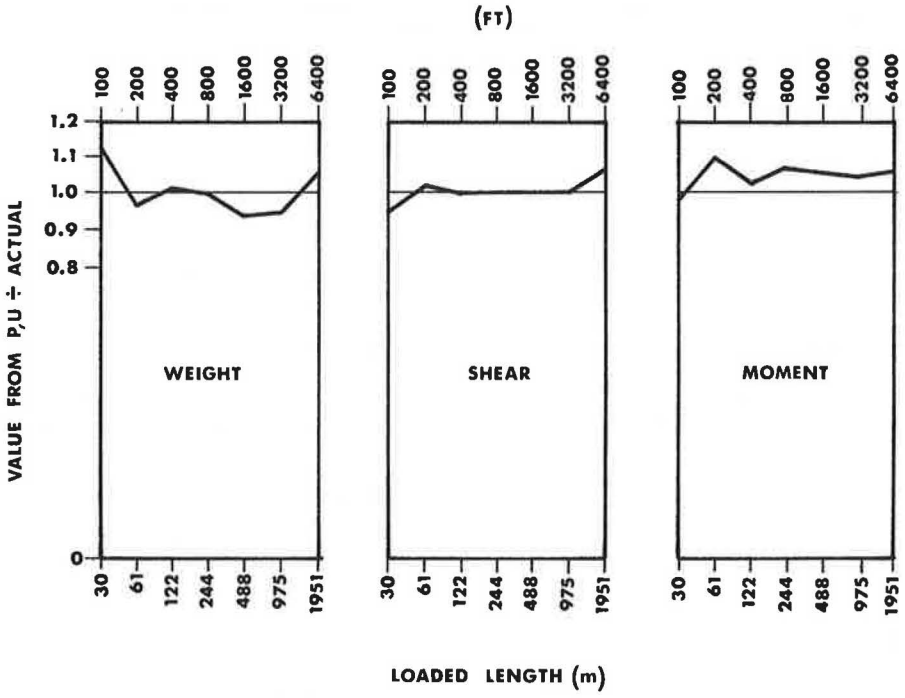

Thus the parameters P, U given in Fig. 2 produce simply supported shears and moments with good accuracy. Justification for their use on non-simple spans can be found in reference 5.

COMPARISON WITH AASHTO AND BS153

A comparison is made in Fig. 4 between the simply supported moments found in the authors' example, and those which would be derived from AASHTO (1) HS-20 loading, which is a common North American loading for bridges up to 122 m (400 ft.) span (and sometimes extrapolated beyond that limit), and British Standard B.S. 153 (3) which gives loadings for spans up to 900 m (2952 ft.). Shears follow a pattern very similar to moments and are therefore not shown separately. It can be seen that between 244 and 488 m (800 and 1600 ft.) all three methods give approximately the same answer, whereas for lower loaded lengths AASHTO underestimates and B.S. 153 overestimates, and above 488 m (1600 ft.) the opposite is true, the errors sometimes exceeding 30%.

FIGURE-4
COMPARISON OF MOMENTS (7.4% H.V.)

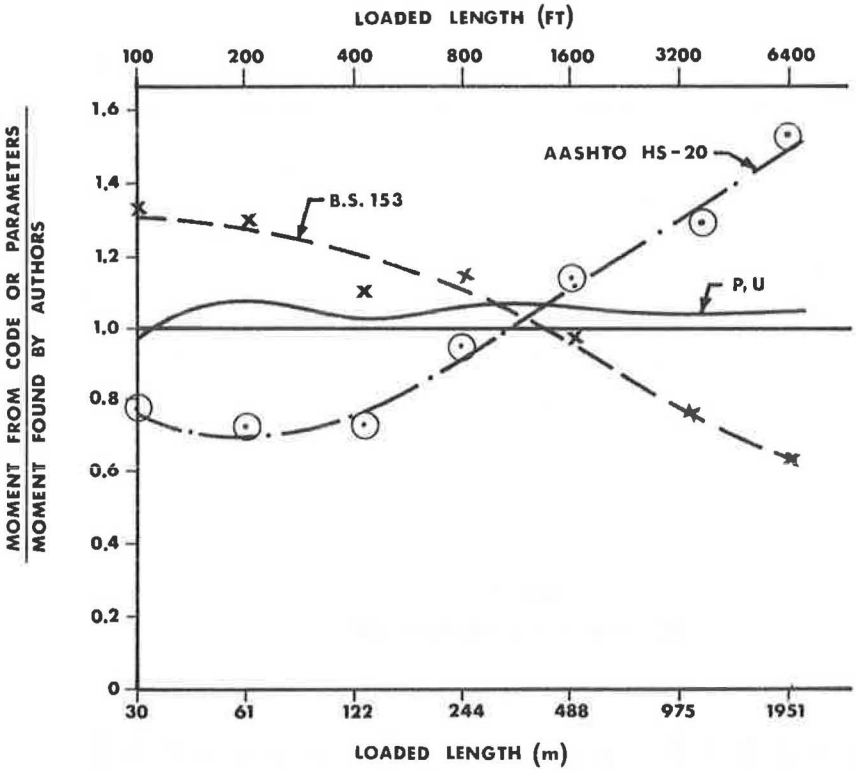

COMPARISON OF TRUCK INTENSITIES

Second Narrows Bridge traffic was chosen for this study as it was thought to be fairly typical. The other theoretical truck intensities were studied, however, in order to determine some upper and lower bounds, should Second Narrows Bridge not be typical.

Fig. 5 compares maximum shears for traffic with 2.4%, 29.6% and 100% heavy vehicles (H.V.) with those for traffic with 7.4% heavy vehicles. It can be seen that at short loaded lengths the three greater loadings tend to converge. This is because they all have the same maximum vehicle weight of 534 kN (120,000 lb.), and at short lengths a single vehicle can govern. The lower curve (2.4% H.V.) has a lesser value at short lengths as its maximum vehicle is only 178 kN (40,000 lb.). At first sight it may appear that the loading at short lengths for 2.4% H.V. should thus be a third of that for the other curves. Such is not exactly the case because the 178 kN (40,000 lb.) truck is shorter than the 534 kN (120,000 lb.) truck, thus resulting in a load intensity somewhat greater than a third.

At longer loaded lengths there is more divergence, but it is interesting that within the range considered even traffic with 100% heavy vehicles produces loading not more than 70% greater than the 7.4% case. When it is considered that at these large lengths the total live load is small relative to the dead load, it can be argued that taking 7.4% H.V. or 29.6% H.V. or somewhere in between will not cause undue errors in stress.

A few cases were considered with a small number of very heavy trucks in the traffic stream, which might represent overloaded logging trucks at 890 kN (200,000 lb.) each. The effect was very small, except at short loaded lengths.

CROSS LANE DISTRIBUTION

A common question to arise in bridge loading is: if the loading on one lane is known, what is the loading on the other lanes? There are several ways in which this can be tackled. One method is to assume that the total loading on two lanes of length L is the same as the loading on one lane of length 2L. In this case the known single lane curves can be used, although the two obvious deficiencies in this line of attack are (a) knowing the loads on two lanes does not indicate how it is distributed between the lanes, and (b) it assumes that all lanes carry identical traffic, which they certainly do not.

AASHTO directs that when several lanes are loaded, the load on every lane shall be reduced to 90% of single lane loading when 3 lanes are loaded, and to 75% of single lane loading when 4 or more lanes are loaded. It can be argued, however, that this is both illogical and erroneous. If a single lane can have a certain load on it, then the addition of two more lanes would tend to increase the load in the curb lane as trucks gravitate towards it. Loads in the second and third lanes may well be reduced, however.

B.S. 153 takes some recognition of this phenomenon by requiring the first two lanes of the bridge to be fully loaded and the remaining lanes to be loaded with one third of the single lane loading.

The fact is that neither standard method is correct because the cross-lane distribution depends on the loaded length. A single ratio independent of loaded length will never be better than approximate. This can be seen by reference to Fig. 6. Making the assumption that all lanes carry identical traffic, two lanes at 30 m (100 ft.) long might carry the same as one lane at 61 m (200 ft.) which is

FIGURE-5
COMPARISON OF MAXIMUM SHEARS FOR DIFFERENT PERCENTAGES OF HEAVY VEHICLES

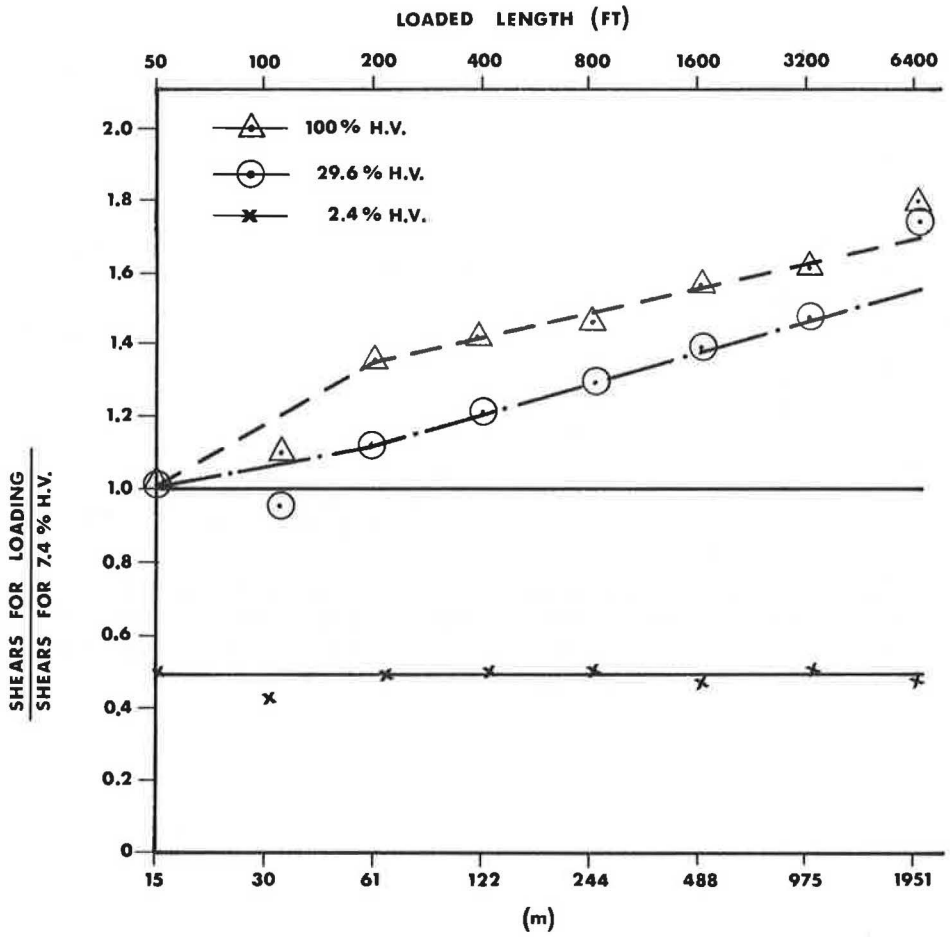

17 kN/m (1180 lb/ft.) of lane, or 34 kN/m (2360 lb/ft.) of bridge. Since one lane could be carrying the maximum load for 30 m (100 ft.) which is 24 kN/m (1640 lb/ft.), the second lane would be carrying 34 - 24 = 10 kN/m (720 lb/ft.) and the ratio of second lane to first lane would be 10 ÷ 24 = 0.42. At a longer loaded length, however, say 488 m (1600 ft.), two lanes would carry the same as 975 m (3200 ft.) of single lane, which is 7.1 kN/m (485 lb/ft.) per lane, or 14.2 kN/m (970 lb/ft.) of bridge. A single lane of 488 m (1600 ft.) could carry 8.2 kN/m (560 lb/ft) leaving the second lane to carry 14.2 - 8.2 = 6.0 kN/m (410 lb/ft.) for a ratio of 6.0 ÷ 8.2 = .73.

Thus the ratio of second lane to first lane can vary depending on the length of bridge considered. The authors' method does not make the simplified assumptions of the previous paragraph, but actually calculates the maximum loads for every length on 1, 2, 3 and 6 lanes, and gives, for each, the amount of load on each lane.

Fig. 7 gives the ratios of second lane to first lane, third lane to first lane and the average of lanes 4, 5 and 6 to the first lane, for total weights in the case of 7.4% heavy vehicles. As expected, the ratios vary considerably, but in the interests of simplicity one could approximate the situation by using lane loading ratios of 0.7 for the second lane, and 0.4 for the remainder. These ratios are compared with those of the other codes in Fig. 8.

When selecting a "general" cross-lane distribution it is important to bear in mind the purpose for which it will be used. Fig. 9 shows four bridge cross sections. Section (a) shows a typical through truss arrangement. The important consideration here is the maximum load which can occur on one truss. A similar case to this would be a suspension bridge where the load on one cable is governing. Section (b) shows two plate girders. Again, the important effect is the maximum load on one girder. Section (c) shows all the lanes carried on a single box girder and section (d) shows a single central support (perhaps cable-stays) and a torsion box. In the last two cases the bending in the box (or the load on the central support) is governed by the total weight on all the lanes, and the torsion in the box is governed by only the lanes on one side of centre-line being loaded.

Thus the main considerations are the total load, the maximum torque, and the maximum load on one support of a double support system. This last depends on the spacing of the supports.

Table 2 compares these three effects using the AASHTO and B.S. 153 distributions with the distribution suggested by the authors. The maximum load on one side is calculated assuming the supports at the outside edges of the outside lanes and no median.

FIGURE - 6
AVERAGE LOAD PER UNIT LENGTH

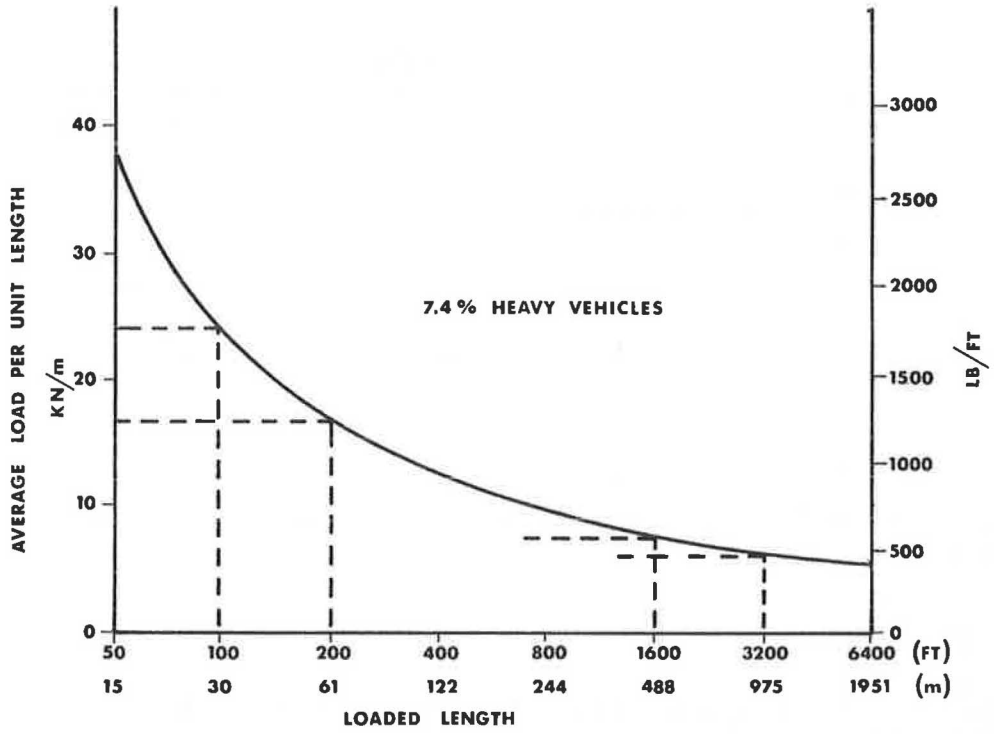

FIGURE - 7
RATIO OF LANE LOADS

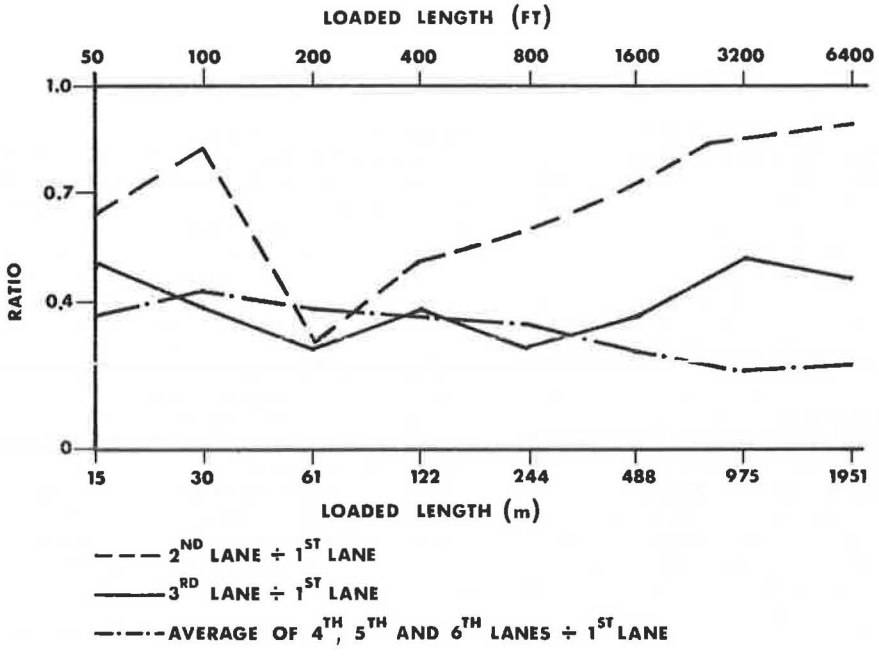

FIGURE - 8
CROSS LANE DISTRIBUTIONS

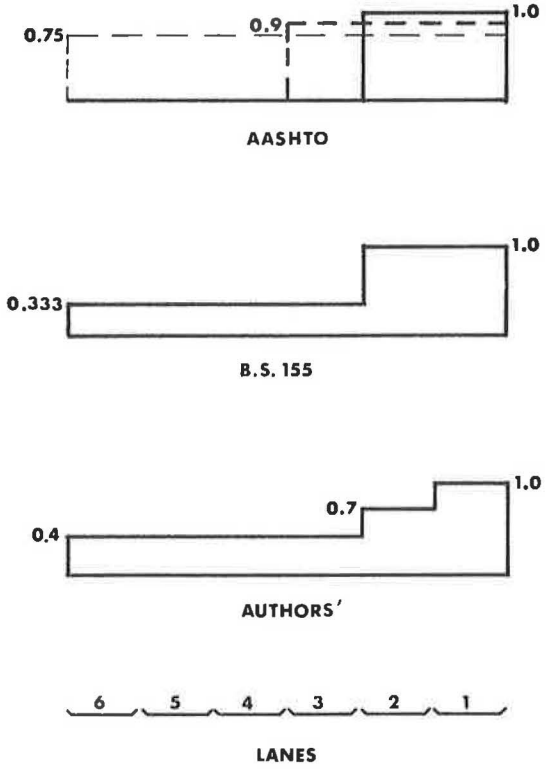

FIGURE - 9
TYPICAL BRIDGE CROSS-SECTIONS

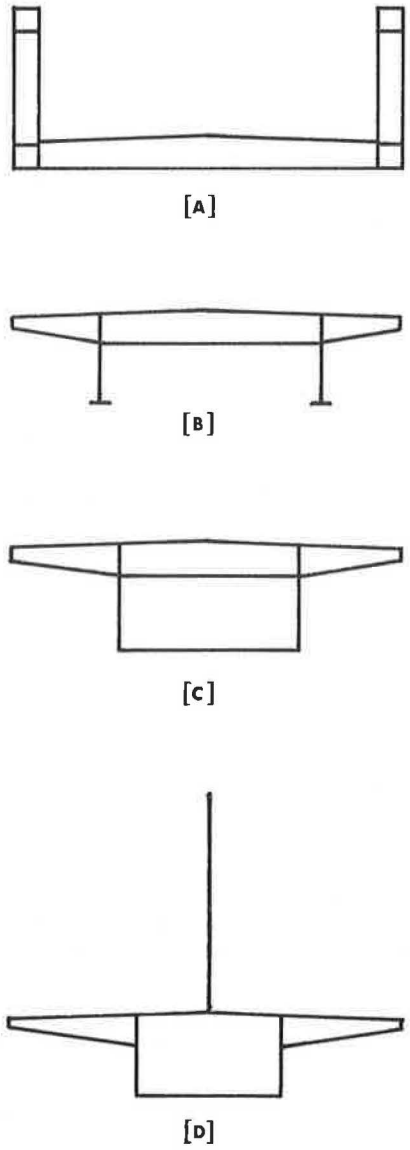

This is a compromise rather than a typical situation, but serves as an illustration. The load in the heaviest laden lane is taken as unity.

It can be seen that there is in practice very little difference in the three methods except that AASHTO tends to overestimate the total load on the bridge by 20 to 36%. This would have been of little concern before the introduction of large box girders and single plane cable stays. Indeed this overestimate has probably discouraged the use of single supports in North America, since there has been no economy to be gained by using them. Whereas in Europe, where the cross-lane distribution is more realistic, they have flourished.

MISCELLANEOUS

Three further opinions can be expressed:

Position in Lane

Most codes state that traffic must be placed in the worst place within a lane. This makes good sense for a short bridge governed by a small number of vehicles, but the authors query its validity for a large bridge carrying many vehicles randomly spaced. They have therefore assumed all traffic at the centre of the lane.

Impact

Impact need not be added to stationary traffic loading. For the moving lanes the authors have also ignored impact on the grounds that (a) impact is random and as some traffic bounces up and some down, the mean effect must be near zero, and (b) moving traffic is the least important anyway, both because of its light weight and its small effect on the major bridge components (see figs. 8 and 9).

Suspension Bridges

Much of this loading will apply to suspension bridges (for which it was originally derived). Because the concentrated load, P, increases with loaded length, it would appear that it can dominate unreasonably. For example, with the entire bridge loaded, P can produce massive shears at the ends of spans, which would seem excessive. It is probable that the best way to handle this is to take the loaded length which produces the worst condition for uniform load only, and then add in the concentrated load, i.e. do not allow U to be applied in the negative region of the influence curve in order to boost P by having a greater loaded length.

TABLE 2. Comparison of cross-lane distributions.

Effect	Number of Lanes	Distribution				
		Authors'	AASHTO	AASHTO % difference[a]	B.S. 153	B.S. 153 % difference[a]
(1)	(2)	(3)	(4)	(5)	(6)	(7)
Total Load	2	1.7	2.0	+18	2.0	+18
	3	2.1	2.7	+29	2.33	+11
	4	2.5	3.0	+20	2.67	+7
	6	3.3	4.5	+36	3.33	+1
Torque[b]	2	0.5	0.5	–	0.5	–
	3	1.0	1.0	–	1.0	–
	4	1.85	2.0	+8	2.0	+8
	6	3.75	4.05	+8	4.17	+11
Maximum Load on Support	2	.93	1.0	+8	1.0	+8
	3	1.25	1.35	+8	1.39	+11
	4	1.51	1.5	-1	1.67	+11
	6	1.98	2.25	+14	2.11	+7

Note: [a]compared to the authors' distribution (column 3).
[b]assuming a lane width of unity.

SUMMARY

The main conclusions to be drawn from this study can be summarized as follows:

1. The facility is now available to calculate the loading on a long span bridge with a fair degree of accuracy. More data are needed about the traffic.
2. The loading can be represented as a uniform load and a concentrated load. The uniform load diminishes as the loaded length increases. The concentrated load increases with loaded length. The same loads produce the maximum shear and the maximum moment, unlike those in AASHTO.
3. Maximum loading conditions will occur with the traffic stationary, therefore no allowance need be added for impact.
4. Guide-line loadings can be derived from fig. 2 or Table 1. Increasing the number of heavy vehicles in the traffic has only a moderate effect on the load.
5. Neither AASHTO HS20 loading nor B.S. 153 are particularly accurate, nor consistent with each other, but they coincide with the authors' loading over a limited length range.
6. No single cross-lane distribution is accurate, but there is little practical difference between the authors' recommended distribution and those of B.S. 153 and AASHTO, except that the latter overestimates the load on a central support system, such as a box girder or cable stays.

ACKNOWLEDGEMENTS

The authors are indebted to Mr. W.A. Bowman, Director of Bridge Engineering of the British Columbia Ministry of Highways and Public Works, who initiated this research, to the Department of Civil Engineering and the Centre for Transportation Studies of the University of British Columbia and to Stanford University, California, for supporting the work, and to Mr. Jacques Beauchamp, Chief Bridge Engineer of the Canadian Department of Public Works who sponsored the generalization of the research which was funded as an "unsolicited proposal" by the Canadian Department of Supply and Services, and administered by Dr. M.S. Cheung, Research Officer, D.P.W.

The authors would also like to thank Dr. Caroline Fisk of the Université de Montréal (formerly of U.B.C.) for her superb programming, Richard Lockhart, formerly of U.B.C., for his contributions to the analytic method, and David Burkholder and Tom Louie of U.B.C. for their enthusiastic assistance.

The conclusions presented in this paper represent the authors' opinions, and are not necessarily endorsed by any of the above parties.

REFERENCES

1. American Association of State Highway Officials. *Standard Specifications for Highway Bridges.* 11th ed. Washington 1973.
2. Asplund, S.O., *Probabilities of Traffic Loads on Bridges.* ASCE Proceedings, separate vol. 585, vol. 81 pages 585-1 to 585-12, Jan. 1955.
3. British Standards Institution, *Specification for Steel Girder Bridges, part 3A Loads.* London 1972.
4. Buckland, P.G., F.P.D. Navin and J.V. Zidek, *Bridge Traffic Loads – Are we Overdesigning?* Roads and Transportation Association of Canada, Proceedings, Sept. 1975.
5. Buckland, P.G. et al, *Proposed Vehicle Loads for Long Span Bridges* presented to ASCE Spring Convention, Pittsburg, April 1978.
6. Henderson, W., *British Highway Bridge Loading* Institution of Civil Engineers Proceedings, Road Paper No. 44 pages 325 to 373, March 1954.
7. Ivy, R.J. et al, *Live Loading for Long-Span Highway Bridges* ASCE Transactions Paper 3708, June 1953.
8. Navin, F.P.D. et al, *Design Traffic Loads for the Lions' Gate Bridge* Transportation Research Board, Washington 1976.
9. Zidek, J.V., F.P.D. Navin and R. Lockhart. *Statistics of Extremes: an Alternate Approach With Application to Bridge Design Codes* Submitted to Technometrics, New York, 1978.

APPLICATION OF PREFABRICATED HOLLOW STEEL DECKS TO BRIDGE CONSTRUCTIONS

Toshikazu Suruga and Kenichi Kushida, Kobe Steel, Ltd., Japan
Yukio Maeda, Osaka University, Japan

At the 10th Congress of International Association for Bridge and Structural Engineering in Tokyo, in 1976, the authors introduced a prefabricated hollow steel deck as a floor system for long-span suspension bridges. In this paper, they are proposing the application of this new deck to the main structure of smaller bridges. This deck has been used in bridges and floor systems in Japan. Here, the authors discuss the structural features and fabrication of this deck and present examples of its application to bridge construction. They also discuss the problems of design and construction of bridges using this deck, the methods of solving these problems, and the experimental studies conducted on the deck. This hollow steel deck is a prefabricated slab structure made up of two face plates with evenly-spaced core plates arranged diagonally between them. Tests have shown that this deck improves a bridge's lateral and torsional rigidity as well as its shearing resistance and fatigue strength. In that this deck is a prefabricated structure, its application facilitates bridge construction.
Furthermore, the total thickness of the bridge structure can be reduced, thus improving its aesthetic appearance.

The steel deck, a light-weight, prefabricated structure, has been used for about twenty years for bridge and floor-system construction not only because of its high strength, but also because it helped to increase economy, safety, and the speed of completion. This conventional orthotropic steel deck, however, having an upper face plate stiffened with longitudinal and lateral ribs, has a low level of lateral and torsional rigidity.

Recently, a new type of steel deck, having two face plates, both a top and a bottom, connected by longitudinal ribs only, was developed by the authors. This prefabricated structure was intended primarily for decks and floor systems, but it is also applicable to bridges with a span of up to about 30 meters, increasing both aesthetic appearance and degree of prefabrication. This hollow steel deck is not applicable to briges with a long span in that they require box girders.

A bridge using this hollow steel deck as its main structure can be referred to as a "slab bridge".

Details concerning the fabrication of this hollow steel deck will be discussed later. It may be helpful at this point, however, to refer breifly to Figure 10. Please note that the bottom plate is actually a series of bands welded longitudinally to the core plates. Thus welding is performed in only one direction.

Figure 1. Completed hollow steel deck showing cross section.

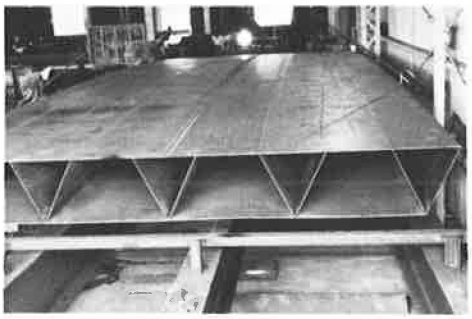

Features and Problems

A bridge using the hollow steel deck has the following advantages:

1. Greater load-carrying capacity, since both top and bottom face plates act effectively against an applied load.
2. Higher accuracy fabrication due to less distortion from welding (less lateral welding).
3. Easier and faster construction.
4. A more slender and aesthetic appearance due to reduced thickness.

There are the following problems in applying the hollow steel deck to bridges:

1. Limitation of application to short-span bridges.
2. Due to the closed nature of the deck:
   a. Splicing units together is difficult.
   b. Inspecting interior welding is difficult.
   c. Interior corrosion may be a problem.

Experimental Studies

Various experimental studies were made to obtain basic data on the behavior and characteristics of the hollow steel deck. Three of these will be discussed here.

Test One—Bending and Torsional Rigidity

In this study the authors intended to determine whether the conventional, practical method of analysis could be applied to the analysis of the hollow steel deck subjected to a concentrated load. That is, the tests were planned to obtain data on the longitudinal bending rigidity (Dx), lateral bending rigidity (Dy), and effective torsional rigidity (H) of the deck. These data required for practical analysis of a slab bridge by the Guyon-Massonnet method.

First, from a test it was concluded that Dx can be calculated by using the moment inertia of the section. Since Dy can not be determined so simply, however, the authors performed an additional test to determine its value.

The test to determine lateral bending rigidity (Dy) of decks with different cross-sectional shapes was carried out using six model specimens. Each was 20 cm wide. Other dimensions are shown in Table 1.

Table 1. Dimensions of model specimens for test of lateral bending rigidity.

(Unit: mm)

Dimension	Test Specimens					
	A	B	C	D	E	F
a	0	100	150	150	225	300
b	135	150	150	150	150	150
h	108	138	141	140	138	138
S	127	158	159.	157	157	157
t_1	6	6	4.5	6	6	6
t_2	6	6	4.5	4.5	6	6
t_3	6	6	4.5	4.5	6	6
L	1350	1500	1800	1800	1875	2250
ℓ	675	750	600	600	750	900

Remarks: 1)

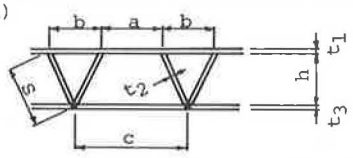

b) L and ℓ are shown in Fig. 2.

Note: 1 mm = 0.03937 in.

Each specimen was loaded as shown in Figure 2. Deflection was measured at several load levels. From these measurements, Dy was calculated for each specimen.

The relationship between rigidity and cross-sectional shape was determined by constructing the graph in Figure 3.

Figure 2. Loading of model specimen for test of lateral bending rigidity.

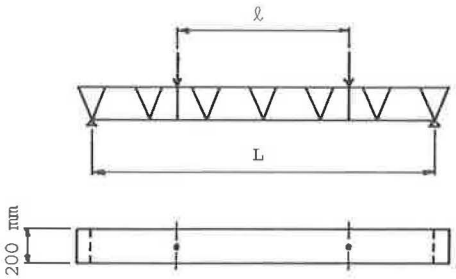

Note: 1 mm = 0.03937 in.

Figure 3. Relationship between rigidity and cross-sectional shape

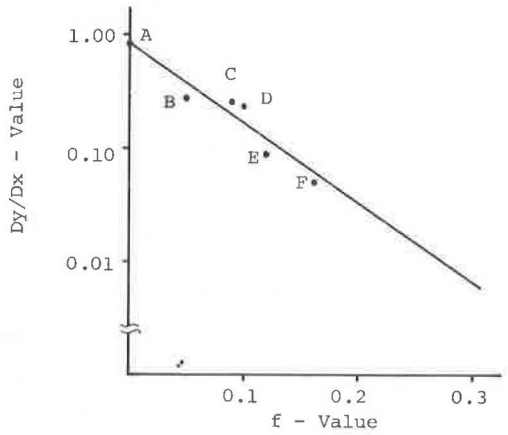

In this graph f is a coefficient calculated from the dimensions of the specimen (Table 1) according to the following formula:

$$f = \frac{a}{h\left(t_1 + \frac{2t_2S}{3(a+b)} + t_3\right)}$$

The f—Dx/Dy curve can be expressed by the following formula:

$$\log \frac{Dy}{Dx} = -0.077 - 6.97f$$

The test to determine torsional rigidity (H) was performed as shown in Figure 4. From the results, the value of H was found to be roughly equal to Dy.

Figure 4. Test for torsional rigidity

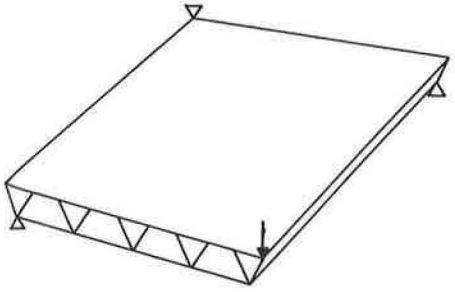

Test Two—Deflection and Stress

The test to determine deflection and stress was performed using the sample deck shown in Figure 5. The position of this load is also shown in Figure 5.

Figure 5. Dimensions and loading of sample deck used in Tests Two and Three.

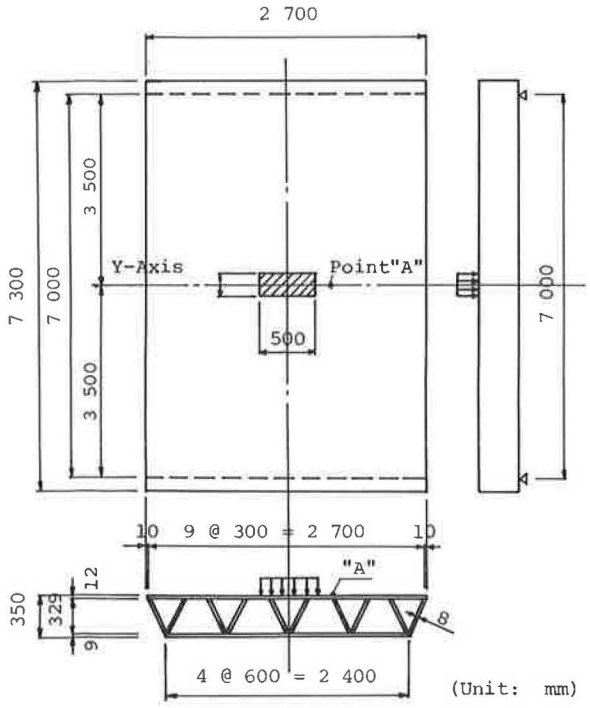

Note: 1 mm = 0.0397 in.

Figures 6 and 7 show the measured values for deflection of top face plate along the X and Y axes, respectively; under a 98 kN (22 kip.) load. Using the data obtained in Test One, deflection for this sample was also calculated according to both the Guyon-Massonnet method and the finite strip method. These values are also shown in Figures 5 and 6.
The values calculated according to the Guyon-Massonnet method are smaller than the measured values presumably, because the calculation in Test One did not take into account the effect of shearing force.

Figure 8 shows both the measured values for strain of the top face plate on the Y-axis under a load of 98 kN (22 kip.) and those calculated according to the finite strip method. One can see from the graph that the top face plate under the load acts on the Y-axis as a continuous plate.

Figure 6. Deflection along X-axis under a load of 98 KN.

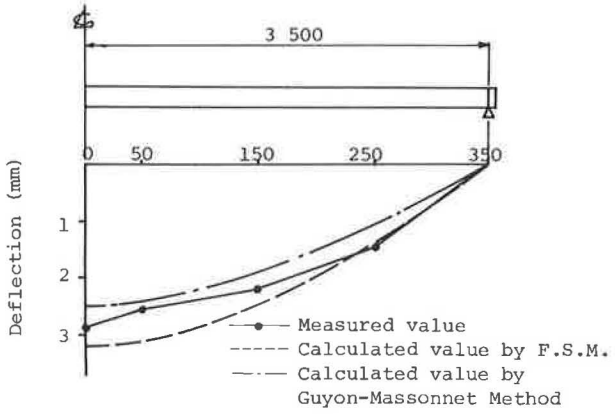

Note: 1 mm = 0.03937 in.

Figure 7. Deflection along Y-axis under a load of 98 kN.

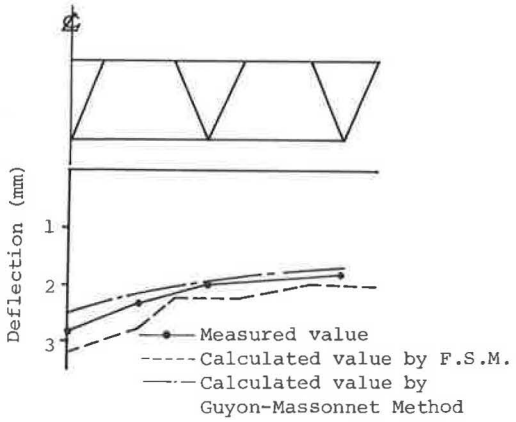

Note: 1 mm = 0.03937 in.

Figure 8. Strain on top plate along Y-axis under a load of 98 kN.

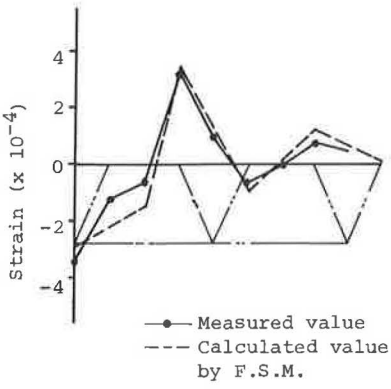

These results suggest that the values for deflection and strain calculated according to the finite strip method are reasonable approximations of the actual values. The authors intend to continue their investigation concerning the application of the Guyon-Massonnet method.

Test Three—Fatigue Strength

To test fatigue strength, the sample deck used in Test Two was subjected to cyclic loads at the same point of loading. First, the deck was subjected to a load of 9.8 kN (2.2 kip.) to 225 kN (50.6 kip.) for 2,000,000 cycles. The maximum load was increased to 343 kN (77.2 kip.) for an additional 1,000,000 cycles. Then, the maximum load was increased to 465 kN (104.7 kip.) for an additional 1,000,000 cycles. The calculated stress from measured strain of the top face plate at paint A under a load of 465 kN was then 164.4 MPa (23,870 $lbf/in.^2$). Finally, the deck was subjected to a more concentrated load with lower maximum for another 5,000,000 cycles at a position on the other side of point A. The stress at point A then reached 226.38 MPa (32,825 $lbf/in.^2$), but no fatigue crack occurred. This test confirms that this hollow steel deck has great fatigue strength.

Design of Slab Bridge

Structural Analysis

The construction and design of a bridge must take into account deflection and stress imposed on each structural member by a live load. When a hollow steel deck is used this analysis becomes complicated by the complicity of elements.

Beam Theory Method. If the bridge will be subjected to a uniform load or if lateral bending moment is not a consideration, stress and deflection can be calculated by using the common beam theory. In this case, the entire assembled deck can be considered as a single beam. Pedstrian bridges are designed by using this method.

Orthotropic Plate Deck Theory Method. If the bridge is to be subjected to a concentrated or nonformly distributed (one-side) load, the beam theory is not applicable. Rather, the hollow deck must be considered as an orthotropic plate. Stress and deflection can be calculated by using the Guyon-Massonnet method. As mentioned earlier, however, values calculated according to this method are less than actual measurements. This problem has not yet been completely solved.

Finite Strip Method. Stress and deflection can be more exactly calculated by using the finite strip method, but the calculations become much more complicated. In this case, each element of a given deck is considered as a finite strip. Stress and deflection are calculated for each strip. This analysis makes use of a computer program designed by the authors specifically for this purpose.

It should be pointed out that the cross-sectional shape and dimensions of the hollow steel deck are determined by allowable deflection, rather than by allowable stress as is the usual case for other bridge structures. In Japan the allowable limitation of deflection due to the live load is $\delta/\ell=1/600$ (δ: deflection due to the live load, ℓ: span length).

Unit Weight and Slab Thickness

Using the Guyon-Massonnet method approximation for designing slab bridges have been calculated. Figure 9 shows the relationship between unit weight and length of span for both roadway and pedestrian bridges. The unit weight here is exclusive of curbs, handrails, shoes, and pavement. Figure 10 shows the relationship between slab thickness and length of span for both types of bridges.

Figure 9. Relationship between unit weight and length of span.

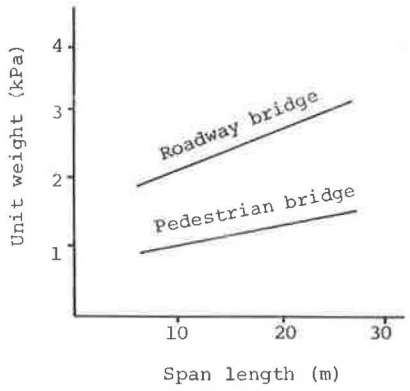

Note: 1 m = 3.28 ft. 1 kPa = 0.145 $lbf/in.^2$

Figure 10. Relationship between slab thickness and length of span.

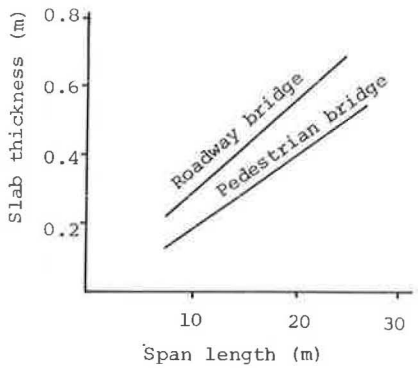

Note: 1 m = 3.28ft.

Structural Details

Steel Plate Thickness. The relationships governing the thickness of each steel plate of hollow steel decks used in roadway and pedestrian bridges are shown in Table 2. Each figure represents the minimum thickness. t_1, t_2, and t_3 are explained in the sketch attached to Table 1.

Table 2. Minimum steel plate thickness of slab bridges.

(Unit: mm)

	Roadway Bridge	Pedestrian Bridge
t_1	0.035a or 12	0.02a or 6
t_2	8	4.5
t_3	0.0125c or 9	0.0125c or 6

Stiffener. Both ends of the slab bridge are closed by stiffeners (Figure 11). Additional stiffeners are placed at the point of each intermediate support of a bridge. These stiffeners, made of steel plate more than 12 mm (15/32 in.) thick, are welded securely to the top and bottom face plate as well as to the core plates. They provide for proper distribution of the reaction force, as well as securing perfect closure to inhibit interior rusting. They also serve as cross beams.

Figure 11. A hollow steel deck under fabrication showing stiffeners and spacing struts.

Pavement

For roadway bridges having steel decks it is a common practice to place a 7-8 cm (2 3/4 — 3 1/8 in.) layer of asphalt on the steel plate. Mastic asphalt is generally preferred. The Honshu-Shikoku Bridge Authority is now studying on the method of coating the steel plate surface with an adhesive, before applying the 3-4 cm (1 3/16 — 1 9/16 in.) layer of mastec asphalt, and then finishing with a 3-4 cm top layer of special asphalt fortified with a selected type of rubber or synthetic resin. Asphalt pavement is known to substantially improve the surface slip resistance.

Pedestrian bridges, on the other hand, are usually paved with a thin layer of asphalt belended with epoxy resin or tiled.

Corrosion

Admittedly, interior corrosion may be problem with the hollow steel deck, but this can be greatly inhibited by the perfect closure at both ends of a bridge with stiffeners, as mentioned earlier. Furthermore, the parts near the abutments at both ends of the bridge, which are not easily accessible for maintenance, can also be coated with a tar epoxy point known for its durable corrosion-inhibiting performance.

The use of weather-resistant steel plates will, of course, be another effective approach to overcome the corrosion problems.

Fabrication and Erection

The fabrication sequence for the hollow steel deck is shown in Figure 12.
Core plates forming evenly-spaced triangles are welded to a steel plate, actually the top face plate of the deck. Next the bottom face plate is welded strip by strip to the core plates.

First each set of two core plates is welded together at the prescribed angle as shown in Figure 13.

Figure 12. Fabrication sequence of hollow steel deck.

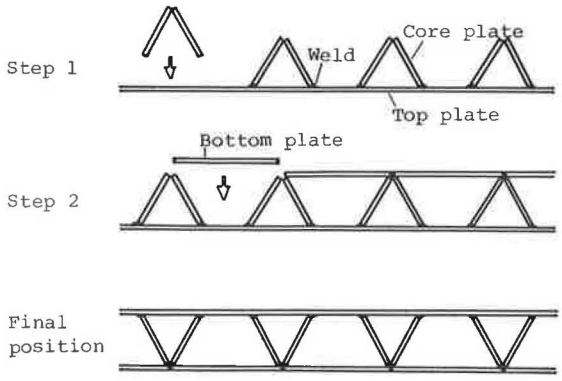

Figure 13. Welding together of core plates.

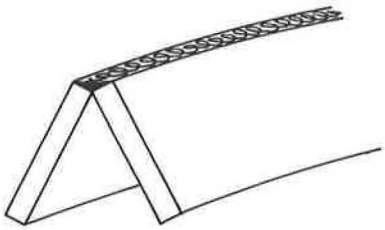

The core plates are then welded to the top face plate either by the full penetration method using backing as shown in Figure 14 or by fillet welding as shown in Figure 15. In this step deformation from welding is relatively small, about the same as in the fabrication of conventional steel decks. If the bridge is to be cambered, the core plates can be cut and curved accordingly.

Figure 14. Full penetration method of welding

Figure 15. Fillet welding

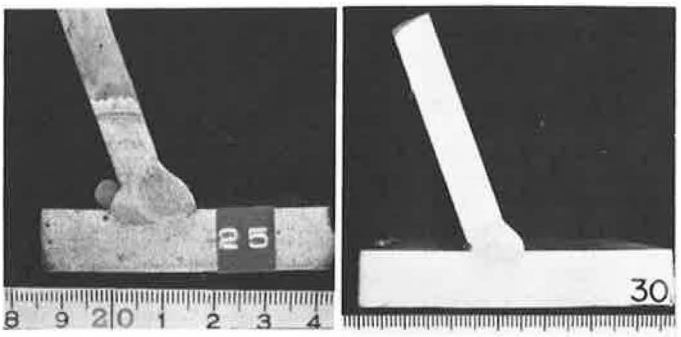

Next, stiffeners are welded where necessary (Figure 11). In order to strengthen the deck against deformation from welding in the next step, spacing struts, also shown in Figure 11, are welded into place. A plate is then welded between the tips of each set of core plates, as shown in Figure 16. These strips from the bottom face plate. The root opening between the strips is roughly equal to the plate thickness.

Figure 16. Welding of bottom face plates into position.

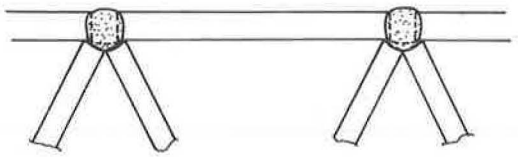

Automatic Welding Machine

Since welding involved in the fabrication of the hollow steel deck can all be performed in one direction, it is relatively easy to automate the welding operation. The authors have developed and tested an automatic welding machine shown in Figure 17.

Figure 17. Automatic welding machine

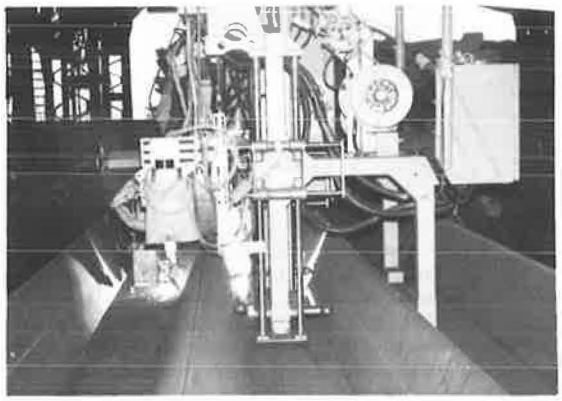

This proto-type can weld only one set of core plates at a time, and is, therefore, not practical for actual use. If further improvements enable automatic, simultaneous welding of a multitude of core plates, however, it will greatly facilitate fabrication of hollow steel decks.

Erection and Spacing

The proper size of the prefabricated units of a slab bridge depends on the mode and conditions of transportation from the shop to the site. In the case of land transportation by truck in Japan, usually, the dimensions of the load are limited to 25 m (33 ft.) in length, 3 m (10 ft.) in width, and 3 m in height. Hence the weight per unit deck does not exceed 200 kN (44 kip.). The most difficult part of the erection work is splicing together the prefabricated units. As shown in Figure 18, there are two modes of splicing involved in the erection of a slab bridge, namely longitudinal or side-on-side splicing and transverse or end on end splicing.

Longitudinal Splicing. Units which are to be longitudinally spliced have a slightly different design from that previously described. Edge core plates are added, resulting in a trapezoidal cross-sectional shape, wide at the bottom rather than at the top, as can be seen in Figure 11. These units are erected side by side with their bottom face plates adjoining, as shown in Figure 19a. First, the bottom face plates are joined by butt welding. Next, a top face plate strip is welded into place, as shown in Figure 19b.

Figure 18. Diagram of splicing.

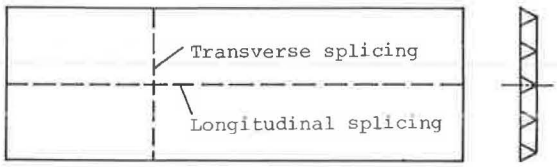

Figure 19. Longitudinal splicing

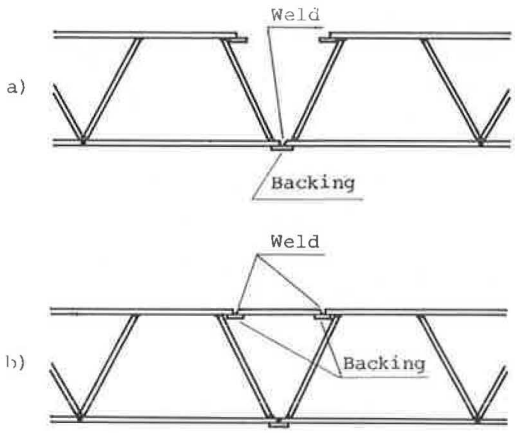

Although deformation caused by welding is small during fabrication, it would be more marked in the process described above, as shown in Figure 20.

Figure 20. Possible distortion due to longitudinal splicing.

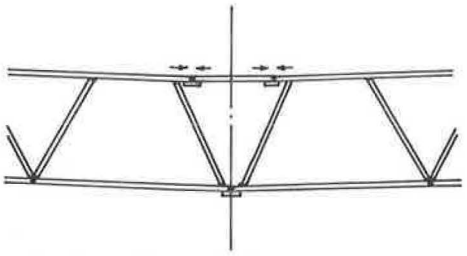

One countermeasure is the addition of splicing ribs, properly spaced, and welded to the core plates during fabrication (Figure 21). Before welding on the top face plates, these ribs can be bolted together. They also help to position the units properly, facilitating the welding.

Transverse Splicing. Transverse splicing of hollow steel decks is very complicated and difficult. It has, however, been successful in all three cases where it has been tried—one pedestrian bridge and two roadway bridges.

Again, the decks must be specially designed. In this case, the top of the end section of each deck to be spliced is left open. After the bottom face plate and the core plates are joined, the top

Figure 21. Splicing rib

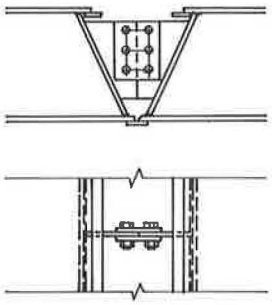

face plates are welded on to the core plates in strips, the same as the bottom face plates in the fabrication sequence. In the case of the roadway bridges, both the bottom face plates and the core plates were bolted. The bottom face plates of the pedestrian bridge, however, were welded, as shown in Figure 22.

Figure 22. Transverse splicing for pedestrian bridge.

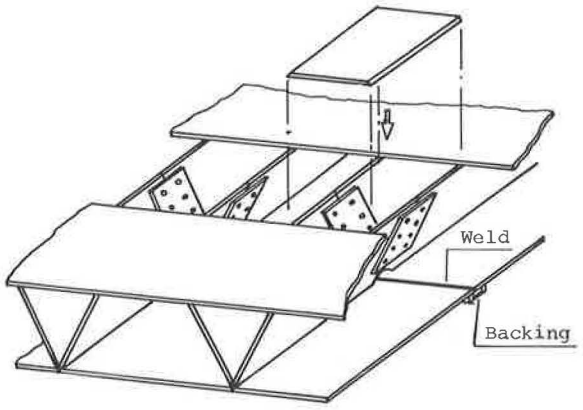

Examples of Application

Pedestrian Bridge

Prefabricated hollow steel decks have been used in the construction of many pedestrian bridges. Figure 23 shows one example.

Figure 23. View of pedestrian bridge.

The dimensions of this bridge are given in Figure 24. This bridge was designed for a uniformly distributed live load of 4.9 kPa (102 PSF).
With a slab thickness of only 1/50 the length of span, the bridge has a very slender and lightweight appearance. The two prefabricated units 19 m (62 ft.) and 12.5 m (41 ft.) long, and each 3 m (9.8 ft.) wide, were transported and erected by truck crane. The decks were joined by two pin-type hinges at the point A in Figure 24, hence no field welding of the decks was required. A circular pipe welded securely into the deck during fabrication, was welded at point B to the same size column pier at the site.

Roadway Bridge

Figure 25 shows the dimensions of a roadway bridge applying the hollow steel deck. This bridge was designed for a 137 kN (30.8 kip.) truck loaded as specified in the Japanese Highway Bridge Specifications. Prefabricated units in sets of two were delivered to the site and joined by longitudinal splicing along the center line of the bridge as described above. Each prefabricated unit was complete with curb and shoes, the latter designed with a sandwiches core of sheet rubber.

Temporary Movable Bridge

Figure 26 shows a temporary movable bridge constructed with a hollow steel deck. This bridge was erected below the high water level across a river for transportation of soil for the construction of an expressway.

Figure 26. View of temporary movable bridge

Special wheels were installed in the decks, and rollers to the top of the pier and the abutment, as shown in Figure 27. Thus, when the river floods, the superstructures can be moved to a higher elevation along rails on the approach road. The use of the hollow steel deck for this kind of bridge allows for a lower and lighter weight structure with greater rigidity.

These three examples of bridges successfully contructed and in use in Japan show the practical application of this hollow steel deck to bridge design. Within the accepted limitations this new type of prefabricated unit has several advantages over those currently in use. The authors are confident that the difficulties involved in designing and contructing bridges with this deck can be effectively overcome. Through continued research and development the authors hope that this prefabricated hollow steel deck will have even wider applications.

Figure 24. General view of pedestrian bridge.

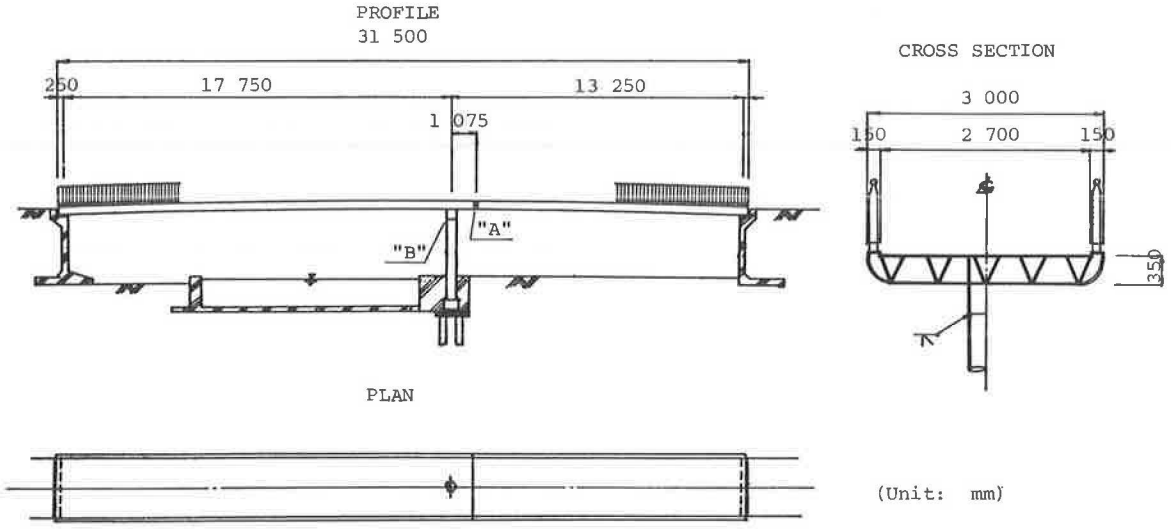

Note: 1 mm = 0.03937 in. 1 m = 3.28 ft.

Figure 25. General view of roadway bridge.

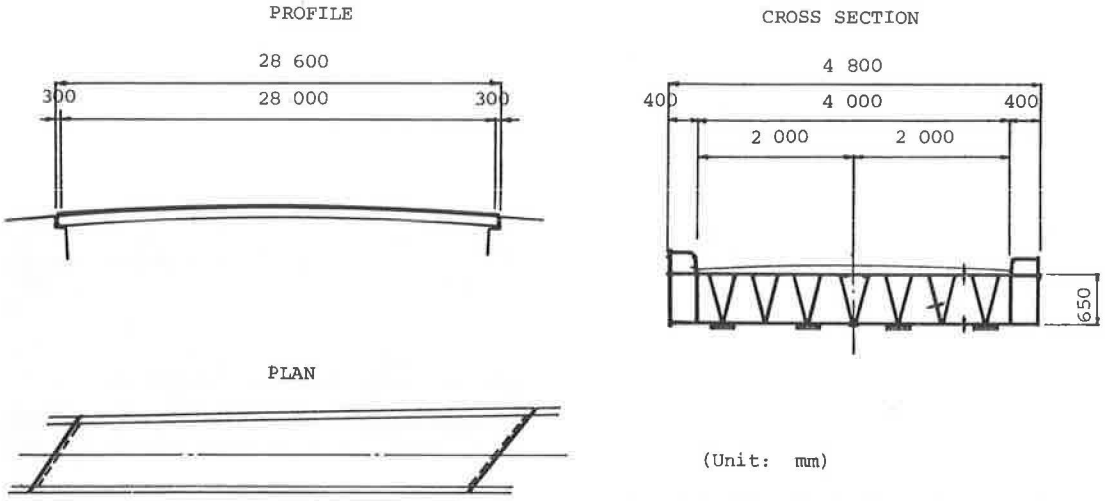

Note: 1 mm = 0.03937 in 1 m = 3.28 ft.

Figure 27. General view of temporary movable bridge.

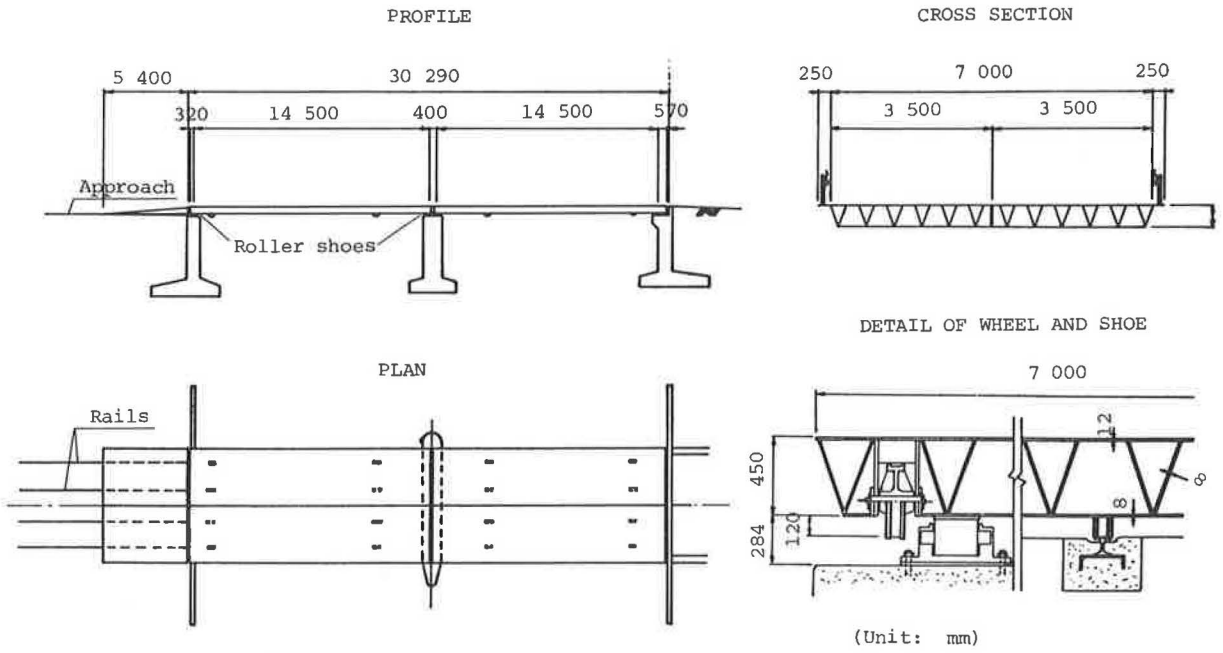

Note: 1 mm = 0.03937 in. 1 m = 3.28 ft.

References

1. T. Suruga and Y. Maeda. Planning of Floor System at Long-Span Suspension Bridges. Preliminary Report of 10th Congress of IABSE, 1976, pp. 149-154.

2. T. Suruga and Y. Maeda. Selection of Hollow Steel Plate Deck for Floor System of Long-Span Suspension Bridges. Final Report of 10th Congress of IABSE, 1976, pp. 19-22.

3. K. Mori and K. Nakaoki. Experimental Study on Strength of Hollow Steel Deck. Kobe Steel Ltd., Research and Development, Vol. 25, No. 1, 1975, pp. 39-45 (in Japanese).

4. H. Yoshida, T. Suruga, and T. Tsutsumi. Experimental Study on Hollow Steel Deck (KOSWECK). 28th Annual conference of the Japan Society of Civil Engineers, Preprints, 1973, pp. 339-340 (in Japanese).

APPLICATION AND DESIGN OF PRESTRESSED DECK PANELS

Robert L. Reed, Texas State Department of Highways and Public Transportation

The purpose of this paper is to review the development of precast prestressed concrete panels as permanent structurally interacting forms in the construction of reinforced concrete decks for stringer type bridges. This system was used on the Illinois Toll Highway in 1957. In 1963 Texas constructed three bridges in this manner. Many bridges have been subsequently completed using this slab construction technique. Precast prestressed concrete panels are placed to form a deck between adjacent stringers. A mat of reinforcing steel is placed and concrete is cast-in-place on top of the panels. The panels support the weight of the wet concrete and then act compositely with it to resist subsequent live loads. Design of the panel deck system is explained and several aspects of fabrication and construction are reviewed.

Early in the modern era of bridges, it became apparent that construction is simplified considerably by using preformed beams (stringers), to span from bent to bent. These stringers usually can be manufactured under a more sheltered environment, delivered to the bridge site by some common mode of transportation and erected without the use of expensive falsework or shoring. First it was timber that was the most readily available stringer material, then steel became economical and lately precast prestressed concrete beams have been developed to accomodate spans of over one hundred feet. A deck must be constructed to span the space between stringers, adjust elevation differences and provide a smooth riding surface. Timber decks were used originally with timber and some steel stringers, but the most popular deck soon became reinforced concrete because of its workability, smoothness and durability. However, construction of a concrete deck has never been easy. Forms must be tight, supported sturdily from the stringers and adjustable for line and grade. The concrete must be strong and durable and it must be placed and consolidated properly. Expert finishing is required to achieve a good riding surface. Early on, the deck would cost half as much as the stringers beneath. This ratio has continued to rise until, in 1977, the decks cost as much as the stringers on Texas bridges. Naturally, there have been attempts to reduce this cost by devising more efficient systems for construction of bridge decks. There have been better forming procedures developed, including stay-in-place metal forms, admixtures introduced to improve the workability of the concrete without injuring the strength and durability, and bigger and better finishing machines marketed to replace the skill required for producing a good surface. One system, which appears to be coming into more widespread use in this country, uses precast prestressed concrete panels to serve as forms and act with a thin cast-in-place slab to provide a bridge deck of sufficient strength to carry the live load (Figure 1).

This development did not occur overnight. As early as 1957 some of the bridges on the Illinois Toll Road were constructed with prestressed panel decks (1). No further activity was reported until 1963 when Texas constructed three grade crossing structures utilizing prestressed concrete panels. Another five year gap in experience followed, broken in 1968 with the letting of Texas' Trinity River Bridge near Trinidad (Figure 2) and others amounting to a total of 130,200m^2 (1,400,000 ft^2) of panel deck let during the four year period ending in 1971. During this time research began with an investigation of the 1963 Texas bridges (Figure 3) and continued through 1975 with projects conducted by Texas A & M University, the University of Florida and Pennsylvania State University on various phases and details of panel deck construction (2). Another two year lapse ensued during which the Texas research was culminated (Figure 4) and some of the restrictions governing panel use imposed by the FHWA were overcome. Since 1974 there have been a steady number of bridges constructed in Texas using prestressed concrete panel decks. Other states have also constructed panel decks lately and inquiries indicate that still others are seriously contemplating their use. It appears that the prestressed deck panel method has become acceptable for construction of decks on prestressed concrete stringers.

The purpose of this paper, after having reviewed the background of panel deck construction, is to briefly recap the design concepts and then discuss various manufacturing and construction

problems that influence the economy of the system.

Design of prestressed panel decks is the same as for conventional slabs on stringers, except for consideration of the prestressed member as it carries the entire deck dead load and then acts compositely with the cast-in-place slab to resist the live load (Figure 7). The selection of prestressed panel thickness is not vital to the structural design. It can be as thin as possible to contain a layer of seven wire strands or as thick as practical to allow a slab with the necessary cover to an imbedded reinforcing steel grid. The Texas approach was to maintain the total panel plus cast-in-place thickness the same as for a full depth reinforced concrete slab, with the panel thickness in one quarter inch increments, approximately one half the total thickness. This has lately been considered a mistake because of the multiplicity of panel thickness which require different side forms. Often two or three different thicknesses would be required for one project or even one bridge due to the variation of stringer spacing.

Once the panel thickness is selected and the topping thickness estimated, the design can proceed to the calculation of required prestressing, mild steel reinforcing and evaluation of the thicknesses selected. A unit strip of panel is analyzed as a plain rectangular beam for stresses due to simple beam moments caused by the weight of the panel plus cast-in-place slab. Live load moment on the unit strip is calculated, using the regular slab on stringer distribution formula of A.A.S.H.T.O. Article 1.3.2(C) and the 80% continuity factor. A rectangular section of the total panel and cast-in-place thickness is analyzed for stress due to this moment. The sum of these two stresses, less any tension allowable, must be counteracted by the prestress. Thus strand size and spacing may be determined. Since there has been some question about the ability of strands to develope themselves for resistance of ultimate moment in the relatively short length of the panels, Texas has always used 9.5mm (3/8" Ø) strands. Research has indicated no problem with development length, however, and a check of the ultimate moment resistance of the positive moment portion of the panel deck will indicate more than adequate strength using the stress that can be developed according to the formula in A.A.S.H.T.O. Article 1.6.18. The negative portion over the stringers is analyzed as a plain reinforced concrete beam for the live load moment as calculated above. The size and spacing of transverse mild steel in the top of the cast-in-place slab is thus calculated. Concrete stress will not be critical at this point. The strength of the panel concrete is higher than for the usual conventional slab and it has been verified by research (3) that compression in the panel due to prestressing does not have to be added to the beam compression due to live load in establishing the required concrete strength. If the results are reasonable and compatible with the original assumptions, the design is complete. Otherwise new thickness assumptions are made and the system re-analyzed until satisfaction is achieved. The amount of reinforcing perpendicular to the prestressing strands is nominal as is the longitudinal reinforcing in the cast-in-place portion, except that temperature requirements must be satisfied. Texas maintains a fairly high amount of longitudinal reinforcing 13mmØ @ 230mm (#4 @ 9") because there is a history of fine transverse cracking with panel decks and since the most conclusive research used this amount of steel. Composite behavior of the panel and cast-in-place slab, with or without steel across the interface has been verified by tests (3,4). The same research failed to disclose any problem with composite action of the deck with the stringers. Consequently, stringer design can be the same with panel decks as with reinforced concrete deck if the two are of the same thickness.

Panels may be designed to extend past the outside stringers into the overhang also (Figure 2). Openings in the panel are provided over the outside beam to match the beam stirrups in order to achieve the composite tie. This system was used in Texas on a few bridges but has since been abandoned due to construction problems considered not justified by the advantages thereof.

Current details for prestressed precast concrete panel deck used in Texas are shown in Figure 8.

Structural design of the panels has been adequately verified by research and use. Problems in manufacture and construction continue to be studied so that the cost of adequate panel decks can remain competitive.

Panel decks are not automatically less expensive than conventional wood formed decks. Prices have fluctuated so that it is impossible to establish the economy of the panel deck without actually taking bids on an alternate or optional basis. Until 1974 the panel deck was offered for an alternate bid on selected Texas projects. The alternate bid items were slab concrete, reinforcing steel and prestressed concrete panels. During the four big years of 1968-71 prices ranged from $1.15 per square foot for panels to $1.53 and from $63 per cubic yard for concrete to $80. In 1974 a large project was bid for $.75 per square foot with $135 concrete but in 1975 another project was bid at $2.58 - $134. During this period panel deck construction was not used by the low bidding contractors on several other projects. Projects selected were usually those with considerable repetition of details and also high above the ground or over water where form removal is more difficult and dangerous.

Manufacturing problems have influenced the cost of panel decks to some degree. Early problems involved the reinforcing that protruded from the top of the panels. In the beginning there were "Z" shaped bars on 457mm (18 in) centers each way, one leg of which was in the plane of the strands under the transverse bar mat with the other leg 38mm (1 1/2 in) above the top of panel (Figure 5). These bars had to be tied in place before concreting, because of being under the top mat, and they interfered with the finishing of the top of the panel. Some fabricators tried leaning the "Z" bars enough to screed over the top and then lifting them to position and patching the tear left in the concrete. Others tried to finish in between bars. Another problem involved removing splashed concrete from the protruding "Z" bars. They always got a liberal coating of concrete, which took too many man hours to remove. These problems were solved by one fabricator by using multiple loop "U" bars that could be tied more securely than the "Z" bars and employing external form vibrators to level the concrete instead of a screed (Figure 6). The rough top finish required to facilitate bond with the cast-in-place deck was provided with a stamp made of expanded metal lath. Currently the rough finish is accomplished with a stiff broom.

On the first project using panels extending past the outside beam into the overhang, there was a considerable problem due to mislocation between the stirrup bars protruding from the beam and the hole in the panel through which these bars

were supposed to be grouted. Where the holes did not match it was necessary to cut off the stirrup bars and drill and grout an anchor bar into the beam to match the hole location. Two other projects did not exhibit the problem, but items that were necessary to cast into the edge of the panels, such as rail parapet bars, anchor bolts, light brackets and deck drains discouraged the use of panels in the overhang. Also, vertical offset between bottoms of adjacent panels made the overhang somewhat rough in appearance. Although overhang panels have proven to be structurally adequate, they are no longer used in Texas.

A nagging problem that continues to occur is cracking of the panels during handling. The panels are weak in the direction parallel to the prestressing strands, since they are thin and have the reinforcing steel in the middle. There is even less than the gross concrete section resisting moment since the strands form a weakened section and may even create a certain amount of splitting stress themselves, as reported by Pennsylvania (4). There have been projects with as many as 10% of the panels rejected because of cracking, but there have been others with practically no rejects. It is possible to deliver crackless panels but very careful handling is required. The method of lifting must not induce severe bending stresses. Panels are usually stacked five or six high for delivery. Four point or two line resilient blocking, properly located, that bears evenly on upper and lower panels must be provided, along with straps or tie-downs located immediately over the blocking. Care is still required by the carrier to avoid unnecessary roughness. It has been necessary to develop acceptance criteria whereby some cracking parallel to strands is permissible.

With the use of panels on more and more projects, the problem caused by several different designs to fit various beam spacings became apparent. Not all projects are big enough to pay for different side forms and pulling heads. A constant panel thickness and strand spacing became highly desirable so that a more permanent type bed could be provided. Texas' standard details have been revised to meet this requirement (Figure 8). It was considered and calculated to be structurally sound to use 102mm (4 in) thick panels with 9.5mm (3/8" Ø) strands on 152mm (6 in) centers for all beam spacings. This represented a departure from original design controls, primarily in the allowance of some tension in the panel under design loads. The thicker panel allowed the transverse mild steel to be placed below the strands without violating cover requirements. Both the thickened panel and bottom reinforcing are expected to reduce the susceptibility to cracking. Mild steel in the form of wire mesh under the strands will overcome another problem caused by the requirement that no form oil be allowed on the strands. Other revisions were made to the details in order to improve production economy, including allowance of saw cutting square panels to form skewed ends.

In addition to fabrication problems, there are some construction problems that have been encountered with panel decks. Texas has always used constant thickness fiber board strips at the beam edges on which to bed the panels. Early attempts to glue this material on the beams in the fabricating plant were unsuccessful. Placing the strips immediately before erecting the panels is more practical (Figure 9). Rough beam tops can close the opening between the panel and slab so much that grout will not flow in for bearing. It was established by trial that grout from regular deck concrete would flow into a 3.2mm (1/8 in) space. On one early project the beam tops were too rough to let grout enter when 13mm (1/2 in) thick strips were used. The thickness of the strips was doubled. On subsequent jobs the tops of the beams outside of the stirrup bars have been trowelled smooth for better grout penetration. The portion within the limits of the stirrup bars is left rough to provide bond between beam and slab. The gap left between bedding strips to allow air escape has sometimes allowed mortar to escape also. This is corrected by placing a short bedding strip behind the gap to block the mortar exit while allowing the air to escape.

After the panels are erected, extensive grading is required (Figure 10). Because the panels on the constant thickness strips follow the camber of the beams, it is necessary to adjust to finished grade by placing a variable thickness cast-in-place slab, usually thicker nearer the bearings and the minimum design thickness in the span center. This extra thickness occurs through the entire width and most of the length of panel deck and can amount to a sizeable increase in concrete quantity. It is desirable to keep this overrun to a minimum, so bottom of panel elevations are taken for several spans ahead of the concrete placement, if practical. Grade lines and slopes can then be adjusted slightly if necessary to provide minimum concrete over the high points while minimizing the extra thicknesses required near the bents. A computer program has been provided to assist in these deliberations. Initially, Texas paid for this extra concrete at bid prices. Then the specifications were changed to pay only invoice price for the extra concrete since forming and placing costs were hardly affected. Now the decks are bid by the square foot so the overrun is not paid for directly. Pennsylvania reported bedding the panels on variable thickness strips of grout in order to reduce the cast-in-place slab thickness. Sealing of the joints between panels has not been a problem. They usually fit together closely so that only a little tape or caulking is necessary to make them mortar tight.

Just prior to placing concrete the panels are cleaned by high pressure water. There should be no free water standing on the panels when concrete is placed. This poses no particular problem and this type of cleaning appears to be sufficient. Occasionally there may be laitance or even adhered pieces of curing fabric which will require sandblasting to remove prior to concrete placement. No grout or paste is required to be scrubbed in before placement (Figure 11). Placement and finishing of the concrete is very similar to the conventional slab except that it doesn't last as long because of the reduced thickness (Figure 12).

In 1975 prestressed panel decks began to be offered as options to conventional decks rather than alternates. Payment was made on the basis of the plan quantities for the conventional deck. This allowed more projects to have panels because it was not necessary to prepare complete plans and calculate accurate quantities for the panel deck. In 1977 Texas published a specification that provided for bridge decks to be bid and paid for by the square foot, with the Contractor having the option to form conventionally, use stay-in-place metal forms or provide a prestressed concrete panel deck. This makes allowance of panels very easy from the plan preparation stand point and has greatly increased the number of projects with panel options. Under this system bridges are built all three ways. Most are still conventional wood formed decks, but some are metal deck and an increasing number seem to be prestressed concrete panel decks. They continue to be favored for long,

repetitive bridges, although safety requirements for solid deck over traveled ways have increased their desirability for shorter structures. It is anticipated that even further usage will occur when the advantage of the current details are fully realized.

In summary, the development of prestressed concrete panels has been reviewed, structural design procedures given, fabrication and construction problems discussed and the latest improvements presented. It appears that panel decks are here to stay. Now is the time for someone to develop an adequate and economical full depth precast deck for stringer bridges.

References

1. Bender, M. E. and J. N. Knoerle, "Prestressed Concrete Bridges for the Illinois Toll Highway," World Conference on Prestressed Concrete, Paper A-11, 1957.
2. Transportation Research Circular Number 181, September 1976.
3. Furr, Howard L. and Leonard L. Ingram, "Cyclic Load Test of Composite Prestressed-Reinforced Concrete Panels," Summary of Research Report 145-4F, Texas A&M University (December 1972)
4. Barnoff, Robert M. and James A. Orndorff, "Construction and Testing of an Experimental Prestressed Concrete Bridge," Research Project #71-8, Report #1, Pennsylvania State University (March 1973).

Figure 1. Prestressed Concrete panel deck schematic.

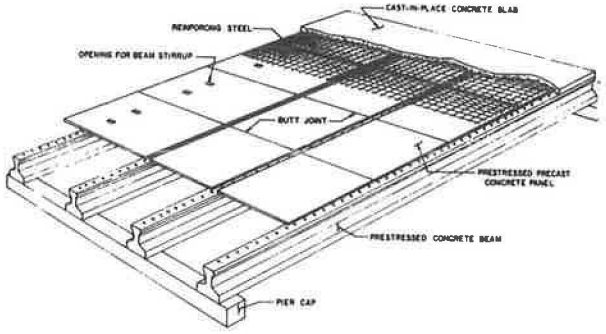

Figure 2. Trinity River Bridge near Trinidad.

Figure 3. Core from 7 year old panel deck.

Figure 4. Full size prestressed concrete beam span with panel deck tested at the University of Texas.

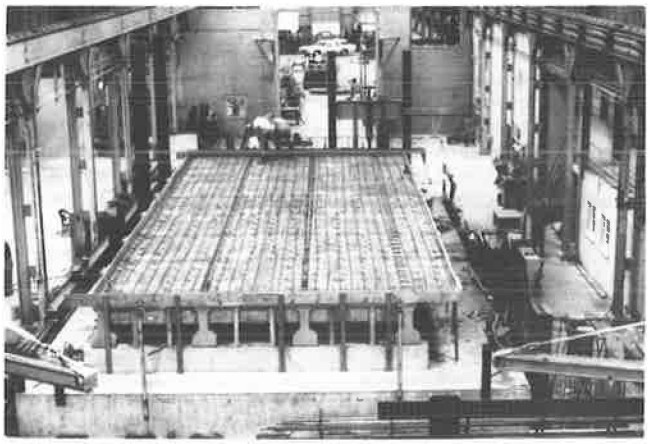

Figure 5. "Z" Bars were difficult to place.

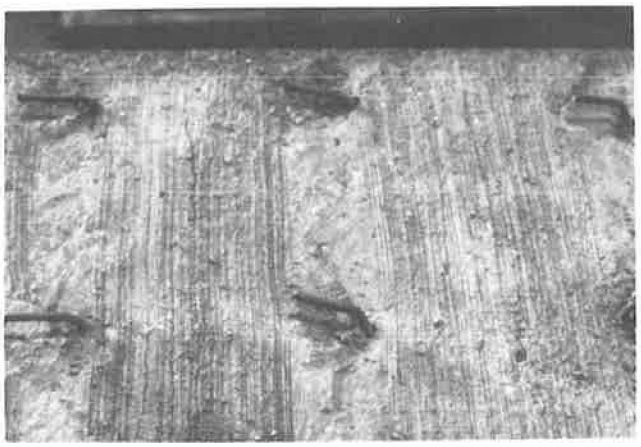

Figure 6. "U" Bars with external vibration are better.

Figure 7. Structural analysis of a panel deck.

DESIGN R.L.R. DATE 6/26/78
CK. DSN. ..... DATE .....
DESIGN FOR PRESTRESSED PANEL DECK

TEXAS
STATE DEPARTMENT OF HIGHWAYS AND PUBLIC TRANSPORTATION
BRIDGE DIVISION

COUNTY .....
CONTROL .....
I.P.E. .....
HIGHWAY .....
SHEET..... OF.....

HS20 Loading 8'-0" Beam Spacing
Standard C.I.P. Slab Thickness

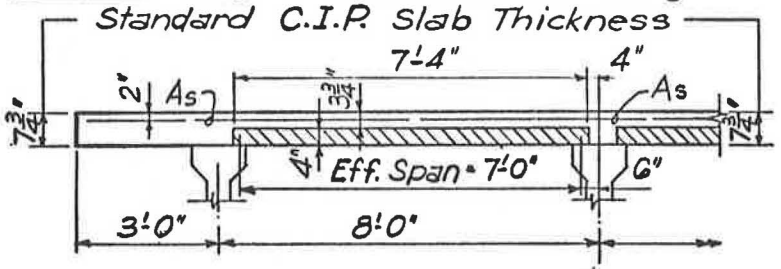

Try Standard Panels
4" Thick
f'_{ci} = 4000 p.s.i.
f'_c = 5000 p.s.i.
⅜"φ 270K Strands @ 6" c.c.
Cast-in-Place
f'_c = 3000 p.s.i.
f_y = 60 k.s.i.

$DLM = \frac{1}{8} \times .0969 \times 7^2 = 0.59^{k'}$
$LLM = \frac{.8(7+2)}{32} 16 \times 1.3 = \pm 4.68^{k'}$

Panels:
DL $S = \frac{12 \times 4^2}{6} = 32\ in^3$
DL $f_c = \frac{.59 \times 12000}{32} = -221$ p.s.i.
LL $S = \frac{12 \times 7.75^2}{6} = 120\ in^3$
LL $f_c = \frac{4.68 \times 12000}{120} = -468$ p.s.i.
Design Total $f_c = -689$ p.s.i.
Prestress $= \frac{16,100 \times .8 \times 2}{4 \times 12} = +538$ p.s.i.
Final Panel $f_c = -151$ p.s.i.
Allow. $= 6\sqrt{5000} = -424$ O.K.

Cast-in-Place Slab:
Req'd d (Overhang) $= \sqrt{\frac{4.68}{.197}} = 4.87"$
2.
6.87"
Provided 7.75" O.K.
$A_s = \frac{4.68 \times 12}{20 \times .875 \times 5.75} = .558\ \square"$
#5 @ 6½" c.c. O.K.

Check Ultimate Moment: +M
$f_{su}^* = f_s' \left(1 - \frac{.5 p^* f_s'}{f'_c}\right)$ AASHTO 1.6.9(C)
$= 270 \left(1 - \frac{.5 \times .0854 \times 2 \times 270}{5.75 \times 12 \times 3}\right) = 240$ k.s.i.
or
$f_{su}^* = \frac{L}{D} + \frac{2 f_{se}}{3}$ AASHTO 1.6.18
$= \frac{44}{.375} + \frac{2 \times .7 \times 270 \times 8}{3} = 218$ k.s.i. Use
$M_u = A_s^* f_{su}^* d \left(1 - \frac{.6 p^* f_{su}^*}{f'_c}\right) \phi$ AASHTO 1.6.9(A)
$= 2 \times .0854 \times 218 \times \frac{5.75}{12} \left(1 - \frac{.6 \times .0854 \times 2 \times 218}{5.75 \times 12 \times 3}\right) .9$
$= 14.3^{k'}$

Check Ultimate Moment: -M
$M_u = A_s f_y d \left(1 - \frac{.6 \rho f_y}{f'_c}\right) \phi$ AASHTO 1.5.32(B)
$= .567 \times 60 \times \frac{5.75}{12} \left(1 - \frac{.6 \times .567 \times 60}{5.75 \times 12 \times 3}\right) .9$
$= 13.2^{k'}$
Req'd $M_u = 1.3(DLM + \frac{5}{3} LLM)$
$= 1.3(.59 + 1.67 \times 4.68) = 10.9^{k'}$ O.K.

Standard Panels Adequate

one foot (') = .3048 m, one inch (") = 2.54 cm, one square inch (□") = 6.45 cm²
one kip foot = 1,356 Nm, one pound per square inch (p.s.i) = 6.895 kPa
one kip per square inch (k.s.i.) = 6.895 MPa

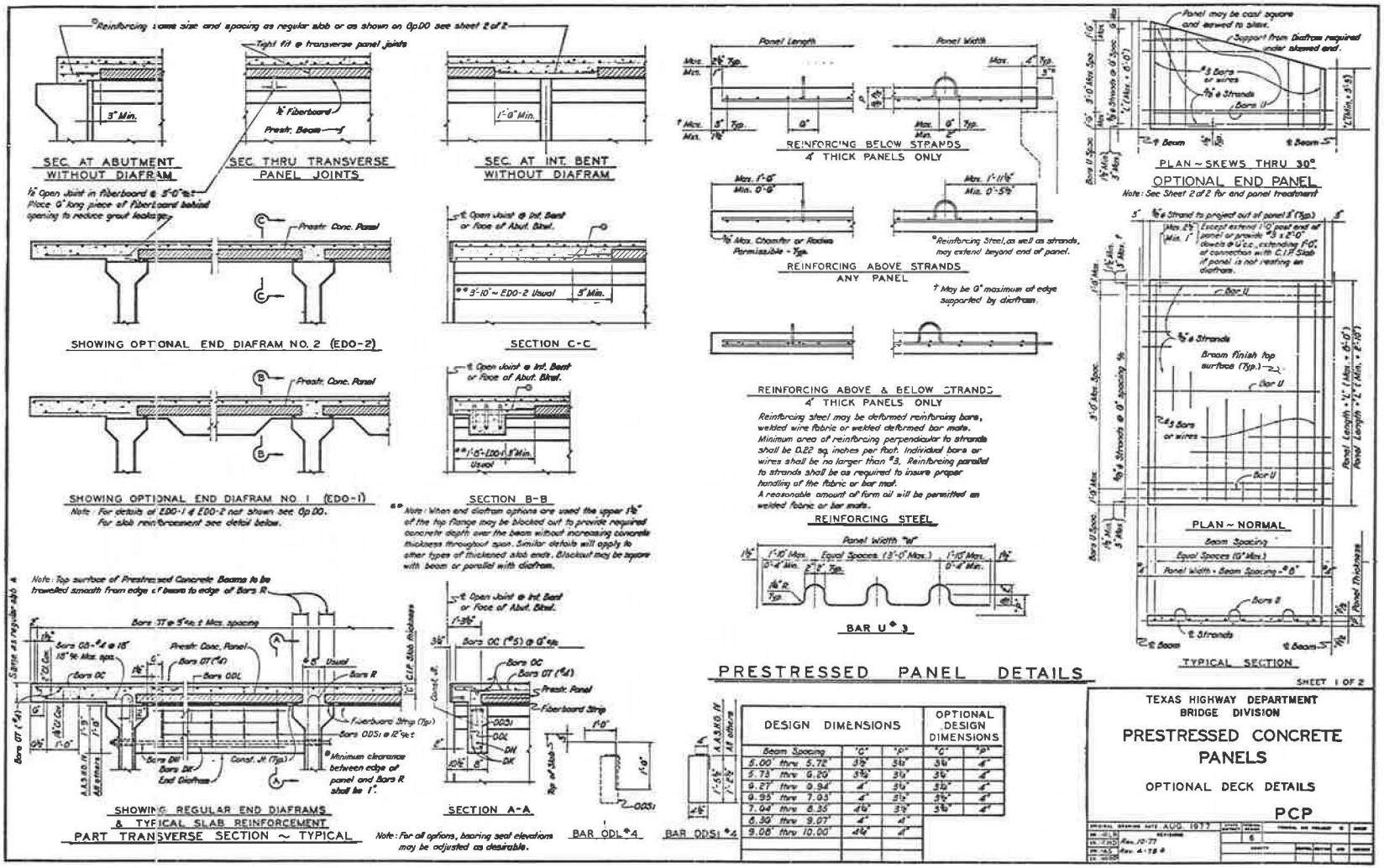

DESIGN DIMENSIONS			OPTIONAL DESIGN DIMENSIONS	
Beam Spacing	"C"	"D"	"C"	"D"
5.00" thru 5.72"	3½"	3½"	3½"	4"
5.73" thru 6.20"	3½"	3½"	3½"	4"
6.21" thru 6.94"	4"	3½"	3½"	4"
6.95" thru 7.03"	4"	3½"	3½"	4"
7.04" thru 8.35"	4½"	3½"	3½"	4"
8.36" thru 9.07"	4"	4"		
9.08" thru 10.00"	4½"	4"		

Figure 8. Current Texas standard panel deck details.

Figure 9. Panels being placed on fiberboard strips.

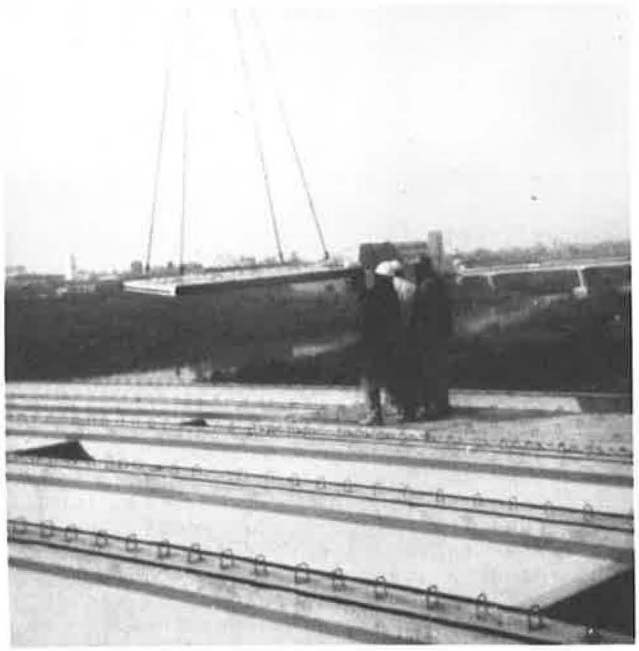

Figure 10. Grading the deck after erection of panels.

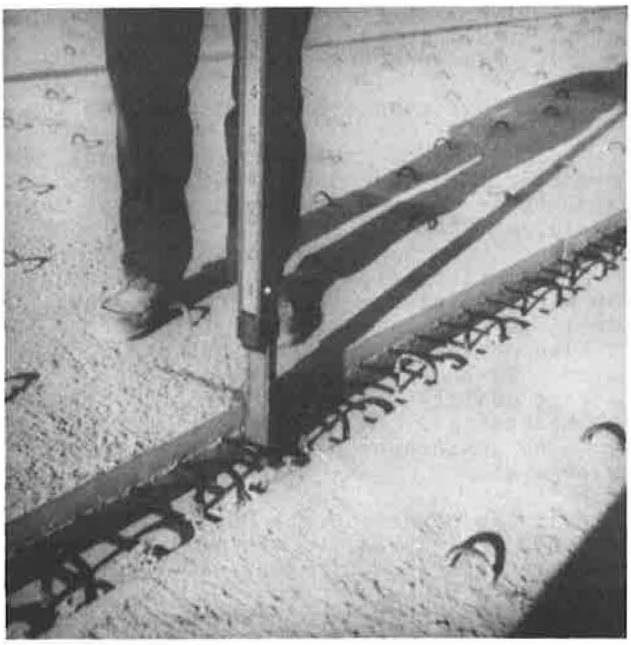

Figure 11. Concrete placement.

Figure 12. Concrete finishing.

RECENT DEVELOPMENT OF CONSTRUCTION TECHNIQUES IN CONCRETE BRIDGES

Man-Chung Tang, P.E., Exec. V.P., DRC Consultants, Inc., N.Y.
Former V.P. and Ch. Eng., Dyckerhoff & Widmann, Inc., N.Y.

It is intended to report about various construction methods developed for concrete bridges. They can be briefly listed as follows: 1) Free Cantilevers, 2) Segmental on Sliding Form, 3) Spanwise Segmental, 4) Incremental Launching, 5) Stage Casting, 6) Cantilever on Falsework, 7) Cable-Stayed Cantilever, 8) Segmental with Gantry or Truss. Most of these methods have been employed in the United States for the first time within the last 5 years. Some are under construction right now. Depending on site conditions and requirements, combinations of these methods can be used. This paper will discuss the advantages as well as the design problems of these methods.

Introduction

The decision of how a bridge should be built depends mainly on local conditions. These include cost of material, available equipment, allowable construction time and environmental restrictions. Since all these vary with location and time, the best construction technique for a given structure may also vary.

In this paper, several popular construction techniques now being used in the United States and Canada are discussed in more detail. Some special methods which are now being used in other parts of the world are also briefly mentioned.

Free Cantilever Construction

The practice of free cantilever construction is quite old. However, it was first systematically developed for concrete by Finsterwalder and was applied in 1952 for the construction of the Lahn Bridge in West Germany. The basic principle of this method is to build the bridge in segments cantilevering from the pier in a balanced manner. The segments under construction are supported by the already completed portion of the bridge. Construction starts by casting on top of a pier a short portion of the superstructure. Two form travelers (Fig. 1) are then erected on this pier table. The form travelers carry the formwork and construction loads for the next segment and advance from segment to segment as construction proceeds. The segments are usually 15' (4.5m) to 16.5' (5m) long. Smaller segments under 10' (3 meters) have also been used.

Each working cycle of a cantilever segment consists of the following steps:

1. Move the form traveler ahead. This also brings the outside forms along.
2. Place rebars and tendons in webs and bottom slab.
3. Pull inside formwork forward.
4. Place rebars and tendons in top slab.
5. Pour concrete after adjusting the formwork.
6. After concrete has reached the predetermined strength, stress tendons and the next cycle can start. Repeat the cycle.

In most cases, the segments are poured in weekly cycles. Shorter cycles, down to 1½ to 2 days are possible if steam curing or special concrete admixture is used. In those cases, however, very strict quality control at the jobsite must be maintained.

The advantages of cantilever construction are:

1. Falsework is not required.
2. The repetitive cycle of the same work in each segment produces high labor efficiency.
3. Form travelers, equipped with hydraulic and mechanical devices for form stripping, moving, and resetting, mechanize the forming work.
4. Each segmental form is used many times, resulting in reduced forming

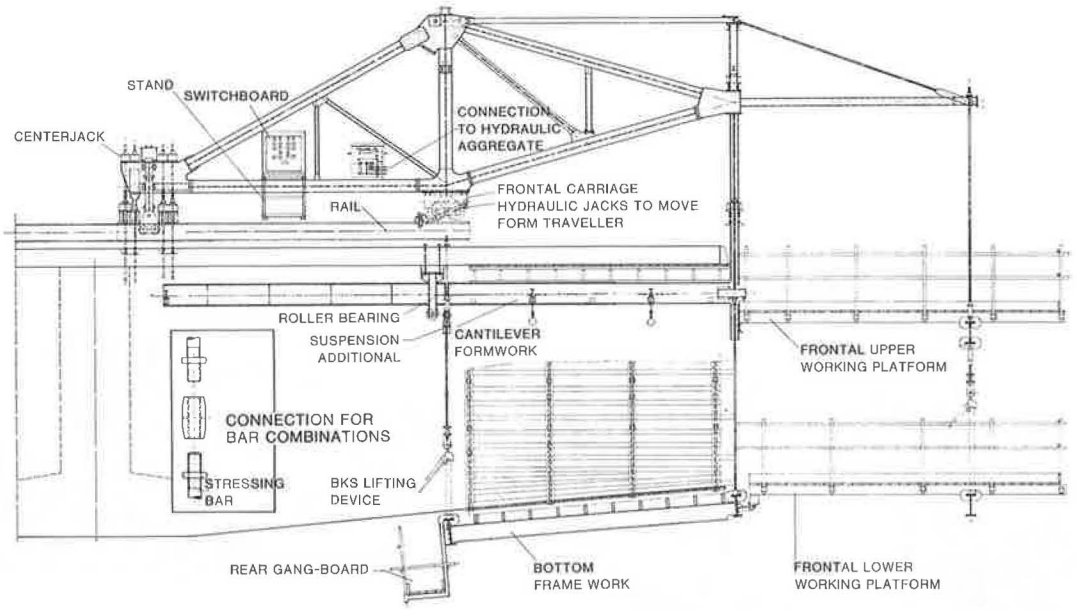

Fig. 1 Form Traveler

material cost.

These advantages have made prestressed concrete bridge construction most economical for the following conditions:

1. Terrain that makes falsework construction very expensive and difficult or even impossible.
2. Clearance requirements for ship, rail or street traffic that forbids falsework.
3. Length of bridge which allows many repetitive segment cycles taking advantage of labor efficiency and small formwork material and elimination of falsework cost.

The first long-span bridge constructed by this method in North America is the Knight Street Bridge (Fig. 2) in Vancouver with 360' (110m) span.

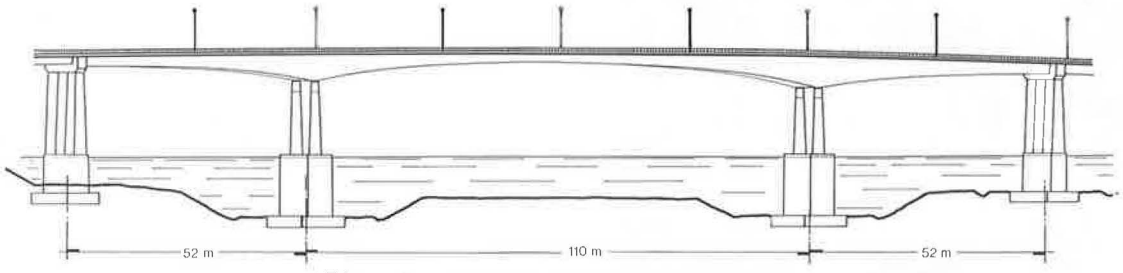

Fig. 2 Knight Street Bridge

The Pine Valley Creek Bridge (Fig. 3) in California is the first in the United States. This spectacular bridge with a 450' (137m) main span and 350' (107m) high piers marks a successful introduction of the cantilever bridge construction to the United States. After the Pine Valley Creek Bridge, there have been a number of free cantilever bridges in the United States and Canada: the Kipapa Stream Bridge in Hawaii, the Grand Mere Bridge in Quebec and the world's record span of Koror-Babelthuap Bridge (Fig. 4) in the U.S. Trust Territory. This latter structure with its 790' span connects the two islands of Koror and Babelthuap. The tidal current of the strait prohibits the construction of any intermediate piers. Cantilever construction is the only possible method for this structure.

Several long-span cantilever bridges are under construction today. The 640' (195m) Parrotts Ferry Bridge in California will be the longest in the continental United States and the 700' (213.4m) Shubenacadie Bridge (Fig. 5) in Nova Scotia will be the longest in Canada.

Fig. 3 Pine Valley Creek Bridge

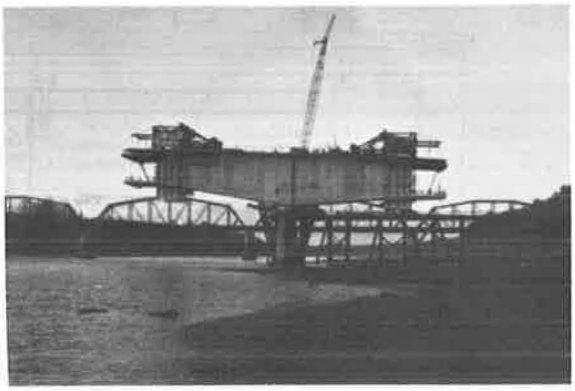

Fig. 5 Shubenacadie Bridge

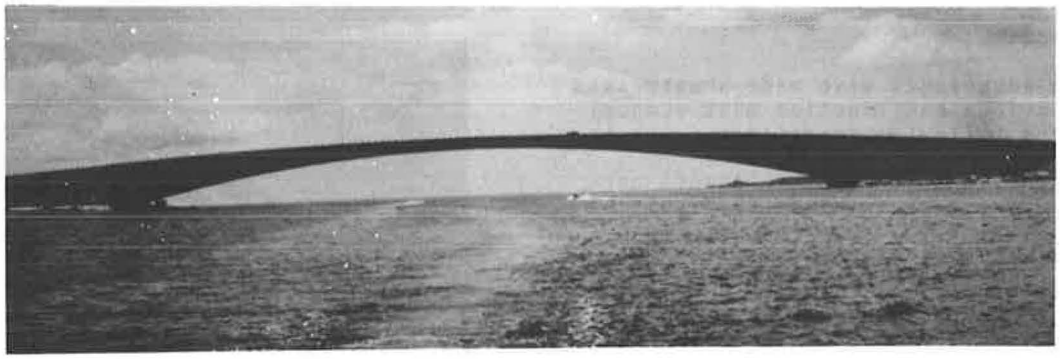

Fig. 4 Koror-Babelthuap Bridge

Fig. 6 Siegtal Bridge

Cantilever Construction with Gantry or Truss

In cantilever construction, the transfer of form travelers from pier to pier is a major expenditure, especially if the spans are small. In the Kipapa Bridge which has 250' (76.2m) spans, the transfer was made easy by use of a large crane which can pick up the whole form traveler and transfer it from one pier to the next without dismantling and reassemblage. If such an equipment is not available, other methods of transferring the form traveler can be used. The Siegtal Bridge (Fig. 6) in West Germany was the first bridge using an overhead gantry. The form travelers were suspended from the gantry and were moved from one pier to the next by winches. The same truss was also used for material and personal transportation. In the Siegtal Bridge, which has rocker bearings at the piers, the unbalanced moment of the cantilevers in the construction stages is also carried by the gantry.

Since the form travelers are transported by the gantry, it is not necessary to have a pier table constructed on local scaffolding. After the form travelers are placed on top of the new pier, they can be connected to each other and thus provide the formwork for the first two segments. The unbalanced moment of the cantilever is transferred to the gantry by tying the finished part of the superstructure to the gantry at both ends.

This method of constructing cantilever bridges has been further developed in recent years. Many varieties are available. Recently Finsterwalder suggested the use of 10' segments and 2-day cycles, a

procedure which might be convenient for many structures.

The writer has suggested to use a double truss running underneath the bridge instead of the overhead gantry. The advantage of using this double truss is that longer segments can be cast because the formwork is supported directly by the truss. Thirty foot (9m) segments are usually found economical for this scheme.

Either the overhead gantry or the underlying trusses can be used for both cast-in-place and precast construction. Because the precast units have to be transported and erected in single pieces, their weight must be kept to a manageable limit. Therefore, the segments in the precast scheme are usually shorter, mostly between 5' to 8' (1.5m to 2.4m).

The Kishwaukee River Bridge (Fig. 7) in Illinois is a precast segmental bridge to be erected by means of a gantry. The typical segments are 7 feet (2.1m) long and all tendons in the bridge are straight.

Fig. 7 Kishwaukee River Bridge

Cantilever Construction with Temporary Supports

If the bridge span is too short for free cantilever construction and the project is too small to warrant the use of a gantry, the bridge still can be built advantageously by the cantilever method but with temporary supports. The Miller Creek Bridge (Fig. 8) at Vail Pass in Colorado is a good example of this type of construction. To eliminate the work of reassemblage of form travelers from pier to pier, the construction of the bridge starts from both abutments and continues segmentally towards the center of the bridge. When the cantilever has reached half the span length, the weight of the subsequent segments is carried by temporary supports which are usually placed under every second segment. These temporary supports can be removed and reused for the next span after the next cantilever has reached approximately half span.

The method is economical if local supports are allowable and the superstructure is not very high above the ground. It retains practically all the advantages of free cantilever construction. In addition, the finished portion of the superstructure can serve for the transportation of material and personnel during construction.

Fig. 8 Vail Pass Bridge

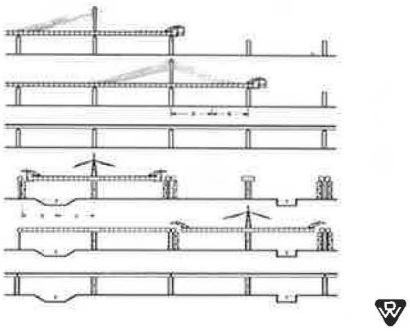

Fig. 9 Use of Staying Cables

Cantilever with Staying Cables

Sometimes, temporary support as described in the last paragraph may not be permitted under local circumstances due to environmental restriction, very high piers or bad soil conditions, In this case staying cables can be used to replace the temporary supports (Fig. 9). This method has been used successfully for many bridges in Europe; one of these is the Berlin Bridge in West Germany. In North America this method has not yet been used. However, a similar system to this construction is actually the cable-stayed bridge, for example, the Pasco-Kennewick Bridge in Washington. This is a precast concrete bridge constructed in the cantilever method, and supplemental cables are used to erect the precast segments which weigh up to 300 tons a piece. The Hoechst Bridge in West Germany is an alternative in the cast-in-place method.

Span-wise Construction

If the bridge span is relatively small, very often a much larger pour, say one whole span, can be justified. In this case, putting the construction joints at about the inflection point appears to be logical. Every time, one span of the bridge from inflection point to inflection point can be constructed at the same time. The formwork can be removed after the post-tensioning of this span has been completed. In this way only one set of formwork equal to the length of one span is required for the whole bridge. This scheme is very suitable for multi-span bridges. One of the first of this type is the Elz Valley Bridge (Fig. 10)

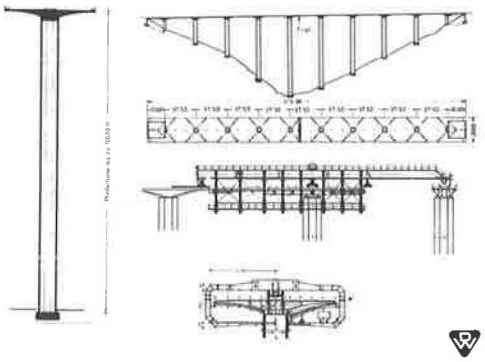

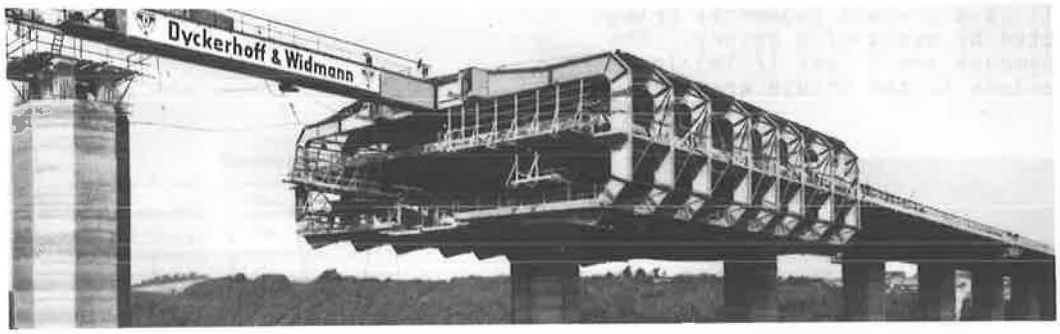

Fig. 10 Elz Valley Bridge - Spanwise Construction

in West Germany. This bridge was 330' (100m) above the valley, which ruled out any kind of falsework support. A form carrier was used to cast one span each time. This early scheme had the shape of a mushroom. The cross-section for this 123' (37.5m) span and 100' (30m) wide bridge was solid and varied from 1'-10" (0.56m) to 8'-0" (2.5m). The form carrier of this bridge was understandably quite heavy.

Fig. 11 Fichera Bridge

However, the construction was speedy. After the initial assemblage and start-up, a two-week cycle for each span was achieved.

After the Erz Valley Bridge had been successfully constructed by this method, a number of other bridges were built in the same manner, notably the Fichera Bridge (Fig. 11) in Italy and the Brenner Autobahn Bridge (Fig. 12) in Austria. Several new bridges in other parts of the world are under construction by a similar method (Fig. 13-15).

If the piers are not very high, falsework can be used instead of the form carrier. This method was used for several smaller bridges in the United States and Canada. For example, the Cumberland Bridge in Maryland, the

Fig. 12 Brenner Autobahn Bridge

Clayton County Bridges (Fig. 16) in Georgia and the Bedford By-Passes No. 1 and No. 2 (Fig. 17) in Nova Scotia are designed and constructed in this method.

To allow for a simple construction in this type of bridge, the layout of tendons should follow a specific pattern so that all tendons can either be termi-

nated or coupled and extended at the construction joint. However, after the construction of so many bridges of this type, various details are available to satisfy these requirements.

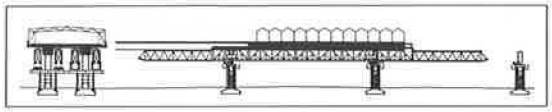

Fig. 13, a & b Ohlstadt Bridge, West Germany - Bridge & Formwork System

Fig. 14 Elevated Highway, Milan

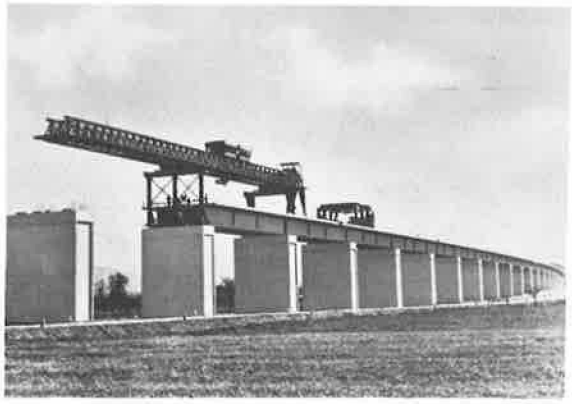

Fig. 15 Expressway, Rome-Florence

Fig. 16 Clayton County Bridge Georgia

Fig. 17 Bedford By-Passes

Segmental Construction on Sliding Forms

When a bridge span becomes larger, span-wise construction becomes inefficient or difficult due to the large quantity of concrete which has to be cast at one time. An alternative to this is the construction using sliding forms.

The bridge span is divided into a number of segments which vary between 40' (12m) and 75' (23m) in length. The main post-tensioning of the span will be done after one span is finished, which is in principle the same as the span-by-span construction. However, partial post-tensioning after construction of each segment must be provided to take care of any bending stresses that may occur due to falsework settlement or other reaons. The best length of segments depends on the local conditions and the size of the bridge. The idea is to limit the quantity of material to be handled in each segment to a manageable dimension. Normally a one-week cycle for each segment is reasonable except for the first few segments.

Fig. 18 Eel River Bridge

The Eel River Bridge (Fig. 18) in northern California was the first in the United States constructed by this method. The segments were about 40' (12m) long. After each segment was poured, the outside formwork was pushed ahead to the next segment, and the inside formwork would follow after the reinforcement and post-tensioning tendons were installed. The construction time had been slightly over 1 week per cycle for a bridge segment. The total length of falsework was about 24% of the total length of the bridge, and the formwork was about 3% of the total contact form area. Considering the high cost of form- and falsework for bridge construction, the saving in this method is evident.

An alternate to this method is shown in (Fig. 19) by using a truss and temporary supports.

Stage Casting

Another alternative to the span-wise construction for longer spans is the stage casting method. In the segmental method on sliding forms, the bridge is separated into segments by vertical construction joints. In the stage casting method the bridge is separated by horizontal construction joints into horizontal slices. For medium-span bridges the falsework for a whole span can be very expensive due to the weights of the bridge, especially if the bridge is high and a gantry has to be used. In order to reduce the weight which is supported by the truss or falsework, the bridge can be designed in such a way that part of it is supported by the previously built parts.

The Denny Creek Bridge is the first bridge designed in this way. It is 2600' (793m) long and has regular spans of 188' (57.3m). The highest pier is about 180' (54.9m). Because of the high piers and because of the soil conditions at the site, falsework is not permitted. Therefore the writer suggested that the bridge be constructed in stages. (Fig. 20)

The bottom part of the box, the U-

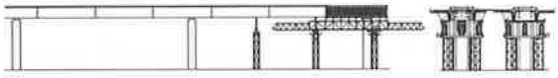

Fig. 19 Sliding Form on Truss

shaped bottom slab and the webs of this bridge, is designed to carry the load of the middle part of the top slab, and the closed box will carry the wing slab. In this way, the truss is required to carry only the weight of the "U" which is approximately 1/3 of the weight of the bridge. After the "U" has been post-tensioned, the truss can be advanced to the next span. (Fig. 21) The top slab of the "U" will be constructed by means of a sliding form which travels inside the box one span after the truss, and then the wing slab will be cast by another form carrier one span after the inside form so that all three parts of the cross-section can be under construction at the same time, but at different locations. It is estimated that a two-week cycle for each span can be achieved after the learning period of a few spans.

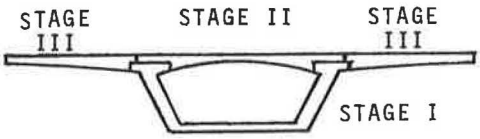

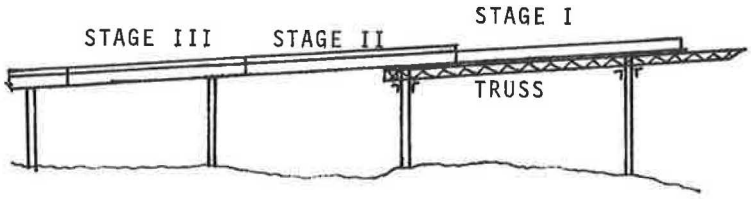

Fig. 20 & 21 Denny Creek Bridge - Stage Construction

Incremental Launching Method

The method as developed by Leonhardt has been applied very successfully to many bridges all around the world. The first of this type of bridge in the United States was built in Indiana (Fig. 22), and it can be anticipated that this method will gain popularity in the United States.

This method can be classified as segmental construction because it is cast in 40'-80' (12m-24m) segments but all at the abutment. It is very similar to an extrusion method used by the aluminum manufacturers. After each segment is cast, the bridge will be pushed out from the abutment so that the next segment can be cast right against the previous one. To simplify the construction, it is normally done in cast-in-place method and the formwork is two segments long. While the webs and top slabs of one segment are being cast, the bottom slab of the next segment will be poured simultaneously so that the use of the labor force can be more efficient. A steel girder is attached to minimize the cantilever moment at the front end of the bridge. (Fig. 23) The post-tensioning of the bridge during launching is mainly centrical post-tensioning because the bending moment in these stages are reversible due to the ever-changing support conditions.

The launching of the bridge is done by mechanism at the abutment. A simple method is to first lift the bridge slightly off the abutment by a hydraulic jack and use another hydraulic jack to push the bridge forward. Pulling devices have also been used for some recent bridges. Teflon pads and steel plates are used at the piers to reduce friction to about 2 to 3% of the vertical load.

There are certain restrictions for this type of construction. It is evident that the foundation at the abutment must be very sturdy. The superstructure must be either completely straight or has a constant curvature. Temporary supports are required for spans over about 160' (49m), and the bridge should be slightly deeper than a comparable bridge built by other methods.

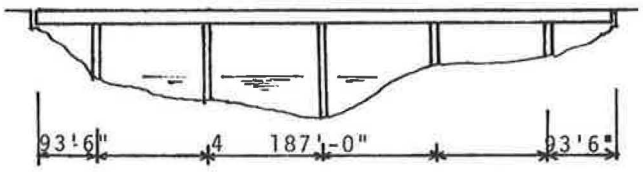

Fig. 22 Wabash River Bridge Indiana

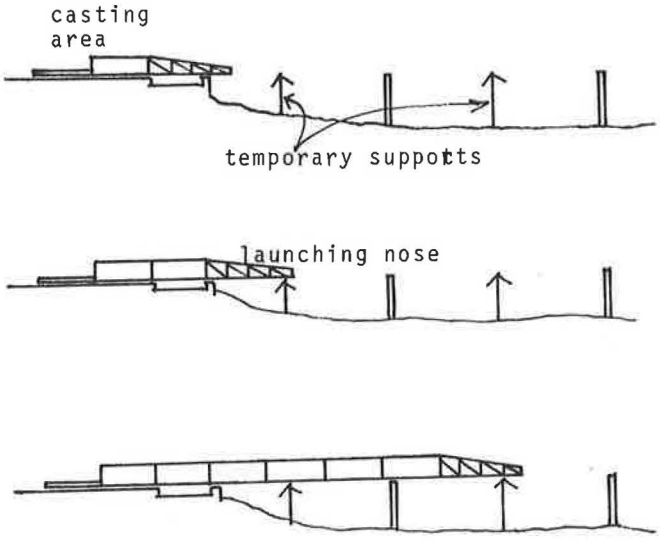

Fig. 23 Incremental Launching

Recently, there have been bridges with more difficult geometric configurations being constructed in Europe by this method. For certain given local conditions, this may be feasible or even economical.

Combinations of Different Methods

The various construction methods discussed can be combined in different ways to suit the local situation. For example, in the Koror-Babelthuap Bridge, while the free cantilever construction was the only method for the main span, the side spans of this bridge were constructed on falsework because the ground level at this area was very close to the soffit of the bridge. Taking further advantage of this local condition, the ground level at the side spans was built up to approximately the soffit level of the bridge with sand-fill and only a very light falsework was required for this part of the bridge. This was especially advantageous because lumber was very expensive in this area and the only available local lumber supplier produces only two-by-fours.

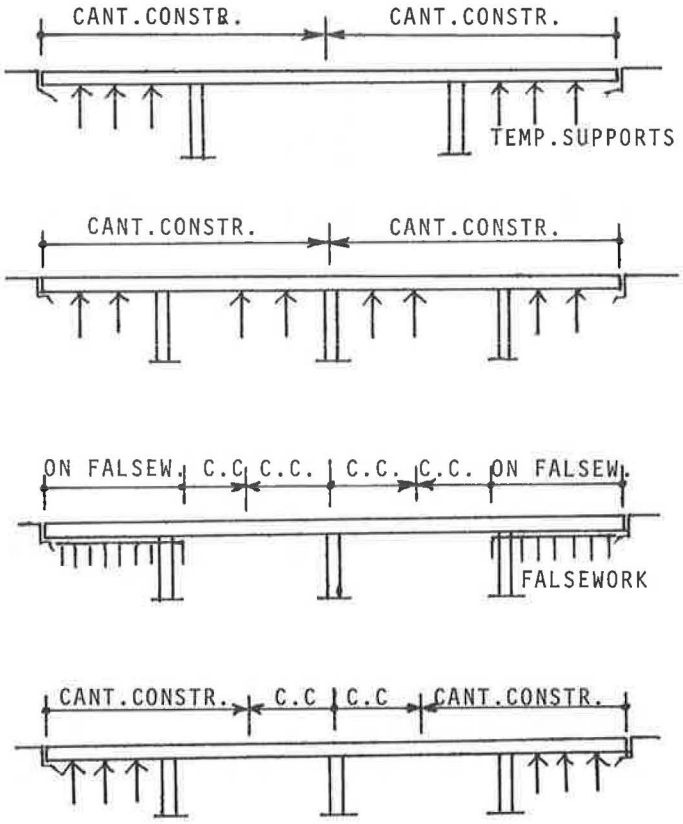

Fig. 24 Vail Pass Bridges

Another example of a combination method is the Vail Pass Bridges. (Fig. 24) There are four bridges of similar size in the same project, however, the topography of these bridges differs. After careful consideration of all local conditions, different construction methods were proposed for these bridges using free cantilevers, temporary supports and falsework construction. It was significant that all four bridges were finished in one season.

An ingenious application of two combined construction methods is the Main-Flingen Bridge in West Germany. This is a girder bridge with a main span of 436' (133m) over a navigational channel. This type of bridge has traditionally been built by the free cantilever method. However, the design and construction team used a combination of cable stays and incremental launching so that the bridge was built in segments at both abutments and launched incrementally over the main span simultaneously.

A similar but significant construction is now under way for the Danube Bridge in West Germany. This cable-stayed bridge will be built by the incremental launching method on temporary supports. The towers and cables will be constructed after the bridge girder has been finished. This combination of methods is in sharp contrast to the last bridge. This is a cable-stayed bridge but built on falsework as a girder bridge, while the Main-Flingen Bridge is a girder bridge but uses temporary cable stays.

This last example shows that the method of construction of any given bridge should be left to the contractor to decide. The best method or the most economical construction depends very much on the experience of the contractor, the equipment he can have available, the environmental constraints of the bridge site, etc. which are mostly unknown to the design engineer who has to work on the structural analysis normally 4 to 5 years before the bridge was out for tender. To restrict the contractor to a specific method using specific types of equipment could only result in a very expensive bridge and very often to inferior quality because this may or may not be in the experienced area of the successful bidder. As an engineer or as an owner, the final product -- the bridge, is of concern but not the intermediate stages of how the bridge is built.

Special Requirements in Advanced Construction Techniques

It is understandable that a certain amount of engineering work is involved in applying any advanced construction technique. A bridge that is built in several stages or in many segments does not behave exactly the same way as a bridge that is built totally on falsework. The reinforcement and post-tensioning requirements may also differ.

There are three important areas that the engineering and construction team has to consider:

1. Stress analysis during construction: Because the loadings and support conditions of the bridge are different from the finished bridge, stresses in each construction stage must be calculated to insure the safety of the structure. For this purpose, realistic construction loads must be used and the site personnel must be informed of all the loading limitations. Wind and temperature are usually signifi-

cant for construction stages.

2. Camber: In order to obtain a bridge with the right elevation, the required camber of the bridge at each construction stage must be calculated. It is required that due consideration be given to creep and shrinkage of the concrete. This kind of calculation, although cumbersome, has been simplified by the use of computers.

3. Quality control: This is important for any method of construction, but it is more so for the complicated construction techniques. Curing of concrete, post-tensioning, joint preparations, etc. are detrimental to a successful structure. The site personnel must be made aware of the minimum concrete strengths required for post-tensioning, form removal, falsework removal, launching and other steps of operations.

Generally speaking, these advanced construction techniques require more engineering work than the conventional falsework type construction, but the saving could be significant.

Closure

As materials and construction equipment are being improved continuously, new ideas of bridge construction will appear from time to time. It is hoped that this paper has made available some of the existing experience which may be helpful for the development of other new approaches.

SEGMENTAL BRIDGE CONSTRUCTION IN WESTERN EUROPE - IMPRESSIONS OF AN IRF STUDY TEAM

Craig A. Ballinger and Walter Podolny, Jr., Department of Transportation

In April of 1977, under the sponsorship of the International Road Federation, a five-man team of U.S. bridge engineers visited Western Europe to study segmental prestressed concrete box girder bridges. The purpose of study was to examine and evaluate the current construction methods and design considerations for this type of bridge. The team visited bridges under construction and completed in West Germany, Austria, Northern Italy, Denmark, Holland, and France. Technical meetings were held with representatives of leading European design firms as well as bridge engineers from the governments of West Germany, Holland, and France. These meetings involved technical discussions of design, construction, and serviceability aspects. This paper presents information gathered during these visits and discussions on the following topics: construction with precast and cast-in-place concrete; erection by balanced cantilever, span-by-span, progressive placing, and incremental launching methods; design considerations relating to live load requirements, segmental joints, allowable tension in concrete, crack control, temperature gradient, shear keys, etc.

In April of 1977, a five-man engineering team sponsored by the International Road Federation, of which the authors were privileged to be members, embarked on a study tour of segmental bridge construction in Western Europe. The objective was to determine and report on the current state-of-the-art and development of segmental bridge construction.

In addition to the authors, the study team was composed of the following representatives of government and private industry: Michael J. Abrahams, Project Engineer, Parsons Brinkerhoff Quade & Douglas, Inc.; Thomas Alberdi, Jr., Deputy Design Engineer, Structures, Florida State Department of Transportation; and Thomas J. D'Arcy, Vice President of Engineering, Research and Development, Rocky Mountain Prestress, Inc.

The group traveled to West Germany, Austria, Northern Italy, Denmark, Holland, and France. Meetings were held with internationally recognized engineers on segmental prestressed concrete bridges including designers, contractors, and government officials. These meetings involved detailed discussions relating to the design, construction, and serviceability of such bridges. The group also visited the sites of numerous segmental bridges; both under construction and completed.

Types of Segmental Construction

Segmental bridges may be categorized by two classifications: (1) the condition of the concrete at the time of erection, that is, precast or cast-in-place; and (2) the method of construction.

In precast segmental construction short segments are cast in a plant or near the job site under factory simulated conditions, but always at some location other than their final position in the structure, and then assembled in place. The cast-in-place segmental construction is such that the bridge is cast in situ in a series of steps. Both precast and cast-in-place construction produce essentially the same final structure, both concepts are viable ones, both have been consummated, and both have been successful.

The second classification of segmental bridges is by the method of construction. Generally, the method of construction can be divided into four types: (1) balanced cantilever, (2) span-by-span, (3) progressive placing, and (4) incremental launching (push-out construction), or what in Germany is called "taktschiebeverfahren."

Balanced Cantilever

The balanced cantilever method simply cantilevers segments from a pier in a balanced fashion on each side of a pier until mid-span is reached and a closure pour is made with a previous half-span cantilever from the preceding pier. Then the procedure is repeated until a structure is completed. At most, the pier will only be out of balance by one segment, which can be accommodated by a moment resistant pier or by a temporary brace.

Until recently, the balanced cantilever method has been the only form of segmental construction used in the United States. It was used on bridges at Corpus Christi, Texas and on the Vail Pass in Colorado. Precast segments were used on both bridges. Cast-in-place segments were utilized on the Pine Valley Bridge in California and the Kipapa Bridge in Hawaii.

For cast-in-place construction, the moveable formwork is supported from a "form traveller" that cantilevers from the previously completed portion of the bridge, Figure 1. New segments are formed, cast, and stressed to the previously erected sections. In some cases, such as the Vejle Fjord Bridge in Denmark, Figure 2, a launching girder may be used to stabilize the structure for segments out of balance and to transport materials to the location of casting. As a cantilever is completed, the launching girder is advanced to the next pier.

Similarly in precast construction, a launching girder may be used to transport the precast segments to the end of the partially erected cantilever for attachment, as indicated in Figure 3 for the Sallingsund Bridge in Denmark.

Figure 1. Form travelers.

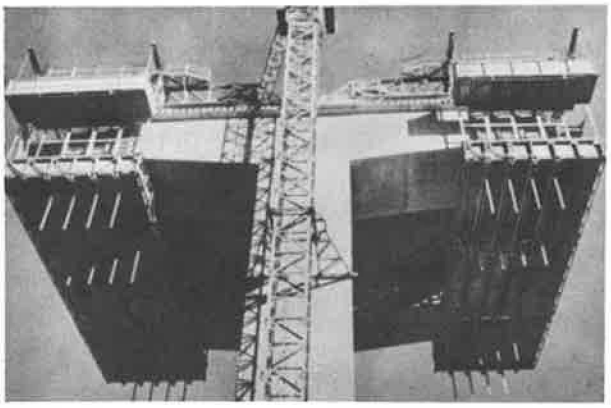

Span-By-Span

In long, viaduct-type structures segmental span-by-span construction is particularly advantageous. The superstructure is executed in one direction, span-by-span, by means of a moveable form carrier, Figure 4. Construction joints or hinges are located at the point of contraflexure. The form carrier, Figure 5, is a type of factory, transplanted to the job site, with all of the advantages of chain production, normally possible only in precast yards, and with the advantage of flexibility in shaping of cast-in-place concrete to suit field conditions. The moveable form carrier may be supported on the piers, Figure 6; or from the edge of the previously completed construction, at the joint location, and at the forward pier. In some cases, as in the approach spans of the Rheinbrucke Dusseldorf-Flehe, the moveable formwork is supported off the ground, Figure 7. The bogies of the form carrier may either run above or below the level of the bridge deck. Bogies below deck are more suitable for bridges close to the ground; for high elevated roadways, the above-deck type is easier to handle. The moveable form carrier consists of a steel superstructure which is moved over the completed bridge. The large formwork elements are suspended from steel rods during concreting and are rolled forward, after the suspension rods have been removed, by means of the structural steel outriggers on both sides of the superstructure, Figure 8.

Figure 2. Launching girder, Vejle Fjord Bridge

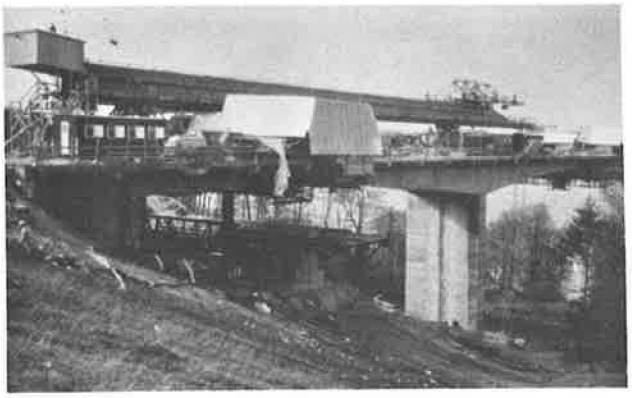

Several rather long bridges using this system of construction were executed on the Brenner Autobahn in Austria near Innsbruck, Figure 9. Footings and piers were placed from a 3-m (9.8-ft) wide path which had been built along the alignment. Construction of a typical 30-m (98.4-ft) span superstructure was 8 calander days. At the Brenner Autobahn, in Italy, sections of elevated highway up to a length of approximately 2.5 km (1 1/2 m) have been constructed using form carriers with bogies above the level of the bridge deck, Figure 10.

Figure 3. Launching girder, Sallingsund Bridge

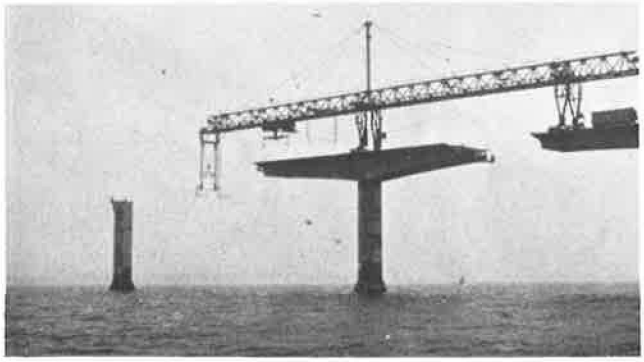

Another typical example for this type construction method is the approximately 7-km (4.3 m) long elevated highway, part of an Autostrade in Sicily, Figure 11. The mushroom-shaped slab of the superstructure, similar to column capitals in flat-plate building construction, is post-tensioned in the longitudinal and transverse directions, Figure 12. The Tangenziale Milano, an intercity elevated highway, was constructed using a form carrier with bogies below the deck, Figure 13. A typical longitudinal and transverse section of the structure is shown in Figure 14. In the longitudinal section, with construction proceeding from left to right, the construction joint is located at the forward edge of the mushroom capital. The span-by-span type of

Figure 4. Moveable form carrier.

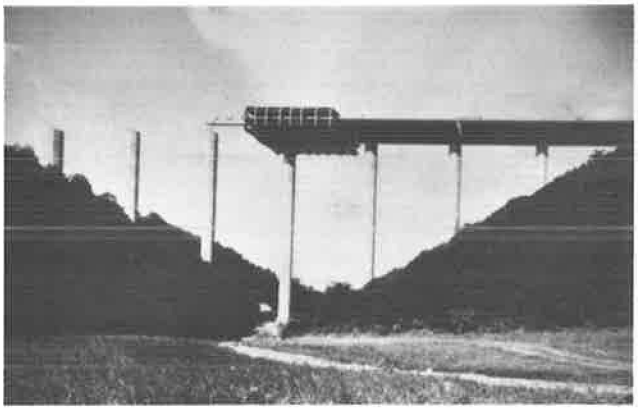

Figure 5. Moveable form carrier.

Figure 6. Moveable form carrier.

Figure 7. Ground supported form carrier, Rheinbrucke-Dusseldorf-Flehe.

Figure 8. Moveable form carrier.

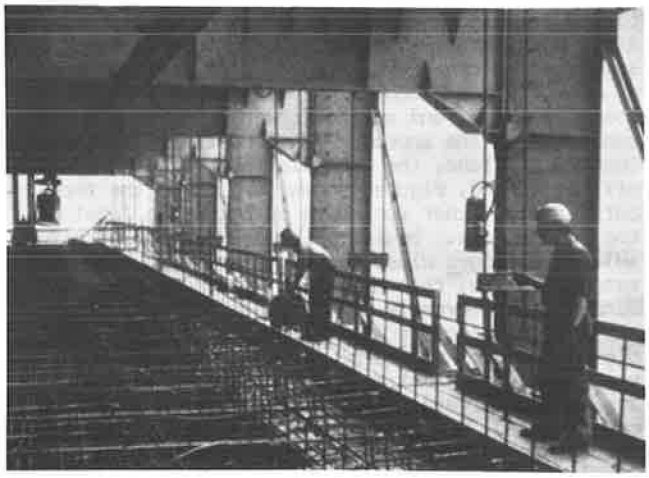

Figure 9. Brenner autobahn - Innsbrucke, Austria.

Figure 10. Atzwang Bridge, Brenner autobahn, Italy.

Figure 11. Viaduct Fichera - Sicily.

Figure 12. Viaduct Fichera - Sicily.

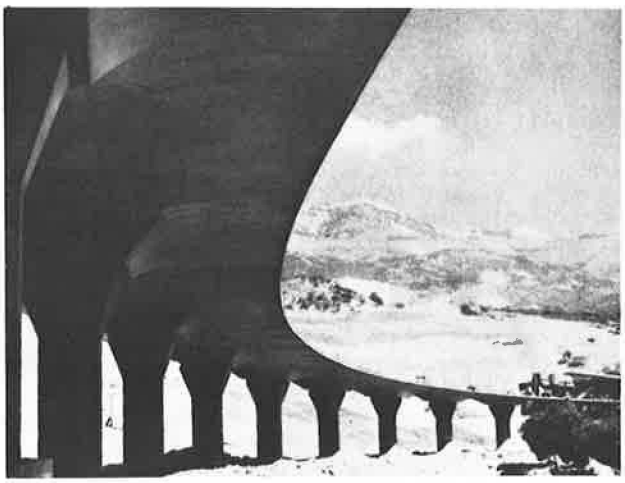

construction is being utilized for the first time in the United States on the Denny Creek project in the State of Washington.

Progressive Placing

Progressive placing is similar to the span-by-span method described above in that construction starts at one end of the structure and proceeds continuously to the other end of the structure. The span-by-span method is used for cast-in-place construction; whereas, the progressive placing method is used for precast construction. The progressive placing method derives its origin from the balanced cantilever concept. However, for this method the precast segments are placed continuously from one end of the structure to the other, in successive cantilevers from the same side of the various piers rather than by balanced cantilevers from both sides of each pier.

At the present time this method appears to be practicable in span ranges from 30 to 50 m (100 to 160 ft), where the balanced cantilever method is generally not economical. Because of the length of cantilever (one whole span) in relation to the construction depth, the stresses become excessive and a movable, temporary stay arrangement must be used to limit the cantilever stresses to a reasonable level. The erection procedure is illustrated in Figure 15. This method of construction was not observed during the study tour.

Incremental Launching

More recently, a new variant, or new generation, of the segmental concept has evolved, which in Germany is called TAKTSCHIEBEVERFAHREN. Litterally translated Taktschiebeverfahren means "phased shoving concept," in this country it is referred to as incremental launching or push-out construction. This concept was first implemented on the Rio Caroni Bridge in Venezuela built in 1962/63 by its originators Willi Baur and Dr. Fritz Leonhardt of the consulting firm Leonhardt and Andra, Stuttgart, West Germany. (1,2)

The bridge superstructure is constructed in an on-site factory in stationary forms behind the abutment in lengths of 10 to 30 m (32.8 to 98.4 ft), Figure 16. Thus, each segment length cast represents one "incremental shoving length" of the superstructure. After a segment reaches sufficient strength, it is post-tensioned to the previous segment and the entire superstructure in pushed out longitudinally one increment length. The succeeding segment is then cast against its predecessor. Normally, a work cycle of 1 week is required to cast and launch a segment, irrespective of its length. Operations are scheduled such that the concrete can attain sufficient strength over a weekend to allow launching at the beginning of the next week, Figure 17. Fabrication of the on-site factory can be in the open or, in the case of inclement weather, a protective covering can be provided. In some instances, the bridge is launched with curbs and rails in place.

Bridge alignment in this type of construction is either straight or on a curve; however, the curve must be a constant radius curve. This requirement of constant rate of curvature applies to both horizontal and vertical curvature. The Val Ristel Bridge in Italy, which was incrementally launched on a radius of 150 m (492 ft), is illustrated in Figure 18.

Figure 13. Tangenziale Milano.

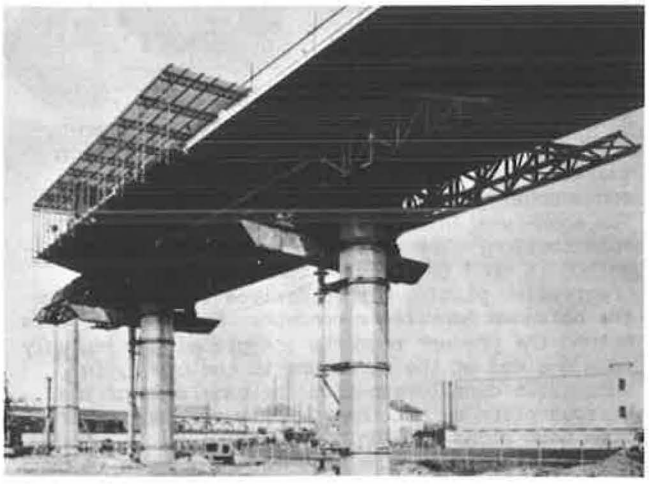

Figure 14. Tangenziale Milano.

Figure 15. Progressive placing erection procedure.

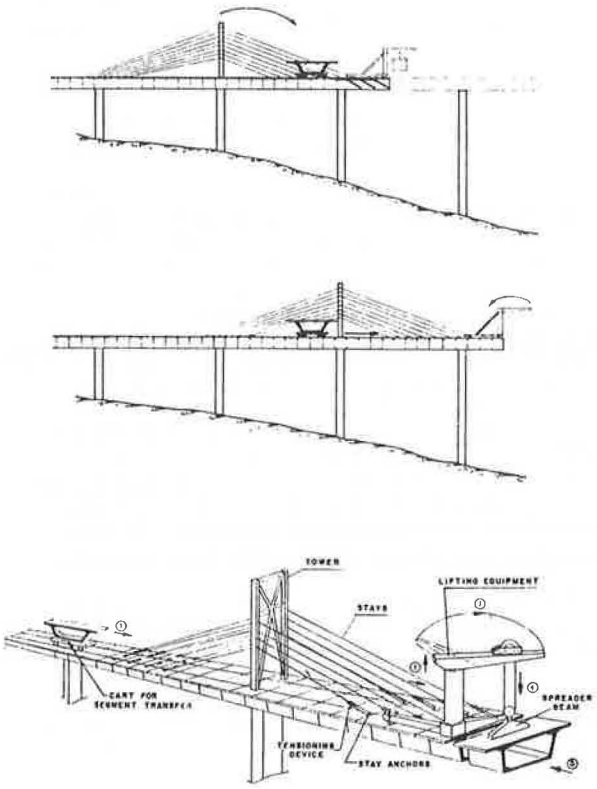

To counteract the varying bending moments that occur during the launching operations, the superstructure is concentrically prestressed. In addition, a launching nose, Figure 17, is provide in order to preclude the development of excessively large bending moments during launching.

The concentrically prestressed superstructure is pushed forward longitudinally in successive increments by means of hydraulic jacks. To accommodate the movement of the superstructure, temporary sliding bearings are installed on the piers. These bearings are made of teflon- (PTFE-) faced steel-reinforced neoprene pads which slide on polished stainless steel plates, Figures 19 and 20.

There are two methods of launching. The method used on the Rio Caroni Bridge has the jack bearing on an abutment face and pulling on a steel rod, which is attached to the last segment cast by launching shoes. The second, and more current, method consists of horizontal and vertical jacks, Figure 21. The vertical jack slides with a teflon plate at its base on a stainless steel plate and has a friction element at the top to engage the superstructure. The vertical jack lifts the superstructure approximately 5 mm (3/16 in) for launching. The horizontal jack then moves the superstructure longitudinally. After the vertical jack has moved one stroke of the horizontal jack, the vertical jack is lowered and the horizontal jack is retracted to restart the cycle. (2)

This construction technique has been used for spans up to 60 m (197 ft) without the use of temporary falsework bents. Spans up to 100 m (328 ft) have been built utilizing temporary supporting bents. Girders must have a constant depth, which is usually 1/12 to 1/16 of the longest span.

An example of this type of construction is the Muhlbachtalbrucke, about 50 km (31 m) southwest of Stuttgart, Figure 22. This structure has an overall length of 580 m (1,903 ft) with 43 m (141 ft) spans. The far-side trapezoidal box girder which has been completed from abutment to abutment, is shown in Figure 22. The near-side trapezoidal box girder has been launched form the left abutment and the launching nose has reached the first pier. There is a horizontal curvature to the bridge. A view of the underside of the twin boxes, Figure 23, showns the longitudinal closure joint that has not yet been poured.

Another example is the Talbrucke Rottweil-Neckarburg Bridge, 80 km (50 m) southwest of Stuttgart, Germany, Figure 24. The bridge deck consists of two incrementally launched box girders supported by cast-in-place segmental arch ribs. The 364.98-m (1,197-ft) long roadway deck is 94.77 m (310.9 ft) above the Neckar Creek. The arch span is 154.4 m (506.6 ft) with a rise of 49.85 m (163.5 ft). The total structure width is 31 m (101.7 ft) constructed in two longitudinal halves.

Figure 24 shows the bridge under construction, just before closure of the first arch rib. During construction, a two-cell arch rib is temporarily tied back to rock anchors by Dywidag bars which pass over a pier, Figure 25. The incrementally launched deck and the launching nose are shown in Figures 26 and 27. The deck spans are 30 m (98.4 ft) in the approach and 22.14 m (72.6 ft) over the arch.

The incremental launching technique was used for the first time in the United States for construction of the Wabash River Bridge at Covington, Indiana.

Figure 16. Casting bed and launching arrangement.

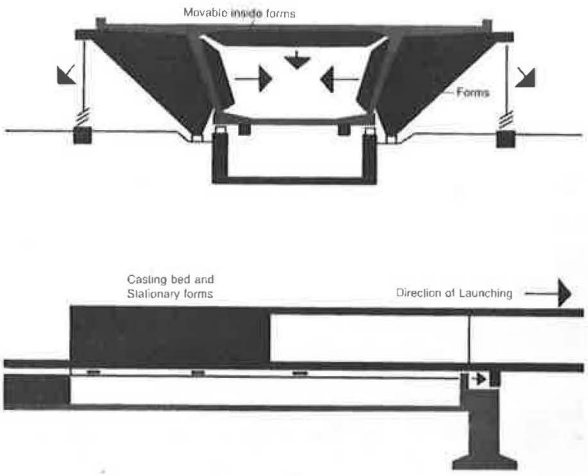

Figure 17. Launching sequence.

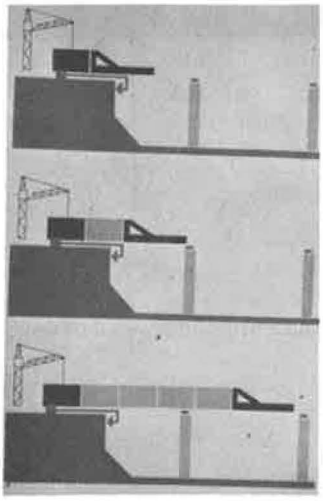

Figure 18. Val Ristel Bridge.

Figure 19. Temporary sliding bearing.

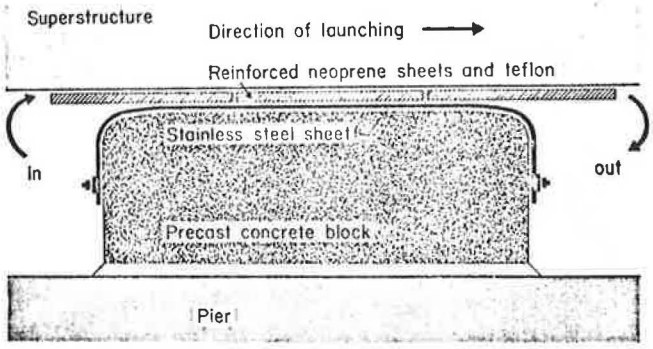

Figure 20. Teflon-faced neoprene pads on temporary sliding bearings.

Figure 21. Push-out jacking arrangement.

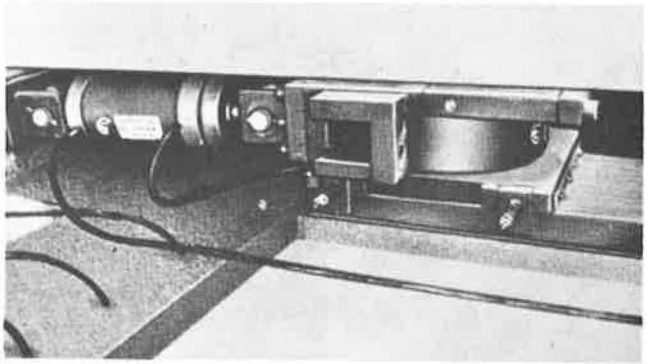

Figure 22. Muhlbachtalbrucke.

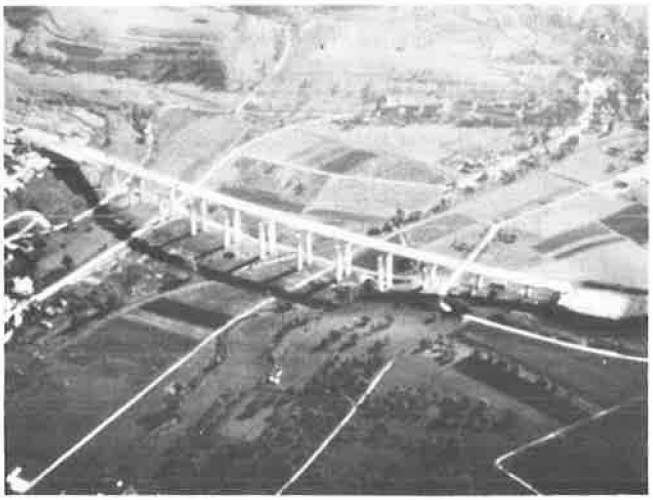

Figure 23. Muhlbachtalbrucke.

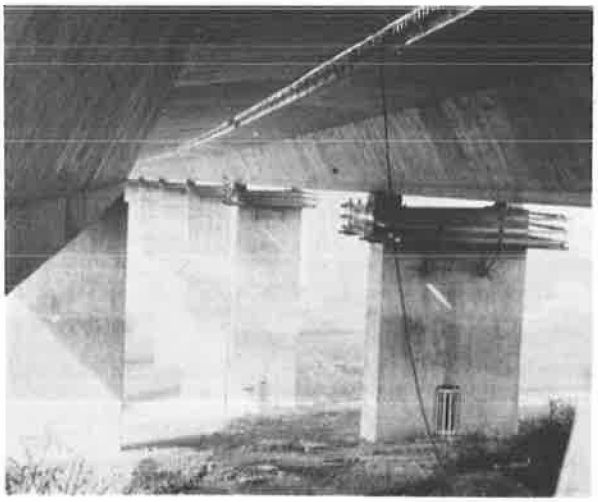

Figure 24. Rottweil-Neckarburg arch bridge.

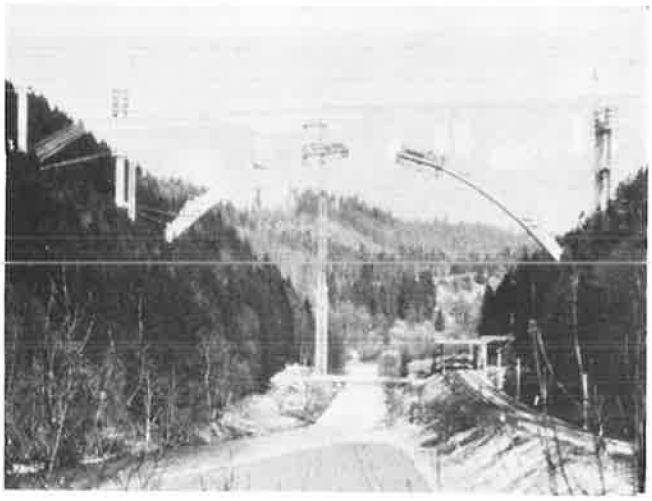

Figure 25. Rottweil-Neckarburg arch bridge.

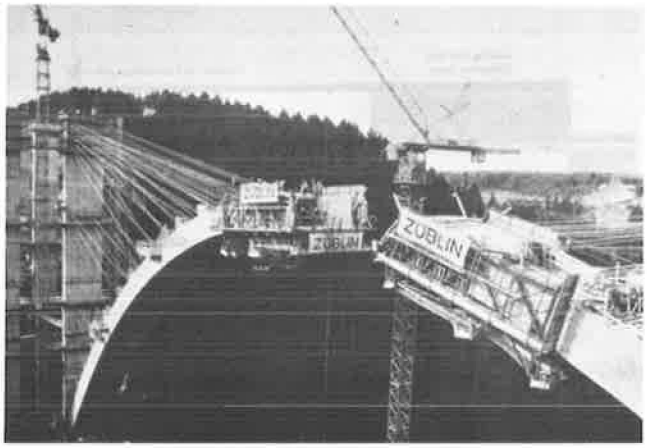

Figure 26. Launching deck on Rottweil-Neckarburg arch bridge.

Figure 27. Closeup of launching nose Rottweil-Neckarburg arch bridge.

Figure 28. Maximum live load moment (simple span).

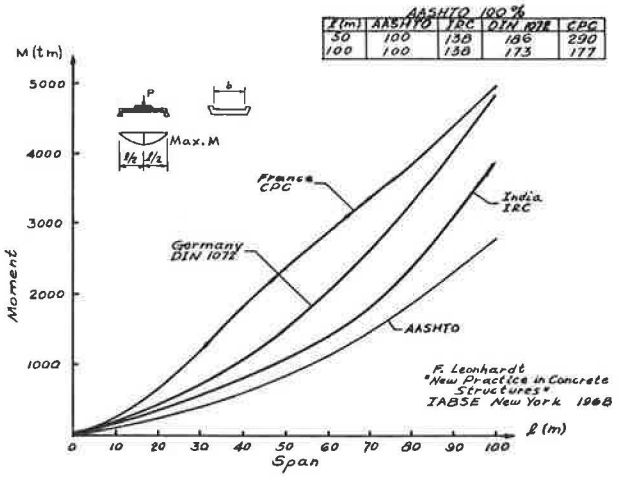

Design Considerations

Design of concrete bridges in the United States conforms with the provisions of AASHTO's "Standard Specifications for Highway Bridges." It should be recognized that, for the most part, the provisions in these specifications were written prior to when segmental construction was considered feasible or practical in the United States.

There has been considerable discussion in the American literature relative to the subject of segmental construction and it will not be repeated here. However, the following will present a discussion of several specific items athat are either controversial or practiced differently in different countries in Europe.

Live Load Requirements

In comparing practices in other countries to that employed in the United States, an important parameter must be kept in mind, that is, live load requirements. Figure 28 illustrates that there is considerable difference in code requirements in various countries. For a simple span of 50 m (164 ft) and width of 7.5 m (24.6 ft) the German specification indicates a moment of 186 percent that of the AASHTO requirements and the French, 290 percent that of AASHTO. (3) There are some Canadian provinces which use the AASHTO specifications, but arbitrarily increase the live load by 25 percent.

The depth-to-span ratio and width-to-depth ratio for segmental construction presently advocated, have been adopted from European practice. The lighter live loads used in the United States should lead to the feasibility of less superstructure depth. This will undoubtedly occur as these concepts are "Americanized."

Segment Joints

In both precast and cast-in-place segmental construction, the segments are reinforced with prestressing tendons and conventional mild steel reinforcement. In both types of construction, the prestressed reinforcement, or at least some of it, crosses the joint. However, the mild steel reinforcement, obviously, can only be continuous across the joint in the cast-in-place method. In precast construction the joint is not reinforced with mild steel although the segments are usually glued together with epoxy. The German code, at the present time, requires mild steel reinforcement across the joint and thus precludes precast construction. The German code is presently under revision and precast construction is under consideration. The joint treatment is a controversial point in Europe and apparently follows nationalistic lines.

Allowable Tension in Concrete

As stated above, in cast-in-place segmental construction, reinforcing steel is extended across the construction joint. For this case, tension is permitted across the joint--in both Germany and France. However, this tension is permitted only when there is a severe combination of loads. In German under a condition of full live and dead load, a 0.14 kg/mm^2 (200 psi) tension is permitted and half of this value, or 0.07 kg/mm^2 (100 psi) is permitted at the joint. However, no tension is

permitted under one-half live and full dead load. During erection, tension is generally not permitted.

For precast segmental construction, no steel extends across the joint and it is difficult to anticipate how this joint will behave under tension. If epoxy is used to glue the joints together, it can be tested to insure that it has adequate tensile strength. The problem is that immediately adjacent to the joint, the concrete is not reinforced and is composed of only a cement and fine aggregate. It is debatable if one can rely on this unreinforced paste to take much tensile stress.

In the design of the precast segmental Sallingsund Bridge in Denmark, no tension was allowed for the load case of dead, temperature, temperature gradient, and settlement. However, for the load case that included the above loads plus redistributed moments, wind, and boat impact on the pier a 0.25 kg/mm^2 (356 psi) tension was allowed.

In Holland, for precast epoxied segmental construction, the goverment engineers design for no tension under dead load, full live load and settlement. Tensile stresses resulting from temperature gradient are not considered.

Crack Control

The question of allowable tension is obviously an improtant one; however, some European engineers felt that this problem should be considered from the point of strain rather than stress. Thus, the problem becomes one of controlling crack widths rather than limiting tensile stress in the concrete. AASHTO has recommendations in the 1974 Interim, Section 1.5.39, for distribution of flexural reinforcement to control cracking for reinforced concrete depending upon exposure. There are no recommendations for prestressed concrete.

One European engineer expressed the opinion that no corrosion will occur if cracks are less than 0.4 mm (0.016 in) and that for prestressed bridge design cracks should be limited to 0.1 mm (0.004 in). He felt that the cracking was most severe the first few days after concrete was cast when there are large shrinkage strains set up by the heat of hydration of the cement and at the same time the concrete was of low strength.

Temperature Gradient

In considering tension stresses, consideration should be given to the tensile stresses produced by a thermal gradient between the top flange and botton flange of the box girder. AASHTO at the present time does not address this problem. Tensile stress in the bottom flange at a first interior support can be as high as 0.35 kg/mm^2 (500 psi). At some point away from the support such temperature stress could easily cause cracks in the bottom flange.

In France, no tension is permitted across the joint for a 5°C (9°F) temperature gradient combined with dead, live (or wind) and settlement. Also, no tension is permitted for a 10°C (18°F) temperature gradient combined with dead load. The German code is being revised following the Franch to consider a 10°C (18°F) temperature gradient in combination with half the live load. For this combination, the section is considered cracked and the prestressing steel is checked for fatigue for 2,000,000 cycles of half live load.

Obviously, another thermal gradient condition that needs consideration in design is that between the outside and inside of exterior webs. Thermal gradient stresses can be developed such that total stress cannot be accommodated by the shear reinforcement provided, which would result in longitudinal cracks in the web.

Shear Keys

Another design consideration about which there was much discussion and difference of opinion was shear transfer across the joint. For cast-in-place construction, the common treatment is to use a form liner which leaves a roughened surface which is considered adequate to provide shear transfer. In one case, a rough broard surface was used as a form liner.

For precast construction shear keys in the webs are used to transfer shear. There are two schools of thought regarding the type of shear key to be used. The Dutch provide a large shear key, Figure 29, which is designed to support two segments and the construction equipment load while the epoxy is setting up and curing. This large shear key is reinforced. Advantages are that, because of the reinforcement in the key, there is reinforcement across the joint, it is less likely to be damaged during handling and erection, and it permits easier details for tendon anchorage in the web. The disadvantage is that it concentrates shear forces at one point.

The French used this type of key in their structures until recently. They are now using a multiple or corrugated type and thus represent a second school of thought, Figure 30. The advantage of this type of shear key is that it provides a more uniform transfer of stress and can be designed to transfer all the web shear during service. Although the small keys cannot be reinforced, the distance between vertical stirrups, if placed close to the ends of the segment, would be less than typical stirrup spacing. If the appearance of the key is undesirable, a relief can be used on the exterior face of the web. Disadvantages are that the keys are more likely to be damaged during handling and erection, and there is a detail problem of providing for tendon anchorages in the webs.

Conclusion

In conclusion, with the exception of the joints, both precast and cast-in-place construction essentially produce the same final structure. Both concepts are viable ones, both have been consummated and have been successful. However, from a designer's point of view, there are questions still to be resolved. We need recommendations as how to accommodate thermal gadient; the question of allowable tensile stress in the concrete apparently needs closer scrutiny; perhaps the concept of crack control needs further investigation; is it better to use large shear keys or smaller ones? It was apparent from the difference of opinion in Europe that there is room for investigation research to provide guidelines and direction to the designer.

Acknowledgments

The following individuals and firms are acknowledged for their hospitality and assistance

in providing data and photographs: Baudirektor Dipl. Irg. Freidrich Standfuss, Bundesministerium fur Verkehr, Bonn; Prof. Fritz Leonhardt, Mr. Zellner, and Mr. Svensson all of the firm Leonhardt and Andra, Stuttgart; Dr. Richard Heinen and Mr. Manfred Bockel of Dyckerhoff & Widmann, Inc., Munich; Mr. P. Allaart and Mr. IR. A. H. Van Rijs, Ministry of Transport and Waterstaat, Bridge Building Department, Holland; Mr. H. E. Westenberg, I.B.I.S., Holland; Mr. M. Le Franc, L'Ingenieur En Chef Des Ponts et Chaussees, Service d'Etudes Techniques des Routes et Autoroutes, France; and Mr. Jean Muller, Europe-Etudes, Paris, France.

References

1. Arvid Grand. Incremental Launching of Concrete Structures. Journal of the American Concrete Institute, Vol. 72, No. 8, August 1975.
2. Willi Baur. Bridge Erection by Launching is Fast, Safe, and Efficient. Civil Engineering-ASCE, Vol. 47, No. 3, March 1977.
3. F. Leonhardt. New Trends in Design and Construction of Long Span Bridges and Viaducts (Skew, Flat Slabs, Torsion Box). International Association for Bridge and Structural Engineering, Eight Congress, New York, September 9-14, 1968.

Figure 29. Large shear key.

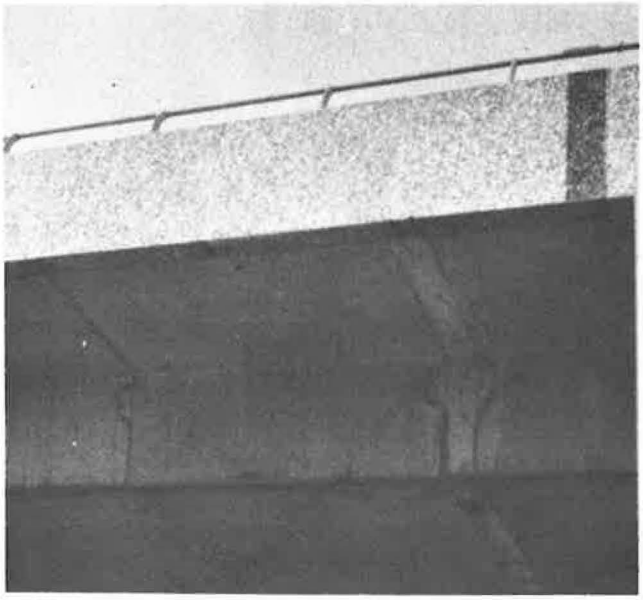

Figure 30. Small shear keys.

SEGMENTAL AND STAGE CONSTRUCTION OF PRESTRESSED CONCRETE BOX GIRDER BRIDGES

Gerald H. Brameld, Queensland Institute of Technology,
Brisbane, Queensland, Australia.

Prestressed Concrete Bridges of uniform or near uniform cross-section are admirably suited to construction by precasting segments and post-tensioning. This form of construction, however, introduces additional design and construction problems - problems of carrying flexure, shear and torsion across joints - the most suitable type of joint, - problems introduced by superelevation and constructional tolerences. As the length of the structure increases, the effective prestress is reduced markedly until it is no longer economical to stress in one operation. The method of stage stressing will overcome these problems, however more complex analysis and design is required. Solutions to these problems are discussed with particular reference to several large prestressed concrete box girder bridges recently constructed in Australia.

The use of prestressed concrete for medium span structures has increased dramatically over the last decade, and now is the predominant material of construction used in the 15m to 40m span range. Geometrics imposed on the bridge designer by the freeway and highway designer have forced the change from straight simply supported bridges to bridges with complex geometry. The hollow box girder bridge is admirably suited to these conditions and has the additional advantage of its aesthetically pleasing lines, a highly desirably property for urban structures.

The simple prestressed concrete box girder has evolved rapidly into the sophisticated bridge with many more design and construction developments. Two of these developments, segmental construction and stage construction will be reviewed. Design and construction problems and solutions to these problems will be discussed with particular reference to recent bridges constructed in Brisbane, Australia.

Two structures will be discussed within this paper.

(a) Nyanda Overpass
(b) Roma Street - South Brisbane Rail Link

Nyanda Overpass

Nyanda Overpass (1) is a 388.3m long elevated prestressed concrete box girder bridge carrying four lanes of traffic over an interstate railway line. The bridge replaced an existing level crossing. Although the natural surface levels suited a tunnel structure under the railway, the railway line being on the crest of a small ridge, the extensive cut required for the approaches seriously affected access to an adjacent heavy engineering works and existing surface streets. The additional construction problems of maintenance of railway and road traffic, and in fact, tunnelling under three railway lines added weight to the final decision to use an elevated structure. The minimum vertical clearance over the railway line of 5.2m had to be provided, and as this was above the crest of the ridge the structure had to be quite long in order to keep the approach grades below 5%. The layout of the overpass is shown in Figure 1.

The superstructure has a basic span of 36.6m with variations to allow for railway and surface street clearances. A multicell hollow box spine with cantilevers was selected for the superstructure, the depth of the box being 1370mm. (Figure 2). The small temporary construction depth allowable over the railway line precluded the use of falsework or erection trusses necessary for insitu construction and therefore, precast segmental construction was selected. To reduce site operations the boxes were cast full width with the exception of the pier diaphragm units. The maximum weight of the units (45 tonnes) was determined by the available lifting equipment. With the exception of the diaphragm units all joints were nominally 125mm wide unreinforced. A uniform external mould was designed to reduce the casting problems.

The use of precast segmental construction offered the following additional advantages:

(a) the units are manufactured under factory conditions, with the resulting higher standard of quality.

(b) at the time of prestressing the units, the losses due to creep and shrinkage are those relevant to fully cured concrete, and will generally be less than for an equivalent insitu design.

(c) Construction time can be reduced as the precasting can be carried out simultaneously with substructure construction.

The superstructure is anchored at each abutment

with all longitudinal movements accommodated at a single expansion joint in the middle of Span 6. This expansion joint is designed as a hinge and carries transverse shear.

With the total length of the superstructure between abutments and the hinge being 169.75m and 218.55m respectively friction losses in the cables as the prestress is applied were excessive, and residual prestress after all losses was at an uneconomically low level.

For this reason the superstructure was designed to be constructed in a number of self contained stages as shown in Figure 3.

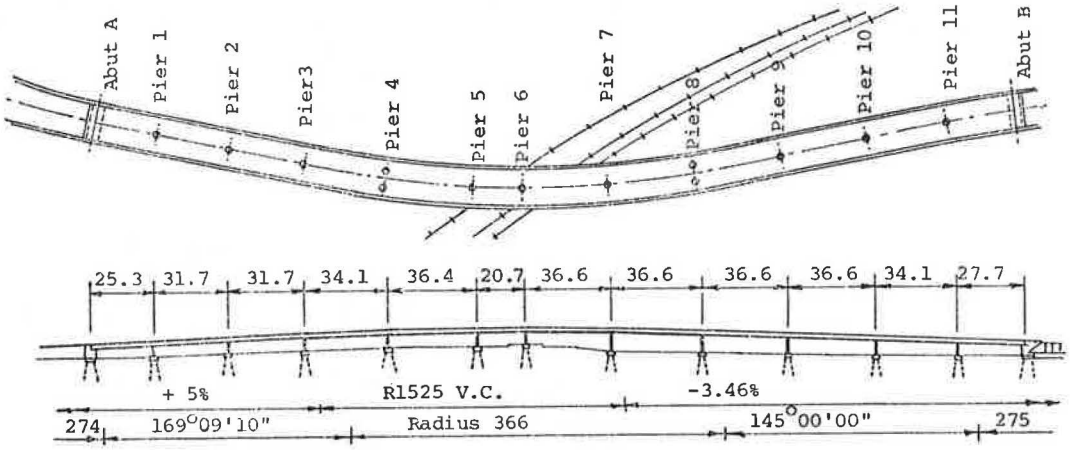

FIGURE 1

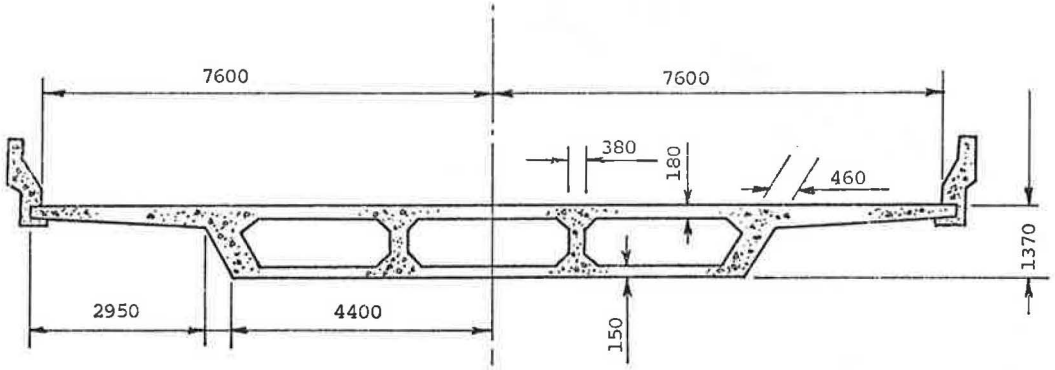

Typical Section

FIGURE 2

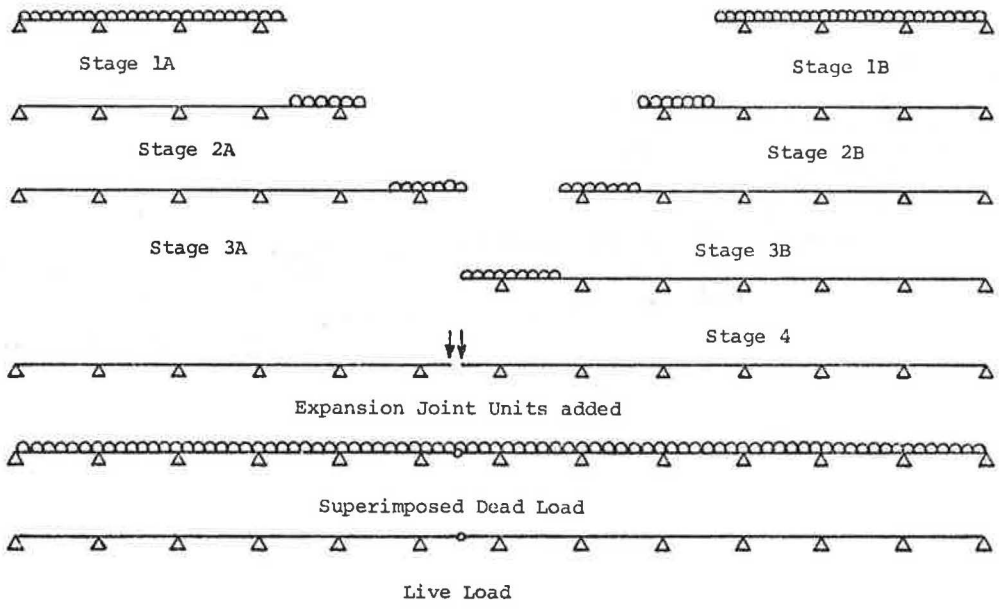

FIGURE 3

Roma Street - South Brisbane Rail Link

The city of Brisbane is located on the Brisbane River which splits the city into two. The city is served by a number of road bridges, however there has been only one railway crossing for many decades. This existing railway crossing carries suburban railway traffic to the western suburbs and western towns. More recently the population expansion has been to the south and south-east of the city, thus imposing heavy demands on public transport. Brisbane has for many years been served by two major railway stations - Roma Street serving the suburban lines on the north side of the river, and all intrastate lines, and South Brisbane serving the suburban lines on the southside of the river, and the interstate line to Sydney. Suburban and intrastate lines are narrow gauge while the interstate line is standard gauge.

The design for the 2km link was commissioned in 1972 and construction is currently in progress. The link consists of 642m of elevated vaiduct, a 132m steel tied arch across the river, two through bridges over surface streets of 60.1m and 29.2m respectively, 117.4m of embankment, and 111.4m of cut and backfill tunnel (see Figure 4).

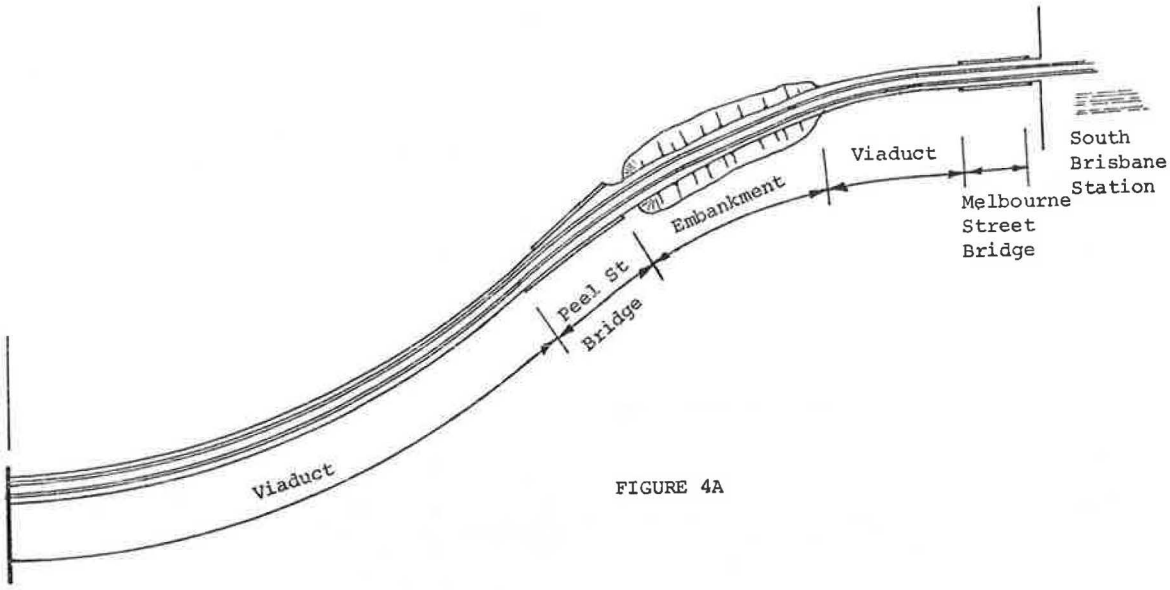

FIGURE 4A

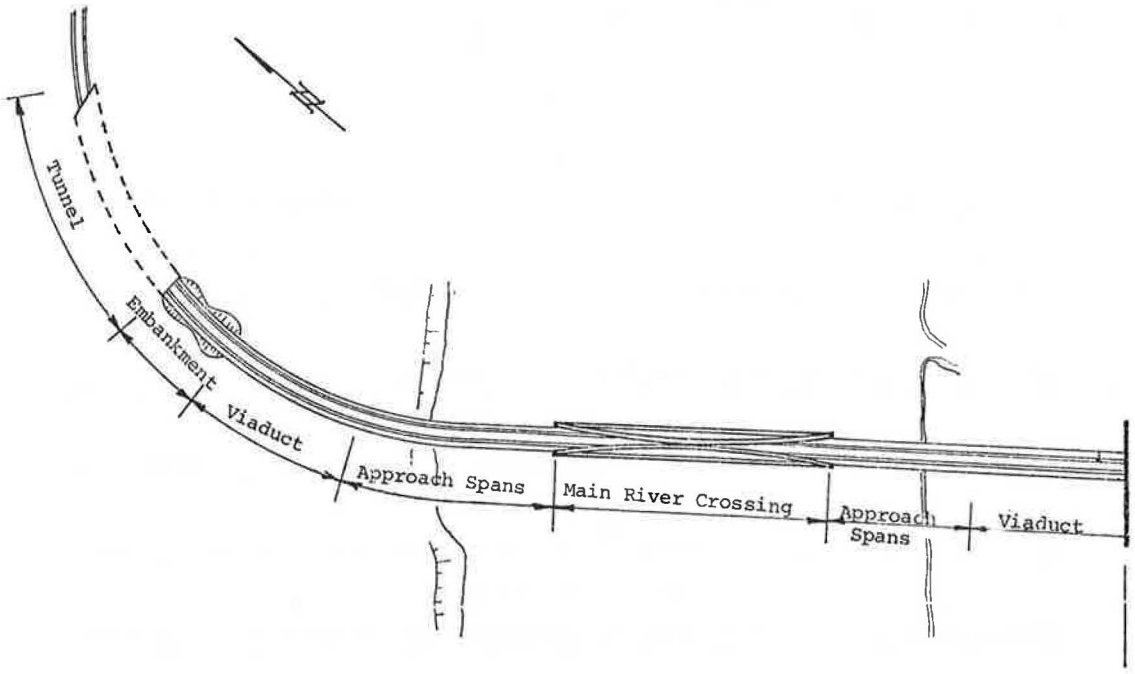

FIGURE 4B

This paper will be concerned with the design aspects of the elevated viaduct sections.

The viaduct has been constructed in a number of sections, these being:-

Section	Span (m)
A	22.5, 25.9, 22.9
B Approach Spans	28.2, 33.9, 33.9
C Approach Spans	33.45, 33.9, 28.2
D	19.1, 30.0, 23.0 22.1, 27.6, 20.0, 20.0
E	7 spans @ 20.0, 1 @ 22.0
F	20.22, 25.0, 20.22

Twin single cell box girders were used for section A, D, E, and F each girder carrying one track, while a single multicell box was used for the longer approach span sections B and C. The boxes had a constant depth of 1830mm, with a spine width of 2500mm for the single cell boxes and of 6500mm for the multicell box. (see Figure 5).

Variations in overall width due to curve widening were accommodated by varying the lengths of the cantilevers. The superstructure was cast insitu and post-tensioned with high capacity cables. The insitu superstructure was selected because it offered a number of advantages:

(a) Only a small proportion of the viaduct crosses surface streets and interruption to road traffic flow would be minimal

(b) Shuttering is simple

(c) Heavy lifting equipment is not required.

(d) Previous experience had shown that insitu construction in urban areas was less costly than precast segmental construction.

Section A, B, C and F were cast and stressed full length, while the stage method of construction was used for sections D and E. The stages are shown in Figure 6.

Segmental Construction

The method of segmental construction offers a number of advantages over the insitu method.

(a) Falsework and shuttering is considerably lighter

(b) Considerable economy in formwork design - particularly for uniform sections

(c) Factory casting conditions allow better quality control and thus higher strength concrete may be used

(d) The majority of the shrinkage has occurred at the time of erection

Contra these advantages there are a number of disadvantages:

(a) Heavy site lifting equipment is required for erecting the units

(b) Effects of horizontal and vertical alignment are difficult to accommodate

(c) Casting facilities must be available in close proximity to the site or transport costs will be excessive.

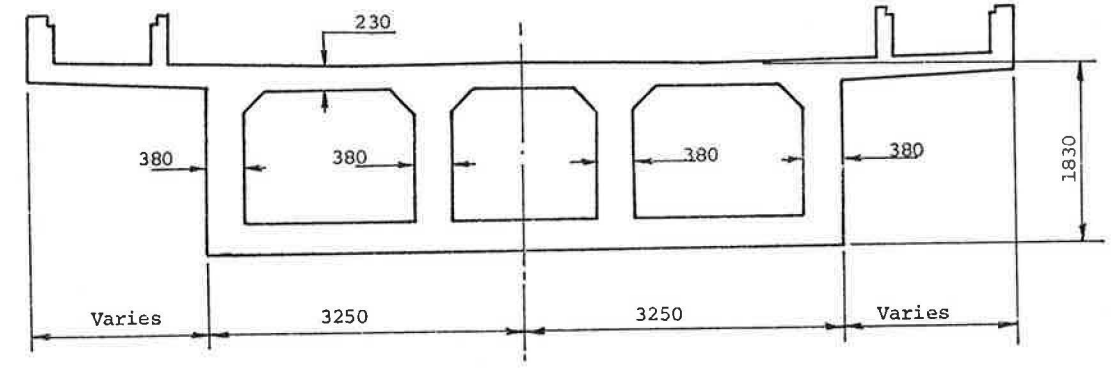

TYPICAL SECTION - APPROACHES

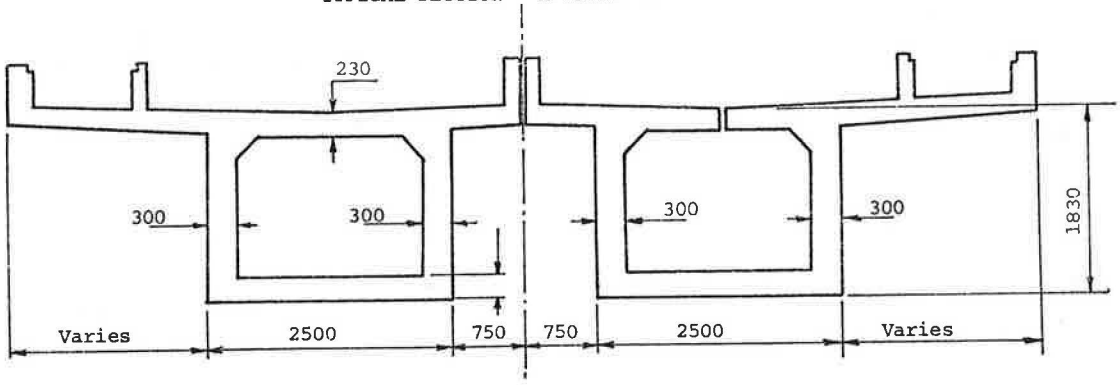

TYPICAL SECTION - VIADUCT

FIGURE 5

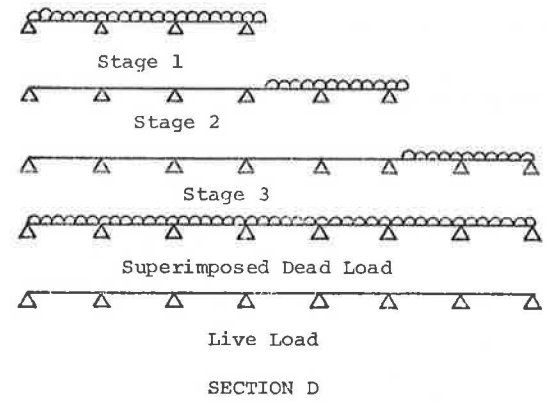

SECTION D

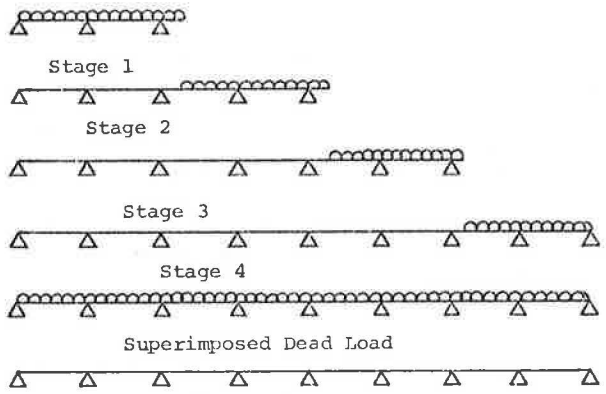

SECTION E

FIGURE 6

Casting of Units

The precast units may be cast either vertically or "right way up". The advantages of casting vertically are:-

(a) Easier to place concrete
(b) Finishing off is easier since only one end of the cross-section need be finished, and this will be sand blasted prior to final assembly.
(c) Storage requirements are less
(d) No windows and chutes are required to enable placing of the concrete in very deep sections.

Advantages of cast "right way up" are:-

(a) Easier to place formwork, since all the soffit forms are fixed
(b) Easier to place reinforcement
(c) Requires less formwork
(d) No turning mechanism is required to rotate the segments to the horizontal.

Both methods of casting are used extensively and it would appear to be purely a matter of preference by the individual contractor which method is used. For long structures with a unifrom cross-section it is often economical to design special purpose formwork. Hydraulically controlled steel formwork has recently been developed in Germany. This formwork may be stripped by only one semi-skilled operator, and formwork is collapsed and retrieved in a matter of minutes.

Joints

Joints between units may be either reinforced or unreinforced. The reinforced joint will allow diagonal tension to be carried across the joint, however, in order that account may be taken of the continuity of reinforcement, a positive tensile splice is required. This may be achieved by the welding of mild steel reinforcement either by a butt weld (with costly preparation) or by fillet welding to an angle of equal tensile strength. The size of the joint in this instance will be determined by the length of fillet weld required to transmit the tensile force in the bar. As welding of cold work reinforcement is not generally permitted, a positive screw type connection would be required to splice cold worked bars. The cost of these connections will far exceed the benefit gained by using cold worked reinforcement in lieu of mild steel reinforcement. The plain unreinforced joint is simpler to form and cast, but cannot be relied on for the transmission of tensile stresses. Joint thicknesses typically vary between 75m and 150mm, however the larger joints have shown a tendency to crack under shrinkage. Although these cracks close on tensioning they do initiate leakage paths for grout and provide an initial crack which is easily propagated by principal tension.

Torsional Strength of Units

The box girder section is used principally for its extensive torsional strength, a property which makes it invaluable for structures with horizontal curvature, and where eccentric live loads produce large torsional moments. Although the webs and to a lesser extent the deck and soffit slabs have physically large dimensions (up to 600mm) their relation to the overall dimensions makes the assumption of thin walls quite valid. Direct shear and torsional shear stresses may then be calculated on the basis of the thin wall theory (2) used for steel box sections assuming the shear stress to be constant across the thickness. Principal tensile stresses should be calculated at the critical points of the webs and flanges as shown in Figure 7.

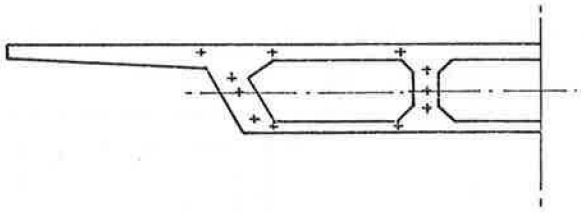

FIGURE 7

On the Nyanda Overpass calculations were made for the co-existing live load longitudinal moments, direct shears and torsion, caused by two lanes, three lanes, and four lanes loaded. The principal tensions were limited to $3\sqrt{Fc'}$. This stress limitation is in itself insufficient, as any principal tension will propogate the existing shrinkage cracks in the joints. The opening of these cracks at the surface and hence the opening

of the unreinforced joint can be minimised by ensuring that the orthogonal plane to the direction of the principal tensile stress is always at an angle, preferably greater than 15°, to the joint.

An additional problem in the segmental construction caused by torsion is the transmission of the longitudinal hoop tension across the joints. This is of particular importance at abutments and those piers where a torsional restraint is supplied. In these areas of high torsion it is necessary to provide continuity of the longitudinal reinforcement across the joint, and a full strength welded connection should be used. where the torsion moments are lower it is not necessary to use continuity reinforcement provided the longitudinals are anchored adequately. The unreinforced joint should be checked for its capacity to resist the applied torsion.

Prestressing Ducts

The use of short precast segments of up to 3m in length enables the cable ducts to be straight with all angle changes in the cable profile accommodated at the joint. The straight ducts can be set extremely accurately by inserting steel mandrels through the ducts, and locating them through prepositioned holes in the end forms. This stiffening of the ducting ensures that there will be no movement of the ducting during the placing and compacting of the concrete and as a consequence the parastic angular deviation (previously known as wobble coefficient) is quite low. Site measurements indicated extremely low values of parasitic angular deviation varying from 0.025 to 0.0025 (or 0.003 to 0.0003 per metre in the old terminology).

Horizontal Alignment and Superelevation

Structures set to horizontal curves, reverse curves or transitions provide additional problems at the joints. If the units are adjusted to take up these effects the economies achieved through uniformity of formwork will be largely reduced as each unit will require special attention to the end forms. The other alternative is to cast the units with identical external forms and take up the length variations in the joint. This was the solution chosen for the Nyanda Overpass, however, many problems were encountered during the erection stage. The Nyanda Overpass is on a reverse curve (see Figure 1) varying from 275m radius to 366m radius. The units were set with their centre lines radial and on the smaller radius the nominal 125m joint reduced to 55mm. The change in superelevation produced a sawtooth appearance with a discontinuity of 6mm to which can be added the construction tolerance of ± 6mm. This effect was even more pronounced on the inside of the curve where the joint width had been reduced. The effect at the tips of the cantilevers is masked by the parapet overhang, however at the spine of the box it is quite noticeable. The change in superelevation gave a discontinuity of 3mm at the main longitudinal cables and 6mm at the slab cables. This discontinuity was particularly important at the slab ducts which were only 19mm thick carrying a 12.5mm strand, thus allowing no tolerance for construction.

Stage Construction

Continuous bridges with more than three spans and total length longer than about 100mm suffer very large friction losses during the stressing operation, and the effective prestress available to resist flexure reaches an uneconomical level. An effective prestress of less than 50% of the Ultimate Tensile Strength is usually considered undesirable. The problem can be overcome to some extent by using low friction ducts and cold drawn strand which has a lower friction coefficient, however this will only marginally increase the economical stressing length.

Coupling

The basis of the stage method is to break the structure into a number of smaller structures with total length of cable restricted to an economical length with regards to friction losses. Each stage is then tied back to the previous stage by coupling the prestressing strands at the previously stressed anchorage. Special coupling anchorages are available from most manufacturers. Since the cables are connected to an anchorage which will be completely enclosed in concrete, it will be possible to stress all stages except the first, from one end only. Thus the economical length for subsequent stages is approximately half that of the first stage.

The coupling anchorages are necessarily bulky and require the webs to be thickened considerably, to carry the splitting forces at the anchorage. The physical size of the couplers ensures that the centre of gravity of the cables will be close to the centroid of the section and thus the logical location for the coupling anchorages will be at a point of contraflexure, i.e. about one fifth of the span length from a pier. The critical point for stresses at the coupler position will be the "dead" end side of the anchorage as the effective prestress will, in general, be less than the effective prestress at the "live" end of the same anchorage (Figure 8).

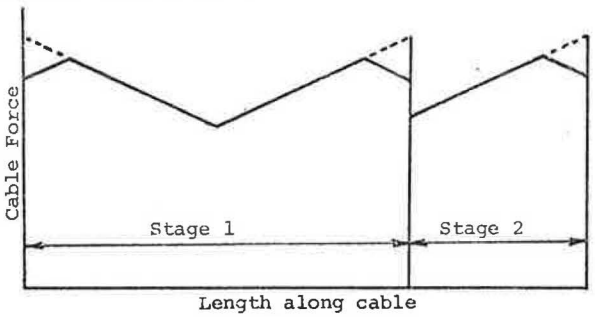

FIGURE 8

Analysis

Each stage must be analysed for self weight moments, shears and torsions, and for the parasitic moments caused by the cable profiles being non-concordant. It is assumed that the structure remains elastic and the principle of superposition may be applied to obtain the final effects. On the completion of stressing the final stage, the structure can then be analysed as a single continuous beam for superimposed dead load and live load effects, and for temperature differentials through the deck slab.

An additional advantage of this method is that as each stage is stressed and becomes self supporting, the erection falsework and formwork can be removed and used for the next stage. This provides a major cost saving for bridges with a large number of spans e.g. sections D and E of the Rail Link viaduct,

where seven and eight spans respectively are involved.

Post Tensioning

The V.S.L. System of post tensioning used for both the Nyanda Overpass and the Rail Link viaduct, the Nyanda Overpass using cables of 48 No. 12.5mm super 7 strands with an ultimate capacity of 8830 kN, and the Rail Link using cables of 27 No. 12.5mm super 7 strands with an ultimate capacity of 2970 kN.

Details of the V.S.L. coupling anchorages are shown in Figure 9.

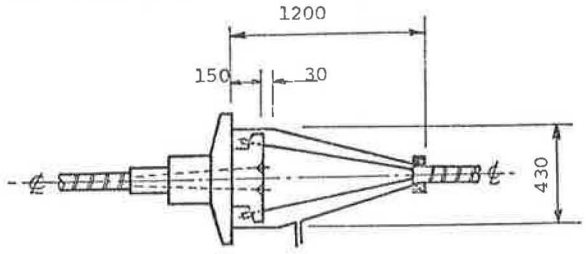

FIGURE 9

The physical size of these anchorages is such that the webs had to be increased in thickness from 300mm to 600mm for the Rail Link and from 450mm and 380mm to 790mm for Nyanda Overpass. With the extensive reinforcement required around these anchorages placing and compacting of the concrete in the webs is difficult and care must be taken on site to ensure adequate compaction of concrete is achieved. In the case of the Nyanda Overpass structure, recesses were left in the webs to allow concrete placement of the anchorages and to facilitate connection of the unstressed strands to the coupler. The recesses were then filled with concrete after the second stressing operation.

When geometric layout requires large variations in span lengths, or precludes the use of shorter end spans, it may not be possible to use the main longitudinal prestress to resist entirely the applied longitudinal moments, and additional capping cables may be required in the deck and soffit slabs. In both the Nyanda Overpass and the Rail Link small cables with four and seven 12.5mm super 7 strands respectively were used. Anchorage of these capping cables will normally occur on the inside of the box, although it is possible to anchor on the outside surfaces of the slabs and infill after stressing. This latter technique has the disadvantage of reducing the effective thickness of the slabs considerably, and this will generally far outweigh the disadvantage of forming anchorages on the inside of the box. Stressing the small cables from within the box is a relatively simple procedure requiring only adequate lighting and more particularly adequate ventilation during the stressing operation. These cables may be stressed from both ends to reduce the effects of friction losses.

Deflections

The stressing of the cantilever on each stage will result in an upwards deflection of the tip of the cantilever as the centroid of prestress will be predominantly above the centroid of the section. To ensure an aesthetically pleasing joint and to prevent an unsightly kink at the joint it is necessary to set the formwork to allow for these deflections and rotations. Allowances must be made, of course, for the final camber profile.

Grouting

It is almost impossible to produce a water tight seal to the duct connections and invariably some leakage will occur from one duct to the next. This loss can be reduced by grouting ducts in pairs. On Nyanda Overpass the length of the cables caused severe head losses during pumping and a loss of workability at the face of the grout, and the grout pump had to be moved along the bridge to the last point where grout had already vented. This process was continued along the bridge until grouting was complete.

General Features of Design

Shear Lag

The assumption of the theory of bending, that plane sections remain plane, is no longer valid for wide flange box girder bridges. The effect of shear lag over the supports may be calculated from the theory of elasticity (3) or some empirical formula. Tests carried out in England (4) produced the simple formula that the shear lag effect can be accounted for by simply ignoring the cantilever at the supports. Thus the effective cross section is only the spine of the box. The effect of the shear lag is taken from the support to a point one fifth of a span length on either side of the support. This approximation has since been checked against the German code (5) and was found to be in good agreement.

Distribution of Prestress

A more important problem in the vicinity of the supports is the distribution of the prestress, particularly through a solid diaphragm. It has been assumed, conservatively, that the axial component of the prestress is distributed over the whole of the cross section, while the eccentric component is distributed over the reduced "shear lag cross section". This assumption has lead to some structures containing unnecessary additional axial prestress in the vicinity of the supports.

Diaphragm Action

The superstructure may be supported at the piers and abutments either by a single bearing allowing transverse rotation, or by a multiple bearing system providing torsional restraint. The large shears carried by the webs must be transmitted to the bearings through the diaphragm. These transverse bending effects are resisted by prestress in both the Nyanda Overpass and the Rail Link. Detailing the intersections between the transverse cables and the main longitudinal cables requires more than ordinary care as during stressing of either the transverse or longitudinal cables there is a distinct possibility of crushing the ungrouted duct running at right angles. It may be necessary in some instances to provide a more solid duct. 6mm thick steel tubing has been used to carry the longitudinal cables through the diaphragm, in order to resist crushing during the stressing of the transverse cables.

The large capacity bearings used exert concentrated forces of up to 15000 kN to the diaphragm. The diaphragms must therefore be designed to resist the bursting and spalling stresses associated with

the application of a large concentrated force. The theories proposed for similar stresses behind post tensioning anchorages may be used to reinforce the diaphragm in the vicinity of the bearings.

Diaphragms at torsion restraint piers and abutments will require heavy reinforcement to carry the applied torsion moments.

When maintenance access is required through the boxes small manholes will be required through the diaphragm, thus complicating the detailing further.

Differential Temperatures

Thermocouple readings taken from existing box girder bridges indicate that, for the climatic conditions of Brisbane (27½°S) an almost linear temperature differential of 11°C can occur between the outside and inside faces of the deck slab (6). This figure was used for design calculation in both the Nyanda Overpass and the Rail Link, although it is expected that the temperature of the outer surface of the deck slab in the Rail Link under 450mm of ballast will be lower than under the 125mm to 150mm of hotmix surface on road bridges.

Thermocouples are being incorporated in sections of the Rail Link to verify the temperature differential.

Large Capacity Post Tensioning Cables

The 48 strand V.S.L. cables used on the Nyanda Overpass at the time of construction were the largest capacity cables to be used in Australia. The bridge contains 120 tonnes of main prestressing strand, and the large capacity cables were adopted because:

(a) There is an economy in minimising labour associated with fixing a smaller number of ducts.

(b) There is an economy in minimising the number of anchorages and couplers

(c) The larger than usual ratio of duct area to strand area indicated that lower friction values could be used, thus decreasing the losses

(d) There is a design economy associated with the force being concentrated in a fewer number of cables, thus allowing larger eccentricity of prestress at points of maximum moment.

There are, however a number of disadvantages in using this system:

(a) Any failure to achieve adequate prestress in a cable (by breaking strands etc.) cannot be rectified by increasing the prestress in other cables, as easily as in a design with a larger number of cables

(b) The jacks are very heavy and cannot be manhandled easily

(c) The large forces at the anchorages require special attention in the design of details to resist bursting stresses

(d) The large anchor plates and couplers require the webs to be thicker than normally would be required for stress considerations.

Despite these disadvantages the use of the large capacity system proved to be worthwhile.

Heavy lengths of cables were pulled through the ducts with an air winch, while for shorter lengths the individual strands were pushed through manually.

Site measurements confirmed the expectation of lower friction values with a measured coefficient of friction of only 0.12, i.e. half of the normal design value.

Conclusion

The prestressed concrete box girder bridge in its many forms provides an aesthetic, structurally sufficient solution to complex crossings. The problems encountered during these designs are no doubt universal, however the solutions discussed are those applicable to the local conditions of construction in Queensland.

Some of the aspects discussed still require further research in order to provide more economical solutions.

Acknowledgements

The author wishes to thank Mr. J. D. Snelling, the Director in charge of the Bridge Section of Cameron McNamara and Partners Pty. Ltd., Consulting Engineers, under whose general direction these designs were carried out.

References

1. Christsen C. J., and Pierce J. M. - "The Design and Construction of the Nyanda Overpass." I.E.Aust. Qld. Div. Tech. Papers. Vol. 17, No. 15, July 1976.
2. Williams D. ' "Theory of Aircraft Structures." Edward Arnold, 1960.
3. Timoshenko S. and Goodier J. ' "Theroy of Elasticity." McGraw-Hill, 1951.
4. Lee D. - "The Mancunian Way." Aust. Prestressed Concrete Group, Lecture Series, 1966.
5. D.I.N. 1050 - "Steel in Building Construction."
6. Maher D. H. - "The Effects of Differential Temperatures on Continuous Prestressed Concrete Bridges." I.E.Aust. Transactions Vol. CE 12, No. 1, April 1970.

CURRENT PRACTICE IN DESIGN AND INSTALLATION OF DRIVEN PILES

Hal W. Hunt, P.E., Associated Pile & Fitting Corp.

Tests have proved that H-piles can dependably carry heavier loads than usually are assigned to them. Concrete and timber piles are being loaded heavier. Prestressed concrete piles benefit from improved splicers. Gaining in use are H-pile extensions for precast. The H end, with cast steel protection, can assure penetration into compact material; it can prevent sliding of sharply battered piles or piles driven on steeply sloping rock; it provides protection to the vulnerable end of a precast pile. An import from Europe is an interlocking deep-web H that can be used with sheet piles for cofferdams or a strong wall. Improved mandrels have increased use of corrugated shell piles. The wave equation is increasingly used for determination of driving stresses and selection of the optimum combination of pile and hammer. Dynamic measurement gives instant pile capacity information at minimum cost. More adequate soils investigation and foundation planning can reduce overall cost.

Recent comprehensive tests have proved that H-piles can dependably carry heavier loads. Use of H-section extensions on precast piles makes it practical to drive on to sloping rock or to penetrate dense materials such as boulder-filled tills. Precast piles--most often prestressed--are gaining in use.

Pipe piles currently are used less than in the past but are preferred by some as the inside of the pile can be checked after driving; especially for waterfront work they can be made large for the loads and lateral strength needed. Corrugated shells, installed with a mandrel and filled with concrete, continue to be a popular design for larger projects where soils are suitable. Timber still is used in quantity for lighter loads. Augering to place concrete as a deep shaft without driving is expanding but is outside the scope of this presentation.

Diesel hammers are used very widely--especially for moderate size bridge projects where a relatively few piles are needed for each of several supports. Steam-air hammers are used extensively in urban areas, following long-established work practices. The heavy ram, and short stroke of the single-acting steam-air hammer has generally been found preferable for driving heavy precast piles. In some soils more rapid strokes may drive even the large displacement piles faster. Diesel hamers require resistance to driving to continue firing. Steam-air hammers may work more satisfactorily where initial driving is through very soft materials. (Ref. 1)

Steam hammers are popular for use on floating rigs where boilers may be part of the equipment for other needs. If a compressor or boiler is conveniently available, it may be preferable to use an on-hand steam-air hammer rather than purchase or rent other equipment. Economy of this should be carefully checked. Drop hammers are not much used in the U.S. but continued satisfactory results elsewhere may result in a resurgence of their use. A Swedish development provides for rapid lifting by hydraulic means, then a free fall for a heavy drop. Load bearing capability of driven piles is being quickly checked by dynamic information fed into a job site computer.

Design loads generally have increased for all types of piles. More dependable subsurface data, more knowledgeable interpretation of test results, plus improved installation methods and inspection procedures have made this practical. This has reduced the factor of safety, which in the past may have been a factor in avoiding unacceptable settlements.

H-piles At 18,000 PSI Working Stress

Under American Iron and Steel Institute (AISI) sponsorship extensive tests on driven long H-piles provided verification for loading A-36 steel to one-half of its 36,000 psi yield strength. This is 248 in SI MPa units. The tests were made at Bethlehem Steel Corp.'s construction of a blast furnace at their Sparrows Point, MD, plant. The tests were planned and conducted under supervision of Thomas D. Dismuke, Chairman of the AISI Subcommittee on Steel Piles and a consultant in the Technical Services Engineering Department of Bethlehem Steel Corp.

Soils under the furnace are sedimentary, mostly sand, gravel, clay and silt. The first dependable bearing strata is at 27 m (88 ft) depth. Test and production piles were driven to 30 to 33 m (100 to 110 ft) to obtain adequate support for the blast furnace. Several piles were test loaded; some were instrumented and a few were pulled. For one, a 560 mm (22 in.) diameter casing was driven to 28 m (90 ft) and cleaned out to 24 m (80 ft) then an HP 360 x 108 (14 x 73) driven inside the pipe to bearing in the sand. This eliminated frictional

support of the upper fine-grained soils to give dependable bearing capabilities. Pile tip movement after driving and test loading, to over 450 tonne (500 tons), was roughly twice as much for the pile driven inside the protective casing. But net settlement after removal of load was less than half as much for the protected pile as for the one driven full-length through the soil. (Ref. 2) Conclusions in the referenced article include:

1. The tested piles can be normally driven to safely support loads at stress levels exceeding 0.5 f_y.
2. The current use of the concept "freeze" is not adequate to predict the load capacity difference between results of pile tests and wave equation solutions.
3. The wave equation was very inaccurate in the prediction of the driving stress.

Properly, many codes and jursidictions are cautious about use of half the yield strength of steel as a safe loading for H-piles driven into unknown obstructions in the underground. After considerable study New York City accepted .35 f_y or 86.8 MPa (12,600 psi) on A 36 steel. This has been in effect for a few years. No problems are known to have developed from this if adequate safeguards and inspection are given to installation. But Boston still has 58.6 MPa (8,500 psi) as the upper limit in its code. The American Association of State Highway and Transportation Officials specifies 6.2 MPa (9,000 psi) where test or other means are not used to prove greater strength value.

Bethlehem Steel Corp. used cast steel point protection on piles driven in critical areas. Such points have become quite common for use on H-piles driven into difficult ground. Observation of pulled H-piles and soldier piles where excavated to below their tips, show that point reinforcement can be most helpful in enabling the pile to penetrate to desired strata in dependable bearing conditions. Close observation at two test sites provide details.

Interlocked H-sections For Deep Cofferdams

From Arbed in Luxembourg come interlocking H-piles arranged for use with steel sheet piles. The H-piles can be used as a high section modulus continuous wall with an interlocking bar connection. Or, they can be used as mater piles with a pair or more of Z type sheet piles between them. This reduces the section modulus per linear length but also the amount and cost of the steel.

The interlocking H-sections are available in several configurations at about 0.58 to 1.00 m (23 to 39 in.) web depth and flange widths of 360 to 460 mm (14 to 18 in.). Sections are available in different web and flange thicknesses. Several shapes of sheet piles from Arbed interlock with the deep H-sections to give a wide choice of section modulus and wall strength.

Figure 1. New from Europe is an interlocking deep section H with high section modulus for cofferdams or dock walls. Interlocking Z sections can be alternated to reduce steel weight and cost.

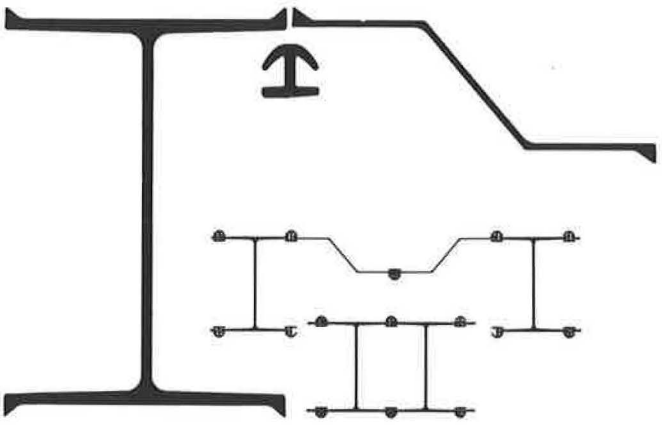

Figure 2. For a bridge over the Columbia River near Portland, cast steel points protect the interlocking H-sections for driving through boulders.

Figure 3. One side of the connecting bar is cut back a little at the top to ease threading of the front and rear interlocks.

Where a continuous H wall is used with the interlocking bar on both face and rear the wall can be exceptionally watertight. For special conditions clays or other materials can be puddled between the H-sections.

Tests Prove H-pile Value

H-piles Replace Caissons

On a project in a mixed limestone area the owner asked that a test be made using H-piles for a parking garage where caissons on a nearby job had far overrun the contract amount. At a shallow area and

at a deep area, some 100 m (330 ft) apart, an HP 250 x 62 (10 x 42) was specified to have cast steel point protection. At the deep area a comparison HP 250 x 85 (10 x 57) was required. The contractor for the test installation elected to drive reaction piles to develop the test load. HP 310 x 79 (12 x 53) were used as tension piles--without end protection.

Figure 4. With cast-steel end protection H-piles can be driven into medium hard rock. Note how the contractor utilized salvaged guard rail.

On the test at the shallow area the HP 10 x 42 with point protection and six HP 310 x 79 (12 x 53) reaction piles were driven to a moderately hard limestone with a Link Belt 440 double-acting diesel hammer, rated at 2520 kg-m (18,210 ft lb). After testing the HP 250 x 62 (10 x 42) to the desired load the seven piles were pulled. All six of the unprotected HP 310 x 79 (12 x 53) were damaged, see photo. The HP 250 x 62 (10 x 42) test pile, with a cast-steel point was the only pile not damaged. Significantly, none of the experienced pile driving crew were aware of the damage to the piles.

At the deeper area of the site the test pile and comparison pile were driven to 90 ft depth. The unprotected HP 250 x 85 (10 x 57) was twisted into a "bow-tie" at the tip, with undependable bearing capability. The HP 250 x 62 (10 x 42)--with a 10 kg (23 lbs) cast steel point but some 590 kg (1,300 lb) less steel--was damaged. Some HP 310 x 79 (12 x 53) reaction piles were mangled on small boulders at 7 m (23 ft) depth--above material resisting only four blows on a standard sampling spoon. Several piles could not be pulled, probably because they were badly distorted by driving onto obstructions. (Ref 3)

Figure 5. Test pile HP 250 x 62 (10 x 42), 3rd from right with point protection was unharmed by driving that damaged all six HP 310 x 79 (12 x 53) driven as reaction piles.

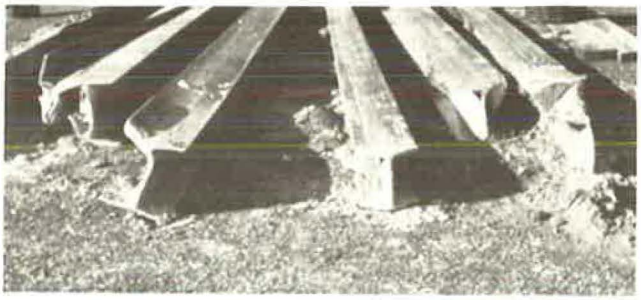

Through Muck To Rock On Ohio DOT Tests

The State of Ohio, with Federal Highway Administration funding, experimentally drove H-piles through 7 to 8 m (23 to 25 ft) of soft silt then directly on to a hard limestone to obtain guidance for foundation design. Three piles were driven with each of five hammers to develop comparisons of driving capabilities and characteristics. (Ref. 4)

Figure 6. Piles were driven with five different hammers. The vertical and adjacent batter pile were driven with a Link Belt 520 (3,640 kg m or 26,300 ft lb). Next pile was driven with a Vulcan 08 (3,600 kg m or 26,000 ft lb). Hammer seen is a Kobe 25 (7,000 kg m or 50,700 ft lb). Case-Goble device for instantaneous determination of pile capacity is seen in the van.

Table 1. Pile hammers used in Ohio DOT Tests. (From manufacturer's published data) The Link Belt is a double-acting diesel; the Vulcan is single-acting, air powered; the Kobe are single-acting diesels; the MKT is double-acting, air powered.

Hammer	Energy		Ram Weight		Total Weight		Strokes
	Kg m	Ft lb	Kg	Lb	Kg	Lb	Minute
Link Belt 520	3,640	26,300	2,300	5,070	5,670	12,550	80-84
Vulcan 08	3,600	26,000	3,630	8,000	7,600	16,750	50
Kobe 13	3,400	24,400	1,300	2,860	3,600	8,025	45-60
Kobe 25	7,000	50,700	2,500	5,510	5,950	13,100	39-60
MKT 9B3	1,210	8,750	720	1,600	3,170	7,000	145

A vertical pile and a pile on a 1:4 batter were driven with each of the five hammers listed in Table 1. An additional HP 250 x 62 (10 x 42) with a cast steel tip reinforcement was driven with each of the four more powerful hammers. It was not thought necessary to protect the end of a pile driven with the 1210 kg-m (8,100 ft lb) hammer; but when pulled both the vertical and batter piles driven with the small hammer were found to be damaged beyond end-bearing capability. (The paper at this seminar by Ray Grover of the Ohio Department of Transportation covers this in more detail.)

Figure 7. Pile at left, with point protection, was driven with the Kobe 25, a 7,000 kg m (50,700 ft lb) hammer as was the third pile. Others in Ohio test were driven with smaller hammers.

Photos show the driving and some of the pulled piles on the Ohio DOT tests. It should be emphasized that these piles were driven through a soft silt then suddenly on to a hard limestone. It has long been recognized that tip protection is essential under this condition. The U.S. Steel Corp. booklet on H-piles states: "If impenetrable rock is overlaid with soft material with little horizontal stability, the pile tip must be built up with points."

Pile Capacity By Dynamic Measurement

The driving was monitored by the Case-Goble method of dynamic pile capacity determination. This is based on the now widely accepted wave equation. The Pile Analyzer records strain and acceleration in a unit that has been developed to a size that can be put into a couple of suitcases for air transport or taken to a job by car. With knowledge of pile type, size, and length an instantaneous determination of total capacity can be made.

This system was developed by Prof. George Goble while at Case-Western Reserve University in Cleveland. Dr. Goble is now Chairman of the Department of Civil, Environmental and Architectural Engineering at the University of Colorado, Boulder, CO. These units are finding increasing use for checking pile capacity; they are available for purchase or rental at moderate cost. More than 20 driven piles can be checked for capacity in half a day with a mobile crane, an efficient hammer, and a crew experienced with the device. It can be used for timber, precast concrete, H and pipe piles.

Transducers are placed on top of the pile or attached to a side and connected to a recording device. The force and acceleration during driving are recorded in analog form on magnetic tape. The tape record can be converted to digital form and further processed using FORTRAN software.

Returning to the Ohio tests, the Case-Goble computer recorded good capacity for all piles at the first blows as each pile struck the limestone. But after a very few blows on piles without end protection the indicated capacity dropped off rapidly; the hammer-pile sound became a dull thud. The pile continued to move down, as if it were penetrating the limestone. When pulled, the piles were found to have the tips badly mangled. (See photo.)

Piles with the protection of cast steel points stopped moving when the limestone was struck. The sound continued to be a live "ring"; the computer showed increasing capacity for each of the piles. Under continued driving with powerful hammers the piles with point protection started to buckle in column failure in the 2.5 m (8 ft) length above the ground. There was no evidence of column bending from driving in the length embedded in the soil on any of the piles.

Another job reported in the Ohio DOT test series involved HP 10 x 42 driven into a shale. Here all piles installed and tested performed satisfactorily. H-piles are being driven into boulder-filled stream beds and through dumped rock. With end proteciton, H-piles can be driven straight enough that they can be used as a single line column support exposed up to the superstructure.

Laboratory Tests Develop Reasons For Pile Deformation

After loading H-piles--with and without point protection--to failure in a laboratory compression machine, Dr. Roger Slutter, director, Fritz Engineering Laboratory at Lehigh University had comments as briefed here.

"The flanges of a steel pile at the tip are very susceptible to buckling when the tip of the flange encounters resistance in driving. The AISC and AREA specifications give limits on the ratio b/2t and the AASHO specifications give a limit of b/t as a means of indicating when the flange width of a section is such that the section can be described as a compact section (b is width, t is thickness of flange). For ASTM A 36 steels the limit of b/2t suggested is 8.5. For all pile sections except HP 250 x 85 (10 x 57) the ratio of b/2t exceeds 8.5.

Figure 8A. Loading under corners of H caused early failure in Lehigh tests.

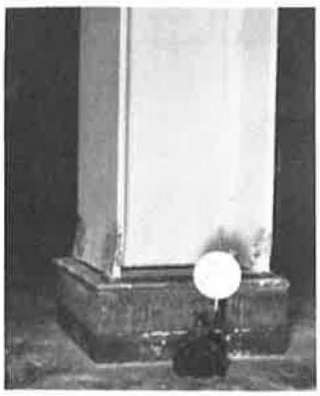

Figure 8B. Loading under web through cast steel point distributed load.

"All rolled sections have residual stresses formed when the section cools after rolling. The flange tips, which cool first, have a compressive residual stress and webs have a tensile residual stress. The compressive residual stress in the

flange tip for light steel sections of similar shape is about 914 k-cm^2 (13 ksi). To this must be added the stress from driving. For a pile cross section the flange could be expected to buckle at a compressive strength of 1406 k-cm^2 (20 ksi) would produce buckling.

"For a load under the web of a pile that has a tensile residual stress of the order of 492 k-cm^2 (7 ksi), it would require an applied stress of 1900 k-cm^2 (27 ksi) to buckle the web. Since pile sections have the same web and flange thickness, the pile tip performs far better when the web is the first to meet resistance in driving. The highest tensile residual stress is found at the junction of the web and flange. When the tensile stress generated by buckling is added to the tensile residual stress the flange will tear from the web at stress levels lower than the yield stress. This explains why driving without end protection is so variable.

"Pile points overcome the unfavorable geometry of the pile cross section in several ways: They have a more favorable b/t ratio than the pile cross section; They do not have the unfavorable residual stress distribution that exists in the pile section; They tend to distribute the load more uniformly over the cross section of the pile regardless of what point first encounters resistance. Finally, they provide bracing for the delicate flange corner." (End of comments by Slutter; Ref. 5)

Additional H-pile Sections

New in the H-pile field are additional sections in the 310 mm (12 in.) depth and a series of 330 mm (13 in.) H. These are, or are to be, rolled by Armco at Houston and Inland in the Chicago area. Neither Armco nor Inland can roll the conventional 360 mm (14 in.) with up to 378 mm (15 in.) wide flanges of the H sections. The fabricators expect to have a sales advantage with the 13 in. H. Some suppliers are equipment makers are unenthused about required additional sizes and inventories. But American Iron and Steel Institute has accepted the new sizes and worked out dimensions for them. Table 2 gives metric and conventional details.

H-piles are available in a wide range of sizes and areas to meet any load-bearing requirement. They are easily handled; they can be extended to any length. If an end or section is damaged, the rest of the length can be salvaged at little cost. Splices can be made by conventional full penetration welding. More popular is a manufactured unit with flared ends, which slips on one end of a pile then safely and quickly aligns the added length and assures that the ends stay in line. The splice is two shop fabricated U sections with an accurately positioned spacer. The outside of the flanges of the top length of H is beveled. The splicer is slipped on the pile; a short fillet weld is made to the flange near each corner of the U-shaped splicer. The new length is positioned on the driven length. A penetration weld is made along the full width of each flange to complete the joint.

Pipe Piles - Driven Open or Closed End

Use of pipe piles in the U.S. varies considerably from year to year. Currently only occasional projects are designed with pipe piles--despite the fact that engineers like the opportunity to look down the tube to assure themselves all is well. Pipe driven open-end, cleaned out to rock and again driven for firm contact, then filled with high quality concrete is allowed high loading under most jurisdictional codes.

Pipe to be driven open-end as a pile should have a minimum outside diameter of 254 mm (10 in.) and wall thickness of 6.3 mm (0.25 in.). Wall thickness for 356 mm (14 in.) and larger pipe should be 7.9 mm (0.310 in.). Pipe more than 450 mm (18 in.) should be at least 9.5 mm (0.375 in.) wall. Stress usually allowed is 0.35 f_y on ASTM A 272, pipe; stress on concrete fill may be 0.33 f_c; in the past a top limit of 6.9 MPa (1,000 psi) has been common, but this has been increased.

Wall thickness must be gaged to driving obstructions and expected end contacts. Driving shoes of cast steel are used to protect the end of the pipe. Such shoes usually are an outside type with perhaps 9.5 mm (3/8 in.) extension beyond the pipe. This may reduce friction while driving; this generally is accepted as being desirable. An inside shoe is available; it is preferred, and needed, in permafrost where the soils do not reform and friction along the pipe is essential. It is difficult to do chopping and cleaning in the pipe when an inside shoe is used.

Both types of cast steel shoes attach with a minimum of welding as they have a square ledge on which driving is done in compression. This contrasts with wrapping a hardened, thick structural plate around the pipe and attaching it by welds in shear. Special techniques and perhaps heat-treating are required.

An extension of the open-end pipe is the Drilled-In-Caisson. The open-end pipe is driven to contact, cleaned out and a hole drilled into the rock at least 30 cm (1 ft) deeper than the diameter of the

Table 2. H-Shapes Table A1.4 From American National Standards Institute/American Society for Testing and Materials publication A6-77b provides details of new H-shapes.

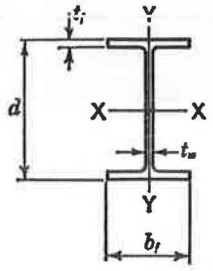

Designation (Nominal Depth in Inches and Weight in Pounds per Linear Foot)	Area A, in.^{2}	Depth d, in.	Flange		Web Thickness t_w, in.	Designation (Nominal Depth in Millimetres and Mass in Kilograms per Metre)	Area A, mm^2	Depth d, mm	Flange		Web Thickness t_w, mm
			Width b_f, in.	Thickness t_f, in.					Width b_f, mm	Thickness, t_f, mm	
HP14X 117	34.4	14.21	14.885	0.805	0.805	HP360X 174	22 200	361	378	20.4	20.4
X 102	30.0	14.01	14.785	0.705	0.705	X 152	19 400	356	376	17.9	17.9
X 89	26.1	13.83	14.695	0.615	0.615	X 132	16 800	351	373	15.6	15.6
X 73	21.4	13.61	14.585	0.505	0.505	X 108	13 800	346	370	12.8	12.8
HP13X 100	29.4	13.15	13.205	0.765	0.765	HP330X 149	19 000	334	335	19.4	19.4
X 87	25.5	12.95	13.105	0.665	0.665	X 129	16 500	329	333	16.9	16.9
X 73	21.6	12.75	13.005	0.565	0.565	X 109	13 900	324	330	14.4	14.4
X 60	17.5	12.54	12.900	0.460	0.460	X 89	11 300	319	328	11.7	11.7
HP12X 84	24.6	12.28	12.295	0.685	0.685	HP310X 125	15 900	312	312	17.4	17.4
X 74	21.8	12.13	12.215	0.610	0.605	X 110	14 100	308	310	15.5	15.4
X 63	18.4	11.94	12.125	0.515	0.515	X 93	11 900	303	308	13.1	13.1
X 53	15.5	11.78	12.045	0.435	0.435	X 79	10 000	299	306	11.0	11.0
HP10X 57	16.8	9.99	10.225	0.565	0.565	HP250X 85	10 800	254	260	14.4	14.4
X 42	12.4	9.70	10.075	0.420	0.415	X 62	8 000	246	256	10.7	10.5
HP8 X 36	10.6	8.02	8.155	0.445	0.445	HP200X 53	6 840	204	207	11.3	11.3

pipe. A heavy H-section may be set into the pipe and socket; it may extend to the surface where a milled contact can be made to directly support major columns of power plants and the like. For lighter loads of H-section or reinforcing bars twice the depth of the rock socket may extend above the rock to transfer load to the pipe. In this arrangement loading has been allowed as high as 0.35 f_y (with f_y taken as not greater than 241 in SI, MPa units or 35,000 psi) on the pipe; 0.45 f_c (up to 13.8 MPa-2,000 psi) on concrete and 0.50 f_y on protected steel in the core.

Conical Points For Closed-End Pipe

Pipe is most often installed with the bottom closed with a conical point or flat plate. Conical points are quite generally preferred. Flat plates may be used because they are cheaper. Pipe thicker than 3.1 mm (1/8 in.) is usually allowed working stress. Pipe with a wall thickness less than 4.7 mm (0.188 in.) generally must be driven with an inside mandrel. Even the 4.7 mm (0.188 in.) wall requires special care; pipe 6.2 mm (0.25 in.) thick will withstand ordinary driving.

Conical points push the soil aside, compressing rather than displacing it so maximum friction is quickly restored. They also distribute the load to the entire periphery of the pipe at obstructions and final bearing. The 60 degree configuration seems best for penetration and for resistance to damage. Flatter points on large diameter piles have been known to have difficulties. Outside-flanged points can be beveled so attachment can be made without welding; swabbing on a little roofing tar will take care of severe water conditions. The inside-flange concial point requires welding as it is not practical to make it to the many inside dimensions of different wall thicknesses. Additionally, the pipe might split from hard driving over an inside flange.

Flat plate closure on pipe piles is said to develop a cone ahead of the driving similar to the conical point. It has been found when testing piles that this compressed cone slowly spreads to the surrounding soil and may permit continuing movement. This delays completion of a test and introduces questions about possible settlement of the structure.

Splice Pipe Piles Without Welding

Like H-piles, pipe can be economically adjusted to different lengths and unexpected conditions. Cut-offs can be salvaged for reuse. Pipe can be extended readily by adding sections. For butt welding the upper sections should have the contact end beveled for good penetration. (The driving end of the pipe should be left square for the hammer.) For welding, a spacer bar with break-off nibs is available for insertion in the pipe for back-up.

A tapered outside splicer, with a square-ledge stop at the center, can be set on the driven length and the added length driven down into it. This swages the two ends tightly into the splicer bar to make a friction joint without welding. The same splicer device is available without taper for welding on the bottom section while in convenient horizontal position. Driving can be done on the splicer. Another length of pipe can be set in and welded down-hand. This is especially useful where headroom for driving is small and several splices must be made adequate to resist uplift. The splicers also are useful for underpinning; here they are usually installed without welding as the jacking is axial on the square end of the pipe.

Corrugated Shells and Uncased Piles

In recent years several mandrels have been developed for installing uniform diameter corrugated shells for silling with concrete. Shells are made by several fabricators and generally are 12 to 18 gage with 12 x 50 mm (½ x 2 in.) corrugations. They are welded or crimped watertight and have a pan or boot for end closure.

Shells are pulled up over the mandrel which is then pneumatically, hydraulically or mechanically expanded to fit into the corrugations, Figure 9. This holds the shell firmly while driving is done and others make mandrels; most of these are available on a rental basis. Step-taper piles generally are driven with a non-expanding core, which drives by contact of shoulders at size changes of the shell--usually 2.4 to 3.6 m (8 to 12 ft). An enlarged precast concrete tip with a corruaged shell cast into its center and extended to lengths needed has proven effective in some soils, Figure 10. An earlier practice of driving a closed-end pipe mandrel, filling it with concrete and withdrawing the pipe to leave an uncased shaft in the ground has been almost entirely replaced by augering a hole for the concrete.

Timber Piles

Timber piles are used for support of many structures and for waterfront needs. Clean-up of pollution in some harbors has made the waters hospitable to marine organisms that destroy piles. Structures in such harbors should be frequently examined to determine that support capacity continues adequate.

The American Wood Preserves Association have been effective in increasing the allowable loads and permissible stress on timber piles. Some engineers feel this may have gone too far. Use of steel to provide end protection for wood piles is increasing. A "boot" that covers the full available area of the pile is substantially more effective than use of a point that requires cutting is not symmetrically done.

Most timber piles installed currently are creosote treated. Piles that will always be below a permanent water table, as for many bridge foundations, can be untreated at a substantial savings. Sometimes untreated

Figure 9. Guild mandrel.

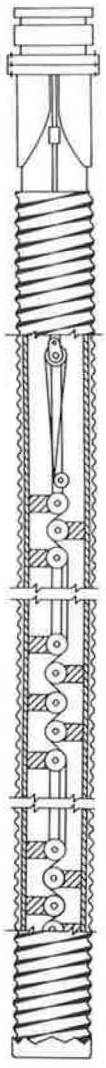

Figure 10. Enlarged precast tapered tip.

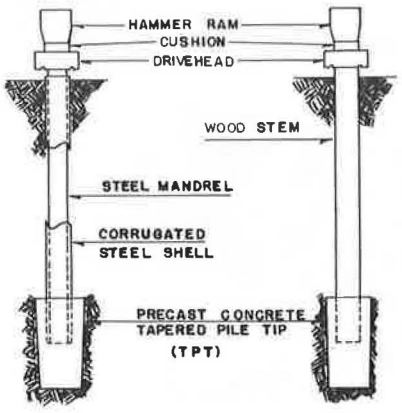

timber may be used for a lower section of pile with cast-in-place concrete for the length above permanent ground water. A casting is available for attachment by welding to corrugated shell; barbs for driving into the top of a driven length of timber. A pipe mandrel is placed inside the shell for driving the timber to greater depth and drawing the shell down with it for filling with concrete. Similar connections are available for pipe or fluted steel lower ends with corrugated tops.

Precast-Prestressed Piles Gain In Use

Precast--and usually prestressed--piles are a growing foundation support material. They have their tip problems as well as splicing difficulties. Splices are avoided where possible.

Big equipment makes it practical to cast and drive in up to 30 m (100 ft) lengths; piles may be substantially longer where they can be set in deep water. In New Orleans in the deep silts of the Mississippi River Delta 20 to 30 m (65 to 100 ft) lengths may be spliced to reach very deep bearing strata. Many means of splicing precast piles have been developed; all concerned with long precast piles keep striving for the perfect splice.

Current practice is covered in a Prestressed Concrete Institute committee report "Recommended Practice for Design, Manufacture and Installation of Prestressed Concrete Piling." This appeared in the March-April 1977 Journal of the Prestressed Concrete Institute (150 N. Wacker Drive, Chicago, IL 60606) and is available as a 32 page reprint. Details of splicers and some comprehensive tests are in a reprint form the PCI Journal, No. 5 and 6 in 1974.

H-Stubs For West Coast Prestress

A recent development with precast piling is use of H-pile extensions for penetration in difficult ground. The H provides a toe hold in rock encountered at a sharp angle to the pile axis as well as protection for the concrete end. With a cast steel point on the H-stub it has been practical to penetrate into boulder-filled glacial till at a dock for the new Trident, the world's largest submarine. For this Pacific Northwest installation 610 mm (24 in.) octagonal prestressed concrete piles had a HP 360 x 152 (14 x 102) extension with cast steel point.

Figure 11. For the home port of the Trident Submarine on Puget Sound, H-stubs on 24 in. prestressed piles provided for driving into dense till.

This could penetrate to develop needed uplift resistance for piles more than 30 m (100 ft) long. The H was connected by welding to a plate that had ten No.11 bars 1.2 m (4 ft) long attached to the other side. The bars were slipped into the 370 mm (14½ in.) center void of the 610 mm pile and grouted in.

A nearby project for the Port of Vancouver, WA, on the Columbia River, utilized HP 360 x 132 (14 x 89) attached to 460 mm (18 in.) octagonal prestressed piles, Figure 12. It was found that with a cast steel shoe an H-pile extension could penetrate very dense gravels of the Troutdale formation for 10 m (30 ft) to develop 40 tons resistance to uplift. Unprotected H-ends were damaged and could not be driven deeply into the till. (Ref. 6)

Figure 12. Prestressed 18 in. octagonal pile with HP 360 x 132 (14 x 89) tip.

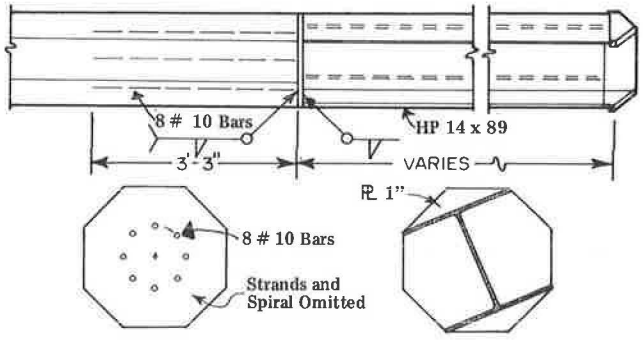

H Protection For Prestress In New York

In New York harbor prestressed concrete is desirable to minimize corrosion in the exposed length. Rock slopes sharply so H-pile ends are needed to secure bearing and minimize breakage. On test piles for a proposed convention center HP 360 x 174 (14 x 117) were cast 2.4 m (8 ft) up into 610 mm (24 in.) square prestressed piles and extended a few feet beyond the end of the concrete. Needed lengths of H were attached as extensions to reach required depth.

Hard driving on sloping rock damaged the end of unprotected piles. With a cast steel point a pile was driven without damage to 342 blows of a 8,300 kg m (60,000 ft lb) hammer for 10 mm (3/8 in.) penetration in a futile attempt to reach a deeper rock line erroneously indicated on plans. Point, pile and hammer all withstood this terrific overdriving.

The Wave Equation

By use of a differential equation that describes the mechanics of force transmission along an elastic rod (pile) that has been subjected to a mass having a specific initial velocity a Wave Equation has been developed. From this the energy transmission and the stress at any point along a pile being driving can be computed. This was first described by E.A. Smith, then Chief Mechanical Engineer of Raymond Concrete Pile Co.

All Elements Are Considered

In the wave analysis the propagation of the stress wave by a particular hammer operating under specific conditions is analyzed. This is done for each finite element of length. An almost infinite

number of computations are required, made practical only by use of a computer.

Elements considered in anaylsis include: the soil into which the pile is to be driven; the piles selected for consideration, their weight, stiffness and length (splices add another element as wave propagation through them changes); the hammers available, the weight of the ram and its impact velocity, plus the characteristics of the driving cap, cushion blocks and the like.

The wave equation is the only method currently in use for determining the stress in a pile while it is being driven. This is a much greater stress than is developed under the static load of a structure.

The wave theory is valuable in planning for installation of large heavy piles, especially in precast concrete. It is helpful in selecting the hammer-cap block-cushion combination that will be most effective in installing big piles.

Wave Equation Has Limits

The wave equation is a theoretical solution rather than the empirical solution of most pile formulas. It describes only the structural dynamics of soil, pile and hammer. It does not solve the associated soils mechanics problems or infallibly predict the length of pile.

Like other foundation aids the wave equation will assist but cannot replace the judgment developed from experience in the field of pile driving by engineers and contractors.

Unsolved Problems

The foundation field probably will always have unsolved problems. Design and construction move out into areas previously thought unusable. Heavier loads are put on longer piles to be driven under tougher conditions. Foundations always area challenge to more economical and dependable solutions. No two sites are alike; even adjacent piles may be substantially different in driving characteristics and resistance to hammer blows. There will always be a need for experienced and competent foundation anaylists.

Negative Friction

Like the weather, everybody talks about downdrag or negative friction on piling, but no one has found a practical solution. It is recognized as a problem in many soils where consolidating clays will grip the bitumen has been placed on precast concrete piles. Handling piles with bitumen soft enough to alleviate friction is difficult and costly. An English contractor, who has installed such piles, has commented that on some work adding piles to carry the downdrag would have cost no more. It would have been less messy and perhaps more dependable. Applying soft bitumen to H-piles is not known to have been done successfully.

At Knoxville, Tennessee, fly-ash was used around HP 250 x 62 (10 x 42) in an attempt to prevent adherence of the weight of 7 m (22 ft) of compacted fill above a compressible strata. The piles were coated with 3 mm (1/8 in.) of rather hard bituminous material. A 25 mm (1 in.) square bar 280 mm (11 in.) long was welded transversely across the outside of each flange of the 3 m (10 ft) above the tip of the 15 m (50 ft) length to open a larger hold as the pile was driven.

Specifications required that fly-ash be mounded up around the H while driving so that it would follow down along the pile. Fly-ash is a hard-burned, microscopic-size waste by-product of coal-fired power plants. It is non-absorptive--essentially small roller bearings. Fly-ash used amounted to 10 mm (3/8 in.) of thickness around the length of the pile to which it was applied. There was no attempt to even-out its distribution. Funds were not available for testing to determine the value or amount of the fly-ash coating. Bentonite was considered for this application but the fly-ash was thought to be easier to handle on the job site.

Pile Corrosion Is Spotty

For piles driven into most ground and capped below the surface corrosion of steel is not a problem. But it should always be a consideration where piles are exposed even in fresh water as alternate wetting and drying and sulphates speed deterioration. Bituminous coatings, preferably shop applied after cleaning to white metal, is effective if it can be kept on during handling and driving.

Exposure in salt water and salt atmospheres frequently causes rapid deterioration of steel. Tie rods holding sheet pile walls are especially vulnerable. Extensive corrosion is often found in the tidal/splash zone. Butt welds deteriorate rapidly under some conditions, due to galvanic action. This has caused complete failure of support for some structures.

Cathodic protection can be used to direct corrosive forces to sacrificial anodes. For some areas it is essential. But it requires monthly inspection and maintenance; this can be expensive. Prestressing concrete piles helps to close cracks and prevents water getting to the steel to cause rusting and progressive spalling of the concrete.

Jacketing Can Be Effective

Concrete jacketing of steel piles can be effective. If practical this should be carried to below the mud line. Galvanic action has been known to occur between steel in contact with concrete and steel at contact with water.

American Seaport, February 1978 issue, reports that the Port of Los Angeles Testing Laboratory has developed a method of heat shrinking a 20 mil polyethylene jacket around the circumference of a wood or other circular pile. There is other information. (Ref 7)

Lessons From Exposed And Pulled Piles

Soldier pile installation is of special interest to pile designers and installers. Where driving and subsequent excavation is to rock the ends of the piles may be exposed *in situ*. The strata and obstructions through which the pile is driven and the conditions of the end can be evaluated. Sheet piling also is often exposed full length inside a cofferdam. Pulled piles, extracted for test observation or for salvage and reuse, give an excellent indication of how all piles fare under similar conditions.

Design for bracing and tie-back systems for cofferdams and excavations are beyond the scope of this paper. Sheet piling booklets of Bethlehem Steel Corp. and United States Steel Corp. have excellent design information. A reprint of a series of articles from CONSTRUCTION METHODS AND EQUIPMENT on "How to Work with Sheet-Piles" is available from

L.B. Foster Co. and some sheet pile manufacturers.

Piling Can Cost Less

Piling can cost the owner less if he can be convinced of a few simple facts from the start:

1. It is his site--with its inherent problems.
2. Adequate subsurface investigation pays off in more economical design, fewer on-site surprises.
3. Test piles should be driven, tested and pulled in advance of final design and results utilized to plan and specify the least costly foundation.
4. All information about the subsurface must be given prospective bidders. Witholding pertinent data that is known--or should have been known--can be a basis for a valid claim.
5. The engineer, with the owner's knowledge--and particiaption, if possible--should discuss field conditions with a reputable local pile contractor in the early stages of design.
6. Specify by name what is wanted. Detail acceptable alternates in preference or addition to "or equal".
7. Do not try to make the contractor responsible for all the unknows of the owner's land or for replacement of piles that meet the specification and are installed as has been specified.
8. If a site can be expected to have installation problems provide for them rather than wealing them to the contractor. A competent contractor will include enough in his proposal to cover unknowns that are not provided for in the bid documents. If there are no troubles, he has an unearned profit. An inexperienced contractor may take a hopeful chance. If there are problems, he goes bankrupt; the bonding company dilly-dallys; the job is delayed; the engineer contributes extra time and energy; and the owner pays.

For jobs where pile driving may be a substantial part of the contract (perhaps not applicable to small bridges) two additional suggestions may be helpful:

9. Provide separate payment for mobilization and moving out pile driving equipment. On a unit pile length contract that overruns the contractor may be entitled to an excessive profit; it lengths substantially underrun, he will be seriously injured and will claim additional payment. The owner pays more. Paying separately for moving on and off keeps the unit price for driving low so inequity from length variation is minimized.
10. Pile installation is one of the early activities. Construction above it may continue for a year or two until the last door is hung and painted. Provide in the contract for payment in full to the foundation contractor within a short time after that part of the work is satisfactorily completed. The general contractor will not have to listen to pleas for payment. The owner will get a better price if prompt, full payment can be planned for.

1. G. Goble, K. Fricke, G.E. Likins, Jr., Driving Stresses in Concrete Piles, Prestressed Concrete Institute Journal, Jan-Feb 1976.
2. T.D. Dismuke. Foundation Pile Tests for Sparrows Point Blast Furance. Preprint PILETALK Seminar, San Francisco, March 1977, pages 29-46, Associated Pile & Fitting Corp., Clifton, NJ 07014. Also, High Capacity Steel H. Piles, American Iron and Steel Institute, 1000 - 16th NW, Washington, DC 20036.
3. Technical Report on H-Piles Driven into Dolomite and Limestone for the Reading, Pennsylvania, Parking Authority. Bulletin HPP 752, Associated Pile & Fitting Corp., Clifton, NJ 07014.
4. G.Goble, G. Likins and W. Teferra. Piles and Pile-Driving Hammer Performance for H-Piles Driven to Rock, 1978. Department of Civil Engineering, Case-Western University, Cleveland, OH 44106.
5. Dr. Roger Slutter. Unpublished report, 1974, Lehigh University to Associated Pile & Fitting Corp.
6. L. Radley Squier and H. Stanley Kelsay. Composite Pile Solves Installation and Uplift Problems for New Wharf. Preprint PILETALK Seminar, Miami, March 1978, pages 115-124, Associated Pile & Fitting Corp., Clifton, NJ 07014.
7. NBS Nomograph 127: National Bureau of Standards Papers on Underground Corrosion of Steel Piling 1962-1971. Supt. of Documents, U.S. Government Printing Office, Washington, DC 20402. Roney A. Heinz. Protection of Piles: Wood, Concrete Steel. Civil Enginering--ASCE, December 1975, pages 59-64.

A CRITICAL EXAMINATION OF THE WAVE EQUATION

Frank Rausche, Goble and Associates, Inc., and
G. G. Goble, University of Colorado

A recent research project sponsored by the Federal Highway Administration produced a new wave equation computer program for the analysis of pile driving (WEAP). While the primary purpose of developing this program was to provide a better model for diesel hammers a number of other improvements were included and an extensive correlation study with dynamic measurements was made. This study together with the authors' extensive field experience pointed out several conditions where wave equation predictions will be inaccurate and unreliable. In this paper the capabilities of the WEAP program will be compared with other commonly used programs. The various factors which can influence the accuracy of a wave equation analysis are considered, evaluated and discussed. The specific topics included are: pile model, soil model, hammer model, and static soil analysis.

The application of the Wave Equation approach to the solution of a variety of pile driving problems has become more and more widespread. For example, the authors have been involved, under a contract with the Federal Highway Administration, in the development of a computer program called WEAP (Wave Equation Analysis of Pile Driving). They also presented a series of eleven seminars around the country as part of FHwA research implementation efforts.

As a result of this work a large number of program copies have been sent out and implementation is proceeding in many State Departments of Transportation and engineering consulting firms. This progress has the advantage of leading to a more realistic preparation of pile driving projects; on the other hand, it may in some instances lead to erroneous conclusions when the basic assumptions of the approach are violated by unusual or unanticipated circumstances.

The Federal Highway Administration sponsored the development of WEAP in response to concerns voiced by wave equation users regarding unsatisfactory results obtained from available programs when applied to diesel hammers. First, it was necessary that the thermodynamic cycle be modeled in complete detail so that combustion chamber forces are determined. Second, since the stroke of a diesel hammer is dependent on the driving resistance and the dynamics of the pile-hammer system it must be determined during the analysis rather than being treated as an input quantity. The WEAP program satisfies these needs.

It is the purpose of this paper to discuss problems that can arise in wave equation analyses. Since many of these problems occur in cases involving high driving resistance, emphasis will be placed on that aspect of wave equation application.

Basic Approach

The wave equation method of solving the pile driving problem as devised by E.A.L. Smith in the 1950's is relatively well known to most engineers involved in pile driving. It gives the designer a rational means of designing a pile for driving stresses; it provides a soil resistance versus blow count relation to be used for construction control purposes; and it allows a check on the feasibility of a hammer-pile system, given a certain profile.

Wave equation analysis is usually conducted in the following manner:

1. From a static soil analysis an ultimate capacity versus depth relation is established.
2. For a particular depth the static resistance distribution and the percentage of bottom resistance are determined and the total ultimate resistance, R_{ut}, is found. Wave equation analysis will determine the blow count associated with R_{ut} for the specified driving system.
3. In general, additional analyses are also made for other possible R_{ut} values and a curve, R_{ut} versus blow count (the result of each individual analysis) is constructed. This curve is called a bearing graph and an example is shown in Figure 1.

The bearing graph is usually the desired result as it indicates what capacity has been obtained at a certain blow count or how the pile would drive in the given situation (blow count from soil resistance). The wave equation is not the only source of a bearing graph; for example, the Engineering News Formula or any other dynamic equation can be plotted in the same manner.

Figure 1. Bearing graph (capacity versus blow count) as constructed from individual wave equation analysis.

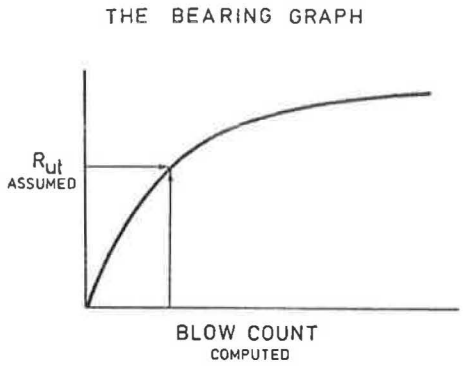

Pile Model

The analysis itself is carried out using a discrete spring mass model of the pile as shown in Figure 2. The pile is divided into segments, each two to at most, ten feet long. The pile accelerations are computed from Newton's Second Law for a given set of forces at an element at a certain time.

Figure 2. The Wave Equation representation of pile driving. A. The system to be analyzed. B. The Wave Equation model. C. The components of the soil resistance model.

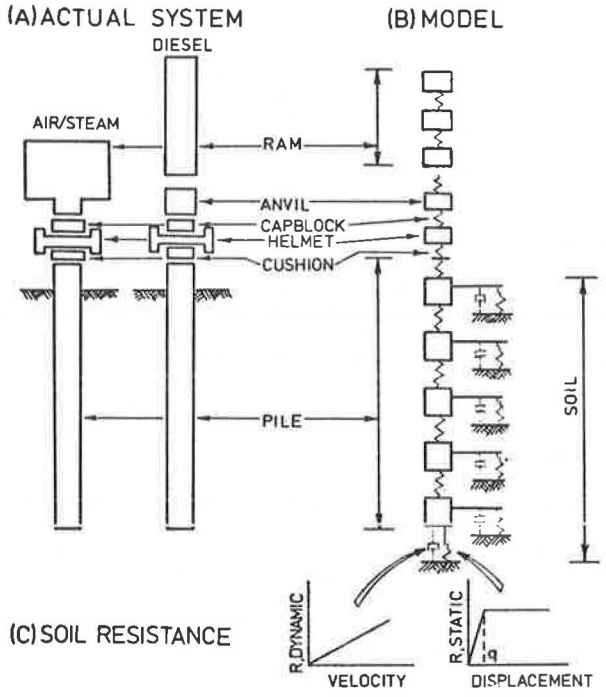

The pile velocities and displacements are obtained by integration of the acceleration over a small time increment. The pile forces are in turn computed from the segment displacements and the spring stiffnesses. The process is then repeated for a new time increment. More elaborate and accurate computational procedures are frequently used but they will not be discussed here in any further detail.

Soil Model

On each embedded pile segment a soil resistance force is acting during driving. This force is dependent on the soil characteristics and is a complex function of both pile and soil motion. A static soil analysis is performed and an ultimate static resistance, R_u, is obtained for each pile element. The sum of all R_u-values is, of course, the total pile bearing capacity, R_{ut}.

Smith's soil model distinguishes an elastic and a plastic portion of soil behavior. It introduces the "quake" as that displacement at which the elastic, static behavior becomes plastic, i.e. that pile displacement at which the ultimate resistance, R_u, is reached. In addition to the static resistance a dynamic resistance force is also modelled. It is treated as proportional to the pile element velocity. The soil resistance forces acting during driving are functions of element displacements and velocities. The characteristics of these forces are shown in Figure 2. The parameters defining these forces must be provided by wave equation program users.

Hammer Model

The wave equation hammer model can be more or less sophisticated depending on the particular computer program used and on the type of hammer employed. If the program does not permit a realistic treatment of hammer operation it cannot be expected that consistent reliable results will be obtained. For the simplest hammer type, such as the drop or the single acting air/steam hammer, the ram is usually modelled as a single mass, striking a capblock that is modelled by a bilinear spring which in turn exerts forces on a helmet that strikes the pile, sometimes through a cushion.

For diesel hammers, the WEAP program uses several elements to represent the more slender rams typical of these machines. An initial stroke is assumed, the ram is allowed to fall past the exhaust ports and impact on the anvil after going through the precompression phase. The combustion chamber pressures are calculated from the Gas Law and the effect of these pressures on impact velocity is included in the computation. The dynamic analysis is continued after impact until ram separation occurs on the upstroke. The ram motion is then computed including the effect of the combustion chamber pressure and the rebound stroke is determined. If the rebound stroke is different than the starting stroke the computation is repeated until convergence. Thus, ram stroke is available as a function of blow count for use in construction control. The WEAP program is the only available program having this capability.

Examples

A few examples of problems that may be encountered when using the Wave Equation approach will be discussed here. It should be understood that these examples are unusual and should not be considered to be proof of a failure of the wave equation but rather an illustration of problems that can occur.

1. The Pile Model

The lumped mass model, representing the pile, is probably the most reliable portion of the wave equation idealization. In the context of high capacity piling the assumption of elastic behavior should be examined. The measured and computed curve of pile top forces shown in Figure 3 were obtained for an HP 10x42 pile driven by a Kobe K25

Figure 3. Pile top forces and velocities both measured and computed by WEAP for a case where stresses exceed yield.

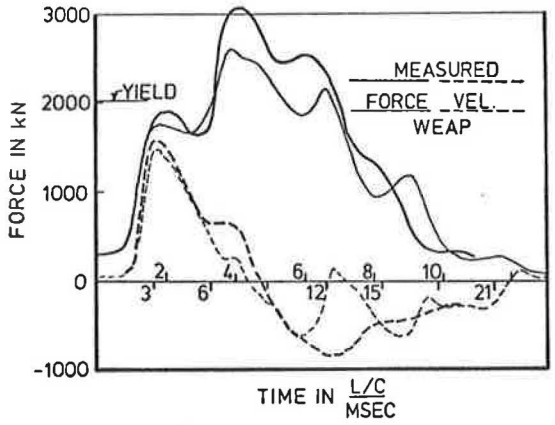

Note: 1 kN = 0.225 kip.

hammer to a hard limestone rock. The measurements were made using strain transducers attached to the pile web. Thus, when yield was reached a force was measured that was higher than actually occurred due to the assumption of a constant elastic modulus. The wave equation showed that the forces at the pile top were smaller since yielding and hence a reduction of the pile strength was not modelled.

2. The Soil Model

Among the various error sources inherent in the simplified soil model used in wave equation analysis those introduced by the assumption of linear elastic - ideal plastic behavior will be discussed. These error sources are of particular interest in hard driving.

First consider differences in bearing graphs when the quake is changed from the usual 0.25 cm. (0.1 in.) to a low value of 0.10 cm. (0.04 in.). The two bearing graphs are shown in Figure 4. At a capacity of 2670 kN (300 tons) the larger quake gives a 35% higher blow count. The errors introduced are smaller when determining a capacity from a given blow count. If the goal is to estimate blow count at a particular depth the error is

Figure 4. Bearing graphs from WEAP for two different quakes.

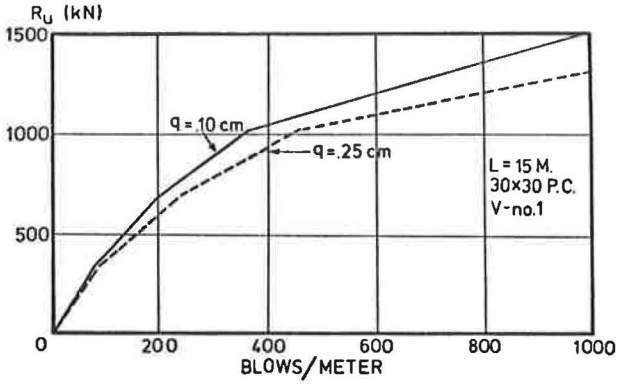

larger. This characteristic is illustrated in Figure 5 where the blow counts are plotted as a function of depth for a given R_u versus depth

Figure 5. Blow counts versus depth from the two bearing graphs of Figure 4 via an assumed R_u versus depth relation.

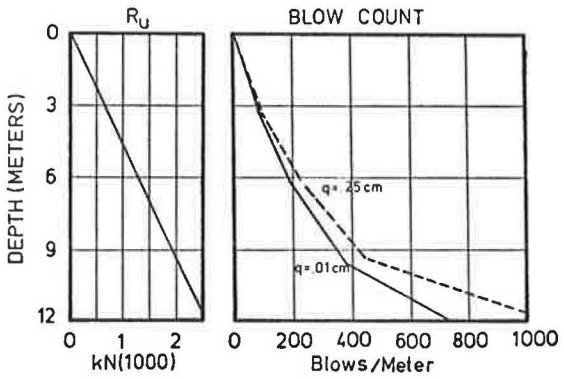

relationship. Since the value of the quake is usually not accurately known and since the usual assumption of 0.25 cm. (0.1 in.) has only proven to give good predictions of capacity for "normal" cases, this factor should be considered when the analysis gives high blow counts or refusal.

Another effect may lead to erroneous results in hard driving cases. This effect, resulting from the real non-linear behavior of the soil is of importance when the final sets during driving become very small; say less than 0.13 cm. (0.05 in.) or more than 790 blows per meter (240 blows per foot). In Figure 6 real force deformation curves are shown together with the wave equation idealization. For these cases it is seen that for Cases a and b the idealization approximates the real curve quite well. For the other two cases the results will be poor. The idealized soil law would predict complete refusal (no permanent set) where actually penetrations still occur. This error source limits the applicability of the wave equation approach since R_u becomes unknown for a high blow count. In fact, at high blow counts higher capacities than those predicted by the wave equation are likely.

Figure 6. Nonlinear static soil resistance law - real and idealized.

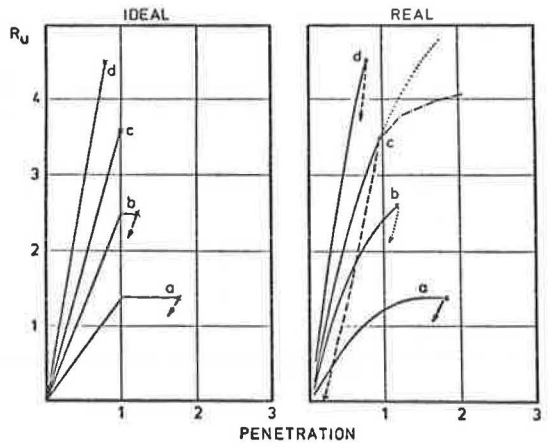

Figure 7. Results from WEAP analyses and from load tests for a pipe pile driven into coarse grained soil.

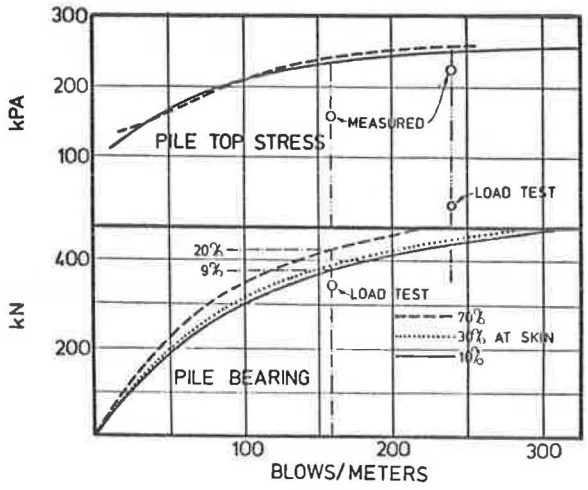

Note: 1 kpa = 0.145 psi.

3. The Hammer Model

Among the various quantities that describe the hammer model the efficiency is probably most important for air/steam hammers. It is very well possible that errors are introduced into results due to an erroneous assumption of hammer energy and that these errors are initially thought to result from improper soil data.

An example is given to illustrate this problem: A 13 meter (43 feet) long pipe pile was driven into coarse grained material that exhibited increasing strength with depth. The hammer was a Vulcan No. 1 single acting air/steam hammer which is commonly thought to supply an energy that is independent of soil resistance. The final blow count was 157 blows per meter (48 blows per foot).

The soil resistance distribution was calculated by a static analysis and the total amount of skin friction was varied using 10, 30 and 70%. Correspondingly three different bearing graphs were obtained that differed from the load test by 9 to 20%. The bearing graphs together with the stress-blow count plots are shown in Figure 7.

The conclusion that an erroneous amount of skin friction was primarily responsible for the difference between dynamic prediction and static capacity is not justified. Note the low magnitude of the measured dynamic stresses suggesting that the hammer was not 80% efficient as assumed in the wave equation input.

A second load test was performed on an almost identical, nearby pile which was driven to 236 blows per meter (72 blows per foot). It indicates a better agreement of stresses and an underprediction of static capacity. Measurements taken during driving of both piles actually did indicate an increase of hammer energy with blow count.

Static Soil Analyses and Driveability

It was shown that an uncertainty in the magnitude of the quake can result in a rather large error in the estimate of the number of blows necessary to drive a pile. In that example of Figures 4 and 5 it had been assumed that the static soil analysis was correct.

Uncertainties in static formulas, however, were the reason why the wave equation approach was developed and accepted. Thus, a driveability study must always be considered with some suspicion since it depends on the ability to make an accurate static analysis.

The next example demonstrates the rather dramatic effect of an unknown resistance force at the pile bottom. The example was taken from a driveability study on an open ended conductor pipe driven into primarily sandy material. The pile had a drive shoe consisting of a portion of pipe having increased wall thickness over the bottom two feet of pile. The pile shoe extended to the inside thus reducing the diameter of the soil entering the pile and the friction on the inside of the pile. Frequently this technique is unsuccessful and a plug may form that activates a soil resistance equal to that of a closed end pile. In Figure 8, blow count versus depth curves are shown for the two cases. A drastic difference results.

Figure 8. R_u versus depth and resulting blow count versus depth from WEAP analysis for an offshore conductor pipe.

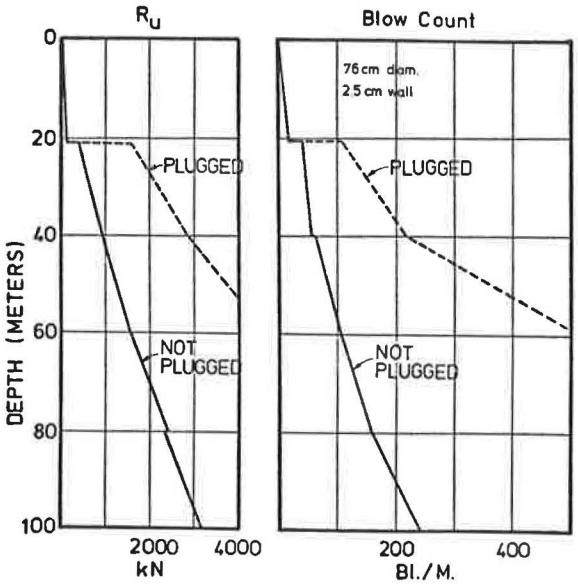

Conclusions

Experience with the WEAP program has shown that it can be an effective tool for evaluating pile driving systems. It is particularly useful in dealing with open end diesel hammers since the total thermo-mechanical system is modelled.

Care must be used in applying WEAP or any other wave equation program in that errors in input parameters or cases where the model contained in the program is not a proper representation of the real physical system can produce poor results. Of particular concern are three problems:

1. The program depends on a knowledge of hammer efficiency and since it can vary from hammer to hammer it is unknown in advance.
2. The soil resistance model of elastic-plastic spring and linear dashpot can produce poor results for high blow count driving.
3. The inability to perform an accurate static soils analysis make driveability studies unreliable.

ECONOMICAL STRUCTURES FOR LOW-VOLUME ROADS

Roy Tokerud, P.E., Federal Highway Administration

Sharp increases in prices and a concurrent decline in highway revenues have forced a re-evaluation of highway projects. Most seriously affected are the old bridges since, unlike the rest of the highway, their life cannot be indefinitely extended by maintenance. A national bridge survey reveals that 105,000 bridges in the U.S. are structurally deficient and/or functionally obsolete and 72,000 of these are on roads that are not on the federal-aid system. The needs on our low-volume roadway system far exceed program funds available. The potential economies suggested in this paper will hopefully lead to better utilization of the funds available. This paper investigates the economics of low-volume structures. It discusses the most economical bridge types being constructed in the Northwest. Although, not primarily addressed to the hydraulics involved in stream crossings, the paper discusses some of the hydraulic considerations that should be made. Attention is directed to actual practice of agencies constructing bridges on low-volume roads. The three principal structural materials of concrete, timber, and steel are discussed. Certain structural details are suggested for economy, as well as structural types. The comments and recommendations contained in this paper are based on a survey made in the Northwestern United States.

For many years our highway and bridge engineers have been well aware that this country has a major bridge problem which daily grows worse, particularly on our low-volume roads. Time has taken its toll, so we are now surrounded by large numbers of deteriorated and dilapidated bridges. Fortunately, as the result of the widespread publicity given to the problem in the past few years, other people - from layman to congressman - have finally been awakened to the seriousness of the situation. Congress is now recognizing this by increasing the funds for bridge replacement to the point where significant progress can be made in years ahead. The present amounts proposed vary from $450 million to $2 billion per year. This is a welcome contrast to the previous allocations which averaged only $120 million per year over the seven-year life of this program. Other improvements in the current bills before Congress would permit rehabilitation of existing bridges as well as replacement and, for the first time would allow bridge replacement funds to be spent on both federal-aid and non-federal aid (off-system routes.) It is estimated that there are 33,500 deficient bridges on federal-aid routes and 72,000 on off-system routes. Estimated replacement cost of these deficient bridges is in excess of $25 billion.

The problem with old deficient bridges is most critical on low-volume roads because that is where the largest percentage of very old narrow bridges are found. Many of these old bridges on the back roads are collapsing, but we hear little or nothing about most of them. Unless the bridge is large or involves fatalities, it is considered just another "fact-of-life" occurrence. An example of one such collapse is shown in Figure 1. It has been estimated that 200 bridges in the U.S. collapse every year.

Figure 1. Collapsed log bridge in Oregon.

In order to determine what was being done in the Northwest, questionnaires were sent to counties and other local jurisdictions in the States of Idaho, Oregon, and Washington. The total number of bridges built, over a three year period, by some 100 responding agencies was 790. Of these 72% were prestressed concrete, 15% were timber, 5% were steel, and 8% were other types including long span culverts. A

further breakdown of the prestressed concrete bridges showed 57% were slab or "rib deck", 39% were bulb tees, and 4% were box beams.

Interestingly, the questionnaire revealed that, of the 790 bridges reported only 55% were contracted. The other 45% were built with the agencies' own forces. These numbers are misleading of the total picture though because the large bridges were contracted and those built by day labor often involved contract purchases of beams and other components.

The initial statement in this paper to the effect that the problem of old deteriorating bridges daily grows worse, needs clarification. While the statement is true of a large number of counties and cities there are many others that are making good progress in replacing their old bridges. In an effort to get an indication of the progress being made we selected Washington State, since the County Road Administration Board (CRAB) in that State maintains good records of all county bridges including the number that are deficient and the number replaced each year. Although our previous survey indicated that most counties in Washington were making good progress replacing deficient bridges, CRAB's bridge inventory records reveal some surprising statistics. The total number of bridges being maintained by the 39 counties in Washington is about 4100. In 1972, 514 of these were rated as structurally deficient. In the ensuing five years 443 of these deficient bridges were replaced. Simple arithmetic would indicate that few deficient bridges remained. Yet in 1977, five years later, the CRAB tabulation shows that the number of structurally deficient bridges had increased by 26, to 540. This makes it appear as though they are losing ground but this is not necessarily true. While most of the increase in the number of deficient bridges is undoubtedly due to the continuing deterioration of the older structures, part of the increase can be attributed to an improved bridge inspection program and a more thorough rating analysis which has caused many older structures, that were previously considered adequate, to now be classified as deficient.

Planning

The first step in planning a bridge replacement program is to establish needs. Since the national bridge inspection program for federal-aid routes has now been in existence for several years, counties and other agencies should be aware of their needs on the federal-aid system. With the new highway bill including funds for off-system bridges, the inspection program will have to be extended to include all bridges and thus needs for the entire highway system will be established. Many counties, at least many of those surveyed in the Northwest, already have an inspection program covering all bridges and thus are well aware of their entire needs. Those who are not that fortunate should get going fast if they hope to get their share of the expanded bridge replacement funds. As the replacement program is planned, the first question should be, how many of the old bridges can be replaced with culverts? If a commercially available size culvert up to 4.6 m (15 ft.) can handle the runoff, and if drift is not a serious problem, the culvert should save money and require minimum maintenance. Other advantages to culverts include: no bridge rails to run into head-on, no bridge icing, and no deck deterioration. Also, the culvert can carry heavier loads and the continuity of riding surface over a culvert eliminates the bump that is often found at bridge ends. For the larger sizes, with spans up to 15 m (50 ft.), the culvert requires special site conditions including adequate depth of embankment to allow space for the structure plus some 1.5 m (5 ft.) of fill over the pipe. (Figure 2.) Over 600 of these larger culverts (termed long-span) have been installed in North America since 1960. They are being used as drainage structures and as grade separations. Six major companies are producing long-span culverts. Culverts can be constructed faster than most bridges and often at substantially less cost. When site conditions are right for these large culverts careful study should be made to determine the relative merits of a culvert or bridge. Structure choice at these locations should be based on comparative cost of construction and maintenance, risk of failure, risk of property damage, traffic safety, fish passage requirements, and environmental and aesthetic considerations. At some sites the culvert seems to be an ideal structure from an environmental standpoint. In other locations, especially in urban areas, the openness of a bridge and the smaller right-of-way make it more desirable.

Figure 2. Horizontal arch-shaped culvert with 12 m (40 ft.) span.

Although this paper is not primarily addressed to the hydraulics involved in stream crossings, this is an area which needs more attention. Such items as skew angle, possible channel changes, streamlining of intermediate piers and bents to avoid excessive scouring and drift hang-up may require special study. Many of the major and costly engineering shortcomings over the years have been due to lack of proper consideration for hydraulics. A hydraulic study should be conducted for those stream crossing where the primary problem is to pass floods of unusual magnitude and frequency. Crossings controlled by high grade lines or those over well-defined or diked channels often require little if any hydraulic study. A nutshell sketch of a hydraulic study where the problem is the determination of an adequate sized structure to pass estimated flood flows would include:

1. A hydrologic analysis of stream flow data to establish the magnitude of the design flood.
2. An evaluation of existing structures over the same river or stream.
3. Identification and location of dwelling and other high-cost development.
4. Documentation of past flood heights complete with location and dates.
5. Hydraulic-sizing of the culvert or bridge so that watersurface elevations during flood flows are kept at acceptable levels.

If funds are not available to build a structure which will carry the anticipated flood flow, there are other possibilities. A low level bridge can be built which will be overtopped during the higher

flows. When designing this type of structure special attention should be given to the elevation of the structure, streamlining of the section, and type of anchorages. Since drift is supposed to pass over the top of low level bridges, it is advisable to omit the railing. Another possibility is to build the approach road low to serve as an overflow or build a portion of the fill with a sand core that will wash out when flooding becomes critical.

Design Considerations

Once the decision has been made to use a bridge with a certain waterway opening, the engineer has numerous choices. The bridge type may depend on how the construction is to be performed. If the construction is to be done with in-house personnel, the bridge crew may be skilled and have equipment for only one type of construction. The responses to the questionnaire indicated that most bridge crews were experienced with timber construction; several used their own forces primarily on short-span concrete construction, and a few specialized in steel construction. When the construction is let to contract the above limitations do not apply and all logical bridge types should be considered. Span lengths and beam spacing need careful study during detail design. As a general rule, maximum economy is obtained by using the minimum number of beams without requiring excessive deck thickness.

Fortunate are the counties that can afford an engineer on their staff who is knowledgeable about bridges. Even though he may not have time to do much design work, he would be available to make studies of needs and programs, deal with problems regarding maintenance and repairs, evaluate foundation conditions and determine the most suitable and economical bridge types. For example there are many choices available in the type of abutment or end support for a bridge. The use of spill-through, half spill-through, or retaining type abutment may significantly affect the cost. The abutment selected will influence the bridge length which in turn may dictate the most logical superstructure type. (Figure 3.) The spill-through type abutment is generally most economical unless, for example, it requires the use of two spans instead of a single span. When pile bents are used the end bent piling can also serve to retain the fill by the addition of timber, steel or concrete planking bearing against the piles. The cheapest way to support a bridge end is to pour a concrete footing, or lay a sill on the ground or on a compacted embankment. The abutment is completed by the addition of a solid diaphragm between the beams or a back wall above the footing or sill. If the bridge is in a remote area where concrete is not readily available and the ground will not support a sill, the weight of the bridge can be spread over a greater bearing area by supporting the sill on gabions, filled binwalls, or reinforced earth. When the structure is not too long, the abutment should be monolithic with, or firmly secured to, the superstructure. This avoids the extra cost and maintenance involved with expansion devices. Monolithic abutment construction has been used successfully on many bridges up to 100 m (328 ft.) long. When retaining-type concrete abutments are used, the walls and wings can be precast to reduce construction time in the field. (Figure 4.) If poured-in-place concrete is used and the wings are not too long they can be cantilevered from the abutment wall. These are just a few items to be considered in the design to get the most economical construction.

Figure 3. Showing the effect abutment type has on bridge length.

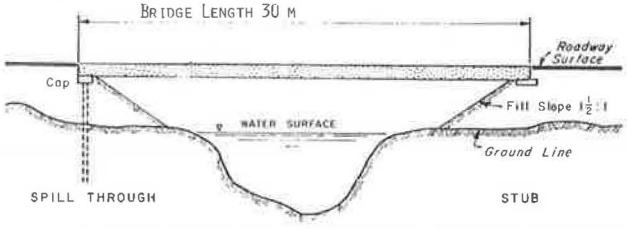

SPILL-THROUGH or STUB TYPE ABUTMENT

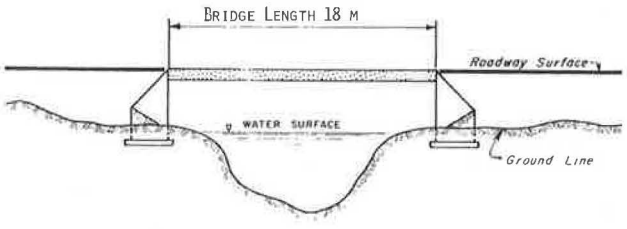

RETAINING TYPE or CLOSED ABUTMENT

Figure 4. Bridge on county road in Washington with precast abutment and wingwalls.

Timber

Approximately 40% of those responding to the questionnaire reported that they build some timber bridges. Some even build untreated timber bridges on extremely low-volume roads. Others use treated timber only for sills, bents, stringers, and headers and untreated timber for the decking and rails. In general untreated timber is unsuitable for bridge construction except for temporary structures or for foundation piling remaining permanently below the water table. Treated timber can and generally does give a long service life varying from 25 to 50 years. A few treated timber bridges have lasted only 10 to 15 years which is obviously unsatisfactory. Such a short life must be due to careless erection or to the manner of construction whereby the effectiveness of treating is lost by drilling, cutting, and nailing during construction. The principal factors contributing to the life of treated timber are environment or location, exposure to the elements, type of treatment, and the care and manner in which the

fabrication and erection are performed. Pressure treatment with oil borne preservatives is recommended for best results.

In recent years there have been many improvements in the fabrication and erection of timber bridges which have made them both more competitive and more long lasting. Modular systems have been developed which consist of completely prefabricated members and require no cutting, drilling, or nailing after treatment. All connections are made by bolts through predrilled holes. The girders, felloe guard, and rail posts are all glu-lam members. Deck panels are also glu-lam in widths of 0.6, 0.9, and 1.2 m (2, 3, and 4 ft.). Structures such as these have been built in the Northwest with spans up to 36.6 m (120 ft.) carrying loadings heavier than HS20. (Figure 5.)

Figure 5. Panelized timber bridge system. Assembly diagram.

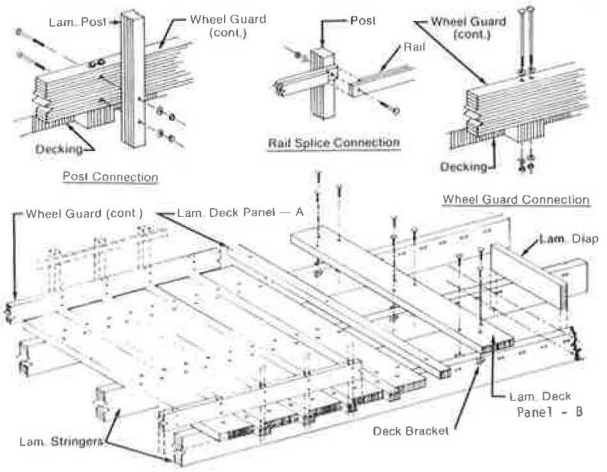

A new concept in timber now being developed by Forest Products Laboratory is a process referred to as "Press-Lam". The system involves rotary cutting of logs into plies up to 1.2 cm thick. The veneers are glued together with all laminations placed vertically to form a continuous sheet of wood which can then be ripped and cross-cut to the desired dimensions for stringers, deck panels, etc. The process involves less waste of material and scatters the defects better which produces higher structural quality from any given grade of log. To date, one small bridge in West Virginia has been constructed using press-lam members. The members were actually fabricated in the Forest Products Laboratory since the necessary manufacturing equipment is not currently available in industry.

Some advantages of timber, or the conditions under which timber seems especially appropriate, include the following:

1. Timber is plentiful in many areas and is a resource that replaces itself and is more conserving of energy than concrete and steel.

2. When used as friction piling, timber will generally be most economical, i.e., will furnish the highest bearing-to-cost ratio. When soil conditions are right it is possible to use high bearing values. On one recent Interstate project in Nevada, timber piles were designed for 64 t (70 tons). A word of caution here, however, many treated timber piles have been damaged during handling and by over-driving so that the effectiveness of treatment is lost and the service life greatly reduced.

3. When existing abutments and piers are to be reused, they may be able to support a superstructure dead load of timber but not concrete. Several old trusses have been replaced with glu-lam girders using existing abutments and piers.

4. Glu-lam panels used for decking apparently are not affected by salts and therefore under some circumstances may be more durable than concrete decks.

Concrete

Cast-in-place concrete, for superstructure members of bridges on low-volume roads, has for the most part been replaced with precast, prestressed construction. Cast-in-place concrete, nevertheless, has certain advantages. Bridges with curves and flares can be built more readily with cast-in-place concrete. Also, for multiple spans, cast-in-place concrete lends itself to continuous design which contributes to smoother riding qualities. In general, however, the cast-in-place bridge has become too expensive due to the on-site labor for falsework, forms, placing resteel, and pouring and finishing concrete. Another disadvantage of the cast-in-place bridge is the extra time required for construction and the additional inspection. The fact that precast work requires less on-site field inspection should not be carried too far. We have seen some precast, prestressed structures which apparently got little or no inspection and the result was poorly placed foundation, poor welded connections and improperly grouted keyways.

For the low-cost, short-to-medium span range, 6 to 40 m (20 to 130 ft.), prestressed concrete is by far the most commonly used bridge material on new construction in the Northwest. In our survey of several Northwest prestress plants, we found that a large number of different forms and sections are being used. The standard bridge sections that were developed by AASHTO and PCI are well known and have been used extensively throughout the country. These standard sections were selected in the hope that they could be used for most precast, prestressed concrete contruction in all of the states. Their goal was only partially successful. Many prestress plants developed their own sections and have successfully promoted their use. Their objective has been to develop cheaper members and a total bridge system that requires the minimum material and field labor. Fortunately, these are not patented, so that any plant can get the forms and compete for the business. The most significant revision in these non-standard sections, and the one which is saving money on many jobs, is the precasting of an integral deck slab along with the beams (Figure 6.) With the standard AASHTO - PCI precast sections, the integral slab is obtained only with the use of slab or box sections. With non-standard sections, integral decks are obtained with many different shapes. Some of the most common non-standard shapes with integral decks being used in the Northwest are shown in Figures 7, 8, and 9.

The use of integral decks on prestress tee beams was pioneered by Concrete Technology in Tacoma, Washington in the early 1950's. A few of these structures are now 25 years old and are giving good service. As their general use spread, other prestress plants followed suit and went on to develop other bridge sections such as the double-tees, channels, and rib deck. The double tees and channels are more stable than single tees during handling and placing and consequently are being selected by some contractors.

Figure 6. Prestressed single tee with integral deck being placed. The end and intermediate diaphragms on this 15 m (50 ft.) span are also integral with the beam. The material stacked on top of the beam includes rail posts and rail members.

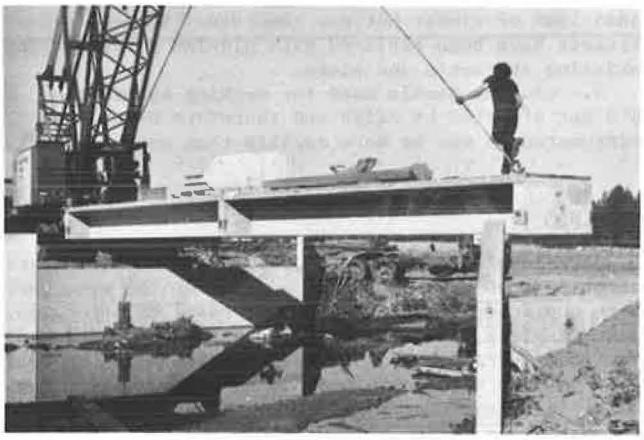

On the other hand, they require heavier handling equipment. The four-stem rib deck section shown in Figure 7, has been very popular for several years in areas where they have been produced. About a year ago a prestress plant in Yakima, Washington introduced a larger rib deck section with three stems (not shown). It varies in depth from 0.5 m (18 in.) to 0.6 m (24 in.) and in width from 1.2 m (4 ft.) to 1.8 m (6 ft.). Their economic span ranges from 12 m to 18 m (40 to 60 ft.). The efficient rib deck shape requires less material and is lighter to handle than solid or voided slabs. When bid as an alternate it is being selected by contractors in preference to slab units. The survey showed that only a few bridges were being constructed with the box beam section shown in Figure 7. This is as it should be because the box shape is inherently less efficient than the tees and channels.

Figure 7. Miscellaneous prestressed shapes.

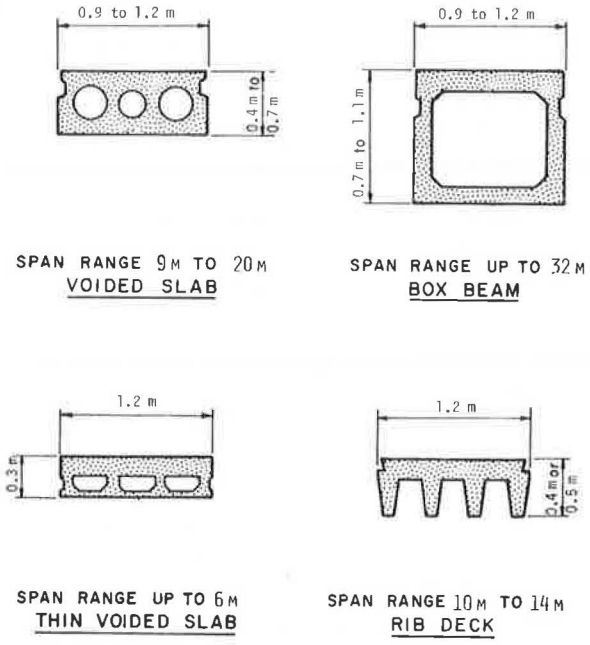

Figure 8. Prestressed single and bulb tee with integral deck.

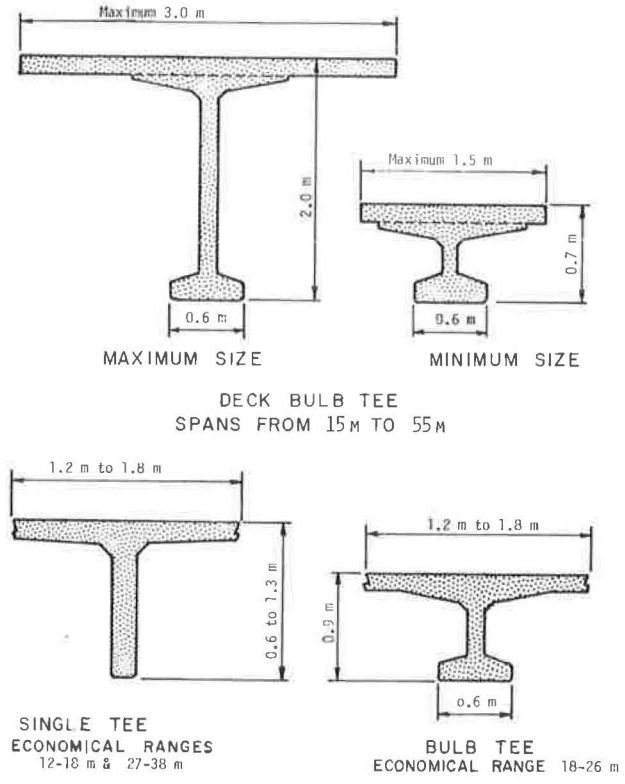

Figure 9. Prestressed double tees and channels.

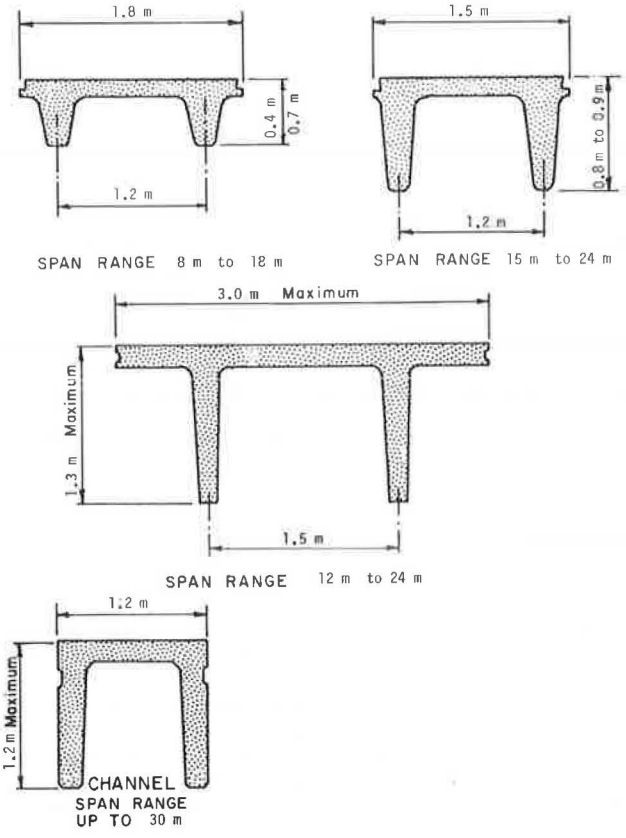

Some counties are getting maximum economy by using sections without any overtopping or extra wearing surface. When this is done it is important that the beams end up with the same camber. One plant obtains closer camber control by applying partial prestressing initially and then following-up with appropriate post-tensioning a couple of weeks later. Another company has devised a system of jacking beams up or down after erection and then tying them together by welding tie bars to insert plates on adjacent precast diaphragms. Many counties prefer to place a bituminous wearing surface over the deck, and when this is done the matter of unequal camber is not so critical.

Some other developments in the precast, prestress business include tilting flange forms on tee beams which allows roadway crown to be built into the precast member. Also, some prestress plants are now renting precast slabs and beams to contractors for use on detours and other temporary structures.

Steel

Steel bridges are also being built on low-volume roads; however, relatively few have been constructed in the Northwest in the past few years due to their higher cost. A few counties in the Northwest have been using their own forces to build all-steel bridges - mainly over irrigation canals with spans of 5 to 7 m (16 to 24 ft.). These are supported on wide-flange sills resting on the ground or on steel pile bents. Steel bridge plank is used for the end bulkhead and extended out as necessary to serve as wing walls. The deck consists of steel plank welded or bolted to the wide-flange stringers and overlaid with a bituminous wearing surface.

Until recently several counties in the Northwest were constructing a prefabricated steel "package" consisting of welded beams, decking, wheelguards, railing, and bracing. They came in span lengths of 6 to 24 m (20 to 80 ft.). Over 200 of these were built in the past several years. Average construction time of a single span bridge, including pile driving, was reported to be 12 days. One of these steel structures in Idaho is shown in Figure 10.

Figure 10. Steel "package" bridge with 24 m (80 ft.) span in Latah County, Idaho.

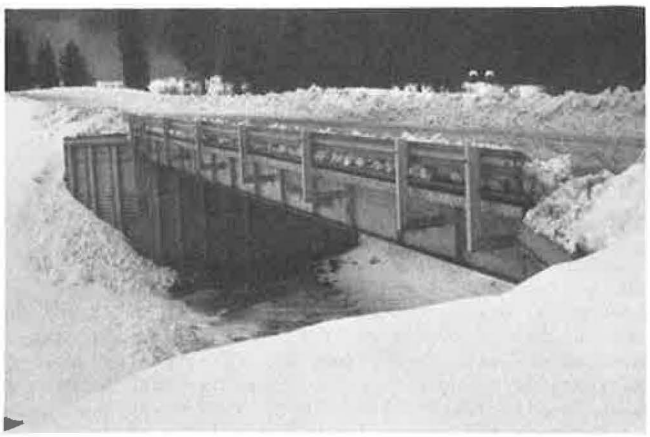

Douglas County in Oregon has had an ambitious and unusual steel bridge replacement program for many years. For their longer girder spans, from 18 to 24 m (60 to 80 ft.), they fabricated castellated beams (Figure 11). Over the years they have built up expertise in welding and steel fabrication within their own bridge crews. They report that economical steel structures are being obtained by careful planning and scheduling of steel fabrication to take advantage of any otherwise slack periods.

Some well-known details of steel construction that result in economies, but are overlooked by some designers and fabricators, include:

1. Keep details as simple as possible.
2. Use automatic welding wherever possible.
3. Place stiffeners on one side only or stagger them, or omit them by using rolled beams or by thickening the webs of welded girders. This suggestion is intended only for moderate span lengths up to 40 m (130 ft.).
4. Use elastomeric bearing pads or, on spans up to about 20 m (65 ft.), use the cheaper milled fiber/rubber bearing pads.
5. Use weathering steel if available, particularly in wet climates, to avoid cost of frequent painting.

Figure 11. Bridge in Douglas County, Oregon with castellated steel beams.

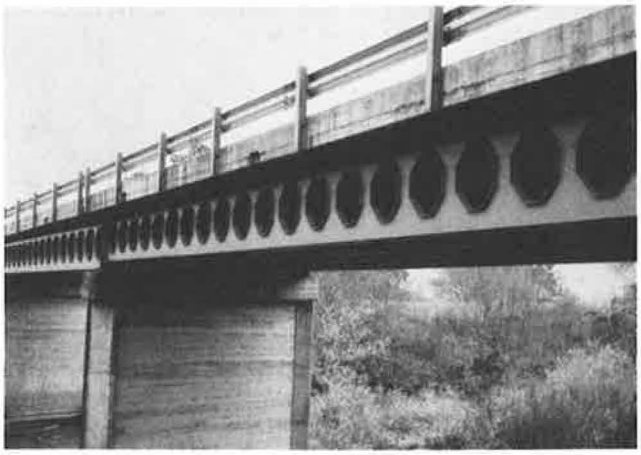

Contracting Methods

Many agencies are using their own forces to build smaller bridges. Since they must have bridge crews to do maintenance work, the crews can be used to advantage on new construction during otherwise slack times. Competitive bidding in these cases is used only for purchase of materials. Substantial savings can be had if bids are taken on carload lots, or on a large number of bridge components at one time. Some counties we surveyed preplan and budget their funds so they can contract for a year's supply of prestressed units at one time. As their designs are finalized, they retain the privilege of revising the number of various lengths and specifying the skew angle, if any, that is desired. This permits the prestress plant to schedule their work more advantageously and therefore bid lower than they would on smaller quantities. As a variation of the above a few counties contract for the furnishing and erection of prestress units and use their own forces for the substructure work and for shear key grouting and rail installation.

When construction is fully contracted the conventional method is to take bids on a single design. This will yield the most economical structure providing the designer has made the best selection. When

a number of small bridges are to be constructed in one area, significant savings can be realized by letting several bridges in one contract.

Some agencies take bids on alternate designs from time to time. While this requires more engineering, it helps establish better comparative costs. One county surveyed has on two occasions taken alternate bids on a prestressed beam design versus long-span culverts. In both instances the successful contractor bid low on the culvert. Some other bidders did not see it that way. In any event the bids were close.

Some counties are using the "design and construct" type contract which is sometimes referred to as the "open competitive" contract. This conforms approximately to what industry calls the "turnkey" system and is similar to the European design competition contracts. The county engineer determines the structural and hydraulic requirements and specifies the gradeline, clearance requirements, roadway width and general design criteria. Caution must be used with this type of contracting as it places the burden on the agency engineer to evaluate the bid proposals to determine whether they are in compliance with the plans and specifications and will provide the desired end product. The principal advantage to this open competition contract is that it encourages maximum innovation and economy by the engineer, supplier, and contractor working as a team.

Geometrics

The main geometric consideration for bridges on low-volume roads is the bridge width. The widths reported by questionnaire respondents varied all the way from 6 to 13 m (20 to 44 ft.) for two-lane bridges. The 6 m (20 ft.) width is not considered satisfactory except when it is located on a road serving only a few families and there is little prospect of the traffic increasing in the future. In farming areas the width may have to be a minimum of 7 m (24 ft.) to accommodate farm machines. The upper limit of 13 m (44 ft.) width would include full shoulders and obviously would not be on a low-volume road. The most common widths reported on new construction were 8 to 10 m (26 to 32 ft.). A few counties reported they were building 4 to 5 m (12 to 16 ft.) single-lane bridges on extremely low-volume roads.

It is desirable to leave the bridge width flexible until the design stage is reached. Often it is possible to add some width at little extra cost. For example, if an 8 m (26 ft.) minimum width is desired and this width would require 5 beams for a particular span length, it may be that 5 beams would also be adequate for a 9 m (30 ft.) width. If so, the extra width could be obtained for relatively little cost. On the other hand, if the wider roadway required an extra beam, the additional cost would be substantial. Several comparative cost studies have been made of various bridge widths. In general the extra width can be obtained for much less cost per square foot than the overall bridge cost, since many bridge costs including overhead, mobilization, and railing, remain the same regardless of width.

Most counties follow state standards which are similar to those in AASHTO publication "Geometric Design Guide for Local Roads and Streets." Our office made a study of bridge widths and came-up with suggestions for new construction. These are shown in Table 1.

Table 1. Suggested bridge width guide.

	Traffic Volume (Current ADT)			
Speed km/h	Over 750	250 to 750	50 to 250	Under 50
>80	12	11	10	9
50 to 80	11	10	9	8
<50	10	9	8	7

Miscellaneous

1. Curbs are expensive and most often unnecessary. The decks on bridges with open rails keep cleaner of snow and debris when no curbs are used.
2. Railings on low-volume bridges may logically be less substantial than those on high-volume roads. Most of the counties responding to the questionnaire were using steel beam rails with posts spaced at 1.9 m (6 ft. 3 in.) centers. Other rails included timber, steel tubes with posts spaced at 2.4 to 3.7 m (8 to 12 ft.) and a few were using the "New Jersey" safety rail. The concrete safety rail with its heavyweight (dead load) is hardly necessary or suitable for low cost bridges on low-volume roads. While many of the rails being used were substandard by AASHTO criteria, they may well be satisfactory for low-volume roads depending on traffic volume, highway alignment and bridge widths.
3. Simple details and realistic specifications that can be met using economical and preferably local materials should be used. As an example, elastomeric neoprene bearing pads or the cheaper milled fiber/rubber pads can be used in lieu of more expensive metal assemblies.
4. Several studies have been made over the years to establish the extra cost to design for HS20 instead of HS15. The difference in cost is nominal, varying from 2% or less for most bridges up to a maximum of about 4%. With this small difference it is advisable to use HS20 for all except the very low-volume roads.
5. Foundation designs should be conservative particularly for bridges crossing bad streams. A little extra expense on the foundation may save the structure when the next flood comes.
6. Concrete piles should be cast with a "jet" hole in the center in case jetting is required to drive them.
7. For the larger structures, the possibility of using drilled shafts in lieu of the more conventional substructure with pile or spread footings should be investigated.

Conclusions and Recommendations

With today's rising prices and declining revenues, the engineer has a challenge to arrive at the most economical bridge system. It appears that, regardless of material used or bridge type selected, maximum economy will be obtained by prefabricating as many bridge components as possible in order to reduce on-site labor costs.

The principal economies suggested are intended to be within acceptable geometric, design, and safety standards. It was considered inappropriate to suggest building in structures as weak links on low-volume roads and thereby furthering substandard design on a system that is in need of substantial upgrading.

Some specific recommendations to keep in mind when planning and designing structures on low-volume roads include the following:

1. Develop a long-range structure replacement program based on findings of a continuing bridge inspection program.
2. Make adequate preliminary studies.
3. Preferably have a bridge engineer on your staff; otherwise seek the services of a consultant or another qualified engineer.
4. Evaluate contract procedures and use one that gives you the best opportunity to save money.
5. Ensure that specifications and special provisions are complete to avoid costly construction claims.
6. Consider replacing bridges with culverts when conditions are right, and particularly when commonly used sizes will handle the runoff.
7. Use spill-through abutments as they generally will be most economical.
8. Use bridge types requiring minimum on-site labor.
9. For bridge lengths of 25 m (85 ft.) or under, consider the use of single spans. They present the minimum obstruction to the waterway and may also be most economical.
10. For long structures over flood plains, consider using span lengths of 15 to 30 m (50 to 100 ft.) as they often will be more economical than shorter spans depending upon bridge height and type of intermediate bents or piers.

Considering the current price situation in the Northwest the most economical bridge type on low-volume roads is precast, prestressed concrete with integrally cast decks. Average cost of these structures in the Northwest (Alaska excluded) ranges from $22 to $28 per square foot. Most counties that construct bridges by both in-house personnel and contract report that they get lower prices using the in-house method since the bridge crew can work on new construction when they are not otherwise occupied with maintenance work. On the other hand, several counties that previously used their own forces on new construction now report that all such work is done by contract.

Acknowledgements

In preparing this paper a large number of agencies and individuals were contacted. Their data and practices served as the detailed basis for this paper. Many individuals contributed considerable time along with their expertise. The author wishes to specially acknowledge some of the major contributors of information, design details, cost figures, photographs, etc.: ARMCO Corp.; Central Premix Concrete Co.; Concrete Technology Corp.; County Road Administration Board, Olympia, Washington; Morse Bros.; OBEC Consulting Engineers; U.S. Forest Service; and Weyerhaeuser Co. Appreciation is expressed to the many counties in Idaho, Oregon, and Washington who responded to the questionnaire and especially those who provided information in addition to the questionnaire.

SYSTEMS CONSTRUCTION TECHNIQUES FOR SHORT-SPAN CONCRETE BRIDGES

Michael M. Sprinkel, Virginia Highway and Transportation Research Council

Systems construction techniques have recently been used in the widening and replacement of numerous substandard or deteriorated short-span bridges in Virginia. The techniques involve the mass production of precast concrete components to one or more standard dimensions. Standard designs have been used for precast slab superstructures in the 3.1 - 9.1 m (10-30 ft.) span range, and for precast, prestressed single T-beams in the 9.1 - 20.1 m (30-66 ft.) span range. A modular precast parapet has been developed to accommodate all span lengths. Other modular concrete components that have been used include the channel beam, box beam, I-beam, and permanent bridge deck form. Evaluations have shown that the use of these mass produced components can minimize bridge costs; the same forms can be used many times and costly on-site forming and form removal are eliminated. Also investigations have shown that the use of precast components enables a reduction in on-site construction time that provides motor vehicle fuel savings for construction personnel and the traveling public. The experience in Virginia suggests that systems construction is an economical and operationally efficient method for widening or replacing short-span bridges.

Systems bridge construction may be defined as the on-site assembly of bridge components mass produced at an off-site plant to one or more standard dimensions. Because systems techniques have been used successfully in other industries to reduce costs by improving production efficiency, it is reasonable to expect that the same techniques could be applied successfully to bridge construction. When compared with conventional bridge construction techniques, systems techniques should improve construction efficiency because the same forms can be used for numerous bridges; fabrication can proceed in a systematic manner; fabrication can often proceed in bad weather, because protection from the elements is usually readily available; fewer man-hours are required for travel to and from the bridge site; and the cost of concrete is usually less, since the concreting operations are more centralized and haul distances are generally shorter. Also, since the systems techniques allow most of the bridge construction to take place at an off-site plant, the appearance and condition of the bridge site is restored in a short time; inconvenience to the motorist is lessened; motor vehicle fuel is conserved because there are fewer work trips to the bridge site, and fewer delays due to traffic detours and closed roadways; and working conditions are improved, as a majority of the work time is spent in the convenience and safety of the fabrication plant. Finally, it is anticipated that systems construction techniques will provide for a reduction in maintenance costs since high quality concrete is generally more readily attained in a fabricating plant than at a bridge site. Recent developments in concrete technology which may enhance the quality of bridge decks, such as vacuum dewatering, superplasticizers, wax beads, and polymer impregnation, may be more easily applied to modular components at the fabrication plant than to a large bridge deck at the bridge site.

Systems bridge construction techniques have been implemented in Virginia after some six years of joint efforts by many individuals, organizations, and committees. The Research Advisory Committee for Industrialized Construction, a committee made up of individuals from the Virginia Department of Highways and Transportation, the Virginia Highway and Transportation Research Council, and private industry, supported the basic concepts and recommended action by the Virginia Department of Highways and Transportation. Through the coordination of the Portland Cement Association, the Virginia Prestress Concrete Association cooperated with bridge contractors in Virginia to provide the Department with designs of bridge systems which could be competitively fabricated and erected in Virginia. The Bridge Division of the Department provided input to the systems design concept and supplied the final design details for the structures. The Research Council is monitoring the implementation of each bridge system.

The modular components that have been used successfully in Virginia, and which are discussed in detail in this paper, are a precast slab, which is used for 3.1 - 9.1 m (10-30 ft.) bridge spans; a precast, prestressed concrete single T-beam used for 9.1 - 20.1 m (30-66 ft.) bridge spans and a precast concrete parapet that is an option on almost all bridge spans. Other modular components include a channel beam, box beam, I-beam, and stay-in-place bridge deck form.

Precast Slab Bridges

For more than two years maintenance forces in the Virginia Department of Highways and Transportation have been using a systems construction technique to upgrade deteriorated and inadequate short-span bridges. The systems technique involves the fabrication of numerous precast concrete slabs in standard 1.2 m (4 ft.) widths and various lengths and skews using one set of forms. The slabs are cast at a district casting yard and stored until the substructure of the bridge on which they are to be used is properly prepared. They are then hauled to the bridge site and installed in a very short time. The modular precast slab members have been successfully used to widen concrete slab superstructures (Figure 1) and to replace substandard steel stringer-timber deck (SS-TD) superstructures (Figure 2).

A solid concrete slab is probably the easiest precast modular component to fabricate. A satisfactory casting bed is very simple to prepare and a systems casting operation is easily implemented. Three men worked about two weeks in preparing one of the first casting beds to be used by maintenance forces in Virginia. The bed was made from railroad ties, 5 cm (2 in.) thick timbers, exterior plywood, and miscellaneous hardware. It is 1.2 m (4 ft.) wide and 24.4 m (80 ft.) long (Figure 3).(1) The sides may be raised or lowered to produce slabs of various depths.

Slabs can be fabricated during the winter when there usually is a surplus of construction manpower. The precast slabs can be more economically heated and protected during curing than can site-cast slab superstructures.

Procedures for providing a rail with precast slab superstructures include casting a few large reinforcing bars into the exterior slabs to provide anchorage for the parapet, with the remainder of the parapet steel and all the concrete being placed at the bridge site; casting all the parapet steel and threaded metal inserts for anchoring the parapet forms into the exterior slabs; or precasting a concrete curb on the exterior slabs and bolting guardrail to the outside of the curb. A parapet is not precast on the exterior slabs because the combined weight of the parapet and slab would cause handling problems, but separately precast parapets can be satisfactorily connected to the exterior slabs at the bridge site.

In a typical widening and replacement project on a secondary road in Virginia, seven modular slabs can be placed and connected in one work day, and usually the road is closed for only a few minutes. A traffic detour usually is eliminated.

Shear transfer between adjacent slabs is provided by using a field weld to connect transverse reinforcing bars in the keyways, or by tensioning threaded metal rods placed through the slabs in the transverse direction. Cement mortar is used to grout the keyways between adjacent slabs.

Whereas precast slabs can be placed to widen a bridge in a few hours, a considerable amount of construction time at the bridge site is necessary to widen a bridge with site cast (SC) concrete. The falsework and forming and the placing of the concrete must be done at the site and in the presence of traffic. A lot of time is lost each day mobilizing the men, equipment, and materials.

As reflected by Table 1, a study of the operations in which maintenance forces widened and replaced 10 bridges in Virginia revealed that the precast slab superstructures were about 25% cheaper than the conventional alternative SS-TD and SC concrete superstructures. (2) Also the precast slabs reduced

Figure 1. Precast slabs used to widen bridge.

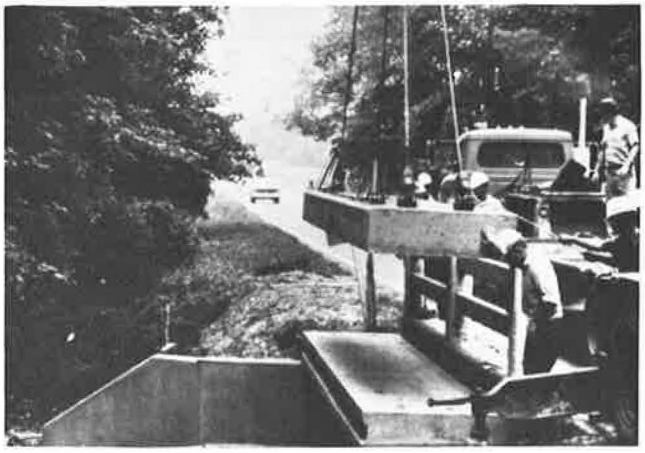

Figure 2. Precast slabs replace substandard steel stringer-timber deck superstructure.

Figure 3. Wood casting bed.

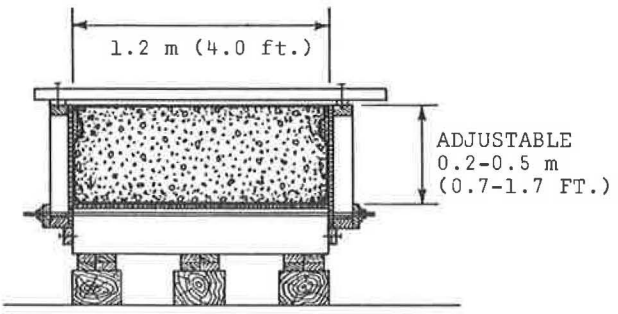

Table 1. Costs, man-hours, and travel required for precast slab construction as compared to SC concrete and SS-TD construction.

	Item	Percentage of Item Required for Precast Slabs	
		Site-Cast Concrete = 100%	Steel Stringer-Timber Deck = 100%
Costs	Labor	63	114
	Equipment	78	115
	Materials	107	40
	Total	77	69
Man-hours	In travel	22	42
	At-site	13	24
	Total	61	113
Travel	Fuel consumed	26	51
	Labor cost	21	38
	Equipment cost	57	117

on-site construction time by about 80%, which significantly benefits the motorist. Since precast slab construction requires fewer trips to the bridge site, less fuel, about 65% less according to the study, is required for moving the men and equipment.

The precast slabs fabricated by state forces are more economical than the conventional alternatives, primarily because of the turnkey concept. State forces design, fabricate, and construct the precast slab superstructures. Slabs designed by the state, fabricated by a subcontractor, and erected by a prime contractor may not be as economical as reported here. With adequate communication between the three parties the precast slabs should prove to be economical when advertised on a competitive basis. From a cost to society viewpoint, the precast slabs will be economical because they reduce delays and inconvenience to the motorist, conserve fuel in travel to and from the bridge site, and provide efficient use of manpower, equipment, and materials.

Precast, Prestressed Single Tee-Beam

The precast, prestressed concrete single T-beam provides for efficient bridge construction for numerous reasons. The shape of the member is particularly suitable for use in systems construction in that by maintaining a constant stem width of 0.3 m (1 ft.) and a flange width of about 1.2 m (4 ft.), only the bottom pallet and end bulkheads of a form have to be adjusted to provide economical beams for spans between 9.1 m (30 ft.) and 20.1 m (66 ft.)long as shown by Figure 4.(3) Since the flanges of the T-beams serve as the lower half of the bridge deck, in one step, which takes only a few hours, the contractor can advance from the bridge seat stage of construction to the forms-in-place stage (see Figure 5). Major deck forming is eliminated. Because of the reduced volume of SC concrete required, more extensive use of high quality concrete mixes that enhance durability may be reasonably justified for the 10.2 cm (4 in.) composite overlay. Usually a local prestressor will fabricate the single T-beams for a bridge and store them until the contractor completes the substructure. A lowboy is used to transport the beams, one or two per trip, to the job site. During 1976 and 1977, nine T-beam bridges

Figure 4. Systems T-beam shape. (1 ft. = 30 cm)

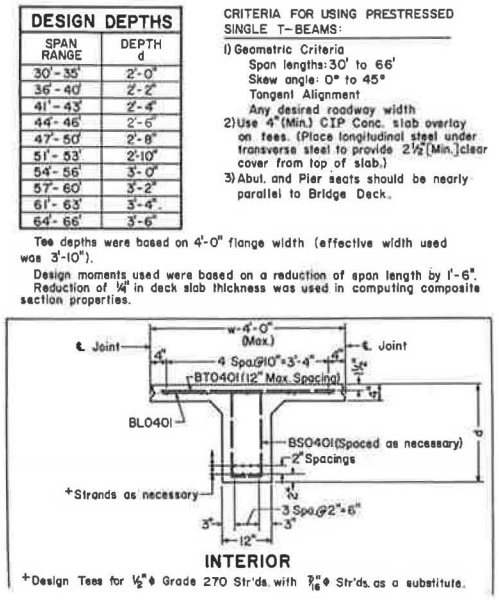

Figure 5. T-beam is placed in position.

were competitively advertised and constructed. In general the T-beam superstructures were about 10% cheaper than the conventional alternative steel-stringer SC concrete deck superstructures.

Figure 6 shows the construction sequence data for a typical 4-span precast, prestressed single T-beam bridge.(4) Working with a bridge crew of two to four men, the contractor erected, connected, and overlaid the T-beams in the 4-span bridge in roughly four weeks. A 4×10^4 kg (45-ton) truck crane and four men erected the eight 10.7 m (35 ft.) T-beams for each span in several hours. Another three days per span were required to form and cast the concrete diaphragms and to grout the keyways between the beams (see Figure 7). The side forms were prepared, the reinforcing steel positioned, and the concrete placed to provide a 10.2 cm (4 in.) overlay in another day and a half.

The amount of site time required to construct a concrete bridge superstructure is the sum of the times required to prepare the formwork, place the steel and concrete, strip the form work, and obtain cylinders with the design strengths. None of these four activities can be completely eliminated unless all SC concrete is completely eliminated. The precast, prestressed single T-beam design reduces site time by eliminating most of the forming and form removal usually required for conventional SC bridge decks and beams. But when the diaphragms are formed and cast at the site, an overlay cannot be placed until the diaphragm concrete has attained 75% of its design strength, which usually takes from three to seven days. Additional spans cannot be overlaid until the concrete in the adjacent overlays has reached 50% of its design strength, which takes from two to three days. If the backwall is used to support the screed, it also must have attained 50% of its design strength. A bridge cannot be opened to traffic until all the concrete in the superstructure has attained its 28-day design strength. The T-beam design reduces site labor considerably, but reduces site time only marginally when compared with more conventional types of construction.

Figure 6. Construction sequence data for Dickenson County bridge. (1 psi = 6.894 Pa)

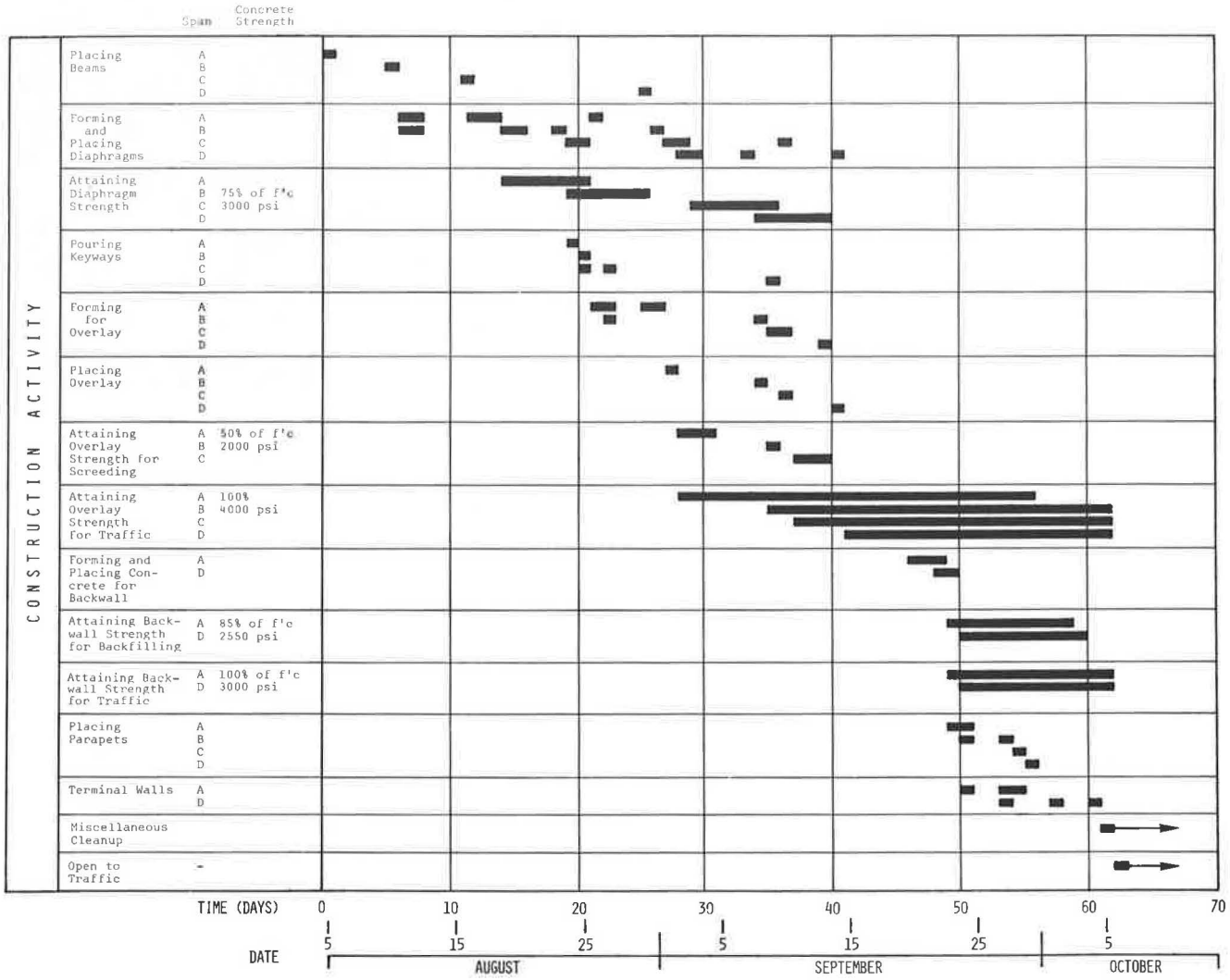

Figure 7. Nonshrinking cement paste is placed between adjacent T-beams.

Site time for a single T-bridge could be reduced if less SC concrete or high early strength SC concrete were used in the structure. For example, the use of precast concrete or steel diaphragms would reduce site labor time by three days, strength development time from three to seven days, and total site time from six to ten days per span. Forming for the overlay could begin the same day that the T-beams are placed and the diaphragms connected. The use of precast backwalls would allow the contractor to screed off the backwall and begin grading operations immediately after the backwall is positioned. Conceivably all the precast pieces could be placed and connected in one day, the overlay could be placed in another day, and grading operations could be completed on a third day. However, until the overlay develops 85% of its design strength, the parapets cannot be placed; and until the overlay develops 100% of its design strength, the bridge cannot be opened to traffic. Only when the single T-flange is designed to provide the full-deck thickness can one hope to open a single T-superstructure to traffic after one work day. A single T-bridge requiring no SC concrete will likely require transverse posttensioning for load distribution, longitudinal posttensioning to accommodate differential camber, and a waterproof membrane and bituminous wearing surface to protect the concrete.

Precast Parapets

Since placing the forms for conventional SC concrete parapets can be a costly and time-consuming job, precast parapets have been used with all of the T-bridges built in Virginia, and on many other bridges. The parapet lends itself ideally to a systems concept as it has a constant shape suitable for mass duplication (Figure 8) and is used in sufficient volume statewide to make precasting economical. The standard 2.4 m (8 ft.) long precast parapets are fabricated upside down to help eliminate honeycombing.

With the aid of a light truck crane, three men can place and connect the 1.8 x 10^3 kg (2 ton) parapet sections on a three-span structure in two or three days. The parapets may be set in cement mortar spread on top of the deck or they may be set on temporary wooden shims (Figure 9). The parapets may be anchored to the bridge deck in several ways,

Figure 8. Modular precast parapets.

Figure 9. Modular precast parapets positioned on shims prior to being anchored in place with grout.

but thus far all the contractors have chosen to make the connection with threaded metal rods which screw into inserts precast into the deck and extend upward through voids cast into the parapet (Figure 10).(4,5) Cement mortar is used to grout the voids and anchor the parapet. From the results of a pull-out test conducted in the laboratory, it was concluded that the spacing of approved inserts on 0.6 m (2.0 ft.) centers anchors the precast parapet sufficiently to satisfy AASHTO rail specifications.

Figure 10. Connection detail for precast parapet.

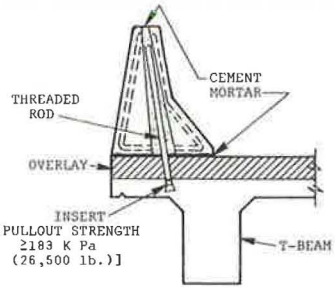

Further Considerations

Quality control and efficiency at the fabrication plant are probably the most essential ingredients for the successful construction of a modular or prefab structure. Precast components will fit together satisfactorily in the field only if they are cast to close tolerances. Since the major portion of a modular construction project takes place in the factory, the major portion of the supervision and inspection also must take place there. Fabrication errors that are not detected at the plant can be very costly and time-consuming to remedy in the field. Precast components cast in a good set of forms and under close supervision will fit together quickly and securely in the field and will provide a structure that is far more economical and of superior quality to one built with more conventional construction techniques.

Systems bridge construction has been initiated in Virginia with an emphasis on bridge superstructures. Since 50% to 80% of total bridge construction time is involved with the substructure, it is believed that considerable savings in time and related costs can be achieved by specifying precast substructure components where their application can contribute to speed off construction. A contractor who has a large crane on hand to install superstructure elements should be able to efficiently and economically erect substructure components. Substructure systems are being considered at this time, but a prototype has not yet been designed in Virginia.

Conclusions

Evaluations of the systems construction techniques have shown that concrete bridge components mass produced in off-site fabrication plants can be used to minimize bridge costs; the same forms can be used many times and costly on-site forming and form removal are eliminated. Also investigations have shown that the erection of precast components enables a reduction in on-site construction time that provides motor vehicle fuel savings for construction personnel. Fuel savings for the traveling public are implied, since detours and traffic congestion are minimized and at times eliminated. The greatest benefits are found in remote areas where haul distances for ready-mix concrete are excessive and in highly congested urban areas where many motorists are inconvenienced by detours, delays, and traffic congestion accompanying the widening or replacement of a bridge. Recent experience and ongoing research indicate that systems bridge construction will have a significant role in Virginia's bridge replacement program. Since transportation officials have estimated that there are over 100,000 short-span bridges in the U. S. that need to be upgraded, it is envisioned that systems bridge construction will have national application in the years ahead.

Acknowledgements

The research reported here was sponsored by the Virginia Highway and Transportation Research Council in cooperation with the Federal Highway Administration. The opinions, findings, and conclusions expressed in this paper are those of the author and not necessarily those of the sponsoring agencies.

References

1. "Sketch of Casting Bed", Staunton District Bridge Division, Virginia Department of Highways and Transportation, 1975.

2. Sprinkel, M. M., "In-house Fabrication of Precast Concrete Bridge Slabs", VHTRC 77-R33, Charlottesville, Virginia, December 1976.

3. "Prestressed Single T-beam Details", Bridge Division, Virginia Department of Highways and Transportation, August 1976.

4. Sprinkel, M. M., "Construction of Prestressed Concrete Single-Tee Bridge Superstructures", VHTRC 77-R50, Charlottesville, Virginia, May 1977.

5. "Precast Concrete Parapet Details", Bridge Division, Virginia Department of Highways and Transportation, 1974.

BEHAVIOR OF ALASKAN NATIVE LOG STRINGER BRIDGES

W. W. Sanders, Iowa State University
F. W. Muchmore and R. L. Tuomi, U.S. Forest Service

For many years, native log stringer bridges have served as the primary bridging system for the Alaska forest transportation network. They are constructed from Sitka spruce or western hemlock logs, placed side by side and decked with blast rock, all locally available materials. These bridges have served for ten years or more, and have been economical as well (average cost $54/sq m, or $5/sq ft). Inspection and load rating as required by the national bridge inspection standards raised questions about wheel-load distribution and physical strength properties of the bridges. The procedures used in their analysis were based on limited information and the evaluations were, at best, approximate. This applied particularly to the load distribution criteria. A research program was undertaken to obtain the information necessary to provide more realistic rating information. This research program included four phases:

1. Strength evaluations of full size logs,
2. Load distribution tests of four "in-service" bridges (spans 11.6 - 28.0 m; 38-92 ft),
3. Laboratory tests of models of typical bridges, and
4. Analytical evaluation of bridge test data and development of revised load distribution criteria.

The field and laboratory test results supported the analytical findings of better distribution than that of current design. The strength tests provided current data on the ultimate bending strength of Sitka spruce and western hemlock logs. The final result of the study are revised design criteria which show that significantly higher loads can be allowed than are permitted under current criteria.

Within the last 20 years, several thousand bridges have been built with native logs in the southeast regions of Alaska (Figure 1). This effort is part of the development of the National Forest Transportation system on the islands of the Alexander Archipelago in the Southeast Alaska Panhandle.

Bridges were needed to span streams, and an abundance of high-quality Sitka spruce logs, up to 1.52 m (5 ft) in diameter, was available locally. Therefore, it proved economically advantageous to build the bridges from these native materials. With trees cut in the proximity of the bridge site, the cost of constructing these bridges was only about $54.00 per sq m ($5.00 per sq ft).

Figure 1. Native log stringer bridge in southeast Alaska: Span--28 m (92 ft); Capacity--72.5 Mg (80 tons).

Typically, logs are not sawn into timbers and planks, but are placed butt-to-tip on log crib abutments and tied together with cables (Figure 2). Blast rock is then placed on the logs and bladed to provide a running surface. Brow logs are placed at the sides of the bridge to serve as curbs and guardrails. Although this may seem primitive, the several hundred bridges of this type currently in use function quite adequately for up to ten years or more. Some of the bridges are quite impressive, with clear spans approaching 30 m (100 ft), and carry off-highway logging trucks with gross vehicle weights exceeding 90 Mg (100 tons).

Figure 2. Log crib abutments and bottomside of log stringer superstructure.

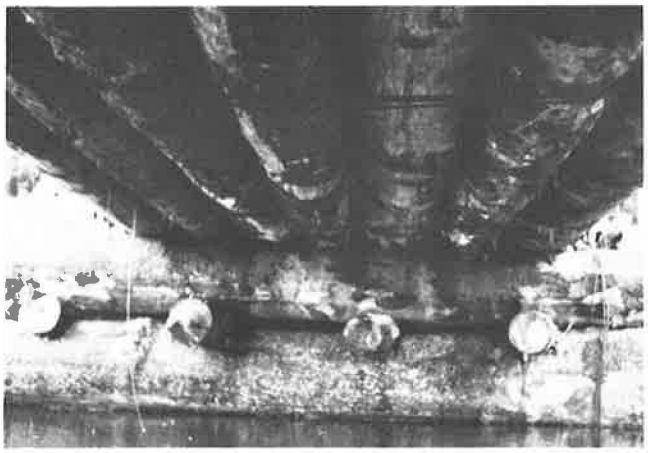

Bridge Safety

As a consequence of the "Silver Bridge" disaster in 1967, Congress included a provision in the Federal Aid Highway Act of 1968 which required the Secretary of Transportation to establish national bridge inspection and load rating standards. Those bridges not meeting the loading criteria must be posted for allowable loads accordingly.

Unfortunately, the current knowledge of log stringer bridge analysis and design (1) is limited. Little is known about the bending strength or expected life of large-diameter logs. The recommended allowable design stresses are based on procedures developed for poles and piles. The manner in which wheel loads are distributed between stringers is not well understood.

Inspecting and load-rating existing bridges by current procedures indicated that many log stringer bridges are being seriously overloaded. In a number of instances, the calculated allowable load is much less than the weight of logging trucks which have regularly been using these bridges for several years. It is apparent that new and reliable design information is needed to properly analyze log stringer bridges.

Cooperative Research Program

To obtain the needed information on the performance of log stringer bridges, the U. S. Forest Service-Alaska Region (Region 10) and the U.S. Forest Products Laboratory (FPL) conducted wheel-load distribution tests on existing bridges, and strength evaluations on both used and green Sitka spruce and green western hemlock logs.

The field test data for load distribution analysis were then analyzed by the Engineering Research Institute of Iowa State University (ISU) under a cooperative agreement with the Forest Products Laboratory. Using this data, ISU developed analytical procedures to study a wide range of variables affecting load distribution that cover all types of log stringer bridges. The results were confirmed by scale-model tests conducted in the ISU laboratory.

The final result of the study are recommendations for new allowable log stresses and load distribution criteria that will more accurately predict the behavior of the bridges. This paper summarizes the studies indicated above.

Field Test of Log Stringers (2)

The testing took place at Thorne Bay on Prince of Wales Island. Twenty-five green Sitka spruce logs, 15 green western hemlock logs, and 28 used Sitka spruce logs were tested to destruction in the field test facility. These are the common species for log stringer bridges, with Sitka spruce being used almost exclusively. The logs for the individual stringer tests were representative of the logs used in existing logging operations in the 16-million-acre Tongass National Forest. Log quality was determined by standard design requirements (1). Lengths ranged from 14.3 to 26.2 m (47 to 86 ft), with diameters of up to 1.47 m (4.8 ft) at the butt end.

The test facility (Figure 3) consisted of a hold-down anchor, support cribs, and a loading system. Sixteen rock anchors, capable of resisting 900 kN (200,000 lbf), were installed. Two movable support cribs (adjusted for log length) were built by cross-stacking large logs to a height of about 4.9 m (16 ft) above ground. Loads were applied by cable through two quadruple sheave blocks to increase the force by about 8 to 1. The strongest green log held up a load in excess of 530 kN (120,000 lbf) before it broke. The green western hemlock logs frequently broke explosively, scattering some of the loading apparatus about the site. Green Sitka spruce logs, on the other hand, failed gradually and stayed up on the supports. However, a few of the old, used spruce logs shattered upon failure.

Figure 3. Test set-up (with log in position) for bending tests.

The current procedure for determining allowable bending stress in logs is contained in ASTM D-2899 (3). With this procedure, a statistical point estimate of minimum strength is established which 95 percent of the population should exceed. It is based on the modulus of rupture of small clear wood specimens with appropriate adjustments for growth, shape, variability, etc. The field tests confirmed that this procedure is reasonably accurate.

The log strength properties for green logs are summarized in Table 1. The frequency distributions

Table 1. Log strength properties.

Source	Number of Specimens	Modulus of Rupture				
		Average MPa	Standard Deviation MPa	Coefficient of variation %	Maximum MPa	Minimum MPa
		Western Hemlock				
False Island	4	33.0	4.8	14.4	39.4	28.0
Zarembo Island	4	31.9	4.4	13.9	37.9	27.6
Prince of Wales Island	7	32.1	6.8	21.2	40.2	21.9
All hemlock	15	32.3	5.4	16.7	40.2	21.9
		Sitka Spruce				
False Island	8	31.3	3.7	12.0	39.0	28.1
Zarembo Island	6	29.9	4.1	13.6	35.0	23.6
Prince of Wales Island	11	31.9	7.3	22.8	47.4	20.8
All spruce	25	31.2	5.5	17.6	47.4	20.8

[a] 1 MPa = 145 lbs/in.^{2}

are skewed somewhat to the right and are best represented by log normal distributions which are common for wood. One-sided tolerance limits for the two species at different confidence levels are presented in Figures 4a and 4b. The current design levels are also shown.

The bridge engineer must decide upon the combination of safety and economics that is appropriate for his design. The breaking strengths shown are generally multiplied by a factor of 0.62 to obtain ten-year duration of load stresses. This is quite conservative, since most bridges are under full design load for only a very short time during their service life.

Modulus of rupture values for Sitka spruce logs after 12 years of service were calculated by two methods. The first method was based on the section modulus of the full log diameter, and produced an average strength of 24.0 MPa (3.48 ksi). The second method subtracted peripheral decay from the gross area to estimate the net sound section. The average modulus of rupture of the sound material was 33.2 MPa (4.82 ksi), essentially the same as for fresh logs.

Load Tests of Actual Bridges (Staney Creek) (2)

Four bridges with clear spans ranging from 11.6 to 28.1 m (38 to 92 ft) were selected for the wheel-load distribution tests. The bridges, located on Prince of Wales Island, were loaded with a large off-highway gravel truck with a gross vehicle weight of 39,000 kg (87,000 lb) (Figure 5). Centerline deflections of each stringer and each brow log were recorded for nine different truck positions. The maximum deflection on the 28 m-span (92 ft) bridge was only 33 mm (0.11 ft). There was significant deflection in the brow logs, indicating that they were contributing structurally to the performance of the bridges.

A plan view and cross-section of a typical log bridge are shown in Figures 6 and 7. Typical deflection data for the two positions of loading (concen-

Figure 4a. Short-term breaking strength of western hemlock logs for various tolerance limits and confidence levels.

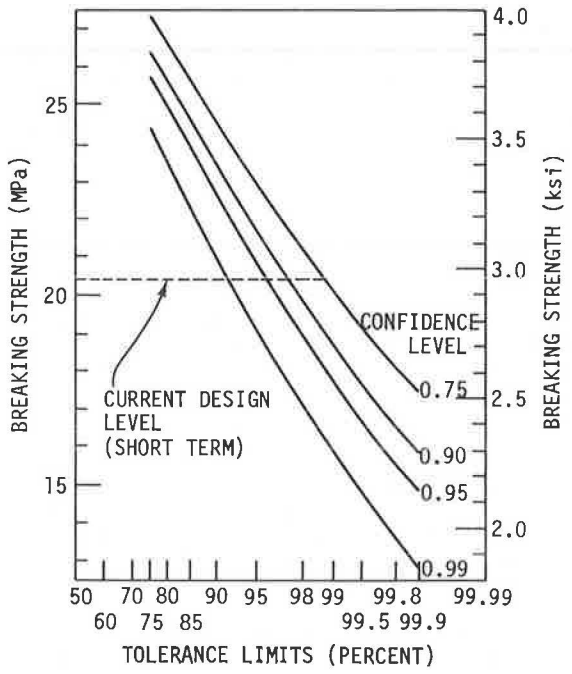

Figure 4b. Short-term breaking strength of Sitka spruce logs for various tolerance limits and confidence levels.

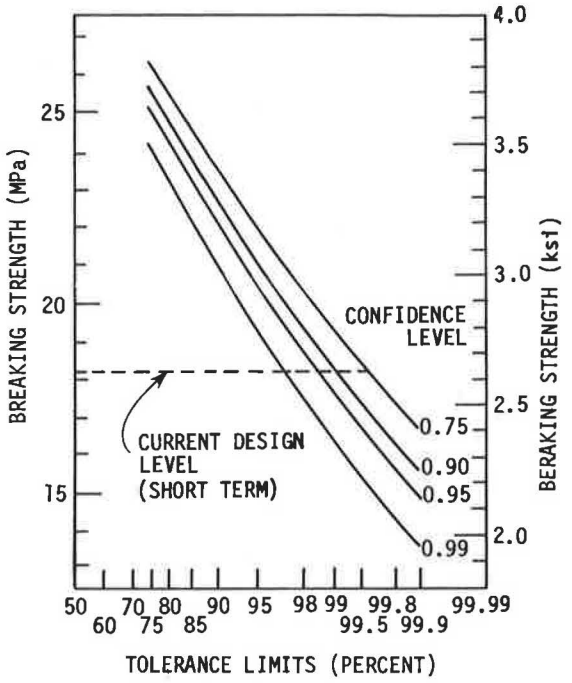

Figure 5. Load test truck (39,000 kg; 87,000 lbs) on bridge.

tric and eccentric) are shown in Figure 8 for the truck at midspan. The deflections give an indication of the load distribution, although adjustments are required due to variations in log diameters.

The results of three of the bridges were used to determine the validity of the analytical procedures used to develop the overall behavior of a wide range of log stringer bridges. The fourth bridge failed during testing.

Analytical Investigation of Bridges

In this portion of the investigation analytical techniques were used to study the load distribution characteristics exhibited by the bridges in the field. The investigation proceded in two parts. First, after a method of theoretical analysis was selected, a means of comparing the load distributions from field tests on the Staney Creek bridges and theoretical load distributions of these same bridges were developed. The second part was the

Figure 6. Plan view of 22 m (72 ft) West Fork Staney Creek Bridge.

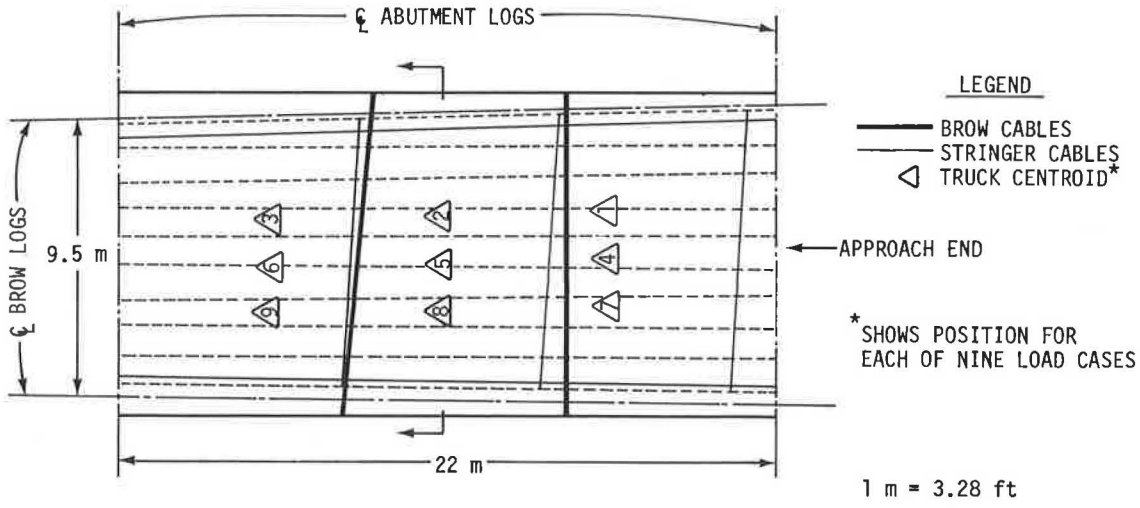

Figure 7. Cross-section of 22 m (72 ft) West Fork Staney Creek Bridge at midspan.

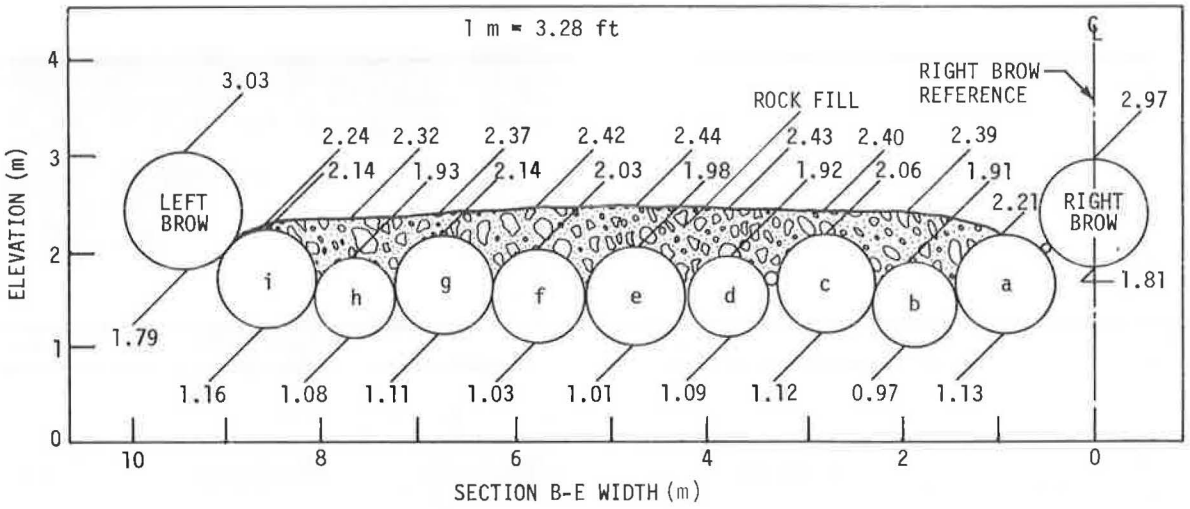

investigation of theoretical load distributions for a range of variable that encompassed the majority of bridges found in Alaska today.

The articulated plate theory (4) was chosen for the analytical investigation, as it is better suited to log bridges because load distribution between stringers is primarily accomplished by friction between logs. This type of behavior indicates a load distribution through shear rather than bending; thus, the selection of the articulated plate theory seemed appropriate. The basic assumption in the theory is that only shear is transferred between bridge elements.

Figure 8. Deflection diagram for 22 m (72 ft) bridge with test truck at midspan.

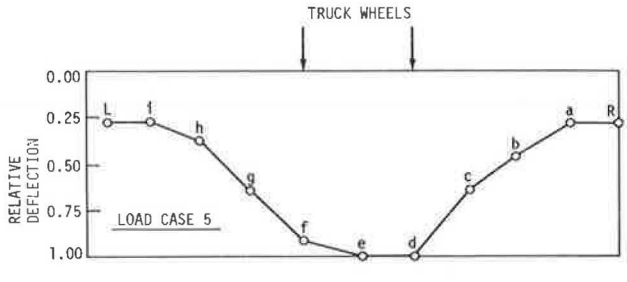

(a) Concentric load position

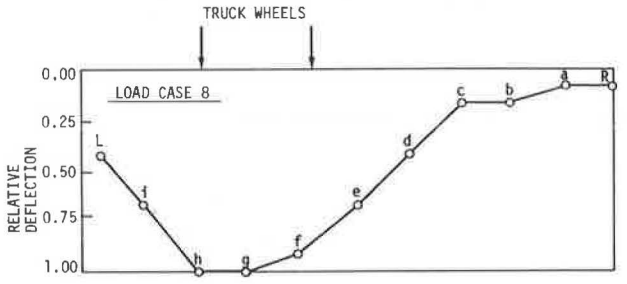

(b) Eccentric load position

The basic comparison between theory and field data is the moment coefficient per foot of log, K_{MPL}. It is the ratio between the moment per foot of bridge width in the log to the average moment per foot of bridge width. To compare theoretical load distribution with the load distribution from field tests, a suitable parametic relationship for use in articulated plate theory was developed. It was shown (4) that the most important cross-section parameter in the determination of transverse wheel load distribution is ϕ, which is approximately

$$\phi = 1.5 \frac{W}{L} \quad (1)$$

where W = effective bridge width, m (width of bridge plus diameter of brow logs) and L = length of span, m.

The values of K_{MPL} for the stringers in the Staney Creek bridges were computed from deflection data received from the field tests. K_{MPL} values in stringer due to all nine load cases were computed for all three Staney Creek bridges. The midspan load cases were of particular interest because the theoretical analysis only considered bridges with midspan loadings. After the values of K_{MPL} had been computed from the field test deflection data, theoretical values for K_{MPL} in the stringers of the same bridges were calculated using articulated plate theory. Typical load distributions from the Staney Creek field test of the 22 m (72 ft) bridge and the computer analysis using articulated plate theory with $\phi = 1.5\ W/L$ are shown in Figure 9.

Comparison of the load distributions curves for the load cases shows that the theoretical analysis favorably models the actual field test results. Not only do the curves follow the same shape in each load case, but the maximum values of K_{MPL} for the theoretical and field test analysis are nearly equal and occur in about the same locations in both analy-

Figure 9. Comparison of K_{MPL} from theory and from field bridge tests, 22 m (72 ft) Staney Creek Bridge.

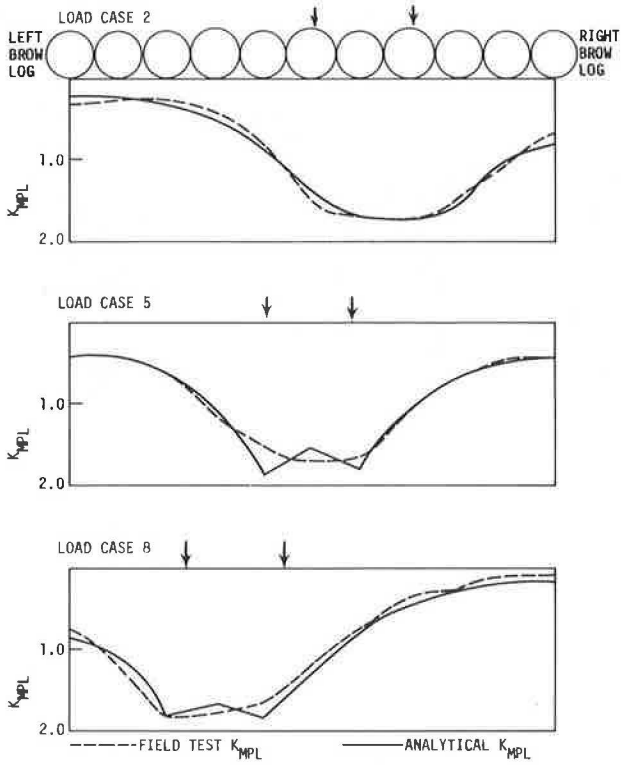

sis. This relationship was typical of all cases studied.

Upon verification of the validity of the theoretical analysis, load distributions were generated for the broad spectrum of bridges. Because the theoretical load distribution in a bridge was based on length and width of the bridge, it was necessary to determine sizes of actual Alaska log bridges. Based upon the results of a field inspection (5), the range of stringer sizes, number of stringers, bridge spans, rock depths, and log configurations were obtained. It was found that the typical bridge had a width of about 4.6 m (15 ft) and a span of 9.1-15.2 m (30-50 ft), and had 8-10 stringers with brow logs.

Using this data, upper and lower bounds were set in width and length of bridges. These bounds set the limits of ϕ (Eq. 1) from 0.25 to 2.50, with a typical value of 0.75.

After determination of the range of sizes of the field bridges in Alaska, theoretical load distributions for bridges within the range were developed. The initial study was limited to bridges without brow logs. The effect of brow logs was determined later.

Computation of these distributions was done using an articulated plate theory computer program. However, instead of using the field truck loading used in generation of theoretical load distribution curves for the Staney Creek bridges, standard loads (unity) were used as the concentrated loads. This standard load computer program (from articulated plate theory) was then used to generate concentric and eccentric load distribution curves for a broad spectrum of bridges. Typical eccentric and concentric load distributions are shown in Figure 10.

Figure 10. Distribution curves for typical log stringer bridges.

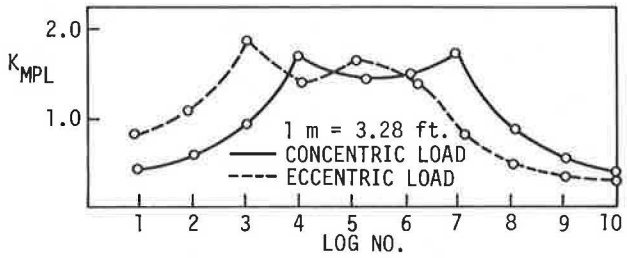

Experimental Investigation of Model Bridges

The experimental investigation of bridges was needed to supplement test data provided by the Forest Service (2) so that confirmation of general design criteria could be obtained. Comparison of the results from the field test data and the computer analysis proved favorable, but experimental work was needed before generalizations on the nature of load distribution in stringers, including the effect of brow logs, could be made. The experimental work consisted of tests of laboratory model bridges.

The model bridges were constructed of 7.6 m (25 ft) utility poles with diameters ranging 20.3-26.7 cm (8-10.5 in.), as shown in Figure 11. The bridges were either at a scale of 1:5 or 1:4, depending on the log diameter in comparison to the span length being modeled. Over 25 model bridges were tested. The significant parameters were the width of the bridge and addition of brow and/or stabilizer (transverse) logs (Figure 12).

The objectives of the experimental investigation were twofold. The first was to gain additional load distribution data to supplement the information provided by the field bridge tests. These additional data were needed to verify the assumptions made in the theoretical load distribution study.

The second objective was to isolate the effect of brow logs and stabilizer logs on load distribution. By the systematic addition and removal of brow logs and stabilizer logs to test bridges of a given length and width combination, their effect on load distribution was determined.

A comparison of the lab test, field test, and theoretical load distribution is shown in Figure 13. The lab test distribution is taken from calculations based on the diameter and deflection of the stringers (Figure 12) in the model bridge. The theoretical distribution is found by using the standard load program with width and number of logs of the model bridge as input. The field test distribution is taken from articulated plate analysis of the Staney Creek bridge. All three curves are approximately the same shape, and the peak percentages of load carried by a stringer in each bridge are close. The peak theoretical and field percentages of total load in a stringer are 18.8 percent and 17.5 percent, respectively, which is a difference of 7 percent. The experimental lab test peak percentage of load in a stringer is slightly higher at 21.5 percent. Comparing all three distributions, the peak percentage of total load in a bridge stringer is about 20 percent.

After comparing the distribution curves (includ-

Figure 11. Laboratory model test bridge ready for test.

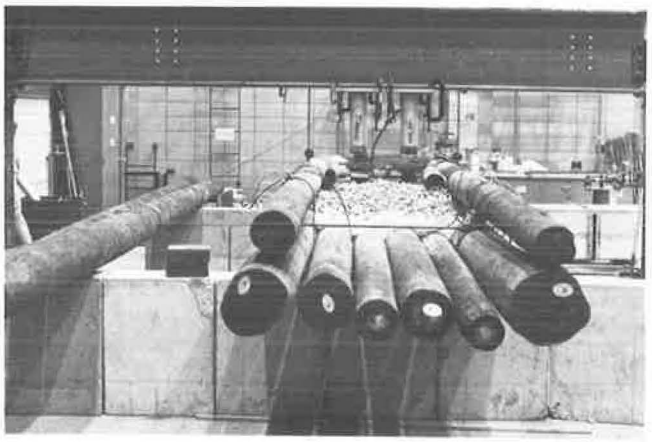

Figure 12. View showing stabilizer log and deflection dials.

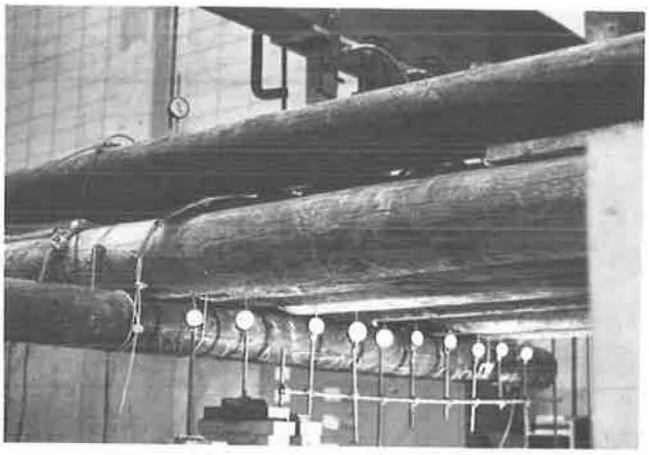

Figure 13. Comparison of theoretical, field test and model test load distribution for 22 m (72 ft) Staney Creek Bridge.

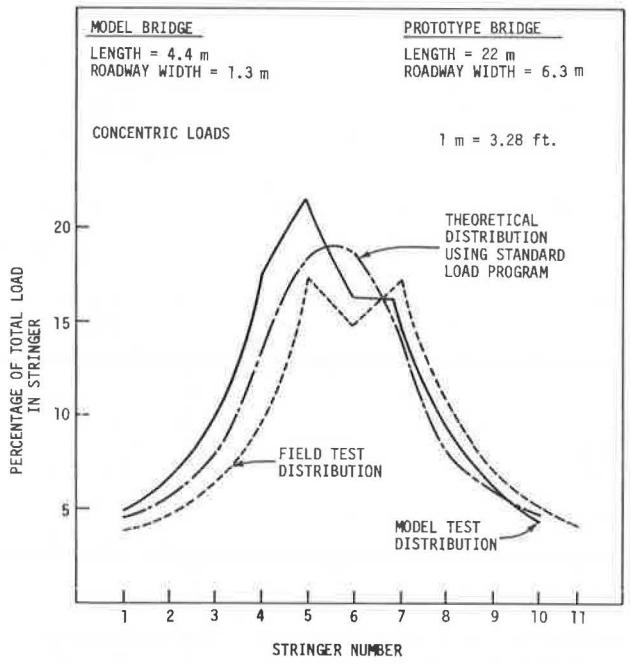

ing Figure 13) for the model bridges, it was seen that the first objective in the experimental investigation had been accomplished, i.e., that the load distributions obtained in the lab tests had consistently matched load distributions from field testing and the theoretical study. Thus, the theoretical results previously outlined could not only be considered valid for bridges similar to those field tested, but also for the entire range of Alaskan bridges as typified by the model bridges. The model bridges also showed the effect of the brow logs and stabilizer logs on load distribution. Reductions in the maximum percentage of load in the critical stringer decreased from about 5 to 15 percent with the addition of brows. Reductions of the percentage of load carried by the critical stringer in the model bridges due to the addition of a stabilizer log ranged from 6 to 27 percent.

Brow logs do much more for a bridge than merely act as a guardrail. It was shown that the brow logs are an essential structural entity of a bridge, since they can decrease the amount of load carried by the critical stringer by an average of 10 percent. Stabilizer logs can also play a role in load distribution. By placing a midspan stabilizer on a bridge, the stiffness of the bridge is increased, which can decrease the amount of load taken by the critical stringer by about ten percent. However, for the stabilizer to distribute the load across the width of the bridge, it is important that the stabilizer logs make contact with all stringers. In reality, this is difficult, thus making their practical use very questionable.

Formulation of Load Distribution Criteria

After completion of the analytical and experimental investigation of load distribution, the final phase of the ISU study was to incorporate the findings of the two investigations into a new rating criteria. The analytical investigation had shown that the behavior of the field bridges in Alaska (2) could be theoretically explained using a modified form of articulated plate theory. Once the load distribution in the Staney Creek bridges had been verified, a series of theoretical load distribution curves were produced to predict the behavior of a range of bridges commonly in use. The experimental investigation provided additional laboratory tests to supplement the actual field tests done in Alaska, and helped justify the assumptions made in the theoretical investigation.

The final step of the analytical investigation was to produce a set of theoretical load distribution curves for the range of bridges used in Alaska. The maximum values of K_{MPL} for the range of bridge sizes were compiled for both concentric and eccentric load cases. For cases with realistic configurations, these values are plotted in Figure 14. The plot relates the distribution factor, K_{MPL}/W, to

the bridge span. It should be noted that this plot is for bridges without brow logs.

A least squares fit for the data relating the distribution factor with span is also shown in Figure 14. This data is being analyzed and will be developed into tabular form so that the engineer can readily determine the final design or rating factor for any bridge to be studied. This final factor will consider the effects of variables such as workmanship and variations in log properties.

Figure 14. $\frac{K_{MPL}}{W}$ vs. L for bridges without brow logs.

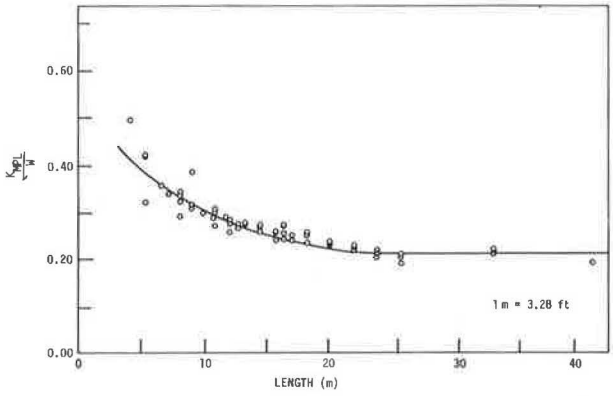

The maximum vehicle moment per log (M_L) can then be computed from

$$M_L = \frac{K_{MPL}}{W} M_v d \qquad (2)$$

where M_v is the maximum applied vehicle moment, d is the diameter of log (m) being rated.

The effect of brow logs has been shown to reduce the maximum moment coefficient as much as 10 percent. This method results in an average stringer moment of about 22 percent of the total truck moment, as compared to 30 percent in the current design and rating criteria (1). Since the dead load in most bridges is relatively low, the use of the revised criteria could result in an increase in rated capacities of about 30 percent.

Summary

This paper presents a summary of the results of a three-part study of Alaskan log stringer bridges. The investigations included the load testing of actual logs to determine ultimate bending stress, field load testing of four log stringer bridges to obtain experimental distribution of live load, and a comprehensive analytical and laboratory model test study of load distribution with the development of a proposed revision to the current load distribution criteria (1).

The results of the project are more accurate ultimate bending stresses for log stringers and a more realistic load distribution criteria for rating of bridges. These results will be used to develop revisions to the current design and rating procedures (1) for Alaskan native log stringer bridges and will be considered by the U.S. Forest Service.

Acknowledgments

The research was funded by the U.S. Forest Service. The field tests and the log property tests were conducted by the Forest Products Laboratory and the Alaska Region of the U.S. Forest Service. The laboratory tests, the analytical investigation and development of the distribution proposals were undertaken by the Engineering Research Institute of Iowa State University. Special recognition should go to R. Wolfe of the U.S. Forest Service and to R. A. LaBoube and J. R. Woodworth of Iowa State University.

References

1. F. W. Muchmore. Design Guide for Native Log Stringer Bridges. U.S. Forest Service (Region 10), 1977, 20 pp.
2. F.W. Muchmore et al. Native Log Stringer Bridge Research in the Alaska Region. U.S. Forest Service Field Notes 9, 1977, pp. 9-17.
3. Standard Method for Design Stresses for Round Timber Piles. ASTM Specification D-2899-74. 1977 ASTM Standards 22, pp. 816-818.
4. W. W. Sanders and H. A. Elleby. Distribution of Wheel Loads on Highway Bridges. NCHRP, Rept. 83, 1970, 56 pp.
5. R. Willis. Log Stringer Bridge Inspection and Analysis in Alaska. U.S. Forest Service Field Notes 7, 1975, pp. 10-16.

TRANSVERSE POST-TENSIONING OF LONGITUDINALLY LAMINATED TIMBER BRIDGE DECKS

R.J. Taylor and P.F. Csagoly, Ontario Ministry of Transportation and Communications

Longitudinally, nail-laminated timber bridge decks are used extensively in northern Canada, where the cold and dry climate discourages the activities of fungi and termites. The load-carrying capacity of these structures is dependent upon their ability to effectively distribute wheel loads among the laminates; this being a function of the friction and the holding power of the nails. Due to overloads, volumetric changes and environmental effects, the holding power tends to diminish resulting in a subsequent reduction in the load-carrying capacity of the bridge. Construction of these nail-laminated systems involves extensive labour, since thousands of nails have to be driven into hundreds of laminates. Quality control is quite difficult as it requires continuous supervision to ensure that all the nails are properly placed and driven. This report describes the application of transverse post-tensioning to an existing longitudinally nail-laminated timber deck structure in Ontario. This 3-span continuous bridge portrayed the delaminating problem, and as such, presented an appropriate test site for a post-tensioning system. Load testing was done before and after post-tensioning to determine its effects on the structure's response. An evaluation of the test results indicated that the structure's load-carrying capacity was increased by at least 100%. Transverse post-tensioning, in effect, replaces the need for nailing and hence reduces the labour required for construction. Quality control extends only to ensuring that adequate post-tensioning forces exist to provide the friction necessary for load distribution, allowing for anticipated losses due to creep. This confined deck system exhibits better resistance to the environment, as it eliminates the penetration of foreign materials between the laminations.

The Ontario Ministry of Transportation and Communications is conducting an ongoing load testing program, in which a varying number of bridges are analyzed and tested each year. The primary objective of the program is to establish a safe load-carrying capacity, while increasing knowledge of the behaviour of bridges under load. Prior to the start of a load testing season, an inspection is undertaken to determine which structures would most benefit from load testing. It is during these inspections that many inherent problems related to specific structural designs become apparent. One such problem concerns the delamination of Longitudinally Nail-Laminated Timber Deck structures (L.N.L.).

Since the L.N.L. system depends extensively on its ability to distribute wheel loads transversely, delamination of the system can cause a severe reduction in the capacity of the structure. In some instances, where some of the nails no longer perform their function, the capacity of the structure rests upon those laminates directly under the applied load.

Hebert Creek Bridge displayed the characteristic problems of a delaminated L.N.L. structure. The bridge was posted for a reduced load of 15 tons (133 kN) and identified for replacement in 1976. This bridge was selected as a test site for the development and testing of a transverse post-tensioning system. This system would create adequate friction to ensure load sharing of the laminations, while closing the deck tightly to prevent further deterioration.

This report is primarily concerned with the design and installation of the post-tensioning system for the Hebert Creek Bridge and the load testing of the structure before and after the system was stressed.

Site Description

Hebert Creek Bridge is a 2-lane structure located on Highway 539 about 5 km (3 mi.) north of Highway 64, near Field, Ontario. The 3-span continuous structure was designed and built for an H20 truck load in 1951.

The 16.76 m (55 ft.) long structure consists of two side spans of 5.33 m (17.5 ft.) and one center span of 6.10 m (20 ft.), as shown in Figure 1. The 51 mm x 305 mm (2 in. x 12 in.) timber laminations were placed on edge and oriented longitudinally, as illustrated in Figure 2. The timbers were so arranged to produce longitudinal discontinuities of the laminates at the one third span points and support points only. In addition, for any one transverse section the joints would occur at every third lamination.

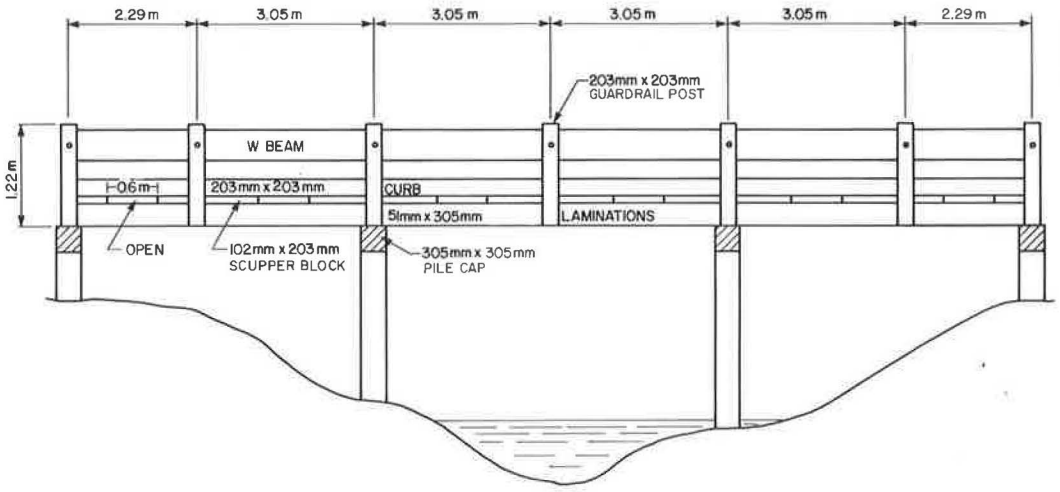

Figure 1. Hebert Creek Hwy. 539 elevation.

Figure 2. Hebert Creek cross section of deck at pier.

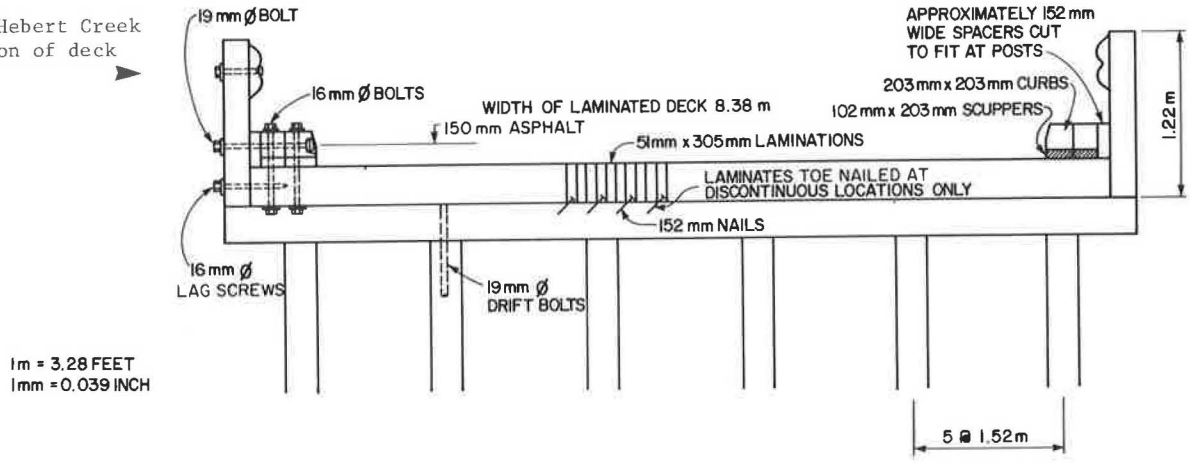

Figure 3. Creep testing machine.

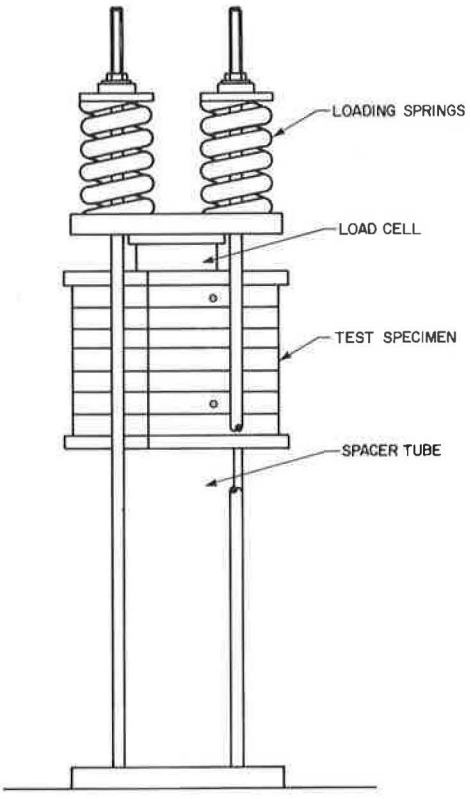

Pre-Testing Evaluation

The structure was initially evaluated according to AASHTO (1) Specifications and the original H20 design loading was confirmed. A precise computer analysis of the structure, prior to post-tensioning, was not feasible due to the non-linear mechanical nature of the deteriorated nail-laminated system.

However, a computer analysis was performed which was intended to represent the post-tensioned structure. The analysis was conducted using a program called ORTHOP (3) assuming that the transverse transfer of load is performed by shear, with no transverse flexural stiffness. The analysis predicted a maximum longitudinal flexural stress of 6200 kPa (900 psi) under the maximum load of a 417 kN (93,800 lb.) tandem of the test vehicle. The maximum transverse vertical shear stress was established as 138 kPa (20 psi) which was incorporated in the design of the post-tensioning system. The maximum anticipated deflection of the post-tensioned structure under the test vehicle was 10 mm (0.4 in.), assuming a modulus of elasticity of 10.3×10^6 kPa (1.5×10^6 psi).

Allowances for support movements were not incorporated in the analysis, therefore, the actual displacements were expected to be higher.

Post-Tensioning

Creep Tests

Creep is considered to be one of the most important considerations in post-tensioning timber perpendicular to the grain. Under sustained stress the timber will creep considerably, reducing the initial stress that was introduced into the system. To evaluate the effects of creep, an investigation was conducted prior to the actual design of a post-tensioning system.

Two test specimens, composed of seven pieces of timber approximately 279 mm x 279 mm x 41 mm (11 in. x 11 in. x 1 5/8 in.), were constructed and installed into the testing apparatus as displayed in Figure 3. Both specimens were stressed to 1034 kPa (150 psi), however, the load springs were removed from one specimen to introduce a variation in the stiffness of the system. Both load and strain measurements were taken over a period of 2000 h.

The results of these tests are displayed in Figures 4 and 5 and indicate that an equilibrium was reached at approximately 1000 h. Plotting the ratio of the initial to the final stress against the stiffness of the test apparatus produces the two points on the curve given in Figure 6. With these points and the two known boundary conditions, an approximate solution to the curve was developed. This relationship was used to account for the effects of creep in the design of the post-tensioning system.

Further creep tests are being performed to gain an understanding of the effects of the environment on the test specimens under sustained load. This is being performed as a separate investigation since it involves a considerable amount of time and special equipment.

Design

An important aspect of the design is the evaluation of the minimum permanent stress required between the timber laminations, to ensure proper load transfer. An analysis was performed using a program called ORTHOP (3), as described in the pre-testing analysis. Under the maximum tandem load of the test vehicle, 417 kN (93,800 lb.), the maximum transverse shear stress was calculated to be 138 kPa (20 psi). Assuming a conservative coefficient of friction between the timber surfaces of 0.5 (4), the required minimum prestress would be 276 kPa (40 psi). Using the relationship for creep developed in the preceding section, and assuming an initial stress of 1034 kPa (150 psi) on the timber, the stiffness of the required post-tensioning system should be about 70 000 kN/m (400,000 lb./in.).

The selection of the post-tensioning system used at Hebert Creek was based upon the following considerations:

1. Ductility - The system must be ductile enough to compensate for losses due to creep. A minimum design strength of 793 MPa (115 ksi) was required to provide a stiffness of 70 000 kN/m (400,000 lb./in.) based upon a modulus of elasticity of steel of 200×10^6 kPa (29×10^6 psi).
2. Adjustability - Since re-prestressing may be a necessary maintenance procedure, it should be entirely readjustable.
3. Protection - Since the system would not be embedded in concrete or grouted, as is the case with concrete design, environmental protection should be provided.
4. Practicality - The system should be such that it can be handled easily by local Ministry personnel and could be installed with little disruption to traffic flow.

After evaluating various systems available, a post-tensioning bar manufactured by Dywidag Canada Ltd. was selected. This system incorporates a high strength bar with spiral deformations, which use anchorage nuts containing complementary deformations. This system can be quickly re-adjusted and can be handled easily by the local Ministry personnel. As well, the 16 mm (5/8 in.) diameter bars have an ultimate strength of 1082 MPa (157 ksi) and can be safely loaded to the required stress of 793 MPa (115 ksi).

The layout of bars shown in Figure 7, with two bars at each station, provides an initial transverse stress of 1034 kPa (150 psi) on the timber decking. The anchorage bulkhead, as shown in Figure 8, consists of new 76 mm x 305 mm (3 in. x 12 in.) select structural Douglas Fir placed the full length of both sides of the timber deck and secured in place with 178 mm (7 in.) spikes. Steel anchorage plates, 305 mm x 457 mm x 38 mm (12 in. x 18 in. x 1½ in.), bear directly against this timber at each post-tensioning station. Protection of the bars is provided by enclosing the bars in grease filled P.V.C. piping, a method which has already been used by Dywidag Canada Ltd. Steel sleeves are welded onto the steel plates and, under relative movement, telescope into the P.V.C. piping to maintain an enclosed environment. Plastic caps are placed over the anchorage nuts and filled with grease to prevent deterioration of the anchorage system.

To facilitate installation, the guardrail posts and curbs were removed from the structure. The top P.V.C. pipes, with the bars inside, were placed into transverse grooves cut in the asphalt. The bottom P.V.C. pipes with bars inside were secured to the underside of the timber deck with standard metal pipe brackets and wood screws, supported at every 0.91 m (3 ft.) along their length. Installation of the system, including the replacement of the curbs and posts but not including the stressing operation, took just over two working days with

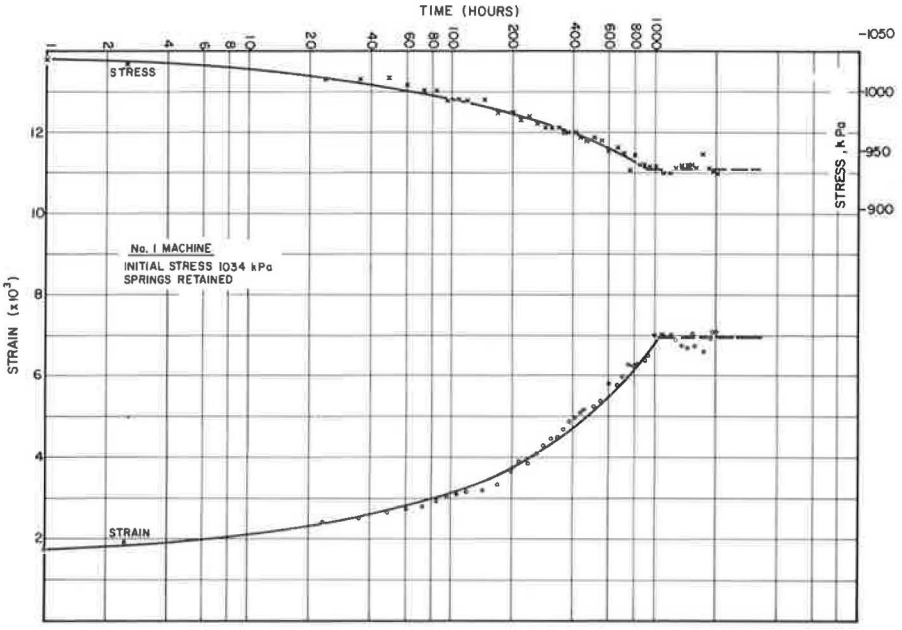

Figure 4. Results of creep tests, 2000 h.

Figure 5. Results of creep tests, 2000 h.

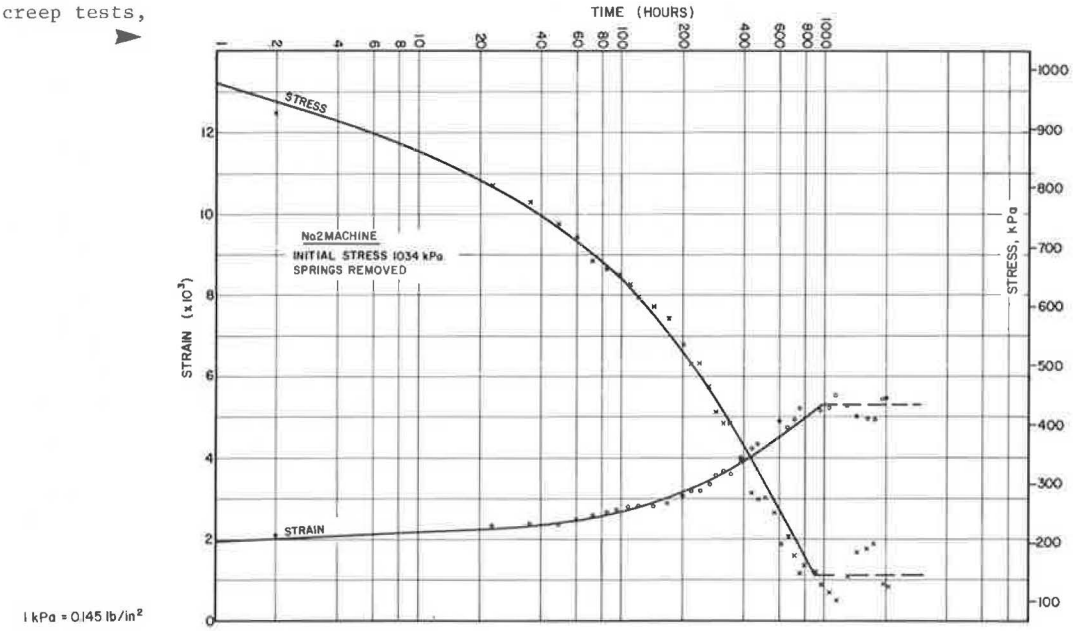

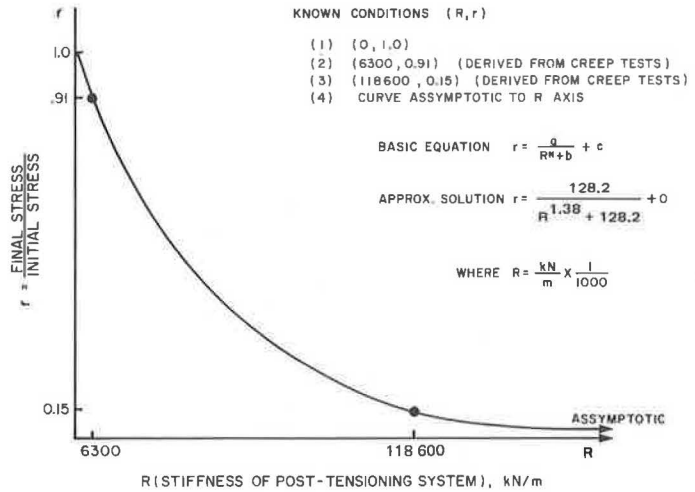

Figure 6. Ratio of final to initial stress versus stiffness of post-tensioning system.

four men (approximately 70 man-hours).

Stressing

Two jacks were used in tandem at one post-tensioning location to stress both the top and bottom bars simultaneously and to maintain a uniform pressure on the steel-timber contact surface.

Each location along the length of the bridge was stressed in turn to one half of the required load. Five complete passes were necessary to maintain some amount of tension at all of the post-tensioning locations. After a further seven passes an average load of 222 kN (50,000 lb.) was obtained at each post-tensioning location, which provided a normal pressure of 827 kPa (120 psi) on the timber deck. Further stressing was not possible as the rotation of some steel plates was causing local crushing of the timber bulkhead.

Though narrowing of the deck was anticipated it was not expected to exceed 150 mm (6 in.). However, a maximum of 450 mm (18 in.) occurred across some locations of the bridge.

It is estimated that about 60% of the movement of the structure occurred during the first five stressing operations. These took a total of 2 full working days to perform. The remaining 40% occurred in the last seven passes which also took two full working days. The stressing operation required the constant participation of at least three men.

Instrumentation and Testing

The instrumentation layout, as shown in Figure 9, consisted of 44 linear displacement transducers used to measure vertical displacements across the center of the north end span and center span, where maximum deflections were anticipated. The remaining transducers were positioned to record the vertical movement of the timber piles at the north abutment and the two interior piers. The south abutment was monitored with dial gauges.

The demac points were used to measure extreme fiber strain on the underside of the timber deck at the location of maximum moment occurring at 2.13 m (7 ft.) from the north abutment. The points were equally spaced from the west edge of the structure to the centerline, and each was oriented longitudinally in the center of the bottom face of a lamination.

The structure was tested in July 1976 using the Ministry's test vehicles, before and after post-tensioning. Testing was repeated 2½ months later in October when the majority of the post-tensioning losses was believed to have occurred. The vehicle was loaded to produce six increasing vehicle weights as indicated in Table 1, and was positioned in 18 static locations, as shown in Figure 10. Dial gauges at the south abutment were monitored whenever the vehicle was placed in the fifth or sixth longitudinal position of each lane.

Few problems were encountered while testing the structure apart from deformation of the asphalt pavement under the heavy wheel loads, which is a common occurrence during load testing.

Post Testing Evaluation

Test Results

Prior to post-tensioning, the load testing was terminated during the application of load level 5. Under this loading, the failure of a timber lamination occurred at vehicle position 2 of lane 1 (Figure 10). Just prior to failure, the maximum deflection and maximum strain were 25 mm (1 in.) and 1470 micro strain, respectively. However, measurements were not taken at the actual time of the failure as the vehicle was being removed to prevent further damage to the bridge. It is believed that the deflections and strains would have been much higher at the time of failure, as visual observation displayed a sudden vertical movement of the laminations directly under the wheels of the vehicle. This vertical movement suggests that a loss of transverse shear capacity occurred which resulted in the overloading of several laminates and the failure of one.

Immediately after post-tensioning was completed, the structure was re-tested and the maximum load level, as shown in Table 1, was reached. No signs of structural deficiency were observed and the maximum deflections and strain were 16 mm (0.62 in.) and 940 micro strain, respectively. These maxima again occurred under the same vehicle position as in the previous test. In comparison to the unpost-tensioned structure the maximum measurements under load level 5 were 14 mm (0.56 in.) and 750 micro strain of deflection and strain, respectively.

Figures 11 and 12 compare some transverse deflection curvatures from the load tests. These curves illustrate clearly the dramatic effects of the structure's response due to post-tensioning and indicate that the maximum deflection was reduced by 40% immediately after post-tensioning. The figures also show an additional 12% reduction in deflections under the final testing of the post-tensioned structure. It is believed that the new asphalt, which adds slightly to the stiffness and increases the load distribution, may account for the additional reduction in vertical displacements.

Table 2 displays the strain results obtained from the load testing of the structure in both cases. Strains were not measured during the final testing when the post-tensioning losses had occurred. Under load level 5 the maximum strain measured was reduced by 50% when the structure was post-tensioned. This reflects directly on the flexural capacity of the structure. Table 3 shows the relative changes in normal stresses in the timber laminates over a period of 1½ years. The table indicates that the normal stress has not changed significantly since the bridge was last tested in October 1976.

Post Testing Analysis

The action of the post-tensioned structure was not correctly represented by the computer analysis performed before testing. Under post-tensioning forces the structure performed similar to an orthotropic plate, with a very small transverse flexural rigidity. An orthotropic (3) analysis was performed assuming the transverse to longitudinal stiffness ratio to be approximately 1/20, based upon figures from the Wood Handbook (4). A shear modulus was estimated at 1/16 (4) of the longitudinal modulus of elasticity. The results of this analysis are displayed in Figures 13 and 14 compared to the test results of July and October 1976. Although the overall displacement diagrams are similar to the test data, there exists definite discrepancies in curvature between the points of load application. Variation of the modulus of rigidity and Poisson's ratio had little apparent effect on the curvatures. However, reducing the

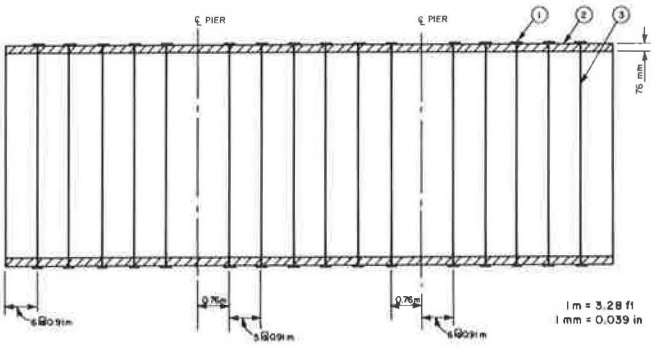

Figure 7. Plan view post-tensioning.

1 Steel Plates 38 mm x 457 mm x 305 mm
   – at 16 post tensioning stations
   – secured by 152 mm spikes

2 Select Structural 76 mm x 305 mm Wood Bulkhead
   – each side comes in 3 pieces
     2 @ 5.5 m and 1 @ 6.10 m
   – secured by 178 mm spikes

3 Bars 16 mm ϕ in 51 mm P.V.C. Sleeve
   – top bars below asphalt
   – bottom bars secured by clamps to underdeck

Figure 8. Details of anchorage and protection.

① METAL SLEEVE ATTACHED TO PLATE
② 51mm P.V.C. SLEEVE FITTED OVER STEEL SLEEVE FILLED WITH GREASE.

1 m = 3.28 ft.
1 mm = .039 in.

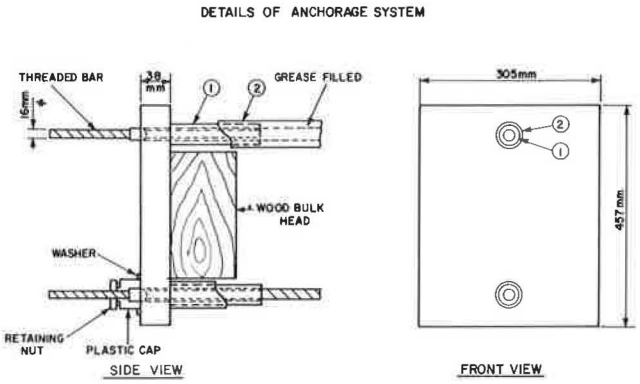

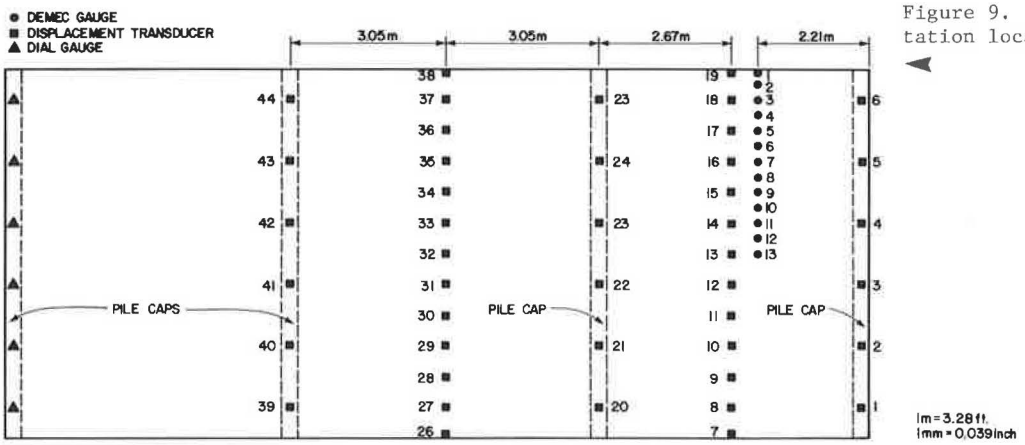

Figure 9. Plan showing instrumentation locations.

Figure 10. Load vehicle positions.

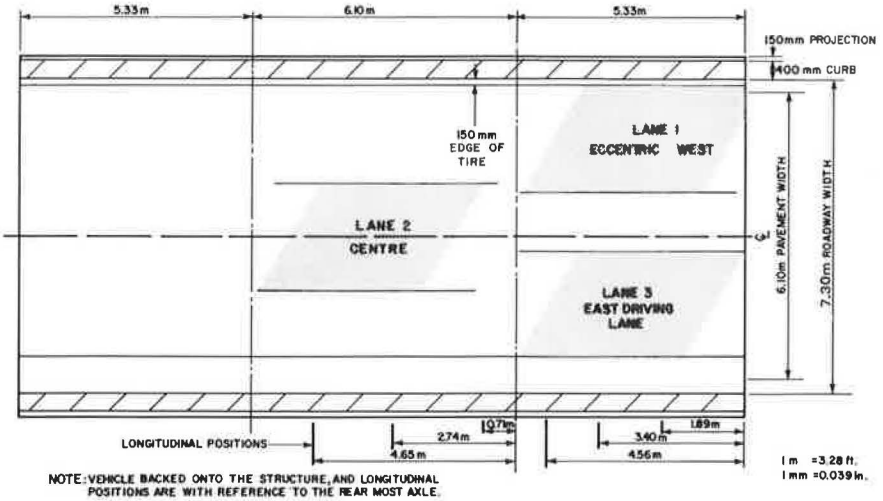

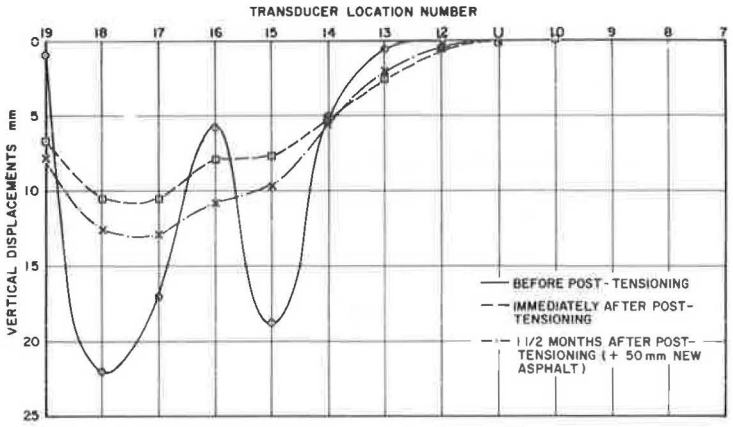

Figure 11. Vertical displacements at L/2 of north end span, load level 4, lane 1, longitudinal position 2.

Figure 12. Vertical displacements at L/2 of north end span, load level 4, lane 2, longitudinal position 2.

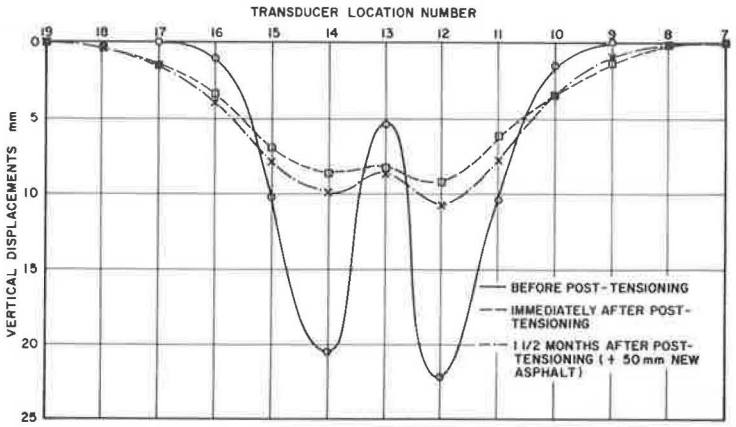

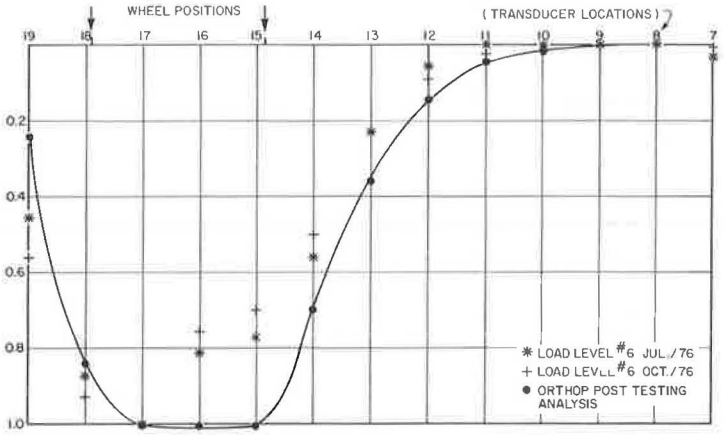

Figure 13. Normalized vertical displacements compared to an orthotropic analysis at L/2 of north end span, load level 6, lane 1, longitudinal position 2.

Figure 14. Normalized vertical displacements compared to an orthotropic analysis at L/2 of north end span, load level 6, lane 2, longitudinal position 2.

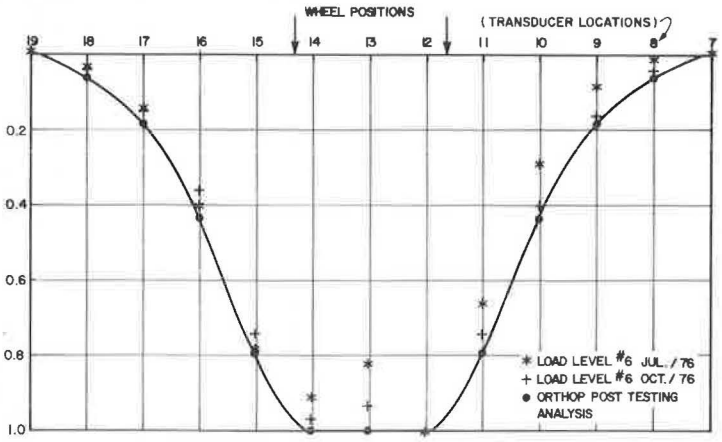

Table 1. Tandem weights of vehicle for testing.

Load Level	Number of Blocks	Vehicle Loading: Weight Rear Tandem (kg)	Vehicle Loading: Weight Front Tandem (kg)
1	8	12400	12400
2	22	18900	19100
3	36	25700	25600
4	52	33100	33300
5	62	37800	37900
6	72	42600	42600

1 kg = 2.20 lb.
1 kg = 9.81 N

Table 2. Test results. Strain (x $10^{-6} \pm 10$) vehicle in longitudinal position 2 of lane 1.

Load Level	Demac Location 1	2	3	4	5	6
Before Post-Tensioning						
3	20	210	710	970	60	180
4	40	280	910	1140	180	270
5	30	310	1080	1470	—	—
After Post-Tensioning						
3	180	230	320	520	330	280
4	270	280	420	670	420	370
5	270	340	490	750	640	470
6	320	330	520	940	530	520

Table 3. Post-tensioning stress (kPa) on timber laminates during survey to date.

Survey	Station Number 1	2	3	4	5	6	7	8	9	10	11	12	13	14	15	16
(1 day after) July 1976 Cloudy 21°C (70°F)	870	760	870	760	760	680	650	710	490	760	680	760	850	850	810	810
Oct. 1976 Overcast 16°C (60°F)	520	490	490	460	460	490	520	490	490	520	490	540	520	540	490	490
Jan. 1977 Snowing -29°C (-20°F)	410	430	430	410	380	410	410	410	410	410	410	410	430	490	460	430
April 1977 Very Wet 18°C (65°F)	460	520	540	520	490	460	490	490	490	460	460	490	490	520	490	490
August 1977 Dry 21°C (70°F)	410	430	430	410	410	390	410	410	410	410	410	410	430	460	430	380
Nov. 1977 Cloudy 13°C (55°F)	410	430	430	410	420	410	420	420	420	410	410	430	460	480	460	410

1 kPa = 0.145 psi

transverse flexural stiffness considerably tended to produce closer agreement with the test results. It is believed that the transverse flexural rigidity is dependent upon the magnitude of the applied transverse moment. When high enough, this moment will begin to separate the laminations as the post-tensioning stress is overcome. This creates the need for a non-linear analysis which not only accounts for this changing transverse flexural stiffness, but also considers the longitudinal discontinuities produced by the butt joints. However, a non-linear analysis is considered beyond the scope of this report.

Although not acceptable for design, the orthotropic analysis does indicate that the actual longitudinal modulus of elasticity of the Hebert Creek Bridge was drastically overestimated in the pre-testing analysis. A more realistic value of 7.6×10^6 kPa (1.1×10^6 psi), as compared to the former value of 10.3×10^6 kPa (1.5×10^6 psi), was needed to produce the overall magnitude of the deflections that were obtained from the field test data. As well, the orthotropic analysis indicates that the maximum transverse shear stress, which was used in the post-tensioning design, was conservative.

Conclusions

The post-tensioning performed on the Hebert Creek Bridge was more than adequate to establish the structure as capable of safely carrying the Ministry's testing vehicle, which represents the heaviest commercial vehicle weights in the province. The flexural capacity, as indicated by the maximum strains in Table 2, was almost doubled. The maximum strain of 940 micro strain provides a stress of 7170 kPa (1040 psi), assuming a modulus of elasticity of 7.6×10^6 kPa (1.1×10^6 psi) as indicated in the previous section. This stress corresponds to an assumed distribution width of at least 1650 mm (66 in.) for flexural design of one line of wheels. This is over twice the design width of 810 mm (32 in.) specified by AASHTO (1),(2). Coupled with this, the maximum stress of 7170 kPa (1040 psi) is less than the original design strength of the timber of 8300 kPa (1200 psi), and yet was induced by a vehicle load which produces a moment 60% larger than the AASHTO design moment.

Existing nail-laminated structures can be adequately upgraded by post-tensioning with a system equivalent to that provided on Hebert Creek. The fact that the structure now becomes overdesigned cannot be accommodated. Only by increasing the spans of the structures, which would only be practical in new bridges, could the extra strength be utilized.

Using this system in new structures, the additional capacity could be utilized by increasing spans and maintaining the present deck thicknesses. This would be most beneficial where multi-span structures are encountered, as it would decrease the number of supports required.

Confinement of the deck system in Hebert Creek and the reduced deflections has virtually eliminated the passage of moisture through the deck. This was confirmed by observing the structure under various climatic conditions during the collection of the data given in Table 3. The reduced deflections lower the tendency of the asphalt to break up which resists the penetration of moisture to the deck below.

Future Research

One of the most important considerations is the development of an analytical understanding of the post-tensioned structure. Presently, an investigation is being formulated, in cooperation with Queen's University in Kingston, Ontario, to establish an acceptable design procedure for new bridges. The program includes the testing of small and large-scale models to establish a better understanding of the flexural and torsional properties of the post-tensioned deck system. As well, further creep tests are to be performed to determine the effects of environmental changes on the post-tensioning forces.

The local failures of the timber bulkhead due to rotation of the steel anchorage plates indicate that a practical design is required which ensures dimensional stability and resists rotation. It is hoped that a continuous anchorage system can be developed which does not require extensive labour or machinery for installation. Along with this, investigations are underway to determine whether a high strength tendon can be manufactured which would not require external protection. This would require less work to install and give better peace of mind, as the physical protection provided at Hebert Creek is never totally dependable.

Finally, tests are to be performed to produce acceptable friction coefficients for design of various timbers. The tests will subject the timber to different environmental conditions and preservative treatments aimed at representing the field conditions.

References

1. AASHTO. Standard Specifications for Highway Bridges. Eleventh Edition, Washington, D.C., 1973.
2. Canadian Standards Association, S6-1974. Design of Highway Bridges. Ontario, 1974.
3. B. Bakht and R.C. Bullen. Analysis of Orthotropic Right Bridge Decks. Highway Engineering Computer Branch/B/15 (ORTHOP), Department of Environment, 1973.
4. U.S. Forest Products Laboratory. Wood Handbook: Wood as an Engineering Material. U.S. Department of Agriculture, Handbook No. 72, Washington, D.C., 1974.

MULTIPLE SERVICE LEVEL BRIDGE RAILINGS--PERFORMANCE AND DESIGN CRITERIA

M. E. Bronstad and J. D. Michie, Southwest Research Institute

The current AASHTO Specification provides designers with static design criteria and/or crash test criteria to qualify a bridge railing system. Accordingly, a bridge railing system meeting the AASHTO specifications is used on any bridge regardless of vehicle mix, traffic volume, and speed and bridge geometry. The Multiple Service Levels Approach (MSLA) procedure for selecting bridge railings is a new approach differing markedly from traditional practice. The objective of the MSLA is to provide a level of motorist protection consistent with the degree of traffic hazards present at a highway site. With the MSLA, the degree of risk is the combined measurement of the probability of an impact occurrence, the probability of collision severity and the consequences of that impact occurrence. Accordingly, the procedures described in this paper consider encroachment rates, traffic volume, vehicle mix, category speed, shoulder widths, and horizontal alignment as these factors relate to probability of an impact occurring and the severity probability of the impacts. Using a collision severity index as an indicator of bridge railing performance requirements, six service levels were established. By setting critical impacts corresponding to a uniform probability factor, service level requirements are determined for a site. Thus, using the MSLA procedures, a designer selects a higher service level device at locations where collisions are numerous and severe; and lower service level devices are indicated for the relatively safe or improbable accident locations. Since the higher service devices are generally more costly to construct, highway safety funds can be more wisely expended by selecting the service level appropriate for each location.

The current AASHTO(1,2) specification provides designers with static design criteria and/or crash test criteria to qualify a bridge railing system. Accordingly, a bridge railing system meeting the AASHTO specifications is used on any bridge regardless of vehicle mix, traffic volume, and speed and bridge geometry. Although not specifically stated, the AASHTO static/elastic design criteria are directed to the passenger-size vehicle with no specific containment goal for heavy vehicles (trucks and buses). Highway engineers are concerned that this single service level bridge railing design approach is not cost-effective for use on roads with low traffic volumes and may be inadequate for highways with high traffic volume or with significant truck traffic. For these reasons, a discriminating approach is needed in the selection of bridge railing installations to improve overall safety performance and cost-effectiveness of particular barrier systems.

Although this paper is concerned with describing the multiple service level selection process, the design and development of lower service level bridge railing hardware is underway at SwRI as part of this same NCHRP project. In addition, further refinement of the Multiple Service Level Approach (MSLA) is a possibility in the near future.

Research Approach

The Multiple Service Levels Approach (MSLA) procedure for selecting bridge railings is a new approach differing markedly from traditional practice. The objective of MSLA is to provide a level of motorist protection consistent with the degree of traffic hazards present at a highway site. Based on this approach, higher service level devices are indicated for the relatively safe or improbable accident locations. Since the higher service level devices are generally more costly to construct, highway safety funds can be more wisely expended by selecting the service level appropriate for each location.

Definition of Safety(3)

The keystone to the MSLA is a clear definition of the term "safety". A simplistic dictionary definition of "safe" is "free from harm or risk." Because nothing can be absolutely free of risk, nothing can be said to be absolutely safe. There are degrees of risk, and, consequently, there are degrees of safety. Safety, then, is a judgment of the acceptability of risk; and risk, in turn, is defined as a measure of the probability and severity of harm to human health. In other words, something is safe if its risks are judged to be acceptable.

In highway applications, the engineer designs hydraulic structures based on a 50-year mean

recurrence interval for rainfall or sign supports for a 25-year mean recurrence interval for wind velocity. He has balanced the probability of an overload condition and its consequences against costs to produce a more conservative design. Although the engineer can design for a 200- or 1000-year mean recurrence interval, the cost of the structure would be judged excessive for the derived benefits.

In the field of traffic barrier systems, the challenge is to select a bridge railing for a particular site based on acceptability of risk. Placing a low performance railing on a heavily used highway would be an unacceptable risk. On the other hand, placing high performance bridge railings on low traffic volume roads where chance for an impact is practically nil is a waste of public funds.

Degree of Risk

In the MSLA, the degree of risk is the combined measurement of the probability of a bridge railing impact occurrence, the probability of collision severity and consequences of that impact occurrence.

Probability of Occurrence. The number of vehicles that inadvertently leave the pavement and collide with a unit length of bridge railing within a specified period of time can be predicted.

Probability of Severity. The severity of collision is determined by vehicle dynamics at impact. Currently, the dynamic performance of bridge railings evaluated by full-scale crash tests is assessed according to three factors: (1) containment of the impacting vehicle, (2) redirection of the vehicle such that the occupants can survive, preferably uninjured, and (3) vehicle post-impact trajectory such that other traffic is not subjected to undue hazard.(4) Unfortunately, the present state of technology does not permit evaluation of a barrier design by the second and third factors with any degree of precision. Therefore for MSLA, the dynamic performance of a bridge railing is evaluated only by its ability to contain the impacting vehicle.

Graduated Containment Capability. Based on the containment standard, a bridge railing can be developed to contain and redirect an array of vehicles that impact the barrier at or below a specified level of dynamic conditions. Graduated levels of vehicle dynamic conditions can be established over the range of all possible impact conditions; these graduated levels are defined as multiple service levels.

Critical Impacts. Thus, given the following factors--a bridge railing installation designed for a specified service level or containment capability, a bridge site with known or projected geometry, traffic characteristics and special environmental conditions--the probable number of impacting vehicles that will be contained and redirected can be estimated. More importantly, the probable number of impacting vehicles with dynamic conditions exceeding the containment capability of the barrier can be estimated. (It is assumed that a large percentage of critical impacts will result in penetration of the barrier by the vehicle.) These vehicle impacts exceeding a particular containment capability threshold are defined as critical impacts. Accordingly, the degree of risk for the MSLA is the estimate of the number of critical impacts that will occur along a unit length of barrier within a specified period of time.

Acceptability of Risk

Acceptability of risk is a subjective judgment that varies with time, region and circumstances. For the MSLA, the acceptability standard for risk is defined in terms of a containment goal. This containment goal is a national, state or regional policy that specifies the maximum number of critical impacts permitted for a unit length of bridge railing over a specified period of time.

Service Levels

Six service levels are presented and defined in terms of vehicle impact conditions that must be contained by each level. It is most likely that a highway agency will not require bridge railing designs that conform to all six service levels. Full-scale vehicle crash testing will be necessary to demonstrate the containment and redirection capabilities of bridge railing designs for the various service levels.

Content

The purpose of this paper is to provide an overview of the MSLA approach [described in detail in NCHRP Project 22-2(2) Phase I Report (5).] The MSLA approach procedures are briefly described in sections to follow. Even though the probabilistic model that predicts occurrence and severity of vehicle impacts is complex, the procedures to be used by design engineers in selecting appropriate service levels are simple and can be accomplished in a matter of minutes.

Bridge railing performance and design considerations are discussed, and the application of findings is presented, respectively, in sections to follow.

Development of Bridge Railing Service Level Selection Criteria

The Multiple Service Level Approach for selecting appropriate bridge railing designs for particular highway sites is presented in this section.

Vehicle Containment

Practical Limitations. It is neither technically nor economically feasible to construct bridge railing that will contain 100 percent of all possible impacts at every site. Unusually large vehicles with peculiar cargos or unpredictable collision conditions make the design of an all-containing barrier structure an impossible task. Furthermore, the cost of installing the "super barrier" structure at over 550,000 bridges in the United States would be over $8 billion [assuming a nominal $30 per linear meter for the 25,000 km (15,400 miles) of bridge railing]; not only is this amount prohibitive, but also the number of forestalled fatalities (about 1000 per year out of 50,000 total highway fatalities) can be achieved more readily by less expensive means, i.e., reduction of speed limits, mandatory use of active restraints for vehicle occupants, etc. Treatments such as pavement deslicking, signing, and delineation are other cost-effective ways of reducing the frequency of accidents.

Achievable Performance. As an alternative to the 100-percent containment ideal, the acceptance of a uniform containment policy would greatly reduce the structural requirements and cost of the barriers. The containment policy could be set on a national, regional or state-wide basis, and it would be adjusted depending on available funding.

Containment Percent or Critical Impacts. In the MSLA, the performance goal of a bridge railing is expressed in terms of a maximum probable vehicle critical impact rate. A convenient scale, based on current performance of bridge railing in the United States, is the number of critical impacts per 16-km (10-mile) length of bridge railing per 10-year period. The fact that a specific bridge railing installation is only 30 m (100 ft) and not 16 km (10 miles) in length is immaterial to application of the MSLA. Using the containment goal expressed in the rate of critical impacts, it can be reasoned that a bridge railing on a high traffic volume road with a great number of vehicle impacts will require a device that contains a high percentage of these vehicle impacts. In contrast, for low traffic volume roads with a small number of probable impacts, the bridge railing installation can contain a lower percentage of colliding vehicles and still satisfy the containment goal.

Although the designer prefers to think in terms of success rather than failure of bridge railing structures, it is necessary in the MSLA to deal with the probable number of **critical impacts** (i.e., possible penetrations) rather than the **percent** of vehicle impacts contained. A percent containment policy would provide essentially the same service level railing for a 100-ADT (average daily traffic) road as for a 100,000-ADT road assuming everything else is equal, even though the number of bridge railing impacts is a direct function of traffic volume. Thus, the same bridge railing would be used at locations where there is less likelihood of vehicle impacts and penetrations as is used at those locations where critical impacts are frequent. For this reason, the performance goal of a barrier expressed in terms of percent of impacting vehicle contained is not meaningful to the MSLA.

Containment Goal. In order to establish reasonable limits on the containment goal, the maximum number of critical impacts considered an acceptable risk can be inferred by safety performance of the existing bridge railing with this performance measured in terms of accident statistics.

Based on analyses of very limited data, it was determined that the current rate for the United States is approximately 2 penetrations per 10 years per 16 km (10 miles). This figure is considered a "ball park" number based on the best data available. Thus, a highway agency could select 2 critical impacts per 16 km (10 miles) per 10 years as its containment goal and maintain the level of containment reflected by the data analysis. By accepting a higher number, i.e., 3, as an acceptable critical impact rate, a highway agency can effect a savings in construction funds by lowering loading requirements on many low traffic volume bridges and increasing strength requirements on a few high traffic volume bridges. On the other hand, a highway agency may opt to use a lower critical impact rate, i.e., 1 or 0.5, and thereby reduce the total number of penetrations; of course, this decision will be more costly to implement. Regardless of the selected containment goal per critical impact rate, this approach will provide a rational and consistent technique for setting bridge railing service level requirements.

Probability of Barrier Impact

The probability of a bridge railing impact occurrence is based on encroachment rate and the lateral distance L_T between the traffic stream and the barrier face.

Encroachment Rate. Encroachment rate data as shown in Table 1 were obtained from Reference 6 and

Table 1. Encroachment rate table(6).

Type of Highway	Description of Collision Direction	Encroachment Rate events/km (mile)/year[a]	Sketch
Divided Urban Arterial Street	One direction each side, each direction separately for median	0.00021 (0.00033) ADT	A
Undivided Urban Arterial Street	Both directions	0.00042 (0.00067) ADT	B
	One direction only	0.00021 (0.00033) ADT	D
Narrow Two-lane Rural Highway (roadbed less than 11 m)	Both directions	0.00037 (0.00060) ADT	C
	One direction only	0.00019 (0.00030) ADT	C
Wide (roadbed of 11 m or greater) Two-lane or Undivided Four-lane Rural Highway	Both directions	0.00023 (0.00037) ADT	C
	One direction only	0.00011 (0.00019) ADT	D
Multi-lane Divided Rural Highway	One direction for each side, each direction separately for median	0.00009 (0.00015) ADT	A
Freeway	One direction for each side, each direction separately for median	0.00014 (0.00023) ADT	A

[a] ADT is for two-way traffic volume.

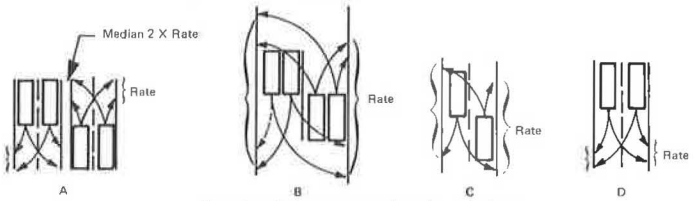

are considered state-of-the-art 1977. These rates are a function of highway type and direction of traffic. The encroachment probability is a linear relationship with traffic volume. MSLA is readily adjusted to other encroachment rate values.

Adverse Conditions. Factors not considered which may affect the encroachment rate at a specific site include the following: skid resistance, horizontal and vertical alignment, stopping sight distance, route discontinuity, narrow lanes, inadequate superelevation on curvature, shoulder surface type, length of grade, lane drops--shoulder drop or reduction, regional differences (climate, driver, etc.), pavement marking and delineation, and shoulder width. Some, if not all, of the above factors can be mutually exclusive (additive or subtractive) in their influence on encroachment rates. In other circumstances, the worst value of one factor alone can be overwhelming because of other associated inconsistencies violating driver expectancy.

Selection of adverse factors was not in the scope of this work; however, the reader is alerted to the existence of such data in the technical literature. It is conjectured that the adverse condition multiplier will generally range between 1 and 2. Since most of the data pertain to roadways, judicious selection procedures should be employed to apply these factors to bridges.

Figure 1. Distribution of lateral displacements.

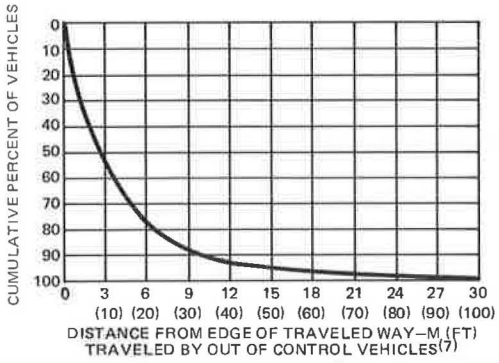

Figure 2. Point mass conditions for straight bridge.

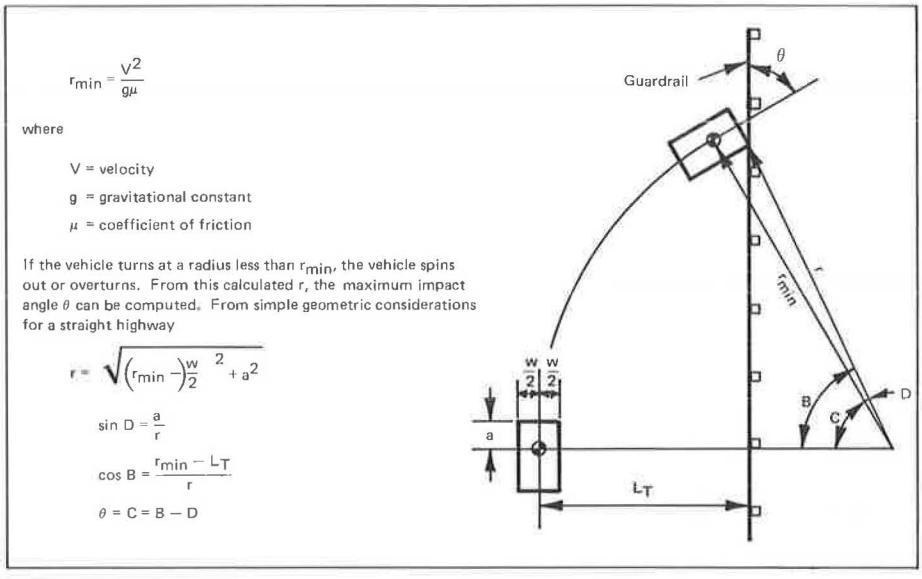

Barrier Offset. The probability of an encroachment becoming an impact is affected by the distance from the pavement edge to the barrier. In general, the greater the offset distance, the greater the opportunity for the errant motorist to regain control of the vehicle and avoid collision. The percentage of encroachments resulting in barrier impacts is determined from the relationship(7) presented in Figure 1.

Probability of Vehicle Impact Conditions

As the vehicle mass, speed and approach angle increase, the collision generally becomes more severe and the containment requirements more difficult to satisfy. Bridge railing collisions consist of a full range of energy impacts. As the structural capability of a bridge railing is increased to contain a higher energy impact, the proportion of impacting vehicles that are contained by the bridge railing is also increased. Thus, a rational design approach is to select a bridge railing system that will contain a threshold vehicle impact energy corresponding to most possible impacts at that particular site in accordance with the containment goal.

To determine probability of vehicle impact conditions, the techniques described in the following sections were used:

Impact Angle (θ). It is widely accepted that maximum automobile impact conditions can be predicted by using a point mass model using a representative value for coefficient of pavement friction as illustrated in Figure 2. For passenger cars, a coefficient of pavement friction of 1.0 is used. Vehicles with high center of gravity have performance limits that increase the minimum possible turning radius, thus decreasing the maximum impact angle. These performance limits are applied to the heavy trucks and buses and can be accommodated in the point mass model by using an effective coefficient of friction of 0.47 determined from vehicle handling studies.

A distribution of impact angles based on the maximum possible angle was determined from field data by Ross. (8) Encroachment trajectory considerations are described in Figure 3.

Figure 3. Vehicle encroachment trajectories.

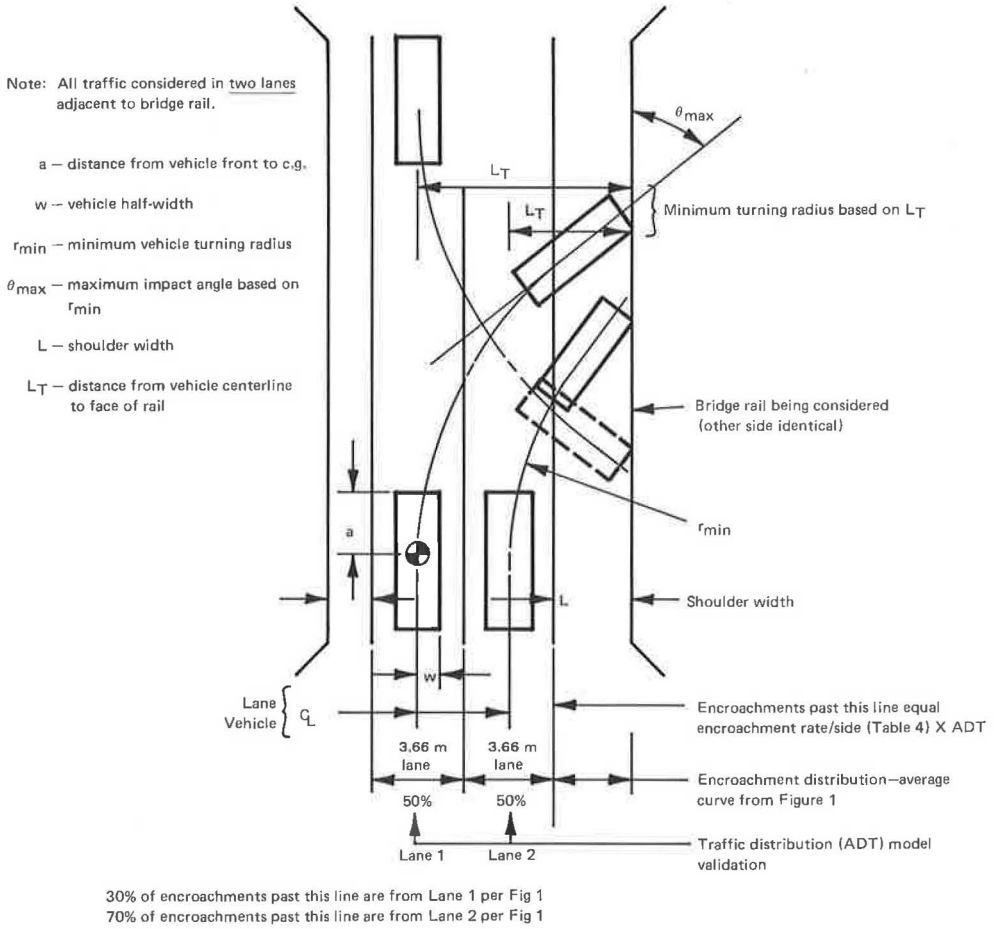

Table 2. Traffic mix description.

Vehicle Type	Traffic Mix Number 1[a]		4[a]		5[a]		6[b]		7[b]	
Passenger Cars										
1200 kg (2700 lb)	17.5		20.0		22.5		50.0		13.3	
1800 kg (4000 lb)	31.0		35.2		39.6		25.5		23.6	
2100 kg (4700 lb)	16.7		19.2		21.6		14.0		12.8	
2700 kg (6000 lb)	4.8		5.6		6.3		4.0		3.7	
Subtotal, %		70		80		90		93.5		53.4
Pickups and Panels										
2200 kg (5000 lb)	6.3		5.0		4.4		2.8		4.8	
3600 kg (8000 lb)	3.7		3.0		2.6		1.7		2.8	
Subtotal, %		10		8		7		4.5		7.6
Other Trucks and Buses										
10,500 kg (23,000 lb)	11.8		7.1		1.8		1.2		9.0	
18,000 kg (40,000 lb)	8.2		4.9		1.2		0.8		30.0	
Subtotal, %		20		12		3		2		39
Total Traffic, %		100		100		100		100		100

[a]Based on traffic count data.
[b]Hypothetical mix.

Vehicle Size. The distribution of vehicle by mass was determined from traffic count data compiled by FHWA and other data sources. Based on analyses of these data, five vehicle mixes (1, 4, 5, 6 and 7) were deemed adequate as described in Table 2.

As shown in this table, vehicles weighing more than 18,000 kg (40,000 lb) were not considered in this study. These heavier vehicles, which are generally tractor-trailer rigs, have performance limits that result in larger minimum radii of curvature and, hence, represent a less formidable impact possibility for a given weight, speed, and offset distance. The mechanics of articulated vehicle impacts are very complex and were not included in this study because of the lack of current information. Based on recent crash test results with the new collapsing ring bridge rail system,(9) the following comparisons can be made:

Vehicle	Vehicle Weight, kg (lb)	Impact Speed, km/h (mph)	Impact Angle, deg	Max Deflection, m (in.)
Intercity Bus	18,000 (40,000)	86.8 (53.9)	15	1.2 (48)
Tractor/Trailer	32,000 (70,000)	71.4 (44.4)	10	0.3 (12)

Thus, the inclusion of a 18,000-kg (40,000-lb) single unit vehicle [as well as the 10,000-kg (23,000-lb) vehicle] gives assurance that single unit vehicles in this weight range are adequately considered; and it can be inferred, as demonstrated above, that articulated vehicles weighing in excess of 18,000 kg (40,000 lb) are included also because of performance limits previously discussed. The inclusion of a 10,000-kg (23,000-lb) vehicle assures that the upper limit of school bus mass has been considered in the vehicle mix.

Impact Speed. Speed distributions for accidents are not available in any degree of precision. Accordingly, four speed categories, 56, 72, 88 and 105 km/h (35, 45, 55 and 65 mph) are used. The designer must select what he considers a representative speed for his site.

Collision Severity Index

To rank the relative severity of all predicted barrier impacts, a Collision Severity Index (CSI) was developed in the program. Essentially, the CSI was developed by curve-fitting results from BARRIER VII(13) computer simulations of 16 vehicle/barrier impact cases. The vehicle size was varied from a passenger vehicle to an intercity bus, the approach angle was varied from 7 to 25 deg and the speed was varied from 65 to 95 km/h (40 to 60 mph). Maximum lateral deflection was the selected measure of impact intensity using an extremely stiff, but deformable barrier.

$$CSI = 2.598 \times 10^{-7} m^{(0.50)} I_z^{(0.82)} V^{(2.50)} \sin\theta^{(3.00)} \quad (1)$$

where

CSI = collision severity index,

m = vehicle mass, kg (slugs)

V = impact speed, m/s (fps)

θ = approach angle, deg

I_z = vehicle mass moment of inertia about vertical axis (yaw) kg-m^2 (slug-ft^2)

Bridge Railing Service Levels

Six bridge service levels are defined in Table 3 on the basis of the Collision Severity Index. Also, impact conditions corresponding to CSI values are shown for each service level. These levels were arbitrarily selected with some preference given to current design performance range and the type of vehicles that may have to be contained. Service Level 2 coincides with the current AASHTO bridge rail crash test option specification; however, test experience has demonstrated that railings designed to the 44.5-kN (10-kip) static force are not significantly damaged when impacted by a 1640-kg (3620-lb) car at 99 km/h (61.4 mph) and a 25-deg angle.(10) Thus, the ultimate containment capacity of this railing design may be much greater than the level indicated by these test conditions. The service levels indicated are based on ultimate containment; large deflections are permissible if containment is achieved. It should be emphasized that these large deflections would occur infrequently if a goal such as 1 critical impact per 10 years per 16 km (10 miles) were adopted.

Bridge Railing Service Level Selection Procedures

All of the factors discussed previously are combined to provide a range of impact conditions based on: five vehicle mixes (Table 2) (eight vehicle weight categories); four category speeds (55, 70, 90, 105 km/h) km/h x 0.62 = mph; four shoulder widths (0.6, 1.8, 3.0 m) m x 0.33 = ft; five alignment variations (horizontal curves of -10, -5, 0, +5, +10 deg); one encroachment rate (0.00037 ADT events/km/year). Note: This encroachment rate value is for one side of the bridge and corresponds to a narrow two-lane rural highway with traffic in both directions. Collision Severity Index values are calculated based on all of these variables. By using a containment goal of 1 critical impact per 10 years per 16 km (10 miles), maximum equivalent ADT values can be obtained that correspond to this goal for each of the conditions. These values are illustrated in Table 4. For the purpose of increasing the encroachment rate due to unusual site conditions, an adverse conditions factor is included; however, no recommendations for these values are presented. For other encroachment frequencies and goals, the adjusted ADT values are linear and can be readily calculated as follows:

Actual (ADT) x (Ratio of Encroachment Rates) x

Environmental Factor/No. of Permissible

Critical Impacts

Typical Selection Procedure--An example problem and worksheet are illustrated in Table 5.

Table 3. Bridge rail service levels.

Service Level	CSI	Performance-Related Impact Conditions, Vehicle Weight, kg (lb)			
		1000 (2250)	2000 (4500)	10,500 (23,000)	18,000 (40,000)
1	4	95 km/h (60 mph) @ 25 deg	95 km/h (60 mph) @ 15 deg	65 km/h (40 mph) @ 7 deg	
2	16		95 km/h (60 mph) @ 25 deg	50 km/h (30 mph) @ 15 deg	80 km/h (50 mph) @ 7 deg
3[a]	60			80 km/h (50 mph) @ 15 deg	55 km/h (35 mph) @ 15 deg
4[a]	100			95 km/h (60 mph) @ 15 deg	70 km/h (45 mph) @ 15 deg
5[a]	400			95 km/h (60 mph) @ 25 deg	65 km/h (40 mph) @ 25 deg
6[a]	1000				95 km/h (60 mph) @ 25 deg

[a]Staging of these systems may be required to provide desirable safety performance for impacting automobiles. Staging is provided by a softer barrier placed in front of a more rigid barrier.

Table 4. Typical MSLA selection guide 1.8-m (6-ft) shoulder.

Shoulder Width, m (ft)	Designated Speed km/h (mph)	Degree of Curve	Vehicle Mix	Maximum Equivalent ADT Barrier Service Level 1	2	3	4	5	6
1.8 (6)	90 (55)	-10							
			1	835	27911	No Limit	No Limit	No Limit	No Limit
			4	901	33691	No Limit	No Limit	No Limit	No Limit
			5	975	41792	No Limit	No Limit	No Limit	No Limit
			6	1407	64585	No Limit	No Limit	No Limit	No Limit
			7	678	17303	No Limit	No Limit	No Limit	No Limit
1.8 (6)	90 (55)	-5							
			1	255	1348	12580	53169	No Limit	No Limit
			4	123	2098	20997	88911	No Limit	No Limit
			5	457	5510	84223	361599	No Limit	No Limit
			6	637	8386	126377	542407	No Limit	No Limit
			7	157	600	4130	15778	No Limit	No Limit
1.8 (6)	90 (55)	0							
			1	159	559	2695	6274	499024	No Limit
			4	203	870	4492	10479	835012	No Limit
			5	294	2296	17885	42368	No Limit	No Limit
			6	399	3486	26840	63553	No Limit	No Limit
			7	100	257	1023	2158	138103	No Limit
1.8 (6)	90 (55)	5							
			1	125	353	1334	2597	57025	No Limit
			4	157	543	2221	4334	95388	No Limit
			5	219	1365	8761	17456	388637	No Limit
			6	290	2067	13152	26185	582955	No Limit
			7	81	169	532	973	16400	No Limit
1.8 (6)	90 (55)	10							
			1	106	268	854	1533	18484	581856
			4	130	407	1420	2557	30905	973672
			5	175	960	5539	10269	125638	No Limit
			6	228	1446	8319	15405	188457	No Limit
			7	72	131	349	597	5609	159899

Table 5. Service level selection example.

Example Problem. A bridge railing system is needed on a divided rural highway with an ADT of 20,000. The traffic mix contains 20 percent trucks corresponding to Mix 1. The traffic on this section moves about the posted speed of 88 km/h (55 mph) and there is a 2-m (6-ft) shoulder. The engineer has been instructed to use a goal of 1 critical impact/10 miles/10 years.

Input

1. Bridge Example 1
2. Total ADT 20,000
3. Vehicle mix (see Table 2) 1
4. Category speed, km/h (55, 70, 90, 105) 90
5. Shoulder width, m (0, 0.6, 1.8, 3.0) 1.8
6. Horizontal curvature, deg (-10, -5, 0, +5, +10) 0
7. Encroachment rate from Table 3 0.00015
8. Adverse conditions factor 1
9. Containment goal (critical impacts/16 km (10 mile)/10 years) 1

Step 1: Calculate maximum equivalent ADT, ADT

$$ADT = (2) \times \frac{(7)}{0.0006} \times (8) \div (9)$$

$$ADT = (20{,}000)\ \frac{0.00015}{0.00060}\ \frac{(1)}{(1)} = 5000$$

Step 2: Enter Table 4 and select lowest service level bridge rail by comparing adjusted ADT with applicable Table 4 value.

$$6274 > 5000 < 2695$$

USE SERVICE LEVEL 4

Bridge Railing Performance and Design Considerations

There is apparently no relationship between the AASHTO load criteria and the crash test requirement. While not stated as a design objective, the static force criterion generally is believed to guarantee little or no damage to the railing system during the severe strength crash test [2040-kg (4500-lb) car, 95 km/h (60 mph), 25 deg].(4) The ultimate containment capacity of these railing systems is not known. Furthermore, the margin of safety to which the system has been designed according to this static criterion will influence its ultimate capacity. In other words, the AASHTO static force is a lower limit, and overdesigned bridge railings are not prohibited. The current AASHTO specification does not specify behavior of the barrier past the elastic range. The failure of a post, for example, could occur either above the deck or within the deck itself. Designs where deck failure controls are considered to be unsatisfactory for a number of reasons:

1. The failure mechanism in the concrete deck is complex and, therefore, cannot be reasonably predicted.
2. Bridge deck repair is a costly item compared to simple replacement of posts and beam.
3. Deck damage may go unnoticed until a more severe impact causes noticeable failure. The weakened structure will not perform as designed.

Other railing components such as beams and hardware also should be considered for ultimate performance. A bridge railing system that performs well in the elastic/small deflection range, but breaks down far below its ultimate capacity because of some undesirable failure mechanism (e.g., lowered system

height allowing vaulting, beam splice failure due to fastener inadequacy, etc.) represents inefficient use of materials.

After 10 years of intensive barrier development and testing using all available tools, design methods, computer simulations, laboratory experiments and full-scale vehicle crash tests, the authors are convinced the prescriptive design approach is inadequate to effect barriers with predictable containment and safety performance. On the other hand, the performance standard approach would encourage the generation of a limited number of carefully developed standard barrier designs, hence, decreasing the time spent by every agency designing their own unique systems, decreasing material costs due to standardization and the smaller number of inventory items, and improving safety performance because of the more comprehensively developed barrier designs.

Performance Predictions

Use of a single force to design a service level traffic barrier is not recommended in this paper. Bridge railing performance beyond the elastic range requires analysis methods that go far beyond the current static method. However, complicated methods of analysis are considered unnecessary when available computer simulations can be employed that actually relate to a vehicle impact and are no more involved to use than a dynamic structural analysis program. Computer simulation programs currently available(11,12,13) provide reasonable assurance that the simulated impact forces are being applied to the barrier during the redirection process. In addition, the use of a rollover vaulting algorithm (RVA),(14) coupled with 2-dimensional barrier models, predicts rollover or vaulting due to insufficient rail height. Wedging under a beam and so-called "pocketing" are difficult phenomena to ascertain from the current programs.

Figure 4. Barrier beam geometry.

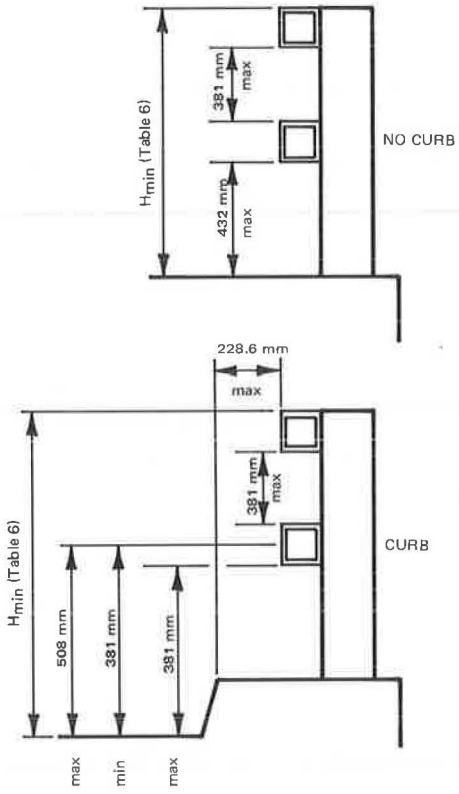

Note: Definitive dimensions shown are based on current AASHTO specification.(2)

Performance and Design Criteria

Vehicle Containment. The proposed bridge railing service levels are related to vehicle impact conditions (presented in Table 3), and containment of the impacting vehicle for these respective impact conditions is recommended as the strength test for each railing category. Ultimate containment is considered to be the most efficient use of bridge railing structure. The ultimate containment approach requires an understanding of the failure mechanisms of the structural system as the ultimate loading threshold is reached. From the knowledge of the ultimate containment capacity, the full range of barrier performance is understood. Although full-scale crash tests at each performance level are necessary, preliminary designs can be formulated using computer simulation models.

Good Design Practice. Recent crash test experiments with both heavy vehicles and automobiles have revealed certain deficiencies in barrier behavior which can be averted by good design practice. These include:

1. Undesirable lowering of barrier height because of ductile post behavior reduces effectiveness of barrier in preventing vaulting/rollover.
2. Beams considered flexural members fail in tension during large inelastic deflections because of inadequate splice or tensile anchorage.
3. Unpredictable failure mechanisms of post/parapets make ultimate loads indeterminate and unrepeatable.
4. Barrier height is too low for heavy vehicle impacts.
5. Beam/vehicle interface is inadequate for full range of automobiles.
6. Beam/post geometry permits wheel snagging at even moderate impact angles.

Bridge railing performance criteria for each service level are suggested in Table 6. The performance test criteria of NCHRP Report 153 recognize the need for providing forgiving redirection to the small passenger cars. This class of vehicle currently constitutes approximately 25 percent of all passenger cars sold. Passenger cars are still the predominate vehicle representing up to 90 percent of the traffic on highways. Crash tests are recommended for performance and strength evaluation. Barrier heights based on rigid barrier RVA simulations are shown. Strength of barrier elements is suggested that encourage efficient ultimate performance. The evaluation criteria of NCHRP Report 153 are also recommended. There has been no systematic study of vertical bridge rail spacing; the current AASHTO recommendations are shown in Figure 4.

Discussion and Application of Findings

Discussion

Bridge Railing Service Levels. The multiple service bridge railing approach is a major change from current recognized practice, both from a

Table 6. Bridge railing performane criteria.

Service Level:	1	2	3	4	5	6
1. Crash Test Requirements						
Impact Conditions						
A. Strength Test						
Vehicle Weight, kg (lb)	1000 (2250)	2000 (4500)	10,500 (23,000)	10,500 (23,000)	10,500 (23,000)	18,000 (40,000)
Impact Speed, km/h (mph)	95 (60)	95 (60)	80 (50)	95 (60)	95 (60)	95 (60)
Impact Angle, deg	25	25	15	15	25	25
B. Redirection Severity Test	1000-kg (2250-lb) auto, 95 km/h (60 mph), 15 deg					
2. Dynamic Performance						
A. Posts/Parapets	Controlled, repeatable failure mechanisms outside bridge deck are required. Ductile failures of posts are discouraged unless separation of beam from post prior to rail lowering is controlled and repeatable. The post anchorage is designed to AASHTO working stresses using ultimate post failure load.					
B. Beam	Full tension of net section should be developed at splice. The AASHTO Standard Specifications for Highway Bridges, (1) Article 1.7.19, provide a good splice specification. Beam should be anchored (expansion joints require special treatment).					
C. Vehicle performance	The preferred vehicle acceleration criteria are found in recommendations of NCHRP Report 153. Values shown in this document are subject to change as technology becomes available. Other requirements specified for automobiles in Report 153 regarding snagging, pocketing, etc. are considered applicable also.					
3. Guidelines						
A. Geometry						
[a]1. Barrier height, m (in.) (min)	0.7 (27)	0.7 (27)	0.7 (27)	0.7 (27)	0.9 (34)	1.0 (40)
2. Beam (see Figure 4)						
B. Maximum dynamic deflection	As a guide for design, the maximum dynamic deflection should not exceed the vehicle half-width. This value may be exceeded during crash test if redirection/containment is achieved.					

[a]Barrier height is a minimum; this height must be increased if beam/post interaction allows beam to drop below this height.

technical and administrative view. Rather than the synthesis design of a bridge railing system, MSLA implies the selection from a group of systems crash tested to specific impact conditions. The creation of unique bridge railing designs from prescriptive specifications using static loading/elastic design results in a proliferation of barrier systems that are not fully analyzed in terms of vehicle containment.

The national trend is toward the adoption of a limited number of carefully developed and demonstrated traffic barrier systems. The movement is prompted by the requirement for increased safety performance of traffic barriers and the realization of cost savings in design, fabrication and maintenance of widely accepted standard systems. These limited number of bridge railing designs can be developed on cooperative programs such as NCHRP where the development costs are shared.

Thus, the multiple service level bridge rail approach takes into account the trend toward standardization of bridge rail systems and presents a technique for selecting the most appropriate system for particular site conditions.

Service Level Selection Parameters. The service level parameters were selected based on what was considered state-of-the-art 1977. Certain parameters in this model are linear in the final product and may be varied or changed by simple multiplication. These linear factors include: ADT, encroachment rate, adverse conditions as related to encroachment rate, and containment goal. Other factors influencing the final results are more complex, and reformulation of probability equations is required if their values are changed. These nonlinear factors include: shoulder width as it relates to encroachment distribution, encroachment distribution (lateral distance traversed), vehicle mix characteristics (mass, geometry, etc.), speed (or speed distribution if available), impact angle distribution, and traffic distribution (e.g., unequal lane distribution, more than two lanes, etc.). It is recognized that parameter values such as encroachment frequencies, vehicle mix characteristics and impact speed and angle distributions are based on tenuous and sometimes scant research data. Undoubtedly refined values for these parameters will be forthcoming from future research efforts. Nevertheless, the authors strongly believe that the lack of precision in the values will not change the systematic method of selection nor should it be a reason to deter or delay the implementation of the MSLA.

Results. Bridges on roadways with high ADT, high speed traffic, horizontal curvature, and large truck percentages will require bridge railing structures with greater containment capacity than that specified by the current AASHTO specification. Conversely, bridges on roadways with low ADT, low traffic speeds and mostly automobile/pickup traffic will require a bridge railing less demanding than the current AASHTO specification. The degree of this variance will depend largely on the containment goal selected. Since this containment goal is new and no specific goal has been used previously, this goal will require study by highway agencies to ascertain influence on implementation funding.

Application of Findings

Service Level Selection. A rational basis has been derived which provides maximum protection where impacts are likely to occur and further accounts

for degrees of collision severity based on a number of factors. The use of this model to evaluate a barrier system on a regional or national basis requires a knowledge of barrier containment capacities both existing and proposed. Containment goals and encroachment frequencies can be varied as policy or better findings permit.

Barrier Design. The shortcomings of simplified barrier design were previously discussed. Currently available barrier simulation computer programs are available to provide insight for existing barrier systems as well as new designs. It is considered necessary to evaluate new and upgraded designs by crash test to prove the containment capacity. Suggested criteria and guidelines are presented for the six service levels of this paper.

The new concept of ultimate containment barriers which deviates from statically designed barriers is considered superior for these dynamically loaded structures. The range of costs among the six service levels cannot readily be determined until some definitive designs are formulated; however, using analyses such as presented in this report will justify high performance bridge railing costs when compared to current expenditures on lower traffic volume roadway bridge railings. The illustration of six service levels should not be construed as a recommendation; the number of levels actually needed will be the product of future investigations.

Acknowledgment

This work was sponsored by the American Association of State Highway and Transportation Officials, in cooperation with the Federal Highway Administration, and was conducted in the National Cooperative Highway Research Program which is administered by the Transportation Research Board of the National Research Council.

References

1. Standard Specifications for Highway Bridges, adopted by The American Association of State Highway and Transportation Officials, Eleventh Edition, Washington, D.C., 1973.
2. Interim Specifications--Bridges 1975, developed by the AASHTO Subcommittee on Bridges and Structures.
3. Lowrance, W.W., Of Acceptable Risk (Science and the Determination of Safety), William Kaufmann, Incorporated, Los Altos, California, 1976.
4. Bronstad, M.E. and Michie, J.D., "Recommended Procedures for Vehicle Crash Testing of Highway Appurtenances," NCHRP Report 153, 1974.
5. Bronstad, M.E. and Michie, J.D., Multiple Service Level Bridge Railings--Performance and Design Criteria, Phase I Report, NCHRP Project 22-2(2), August 1977.
6. Glennon, J.C. and Wilton, C.J., Effectiveness of Roadside Safety Improvements, Vol. 1 Final Report, Report No. FHWA-RF-75-23, November 1974.
7. Calcote, L.R., The Development of a Cost-Effectiveness Model for Guardrail Selection, Interim Progress Report, FHWA Contract DOT-FH-11-8827, July 1976.
8. Ross, H.E., Jr., Impact Performance and a Selection Criterion for Texas Median Barriers, Texas Transportation Institute Research Report 140-8, April 1974.
9. Kimball, C.E., et al, Development of a Collapsing Ring Bridge Railing System, Final Report FHWA Contract DOT-FH-11-7985, 1976.
10. Olson, R.M., et al, Texas T1 Bridge Rail Systems, Technical Memorandum 505-10, Texas Transportation Institute, April 1971.
11. Powell, G.H., BARRIER VII: A Computer Program for Evaluation of Automobile Barrier Systems, Report No. FHWA-RD-73-51, April 1973.
12. McHenry and Deleys, N.J., Highway Vehicle Object Simulation Model (HVOSM), "Vehicle Dynamics in Single-Vehicle Accidents," Volumes 1-10.
13. Bruce, R.W. and Hahn, E.E., GUARD, Guardrail/Vehicle Dynamic Interaction, Final Report FHWA Contract DOT-FH-11-8520, 1976.
14. Labra, John J., et al, A Rollover Vaulting Algorithm (RVA) for Simulating Vehicle/Barrier Collision Behavior, presented at Transportation Research Board Annual Meeting, 1975.

REDUCING THE RISK OF CATASTROPHIC BRIDGE FAILURES

Lester A. Herr, Chief, Bridge Division,
Federal Highway Administration, Washington, D.C.

The public and engineers alike have become accustomed to the use of a factor of safety to prevent failures. Unfortunately, such factors do not prevent catastrophic failures because of rare or unusual events or circumstances. Such failures could be caused by large floods, earthquakes, poor workmanship, inferior materials, errant sea vessels or insufficient knowledge on which to make design judgments. This paper presents a philosophy, and briefly describes methods, for reducing the risk of catastrophic bridge failures.

Catastrophic failures have a great impact on the public and the engineering profession. The collapse of a bridge, although infrequent, always makes the news headlines. Such failures are not expected because the bridge engineer is a respected public servant who has done his job well. We must keep this public trust, therefore, it is important that the subject of reducing the risk of catastrophic bridge failures be discussed at this meeting.

A catastrophe, according to the dictionary, is any great and sudden calamity, disaster or misfortune. The collapse of a bridge is a catastrophe. Catastrophic failures of bridges are caused by: (1) the occurrence of unusual or rare events such as floods or earthquakes, (2) the limited understanding of our materials and engineering principles, (3) failure to provide adequate maintenance or timely replacement (4) load limit violations or (5) impact from naval vessels.

In reducing the risk of failures, one might conclude that this can be accomplished by increasing the factor of safety. No, this reduction of risk is not necessarily one of making a bridge larger or stronger but one of designing with the recognition that the unusual and unexpected can occur and that no one individual has all the answers in this complex engineering profession.

As evidenced by all the excellent papers on new technology in the use of materials for bridge construction given at this meeting, we are making tremendous progress in designing new type structures and in doing a better job on our conventional designs. Nothing in this discussion on reducing the risk of failures should detract from the technical experts who so ably have made such significant contributions. We need, however, to recognize that catastrophic failures are a concern of all of us and we must cope with this eventuality in the design of a bridge and throughout its service life.

Unfortunately, it took the failure of the Silver Bridge over the Ohio River in 1967, killing 46 people, to bring about the National Bridge Inspection Program. Inspection of existing projects is quite important and hopefully such inspections can prevent other catastrophic failures. My objective here, however, is to stress the importance of making engineering decisions from the inception of a project, as well as throughout its service life, that will give the best chance of survival of our bridge structures should the unusual and unexpected occur.

The recent failure of dams in Idaho and Georgia are good examples of the risk assumed in building such structures. There is always the possiblity of failure from rare floods, earthquakes or inadquate inspections, even though the probability of such an occurrence is small indeed. In these cases we reduce the risk of failure by doing a good job of design and construction but we must be aware that a failure can occur. It might be prudent to evaluate the alternatives of building no dam or permitting no town downstream. One can easily see by this extreme example what is meant by reducing the risk of catastrophic failures.

The idea of reducing the risk of catastrophic bridge failures is somewhat more subtle. Possibly the best way to illustrate the point is to present several examples that might apply during plan development and operation of a bridge project, namely through the customary planning, design, construction and maintenance phases.

Planning

Good planning is essential in building a bridge. The bridge engineer should be involved in the planning process as well as in the operation of the bridge after it is completed. Some bridge engineers believed that the environmental impact statement process would give them more input into the planning and development phases. Such input should reduce the constraints in modifying structural proposals and locations as design plans develop. It is doubtful that such an ideal arrangement has come about, since many environmental impact statements tend to be quite restrictive on the designer.

The whole thought process in reducing the risk of a catastrophic failure is to evaluate the chance of a bridge to survive if the unusual occurs. Planning decisions that avoid landslides, avalanches, floods or poor foundations are steps in the right direction. Planning and design advisory panels composed of selected expertise have proven their worth over the years, particularly in designing large, new-type bridge structures. The advisory panel for the first Lake Washington floating bridge is an excellent example. One member of this panel once related that one of their major concerns was whether or not the concrete pontoons used could be built to withstand water for a long period of time. One wonders if this concern over such a mundane matter did not have some bearing on the fact that you can sweep dust in the cells of the pontoons after 40 years of service. To further emphasize the desirability of setting up of such panels, the designer of the more complicated Hood Canal floating bridge did not have the benefit of a panel and the project nearly ended in a catastrophic failure of both the bridge and the chief engineer.

Design

As a result of the planning process, the bridge engineer usually has to accept some compromise to his idea of the ideal solution. Hopefully the planning decisions provide for some latitude to study alternatives as the more detailed design develops. Crossing a river usually offers no compromise, but where and how we cross usually give some latitude on the selection of the location and grade of a structure.

In considering a reduction to risk of failure stream crossings are particularly important because of the number of bridges lost annually due to floods. Many are designed to pass 50- or 100-year floods, but larger floods are usually the cause of a washout. It is time we stand back and look at our designs and follow the suggestion of one college professor when he tells his students to ask, "What if?" What if a larger flood occurs (and it will)? What if there is a flaw in my material or my workmanship is poor? In answering these questions, must I admit that my structure will collapse or will I just have a minor repair?

Providing structures adequate to pass rare floods and maintain traffic at the same time is both difficult and uneconomical. It is then a challenge to construct a crossing that accommodates the rare flood with minimal damage. Such designs mean providing waterway over bridge approaches, building relief openings and even submerging the bridge itself. This type of design has worked satisfactorily in the past, and more common use of such features can do much in reducing the risk of catastrophic failures.

What is involved in designing a crossing that can accommodate such large floods? First, the designer must have a good concept of the hydraulic principles of stream flow, the characteristics of stream scour (realizing the limitations in the state-of-the-art), the effects of bridge and approach geometry on flow and an appreciation of problems caused by drift and debris. This knowledge must be applied to design the many features of the entire crossing or our bridge could be washed out before overflow is accomplished. Some of the features to be considered are: pier type and orientation, use of spur dikes and abutment treatment, pile penetration, size and location of main span and relief openings, and resistance of the structure to forces of water and debris, including floatation. Usually each crossing has a unique set of problems. Often the type of construction proposed here is not a matter of more cost, but rather more design time and much engineering ingenuity.

Another design aspect that is less obvious than floods, but nevertheless a major factor in catastrophic failures, is the problem of the brittle fracture of critical structural members. Recently there have been several failures of such members, nearly causing complete collapse of major bridges. The risk of this type of failure can be reduced in two ways: (1) avoid this type of design or (2) recognize the risk and design accordingly.

Fracture critical structural members are single load-path (nonredundant) elements of a structure whose unfailing performance is necessary to prevent collapse of the structure. As compared to a multiple load-path (redundant) member, there is no alternate member to carry the load if one of these fracture critical members should fail. Two examples of fracture critical members are the tie-girder of a tied arch and the girders of a two-girder simple-span bridge.

Obviously, safety can be built into a structure by designing a multiple-load-path system or one that can transfer load from one member to another should one break. Such a system is sometimes called a back-up system. A multiple girder superstructure is this type of system. If, however, a non-redundant system is to be built, the designer must understand the detailing of such a design and the limitations of the materials to be used. He must also understand the constraints on perfection in the construction of his project. Provisions must be made for access to critical members to facilitate inspection and maintenance.

To reduce the risk of collapse of a steel bridge containing fracture-critical members, the Federal Highway Administration is proposing a facture control plan for use by the designer, contractor and inspector. The fracture control plan specifies higher toughness steel, more stringent weld-procedure qualification and high quality inspection during fabrication.

Construction

Assuming we have an adequate design, including specifications, it then behooves us to construct the project according to plans. When fracture critical members and other vulnerable features are involved in our construction, extra-special care must be taken as to how the job is constructed. The pressures of both political and economic competition make it attractive to cut corners

either to expedite the project or to make more profit. We must guard against all irregularities on projects or portions of projects identified to be critical.

The most productive and obvious way to construct a good project is through the cooperative efforts of the contractor and the project engineer. Both of these individuals must have a thorough understanding of the project, including the identification of items that require special attention and unusual inspection. Although it is difficult to list all the steps or procedures needing attention on critical projects, the following list can be used as a guide.

1. Arrange a preconstruction conference and subsequent conferences as required to assure that all parties involved in the construction of a project are informed of responsibilities.
2. Review the contractor's schedule of work and discuss critical items with the project supervisor.
3. Check all items on the fracture control plan and confirm with the contractor the assignment of responsibilites. Quality control and quality assurance programs are an essential part of the fracture control plan.
4. All changes in plans of identified critical items should be checked by the designer before approved.

Maintenance

No mention has been made to this point about the disregard of load limits on structures as being a cause of catastrophic failures. Each year a number of drivers of large trucks ignore load-limit or clearance signs and cause bridges to collapse. Nothing in this discussion is meant to imply that we should design to eliminate the need for weight-limit controls. We know that overloads shorten the fatigue life of structures, therefore, load-limit posting commensurate with the structural strength of a bridge is important to prevent catastrophic failure.

To assure fail-safe bridges that are in service, we need adequate periodic inspections by qualified personnel. Criticial parts of each bridge, including foundation piling, fracture critical members, rockers and bearings should be identified and receive special attention in order to reduce the risk of collapse. All deficiencies at critical locations should be reported, evaluated, and remedial action taken for immediate repair or possible closure of the structure. It must be stated that periodic inspections of existing bridges is an important step toward preventing catastrophic bridge failure. Also, inspections during and after highwater have helped considerably in correcting deficiencies.

Recently we have experienced a rash of bridge failures from the impacts of large ships and barges. Fender systems, navigation aids, warning devices and clearances must be maintained as an effort to protect our bridges from such catastrophic failures. Navigation controls, passage clearances, and pier fendering systems are subjects needing further study and research.

Conclusion

In the short time of this presentation you have thought of some additional ways you could design your bridges to give them a better chance of survival. Only highlights have been presented here. Designing to withstand earthquakes is certainly a subject worthy of consideration. Avalanches, earth slides and wind deserve some attention too. None of us, as individual engineers or collectively as a profession, want our structures to fail. We cannot predict the so-called "Acts of God," but we can minimize their impact.

CONSIDERATIONS IN THE DEVELOPMENT OF AN EARLY WARNING VESSEL/BRIDGE COLLISION SYSTEM

Eugene F. Greneker, Jerry L. Eaves, and Melvin C. McGee, Georgia Institute of Technology

Overview

Highway and railway bridges spanning navigable waterways face the real possibility of being accidentally struck by large ocean-going vessels or large barge trains. In many cases, these accidents can result in serious damage to the bridges, blockage of the waterways, economic losses to communities served by the bridges and waterways, and loss of property and life.

Two basic types of systems might be used to help prevent ships from striking bridge supports. The fender system is sometimes deployed around vulnerable bridge supports, but this approach is not always practical nor cost effective. Moreover, the fender system is not always effective in preventing damage to ships and bridge structures. Since it provides no warning to alert the ship crew that the ship is on a collision course, the fender system can at best only reduce the damage; it is a brute-force, last-ditch protection device.

An electronic warning system is a viable alternative or complement to the fender system. The electronic system could continuously monitor the ship position relative to a safe corridor for passage under the bridge and issue an immediate warning of any deviation from a safe-passage course. The system could also issue warnings to the bridge tender and people on the bridge when a collision is determined to be unavoidable. An advanced design concept of such a system was developed by the Georgia Institute of Technology Engineering Experiment Station (GIT/EES) during a recent study.

Equipment failure and human negligence are the primary causes of accidental damage to bridges by ships, but any system designed to prevent such accidents must also consider other factors; e.g., bridge-waterway configuration, ship navigation characteristics and the effects of wind and tide conditions, system reliability, and liability for accidents attributed to system failure. These design considerations led to selection of a system that uses a shore-based radar and shore-based displays as the most practical concept for an electronic collision avoidance/warning system. The radar would determine the ship's position, and the displays would inform the ship's pilot of the ship's position relative to a safe-passage corridor. The system would continuously assess the potential for collision during the various stages of the ship's passage. Ship speed and trajectory would be monitored as the ship approached the bridge; this information could be displayed for use by the ship crew in navigating the channel. When the ship approached closer to the bridge and entered a critical maneuver zone, the system would continue displaying the ship position while performing trajectory calculations to determine the possibility of a collision with the bridge. Should the system determine that a collision is possible (given the ship's handling characteristics and position in the channel, tide and wind conditions, and distance from the bridge), an alarm would be sounded to alert the ship crew, the bridge tender, and those on the bridge. Safety systems such as gates could be activated to keep additional traffic off the endangered bridge span.

Although the design concept was developed for the protection of highway bridges, it could be easily adapted for the protection of railway bridges.

Design Considerations

Effects of Ship/Bridge Collisions

Human lives, property, and income are often affected by ship/bridge collisions. The GIT/EES became involved in the design and development of ship/bridge collision warning systems shortly after the freighter **African Neptune** rammed the Sidney Lanier Bridge near Brunswick, Georgia, on 7 November 1972. Ten people were killed when an entire bridge span was severed from its support system and dumped into the river. The bridge was closed to vehicle traffic for seven months while repairs were being made to the damaged parts of the bridge span. This was not an isolated incident.

A similar accident occurred during January 1975 when the freighter Illawarra struck the Tasman Bridge spanning the Derwent River at Hobart on the Australian island of Tasmania. The collision collapsed an entire bridge span, sinking the vessel and killing at least six persons. Four of the dead were motorists who plunged from the broken span into the river.

Since 1955, the Lake Pontchartrain Causeway in Louisiana has been damaged by waterway traffic 13 times. Nine persons were killed in these accidents.

On 13 September 1976, one motorists was killed and two were injured when the tugboat Leander, Jr. lashed to several barges collapsed a span of the Highway 51 bridge near Pass Manchac, Louisiana, after colliding with the structure.

On 24 February 1977, the sulpher carrier Marine Floridian smashed into the Benjamin Harrison lift bridge, dumping vehicles into the James River near Hopewell, Virginia. The river channel was closed to shipping traffic for 20 days, and the bridge was closed to vehicle traffic until the latter quarter of 1978.

These (and many more documented ship/bridge collisions) accidents indicate a definite need for a collision avoidance/warning system.

Cause of Ship/Bridge Collisions

Equipment failure and human negligence are the primary causes of ship/bridge collisions. Human error caused the collision of the African Neptune with the Sidney Lanier Bridge. During the approach to the bridge, the harbor pilot ordered 20-degrees left rudder. The helmsman mistakenly put the rudder 20-degrees to the right. The mistake was noticed too late for compensating actions to prevent the collision.

Eight of the accidnets involving the Lake Pontchartrain Causeway Bridge were caused by human negligence; five were caused by equipment failure. All but one of the accidents caused by negligence occurred at night or under twilight conditions. One accident occurred when the helmsman passed out, another occurred when the helmsman fell asleep.

Mitigation of Losses

A study of ship/bridge collision reports indicates that suitable warning could substantially reduce accidental losses, particularly human lives. Newspaper accounts of the Sidney Lanier Bridge accident credit three boys with saving the lives of several persons. The boy's cars were stopped with other traffic on the bridge waiting for the African Neptune to pass through the lift. One of the boys realized that the ship was on a collision course with the bridge even before the ship began to sound it's whistle as a warning. The boys began beating on the windows of other cars and shouting warnings of the impending collision. Several motorist left their cars and ran with the boys to safety; others, perhaps thinking the boys were joking, rolled up their windows and locked their doors.

Analysis of other similar accident reports revealed several common factors which must be considered in designing a warning system. It appears that when human factors cause a collision the ship crew either can not or does not sound a warning in time for all persons on the bridge to reach safety. In the case where a warning was sounded, few motorist associated the warning whistle with danger. In most accidents, the ships were well outside of a narrowly-defined approach corridor sometimes minutes before the collisions.

These analyses indicate that a warning system designed to prevent or reduce the potential for losses due to ship/bridge collisions should:

1. Notify the ship crew of the ship position relative to the channel centerline.
2. Sense when a ship is on a non-correctible collision course with the bridge.
3. Warn the bridge tender and motorists of the impending collision and give instructions on where to seek safety.
4. Actuate gates and other barriers to prohibit vehicles from entering onto the endangered bridge span.
5. Record the track of the ship as it navigates the waterway for later analysis and court evidence.

Bridge-Waterway Configuration

The bridge-waterway configuration affects the need for and the design of a collision avoidance/warning system. Wide waterways offering a straight approach to the bridge reduce the changes of ship/bridge collisions, but these are not always practical. The Sidney Lanier Bridge chosen by the GIT/EES for development of the electronic warning system concept represents a more dangerous configuration, particularly for ships sailing from Brunswick Harbor. Ships approaching the bridge from the southeast (i.e., sailing up the Turtle (Brunswick) River) make a straight approach to the bridge for a distance of approximately 3.3 km (1.8 nmi); very little maneuvering is done by ships approaching from this direction since only minor course corrections are normally required.

The critical part of navigating the channel occurs between the Sidney Lanier Bridge and the Brunswick Port Authority docks. Approximately 457m (1500 feet) north-northeast of the bridge, the channel forms a Y intersection. The right fork goes to the dock area; the left fork continues up-river. The angle formed by the intersection of the river and dock area channel is about 50 degrees. Thus, all large vessels entering or leaving the Brunswick dock area must negotiate a 50-degree turn over a distance of less than approximately four ship lengths. It is during the performance of this maneuver by outbound ships that almost all problems occur that lead to potential collisions with the bridge.

Ship Navigation Characteristics

Ship navigation characteristics and the effects of wind and tide conditions combine with the bridge-waterway configuration to increase the possibility of a ship/bridge collision. Large ships, by virtue of their size, are not highly maneuverable. Each ship has a design turning radius that cannot be reduced at will. The turning performance is further degraded when the current vectors of the surrounding water are aligned with the thrust vectors of the ship (ebb tide). Wind can combine with current vectors to further degrade a ship's maneuvering ability.

The rudder size of large ships requires the use of hydrolic systems to relay steering commands to the rudder. This can account for a delay of up to 15 seconds in the ship's response to a steering command. The effectiveness of the rudder is also affected by ship speed; the faster the ship moves, the more effect the rudder has for any given degree of rudder offset.

For ships such as those leaving the Brunswick Harbor, these characteristics pose a paradox. The ship must maintain speed for maximum rudder effectivenesss while making the critical turn; yet, the speed cannot be so great that the ship cannot be stopped should the ship fail to navigate for proper alignment with the bridge opening. The range of speed that must be maintained to ensure the proper balance between ship maneuverability and safety is

very narrow. Any system designed to help in avoiding ship/bridge collisions should, therefore, have the capability of displaying the ship's true speed to the pilot.

Operational Requirements

The electronic system must function in adverse weather and must provide position information to the ship pilot without distracting the pilot. The use of the radar aboard the ships was rejected as an element in the warning system because the operational performance of shipboard radars varies significantly and requires that the local pilot become familiar with each particular ship radar peculiarities. In addition, it was determined that the pilot should have a system that he can depend on and learn to use skillfully. This requirement dictates that the system must be a permanent fixture having known performance standards. Furthermore, the system should not require that the pilot rig the system for each ship. Thus, the primary requirements are for a shore-based radar system and shore-based displays.

System Concept

The system concept developed for protection of the Sidney Lanier Bridge is based on the use of a shore-based radar to determine the ship's position and shore-based displays to inform the ship's pilot and the bridge tender of the ship's position relative to a safe-passage corridor. The system concept is illustrated in Figure 1.

The radar would be located so that it would have a clear view of the entire river channel from the mouth of the Brunswick dock area to the bridge, and the antenna would be operated in a sector scan mode to provide an angular coverage of approximately 90 degrees. The radar would track the ship as it left the Brunswick dock area until it reached the bridge. The radar would supply information concerning the location of the ship bow and stern (i.e., orientation of the ship in the channel).

The pilot's display would be a billboard system to provide a heads-up indication of ship speed and distance from channel centerline. The Sidney Lanier Bridge system would require the use of two pilot's displays; one located on the bank and one located on the bridge. Two displays would be used because it is important that the pilot look down the center of the ship bow during turning maneuvers. The pilot would use the shore-based display while emerging from the dock area until reaching a point halfway through the 50-degree mid-river turn. Halfway through the mid-river 50-degree turn, the pilot's field of view would shift to a point near the center of the bridge. At this point, the pilot would use the display mounted in the center of the bridge.

The display system used by the bridge tender would be a miniature version of the pilot's display system and would be mounted on a panel in the bridge control room. Thus, the bridge tender would have access to the same information as the ship pilot. It was reasoned that the bridge tender would eventually learn the proper channel position for the ship as a function of distance from the bridge. The ability of the bridge tender to use his display to warn of a collision would not be left to chance. The radar signal processor would automatically sound an alarm when the ship posed a danger to the bridge. This danger criteria would be computed on the basis of the ships location in the channel, heading, speed, size, and interactions with tide, current and wind conditions. A second alarm would be sounded if the ship reached a point where collision were imminent. A plan of action could be developed to warn motorists and the pilot, given the two levels of warning available to the bridge tender. This warning would be in verbal form given to motorists (by loudspeaker or other communication device) with instructions on the evasive action to be taken. The evaisve action tape recording message would be selected by the radar signal processor.

Figure 1. System concept for Sidney Lanier Bridge.

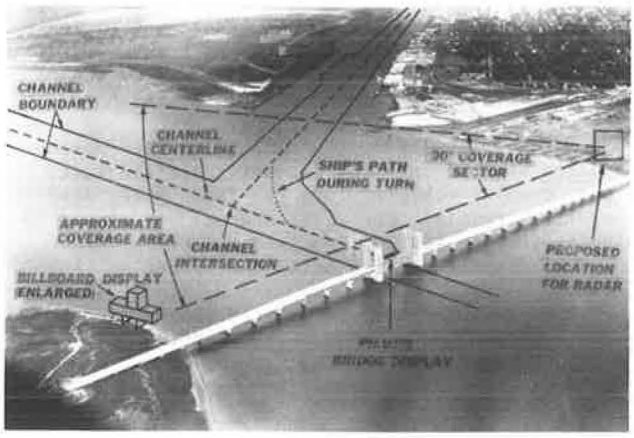

Conclusions

Highway and railway bridges are vulnerable to damage by ships. The consequences of ship/bridge collisions can be far reaching, including the loss of human life. The primary causes of accidental ship/bridge collisions are equipment failure and human negligence. Therefore, an electronic system that reduces the chances of or the losses from such accidents should be given serious consideration.

The system concept developed by the GIT/EES for protection of the Sidney Lanier Bridge represents a near worst case condition. The concept can be readily adpated to provide protection of less vulnerable bridges.

An automated detection and warning system may **be a cost-effective alternative to fenders for protection of certain bridges. The system could in many cases provide a warning to motorist much earlier than a ships crew. It could also provide a warning message tailored to get an optimum response as well as provide accurate data for post accident inquiry boards. Ships crews could be given information to improve their navigation and thus decrease the probability of collision. The same system could operate safety barriers to close traffic lanes after collision.**

Acknowledgements

The original research from which this report was generated was sponsored by the Georgia Department of Transportation under R&D Contract No. 6-73.